UCLA
UCLA Electronic Theses and Dissertations

Title

The gut microbiota mediates dietary and stressor-induced risk for murine neurological dysfunction

Permalink

Author

Olson, Christine

Publication Date

2021

Peer reviewed|Thesis/dissertation

UNIVERSITY OF CALIFORNIA

Los Angeles

The gut microbiota mediates dietary and stressor-induced risk for murine neurological

dysfunction

A dissertation submitted in partial satisfaction of the

requirements for the degree Doctor of Philosophy

in Molecular, Cellular, and Integrative Physiology

by

Christine Ann Olson

2021

ABSTRACT OF THE DISSERTATION

The gut microbiota mediates dietary and stressor-induced risk for murine neurological dysfunction

by

Christine Ann Olson

Doctor of Philosophy in Molecular, Cellular, and Integrative Physiology

University of California, Los Angeles, 2021

Professor Elaine Hsiao, Chair

The gut microbiota varies in a host of human neurological disorders and in murine models is critical to proper neurodevelopment and in neuropathologies. However, current mechanistic evidence is lacking for how microbes related to homeostatic and/or pathological signaling affect these processes. The incidence of neurological disorders without viable treatment options, including epileptic disorders and cognitive impairment, is increasing which raises the impetus in searching for novel biological pathways and mechanisms by which these disorders may be prevented or treated. The gut microbiota has gained attention as a modifier of neurological risk for disorders in development, adulthood, and aging. The work described in this thesis isolates molecular mechanisms by which the gut microbiota mediates environmental protection or risk in murine models

of epileptic episodes, cognitive impairment, and host metabolic dysfunction. Specifically, we report that the ketogenic diet, which provides protection against intractable epileptic seizures, mediates this effect in mice through the gut microbiota, more specifically through modifying gamma-glutamylated amino acids. We characterize cognitive and neurophysiological responses in mice mediated by dietary and stressor-induced changes in the gut microbiota, which is mediated by microbial changes in host immune pathways. Together, our findings provide mechanistic evidence that the host microbiota prevents and contributes to murine neurological dysfunction.

The dissertation of Christine Ann Olson is approved.

Alcino Jose Silva

Xia Yang

Jonathan P. Jacobs

Yvette Tache

Elaine Yih-Nien Hsiao, Committee Chair

University of California, Los Angeles

2021

PREFACE

This dissertation was supported in part by National Institutes of Health (NIH) National Research Service Award Institutional Training Grant (T32), NIH Individual Predoctoral Fellowship (F31), the UCLA Graduate Division Dissertation Year Fellowship, and the UCLA Edith L. Hyde Award. All the work was performed primarily by me with the exception of co-authored work in Chapters 1, 2, 4, 6, 8 and Appendix 2. Specific author contributions are indicated in each Chapter. The Chapters listed below are reprints or versions of published or submitted manuscripts, reproduced with permission.

Chapter 1 is a version of:

Jameson, K.G., Olson, C.A., Kazmi, S.A., Hsiao, E.Y. Toward Understanding Microbiome-Neuronal Signaling. *Molecular Cell*. (2020).

Chapter 2 is a version of:

Lum, G.R., Olson, C.A., Hsiao, E.Y. Emerging roles for the intestinal microbiome in epilepsy. *Neurobiology of Disease*. (2019).

Chapter 4 is a version of:

Fung, T. C., Olson, C. A., Hsiao, E. Y. Interactions between the microbiota, immune and nervous systems in health and disease. *Nature Neuroscience* 20, 145-155, PMID: 28092661 (2017).

Chapter 5 is a version of:

Olson, C.A., Vuong, H.E., Yano, J.M, Liang, Q.L., Nusbaum, D.J., Hsiao, E.Y. The gut microbiota mediates the anti-seizure effects of the ketogenic diet. *Cell*. 173(7):1728-1741.e13. PMID: 29804833 (2018).

Chapter 6 is a version of:

Olson, C.A., Iñiguez, A.J., Yang, G.E., Fang, Ping, Pronovost G.N., Jameson, K.G., Rendon, T.K., Paramo, J., Barlow, J.T., Ismagilov, R.F., Hsiao E.Y. The gut microbiota modulates environmental risk for cognitive impairment. *Cell Host and Microbe* (2021).

Chapter 7 is a version of:

Ahn, I., Lang, J., Olson, C.A., Ying, Z., Zhang, G., Byun, H., Zhao, Y., Kurt, Z. Lusis, A.J., Hsiao, E.Y., Gomez-Pinilla, F., Yang, X. Host Genetic Background and Gut Microbiota Contribute to Differential Metabolic Responses to High Fructose Consumption in Mice. *Journal of Nutrition*. (2020).

Chapter 8 is a version of:

Noble, E., Olson, C.A., Davis, E., Tsan, L., Chen, Y., Schade, R., Liu, Clarissa, Suarez, A., Jones, R., Goran, M., de la Serre, C., Yang, X., Hsiao, E.Y., Kanoski, S. Gut microbial taxa elevated by dietary sugar disrupt memory function. *Translational Psychiatry* (2021).

Appendix 1 is a version of:

Ulzee, A., Shenhav, L., Olson, C.A., Hsiao, E.Y., Halperin, E., Sankararaman, S. STENSL: microbial Source Tracking with ENvironment SeLection. *RECOMB*. (2021).

Table of contents

VITA

EDUCATION

Ph.D. Candidate
> University of California, Los Angeles
> Molecular, Cellular and Integrative Physiology

Bachelor of Science, June 2013
> University of California, Davis
> Neurobiology, Physiology, and Behavior; English Minor

FELLOWSHIPS AWARDED

- 2020-2021, UCLA Graduate Division Dissertation Year Fellowship
- 2019-2021, NIH/NRSA Ruth L. Kirschstein Predoctoral Fellowship (1F31AG064844-01)
- 2019-2021, Advanced Predoctoral Fellowship in Neurobehavioral Genetics (T32NS048004)
- 2017-2018, Edith I. Hyde Fellowship, UCLA
- 2015-2017, NIH Institutional Predoctoral Fellowship, Molecular, Cellular and Integrative Physiology (T32GM065823), 2015-2017

AWARDS

- 2019 Best Talk, UCLA Molecular, Cellular, Integrative Physiology Annual Retreat
- 2017 Society for Neuroscience Nancy Rutledge Zahniser Trainee Professional Development Award
- 2017 BRI/Semel Institute Society for Neuroscience Meeting Travel Grant
- 2017 Best Poster Presentation, UCLA Molecular, Cellular, Integrative Physiology Annual Retreat
- 2017 Travel Grant, Attendance to Microbiome Analysis in the Cloud Seminar; Baltimore, MD

PRIMARY RESEARCH PUBLICATIONS

- Olson, C.A., Iñiguez, A.J., Yang, G.E., Fang, Ping, Pronovost G.N., Jameson, K.G., Rendon, T.K., Paramo, J., Barlow, J.T., Ismagilov, R.F., Hsiao E.Y. The gut microbiota modulates environmental risk for cognitive impairment. Under review (2021).
- Olson, C.A., Vuong, H.E., Yano, J.M, Liang, Q.L., Nusbaum, D.J., Hsiao, E.Y. The gut microbiota mediates the anti-seizure effects of the ketogenic diet. *Cell*. 173(7):1728-1741.e13. PMID: 29804833 (2018).
  - o Recipient of the 2019-20 Life Sciences Excellence Award for Outstanding Research Publication from UCLA Life Sciences
- Noble, E., Olson, C.A., Davis, E., Tsan, L., Chen, Y., Schade, R., Liu, Clarissa, Suarez, A., Jones, R., Goran, M., de la Serre, C., Yang, X., Hsiao, E.Y., Kanoski, S. Gut microbial taxa elevated by dietary sugar disrupt memory function. *Translational Psychiatry* (2021).
- Ulzee, A., Shenhav, L., Olson, C.A., Hsiao, E.Y., Halperin, E., Sankararaman, S. STENSL: microbial Source Tracking with ENvironment SeLection. *RECOMB*. (2021).
- Ahn, I., Lang, J., Olson, C.A., Ying, Z., Zhang, G., Byun, H., Zhao, Y., Kurt, Z. Lusis, A.J., Hsiao, E.Y., Gomez-Pinilla, F., Yang, X. Host Genetic Background and Gut Microbiota Contribute to Differential Metabolic Responses to High Fructose Consumption in Mice. *Journal of Nutrition*. (2020).
- Orbay, H., Little, C.J., Lankford, L., Olson, C.A., Sahar, D.E., The Key Components of Schwann Cell Differentiation Medium and the Effects on Gene Expression Pattern of Adipose Derived Stem Cells. *Annals of Plastic Surgery*, 74, 584-588, doi:10.1097/sap.0000000000000436 (2015).
- Hinchcliff, K., Olson, C.A., Little, C.J., Orbay, H., Sahar, D.E. Irradiated Superficial Femoral Artery Rupture after Free Flap: A Case Report and Review of the Literature. *Annals of Plastic Surgery* 74 Suppl 1, S15-18, doi:10.1097/sap.0000000000000432 (2015).

REVIEWS, PERSPECTIVES, AND PREVIEWS

- Olson, C.A., Lum, G.R., Hsiao, E.Y. Ketone Bodies Exert Ester-Ordinary Suppression of Bifidobacteria and Th17 Cells. *Cell Metabolism* (2020).

- Jameson, K.G., <u>Olson, C.A.</u>, Kazmi, S.A., Hsiao, E.Y. Toward Understanding Microbiome-Neuronal Signaling. *Molecular Cell.* (2020).
- Lum, G.R., <u>Olson, C.A.</u>, Hsiao, E.Y. Emerging roles for the intestinal microbiome in epilepsy. *Neurobiology of Disease.* (2019).
- Fung, T. C., <u>Olson, C. A.,</u> Hsiao, E. Y. Interactions between the microbiota, immune and nervous systems in health and disease. *Nature Neuroscience* 20, 145-155, PMID: 28092661 (2017).
- <u>Olson, C. A.</u>, Vuong, H. E., Hsiao, E. Y. Microbial Olympics: Equestrian Event. *Nature Microbiology* doi:10.1038/nmicrobiol.2016.122 (2016).

PRESENTATIONS AND INVITED TALKS

- Invited talk for American Epilepsy Society 2021, cannot attend due to COVID
- Invited talk for Global Keto Meeting 2020, cancelled due to COVID
- Invited talk for International Society for Neurochemistry delayed to 2021 because of COVID
- <u>Olson, C.A.</u>, Vuong, H.E., Yano, J.M., Liang, Q.L., Nusbaum, D.J., Hsiao, E.Y. Indigenous bacteria of the gut microbiota mediate antiseizure effects of the ketogenic diet. Society for Neuroscience 2017.
  o Selected for publication and presentation in the 2017 Society for Neuroscience *Hot Topics in Neuroscience* book
- Ahn, I.S., Lang, J., Ying Z., Byun, H.R., Zhang, G., <u>Olson, C.A.,</u> Hsiao, E.Y., Lusis, A.J., Gomez-Pinilla, F., Yang, X. "Host Genetic Background and Gut Microbiota Contribute to Differential Metabolic Responses to High Fructose Consumption in Mice". American Diabetes Association, 2018.
- Irradiated Superficial Femoral Artery Rupture after Free Flap: A Case Report and Review of the Literature. Presented to the California Society of Plastic Surgeons 2014 in Newport Beach, CA

MENTORSHIP EXPERIENCE

- **Alonso Iniguez *(Sept 2017-July 2019)***: Masters student in Integrative Biology and Physiology program. Studying microbiota-based effects on hippocampal gene expression. Current employee of Pivot Bio, Inc.
- **Grace Yang (*Jun 2019-present)*** Undergraduate student interested in dissecting microbiome-brain interactions.
- **Gregory Lum (*Jan 2019- Mar 2019*)** PhD student studying the consequences of ketogenic diet-associated microbes on seizure susceptibility. Mentored as a rotation student and now occasionally as a PhD student in our laboratory.
- **Julia Barnett (*Jun 2017-Aug 2018*)**: High school student interested in studying QIIME and correlations between cognition and microbiome.
- **Qingxing Liang (*Jan 2016-Jun 2018)***: Neuroscience undergraduate student engaged in biochemical assays, dissections, growth curves, qPCR, behavioral analysis. Accepted to the Undergraduate Research Scholars Program and presented a poster in her junior and senior years. Current medical student at University of California, Irvine.
- **Benita Jin (*Nov 2018-Jun 2019*)** PhD student in the Molecular, Cellular, and Integrative Physiology program. Mentoring regarding choosing a thesis laboratory and tips for beginning graduate school.

PATENTS

- <u>Olson CA</u>, Iniguez, A., Hsiao EY (2019) Compositions and Methods for Modulating Cognitive Behavior. UCLA. Provisional Application Number: 62/855,290.
- <u>Olson CA</u>, Vuong HE, Yano JM, Hsiao EY (2016) Compositions and Methods for Inhibiting Seizures. UCLA. Provisional Application Number: 62/436,711, 62/447,992.

Acknowledgements

Shakespeare wrote in *The Tempest*, "What is past is prologue". With that, I would first like to thank the individuals responsible for the prologue of this story: Dr. Marc Facciotti, Dr. Brian Mulloney, Dr. Jim Trimmer and Dr. Belvin Gong, without whom I would have never started my Ph.D. work. Dr. Facciotti sponsored my participation in the international undergraduate synthetic biology competition iGEM in 2012, which first convinced me I would love doing and sharing research. Dr. Mulloney helped begin a Neurobiology laboratory course at my undergraduate institution UC Davis, and I was a student in the first class. Through a humorous and serendipitous event, I met Dr. Trimmer through him, who gave me my first post-graduation job producing antibodies for neuroscience under Dr. Belvin Gong. Without these four people in particular, I would not have the courage to begin this work in the first place, and to them I am forever grateful. This past was the prologue to prepare me for studying how specific microbes affect the brain. I fulfilled a dream by embarking on this journey, and I repeatedly reminded myself that even starting my Ph.D. required a good deal of luck and failure in equal measures.

To my friend and classmate Dr. Taylor Brown, who never got the chance to experience being a doctorate, may you forever rest in peace. I will cherish knowing you and value the mental health of those I come in contact with for the rest of my life.

I would like to thank my primary mentor Dr. Elaine Hsiao. I am grateful I got to experience the highs and lows of being your first graduate student, and I learned so much more than

I would have elsewhere. I saw firsthand just how hard you worked to put a laboratory together from the ground up, and it is amazing to consider where the lab is today due to your efforts. This experience in graduate school has transformed my life, and I hope you will agree with me when I say that I have grown through this time. Thank you for your patience with me and for encouraging us to push ourselves and to pursue rigorous science. If I am incredibly fortunate, one day I will have a first graduate student in my own lab, and I will take the lessons I learned here onward to help them. Graduate school can be a highly formative and therefore challenging experience, and I hope to help others through that journey now that mine is coming to an end.

helped me through thick and thin for 12 years now. I would like to thank Dr. Xuan Tran, Dr. Aanand Patel, and Dr. Lynn Yi for helping me laugh along the way, for the times we baked new things, and for our book club that eventually became an excuse to play board games.

As I write this, we are in the midst of the deadly coronavirus pandemic. This crisis has highlighted the critical societal need for basic biological research and for a strong public health program. If there is any wish I have aside from keeping the public as healthy as possible, it is to be able to thank each of these contributors in person. There are additionally many people not listed here who also contributed to my journey. Every experience I had helped me deal with painful rejection, fears of not finishing the work I started, and anxiety about simply not being good enough. Thank you for every warm improvement and interesting turn you have provided to my life. I am forever grateful to each of you. I do not know what the future holds, but I do know that this past has been a beautiful prologue and for that, I am grateful.

Overview

The focus of my doctoral research has been to study mechanisms of host-microbe interactions critical for neurological homeostasis or disease, and this falls under several categories of questions: (i) how does the ketogenic diet associated microbiota affect murine seizure susceptibility? (ii) how does the microbiota affect cognitive responses to ketogenic diet and an environmental stressor? (iii) How do microbiota-immune interactions contribute to cognitive impairment? (iv) Do gut microbes associated with increased sugar consumption sufficiently impair behavioral performance and host metabolism? (v) Are microbes associated with aging-related frailty? In Chapter 1-4, we discuss how microbes interact with neurons, associations of the gut microbiota with epileptic disorders, how bacteria can modulate neurotransmitters, and how microbes interact with both the immune and nervous systems, which serve as primers to understand the work in Chapter 5 on how the ketogenic diet-associated microbiota protect against murine seizure susceptibility. Chapter 7 focuses on how the gut microbiota associated with differing genetic backgrounds contributes to varied metabolic responses to high fructose consumption. Following these works, we were interested in furthering our understanding of how ketogenic diet associated microbes in the context of environmental challenge can affect host cognition, which is discussed in Chapter 6. These findings are furthered by Chapter 8 which demonstrates microbes associated with high sugar consumption which sufficiently impair behavioral performance. In the Appendices are preliminary findings relevant to this doctoral work. Appendix 1 focuses on STENSL, a microbial source tracking methodology, and Appendix 2 focuses on how the microbiota affects aging-related frailty.

This study began with a focus on the ketogenic diet (KD), a high fat, low carbohydrate diet that has been well-validated to be protective in drug resistant epilepsy disorders. Our laboratory demonstrated that in specific pathogen free mice (SPF), KD-mediated seizure protection is lost with antibiotic-induced microbiome depletion (Abx) or in mice that are raised germ free using the 6-Hz psychomotor seizure assay, which is a well-validated test for intractable seizures. These findings demonstrate that the gut microbiota is required for KD seizure protection. Additionally, we had shown that gastrointestinal colonization of Abx mice with microbial taxa enriching on the KD (Akkermansia muciniphila and Parabacteroides spp., AkkPb KD) was sufficient for restoration of KD seizure protection. Seizure was only noted with AkkPb colonized together, as Akk or Pb colonization alone had no significant effect on seizure protection. We asked whether probiotic treatment of AkkPb in mice fed the control diet (CD SPF) could confer seizure protection and found that after 28 consecutive days of AkkPb administration, seizure protection significantly increased. Protection was not conferred to mice treated with Akk alone, and seizure protection decreased when mice were treated with heatkilled AkkPb (hk-AkkPb). I focused on dissecting which host metabolomic changes imparted by the gut microbiota mediate KD seizure protection. To answer this question, we first compared colon content and serum metabolomes for CD SPF KD SPF, Abx KD, and AkkPb KD mice, and identified that both ketogenic γ-glutamylated amino acids and unmodified ketogenic amino acids generally decreased in the seizure protected groups (KD SPF and AkkPb KD) relative to the unprotected groups (CD SPF and Abx KD). We next hypothesized that decreased γ-glutamylation in unprotected mice would produce an antiseizure effect. The enzyme γ-glutamyl transpeptidase (GGT) is

3

ubiquitously expressed across every kingdom and transfers γ-glutamyl groups from glutathione to amino acids. GGT activity is specifically inhibited by GGsTop, and after oral gavage with GGsTop in CD SPF mice, seizure protection significantly increased. We also demonstrated that injection of ketogenic amino acids in AkkPb KD mice reduced seizure protection. We concluded that reductions in ketogenic γ-glutamylated amino acids is sufficient for seizure protection and next aimed to identify how the KD-associated gut microbiota modulates γ-glutamylation and how this process affects the brain. To address whether the CD SPF microbiota directly modulates γ-glutamylation, we performed a GGT activity assay on CD SPF fecal samples and found significantly increased GGT activity compared to KD SPF samples. We were interested to find that AkkPb colonization in mice fed KD further reduced GGT activity, which indicated that AkkPb may have a direct modulatory effect on GGT enzymatic activity. After performing the same activity assay on samples from the probiotic study, we also found that GGT activity was reduced in fecal samples for CD SPF mice after 28 days of AkkPb treatment. To isolate whether KD-associated microbes directly affect GGT activity, we firstly performed in vitro growth assays with Akkermansia and/or Parabacteroides merdae in either CD or KD-based media. We determined that while Akkermansia growth rates are not directly affected by Parabacteroides merdae, Parabacteroides merdae growth significantly increased with Akkermansia presence. We performed GGT activity assays and found that Parabacteroides merdae has GGT activity that is abolished with the presence of Akkermansia in both CD and KD. These findings led us to conclude that KD-associated microbes and the KD itself modulate GGT activity, which is one mechanism for seizure protection. To better understand how the central nervous system is affected by the gut

4

microbiota, we performed metabolomics on CD SPF, KD SPF, KD Abx, and Abx-AkkPb KD mice in the hippocampus, an important seizure gate. We identified that γ-aminobutyric acid (GABA), the primary inhibitory neurotransmitter, increased relative to proportions of glutamate, the primary excitatory neurotransmitter for the seizure protected groups (KD SPF and Abx-AkkPb KD). We hypothesize that decreased γ-glutamylation enhances the proportion of GABA to glutamate and that this process is directly cause by the gut microbiota. In the future, targeted microbiota-based therapies could serve as a novel therapeutic against neurological diseases, including intractable epilepsies.

Impaired cognition is one side-effect of intractable pediatric epilepsies, which has demonstrated some improvement with dietary KD administration. These findings led to researchers' increased interest in the KD as a therapeutic for a broad host of neurological disorders, including Alzheimer's disease and Parkinson's disease, however the data is mixed in early clinical trials. These findings led us to next consider how the KD-associated microbiota affects cognition in the context of an environmental stressor.

Cognitive impairment, defined by reduced attention, diminished learning and memory, and impaired reasoning, is a common and pressing public health concern, afflicting 16 million Americans and increasing globally (CDC 2011). Aging constitutes the greatest risk factor for cognitive impairment, and the American aging population is expected to increase to 88.5 million people by 2050. There is a pressing public health need to identify clinically tractable targets for prevention and/or treatment of cognitive impairment arising from both the lack of current treatment options and the rising aging population. Environmental factors including hypoxic insult and dietary consumption contribute to cognitive impairment probability, but precise mechanisms for how

environmental factors interact with impairment risk remains poorly understood. The gut microbiota mediates environmental contributions to host health and disease and causally modulates cognitive behavior in the novel object recognition, Barnes maze, and Morris water maze tasks. Together, this evidence warrants investigation into whether the gut microbiota modulates cognition during adulthood and aging. Our data support our central hypothesis that the gut microbiota is important for mediating detrimental effects of hypoxia (Hyp) murine hippocampal-dependent cognitive performance under ketogenic diet (KD) consumption. Given the similarities between molecular mechanisms for Hyp-induced and aging-induced cognitive impairment, we further hypothesize that select microbes modify aging-induced cognitive deficits. Our rationale is that identification of gut microbes contributing to cognition through changes in hippocampal and/or vagal nerve signaling pathways will offer new therapeutic opportunities for aging-induced cognitive impairment. We tested the hypothesis that specific microbial taxa mediate effects of the ketogenic diet (KD) and hypoxia (Hyp) on cognitive behavior and test whether treatment with select microbes modifies cognitive deficits; determine roles for the gut microbiota in modulating hippocampal activity relevant to cognitive behavior; assess the contribution of immune cell signaling to microbiota-dependent modulation of cognitive behavior. Upon conclusion, we hope this work contributes to better understanding of how the gut microbiota modulates cognitive behavioral outcomes.

Future studies will analyze the role microbiota-gut-brain circuits play in microbial modulation of host cognition and focus on identifying precise microbial molecules responsible for cognitive behavioral changes.

Chapter 1

Toward understanding microbiome-neuronal signaling

Kelly G. Jameson, Christine A. Olson, Sabeen A. Kazmi, Elaine Y. Hsiao

Summary

Host-associated microbiomes are emerging as important modifiers of brain activity and behavior. Metabolic, immune and neuronal pathways are proposed to mediate communication across the so-called microbiota-gut-brain axis. However, strong mechanistic evidence, especially for direct signaling between microbes and sensory neurons, is lacking. Here, we discuss microbial regulation of short-chain fatty acids, neurotransmitters, as yet uncharacterized biochemicals, and derivatives of neuromodulatory drugs as important areas for assessing microbial interactions with the nervous system.

Introduction

We have co-evolved with trillions of indigenous microorganisms that comprise the human microbiota. Over the past decade, the notion that the microbiome is a key regulator of host physiology and behavior has skyrocketed with the advancement of multi'omics technologies, gnotobiotic tools, intersectional genetics, and live imaging. Early studies linking alterations in the gut microbiome with neurobehavioral phenotypes launched the concept of a microbiota-gut-brain axis, whereby intestinal microbes influence brain and behavior through immune, neuronal, and metabolic pathways. In particular, emerging evidence suggests that select members of the microbiota have the ability to synthesize and/or regulate various neurochemicals known to modulate neurotransmission, as well as a vast milieu of other metabolites that may directly or indirectly impact neuronal activity.

As such, the role of mutualistic microbes in regulating sensory neuronal communication along the gut-brain axis is of active scientific interest. Microbial modulation of dietary molecules, neurotransmitters, as yet uncharacterized metabolites, and neurological drugs represent major areas for research, toward uncovering mechanisms for microbial modulation of neuronal activity (Figure 1).

Microbial Regulation of Short-Chain Fatty Acids

Early studies on feeding behavior, led by such pioneers as Claude Bernard and Ivan Pavlov, laid the foundation for the concept of a brain gut axis through dietary modulation (Leulier et al., 2017). With the advent of germ-free rodent models in the 1920s (Gustafsson, 1946), gut microbes were identified as important mediators of dietary metabolism and host nutrition. Germ-free animals exhibited substantially deficient levels of the short-chain fatty acids (SCFAs) butyrate, propionate, acetate and valerate in the intestine and blood, indicating a crucial role for the microbiota in regulating local and systemic SCFA bioavailability in the host (Hoverstad and Midtvedt, 1986). Continued research in this area has uncovered molecular mechanisms underlying microbial production of SCFAs through their fermentation of complex polysaccharides, propelled by the discovery and characterization of polysaccharide utilization loci present in *Bacteroidetes* (Bjursell et al., 2006).

A wealth of evidence has further demonstrated that alterations in the microbiota and SCFAs are associated with conditions in which food intake behaviors are dysregulated (Byrne et al., 2015). In particular, alterations in the gut microbiota are seen in obese mice and humans, which correlate with alterations in the levels of acetate and butyrate (Ridaura et al., 2013; Turnbaugh et al., 2006). Propionate administration to

9

patients with obesity enhanced gut hormone secretion while reducing adiposity and overall weight gain (Chambers et al., 2015). While some of the animal studies highlight microbial regulation of appetite as a basis for the observed differences in weight gain, exactly how microbial regulation of SCFAs impacts host feeding behaviors remains unclear. The SCFA receptors free fatty acid receptors 2 and 3 (FFAR2, FFAR3) are expressed in the enteric nervous system, the portal nerve, as well as various sensory ganglia (De Vadder et al., 2014; Egerod et al., 2018), suggesting a role for activation of the nervous system in mediating these effects. Consistent with this, propionate feeding induces *fos* expression in the dorsal vagal complex of the brainstem, the hypothalamus, as well as in the spinal cord (De Vadder et al., 2014), raising the question of whether SCFA-induced stimulation of peripheral sensory neuronal activity could mediate the effects of SCFAs on host feeding behavior.

As the list of host behaviors that are modified by the gut microbiome continues to grow (Vuong et al., 2017), a key open question is the extent to which microbial regulation of molecules relating broadly to nutrition underlie reported effects of the microbiome on complex host behaviors, spanning homeostatic feeding, social, stress-related and cognitive domains. SCFAs are fundamental molecules involved in regulating energy homeostasis, and SCFA receptors are expressed by a wide variety of non-neuronal cell subtypes as well. In immune cells, for example, SCFAs can regulate T regulatory cell differentiation (Arpaia et al., 2013; Furusawa et al., 2013; Smith et al., 2013) and microglial maturation (Erny et al., 2017), whereas in enteroendocrine cells, SCFAs can stimulate the release of gut hormones (Larraufie et al., 2018). In addition to promoting SCFAs, the gut microbiota is integral to secondary metabolism of bile acids, another class

of diet-related metabolites for which cognate receptors are expressed by various cell types, including subsets of sensory neurons, to regulate diverse host phenotypes (Mertens et al., 2017). In light of their pleiotropic effects, studies that dissect the precise signaling pathways by which SCFAs and bile acids alter host behaviors are warranted. Efforts to determine the functional roles of specific neuronal pathways in SCFA and bile acid signaling would be particularly illuminating toward uncovering roles for the microbiota in regulating neuronal activity via dietary metabolism.

Microbial Regulation of Neurochemicals

While the gut microbiota may affect host behavior through the regulation of dietary metabolites, like SCFAs and bile acids, emerging research indicates that select gut microbes also regulate levels of host neurotransmitters. The finding that microbes can directly synthesize neurotransmitters is rooted in the first discovery of chemical transmitters by Sir Henry Dale in the early 1900s (Valenstein, 2002). In studying ergot on wheat rye, he discovered the transmitter acetylcholine over a decade before it was extracted from mammalian tissue. Together with George Barger, Dale found that acetylcholine mimicked the effects of parasympathetic nerve stimulation, suggesting chemically-mediated neurotransmission. It was realized later that the acetylcholine itself was likely derived from *Bacillus* contaminants in the ergot, rather than from the ergot itself. Since this landmark discovery, additional neurotransmitters, including norepinephrine (NE), serotonin (5-HT), γ-aminobutyric acid (GABA) and dopamine (DA) have been found to be produced by bacteria in culture and to be regulated by the microbiota in animals (Strandwitz, 2018). Despite these tantalizing associations, all kingdoms of life produce the amino acid derivatives that form common "neurotransmitters", raising the questions:

what are the functional roles of neurotransmitters in microbes, and can host-associated microbes impact the nervous system through neurotransmitter modulation?

As yet, only a few studies have examined the effects of canonical neurotransmitters on bacterial physiology. One relatively early series of studies revealed that the catecholamines NE and epinephrine exhibit structural similarity to the quorum sensing molecule autoinducer-3, and therefore each stimulates enterohemorrhagic *E. coli* motility and virulence (Clarke et al., 2006). Researchers hypothesize that this direct effect of NE and epinephrine on bacterial pathogenesis may contribute to the ability of stress to increase susceptibility to infection. More recently, a study utilizing *in vitro* co-culture screens and metagenomic datasets revealed GABA-producing vs. GABA-consuming bacteria from the human gut microbiota (Strandwitz et al., 2019). In particular, GABA synthesized by *Bacteroides fragilis* supported the growth of KLE1738, suggesting that select neurotransmitters may serve as growth substrates for bacteria. A separate study found that 5-HT promotes intestinal colonization of the bacterium *Turicibacter sanguinis*, similarly suggesting a role for a neurotransmitter in promoting microbial fitness (Fung et al., 2019). Beyond these initial findings, little is known regarding the extent of neurotransmitter modulation across various members of the gut microbiota, the specific microbial genes and gene products used for their synthesis and catabolism, and the molecular pathways underlying microbial sensing and response to neurotransmitters. Integrated microbiological, biochemical and bioinformatic approaches are needed to support *in silico* predictions informed by multi'omic datasets, *in vitro* determination of microbial gene and protein function and *in vivo* investigation of microbial community responses. Identifying the molecular underpinnings for microbial synthesis,

transformation and physiological response to neurotransmitters would further enable mechanistic interrogation of the potential consequences of microbiota-dependent neurotransmitter modulation on host physiology.

Despite evidence that select host-associated bacteria regulate neurotransmitter levels locally in the intestine, and in some cases, systemically in the blood or distantly in the brain itself, whether microbial modulation of neurotransmitters actually influences neuronal activity and behavior remains poorly understood. In mice, the gut microbiota is responsible for promoting the biosynthesis of up to 60% of colonic and blood 5-HT levels by enterochromaffin cells (ECs) in the intestinal epithelium (Yano et al., 2015). In the intestine, microbially-modulated 5-HT activates intrinsic afferent primary neurons of the myenteric plexus to promote gastrointestinal motility, but whether extrinsic intestinally-innervating nerves are also affected remains unknown. Separate studies suggest that subsets of ECs may synapse with 5-HT-receptive afferent fibers of chemosensory vagal or dorsal root neurons (Bellono et al., 2017; Bohórquez et al., 2015), suggesting a direct path for microbial regulation of local 5-HT to impact the central nervous system. While evidence for microbiome-gut-sensory neuronal signaling is currently lacking, a growing number of studies reporting effects of the microbiome on host behavior have applied subdiaphragmatic vagotomy to demonstrate that severely impaired vagal signaling abrogates microbial effects on behavior (Bravo et al., 2011; Sgritta et al., 2019). Additional studies that circumvent the confounds of vagotomy and that carefully examine functional neuronal responses to microbially modulated neurochemicals are needed to evaluate the potential for microbes to directly affect neural activity. These efforts would be aided greatly by the development of synthetic biological tools to identify, regulate and

13

manipulate microbial genes for neurochemical modulation, coupled with host gnotobiotic and intersectional genetic tools for selective microbial colonization and targeted neurophysiological assessments. In addition to evaluating sensory neuronal pathways, efforts to examine the humoral transport of microbially-modulated neurochemicals or their precursors are warranted. Consistent with this possibility, heavy isotope-labeled acetate in the colon enters the bloodstream, crosses the blood-brain barrier, elevates hypothalamic acetate, and feeds into GABA neuroglial cycling to increase central GABA production (Frost et al., 2014). Novel tools to selectively label target neuromodulators that are produced or regulated by the microbiota, along with technologies for spatiotemporal tracking in animals, would help enable efforts to evaluate the ability of the microbiota to impact distant sites in the central nervous system.

Uncharacterized Microbial Products and the Nervous System

Aside from SCFAs, bile acids and neurotransmitters, there are likely many additional microbiota-dependent biochemicals that have the potential to interact with neurons. The human microbiota regulates a vast repertoire of metabolites not only in the intestinal lumen, but also in the circulating blood and various organ systems of the host. However, the identity, cognate receptors, signaling pathways and physiological functions of many microbially modulated metabolites remain poorly understood (Milshteyn et al., 2018). Recent functional metagenomics studies have begun to reveal the scope of bacterial genes for metabolite synthesis and signaling to the host. By screening cosmid metagenomic libraries, researchers identified host-associated bacterial effector genes, which upon bioassaying the gene products, resulted in the discovery of commendamide, an N-acyl amide capable of activating the host G-protein coupled receptor (GPCR/GPR)

14

G2A (Cohen et al., 2015). Continuing their work on N-acyl amides, the researchers also demonstrated that bacterially produced N-acyl serinol activated the endocannabinoid receptor GPR119A (Cohen et al., 2017). These studies illustrate that functional metagenomics can be a powerful tool, not only to discover novel bacterial metabolites, but also to reveal how bacterial metabolites can affect host physiology through mimicking endogenous GPCR ligands.

Recent studies have begun to identify GPCRs and orphan receptors that are activated by bacterial metabolites *in vitro*. In a screen of supernatants from individually-cultured bacteria from the human gut microbiota, receptors for DA, histamine, and 5-HT were highly responsive to soluble bacterial products. Among many additional candidates, bacterially-derived phenethylamine and tyramine activated DA receptors while bacterial production of histamine itself activated histamine receptors (Chen et al., 2019). In addition to these, as yet unidentified bacterial products activated a wide range of other neuropeptide and hormone receptors, classically known to be expressed in the nervous system. In another study, fractionated supernatants from a simplified human microbiome consortium were similarly found to robustly activate neurotransmitter GPCRs. In addition to histamine itself, bacterially produced cadaverine, putrescine, and agmatine also activated histamine receptors (Colosimo et al., 2019). Bacterial supernatants containing 9,10-methylenehexadecanoic acid activated brain angiogenesis factor 1, while 12-methyltetradecanoic acid activated neuromedin receptor 1. Overall, these studies provide proof-of-concept that select microbial products could activate GPCRs known to be expressed by neurons.

Further research is required to identify specific microbial metabolites that are capable of signaling to neurons and to determine whether they are bioavailable to the host when produced by microbes within complex host-associated communities. While existing studies demonstrate the potential for bacteria to activate select GPCRs, the authentic identities of the bacterial molecules that affect individual receptors remain largely unknown. Additionally, our knowledge as yet relies primarily on bacteria grown in culture, alone or in limited communities, raising the question of whether there are additional molecules left unassayed from microbes that were not cultured and whether the data captures physiologically-relevant outputs of complex microbial community interactions. Culture-independent approaches to screen metabolites directly from host biospecimens would greatly aid in this regard. Beyond bacteria from the microbiome, the roles for the mycobiome and virome in altering neuronal activity remain understudied. While sensory nerve fibers in the skin directly sense infectious *Candida albicans* (Kashem et al., 2015), whether non-pathogenic members of the mycobiome influence neuronal activity is poorly understood. Moreover, bacteriophages alter levels of the neurotransmitters tryptamine and tyramine in the gut (Hsu et al., 2019), but whether these alterations ultimately impact neuronal activity is unclear. These studies highlight a need for novel tools to selectively modulate non-bacterial members of the microbiome in order to fully understand the complex role of the entire microbiome in modulating the host nervous system.

While initial evidence suggests that microbes are capable of synthesizing molecules that could directly bind to neuron-relevant GPCRs *in vitro*, additional research is needed to determine whether they bind neuronal GPCRs in host tissues and to further

evaluate the physiological consequences of their signaling. Accordingly, greater attention to spatial variations in metabolite production and receptor activation *in vivo* is warranted. Microbial communities exhibit distinct spatial structures, or "microbiogeographies", along and across the gastrointestinal tract (Donaldson et al., 2016). In addition, recent single-cell RNA sequencing studies suggest that there is cellular, and potentially spatial, heterogeneity in the receptor profiles of intestinally-innervating dorsal root and vagal neurons (Hockley et al., 2019; Kupari et al., 2019). Advances in technologies for high throughput *in situ* microbial imaging, metabolite profiling, and GPCR mapping would help to establish the physiological landscape of the intestine to inform functional microbiome-nervous system interactions.

Microbial Interactions with Drugs for Neurological Disease

The finding that select microbes can synthesize, modulate, sense and/or respond to neurochemicals raises the question of whether they would additionally interact with medical drugs that modulate neurotransmission. The gut microbiota encodes a diverse array of enzymes capable of metabolizing pharmacological agents, thus potentially influencing their bioavailability to the host and contributing to the wide range of intra-patient variability in drug efficacy. Early work describing how the process of glucuronidation promotes drug clearance, coupled with the identification of bacterial beta-glucuronidases from gut microbes, have set the foundation for pioneering studies on microbiomes as modulators of xenobiotic metabolism (Wallace et al., 2010). Since then, xenobiotic metabolism by the microbiome has been extended to numerous drugs targeting neurological indications. In sequencing studies of the human microbiota and culture-based screens of bacterial interactions with common medications, many

antipsychotics, antidepressants, opioids and anticholinergic drugs greatly affected bacterial physiology and correlated with alterations in the composition of the gut microbiota (Jackson et al., 2018; Maier et al., 2018; Zimmermann et al., 2019a). While the distinct contribution of the microbiota to the metabolism of drugs can be difficult to quantify alongside host-derived enzymes carrying out the same metabolic functions, a recent study utilized gnotobiotic, pharmacological and bacterial genetic approaches to disentangle microbial vs. host xenobiotic transformations. By comparing the metabolism of the antiviral drug brivudine in multiple tissues of germ-free mice that vary in a single microbiome-encoded enzyme, researchers were able to generate a pharmacokinetic model to predict the contribution of the microbiota to features of drug metabolism, including oral bioavailability, host drug-metabolizing activity, metabolite absorption, and intestinal transit (Zimmermann et al., 2019b). This modeling approach was further applied to dissect microbiota contributions to the metabolism of the antiviral drug sorivudine and the benzodiazepine clonazepam (Zimmermann et al., 2019b).

Separate studies have utilized biochemical and metagenomic approaches to identify particular bacterial species and novel bacterial enzymes that modulate the metabolism of drugs, including those for neurodegenerative diseases. The mainstay treatment for Parkinson's disease, levodopa (L-dopa), is a natural precursor of DA that, when administered peripherally, is able to cross the blood-brain barrier for local conversion to DA in the brain. However, the gastrointestinal tract is a site of extensive metabolism of the drug, leading to reduced bioavailability and unwanted side effects caused by elevations in peripheral DA. Informed by mechanisms for host metabolism of DA, a recent study identified a novel interspecies pathway for microbial metabolism of L-

dopa, whereby *Enterococcus faecalis* decarboxylates L-dopa to DA, which is subsequently dehydroxylated by *Eggerthella lenta* to m-tyramine (Maini Rekdal et al., 2019). Remarkably, the presence of a single nucleotide polymorphism in the bacterial gene encoding dopamine dehydroxylase was predictive of the capacity for certain patients to metabolize the drug. As such, the field has begun to appreciate the microbiota as a potential therapeutic target not only to aid in drug efficacy for the treatment of neurological disorders, but also as a means for developing additional personalized medical treatments.

Despite these exciting advancements toward our understanding of the molecular mechanisms behind the microbial metabolism of neuromodulatory drugs, a gap remains in our understanding of the relevance of these findings to the clinic. Few, if any, studies to date have rigorously assessed the symptomatic outcomes resulting from altering microbial metabolism of drugs for neurological disorders. As a result, it remains unclear whether or not these mechanisms are ultimately impactful for clinically-relevant outcomes in the host. Experiments utilizing genetically-tractable bacterial species alongside gnotobiotic tools in animal models of disease are needed to assess the role of microbe-specific functions on drug bioavailability and neurobehavioral outcomes. Advancements such as these are paramount for our ability to better understand roles for the microbiome in regulating inter-patient variability in responsiveness to drugs for neurological conditions, and to assess the potential to inform tractable strategies for clinical intervention.

Conclusion

A growing body of evidence indicates that disruptions in host-associated microbiomes can modify animal behavior and further supports the notion of signaling across a microbiota-gut-brain axis. To date, several studies highlight sensory neuronal signaling, humoral metabolic communication, and immunomodulation as likely direct and indirect pathways that mediate microbiota-nervous system interactions, but studies that clearly evaluate and dissect these signaling mechanisms are lacking. Recent advances in sequencing, viral targeting, intersectional genetic and imaging tools, combined with gnotobiotic and bacterial genetic systems, can improve or provide new insight of the molecular and cellular mechanisms underlying microbiota-gut-brain communication and the nuances that arise from the coordinated signaling of heterogeneous cell types in response to pleiotropic microbial cues. In particular, studies profiling sensory neurons and intestinal epithelial cells have uncovered the possibility for both direct and indirect activation of sensory neurons by microbiota-dependent dietary products, neurotransmitters and as yet uncharacterized metabolites either through binding of receptors on afferent fibers themselves or via signaling to enteroendocrine cells in the gut epithelium. However, experiments employing the use of conditional receptor knockouts in specific neuronal or epithelial subpopulations and gain or loss-of-function constructs in bacteria may aid in identifying pathway-specific effects of microbial signals in regulating host brain function and behavior. Additionally, few studies to date have employed the use of *in vivo* electrophysiological- and genetically-encoded calcium indicator-based tools in order to directly assess the functional role of microbial-metabolite effects on neuronal activity. Understanding the distinct circuitry and functional signatures involved in mediating neuronal communication along the gut-brain axis is imperative for our

understanding of how the gut microbiota modifies host physiology. While such studies can be performed in animal models, an added challenge is in assessing the relevance of findings to human health outcomes. Interrogating whether microbes from the human microbiota interact with neuromodulatory drugs, and whether such interactions have measurable consequences on drug efficacy and clinical outcomes, may serve a tractable context. Overall, the future offers the exciting prospect of uncovering fundamental principles for how microbes and microbial products are detected and interpreted by host sensory systems, toward understanding the co-evolution of animals with their associated microbiomes.

Figure and Figure Legend
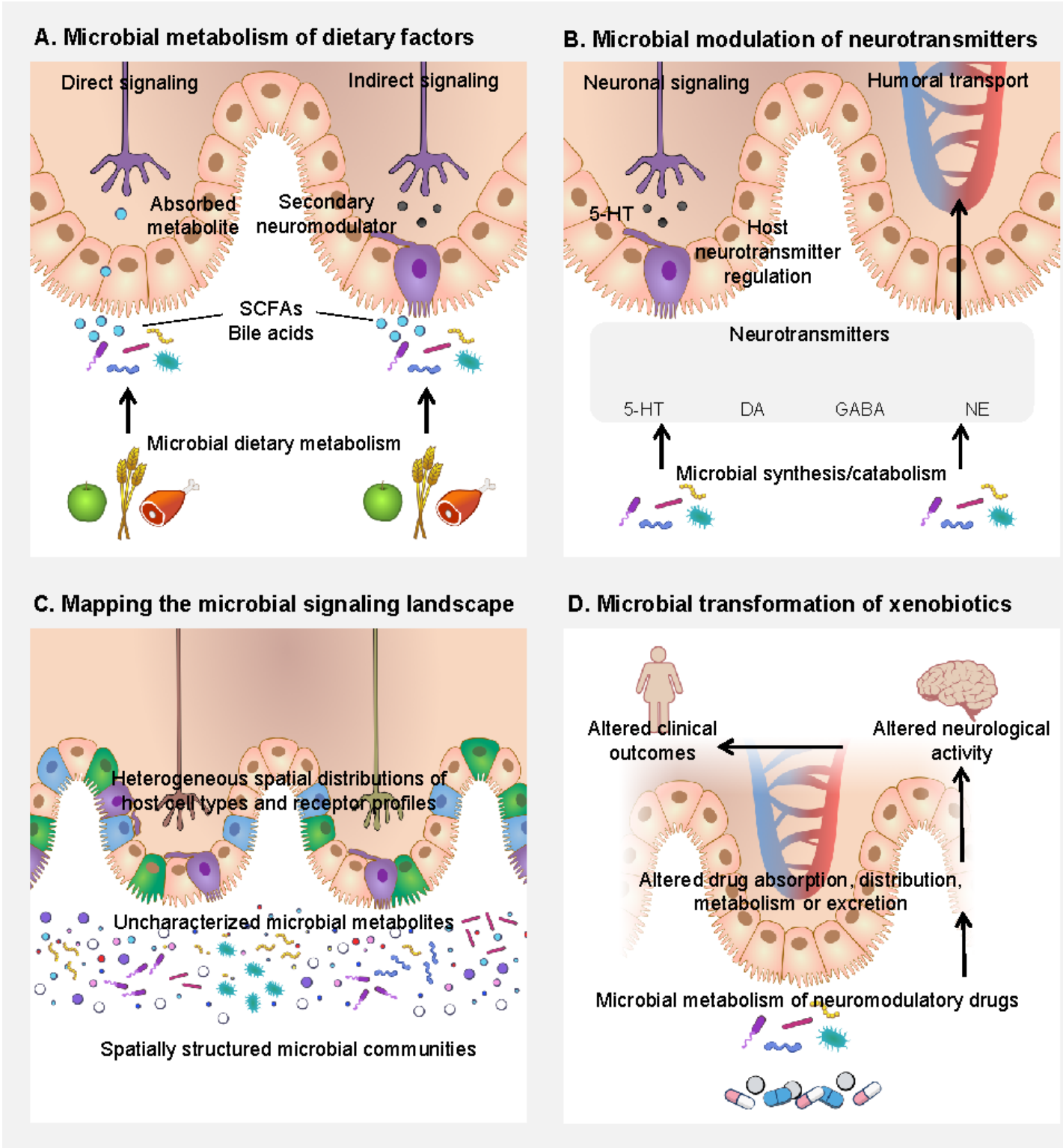
Figure 1: Microbial interactions with the nervous system through the regulation of dietary products, neurotransmitters, uncharacterized biochemicals, and

neuromodulatory drugs. A. Select bacteria from the gut microbiota produce short chain fatty acids (SCFAs) and modify bile acids through dietary metabolism. Metabolites from the microbiota can signal directly to mucosal afferent fibers of sensory neurons (left) or can signal to neurons via intermediate interactions with enteroendocrine or epithelial cells (right). **B.** Select bacteria from the gut microbiota can directly synthesize, consume or sense neurotransmitters, such as serotonin (5-HT), dopamine (DA), gamma-aminobutyric acid (GABA) and norepinephrine (NE) (center) or regulate host biosynthesis of neurotransmitters, like serotonin (5-HT) (center left). Microbially modulated neurotransmitters have the potential to interact with sensory neurons (left) or be circulated humorally (right) to reach the blood-brain barrier. **C.** The physiological landscape for microbial interactions with the nervous system is complex. Emerging evidence suggests that microbial communities are spatially structured (bottom), which yields "microbiogeographies" that vary in physiological function. In addition, the microbiome regulates various metabolites in the host, many of which remain uncharacterized (center). Further complexity is introduced when considering the heterogeneity of host cell types within the intestine, spanning various types of epithelial, endocrine, immune, and neuronal cells that are also spatially distributed and can vary temporally in their localization via turnover and remodeling. Spatial maps of signaling receptors, especially those available for mediating neural communication across intestinal cell types, will help inform functional pathways for microbe-host interactions. **D.** The microbiome is increasingly appreciated as an important modulator of xenobiotic metabolism, particularly for neuromodulatory drugs, including antipsychotics, anticholinergics, antidepressants and opioids. Microbial transformation of drugs for neurological conditions could alter their

absorption, distribution, metabolism and/or excretion in the host with potential downstream consequences on host neural activity and symptoms of neurological disease.

References

Arpaia, N., Campbell, C., Fan, X., Dikiy, S., van der Veeken, J., deRoos, P., Liu, H., Cross, J.R., Pfeffer, K., Coffer, P.J*., et al.* (2013). Metabolites produced by commensal bacteria promote peripheral regulatory T-cell generation. Nature *504*, 451-455.

Bellono, N.W., Bayrer, J.R., Leitch, D.B., Castro, J., Zhang, C., O'Donnell, T.A., Brierley, S.M., Ingraham, H.A., and Julius, D. (2017). Enterochromaffin Cells Are Gut Chemosensors that Couple to Sensory Neural Pathways. Cell *170*, 185-198.e116.

Bjursell, M.K., Martens, E.C., and Gordon, J.I. (2006). Functional genomic and metabolic studies of the adaptations of a prominent adult human gut symbiont, Bacteroides thetaiotaomicron, to the suckling period. J Biol Chem *281*, 36269-36279.

Bohórquez, D.V., Shahid, R.A., Erdmann, A., Kreger, A.M., Wang, Y., Calakos, N., Wang, F., and Liddle, R.A. (2015). Neuroepithelial circuit formed by innervation of sensory enteroendocrine cells. The Journal of clinical investigation *125*, 782-786.

Bravo, J.A., Forsythe, P., Chew, M.V., Escaravage, E., Savignac, H.M., Dinan, T.G., Bienenstock, J., and Cryan, J.F. (2011). Ingestion of Lactobacillus strain regulates emotional behavior and central GABA receptor expression in a mouse via the vagus nerve. Proceedings of the National Academy of Sciences of the United States of America *108*, 16050-16055.

Byrne, C.S., Chambers, E.S., Morrison, D.J., and Frost, G. (2015). The role of short chain fatty acids in appetite regulation and energy homeostasis. Int J Obes (Lond) *39*, 1331-1338.

Chambers, E.S., Viardot, A., Psichas, A., Morrison, D.J., Murphy, K.G., Zac-Varghese, S.E., MacDougall, K., Preston, T., Tedford, C., Finlayson, G.S.*, et al.* (2015). Effects of targeted delivery of propionate to the human colon on appetite regulation, body weight maintenance and adiposity in overweight adults. Gut *64*, 1744-1754.

Chen, H., Nwe, P.K., Yang, Y., Rosen, C.E., Bielecka, A.A., Kuchroo, M., Cline, G.W., Kruse, A.C., Ring, A.M., Crawford, J.M.*, et al.* (2019). A Forward Chemical Genetic Screen Reveals Gut Microbiota Metabolites That Modulate Host Physiology. Cell *177*, 1217-1231 e1218.

Clarke, M.B., Hughes, D.T., Zhu, C., Boedeker, E.C., and Sperandio, V. (2006). The QseC sensor kinase: a bacterial adrenergic receptor. Proc Natl Acad Sci U S A *103*, 10420-10425.

Cohen, L.J., Esterhazy, D., Kim, S.H., Lemetre, C., Aguilar, R.R., Gordon, E.A., Pickard, A.J., Cross, J.R., Emiliano, A.B., Han, S.M.*, et al.* (2017). Commensal bacteria make GPCR ligands that mimic human signalling molecules. Nature *549*, 48-53.

Cohen, L.J., Kang, H.S., Chu, J., Huang, Y.H., Gordon, E.A., Reddy, B.V., Ternei, M.A., Craig, J.W., and Brady, S.F. (2015). Functional metagenomic discovery of bacterial effectors in the human microbiome and isolation of commendamide, a GPCR G2A/132 agonist. Proc Natl Acad Sci U S A *112*, E4825-4834.

Colosimo, D.A., Kohn, J.A., Luo, P.M., Piscotta, F.J., Han, S.M., Pickard, A.J., Rao, A., Cross, J.R., Cohen, L.J., and Brady, S.F. (2019). Mapping Interactions of Microbial

Metabolites with Human G-Protein-Coupled Receptors. Cell Host Microbe *26*, 273-282 e277.

De Vadder, F., Kovatcheva-Datchary, P., Goncalves, D., Vinera, J., Zitoun, C., Duchampt, A., Backhed, F., and Mithieux, G. (2014). Microbiota-generated metabolites promote metabolic benefits via gut-brain neural circuits. Cell *156*, 84-96.

Donaldson, G.P., Lee, S.M., and Mazmanian, S.K. (2016). Gut biogeography of the bacterial microbiota. Nat Rev Microbiol *14*, 20-32.

Egerod, K.L., Petersen, N., Timshel, P.N., Rekling, J.C., Wang, Y., Liu, Q., Schwartz, T.W., and Gautron, L. (2018). Profiling of G protein-coupled receptors in vagal afferents reveals novel gut-to-brain sensing mechanisms. Mol Metab *12*, 62-75.

Erny, D., Hrabe de Angelis, A.L., and Prinz, M. (2017). Communicating systems in the body: how microbiota and microglia cooperate. Immunology *150*, 7-15.

Frost, G., Sleeth, M.L., Sahuri-Arisoylu, M., Lizarbe, B., Cerdan, S., Brody, L., Anastasovska, J., Ghourab, S., Hankir, M., Zhang, S.*, et al.* (2014). The short-chain fatty acid acetate reduces appetite via a central homeostatic mechanism. Nature communications *5*, 3611.

Fung, T.C., Vuong, H.E., Luna, C.D.G., Pronovost, G.N., Aleksandrova, A.A., Riley, N.G., Vavilina, A., McGinn, J., Rendon, T., Forrest, L.R.*, et al.* (2019). Intestinal serotonin and fluoxetine exposure modulate bacterial colonization in the gut. Nat Microbiol *4*, 2064-2073.

Furusawa, Y., Obata, Y., Fukuda, S., Endo, T.A., Nakato, G., Takahashi, D., Nakanishi, Y., Uetake, C., Kato, K., Kato, T.*, et al.* (2013). Commensal microbe-derived butyrate induces the differentiation of colonic regulatory T cells. Nature *504*, 446-450.

Gustafsson, B. (1946). Germ-free rearing of rats. Acta Anat (Basel) *2*, 376-391.

Hallen-Adams, H.E., and Suhr, M.J. (2017). Fungi in the healthy human gastrointestinal tract. Virulence *8*, 352-358.

Hockley, J.R.F., Taylor, T.S., Callejo, G., Wilbrey, A.L., Gutteridge, A., Bach, K., Winchester, W.J., Bulmer, D.C., McMurray, G., and Smith, E.S.J. (2019). Single-cell RNAseq reveals seven classes of colonic sensory neuron. Gut *68*, 633-644.

Hoverstad, T., and Midtvedt, T. (1986). Short-chain fatty acids in germfree mice and rats. J Nutr *116*, 1772-1776.

Hsu, B.B., Gibson, T.E., Yeliseyev, V., Liu, Q., Lyon, L., Bry, L., Silver, P.A., and Gerber, G.K. (2019). Dynamic Modulation of the Gut Microbiota and Metabolome by Bacteriophages in a Mouse Model. Cell Host Microbe *25*, 803-814 e805.

Jackson, M.A., Verdi, S., Maxan, M.E., Shin, C.M., Zierer, J., Bowyer, R.C.E., Martin, T., Williams, F.M.K., Menni, C., Bell, J.T.*, et al.* (2018). Gut microbiota associations with common diseases and prescription medications in a population-based cohort. Nat Commun *9*, 2655.

Kashem, S.W., Riedl, M.S., Yao, C., Honda, C.N., Vulchanova, L., and Kaplan, D.H. (2015). Nociceptive Sensory Fibers Drive Interleukin-23 Production from CD301b+ Dermal Dendritic Cells and Drive Protective Cutaneous Immunity. Immunity *43*, 515-526.

Kupari, J., Haring, M., Agirre, E., Castelo-Branco, G., and Ernfors, P. (2019). An Atlas of Vagal Sensory Neurons and Their Molecular Specialization. Cell Rep *27*, 2508-2523 e2504.

Larraufie, P., Martin-Gallausiaux, C., Lapaque, N., Dore, J., Gribble, F.M., Reimann, F., and Blottiere, H.M. (2018). SCFAs strongly stimulate PYY production in human enteroendocrine cells. Sci Rep *8*, 74.

Leulier, F., MacNeil, L.T., Lee, W.J., Rawls, J.F., Cani, P.D., Schwarzer, M., Zhao, L., and Simpson, S.J. (2017). Integrative Physiology: At the Crossroads of Nutrition, Microbiota, Animal Physiology, and Human Health. Cell Metab *25*, 522-534.

Maier, L., Pruteanu, M., Kuhn, M., Zeller, G., Telzerow, A., Anderson, E.E., Brochado, A.R., Fernandez, K.C., Dose, H., Mori, H.*, et al.* (2018). Extensive impact of non-antibiotic drugs on human gut bacteria. Nature *555*, 623-628.

Maini Rekdal, V., Bess, E.N., Bisanz, J.E., Turnbaugh, P.J., and Balskus, E.P. (2019). Discovery and inhibition of an interspecies gut bacterial pathway for Levodopa metabolism. Science *364*.

Mertens, K.L., Kalsbeek, A., Soeters, M.R., and Eggink, H.M. (2017). Bile Acid Signaling Pathways from the Enterohepatic Circulation to the Central Nervous System. Front Neurosci *11*, 617.

Milshteyn, A., Colosimo, D.A., and Brady, S.F. (2018). Accessing Bioactive Natural Products from the Human Microbiome. Cell Host Microbe *23*, 725-736.

Mukhopadhya, I., Segal, J.P., Carding, S.R., Hart, A.L., and Hold, G.L. (2019). The gut virome: the 'missing link' between gut bacteria and host immunity? Therap Adv Gastroenterol *12*, 1756284819836620.

Ridaura, V.K., Faith, J.J., Rey, F.E., Cheng, J., Duncan, A.E., Kau, A.L., Griffin, N.W., Lombard, V., Henrissat, B., Bain, J.R.*, et al.* (2013). Gut microbiota from twins discordant for obesity modulate metabolism in mice. Science *341*, 1241214.

Sgritta, M., Dooling, S.W., Buffington, S.A., Momin, E.N., Francis, M.B., Britton, R.A., and Costa-Mattioli, M. (2019). Mechanisms Underlying Microbial-Mediated Changes in Social Behavior in Mouse Models of Autism Spectrum Disorder. Neuron *101*, 246-259 e246.

Smith, P.M., Howitt, M.R., Panikov, N., Michaud, M., Gallini, C.A., Bohlooly, Y.M., Glickman, J.N., and Garrett, W.S. (2013). The microbial metabolites, short-chain fatty acids, regulate colonic Treg cell homeostasis. Science *341*, 569-573.

Strandwitz, P. (2018). Neurotransmitter modulation by the gut microbiota. Brain research *1693*, 128-133.

Strandwitz, P., Kim, K.H., Terekhova, D., Liu, J.K., Sharma, A., Levering, J., McDonald, D., Dietrich, D., Ramadhar, T.R., Lekbua, A.*, et al.* (2019). GABA-modulating bacteria of the human gut microbiota. Nat Microbiol *4*, 396-403.

Takeuchi, O., and Akira, S. (2009). Innate immunity to virus infection. Immunol Rev *227*, 75-86.

Turnbaugh, P.J., Ley, R.E., Mahowald, M.A., Magrini, V., Mardis, E.R., and Gordon, J.I. (2006). An obesity-associated gut microbiome with increased capacity for energy harvest. Nature *444*, 1027-1031.

Valenstein, E.S. (2002). The discovery of chemical neurotransmitters. Brain Cogn *49*, 73-95.

Vuong, H.E., Yano, J.M., Fung, T.C., and Hsiao, E.Y. (2017). The Microbiome and Host Behavior. Annu Rev Neurosci *40*, 21-49.

Wallace, B.D., Wang, H., Lane, K.T., Scott, J.E., Orans, J., Koo, J.S., Venkatesh, M., Jobin, C., Yeh, L.A., Mani, S.*, et al.* (2010). Alleviating cancer drug toxicity by inhibiting a bacterial enzyme. Science *330*, 831-835.

Yano, Jessica M., Yu, K., Donaldson, Gregory P., Shastri, Gauri G., Ann, P., Ma, L., Nagler, Cathryn R., Ismagilov, Rustem F., Mazmanian, Sarkis K., and Hsiao, Elaine Y. (2015). Indigenous Bacteria from the Gut Microbiota Regulate Host Serotonin Biosynthesis. Cell *161*, 264-276.

Zheng, Y.M., Lin, F.L., Gao, H., Zou, G., Zhang, J.W., Wang, G.Q., Chen, G.D., Zhou, Z.H., Yao, X.S., and Hu, D. (2017). Development of a versatile and conventional technique for gene disruption in filamentous fungi based on CRISPR-Cas9 technology. Sci Rep *7*, 9250.

Zimmermann, M., Zimmermann-Kogadeeva, M., Wegmann, R., and Goodman, A.L. (2019a). Mapping human microbiome drug metabolism by gut bacteria and their genes. Nature *570*, 462-467.

Zimmermann, M., Zimmermann-Kogadeeva, M., Wegmann, R., and Goodman, A.L. (2019b). Separating host and microbiome contributions to drug pharmacokinetics and toxicity. Science *363*.

Chapter 2

Emerging roles for the intestinal microbiome in epilepsy

Gregory R. Lum, Christine A. Olson, Elaine Y. Hsiao

Published 2019 in *Neurobiology of Disease*

Abstract

The gut microbiome is emerging as a key regulator of brain function and behavior and is associated with symptoms of several neurological disorders. There is emerging evidence that alterations in the gut microbiota are seen in epilepsy and in response to seizure interventions. In this review, we highlight recent studies reporting that individuals with refractory epilepsy exhibit altered composition of the gut microbiota. We further discuss antibiotic treatment and infection as microbiome-related factors that influence seizure susceptibility in humans and animal models. In addition, we evaluate how the microbiome may mediate effects of the ketogenic diet, probiotic treatment, and anti-epileptic drugs on reducing both seizure frequency and severity. Finally, we assess the open questions in interrogating roles for the microbiome in epilepsy and address the prospect that continued research may uncover fundamental insights for understanding risk factors for epilepsy, as well as novel approaches for treating refractory epilepsy.

Introduction

Epilepsy is a chronic neurological disorder affecting more than 50 million people worldwide and accounting for 0.6% of the global economic disease burden (WHO, 2016). It is defined as a brain pathology "characterized by an enduring predisposition to generate seizures" (Fisher, 2014). An estimated 2.4 million patients are diagnosed with epilepsy

every year. These diagnoses include various subtypes of seizures, such as focal, generalized, combined generalized and focal, or unknown, which indicate their localization to specific brain regions or generalization across both cerebral hemispheres (Scheffer, 2017). Seizures occur when excitation and inhibition are imbalanced in the brain, which can be triggered by pathologies affecting synaptic connectivity, ionic channel function, and neurotransmitter reception, among several other pathways (Stafstrom, 2015). Additionally, seizures can occur after cerebral insult or damage, as in the case of febrile seizures, traumatic brain injury, or stroke (Herman, 2002).

While the WHO estimates that 70% of epileptic patients could be seizure-free with appropriate medication, in developing regions, less than half of the epileptic patient population has access to anti-epileptic drugs. Additionally, an estimated 15 million patients exhibit refractory epilepsy, based on their non-responsiveness to existing anti-epileptic drugs. Both genetic and environmental factors contribute to individual predisposition to epilepsy, but the exact causes of most epilepsy cases remain unclear. It is estimated that 35% of epilepsy cases can be directly attributed to genetic risk, while the remaining cases may involve both genetic risk and environmental exposures, such as head trauma or infections that lead to meningitis or encephalitis (Shorvon, 2014). Exactly how environmental factors contribute to long-term susceptibility to epilepsy remains unclear. The gut microbiota, comprising trillions of microorganisms indigenous to the gastrointestinal tract, is increasingly recognized as an important mediator of environmental risk factors on host risk for disease. The composition and function of the gut microbiota is shaped by environmental factors, such as diet, stress and medication, and also informed by human genetics. The microbiota plays a critical role in guiding brain

development and neurobehavior in animal models (Vuong et al., 2017). Of particular

relevance to epilepsy, the gut microbiota significantly alters carbohydrate and amino acid

metabolism, microglial and astrocytic function, vagal neuronal activity, and hippocampal

neurotransmitter levels (Fung, 2017 #395). In this review, we discuss current evidence

for microbiome alterations in epilepsy and potential roles for the microbiome in mediating

risk for epilepsy and the effects of seizure interventions.

Alterations of the Gut Microbiota in Human Epilepsy

Alterations in the gut microbiome have been reported across several

neurodevelopmental, neuropsychiatric and neurodegenerative disorders, but very little is

known regarding microbiome associations with human epilepsy. Only a few recent studies

have highlighted differences in fecal microbiota profiles from select epileptic individuals

as compared to healthy controls (**Table 1**) (Lindefeldt et al., 2019; Peng et al., 2018; Xie

et al., 2017). In a cohort of 42 individuals with refractory epilepsy, 49 with drug-sensitive

epilepsy, and 65 matched family members without epilepsy from West China Hospital of

Sichuan University, 16S rDNA sequencing revealed distinct fecal microbiota alterations

for refractory epileptic patients relative to both drug-sensitive epileptic patients and

controls without epilepsy. In particular, microbiota profiles from the refractory epilepsy

group exhibited elevated α-diversity, as measured by the Chao1 diversity index for

species richness, which was reportedly particular to refractory epileptic patients with 4 or

more seizures per year and not for those with less than 4 seizures per year (Peng et al.,

2018). While samples from refractory epileptic patients exhibited no overt group clustering

by weighted principal coordinate analysis, linear discriminant analysis (LDA) effect size

analysis revealed increases in the relative abundances of select members of the phylum *Firmicutes*, including *Roseburia*, *Coprococcus*, *Ruminococcus*, and *Coprobacillus*, and decreases in *Bacteroides* relative to controls*.* Relative abundances of *Methanobrevibacter*, *Fusobacterium, Neisseria,* and *Akkermansia* were also increased in the refractory epilepsy group relative to the drug-sensitive epilepsy group. Notably, the study design matched group representation by age (mean 25.1-29.4), sex, and exposure to medication, and excluded individuals who had taken antibiotics or probiotics within the past 3 months or who had a history of another chronic disease. Primary differences between refractory and drug-sensitive groups were in seizure frequency and type (generalized, partial, or multiple), which would be expected based on the inherent biological features of the classifications.

In another human study, fecal microbiota were profiled by 16S rDNA sequencing of stool samples collected from 14 infants with refractory epilepsy, ranging from 1-4 years old, and 30 matched healthy infants from Shenzhen Children's Hospital (Xie et al., 2017). In this case, there was no significant difference in α-diversity between groups when measured by the Shannon index for evenness. However, principal component analysis showed clustering of 16S rDNA data from refractory epilepsy infants distinctly from healthy infant controls, indicating substantial differences in fecal microbial beta-diversity. Similar to results from the Peng et al. study, LEfSe analysis revealed elevated relative abundance of *Firmicutes* and *Proteobacteria,* and reduced *Bacteroidetes* and *Actinobacteria,* in infants with refractory epilepsy. At the genus level, *Cronobacter* was highly enriched in epileptic infants and not detected in healthy infants, while relative levels of *Bacteroides, Prevotella* and *Bifidobacterium* were decreased in infants with refractory

35

epilepsy relative to controls. While the study required participants to not have taken antibiotics 1 month prior to the study and excluded those with chronic illness or metabolic disease, baseline differences in infant diet which could confound the study in the absence of matched household controls were not considered.

A third human study of 12 children with refractory epilepsy, aged 2-17 years, and 11 healthy parent controls from Astrid Lindgren Children's Hospital of Karolinska Institute examined fecal microbiomes by shotgun metagenomic sequencing (Lindefeldt et al., 2019). Fecal microbiota samples of children with refractory epilepsy exhibited decreased α-diversity, as measured by Shannon index, compared to microbiota samples from the healthy control parents. Principal component analysis of taxonomic and functional profiles revealed clear clustering of microbiomes from healthy control parents, whereas those from children with refractory epilepsy exhibited larger variation and minor shifts along the first principal component. In general, taxonomic analysis indicated that microbiota from children with refractory epilepsy displayed decreased relative abundances of *Bacteroidetes* and *Proteobacteria* and increased relative abundances of *Firmicutes* and *Actinobacteria*, when compared to control parent samples. Particular differences in functional potential were reported, with refractory epilepsy microbiomes harboring decreased gene content for β-hydroxybutyryl-CoA dehydrogenase and crotonase, genes involved in the acetyl-CoA pathway, as compared to parent control microbiomes. In light of known age-dependent changes in the gut microbiome, a key caveat of these comparisons is the lack of age-matched controls.

Overall, all three of these human studies report alterations in the fecal microbiota of individuals with refractory epilepsy relative to varied non-epileptic controls (Lindefeldt

et al., 2019; Peng et al., 2018; Xie et al., 2017). While they each report increased *Firmicutes* relative to *Bacteroides* in individuals with refractory epilepsy, the reported microbial alterations varied highly across taxonomic levels more resolved than phylum. In addition, the results were conflicting with regard to whether α-diversity is altered in the epilepsy microbiota. These studies are difficult to cross-compare due to variations in study design, age differences of subjects, relatively small samples sizes, as well as a lack of data on genetic and environmental factors that could influence the structure and function of the gut microbiome. Additionally, these studies differ by sequencing methodology and analytical tools used to profile the gut microbiota, where shotgun metagenomics, as in the Lindefeldt study, delivers both strain specificity and microbiome functional profiling, while 16S rDNA taxonomic profiling captures broader, less specific levels of diversity (Poretsky et al, 2014). Larger efforts are needed to achieve adequately powered patient and control populations and to account for variables such as age, human genetics, medication, and diet.

Microbiome Associations with Epileptogenesis

The Gut Microbiota and Seizure Susceptibility in Animal Models

In addition to the existing human studies reporting a correlation between refractory epilepsy and altered gut microbiota, a few animal studies highlight a causal role for the microbiome in modulating seizure susceptibility. Animal models for studying epilepsy include the use of chemoconvulsants such as kainic acid, electrical stimulation using the 6Hz seizure model, or seizure kindling which applies repeated stimulation to increase seizure susceptibility. One in particular drew upon a wealth of literature reporting that

37

physical and psychological stressors alter the gut microbiota (Vuong et al., 2017) to further investigate whether stress-induced alterations in the gut microbiota impact the development of seizures (Medel-Matus et al., 2018). Sprague-Dawley rats were subjected to sham stress or chronic restraint stress for two 2-hour long sessions per day for 2 weeks, and cecal contents from each group were then transplanted into naïve recipient rats that were pre-treated with antibiotics to first deplete the gut microbiome. As expected, rats exposed to chronic restraint stress required fewer number of trials of basolateral amygdalar stimulation in order to induce a full seizure response and longer seizure duration, when compared to sham stress controls. This is consistent with prior studies revealing that stress promotes epileptogenesis. Notably, transplantation of the microbiome from a stressed rat into non-stressed recipient sufficiently conferred the stress-related increases in susceptibility to kindling and duration of seizures. In contrast, transplantation of the microbiome from a non-stressed rat into a stressed rat sufficiently reduced seizure duration and increased the number of kindling trials toward levels seen in the native sham controls. These results suggest that the microbiome mediates stress-induced increases in seizure susceptibility in a rat kindling model. Limitations of the study include the small sample size of 6 rats per group, the lack of companion sequencing data to identify taxonomic and functional differences in the microbiome that underlie their pro- versus anti-epileptic effects, and the lack of sequencing data of donor and recipient microbiota to confirm high fidelity transplantation. Additionally, mechanisms underlying the effects of transplantation on seizure susceptibility remain unclear; it is possible that metabolites contained within the transplant material, rather than the microbiome itself,

could play a role, as could any indirect effects of the procedure on the host stress response.

A separate study examined links between the microbiome and the formation of cerebral cavernous malformations (CCMs), structural abnormalities in brain capillaries that predispose to stroke and seizures (Tang et al., 2017). Initial observations in endothelial specific *Krit1^{ECKO}* and *Ccm2^{ECKO}* knockout mice, which are theoretically susceptible to CCM formation, revealed that differences in the breeding vivarium and unexpected infections modulated resistance vs. susceptibility to CCM formation. Follow-up experiments demonstrated that intraperitoneal injection of the gram-negative bacterium *B. fragilis* or lipopolysaccharide were each sufficient to drive CCM formation through TLR4 signaling. These results suggest that infection with gram negative bacteria (GNB) or systemic injection of GNB-associated antigens accelerates CCM formation. Further supporting a role for the gut microbiome on CCM formation, *Krit1^{ECKO}* mice raised as germ-free failed to form CCM lesions, whereas those raised conventionally colonized developed CCMs by P10. Consistent with this, maternal antibiotic treatment yielded offspring that were resistant to CCM formation, a phenotype that was transmitted transgenerationally to mice in the absence of antibiotic treatment. In contrast, conventionalization of the microbiome by cross-fostering to conventionally-colonized mothers restored susceptibility to CCM formation. 16S rDNA sequencing of fecal samples from CCM susceptible versus resistant *Krit1^{ECKO}* and *Ccm2^{ECKO}* mice revealed distinct group clustering of microbiota profiles by principal coordinates analysis. Taxonomic analysis highlighted significantly increased relative abundance of *Bacteroidetes* S24-7 in mice susceptible to CCM formation, as compared to resistant

controls. Whether this particular taxon is sufficient to modulate CCM formation is unclear.

However, the several experiments performed in the study reveal a causal relationship

between the gut microbiota and formation of CCMs, a primary risk factor for seizures.

Altogether, mechanistic studies in animal models have begun to highlight how the gut

microbiota could modify seizure vulnerability.

Infection and Risk for Epilepsy

Several large epidemiological and case studies associate infections with increased

risk for epilepsy. A singleton cohort study of all children born in northern Denmark from

1998 to 2008 reported increased risk for epilepsy in children born from mothers that

experienced infection during pregnancy (Ahlers et al., 2019; Norgaard et al., 2012).

Similarly, in a nationwide population-based cohort study of all individuals born in Denmark

from 1982 to 2012, childhood infection with hospitalization was associated with a 78%

increase in risk for epilepsy (Ahlers et al., 2019). Consistent with this, infants infected with

Group B streptococcus, a leading cause of neonatal morbidity, are more likely to be

hospitalized and diagnosed with epilepsy or other neurological conditions during their

childhood years (Yeo et al., 2019). A study conducted by the Norwegian Institute of Public

Health reported an increase in febrile seizures characteristic of febrile infection-related

epilepsy syndrome (FIRES) following the 2009 influenza A (H1N1) pandemic (Bakken et

al., 2015). In addition, human herpesvirus (HHV)-6 infection has been associated with

mesial temporal sclerosis (MTS), a common pathological marker in mesial temporal lobe

epilepsy (MTLE), and the HHV6-B virus in particular is linked with childhood epilepsy

(Leibovitch and Jacobson, 2015; Vezzani et al., 2016). In a study of 75 MTLE patients,

52 patients displaying MTS and 23 non-MTS patients, MTS patients exhibited a greater

number of seizures, increased HHV-6 viral DNA load and increased markers of inflammation compared to non-MTS controls (Kawamura et al., 2015). Other studies have also suggested that HHV-6 drives MTS/MTLE pathogenesis by inducing abnormal immune or inflammatory responses (Bartolini et al., 2019; Wipfler et al., 2018). Additional human studies of bacterial and parasitic infections also suggest links between infection and seizure susceptibility. *Taenia solium*, a tapeworm with prevalence in the regions around Burkina Faso causes neurocysticercosis in infected humans, which correlates with the prevalence of epilepsy in low income countries (Sahlu et al., 2019; Vezzani et al., 2016). Overall, the diversity of infections implicated in epilepsy has led to the notion that generalized immune activation or inflammation promotes susceptibility to seizures (Pardo et al., 2014; Tan, 2018).

Animal models of various infections support a causal role for inflammation in promoting seizure vulnerability. As a model of limbic epilepsy, mice injected intracortically with Theiler's murine encephalomyelitis virus (TMEV) exhibited seizures and neuroinflammation characterized by elevated pro-inflammatory cytokines including interleukin (IL)-6 and tumor necrosis factor (TNF)α in the hippocampus, a focal region for seizure initiation (Cusick et al., 2017; Patel et al., 2017). Notably, blocking TNF signaling by TMEV injection into TNF$\alpha^{-/-}$ or TNFR1$^{-/-}$TNFR2$^{-/-}$ mice sufficiently reduced seizures, suggesting that TNF signaling is required for mediating the pro-epileptic effects of TMEV infection. The study provided evidence that TNFα modulates glutamate receptor trafficking via TNF receptor 1 to increase excitatory synaptic transmission, which could underlie the elevated seizure incidence seen in response to TMEV. In a separate study, Wistar rats injected systemically with the bacterial cell wall component lipopolysaccharide

(Veitenhansl et al.) exhibited elevated levels of pro-inflammatory cytokines TNFα, IL-6, and IL-1β in the brain and decreased thresholds for chemically- and electrically-induced seizures by pentylenetetrazole (PTZ) and corneal shock, respectively (Sewal et al., 2017). In addition, toxoplasma-infected mice displayed reduced PTZ-induced seizures as well, which were partially abrogated by blocking the dopamine receptors D1 and D2 (Babaie et al., 2017). Altogether, these animal studies corroborate human association studies by revealing that a broad range of bacteria, viruses, and parasites can similarly promote seizure propensity. Research further suggests that inflammatory responses associated with cytokines and chemokines such as TNFα (Cusick et al., 2017; Patel et al., 2017; Sewal et al., 2017) and MCP-1(Kawamura et al., 2015) could mediate the pro-epileptic effects of infection.

Antibiotic Treatment and Seizure Susceptibility

Antibiotics are commonly prescribed for treating bacterial infections (Tamma et al., 2017) but despite their widespread use, many can elicit adverse side effects, including neurological symptoms (Mattappalil and Mergenhagen, 2014). A large epidemiological study of the Danish registry reported that increased numbers of antibiotic prescriptions for a single patient correlate with increased risk for epilepsy (Norgaard et al., 2012). Another study reported increased seizure risk in hemodialysis patients that were administered cephalosporin antibiotics (Zhang et al., 2019). A meta-analysis of all randomized controlled human trials of carbapenem antibiotics reported a significant increase in seizure risk associated with carbapenem usage (Cannon et al., 2014). Imipenem and meropenem antibiotics were also highly correlated with epileptogenesis (Leibovitch and Jacobson, 2015; Owens, 2008). While the majority of studies point to

neurotoxic effects of antibiotics, such as β-lactams, unsubstituted penicillins, carbapenems, and 4th generation cephalosporins (Esposito et al., 2017; Sutter et al., 2015), a few small cohort and case studies have explored antibiotics as potential treatments for epilepsy (Braakman and van Ingen, 2018; Ghanizadeh and Berk, 2015; Raposo et al., 2016; Zhu and Wang, 2018). One found that treatment with a combination of penicillin derivative and macrolide antibiotics coincided with temporary seizure-free periods in six epileptic individuals (Braakman and van Ingen, 2018). Another reported that cefixime usage correlated with seizure-free bouts in a 9 year old boy with epilepsy and comorbid autism (Ghanizadeh and Berk, 2015). A challenge to interpreting the existing human data is the inability to distinguish potential off-target effects of antibiotics from their indicated anti-bacterial effects.

Findings from laboratory models have studied potential pathways by which antibiotics regulate seizure susceptibility. Particular β-lactam antibiotics are sufficient to elicit focal seizures in mice when injected intracortically or intracerebroventricularly. For example, penicillin-inducible seizure models have been used in multiple studies to understand epileptogenesis (Arslan et al., 2017; Han et al., 2015; Marangoz et al., 2018; Tubas et al., 2017; Zhu et al., 2018). The epileptogenic potential of penicillin, among other antibiotics, has been attributed to the antagonism of gamma-aminobutyric acid (GABA) - A receptors by the β-lactam ring (Veitenhansl et al.). Non-competitive inhibition in this manner and voltage-dependent alterations are thought to reduce GABAergic inhibition and thereby permit excitatory signaling to trigger epileptiform bursts. In addition to inhibiting GABA-A receptors, quinolones can also bind to benzodiazepine receptors in the GABA complex. Moreover, both quinolones and cephalosporins further display agonistic

effects on glutamatergic N-methyl-D-aspartate (NMDA) receptors, which further promote seizure susceptibility. Carbapenems, which are most frequently associated with seizures, have a higher potential to promote seizures due to their greater ability to cross the blood brain barrier and to interfere with the action of antiepileptic drugs such as valproic acid.

In contrast to these direct effects of particular antibiotics on promoting neuronal activity underling seizures, some drugs with antimicrobial properties are being pursued for their anti-epileptic effects. Rapamycin, an mTOR inhibitor and antibiotic, reduced mTOR activation, overexpression of P-glycoprotein, and seizure susceptibility in a rat Coriaria lactone kindling model of temporal lobe epilepsy (Mazumder et al., 2016; Plovier et al., 2017). Minocycline, an inhibitor of microglial activation and antibiotic, reduced sympathetic nerve activity and increased seizure thresholds in rat kainic acid and amygdalar kindling seizure models (Beheshti Nasr et al., 2013; Bhandare et al., 2017). In addition, the antibiotic gentamicin increased latency to seizure and reduced total seizure duration when injected intracerebroventricularly into rats treated with kainic acid (Zhao et al., 2018). Overall, both human and animal studies have reported opposing effects of different antibiotics on seizure susceptibility. The findings warrant increased attention to whether the particular type, dose and route of antibiotic treatment may elicit disparate influences on vulnerability to particular subtypes of seizures.

Microbiome Implications for Epilepsy Treatments

The Microbiome and Ketogenic Diet

The high-fat, low-carbohydrate ketogenic diet (KD) is used as a clinical treatment for refractory epilepsy in individuals who do not respond to existing anti-epileptic drugs. While the KD has been used for almost a century for reducing seizures, the exact

mechanisms by which the diet ameliorates seizures remains unclear. A few recent studies have investigated effects of the clinical KD on the composition of the gut microbiome in epilepsy patients, drawing the attention to whether alterations in the gut microbiome may contribute to the protective effects of the KD against seizures. In a study of 12 children diagnosed with drug-resistant epilepsy, 5 out of 12 children displayed a > 50% decrease in seizure reduction and 10 out of the 12 children exhibited improved cognition and motor functions after 3 months on classical KD (Lindefeldt et al., 2019). When comparing the gut microbiome samples collected before initiation of the KD to those taken after 3 months on KD, there was no significant difference in α-diversity. However, β-diversity analysis revealed compositional differences characterized by decreases in relative abundances of *Actinobacteria* and *Bifidobacterium* and an increase in *Proteobacteria*. Another study of 20 children with refractory epilepsy reported KD-associated reductions in epilepsy symptoms that were correlated with reduced α-diversity of the microbiome, decreases in *Actinobacteria* and *Firmicutes* relative to *Bacteroidetes* after 6 months of dietary treatment (Zhang et al., 2018). A third study of 14 epileptic infants reported reductions in *Proteobacteria* and elevations in *Bacteroides, Prevotella,* and *Bifidobacterium* after at least 1 week on the KD (Xie et al., 2017). There was little consistency across these studies in the particular microbial taxa that were affected, which could be due to variations in study design, such as the length of KD treatment, the specific KD dietary regimen implemented, and the subtypes of epilepsy and seizure semiologies represented by the patient cohorts. One study examined 6 patients diagnosed particularly with glucose transporter 1 deficiency syndrome (GLUT1 DS) (Tagliabue et al., 2017). 3 months of KD treatment correlated with alterations in the gut microbiome that were characterized by a

decrease in the relative abundance of *Desulfovibrio*. Overall, these studies warrant continued efforts to examine the effects of the KD on the gut microbiome across a large cohort of epileptic individuals. In particular, profiling microbial function rather than taxonomy, and examining associations with particular dietary, seizure semiology, medical history, and demographic data may yield greater insight across studies.

Additional studies in animal models of epilepsy similarly reveal functional roles for the gut microbiome in mediating the anti-seizure effects of the diet. In a 6 Hz acute electrically-induced seizure model of refractory epilepsy, depletion of the gut microbiome by antibiotic treatment or germ-free rearing abrogated the protective effects of the KD (Olson et al., 2018). Moreover, promoting the KD-associated microbiome in naïve mice fed a control diet sufficiently conferred seizure protection. 16S rDNA sequencing revealed that the KD decreased α-diversity of the gut microbiome within 4 days of dietary treatment and increased the relative abundance of *Akkermansia muciniphila, Parabacteroides, Sutterella,* and *Erysipelotrichaceae* relative to controls. Selective enrichment of *A. muciniphila* and *Parabacteroides* conferred protection against 6 Hz seizures. These findings were further replicated in the *Kcna1$^{-/-}$* genetic mouse model for sudden unexpected death in epilepsy (SUDEP), where depletion of the gut microbiome promoted spontaneous tonic-clonic seizures whereas selective enrichment of KD-associated bacterial taxa reduced seizure frequency and duration. Metabolomic data revealed decreases in peripheral ketogenic gamma-glutamylated amino acid concentrations, which correlated with higher hippocampal GABA/glutamate ratios in seizure protected mice, suggesting a role for microbial regulation of peripheral metabolites and central neurotransmitter metabolism in regulating seizure susceptibility. These findings align with

increasing interest in select microbes that regulate the biosynthesis of GABA within the gut (Strandwitz, 2018; Yunes et al., 2016), and the use of other microbiota-related metabolites to modulate seizure susceptibility. For example, ginsenoside compound K was reported to decrease seizure intensity and latency in rats challenged with pentylenetetrazole to induce seizures (Zeng et al., 2018), and GPR40, a receptor for free fatty acids, has been shown to also regulate NMDA receptor function to reduced seizure susceptibility (Yang et al., 2018). Additional studies are needed to examine mechanisms by which microbes and microbiome-dependent metabolites influence brain activity and behavior related to epilepsy.

Probiotic Treatment in Human Epilepsy

Although there have been only a few small studies to date that report alterations in the gut microbiome in human epilepsy (Liang et al., 2017; Lindefeldt et al., 2019; Xie et al., 2017), the links between epilepsy and infection, inflammation and antibiotic treatment raise the question of whether microbial alterations under those conditions may play a role. Two recent human studies examined the effects of probiotics on seizures. In an observational study of neonates infected with rotavirus at the Gyeongsang National University Hospital (Yeom et al., 2019), 32 out of the 78 rotavirus positive neonates and 100 out of 150 rotavirus negative neonates were treated with *Saccharomyces boulardii* or *Lactobacillus casei* as a probiotic within 24 hours of birth**.** The authors proposed that *S. boulardii* reduces seizures through inhibition of rotavirus structural protein 4, a viral enterotoxin which increases reactive oxygen species and white matter injurty, or through suppressing the inflammatory response overall. The study reported that probiotic administration within 24 hours of birth was associated with a 10-fold decreased risk for

seizures (odds ratio of 0.09) while rotavirus infection remained a risk factor only in neonates not given probiotics (odds ratio of 4.83). Seizure reduction was also reported in a pilot open label study of 43 adults with drug-resistant epilepsy treated daily for 4 months with a cocktail of *Lactobacillus acidophilus*, *L. plantarum*, *L. casei*, *L. helveticus*, *L. brevis, Bifidobacterium lactis*, and *Streptococcus salivarius* (Gomez-Eguilaz et al., 2018). 13 out of 43 (30%) of individuals reported >50% reduction in seizure frequency in the 4 months post treatment; however, a major limitation is the small study size and lack of placebo control. In addition to probiotic treatment, one recent case study from the Second Affiliated Hospital of Nanjing Medical University performed fecal microbiota transplantation (FMT) to treat Crohn's disease (CD) in a 22-year-old individual with refractory epilepsy (He et al., 2017). After 3 treatments, there was a decrease in the patient's CD index score from 361 (pre FMT) to 131 (20 months post-FMT). In addition, the patient reportedly experienced no epileptic seizures during the 20 months after FMT during which no antiseizure medications were taken. Consistent with this potential role for select probiotics to modulate seizure susceptibility, two studies in rodent models reported that probiotic treatment with *L. rhamnosus* alone or together with *B. longum* modulated expression of select GABA receptor subunits in various brain regions (Bravo et al., 2011; Liang et al., 2017). Overall, the promising results from the limited human and animal studies performed to date suggest that additional studies are needed to examine whether manipulation of the gut microbiome may serve as a tractable strategy for reducing seizures.

Anti-Epileptic Drugs and The Gut Microbiota

Non-antibiotic medications, including anti-epileptic drugs, can interact directly with gut microbes that modify their metabolism and thereby impact drug efficacy and toxicity. A recent study of 1197 medications reported that 27% of non-antibiotic drugs inhibited the growth of at least one of 40 bacterial isolates (Maier et al., 2018). An additional study reported that the anticonvulsant drug clonazepam is metabolized by intestinal microbes, which can contribute to drug toxicity (Zimmermann et al., 2019). Other studies report mild effects of anti-seizure treatments such as carbamazepine on select gut microbes (Gomes et al., 2018; Vasiliadou et al., 2018; Watkins et al., 2017). Moreover, in a mouse study of maternal treatment with the antiepileptic drug valproic acid (Veitenhansl et al.), offspring of valproic acid **(VPA)-**treated mothers exhibited fecal microbiota with decreased *Firmicutes* and increased *Bacteroidetes* when compared to vehicle-exposed control mice (Sgritta et al., 2019). Additional animal studies similarly report that maternal exposure to VPA alters offspring gut microbiota composition (de Theije et al., 2014; Lim et al., 2017; Liu et al., 2018). Notably, VPA during pregnancy has known teratogenic effects, which raises the question of whether select VPA-induced phenotypes occur via microbiome alterations as opposed to other direct effects of VPA on host physiology. These studies highlight the importance of considering drug-induced gut microbiota changes and direct xenobiotic interactions with gut microbes. Large well-controlled population studies are needed to determine whether there is a clear signature of microbiome alterations in human epilepsy, and further, whether any anti-epileptic drugs may alter the microbiome in a reproducible manner.

Conclusion

The gut microbiota is increasingly recognized as an important factor in epilepsy. Epilepsy is a highly heterogeneous disorder requiring understanding of interactions between genetic and environment risk. The gut microbiota regulates immunity and inflammation, metabolism, and peripheral and central neuronal signaling, pathways independently linked to epileptogenesis. Continued studies are warranted to understand the gut microbiota as a mediator of environmental variables, like diet, stress, and immune challenge, on seizure outcomes. Despite human studies demonstrating that changes in the composition of the microbiota correlate with epilepsy, there is as yet little consistency in the exact microbial taxa implicated across studies. The microbiome studies in epileptic patients to date are few, underpowered, and focus largely on bacterial taxa rather than function. Future studies that evaluate functional metagenomic profiles of the microbiome in large cohorts of epileptic individuals and age-matched controls, with careful consideration of seizure semiologies, demographic, medical and dietary information, could reveal whether there are consistent functional microbial signatures for subtypes of epilepsy. Such studies have the potential to uncover whether the gut microbiome can serve as a novel biomarker of subtypes of epilepsy. Absent of consistent microbiome implications with epilepsy pathogenesis, the gut microbiome could influence efficacy of seizure treatments, such as the ketogenic diet and anti-epileptic drugs. Further study of how the microbiome is impacted by seizure interventions could identify microbial markers for treatment responsiveness or form the foundation for novel microbiome-based treatments for epilepsy. Finally, detailed studies in animal models, for how microbes impact brain metabolism, neuroimmunity and neuronal activity promise to uncover fundamental principles for host-microbiome interactions that impact brain and behavior.

Overall, further investigation into roles for the microbiome in epilepsy could help to uncover mechanistic underpinnings of epilepsy pathogenesis, biomarkers for disease and therapeutic responsivity, and novel approaches for treatment of refractory epilepsy.

Study	Location of Study	Subject	Type of Epilepsy or Disease	n	Baseline Alterations in a Refractory Epilepsy Microbiome	Baseline α-Diversity Alterations	Intervention	Results after intervention
Lindefeldt, M., Eng, A., Darban, H., Bjerkner, A., Zetterstrom, C.K., Allander, T., Andersson, B., Borenstein, E., Dahlin, M., and Prast-Nielsen, S. (2019). The ketogenic diet influences taxonomic and functional composition of the gut microbiota in children with severe epilepsy. NPJ Biofilms Microbiomes 5, 5.	Astrid Lindgren Children's Hospital of Karolinska Institute, Sweden	Children (2-17 yrs)	Refractory	12	Increase in *Firmicutes* and *Actinobacteria* Decrease in *Bacteroidetes* and *Proteobacteria*	Reduced α-diversity between refractory epilepsy group and healthy group	3 months KD	Increase in *Bacteroidetes* and *Proteobacteria* Decrease in *Firmicutes* and *Actinobacteria* After 3 months KD, 5 children showed >50% decrease in the number of seizures and 83% showed improved cognition and motor functions
Peng, A., Qiu, X., Lai, W., Li, W., Zhang, L., Zhu, X., He, S., Duan, J., and Chen, L. (2018). Altered composition of the gut microbiome in patients with drug-resistant epilepsy. Epilepsy research 147, 102-107.	West China Hospital of Sichuan Univeristy, China	Children and Adults (0-52 yrs, avg age 28.4)	Refractory/ Drug-Sensitive	42/49	Increase in *Firmicutes* and other rare species: *Akkermansia, Clostridium, Ruminococcus,* and *Coprobacillus* Decrease in *Bacteroidetes* and normal commensal bacteria	Increased α-diversity in the refractory epilepsy group compared to the drug-sensitive and healthy groups	N/A	Altered gut microbiome composition in refractory epilepsy patients compared to healthy control patients *Lactobacillus* and *Bifidobacteria* could be protective factors against for epilepsy
Tagliabue, A., Ferraris, C., Uggeri, F., Trentani, C., Bertoli, S., de Giorgis, V., Veggiotti, P., and Elli, M. (2017). Short-term impact of a classical ketogenic diet on gut microbiota in GLUT1 Deficiency Syndrome: A 3-month prospective observational study. Clin Nutr ESPEN 17, 33-37.	Department of Child Neurology at the University of Pavia, Italy	Children and Young Adults (8-34 yrs)	GLUT1 DS	6	N/A	N/A	3 months KD	Increase in *Disulfovibrio* No significant change in abundance of *Bacteroidetes, Firmicutes, Lactobacillus, Bifidobacterium, Enterobacteriaceae,* or *Clostridium*
Xie, G., Zhou, Q., Qiu, C.Z., Dai, W.K., Wang, H.P., Li, Y.H., Liao, J.X., Lu, X.G., Lin, S.F., Ye, J.H., et al. (2017). Ketogenic diet poses a significant effect on imbalanced gut microbiota in infants with refractory epilepsy. World J Gastroenterol 23, 6164-6171.	Shenzhen Children's Hospital, China	Children (1-4 yrs)	Refractory	14	Increase in *Firmicutes, Cronobacter,* and *Proteobacteria* Decrease in *Bacteroidetes, Actinobacteria, Prevotella,* and *Bifidobacterium*	No significant difference in α-diversity between any groups	1 week KD	Increase in *Bacteroidetes, Prevotella,* and *Bifidobacterium* Decrease in *Proteobacteria* and *Cronobacter* After 1 week KD, 64% of children showed >50% decrease in seizure frequency
Zhang, Y., Zhou, S., Zhou, Y., Yu, L., Zhang, L., and Wang, Y. (2018). Altered gut microbiome composition in children with refractory epilepsy after ketogenic diet. Epilepsy research 145, 163-168	Children's Hospital of Fudan University, China	Children (1-10 yrs)	Refractory	20	N/A	Reduced α-diversity between pre-KD and post-KD time points	6 months KD	Increase in *Bacteroidetes, Bacteroidia,* and *Bacteroidales* Decrease in *Firmicutes* and *Actinobacteria* During KD treatment 2 children were seizure free, 3 children had 90-99% reduction in seizure frequency, 5 children had 50-89% reduction in seizure frequency

Table 1: Reported alterations in the gut microbiota in human epilepsy. KD= ketogenic diet, GLUT1 DS= glucose transporter type 1 deficiency syndrome
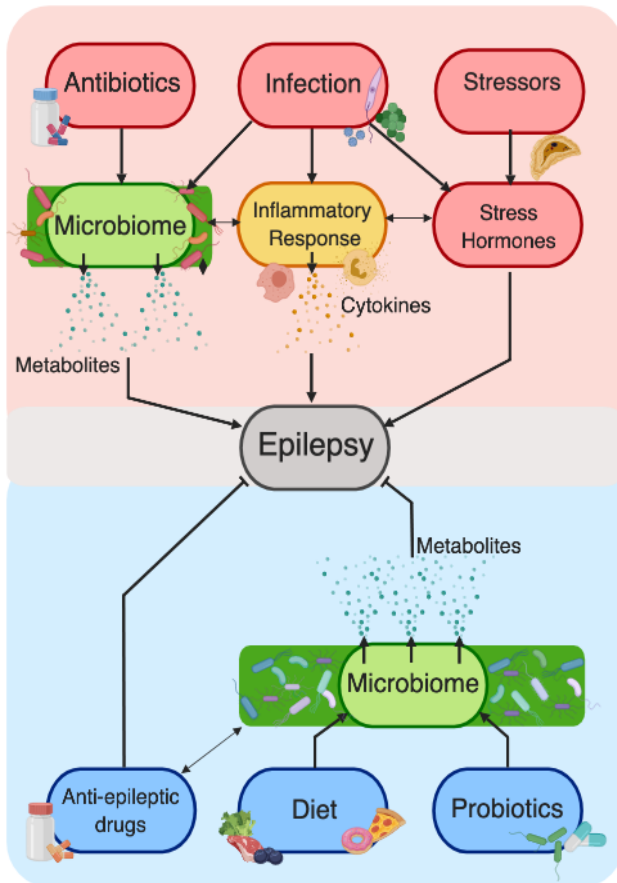
Figure 2: Potential roles for the gut microbiome in mediating risk factors (red) and interventions (blue) for epilepsy. Factors associated with increased susceptibility to seizures, including antibiotics, infection, and psychological and physical stressors, also perturb the gut microbiota. Antibiotics can promote seizures directly through modulation of neuronal activity, or indirectly through modification of the microbiome. Pro-inflammatory cytokines and stress hormones that promote seizure risk can be induced by microbial antigens and can modify the gut microbiome. Particular gut microbes may alter the metabolism of antiepileptic drugs or be directly inhibited by antiepileptic drugs. The

ketogenic diet is used to treat refractory epilepsy and is associated with changes in both the human and mouse gut microbiome. In two human studies, probiotic treatment was associated with reduced seizure risk. Separate animal studies report that probiotics modulate brain expression of gamma-aminobutyric acid (GABA) receptors, levels of GABA relative to glutamate, and seizure susceptibility.

Acknowledgments

References

Ahlers, F.S., Benros, M.E., Dreier, J.W., and Christensen, J. (2019). Infections and risk of epilepsy in children and young adults: A nationwide study. Epilepsia *60*, 275-283.

Arslan, G., Alici, S.K., Ayyildiz, M., and Agar, E. (2017). Interaction between urethane and cannabinoid CB1 receptor agonist and antagonist in penicillin-induced epileptiform activity. Acta Neurobiol Exp (Wars) *77*, 128-136.

Babaie, J., Sayyah, M., Fard-Esfahani, P., Golkar, M., and Gharagozli, K. (2017). Contribution of dopamine neurotransmission in proconvulsant effect of Toxoplasma gondii infection in male mice. J Neurosci Res *95*, 1894-1905.

Bakken, I.J., Aaberg, K.M., Ghaderi, S., Gunnes, N., Trogstad, L., Magnus, P., and Haberg, S.E. (2015). Febrile seizures after 2009 influenza A (H1N1) vaccination and infection: a nationwide registry-based study. BMC Infect Dis *15*, 506.

Bartolini, L., Libbey, J.E., Ravizza, T., Fujinami, R.S., Jacobson, S., and Gaillard, W.D. (2019). Viral Triggers and Inflammatory Mechanisms in Pediatric Epilepsy. Mol Neurobiol *56*, 1897-1907.

Beheshti Nasr, S.M., Moghimi, A., Mohammad-Zadeh, M., Shamsizadeh, A., and Noorbakhsh, S.M. (2013). The effect of minocycline on seizures induced by amygdala kindling in rats. Seizure *22*, 670-674.

Bhandare, A.M., Kapoor, K., Powell, K.L., Braine, E., Casillas-Espinosa, P., O'Brien, T.J., Farnham, M.M.J., and Pilowsky, P.M. (2017). Inhibition of microglial activation with minocycline at the intrathecal level attenuates sympathoexcitatory and proarrhythmogenic changes in rats with chronic temporal lobe epilepsy. Neuroscience *350*, 23-38.

Braakman, H.M.H., and van Ingen, J. (2018). Can epilepsy be treated by antibiotics? J Neurol *265*, 1934-1936.

Bravo, J.A., Forsythe, P., Chew, M.V., Escaravage, E., Savignac, H.M., Dinan, T.G., Bienenstock, J., and Cryan, J.F. (2011). Ingestion of Lactobacillus strain regulates emotional behavior and central GABA receptor expression in a mouse via the vagus nerve. Proceedings of the National Academy of Sciences of the United States of America *108*, 16050-16055.

Cannon, J.P., Lee, T.A., Clark, N.M., Setlak, P., and Grim, S.A. (2014). The risk of seizures among the carbapenems: a meta-analysis. J Antimicrob Chemother *69*, 2043-2055.

Cusick, M.F., Libbey, J.E., Doty, D.J., DePaula-Silva, A.B., and Fujinami, R.S. (2017). The role of peripheral interleukin-6 in the development of acute seizures following virus encephalitis. J Neurovirol *23*, 696-703.

de Theije, C.G., Wopereis, H., Ramadan, M., van Eijndthoven, T., Lambert, J., Knol, J., Garssen, J., Kraneveld, A.D., and Oozeer, R. (2014). Altered gut microbiota and activity in a murine model of autism spectrum disorders. Brain, behavior, and immunity *37*, 197-206.

Esposito, S., Canevini, M.P., and Principi, N. (2017). Complications associated with antibiotic administration: neurological adverse events and interference with antiepileptic drugs. Int J Antimicrob Agents *50*, 1-8.

Ghanizadeh, A., and Berk, M. (2015). Beta-lactam antibiotics as a possible novel therapy for managing epilepsy and autism, a case report and review of literature. Iran J Child Neurol *9*, 99-102.

Gomes, I.B., Simoes, L.C., and Simoes, M. (2018). The effects of emerging environmental contaminants on Stenotrophomonas maltophilia isolated from drinking water in planktonic and sessile states. Sci Total Environ *643*, 1348-1356.

Gomez-Eguilaz, M., Ramon-Trapero, J.L., Perez-Martinez, L., and Blanco, J.R. (2018). The beneficial effect of probiotics as a supplementary treatment in drug-resistant epilepsy: a pilot study. Benef Microbes *9*, 875-881.

Han, Y., Ma, F., Li, H., Wang, Y., and Xu, K. (2015). Optogenetic control of thalamus as a tool for interrupting penicillin induced seizures. Conf Proc IEEE Eng Med Biol Soc *2015*, 6606-6609.

He, Z., Cui, B.T., Zhang, T., Li, P., Long, C.Y., Ji, G.Z., and Zhang, F.M. (2017). Fecal microbiota transplantation cured epilepsy in a case with Crohn's disease: The first report. World J Gastroenterol *23*, 3565-3568.

Kawamura, Y., Nakayama, A., Kato, T., Miura, H., Ishihara, N., Ihira, M., Takahashi, Y., Matsuda, K., and Yoshikawa, T. (2015). Pathogenic Role of Human Herpesvirus 6B Infection in Mesial Temporal Lobe Epilepsy. J Infect Dis *212*, 1014-1021.

Leibovitch, E.C., and Jacobson, S. (2015). Human Herpesvirus 6 as a Viral Trigger in Mesial Temporal Lobe Epilepsy. J Infect Dis *212*, 1011-1013.

Liang, L., Zhou, H., Zhang, S., Yuan, J., and Wu, H. (2017). Effects of gut microbiota disturbance induced in early life on the expression of extrasynaptic GABA-A receptor alpha5 and delta subunits in the hippocampus of adult rats. Brain Res Bull *135*, 113-119.

Lim, J.S., Lim, M.Y., Choi, Y., and Ko, G. (2017). Modeling environmental risk factors of autism in mice induces IBD-related gut microbial dysbiosis and hyperserotonemia. Mol Brain *10*, 14.

Lindefeldt, M., Eng, A., Darban, H., Bjerkner, A., Zetterstrom, C.K., Allander, T., Andersson, B., Borenstein, E., Dahlin, M., and Prast-Nielsen, S. (2019). The ketogenic diet influences taxonomic and functional composition of the gut microbiota in children with severe epilepsy. NPJ Biofilms Microbiomes *5*, 5.

Liu, F., Horton-Sparks, K., Hull, V., Li, R.W., and Martinez-Cerdeno, V. (2018). The valproic acid rat model of autism presents with gut bacterial dysbiosis similar to that in human autism. Mol Autism *9*, 61.

Maier, L., Pruteanu, M., Kuhn, M., Zeller, G., Telzerow, A., Anderson, E.E., Brochado, A.R., Fernandez, K.C., Dose, H., Mori, H.*, et al.* (2018). Extensive impact of non-antibiotic drugs on human gut bacteria. Nature *555*, 623-628.

Marangoz, A.H., Kocacan, S.E., Him, A., Kuruoglu, E., Cokluk, C., and Marangoz, C. (2018). Proconvulsant Effect of Papaverine on Penicillin-Induced Epileptiform Activity in Rats. Turk Neurosurg *28*, 479-482.

Mattappalil, A., and Mergenhagen, K.A. (2014). Neurotoxicity with antimicrobials in the elderly: a review. Clin Ther *36*, 1489-1511 e1484.

Mazumder, A.G., Padwad, Y.S., and Singh, D. (2016). Anticancer Mammalian Target of Rapamycin (mTOR) Signaling Pathway Inhibitors: Current Status, Challenges and Future Prospects in Management of Epilepsy. CNS Neurol Disord Drug Targets *15*, 945-955.

Medel-Matus, J.S., Shin, D., Dorfman, E., Sankar, R., and Mazarati, A. (2018). Facilitation of kindling epileptogenesis by chronic stress may be mediated by intestinal microbiome. Epilepsia Open *3*, 290-294.

Norgaard, M., Ehrenstein, V., Nielsen, R.B., Bakketeig, L.S., and Sorensen, H.T. (2012). Maternal use of antibiotics, hospitalisation for infection during pregnancy, and risk of childhood epilepsy: a population-based cohort study. PLoS One *7*, e30850.

Owens, R.C., Jr. (2008). An overview of harms associated with beta-lactam antimicrobials: where do the carbapenems fit in? Crit Care *12 Suppl 4*, S3.

Pardo, C.A., Nabbout, R., and Galanopoulou, A.S. (2014). Mechanisms of epileptogenesis in pediatric epileptic syndromes: Rasmussen encephalitis, infantile spasms, and febrile infection-related epilepsy syndrome (FIRES). Neurotherapeutics *11*, 297-310.

Patel, D.C., Wallis, G., Dahle, E.J., McElroy, P.B., Thomson, K.E., Tesi, R.J., Szymkowski, D.E., West, P.J., Smeal, R.M., Patel, M.*, et al.* (2017). Hippocampal TNFalpha Signaling Contributes to Seizure Generation in an Infection-Induced Mouse Model of Limbic Epilepsy. eNeuro *4*.

Peng, A., Qiu, X., Lai, W., Li, W., Zhang, L., Zhu, X., He, S., Duan, J., and Chen, L. (2018). Altered composition of the gut microbiome in patients with drug-resistant epilepsy. Epilepsy research *147*, 102-107.

Plovier, H., Everard, A., Druart, C., Depommier, C., Van Hul, M., Geurts, L., Chilloux, J., Ottman, N., Duparc, T., Lichtenstein, L.*, et al.* (2017). A purified membrane protein from Akkermansia muciniphila or the pasteurized bacterium improves metabolism in obese and diabetic mice. Nat Med *23*, 107-113.

Raposo, J., Teotonio, R., Bento, C., and Sales, F. (2016). Amoxicillin, a potential epileptogenic drug. Epileptic Disord *18*, 454-457.

Sahlu, I., Carabin, H., Ganaba, R., Preux, P.M., Cisse, A.K., Tarnagda, Z., Gabriel, S., Dermauw, V., Dorny, P., Bauer, C.*, et al.* (2019). Estimating the association between being seropositive for cysticercosis and the prevalence of epilepsy and severe chronic headaches in 60 villages of rural Burkina Faso. PLoS Negl Trop Dis *13*, e0007101.

Sewal, R.K., Modi, M., Saikia, U.N., Chakrabarti, A., and Medhi, B. (2017). Increase in seizure susceptibility in sepsis like condition explained by spiking cytokines and altered

adhesion molecules level with impaired blood brain barrier integrity in experimental model of rats treated with lipopolysaccharides. Epilepsy Res *135*, 176-186.

Sgritta, M., Dooling, S.W., Buffington, S.A., Momin, E.N., Francis, M.B., Britton, R.A., and Costa-Mattioli, M. (2019). Mechanisms Underlying Microbial-Mediated Changes in Social Behavior in Mouse Models of Autism Spectrum Disorder. Neuron *101*, 246-259 e246.

Shorvon, S. (2014). The concept of symptomatic epilepsy and the complexities of assigning cause in epilepsy. Epilepsy & Behavior *32*, 1-8.

Strandwitz, P. (2018). Neurotransmitter modulation by the gut microbiota. Brain Res *1693*, 128-133.

Sutter, R., Ruegg, S., and Tschudin-Sutter, S. (2015). Seizures as adverse events of antibiotic drugs: A systematic review. Neurology *85*, 1332-1341.

Tagliabue, A., Ferraris, C., Uggeri, F., Trentani, C., Bertoli, S., de Giorgis, V., Veggiotti, P., and Elli, M. (2017). Short-term impact of a classical ketogenic diet on gut microbiota in GLUT1 Deficiency Syndrome: A 3-month prospective observational study. Clin Nutr ESPEN *17*, 33-37.

Tamma, P.D., Avdic, E., Li, D.X., Dzintars, K., and Cosgrove, S.E. (2017). Association of Adverse Events With Antibiotic Use in Hospitalized Patients. JAMA Intern Med *177*, 1308-1315.

Tan, A.P. (2018). Febrile Infection-Related Epilepsy Syndrome (FIRES) with Multifocal Subcortical Infarcts, A New Imaging Phenotype. Neuropediatrics *49*, 347-352.

Tang, A.T., Choi, J.P., Kotzin, J.J., Yang, Y., Hong, C.C., Hobson, N., Girard, R., Zeineddine, H.A., Lightle, R., Moore, T.*, et al.* (2017). Endothelial TLR4 and the microbiome drive cerebral cavernous malformations. Nature *545*, 305-310.

Tubas, F., Per, S., Tasdemir, A., Bayram, A.K., Yildirim, M., Uzun, A., Saraymen, R., Gumus, H., Elmali, F., and Per, H. (2017). Effects of Cornus mas L. and Morus rubra L. extracts on penicillin-induced epileptiform activity: an electrophysiological and biochemical study. Acta Neurobiol Exp (Wars) *77*, 45-56.

Vasiliadou, I.A., Molina, R., Martinez, F., Melero, J.A., Stathopoulou, P.M., and Tsiamis, G. (2018). Toxicity assessment of pharmaceutical compounds on mixed culture from activated sludge using respirometric technique: The role of microbial community structure. Sci Total Environ *630*, 809-819.

Veitenhansl, M., Stegner, K., Hierl, F.X., Dieterle, C., Feldmeier, H., Gutt, B., Landgraf, R., Garrow, A.P., Vileikyte, L., Findlow, A*., et al.* (2004). 40th EASD Annual Meeting of the European Association for the Study of Diabetes : Munich, Germany, 5-9 September 2004. Diabetologia *47*, A1-a464.

Vezzani, A., Fujinami, R.S., White, H.S., Preux, P.M., Blumcke, I., Sander, J.W., and Loscher, W. (2016). Infections, inflammation and epilepsy. Acta Neuropathol *131*, 211-234.

Vuong, H.E., Yano, J.M., Fung, T.C., and Hsiao, E.Y. (2017). The Microbiome and Host Behavior. Annu Rev Neurosci *40*, 21-49.

Watkins, C., Murphy, K., Yen, S., Carafa, I., Dempsey, E.M., O'Shea, C.A., Vercoe, E.A., Ross, R.P., Stanton, C., and Ryan, C.A. (2017). Effects of therapeutic hypothermia on the gut microbiota and metabolome of infants suffering hypoxic-ischemic encephalopathy at birth. Int J Biochem Cell Biol *93*, 110-118.

Wipfler, P., Dunn, N., Beiki, O., Trinka, E., and Fogdell-Hahn, A. (2018). The Viral Hypothesis of Mesial Temporal Lobe Epilepsy - Is Human Herpes Virus-6 the Missing Link? A systematic review and meta-analysis. Seizure *54*, 33-40.

Xie, G., Zhou, Q., Qiu, C.Z., Dai, W.K., Wang, H.P., Li, Y.H., Liao, J.X., Lu, X.G., Lin, S.F., Ye, J.H.*, et al.* (2017). Ketogenic diet poses a significant effect on imbalanced gut microbiota in infants with refractory epilepsy. World J Gastroenterol *23*, 6164-6171.

Yang, Y., Tian, X., Xu, D., Zheng, F., Lu, X., Zhang, Y., Ma, Y., Li, Y., Xu, X., Zhu, B.*, et al.* (2018). GPR40 modulates epileptic seizure and NMDA receptor function. Sci Adv *4*, eaau2357.

Yeo, K.T., Lahra, M., Bajuk, B., Hilder, L., Abdel-Latif, M.E., Wright, I.M., and Oei, J.L. (2019). Long-term outcomes after group B streptococcus infection: a cohort study. Arch Dis Child *104*, 172-178.

Yeom, J.S., Park, J.S., Kim, Y.S., Kim, R.B., Choi, D.S., Chung, J.Y., Han, T.H., Seo, J.H., Park, E.S., Lim, J.Y.*, et al.* (2019). Neonatal seizures and white matter injury: Role of rotavirus infection and probiotics. Brain Dev *41*, 19-28.

Yunes, R.A., Poluektova, E.U., Dyachkova, M.S., Klimina, K.M., Kovtun, A.S., Averina, O.V., Orlova, V.S., and Danilenko, V.N. (2016). GABA production and structure of gadB/gadC genes in Lactobacillus and Bifidobacterium strains from human microbiota. Anaerobe *42*, 197-204.

Zeng, X., Hu, K., Chen, L., Zhou, L., Luo, W., Li, C., Zong, W., Chen, S., Gao, Q., Zeng, G.*, et al.* (2018). The Effects of Ginsenoside Compound K Against Epilepsy by Enhancing the gamma-Aminobutyric Acid Signaling Pathway. Front Pharmacol *9*, 1020.

Zhang, P., Lu, K., and Xia, H. (2019). Multiple Factors Including Infections and Antibiotics Affecting New-Onset Epilepsy in Hemodialysis Patients. Ther Apher Dial.

Zhang, Y., Zhou, S., Zhou, Y., Yu, L., Zhang, L., and Wang, Y. (2018). Altered gut microbiome composition in children with refractory epilepsy after ketogenic diet. Epilepsy research *145*, 163-168.

Zhao, Y., Wang, Z., Lao, W., Kuang, P., Jiang, N., Yin, T., Lin, W., Zhu, H., and Ji, Y. (2018). Anticonvulsant effect of gentamicin on the seizures induced by kainic acid. Neurol Res *40*, 45-52.

Zhu, L., and Wang, H. (2018). Commentary on "Beta-Lactam Antibiotics as A Possible Novel Therapy for Managing Epilepsy and Autism. Iran J Child Neurol *12*, 139-140.

Zhu, X., Chen, Y., Du, Y., Wan, Q., Xu, Y., and Wu, J. (2018). Astragaloside IV attenuates penicillin-induced epilepsy via inhibiting activation of the MAPK signaling pathway. Mol Med Rep *17*, 643-647.

Zimmermann, M., Zimmermann-Kogadeeva, M., Wegmann, R., and Goodman, A.L. (2019). Separating host and microbiome contributions to drug pharmacokinetics and toxicity. Science *363*.

Chapter 3

Bacterial modulation of neurotransmitters for microbiota-nervous system interactions

Christine A. Olson, David J. Nusbaum, Elaine Y. Hsiao

Unpublished

Abstract

Neurotransmitters are widely distributed throughout all domains of life, with diverse functions that precede their use for neurotransmission in vertebrates. Increasing evidence for co-evolution and co-speciation of vertebrate hosts with their microbiomes suggests that neurotransmitters enable both intra- and interkingdom signaling. Particular bacteria have the capacity to synthesize and respond to neurochemicals, which affect growth, quorum sensing, motility, and virulence. The gut microbiota regulates both the enteric and central nervous systems, likely through pathways involving modulation of neurotransmitters, among other neuroactive molecules, in the intestine, blood and brain. Herein we review bacterial synthesis and utilization of neurotransmitters, focusing on serotonin (5-HT), γ-aminobutyric acid (GABA), dopamine (DA), norepinephrine (NE), and epinephrine. We discuss roles for the gut microbiota in modulating host metabolism of neurotransmitters in the gastrointestinal tract and brain. We further assess evidence suggesting that microbial modulation of host neurochemicals may be relevant to neurological disorders—anxiety and depression, Parkinson's disease, and autism spectrum disorder in particular. Finally, we examine the notion that microbial modulation of neurotransmitters is important for communication along the microbiota-gut-brain axis.

Introduction

Neurotransmitters are chemical messengers that enable signal transmission between a neuron and another cell. The majority of neurotransmitters are amino acids and amino acid derivatives- trace amines and monoamines-though some gases, peptides and other

64

molecules mediate neurotransmission as well. Given that many neurotransmitters are produced from simple dietary and metabolic precursors, it is perhaps not surprising that the synthesis and metabolism of neurotransmitters has been reported across several bacterial taxa. Serotonin (5-HT), γ-aminobutyric acid (GABA), dopamine (DA), norepinephrine (NE) and epinephrine, among other transmitters, have been detected in cultures of many pathogenic and mutualistic bacteria. Particular species respond to neurotransmitters as growth substrates, quorum sensing molecules, and virulence factors. That both neurons and particular bacteria can synthesize and utilize neurotransmitters raises the fascinating question of whether neurotransmitters serve as interkingdom signaling molecules, enabling communication between bacterial members of the indigenous microbiota and the host nervous system.

The gut microbiota fundamentally impacts the development and function of both the enteric and central nervous systems[1]. The enteric nervous system (ENS) is comprised of a vast network of plexuses- myenteric and submucosal- that contain an estimated 100 million neurons in humans, equally abundant to those forming the spinal cord[2]. As such, a wide array of neurotransmitters are produced within the gastrointestinal (GI) tract[3] that modulate functions such as sensation, motility, secretion, and circulation. Bacterial regulation of metabolic signals, including neurotransmitters, from the intestinal epithelium, mucosal immune system, and enteric neurons themselves, could contribute to alterations in the ENS.

Still unclear are the molecular mechanisms underlying how the gut microbiota modulates the central nervous system (CNS). Numerous animal studies reveal effects of the microbiota on brain neurophysiology, including neuronal morphology, myelination, and synaptic transmission, in addition to several complex behaviors, such as social interaction, communication, and anxiety. Bacterial modulation of neuroactive molecules, including neurotransmitters, is hypothesized to mediate communication across the microbiota-gut-brain axis (Figure 3). Several neurochemicals produced in the intestine enter circulation to other body systems through the intestinal, mesenteric and gastroepiploic conduits that converge at the portal vein. Some may be able to cross the blood brain barrier (BBB) to access the brain itself, though the extent to which microbially-modulated metabolites enter the brain has not yet been thoroughly delineated. In addition, vagal efferent fibers signal from the CNS to the periphery via the nucleus of the solitary tract (NTS) in the brainstem, while vagal afferent fibers, which are approximately 9 times more abundant than efferent fibers, transmit sensation from the viscera to the NTS and its projection sites[4]. While activation of vagal afferents by intestinal neurotransmitters, such as glutamate, 5-HT and GLP-1, has long been recognized to mediate appetite, satiety and nausea, whether this pathway is modulated by the gut microbiota to modify brain function and behavior remains poorly understood. Potential effects of the microbiota on vagal activity, neuroendocrine signaling and neuroimmunity are thought to underlie the ability of the microbiota to modify a variety of host phenotypes, including complex behavioral and neurophysiological symptoms of disease. Microbial modulation of neurotransmitters is relevant to each of these pathways for communication between the microbiota and nervous system. In the following sections, we discuss roles for bacteria in

the synthesis and/or modulation of host-derived neurotransmitters-- 5-HT, GABA, DA, NE, and epinephrine. We further highlight how microbial changes in neurotransmitter signaling may impact the host nervous system, with implications for neurological disease.

Serotonin (5-HT)

Bacterial Synthesis of 5-HT

In addition to its important roles in the CNS, 5-HT is a key neurotransmitter and hormone in the GI tract and across peripheral organ systems. In mammals, over 90% of 5-HT is found in the gut, where it is synthesized by enterochromaffin (EC) cells and serotonergic neurons of the enteric nervous system (ENS) to stimulate intestinal motility, secretion and absorption[5]. 5-HT also modulates sensory transmission to the CNS, activating vagal afferents in the stomach and superior duodenum to regulate gastric emptying, satiety, nausea, and discomfort[6]. Although much of the 5-HT in the GI tract is thought to be host-derived, several microbes are capable of producing 5-HT *de novo*, raising the possibility that GI 5-HT levels may be affected by contributions from both host cells and gut microbes. The first report of bacterial 5-HT found detectable levels of 5-HT in cultures of many taxa from the helminth *Ascaris suum* intestine[7] (Table 1). 5-HT was also found in cultures of *Bacillus cereus*[8]. Moreover, *Morganella morganii*, *Klebsiella pneumoniae*, and *Hafnia alvei* produced 5-HT when grown in a histidine-supplemented medium[9], and *Lactobacillus plantarum, L. lactis,* and *S. thermophilus* produced 5-HT when grown in broth supplemented with arginine[10]. These results suggest that several groups of bacteria harbor enzymes capable of synthesizing 5-HT from amino acid precursors.

Despite detection of 5-HT from live cultures of bacteria, little is known regarding bacterial mechanisms for 5-HT synthesis. One study identified a tryptophan hydroxylase (Tph) in *C. violaceum*[11], which was hypothesized to catalyze the synthesis of the microbe's characteristic pigment, violacein. 5-HT has been detected in *Chromobacterium* cultures[7], but it is unclear whether this bacterium synthesizes 5-HT using endogenous Tph or via an alternative pathway. Nevertheless, the existence of a Tph enzyme in *C. violaceum* supports the notion that some species harbor orthologous hydroxylases for 5-HT synthesis. Similarly, *E. coli* is reported to synthesize 5-HT, but *para*-chlorophenylalanine (PCPA), an inhibitor of Tph1, the rate-limiting enzyme for 5-HT biosynthesis in animals, had no effect on the growth of *E. coli*, suggesting that some bacteria may utilize Tph-independent processes for 5-HT biosynthesis[12].

Plants synthesize 5-HT via an alternative pathway involving the decarboxylation of tryptophan to tryptamine, followed by hydroxylation of tryptamine to 5-HT[13]. In recent work, *Clostridium sporogenes* and *Ruminococcus gnavus* synthesized tryptamine using tryptophan decarboxylases, providing evidence that microbial genomes encode enzymes capable of synthesizing bioactive tryptophan derivatives that function as eukaryotic neurotransmitters[14]. Although this activity is rare among bacteria, analysis of metagenomic DNA from human stool samples revealed that at least 10% of the human population harbors gut bacteria that encode a tryptophan decarboxylase. It is possible that this pathway is used by some bacteria for 5-HT production, but whether the gut microbiome encodes this function is unclear.

Melatonin, a tryptophan-derived hormone involved in the maintenance of circadian rhythms, has also been detected in bacteria[15, 16]. Arylalkylamine *N*-acetyltransferases catalyze the conversion of 5-HT to melatonin in vertebrates, and these enzymes have been found in Gram-positive bacteria[17]. Interestingly, some gut bacteria were responsive to melatonin and expressed circadian rhythmicity with respect to swarming and motility, indicating that tryptophan derivatives may be utilized by the host to regulate the gut microbiota[18]. Together, these studies suggest that the ability to synthesize 5-HT and 5-HT derivatives is widely distributed among bacteria, although additional work is required to elucidate various mechanisms for 5-HT production.

Despite high levels of 5-HT in the GI tract and reported synthesis of 5-HT by particular gut microbes, how 5-HT influences bacterial physiology remains poorly understood. 5-HT stimulated growth of *S. faecalis*[19], *E. coli* and *Rhodospirillum rubrum*[9, 20, 21] at concentrations between 2×10^{-7} and 2×10^{-5} M. In addition, 5-HT promoted cell aggregation in *E. coli* and *Polyangium* spp.[9, 12], suggesting a role for 5-HT as a bacterial signaling molecule. A recent study revealed a role for 5-HT as a quorum sensing molecule, promoting biofilm formation and virulence of *P. aeruginosa*[22]. Additional studies are needed to examine effects of 5-HT on bacterial growth, metabolism, and function.

Although there is evidence for bacterial biosynthesis of 5-HT in culture, it is possible that microbiota-derived 5-HT contributes little to overall gut 5-HT levels *in vivo*. Luminal levels of 5-HT are substantially lower than tissue-derived concentrations, suggesting a minor

contribution of microbiome-derived 5-HT to total 5-HT content in the gut. In addition, Tph1 knockout mice, which lack the host enzyme required for peripheral 5-HT synthesis, exhibit significant deficiencies in blood and intestinal 5-HT levels[23-25]. Findings across three independent studies suggest that ~7% of blood 5-HT and ~3% of intestinal 5-HT may be accounted for by non-host cells, including the microbiome, and any host cells that utilize enzyme isoforms other than Tph1 for 5-HT synthesis, such as Tph2+ neurons. Whether the microbiota itself is altered in Tph1 knockout animals is unclear, though any changes in microbiota composition may misrepresent the amount of 5-HT that is contributed by a conventional microbiota. Future research is needed to distinguish between 5-HT derived from microbial synthesis, microbe-dependent host synthesis and microbe-independent host synthesis.

Bacterial Modulation of Host 5-HT

The gut microbiota plays an important role in modulating host metabolism of 5-HT. Mice that are raised in the absence of microbial colonization (germ free, GF) display substantial decreases in blood, fecal, and colonic 5-HT levels relative to conventionally-colonized (specific pathogen free, SPF) controls[26]. Select spore-forming bacteria (Sp) from the gut microbiota stimulated Tph1-mediated 5-HT production by colonic ECs. Colonization of GF mice with Sp elevated serum and colon 5-HT to levels seen in SPF controls, reducing colonic transit time and promoting platelet activation and aggregation in a 5-HT-dependent manner. In addition to affecting 5-HT biosynthesis, there is some evidence that microbes can alter host 5-HT bioavailability by regulating 5-HT uptake. Enteropathogenic *E. coli* (EPEC) reduced 5-HT transporter (SERT) function in Caco-2

cells, a human epithelial colorectal carcinoma cell line[27]. Mice infected with EPEC exhibited reduced SERT mRNA expression and decreased 5-HT cellular uptake in small intestine apical membrane vesicles. These data suggest an important role for particular subsets of bacteria in regulating levels of host colonic and blood 5-HT that are relevant to normal GI, ENS and platelet physiology.

While molecular mechanisms underlying how particular gut bacteria modulate host 5-HT levels are unclear, paracrine metabolic signaling may be involved. Short-chain fatty acids (SCFAs, specifically acetate and butyrate), which are products of bacterial fermentation and enriched in response to 5-HT-inducing Sp bacteria, induced Tph1 expression in BON cells, a human EC cell line[28]. A separate study corroborated the relationship between SCFAs and 5-HT *in vivo*, where rats treated with SCFAs exhibited increased colonic transit time, an effect abolished by PCPA treatment[29]. Other microbial metabolites, including deoxycholic acid, tyramine and alpha-tocopherol, have also been implicated[26]. Studies are needed to identify signal transduction pathways by which various microbial metabolites induce host 5-HT synthesis.

The gut microbiome also significantly impacts the host brain serotonergic system. Compared to SPF controls, GF mice exhibited increased hippocampal 5-HT and decreased 5HT1A receptor expression in the hippocampal dentate granule layer[30]. These differences were only significant for male GF mice[31], highlighting a role for sex differences in microbiome-induced changes in host brain neurochemicals. GF mice also had a higher degree of 5-HT turnover in the striatum, which possibly impacts anxiety-like behavior[32].

One study supported this notion of microbiome-mediated changes in anxiety and 5-HT by demonstrating that probiotic treatment with *Lactobacillus helveticus* NS8 corrected deficits in hippocampal 5-HT in a chronic restraint model of anxiety[33]. In zebrafish, treatment with *L. rhamnosus* IMC 501 increased expression of the tryptophan hydroxylases Tph1a, Tph1b and Tph2 in the brain[34]. In rats, probiotic treatment with *Bifidobacterium infantis* decreased 5-hydroxyindole acetic acid (5-HIAA), a 5-HT breakdown product, in the frontal cortex[35]. While evidence suggests that 5-HT does not readily cross the blood-brain barrier (BBB)[36], its precursors tryptophan and 5-hydroxytryptophan (5-HTP) can[37], raising the question of whether microbiome-mediated changes in CNS 5-HT levels are mediated by microbial effects on peripheral 5-HT precursors. Future studies are needed to determine the extent of interactions between peripheral and brain levels of neurotransmitters, including 5-HT, and importantly, to uncover mechanisms by which the gut microbiota impacts CNS 5-HT and downstream functions.

γ-aminobutyric Acid (GABA)

Bacterial Synthesis of GABA

GABA is the primary inhibitory neurotransmitter in the CNS. In addition to modulating neuronal excitability[38], GABA affects the immune system, blood pressure, and stress tolerance[39]. In the GI tract, GABA regulates intestinal secretion and peristalsis through modulation of acetylcholine, another neurotransmitter, and non-adrenergic, non-cholinergic (NANC) enteric neurons[40]. In addition, many immune cells, including dendritic cells, macrophages, and T cells express GABA receptors and enzymes for GABA

synthesis[40, 41], suggesting an important role for intestinal GABA in immunomodulation. Abnormalities in brain GABA metabolism are associated with mental health disorders including depression, anxiety, and autism, raising the question of whether modulation of GABA levels by the microbiota may impact host health and disease.

Microbial biosynthesis of GABA has been widely reported (Table 1). *Bacteroides fragilis* and *E. coli* were capable of producing GABA in culture, suggesting that the microbiota may contribute to GABA levels in the host[42]. GABA production has also been observed in *Pseudomonas aeruginosa*, *P. fluorescens*, *Bifidobacterium*, and *Lactococcus* strains[43-46]. Moreover, an HPLC-based screening method identified 9 high GABA-producing strains of *L. brevis*[47]. Interestingly, GABA synthesis is not limited to commensal microbes, as at least eight common bacterial pathogens also produced this neurochemical[48].

Several studies have explored GABA metabolism in bacteria. The glutamate decarboxylase (GAD) system is important for promoting acid tolerance[49]. GAD catalyzes glutamate conversion to GABA by consuming protons, and a glutamate/GABA antiporter couples glutamate influx to GABA efflux. Many bacteria metabolize GABA to succinate, which can be utilized for energy production. GADs have been identified in a variety of bacteria, including *E. coli*, *Lactobacillus* sp., and *Streptococcus* sp.[50-54], and draft genome sequences for the GABA-producing bacteria *L. plantarum*, *L. brevis*[55, 56], *B. angulatum*, and *B. adolescentis*[57] have revealed genes for the transport of GABA. Moreover, the glutamate decarboxylase GadB is reportedly more highly enriched in human stool

samples than in any other body site[39]. This evidence indicates that select members of the gut microbiota have the genomic potential for GABA synthesis.

Aside from directly synthesizing GABA, some gut microbes directly respond to it. The first report of a neurotransmitter receptor in bacteria was that of a GABA uptake system in *P. fluorescens*[58]. *Pseudomonas* harbored enzymes for GABA metabolism, but was unlikely to utilize GABA as a primary nutrient source due to the inefficiency of this pathway, suggesting that GABA functions as a signaling molecule. When cultures were pretreated with GABA during early growth phase, strains of *P. fluorescens* exhibited increased cytotoxicity, altered LPS structure, and reduced biofilm formation[45]. In a separate study, a gut *Flavonifractor* sp. was found to utilize GABA produced by *B. fragilis* as a growth factor[59]. A co-culture screening assay subsequently identified several other GABA-producing gut microbes that induced *Flavonifractor* growth, including *Alistipes putredinis*, *B. ovatus*, *L. brevis*, and *B. longum*. These results highlight the importance of studying microbe-microbe interactions within the gut in addition to host-microbe interactions. Future studies utilizing these methodologies may elucidate neurochemical-based signaling networks between gut bacteria and provide insight into the key microbial players in neurochemical biosynthesis and utilization in the GI tract.

Bacterial Modulation of Host GABA

Additional studies have revealed important roles for the gut microbiota in modulating host levels of GABA. Compared to SPF mice, mice raised as GF exhibited substantial deficiencies in levels of luminal GABA that were restored by postnatal conventionalization

with an SPF microbiome or colonization with Sp bacteria. In another study, site-directed mutagenesis of *GadB* in *B. dentitium* decreased GABA:glutamate ratios *in vitro*[39]. As such, probiotic treatment with *B. dentitium* significantly diminished visceral hypersensitivity in rats, consistent with the important role for GABA in regulating pain perception from visceral sensory afferent neurons. These studies highlight the potential use of bacterial modulators of host GABA levels as probiotic treatments for symptoms of intestinal disorders.

Like for 5-HT, whether microbiome-mediated changes in peripheral GABA contribute to alterations in brain GABA is unclear. Studies examining whether GABA can cross the BBB have rendered conflicting results[60], though evidence suggests that glutamate, its precursor, does cross the BBB[61]. This raises the question of whether the microbiome can modulate glutamate concentrations to indirectly impact CNS GABA levels. Microbial metabolites have been implicated in glutamate-glutamine and GABA cycling in the hypothalamus of fasted rats. Rats orally gavaged with (U-^{13}C) inulin exhibited microbiome-dependent fermentation of the compound into labeled acetate, with corresponding alterations in hypothalamic GABA metabolism[62]. Acetate was metabolically oxidized by astrocytes through the tricarboxylic acid cycle and fed into hypothalamic GABA cycling, thereby increasing GABA production. Consistent with this, *L. rhamnosus* (*JB-1*) increased brain GABA concentrations after four weeks of treatment[63], suggesting indirect effects of the bacterium on host GABA metabolism. *JB-1* probiotic treatment also modulated expression of GABA receptors GABA$_{a\alpha2}$, GABA$_{a\alpha1}$, and GABA$_{B1b}$ across different brain regions[64]. Alterations in these particular classes of

GABA receptors have been implicated in anxiety disorders. Indeed, *JB-1* treatment improved performance in the elevated plus maze and forced swim test (FST), behavior tests for anxiety- and depression-related behaviors in rodents. Notably, the effects on performance in the FST required active vagal nerve function. Additional studies are needed to identify specific endocrine and/or vagal pathways that may link microbiome-mediated GABAergic signaling in the GI tract and the brain, and to further elucidate how microbial modulation of neurotransmitters including GABA may affect brain and behavior.

Catecholamines: Dopamine (DA), Norepinephrine (NE), and Epinephrine

Bacterial Synthesis of Catecholamines

NE and DA within the GI tract account for approximately half of bodily levels, while epinephrine is low to undetectable[65] [66]. They impart various effects on GI physiology. NE decreases motility through the sympathetic division of the autonomic nervous system (ANS) and is also known to regulate sensory, motor and secretory function[67]. Epinephrine slows GI motility by causing smooth muscle relaxation through beta adrenergic receptors[68]. NE, DA, and epinephrine alter GI nutrient absorption rates, although DA is believed to have a smaller contribution. Catecholamines in the GI tract also modulate blood flow, as NE induces vasoconstriction, epinephrine promotes vasodilation, and DA elicits concentration-dependent vasodilation or vasoconstriction.

DA and NE have been detected in culture media of several bacteria (Table 1). Interestingly, the reported concentrations of catecholamines from bacterial culture are higher than in human blood[21], suggesting that microbe-derived catecholamines play an

important role in signaling between bacteria as well as between the microbiota and the host. L-DOPA is a DA, NE, and epinephrine precursor, and bacterial synthesis of L-DOPA via several enzymatic pathways has been well-documented. *E. intermedia* generated L-DOPA via beta-tyrosinase activity using L-tyrosine and pyrochatecol as substrates[69]. Tyrosinase activity also efficiently converted L-tyrosine to L-DOPA in a soil *Bacillus* species[70]. Alternative enzymatic pathways of L-DOPA production in bacteria include tyrosine phenol lyase, which was identified in *Erwinia herbicola* and several other species[71], a transaminase pathway in several bacteria[72], and synthesis from pyruvate, ammonia, and catechol/pyrocatechol in *E. intermedia* [73]. These findings suggest that L-DOPA production capacity is widely distributed among bacteria, but microbial pathways for the conversion of L-DOPA to catecholamine neurotransmitters remain poorly understood. Interestingly, an L-DOPA decarboxylase was identified in *Sorangium cellulosum*[74], suggesting that some bacteria may produce DA via the same mechanism utilized by eukaryotes.

Several studies have explored the effects of NE on the growth and virulence of pathogenic bacteria. NE stimulated the growth of *E. coli*, *Yersinia enterocolitica*, *K. pneumoniae, S. aureus* and *P. aeruginosa* in culture[75, 76]. NE also increased the growth and virulence of *Streptococcus pneumonia*[77], *Vibrio campbellii*, *V. anguillarum*[78], *Campylobacter jejuni*[79], and *Salmonella typhimurium*[80]. In contrast, NE inhibited the growth of *P. gingivalis* and *B. forsythus*, suggesting that particular bacteria produce NE to regulate others. For *P. aeruginosa,* NE increased virulence and swimming motility, likely via the *las* quorum sensing pathway[81]. The virulence of pathogenic *E. coli* and *Y. enterocolitica* was also

enhanced by NE, which stimulated production of adhesin and shiga-like toxin[82-84].

Notably, flagellar and motility genes of enterohemorrhagic *E. coli* (EHEC) was controlled

by a quorum sensing mechanism involving production of AI-3 by gut commensals and

epinephrine/NE by the host. Structurally similar, AI-3, epinephrine and NE, each bound

to QseC, a sensor kinase involved in the regulation of virulence and motility [85-87]. It is

hypothesized that AI-3 is capable of signaling to eukaryotic adrenergic receptors,

supporting bidirectional signaling between bacteria and eukaryotes[88]. Aside from known

pathogens, particular Enterobacteriaceae, Pseudomonadoceae, *Actinomyces*, *Eikenella*,

and *Campylobacter* members of the indigenous microbiota also exhibited increased

growth in response to NE[82]. Epinephrine enhanced *P. fluorescens* chemotaxis[89], but

much less is known about effects of epinephrine and dopamine on bacterial physiology.

Future studies are needed to examine effects of catecholamines on bacterial function and

genes involved in bacterial metabolism of neurotransmitters.

Bacterial Modulation of Host Catecholamine Synthesis

Animal studies have shown that the gut microbiota plays an important role in the

production of catecholamines found in the intestinal lumen[65]. Compared to SPF controls,

reduced levels of free luminal catecholamines were detected in the luminal contents, but

not intestinal tissue, of GF mice, where over 90% of the DA and 40-50% of the NE was

in the biologically inactive glucuronidated form. This suggests that gut microbes are

necessary for producing the free, physiologically active forms of NE and DA, consistent

with known β-glucuronidase activity of the microbiota. Colonization of GF mice with *E.*

coli and Clostridia bacteria resulted in an increase in free gut NE and DA levels,

suggesting an important role for particular gut microbes in the de-glucuronidation of catecholamines.

The gut microbiota can also stimulate host production of catecholamines[90]. Tyrosine hydroxylase (TH), the rate limiting enzyme in catecholamine production, is transcriptionally regulated by the SCFA butyrate in PC12 cells, a cell line derived from the neural crest that can differentiate into neuron-like cells, which hints at a direct mechanism for microbial modulation of host catecholamine production[91]. Consistent with this, prebiotic treatment of piglets increased TH expression in the duodenum[92]. Further studies are required to elucidate whether butyrate-producers in particular alter TH expression, whether butyrate production regulates TH transcription *in vivo*, and how this affects host physiology.

One study suggests that microbial regulation of gut DA levels is involved in intestinal disease. Active colitis is associated with dysbiosis of the gut microbiota, including increases in Enterobacteriaceae. Interestingly, treatment of colitic mice with vancomycin, which enriched Enterobacteriaceae, resulted in reduced fecal DA concentrations compared to mice treated with gentamicin, which decreased the abundance of Enterobacteriaceae[93]. These findings suggest a link between particular subsets of gut bacteria and intestinal DA levels. Additional experiments are required to determine which bacterial taxa are responsible for modulating DA concentrations, and whether this modulation occurs by direct synthesis/metabolism by bacteria, or via signaling to the host.

Importantly, whether microbiota-mediated changes in catecholamines sufficiently mediate particular symptoms of intestinal disease remains unclear.

The BBB is generally impermeable to catecholamines, but L-DOPA and tyrosine, precursors for NE, DA, and epinephrine do cross the BBB[94]. Cerebral DA levels were approximately two times higher in GF mice compared to conventionalized controls[95]. GF mice also exhibited increased striatal turnover of DA and NE and higher levels of DA in the prefrontal cortex and brainstem as compared to conventionalized mice [32, 96]. Further supporting microbiome-mediated regulation of brain catecholamine levels, probiotic administration of *L. helveticus* NS8 restored hippocampal NE levels in a chronic restraint model [33]. In addition, probiotic administration of *B. infantis* decreased levels of 3,4-dihydroxyphenylacetic acid (DOPAC) without altering DA levels significantly, suggesting abnormal DA metabolism[35]. Further studies are needed to evaluate microbial modulation of brain catecholaminergic derivatives and assess the consequences of microbe-based increases in DOPAC and NE on neurophysiology.

Microbial Modulation of Neurotransmitters and Neurological Disease

Changes in the gut microbiome are implicated in several neurodevelopmental, neurological and neurodegenerative diseases, including autism spectrum disorder (ASD), anxiety disorder, depression, Parkinson's disease (PD), and Alzheimer's disease (Table 2). Additionally, animal studies reveal fundamental effects of microbiome manipulations on the development of neurophysiological and behavioral endophenotypes of disease. In

the following sections we focus on emerging roles for the microbiota and neurotransmitter dysregulation in anxiety and depression, PD and ASD.

Microbial Effects on 5-HT and Implications for Anxiety and Depression

Anxiety and major depressive disorder are associated with dysfunctions in serotonergic neurotransmission, including alterations in 5-HT synthesis, reuptake, and metabolism[97, 98]. Interestingly, these disorders are often comorbid with GI problems, which has prompted interest in the role of the microbiota and GI dysfunction on core symptoms of disease. GF mice exhibit altered anxiety- and depression-related behavior compared to conventionally-reared mice[31, 32, 99], and conventionalization of GF mice restores behavior to that of SPF mice[31]. In light of several studies reporting corresponding changes in peripheral and brain 5-HT metabolism (Table 2), additional research is required to determine whether any microbiota-associated changes in anxiety- and depression-related behavior are sufficiently mediated by microbial modulation of 5-HT. Dysfunctions in GABAergic signaling are also associated with the development of depression and anxiety[64, 100]. Administration of *L. rhamnosus* modulated brain GABA receptor expression and reduced anxiety and depression-like behavior in mice. Interestingly, vagotomized mice did not respond to treatment, indicating that microbial signals may be conveyed via the vagus nerve. Overall, animal studies provide strong evidence that changes in the gut microbiota are associated with aberrant neurotransmission and altered behavioral phenotypes.

Several studies have reported changes in the composition of the gut microbiota in human depression patients relative to healthy controls [101-105] (Table 2). One found that depression-like behaviors could be induced in GF mice by fecal microbiota transplantation from depressed human patients[105], suggesting that endophenotypes of depression are transmissible via the gut microbiota. Furthermore, administration of *L. helveticus* and *B. longum* reduced anxiety-like behavior in rats and alleviated psychological distress in human volunteers[106]. Additional research is necessary to determine whether specific alterations to the gut microbiota disrupt serotonergic neurotransmission in humans. Because independent studies have reported differential changes in microbiota composition associated with depression, well-powered cohorts with clinical sub-classification based on background, symptom severity, medical co-morbidities and pharmacological exposure, among other variables, are needed to determine whether defined microbial signatures exist for subsets of patients with depression.

The Microbiome and Dopamine in Parkinson's Disease (PD)

PD is a neurodegenerative disorder characterized by the aggregation of alpha-synuclein and loss of dopaminergic neurons in the substantia nigra, resulting in symptoms including tremor, rigidity, and bradykinesia. GI dysfunction is associated with PD[107, 108], but it is unclear whether this is an effect of altered physiology or a causative factor implicated in the pathogenesis of the disease. Recent work suggested a link between microbial dysbiosis and PD. A study comparing the fecal microbiota of 72 PD patients to 72 control subjects found differences in gut microbiota characterized by decreased Prevotellaceae [109]. In addition, the relative abundance of Enterobacteriaceae was positively correlated

with motor symptoms of PD patients. Although a causal link between the gut microbiota and PD has not been established, these findings suggest that microbial dysbiosis is associated with PD disease progression.

There are several proposed pathways by which gut microbes could influence PD etiopathogenesis. One hypothesis is that particular gut bacteria influence intestinal bioavailability of L-DOPA, a common treatment for PD. Eradication of *Helicobacter pylori* in PD patients increased absorption of L-DOPA[110], suggesting that *H. pylori* utilizes L-DOPA and thereby reduces bioavailability to the host[111]. L-DOPA interacted with *H. pylori* surface adhesins *in vitro*[112] and increased bacterial growth[111]. Another route by which the microbiota may affect PD is by modulation of circulating lipopolysaccharide (LPS). In animal studies, LPS exposure damaged the substantia nigra, leading to endophenotypes of PD[113]. PD patients exhibited increased gut permeability compared to controls, which could contribute to the microbial dysbiosis observed in PD[114]. Additional work is necessary to determine whether particular changes in the gut microbiota actually contribute to disease. Experimental trials testing the efficacy of probiotics that produce L-DOPA and/or DA are warranted.

The Microbiome, Neuroactive Molecules and Autism Spectrum Disorder (ASD)

ASD is an increasingly prevalent neurodevelopmental disorder characterized by stereotyped behaviors, social impairment and communication deficiencies[115]. ASD is comorbid with several medical conditions, including immune dysregulation, GI disorders, and altered metabolism, raising the question of whether these peripheral alterations

contribute to core behavioral symptoms of the disorder. According to several reports, the microbiome is significantly altered in autistic patients (Table 2).

Evidence for microbial dysbiosis in contributing to core ASD behaviors have largely been provided by animal models. Compared to SPF controls, GF mice exhibit abnormalities in social interactions and communication, endophenotypes of ASD[32, 116]. In a mouse model of an autism risk factor, maternal immune activation (MIA), treatment of mice exhibiting behavioral symptoms of ASD with the *B. fragilis* corrected abnormalities in anxiety-like behavior, ultrasonic vocalizations, repetitive behavior and sensorimotor gating[117]. Notably, other deficits in sociability and social preference were not corrected. Although mechanisms underlying the beneficial effects of treatment are unclear, microbial modulation of the serum metabolome may contribute. In particular, increased in blood 4-ethylphenylsulfate (4EPS) sufficiently induced anxiety-like behavior, and 4EPS was reduced by probiotic treatment. This suggests that microbiome-mediated alterations in neuroactive metabolites could modify particular ASD-related behaviors. In another model for ASD, offspring of maternal high fat diet (MHFD) mice exhibited ASD-related behaviors and deficits in oxytocin, a neuropeptide that promotes bonding and sociability, in the paraventricular nucleus[118]. Remarkably, probiotic treatment with live, but not heat-killed, *L. reuteri* sufficiently corrected deficits in social behavior and brain oxytocin. Additionally, since hypothalamic oxytocin activates dopaminergic neurons in the ventral tegmental area (VTA), MHFD offspring exhibited deficits in long term potentiation of VTA dopaminergic neurons that were ameliorated by *L. reuteri*. It will be interesting to evaluate whether combined probiotic formulations would effectively treat the characteristic

abnormalities in social, communicative and repetitive associated with ASD, and importantly, to determine whether these treatments in mice also ameliorate symptoms in humans.

Conclusion: Neurotransmitters as interkingdom signaling molecules

Produced from simple precursors, the evolutionary origins of neurotransmitters likely precede their use for neurotransmission in vertebrates[119], as they are widely distributed throughout all domains of life. The synthesis and metabolism of neurotransmitters by both bacteria and eukaryotic host cells suggests that neurotransmitters are important factors for both intra- and interkingdom signaling. Particular bacteria, including members of the gut microbiota, synthesize and respond to neurochemicals, which exert varying effects on growth, quorum sensing, motility, and virulence. The gut microbiota further regulates both the ENS and CNS, by metabolic neuroendocrine signaling, modulation of the neuroimmune system, and innervation of sensory neurons that project to the brain or spinal cord. Neurotransmitters are key candidate signaling molecules for each of these pathways. As increasing evidence supports the importance of the gut microbiota for host brain and behavior, a greater understanding of the molecular mechanisms of communication along the microbiota-gut-brain axis is required. Further research is needed to elucidate the specific bidirectional interactions between indigenous microbes and host tissues, via factors such as neurotransmitters. Ultimately, understanding the mechanisms by which neurotransmitter signaling shapes and is shaped by the gut microbiota may lead to novel treatment strategies for a variety of GI, neurobehavioral, and neurological disorders.
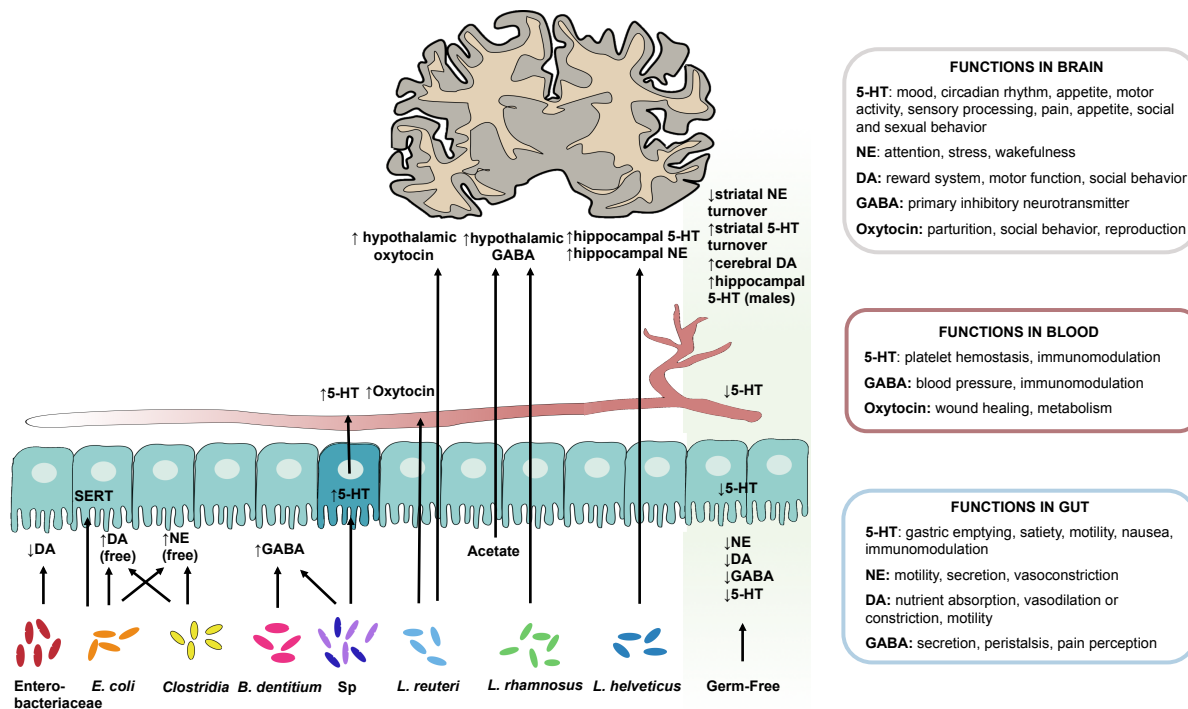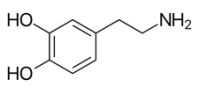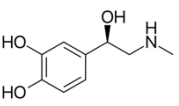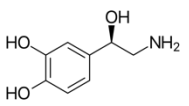
Figure 3: Microbial modulation of neurotransmitters in the host. Treatment of animal models with indigenous gut microbes alters luminal, epithelial, blood and brain neurochemical levels. Mice raised germ-free (GF) exhibit decreased levels of catecholamines, GABA and 5-HT in the intestinal lumen, which correlates with decreased blood 5-HT and altered NE, 5-HT and DA metabolism in the brain. Colonization of GF with a consortium of spore-formers (Sp) restores levels of luminal and blood 5-HT by stimulating synthesis in colonic enterochromaffin (EC) cells. Mice colonized with either Sp, *B. dentitium*, or a full specific pathogen free (SPF) microbiome display increases in luminal GABA levels. While increased Enterobacteriaceae levels in the colon corresponded with decreased DA, colonization with *Clostridia* and *E. coli* increased free

DA levels. GABA, the primary source of neurotransmitter inhibition in the CNS, is increased in the hypothalamus of mice treated with acetate, an SCFA produced by microbial fermentation of dietary fiber. Treatment of mice with *L. helveticus* restored levels of hippocampal 5-HT and NE in a chronic mild stress model of anxiety, implicating the microbiome in modulating anxious behavior. *L. reuteri* colonization not only increased serum levels of oxytocin, *L. reuteri* also increased paraventricular nucleus oxytocin-positive neurons and corrected deficits in social behavior.

Neurotransmitter	Microbial Producers	Microbial Responders
Dopamine (DA)	*B. cereus, B. mycoides, B. subtilis, E. coli, Hafnia alvei, Lactobacillus helveticus, Morganella morganii, Klebsiella pneumonia, Proteus vulgaris, Pseudomonas* aeruginosa, *Serratia marcescens, Staphylococcus aureus*[9, 1]	Enhanced growth: *E. coli*, Y. *enterocolitica*[2, 3], *Klebsiella pneumoniae, P. aeruginosa*[4], *S. epidermidis*[5], *S. enterica*[6]. Enhanced swimming motility and virulence of *Vibrio campbellii* and *Vibrio anguillarum*[7].
Epinephrine	N/A	Enhanced growth: *E. coli*[3], *Klebsiella pneumoniae, Pseudomonas aeruginosa, S. aureus*[2], *S. epidermidis*[5], *S. enterica*[6]. Some *Actinomyces, Eikenella corrodens*, and *Campylobacter*[1]. Inhibited growth: *Porphyromonas gingivalis* and *Bacteroides forsythus*[1]. Enhanced chemotaxis: *Pseudomonas fluorescens*[8], *E. coli* O157:H7[9] (plus biofilm formation and upregulation of virulence genes)
Norepinephrine (NE)	*B. cereus, B. mycoides, B. subtilis, B. mycoides, E. coli, Proteus vulgaris, Serratia marcescens*[9, 10]	Enhanced growth: *E. coli, Klebsiella pneumoniae, Pseudomonas aeruginosa, S. aureus* [2], *S. epidermidis*[5], *Yersinia enterocolitica*[3], *S. enterica*[6], and *Streptococcus pneumoniae*[6]. Some *Actinomyces, Eikenella corrodens*, Enterobacteriaceae, Pseudomonadaceae, and Enterococcus[11]. Inhibited growth: *Porphyromonas gingivalis* and *Bacteroides forsythus*[1]. Enhanced chemotaxis: *E. coli* O157:H7[9] (plus biofilm formation and upregulation of virulence genes such as K99 pilus adhesin[12] and Shiga-

		like toxin[13]). Regulation of flagellar and motility genes: enterohemorrhagic *E. coli* (EHEC)[8, 14, 15].
		Enhanced the growth, swimming motility, and virulence of *Vibrio campbellii*, *Vibrio anguillarum[7]*, and *Pseudomonas aeruginosa*, likely via the *las* quorum sensing pathway[16]. Enhanced virulence of *Campylobacter jejuni[17]*. Increased the growth and enterotoxin production of *Salmonella typhimurium[18]*.
Acetylcholine (ACh)	*B. subtilis, E. coli, Lactobacillus plantarum[19], S. aureus[20, 21]*	Inhibition of chemotaxis in *P. fluorescens[8]*. *P. aeruginosa* encodes an acetylcholinesterase enzyme (hydrolyzes acetylcholine)[22].
γ-Aminobutyric acid (GABA)	*Bacteroides fragilis, Bifidobacterium longum, Enterococcus, E. coli[23], H. influenza, K. pneumoniae[24], Lactobacillus brevis, L. rhamnosus, Lactococcus lactis[25-29], P. aeruginosa, P. fluorescens, P. mirabilis, , S. aureus*	Enhanced growth: Gut *Flavonifractor* sp. (utilizing GABA produced by other bacteria)[30]. Glutamate decarboxylases: *E. coli, Lactobacillus* sp., and *Streptococcus* sp.[31-34]. GABA transport genes: *L. plantarum, L. brevis*[29, 35], *B. angulatum*, and *B. adolescentis[36]*. *P. fluorescens* has a GABA uptake system[37], and GABA causes increased cytotoxicity, altered LPS structure, and reduced biofilm formation[26].
Serotonin (5-HT)	Detected in *Ascaris suum* intestine: Achromobacter*, Acinetobacter, Aeromonas, Chromobacterium, Citrobacter, Corynebacterium, Enterobacteria agglomerans, Escherichia coli, Klebsiella pneumoniae, Listeria monocytogenes, Shigella, Staphylococcus aureus, Streptococcus[38]. Morganella morganii, Klebsiella pneumoniae, Hafnia alvei[39, 40]. Lactobacillus plantarum, Lactococcus lactis, Streptococcus thermophilus[41]*	Enhanced growth: *Streptococcus faecalis[4]*, *Escherichia* coli[42], *Enterococcus faecalis,* and *Rhodospirillum rubrum[39, 42-44]*. Quorum sensing (promotion of biofilm formation and virulence): *P. aeruginosa[45]*. Cell aggregation in *E. coli* and *Polyangium* spp.[39, 43].
Tryptamine	*Clostridium sporogenes, Ruminococcus gnavus[46]* (using tryptophan decarboxylases)	N/A

Table 2 Microbial Production and Utilization of Neurotransmitters

			ANXIETY AND DEPRESSION		
Model	**Perturbation**	**Microbiome Change**	**Associated Neurochemical/Neurochemical Precursor/Receptor Changes**	**Changes in Behavior**	**Reference**
Mouse: BALB/c	treatment with *L. rhamnosus (JB-1)*	Not reported	↑GABA$_{A\alpha2}$R in hippocampus ↓GABA$_{A\alpha2}$R PFC, amygdala ↑GABA$_{B1b}$R in cingulate 1, prelimbic cortices ↓GABA$_{B1b}$R in basolateral amygdala, central amygdala, locus coeruleus, cornus ammonis region 1	↓corticosterone-induced stress, anxiety, depression	[64]
Mouse: NMRI	GF vs. SPF	No bacteria in GF	↑5-hydroxytryptophan (5-HTP) and 5-hydroxyindoleacetic acid (5-HIAA) in hippocampus for males, ↑plasma tryptophan for males	↓anxiety and depression-related behavior	[31, 32]
Mouse: Female Swiss Webster	GF vs. SPF	No bacteria in GF	↓N-methyl-D-aspartate (NMDA) receptor subunit NR2B expression in amygdala, ↑brain derived neurotrophic factor (BDNF) and ↓5-hydroxytryptophan 1A receptor (5HT1AR) expression in dentate layer of hippocampus	↑anxiety-like behavior	[99]
Mouse: Male Swiss	GF vs. SPF	No bacteria in GF	↑delta FBJ murine osteosarcoma viral oncogene homolog B (ΔFosB) expression in dorsal raphe nucleus, indirectly implicates effects on serotonergic neurotransmission	↑anxiety-like behavior	[129]
Mouse: BALB/c	GF vs. EX-GF	No bacteria in GF vs. full microbiome in EX-GF	↑norepinephrine (NE), ↑dopamine (DA) turnover in brainstem and medial prefrontal cortex, ↑serotonin (5-HT) turnover rates in striatum	↓anxiety-like behavior in EX-GF mice	[96]
Mouse: NIH Swiss	SPF vs. antibiotic-treated	Bacterial depletion with antibiotic treatment	↑serum tryptophan, ↓serum kynurenine, ↓BDNF expression in hippocampus, ↓hypothalamic oxytocin and vasopressin, ↑hippocampal NE and 5-HIAA, ↑l-3,4-dihydroxyphenylalanine(L-DOPA) in amygdala	↓anxiety-like behavior in antibiotic-treated mice	[116]
Mouse: BALB/c; NIH Swiss	GF vs. SPF vs. EX-GF	No bacteria in GF vs. administration of full	No change in DA, 5-HT, or NE level in small intestine and colon	↓anxiety-like behavior in antimicrobial-treated mice	[130]

		microbiome in EX-GF			
Mouse: Female C57BL/6	Olfactory Bulbectomy (OBx) model	Alteration in OBx microbiome relative to sham control	↑central corticotropin-releasing hormone (CRH) expression, ↑colon 5-HT	↑anxiety and depression-related behavior	131
Mouse: Male CF-1	*Campylobacter jejuni* infection	↑cecal *Campylobacter jejuni*	↑c-Fos immunoreactivity for catecholaminergic neurons in ventrolateral medulla and NTS , activation of noradrenergic neurons in locus coerculus, activation of dorsal raphe neurons (minor proportion of these serotonergic), activated serotonergic neurons in ventromedial medulla lateral to raphe magnus	↑anxiety-like behavior	132
Rat: Male F344	GF vs. SPF	No bacteria in GF	↓DA turnover rate in frontal cortex, hippocampus, striatum in GF relative to SPF	↑anxiety-like behavior	133
Rat: Sprague-Dawley	treatment with *L. helveticus*	Not reported	↑BDNF expression, 5-HT, NE in hippocampus	↓anxiety-like behavior	33
Rat: Wistar	treatment with *L. helveticus* and *B. longum*	Not reported	Not reported	↓anxiety-like behavior	106
Rat: Maternal Separation Model	treatment with *Bifidobacterium infantis*	Not reported	Correction of NE brainstem deficits	↓depressive behavior	35
Rat: Flinders Sensitive vs. Control Line	Sodium butyrate	Not reported	↑BDNF expression in prefrontal cortex	↓depressive behavior	134
Human	treatment with *L. helveticus* and *B. longum*	Not reported	Not reported	↓psychological distress	106
Human: Depression vs. Control	None	Association with *Faecalibacterium, Alistipes, Ruminococc*	Particular bacterial taxa associated with isovaleric acid, which can cross the BBB and inhibit Na+/K+-ATPase	Not reported	135

Model	Perturbation	Microbiome Change	Associated Neurochemical/Neurochemical Precursor/Receptor Change	Changes in Behavior	Reference
		us, Oscillibacter			
Human: Depression vs. Control	None	↑*Bacteroidales*, ↓*Lachnospiraceae* association with *Alistipes* and *Oscillibacter*	*Oscillibacter* produces valeric acid, which is structurally similar to GABA and binds to GABA$_A$ receptors	Not reported	[103]

			AUTISM		
Model	**Perturbation**	**Microbiome Change**	**Associated Neurochemical/Neurochemical Precursor/Receptor Change**	**Changes in Behavior**	**Reference**
Mouse: Maternal High Fat (MHFD) vs. Control Diet	Probiotic treatment with *L. reuteri*	Prior to probiotic, MHFD offspring exhibit reduced microbiome diversity	Restoration of paraventricular nucleus oxytocin deficits seen in MHFD offspring	Corrected social behavior deficits seen in MHFD offspring	[118]
Mouse: Autism (Maternal Immune Activation (MIA) Model)	Probiotic treatment with *B. fragilis*	↑*Porphyromonadaceae, Prevotellaceae,* Bacteroidales, *Lachnospiracea*; *B. fragilis* in MIA	Not reported	Corrected anxiety-like behavior, communicative, repetitive, sensorimotor behavior	[117]
Mouse: Autism (Prenatal Exposure to Valproic Acid (VPA))	VPA Exposure	↓Bacteroidetes, ↑Firmicutes	↓5-HT in amygdala and prefrontal cortex in males, ↓intestinal 5-HT in males, ↓prefrontal dopaminergic activity without alteration of DA level in males, ↓DA D1 and D2 receptors in males	↓social interaction, ↑stereotyped behavior, ↑anxiety-like behavior, ↓communication, ↓spatial learning, ↓object exploration	[136]
Rat: Autism (Prenatal Exposure to VPA)	VPA Exposure	Not reported, but altered in murine models	Abnormal distribution of serotonergic neurons in embryos, ↓ and ↑5-HT measurements in hippocampus depending on study, ↑frontal cortex dopamine, hyperserotonemia	↓Performance on cognitive tasks, ↓social interaction	[137-141]

Model	Perturbation	Microbiome Change	Associated Neurochemical Change	Changes in Behavior	Reference
Human: Pediatric Autism vs. Control	None	↑Clostridaceae, ↓*Faecalibacterium,* ↑*Bacteroidetes,* ↓*Bifidobacterium,* ↑*Akkermansia muciniphila,* ↑*Sutterella*	↑Glutamate in fecal samples of children with autism	N/A	142 143

PARKINSONS DISEASE (PD)					
Model	**Perturbation**	**Microbiome Change**	**Associated Neurochemical Change**	**Changes in Behavior**	**Reference**
Human: Eradication therapy vs. antioxidant control	Eradication (omeprazole, amoxicillin, chlarithromycin)	Depletion of *H. pylori*	↑L-DOPA intestinal absorption relative to antioxidant control, measured in plasma	↓Global Clinical Score, indicating reduced PD symptoms	110
Rat: SHR	Intranigral injection of lipopolysaccharide (LPS) from *E. coli*	Not reported	↓Substantia nigral dopaminergic neurons and DA levels, ↓striatal DA and DA metabolite levels	Not reported	144, 145
Human: PD vs. Control	None	↓Prevotellaceae, ↑Lactobacillaceae	↓Ghrelin, which regulates dopaminergic function in the substantia nigra	N/A	109

Table 3: Associations between Microbial Alterations, Neurochemical Changes, and Symptoms of Neurological Disease

References

1.   Collins, S.M., Surette, M. & Bercik, P. The interplay between the intestinal

microbiota and the brain. *Nat Rev Micro* **10**, 735-742 (2012).

2. Gershon, M.D. The enteric nervous system: a second brain. *Hospital practice (1995)* **34**, 31-32, 35-38, 41-32 passim (1999).

3. Hall, J.E. *Guyton and Hall textbook of medical physiology*. (Elsevier Health Sciences, 2015).

4. de Lartigue, G. Putative roles of neuropeptides in vagal afferent signaling. *Physiology & Behavior* **136**, 155-169 (2014).

5. Gershon, M.D. Review article: serotonin receptors and transporters — roles in normal and abnormal gastrointestinal motility. *Alimentary Pharmacology & Therapeutics* **20**, 3-14 (2004).

6. Mawe, G.M. & Hoffman, J.M. Serotonin signalling in the gut--functions, dysfunctions and therapeutic targets. *Nature reviews. Gastroenterology & hepatology* **10**, 473-486 (2013).

7. Hsu, S.C., Johansson, K.R. & Donahue, M.J. The bacterial flora of the intestine of Ascaris suum and 5-hydroxytryptamine production. *The Journal of parasitology* **72**, 545-549 (1986).

8. Tsavkelova, E.A., Botvinko, I.V., Kudrin, V.S. & Oleskin, A.V. Detection of neurotransmitter amines in microorganisms with the use of high-performance liquid chromatography. *Doklady biochemistry : proceedings of the Academy of Sciences of the USSR, Biochemistry section / translated from Russian* **372**, 115-117 (2000).

9. Oleskin, A.V., El'-Registan, G.I. & Shenderov, B.A. Role of neuromediators in the functioning of the human microbiota: "Business talks" among microorganisms and the microbiota-host dialogue. *Microbiology* **85**, 1-22 (2016).

10. Ouml *et al.* The Function of Lactic Acid Bacteria on Biogenic Amines Production by Food-Borne Pathogens in Arginine Decarboxylase Broth. *Food Science and Technology Research* **18**, 795-804 (2012).

11. Letendre, C.H., Dickens, G. & Guroff, G. The tryptophan hydroxylase of Chromobacterium violaceum. *The Journal of biological chemistry* **249**, 7186-7191 (1974).

12. Oleskin, A.V., Kirovskaia, T.A., Botvinko, I.V. & Lysak, L.V. [Effect of serotonin (5-hydroxytryptamine) on the growth and differentiation of microorganisms]. *Mikrobiologiia* **67**, 305-312 (1998).

13. Kang, K., Kang, S., Lee, K., Park, M. & Back, K. Enzymatic features of serotonin biosynthetic enzymes and serotonin biosynthesis in plants. *Plant Signaling & Behavior* **3**, 389-390 (2008).

14. Williams, Brianna B. *et al.* Discovery and Characterization of Gut Microbiota Decarboxylases that Can Produce the Neurotransmitter Tryptamine. *Cell Host & Microbe* **16**, 495-503 (2014).

15. Tilden, A.R., Becker, M.A., Amma, L.L., Arciniega, J. & McGaw, A.K. Melatonin production in an aerobic photosynthetic bacterium: an evolutionarily early association with darkness. *Journal of pineal research* **22**, 102-106 (1997).

16. Hardeland, R. & Poeggeler, B. Non-vertebrate melatonin. *Journal of pineal research* **34**, 233-241 (2003).

17. Klein, D.C. Arylalkylamine N-acetyltransferase: "the Timezyme". *The Journal of biological chemistry* **282**, 4233-4237 (2007).

18. Paulose, J.K., Wright, J.M., Patel, A.G. & Cassone, V.M. Human Gut Bacteria Are Sensitive to Melatonin and Express Endogenous Circadian Rhythmicity. *PLoS ONE* **11**, e0146643 (2016).

19. Strakhovskaia, M.G., Ivanova, E.V. & Frainkin, G. [Stimulatory effect of serotonin on the growth of the yeast Candida guilliermondii and the bacterium Streptococcus faecalis]. *Mikrobiologiia* **62**, 46-49 (1993).

20. Anuchin, A.M., Chuvelev, D.I., Kirovskaya, T.A. & Oleskin, A.V. Effects of monoamine neuromediators on the growth-related variables of Escherichia coli K-12. *Microbiology* **77**, 674-680 (2008).

21. Lyte, M. & Freestone, P.P. *Microbial endocrinology: interkingdom signaling in infectious disease and health*. (Springer, 2010).

22. Knecht, L.D. *et al.* Serotonin Activates Bacterial Quorum Sensing and Enhances the Virulence of Pseudomonas aeruginosa in the Host. *EBioMedicine* **9**, 161-169 (2016).

23. Côté, F. *et al.* Disruption of the nonneuronal tph1 gene demonstrates the importance of peripheral serotonin in cardiac function. *Proceedings of the National Academy of Sciences of the United States of America* **100**, 13525-13530 (2003).

24. Izikki, M. *et al.* Tryptophan hydroxylase 1 knockout and tryptophan hydroxylase 2 polymorphism: effects on hypoxic pulmonary hypertension in mice. *American journal of physiology. Lung cellular and molecular physiology* **293**, L1045-1052 (2007).

25. Savelieva, K.V. *et al.* Genetic Disruption of Both Tryptophan Hydroxylase Genes Dramatically Reduces Serotonin and Affects Behavior in Models Sensitive to Antidepressants. *PLoS ONE* **3**, e3301 (2008).

26. Yano, Jessica M. *et al.* Indigenous Bacteria from the Gut Microbiota Regulate Host Serotonin Biosynthesis. *Cell* **161**, 264-276 (2015).

27. Esmaili, A. *et al.* Enteropathogenic Escherichia coli infection inhibits intestinal serotonin transporter function and expression. *Gastroenterology* **137**, 2074-2083 (2009).

28. Reigstad, C.S. *et al.* Gut microbes promote colonic serotonin production through an effect of short-chain fatty acids on enterochromaffin cells. *FASEB journal : official publication of the Federation of American Societies for Experimental Biology* **29**, 1395-1403 (2015).

29. Fukumoto, S. *et al.* Short-chain fatty acids stimulate colonic transit via intraluminal 5-HT release in rats. *American journal of physiology. Regulatory, integrative and comparative physiology* **284**, R1269-1276 (2003).

30. Neufeld, K.M., Kang, N., Bienenstock, J. & Foster, J.A. Reduced anxiety-like behavior and central neurochemical change in germ-free mice. *Neurogastroenterology and motility : the official journal of the European Gastrointestinal Motility Society* **23**, 255-264, e119 (2011).

31. Clarke, G. *et al.* The microbiome-gut-brain axis during early life regulates the hippocampal serotonergic system in a sex-dependent manner. *Molecular psychiatry* **18**, 666-673 (2013).

32.   Diaz Heijtz, R. *et al.* Normal gut microbiota modulates brain development and behavior. *Proceedings of the National Academy of Sciences of the United States of America* **108**, 3047-3052 (2011).

33.   Liang, S. *et al.* Administration of Lactobacillus helveticus NS8 improves behavioral, cognitive, and biochemical aberrations caused by chronic restraint stress. *Neuroscience* **310**, 561-577 (2015).

34.   Borrelli, L. *et al.* Probiotic modulation of the microbiota-gut-brain axis and behaviour in zebrafish. *Scientific reports* **6**, 30046 (2016).

35.   Desbonnet, L., Garrett, L., Clarke, G., Bienenstock, J. & Dinan, T.G. The probiotic Bifidobacteria infantis: An assessment of potential antidepressant properties in the rat. *Journal of psychiatric research* **43**, 164-174 (2008).

36.   El-Merahbi, R., Loffler, M., Mayer, A. & Sumara, G. The roles of peripheral serotonin in metabolic homeostasis. *FEBS letters* **589**, 1728-1734 (2015).

37.   Birdsall, T.C. 5-Hydroxytryptophan: a clinically-effective serotonin precursor. *Alternative medicine review : a journal of clinical therapeutic* **3**, 271-280 (1998).

38.   Krnjević, K. Chemical Nature of Synaptic Transmission in Vertebrates. *Physiological Reviews* **54**, 418-540 (1974).

39.   Pokusaeva, K. *et al.* GABA-producing Bifidobacterium dentium modulates visceral sensitivity in the intestine. *Neurogastroenterology and motility : the official journal of the European Gastrointestinal Motility Society* (2016).

40.   Auteri, M., Zizzo, M.G. & Serio, R. GABA and GABA receptors in the gastrointestinal tract: from motility to inflammation. *Pharmacological Research* **93**, 11-21 (2015).

41.   Jin, Z., Mendu, S.K. & Birnir, B. GABA is an effective immunomodulatory molecule. *Amino acids* **45**, 87-94 (2013).

42.   Schafer, D.F., Fowler, J.M. & Jones, E.A. Colonic bacteria: a source of gamma-aminobutyric acid in blood. *Proceedings of the Society for Experimental Biology and Medicine. Society for Experimental Biology and Medicine (New York, N.Y.)* **167**, 301-303 (1981).

43.   Higuchi, T., Hayashi, H. & Abe, K. Exchange of glutamate and gamma-aminobutyrate in a Lactobacillus strain. *Journal of bacteriology* **179**, 3362-3364 (1997).

44.   Barrett, E., Ross, R.P., O'Toole, P.W., Fitzgerald, G.F. & Stanton, C. gamma-Aminobutyric acid production by culturable bacteria from the human intestine. *Journal of applied microbiology* **113**, 411-417 (2012).

45.   Dagorn, A. *et al.* Effect of GABA, a bacterial metabolite, on Pseudomonas fluorescens surface properties and cytotoxicity. *International journal of molecular sciences* **14**, 12186-12204 (2013).

46.   Franciosi, E. *et al.* Biodiversity and γ-Aminobutyric Acid Production by Lactic Acid Bacteria Isolated from Traditional Alpine Raw Cow's Milk Cheeses. *BioMed Research International* **2015**, 11 (2015).

47.   Wu, Q. & Shah, N.P. Gas release-based prescreening combined with reversed-phase HPLC quantitation for efficient selection of high-γ-aminobutyric acid (GABA)-producing lactic acid bacteria. *Journal of Dairy Science* **98**, 790-797 (2015).

48.   Minuk, G.Y. Gamma-aminobutyric acid (GABA) production by eight common bacterial pathogens. *Scandinavian journal of infectious diseases* **18**, 465-467 (1986).

49.   Feehily, C. & Karatzas, K.A. Role of glutamate metabolism in bacterial responses towards acid and other stresses. *Journal of applied microbiology* **114**, 11-24 (2013).

50.   Capitani, G. *et al.* Crystal structure and functional analysis of Escherichia coli glutamate decarboxylase. *The EMBO journal* **22**, 4027-4037 (2003).

51.   Li, H., Gao, D., Cao, Y. & Xu, H. A high γ-aminobutyric acid-producingLactobacillus brevis isolated from Chinese traditionalpaocai. *Annals of Microbiology* **58**, 649-653 (2008).

52.   Yang, S.Y. *et al.* Production of gamma-aminobutyric acid by Streptococcus salivarius subsp. thermophilus Y2 under submerged fermentation. *Amino acids* **34**, 473-478 (2008).

53.   Komatsuzaki, N., Nakamura, T., Kimura, T. & Shima, J. Characterization of Glutamate Decarboxylase from a High γ-Aminobutyric Acid (GABA)-Producer, Lactobacillus paracasei. *Bioscience, Biotechnology, and Biochemistry* **72**, 278-285 (2008).

54.   Li, H. & Cao, Y. Lactic acid bacterial cell factories for gamma-aminobutyric acid. *Amino acids* **39**, 1107-1116 (2010).

55.   Wu, Q., Law, Y.-S. & Shah, N.P. Dairy Streptococcus thermophilus improves cell viability of Lactobacillus brevis NPS-QW-145 and its γ-aminobutyric acid biosynthesis ability in milk. *Scientific reports* **5**, 12885 (2015).

56.   Yunes, R.A. *et al.* Draft Genome Sequences of Lactobacillus plantarum Strain
        90sk and Lactobacillus brevis Strain 15f: Focusing on Neurotransmitter Genes.
        Genome Announcements **3** (2015).

57.   Dyachkova, M.S. *et al.* Draft Genome Sequences of Bifidobacterium angulatum
        GT102 and Bifidobacterium adolescentis 150: Focusing on the Genes Potentially
        Involved in the Gut-Brain Axis. *Genome Announc* **3** (2015).

58.   Guthrie, G.D. & Nicholson-Guthrie, C.S. gamma-Aminobutyric acid uptake by a
        bacterial system with neurotransmitter binding characteristics. *Proceedings of the
        National Academy of Sciences* **86**, 7378-7381 (1989).

59.   Strandwitz, P. *et al.* Gaba Modulating Bacteria of the Human Gut Microbiome.
        (2016).

60.   Boonstra, E. *et al.* Neurotransmitters as food supplements: the effects of GABA
        on brain and behavior. *Frontiers in Psychology* **6** (2015).

61.   Hans Christian Cederberg, H., Carsten Uhd, N. & Brodin, B. Glutamate Efflux at
        the Blood–Brain Barrier: Cellular Mechanisms and Potential Clinical
        Relevance. *Archives of Medical Research* **45**, 639-645.

62.   Frost, G. *et al.* The short-chain fatty acid acetate reduces appetite via a central
        homeostatic mechanism. *Nat Commun* **5** (2014).

63.   Janik, R. *et al.* Magnetic resonance spectroscopy reveals oral Lactobacillus
        promotion of increases in brain GABA, N-acetyl aspartate and glutamate.
        NeuroImage **125**, 988-995 (2016).

64.   Bravo, J.A. *et al.* Ingestion of Lactobacillus strain regulates emotional behavior
        and central GABA receptor expression in a mouse via the vagus nerve.

Proceedings of the National Academy of Sciences of the United States of America **108**, 16050-16055 (2011).

65. Asano, Y. *et al.* Critical role of gut microbiota in the production of biologically active, free catecholamines in the gut lumen of mice. *American Journal of Physiology - Gastrointestinal and Liver Physiology* **303**, G1288-G1295 (2012).

66. Freestone, P.P., Haigh, R.D. & Lyte, M. Specificity of catecholamine-induced growth in Escherichia coli O157:H7, Salmonella enterica and Yersinia enterocolitica. *FEMS microbiology letters* **269**, 221-228 (2007).

67. O'Mahony, S., Dinan, T.G., Keeling, P.W. & Chua, A.S. Central serotonergic and noradrenergic receptors in functional dyspepsia. *World journal of gastroenterology* **12**, 2681-2687 (2006).

68. Mittal, R. *et al.* Neurotransmitters: The Critical Modulators Regulating Gut-Brain Axis. *Journal of Cellular Physiology* (2016).

69. Kumagai, H. *et al.* Synthesis of 3,4-dihydroxyphenyl-l-alanine from l-tyrosine and pyrocatechol by crystalline β-tyrosinase. *Biochemical and Biophysical Research Communications* **34**, 266-270 (1969).

70. Surwase, S.N. & Jadhav, J.P. Bioconversion of l-tyrosine to l-DOPA by a novel bacterium Bacillus sp. JPJ. *Amino acids* **41**, 495-506 (2011).

71. Enei, H., Matsui, H., Okumura, S. & Yamada, H. Enzymatic preparation of L-tyrosine and 3,4-dihydroxyphenyl-L-alanine. *Biochem Biophys Res Commun* **43**, 1345-1349 (1971).

72.   Nagasaki, T., Sugita, M. & Fukawa, H. Screening of 3,4-Disubstituted Phenyl-L-alanine-producible Microorganisms. *Agricultural and Biological Chemistry* **37**, 587-591 (1973).

73.   Para, G. & Baratti, J. Synthesis of l-dopa by escherichia intermedia cells immobilized in a polyacrylamide gel. *Applied Microbiology and Biotechnology* **28**, 222-228 (1988).

74.   Müller, R., Gerth, K., Brandt, P., Blöcker, H. & Beyer, S. Identification of an l-dopa decarboxylase gene from Sorangium cellulosum So ce90. *Archives of Microbiology* **173**, 303-306 (2000).

75.   Lyte, M. & Ernst, S. Catecholamine induced growth of gram negative bacteria. *Life Sciences* **50**, 203-212 (1992).

76.   Belay, T. & Sonnenfeld, G. Differential effects of catecholamines on in vitro growth of pathogenic bacteria. *Life Sciences* **71**, 447-456 (2002).

77.   Sandrini, S., Alghofaili, F., Freestone, P. & Yesilkaya, H. Host stress hormone norepinephrine stimulates pneumococcal growth, biofilm formation and virulence gene expression. *BMC microbiology* **14**, 180 (2014).

78.   Pande, G.S., Suong, N.T., Bossier, P. & Defoirdt, T. The catecholamine stress hormones norepinephrine and dopamine increase the virulence of pathogenic Vibrio anguillarum and Vibrio campbellii. *FEMS microbiology ecology* **90**, 761-769 (2014).

79.   Cogan, T.A. *et al.* Norepinephrine increases the pathogenic potential of Campylobacter jejuni. *Gut* **56**, 1060-1065 (2007).

80. Rahman, H., Reissbrodt, R. & Tschape, H. Effect of norepinephrine on growth of Salmonella and its enterotoxin production. *Indian journal of experimental biology* **38**, 285-286 (2000).

81. Hegde, M., Wood, T.K. & Jayaraman, A. The neuroendocrine hormone norepinephrine increases Pseudomonas aeruginosa PA14 virulence through the las quorum-sensing pathway. *Applied Microbiology and Biotechnology* **84**, 763-776 (2009).

82. Tsavkelova, E.A., Klimova, S.Y., Cherdyntseva, T.A. & Netrusov, A.I. Hormones and hormone-like substances of microorganisms: A review. *Applied Biochemistry and Microbiology* **42**, 229-235 (2006).

83. Lyte, M., Arulanandam, B.P. & Frank, C.D. Production of Shiga-like toxins by Escherichia coli O157:H7 can be influenced by the neuroendocrine hormone norepinephrine. *The Journal of laboratory and clinical medicine* **128**, 392-398 (1996).

84. Lyte, M. *et al.* Norepinephrine-induced expression of the K99 pilus adhesin of enterotoxigenic Escherichia coli. *Biochem Biophys Res Commun* **232**, 682-686 (1997).

85. Sperandio, V., Torres, A.G., Jarvis, B., Nataro, J.P. & Kaper, J.B. Bacteria-host communication: the language of hormones. *Proc Natl Acad Sci U S A* **100**, 8951-8956 (2003).

86. Clarke, M.B., Hughes, D.T., Zhu, C., Boedeker, E.C. & Sperandio, V. The QseC sensor kinase: A bacterial adrenergic receptor. *Proceedings of the National Academy of Sciences* **103**, 10420-10425 (2006).

87.   Kendall, M.M., Rasko, D.A. & Sperandio, V. Global effects of the cell-to-cell signaling molecules autoinducer-2, autoinducer-3, and epinephrine in a luxS mutant of enterohemorrhagic Escherichia coli. *Infection and immunity* **75**, 4875-4884 (2007).

88.   Hughes, D.T. & Sperandio, V. Inter-kingdom signalling: communication between bacteria and their hosts. *Nat Rev Micro* **6**, 111-120 (2008).

89.   Chet, I., Henis, Y. & Mitchell, R. Effect of biogenic amines and cannabinoids on bacterial chemotaxis. *Journal of bacteriology* **115**, 1215-1218 (1973).

90.   Kendall, M.M. & Sperandio, V. What a Dinner Party! Mechanisms and Functions of Interkingdom Signaling in Host-Pathogen Associations. *mBio* **7**, e01748 (2016).

91.   Patel, P., Nankova, B.B. & LaGamma, E.F. Butyrate, a gut-derived environmental signal, regulates tyrosine hydroxylase gene expression via a novel promoter element. *Brain research. Developmental brain research* **160**, 53-62 (2005).

92.   Berding, K. *et al.* Prebiotics and Bioactive Milk Fractions Affect Gut Development, Microbiota and Neurotransmitter Expression in Piglets. *Journal of pediatric gastroenterology and nutrition* (2016).

93.   Rooks, M.G. *et al.* Gut microbiome composition and function in experimental colitis during active disease and treatment-induced remission. *ISME J* **8**, 1403-1417 (2014).

94.   Kostrzewa, R.M. The blood-brain barrier for catecholamines - revisited. *Neurotoxicity research* **11**, 261-271 (2007).

95.   Matsumoto, M. *et al.* Cerebral low-molecular metabolites influenced by intestinal microbiota: a pilot study. *Frontiers in systems neuroscience* **7**, 9 (2013).

96.   Nishino, R. *et al.* Commensal microbiota modulate murine behaviors in a strictly contamination-free environment confirmed by culture-based methods. *Neurogastroenterology and motility : the official journal of the European Gastrointestinal Motility Society* **25**, 521-528 (2013).

97.   Owens, M.J. & Nemeroff, C.B. Role of serotonin in the pathophysiology of depression: focus on the serotonin transporter. *Clinical chemistry* **40**, 288-295 (1994).

98.   Foster, J.A. & McVey Neufeld, K.-A. Gut–brain axis: how the microbiome influences anxiety and depression. *Trends in Neurosciences* **36**, 305-312 (2013).

99.   Neufeld, K.-A.M., Kang, N., Bienenstock, J. & Foster, J.A. Effects of intestinal microbiota on anxiety-like behavior. *Communicative & Integrative Biology* **4**, 492-494 (2011).

100.   Cryan, J.F. & Kaupmann, K. Don't worry 'B' happy!: a role for GABAB receptors in anxiety and depression. *Trends in Pharmacological Sciences* **26**, 36-43 (2005).

101.   O'Mahony, S.M., Clarke, G., Borre, Y.E., Dinan, T.G. & Cryan, J.F. Serotonin, tryptophan metabolism and the brain-gut-microbiome axis. *Behavioural Brain Research* **277**, 32-48 (2015).

102.   Dinan, T.G. & Cryan, J.F. Melancholic microbes: a link between gut microbiota and depression? *Neurogastroenterology and motility : the official journal of the European Gastrointestinal Motility Society* **25**, 713-719 (2013).

103.   Naseribafrouei, A. *et al.* Correlation between the human fecal microbiota and depression. *Neurogastroenterology & Motility* **26**, 1155-1162 (2014).

104.   Jiang, H. *et al.* Altered fecal microbiota composition in patients with major depressive disorder. *Brain, Behavior, and Immunity* **48**, 186-194 (2015).

105.   Zheng, P. *et al.* Gut microbiome remodeling induces depressive-like behaviors through a pathway mediated by the host/'s metabolism. *Molecular psychiatry* **21**, 786-796 (2016).

106.   Messaoudi, M. *et al.* Assessment of psychotropic-like properties of a probiotic formulation (Lactobacillus helveticus R0052 and Bifidobacterium longum R0175) in rats and human subjects. *The British journal of nutrition* **105**, 755-764 (2011).

107.   Pfeiffer, R.F. Gastrointestinal dysfunction in Parkinson's disease. *The Lancet Neurology* **2**, 107-116 (2003).

108.   Mulak, A. & Bonaz, B. Brain-gut-microbiota axis in Parkinson's disease. *World Journal of Gastroenterology : WJG* **21**, 10609-10620 (2015).

109.   Scheperjans, F. *et al.* Gut microbiota are related to Parkinson's disease and clinical phenotype. *Movement disorders : official journal of the Movement Disorder Society* **30**, 350-358 (2015).

110.   Pierantozzi, M. *et al.* Helicobacter pylori eradication and l-dopa absorption in patients with PD and motor fluctuations. *Neurology* **66**, 1824-1829 (2006).

111.   Lyte, M. Microbial endocrinology as a basis for improved l-DOPA bioavailability in Parkinson's patients treated for Helicobacter pylori. *Medical Hypotheses* **74**, 895-897 (2010).

112. Niehues, M. & Hensel, A. In-vitro interaction of l-dopa with bacterial adhesins of Helicobacter pylori: an explanation for clinicial differences in bioavailability? *Journal of Pharmacy and Pharmacology* **61**, 1303-1307 (2009).

113. Niehaus, I. & Lange, J.H. Endotoxin: is it an environmental factor in the cause of Parkinson's disease? *Occupational and environmental medicine* **60**, 378 (2003).

114. Forsyth, C.B. *et al.* Increased intestinal permeability correlates with sigmoid mucosa alpha-synuclein staining and endotoxin exposure markers in early Parkinson's disease. *PLoS One* **6**, e28032 (2011).

115. Tomova, A. *et al.* Gastrointestinal microbiota in children with autism in Slovakia. *Physiology & Behavior* **138**, 179-187 (2015).

116. Desbonnet, L., Clarke, G., Shanahan, F., Dinan, T.G. & Cryan, J.F. Microbiota is essential for social development in the mouse. *Molecular psychiatry* **19**, 146-148 (2014).

117. Hsiao, Elaine Y. *et al.* Microbiota Modulate Behavioral and Physiological Abnormalities Associated with Neurodevelopmental Disorders. *Cell* **155**, 1451-1463.

118. Buffington, S.A. *et al.* Microbial Reconstitution Reverses Maternal Diet-Induced Social and Synaptic Deficits in Offspring. *Cell* **165**, 1762-1775 (2016).

119. Roth, J. *et al.* Evolutionary origins of neuropeptides, hormones, and receptors: possible applications to immunology. *Journal of immunology (Baltimore, Md. : 1950)* **135**, 816s-819s (1985).

120.   Neal, C.P. *et al.* Catecholamine inotropes as growth factors for Staphylococcus
        epidermidis and other coagulase-negative staphylococci. *FEMS microbiology
        letters* **194**, 163-169 (2001).

121.   Bansal, T. *et al.* Differential effects of epinephrine, norepinephrine, and indole on
        Escherichia coli O157:H7 chemotaxis, colonization, and gene expression.
        Infection and immunity **75**, 4597-4607 (2007).

122.   Roshchina, V.V. New Trends and Perspectives in the Evolution of
        Neurotransmitters in Microbial, Plant, and Animal Cells. *Advances in
        experimental medicine and biology* **874**, 25-77 (2016).

123.   Freestone, P.P., Haigh, R.D., Williams, P.H. & Lyte, M. Stimulation of bacterial
        growth by heat-stable, norepinephrine-induced autoinducers. *FEMS microbiology
        letters* **172**, 53-60 (1999).

124.   Stephenson, M. & Rowatt, E. The production of acetylcholine by a strain of
        Lactobacillus plantarum. *Journal of general microbiology* **1**, 279-298 (1947).

125.   Kawashima, K. *et al.* Ubiquitous expression of acetylcholine and its biological
        functions in life forms without nervous systems. *Life Sci* **80**, 2206-2209 (2007).

126.   Horiuchi, Y. *et al.* Evolutional study on acetylcholine expression. *Life Sci* **72**,
        1745-1756 (2003).

127.   Sanchez, D.G. *et al.* A Pseudomonas aeruginosa PAO1 acetylcholinesterase is
        encoded by the PA4921 gene and belongs to the SGNH hydrolase family.
        Microbiological research **167**, 317-325 (2012).

128. Özoğul, F. Production of biogenic amines by Morganella morganii, Klebsiella pneumoniae and Hafnia alvei using a rapid HPLC method. *European Food Research and Technology* **219**, 465-469 (2004).

129. Campos, A.C. *et al.* Absence of gut microbiota influences lipopolysaccharide-induced behavioral changes in mice. *Behavioural brain research* **312**, 186-194 (2016).

130. Bercik, P. *et al.* The intestinal microbiota affect central levels of brain-derived neurotropic factor and behavior in mice. *Gastroenterology* **141**, 599-609, 609 e591-593 (2011).

131. Park, A.J. *et al.* Altered colonic function and microbiota profile in a mouse model of chronic depression. *Neurogastroenterology and motility : the official journal of the European Gastrointestinal Motility Society* **25**, 733-e575 (2013).

132. Goehler, L.E. *et al.* Activation in vagal afferents and central autonomic pathways: early responses to intestinal infection with Campylobacter jejuni. *Brain, behavior, and immunity* **19**, 334-344 (2005).

133. Crumeyrolle-Arias, M. *et al.* Absence of the gut microbiota enhances anxiety-like behavior and neuroendocrine response to acute stress in rats. *Psychoneuroendocrinology* **42**, 207-217 (2014).

134. Wei, Y., Melas, P.A., Wegener, G., Mathe, A.A. & Lavebratt, C. Antidepressant-like effect of sodium butyrate is associated with an increase in TET1 and in 5-hydroxymethylation levels in the Bdnf gene. *Int J Neuropsychopharmacol* **18** (2015).

135. Szczesniak, O., K, A.H., Hanssen, J.F. & Rudi, K. Isovaleric acid in stool correlates with human depression. *Nutritional neuroscience* (2015).

136. de Theije, C.G. *et al.* Altered gut microbiota and activity in a murine model of autism spectrum disorders. *Brain, behavior, and immunity* **37**, 197-206 (2014).

137. Kuwagata, M., Ogawa, T., Shioda, S. & Nagata, T. Observation of fetal brain in a rat valproate-induced autism model: a developmental neurotoxicity study. *International journal of developmental neuroscience : the official journal of the International Society for Developmental Neuroscience* **27**, 399-405 (2009).

138. Oyabu, A., Narita, M. & Tashiro, Y. The effects of prenatal exposure to valproic acid on the initial development of serotonergic neurons. *International journal of developmental neuroscience : the official journal of the International Society for Developmental Neuroscience* **31**, 202-208 (2013).

139. Martin, H.G. & Manzoni, O.J. Late onset deficits in synaptic plasticity in the valproic acid rat model of autism. *Frontiers in cellular neuroscience* **8**, 23 (2014).

140. Cohen, O.S., Varlinskaya, E.I., Wilson, C.A., Glatt, S.J. & Mooney, S.M. Acute prenatal exposure to a moderate dose of valproic acid increases social behavior and alters gene expression in rats. *International journal of developmental neuroscience : the official journal of the International Society for Developmental Neuroscience* **31**, 740-750 (2013).

141. Narita, N. *et al.* Increased monoamine concentration in the brain and blood of fetal thalidomide- and valproic acid-exposed rat: putative animal models for autism. *Pediatric research* **52**, 576-579 (2002).

142. De Angelis, M., Francavilla, R., Piccolo, M., De Giacomo, A. & Gobbetti, M. Autism spectrum disorders and intestinal microbiota. *Gut microbes* **6**, 207-213 (2015).

143. Finegold, S.M. *et al.* Pyrosequencing study of fecal microflora of autistic and control children. *Anaerobe* **16**, 444-453 (2010).

144. Liu, B. *et al.* Systemic infusion of naloxone reduces degeneration of rat substantia nigral dopaminergic neurons induced by intranigral injection of lipopolysaccharide. *The Journal of pharmacology and experimental therapeutics* **295**, 125-132 (2000).

145. Herrera, A.J., Castano, A., Venero, J.L., Cano, J. & Machado, A. The single intranigral injection of LPS as a new model for studying the selective effects of inflammatory reactions on dopaminergic system. *Neurobiology of disease* **7**, 429-447 (2000).

Chapter 4

Microbiome, nervous and immune system interactions in health and disease

Thomas C. Fung, Christine A. Olson, Elaine Y. Hsiao

Abstract

The diverse collection of microorganisms that inhabit the gastrointestinal tract, collectively called the gut microbiota, profoundly influences multiple aspects of host physiology including nutrient metabolism, resistance to infection and immune system development. An emerging concept known as the "microbiota-gut-brain axis" illustrates a critical role for the gut microbiota in orchestrating brain development and behavior and the function of the neuroimmune system. The gut microbiota regulates the maturation and function of tissue-resident immune cells in the central nervous system such as microglia. Microbes also influence the activation of immune cells in periphery, which regulate responses to neuroinflammation, brain injury, autoimmunity and neurogenesis. Accordingly, both the gut microbiota and immune system have been implicated in the etiology and pathogenesis of neurodevelopmental, psychiatric and neurodegenerative diseases, such as autism spectrum disorder, depression, Alzheimer's disease and Parkinson's disease. Furthermore, associations between microbial dysbiosis and clinical readouts also suggest a role for the gut microbiota and immune system in human neurological diseases. In this review, we discuss the complex interplay between the gut microbiota, nervous and immune systems, which collectively impact brain health and disease.

Introduction

Far from an immune privileged site, the brain harbors resident immune cells that defend against infection and injury, while also supporting neurons in remodeling circuit connectivity and regulating plasticity. Molecules traditionally acknowledged for their roles in the peripheral immune system are now being recognized for their importance in normal neurodevelopment. Cytokines regulate neuronal differentiation and axonal pathfinding[1]; the complement system tags target cells for synaptic pruning[2], and MHC class I proteins modulate neurite outgrowth and synaptic plasticity[3], redefining immune molecules as fundamental signaling factors in normal brain development. Conversely, several factors traditionally acknowledged for their roles in the central nervous system (CNS) are becoming increasingly recognized for their roles in the immune system. Various leukocyte subtypes produce and respond to common neurotransmitters[4,5,6,7], and stimulated subsets of brain neurons modify peripheral responses to immune activation[8]. Bidirectional communication between the nervous and immune systems is further facilitated by the recently defined brain lymphatic system, which connects peripheral lymphatic tissues to the CNS, and the blood brain barrier (BBB), which regulates passage of immune factors and cells[9,10].

The diverse collection of microorganisms that inhabit the gastrointestinal tract, collectively called the gut microbiota, profoundly influences the maturation and function of the immune system, as well as brain development and behavior. There is an increasing

appreciation that the gut microbiota fundamentally regulates interactions between the nervous and immune systems. Key pathways and factors for signaling between the immune system and CNS are modulated by the gut microbiota. The development and function of resident brain immune cells are altered in response to changes in the gut microbiome. Particular microbial products synthesized *de novo* or induced by stimulation of host cells act directly on resident immune cells. Moreover, the microbiome can activate peripheral immune cells, which then send signals to neural cells or traffic into the brain itself. Such effects of indigenous gut bacteria on nervous-immune system communication have important implications for normal neurophysiology and neurological disease.

Development and function of brain resident immune cells

Microglia

Microglia are the most abundant resident immune cells in the CNS, comprising 5-20% of glial cells[11,12]. Derived from yolk sac erthyromyeloid progenitors that enter the neuroepithelium during mid-gestation and continuously self-renew under typical circumstances[11,12,13], microglia perform canonical functions of myeloid cells, including phagocytosis, antigen presentation, cytokine signaling and inflammatory activation[12,14]. However, microglia are also unique in several respects. Their extensive ramified processes enable rapid immune surveillance and clearance of debris and infectious agents, taking an estimated 2-5 hours to survey the entire brain with limited physical migration[14,15]. Microglia exhibit a wide spectrum of activation states, where those that

display an M1 phenotype generally exhibit pro-inflammatory features, while those that align with an M2 phenotype are generally associated with neuroprotective responses[16,17]. Microglia also perform specific functions during neurodevelopment, tagging and clearing synapses for pruning, promoting neuronal circuit wiring and producing cytokines and chemokines that guide neuronal differentiation[11,12,17,18].

The microbiome influences microglial maturation and function (**Fig. 1a**) . Germ free (GF) mice, raised in the absence of microbial colonization, had increased numbers of immature microglia across gray and white matter of the cortex, corpus callosum, hippocampus, olfactory bulb and cerebellum[19]. These microglia exhibited longer processes and increased branching, with elevated expression of CSF1R, F4/80, and CD31, factors which typically decrease with progressive development toward an adult-stage phenotype[19]. Similar increases in immature microglia were observed after antibiotic treatment of conventionally-raised mice, though the overall number of microglia remained unchanged[19]. This suggests differential effects of the microbiota on microglia that are dependent upon developmental timing and/or duration of microbial colonization. Consistent with this, newborn differed from adult microglia in GF mice with respect to gene expression compared to their age-matched conventionally-colonized controls[13]. Several genes were downregulated in GF microglia, but a greater number of genes were more substantially downregulated in microglia from adult GF mice compared to those from newborns. The finding that microglia from newborn GF mice display altered gene expression profiles compared to those from newborn conventionally-colonized mice

raises the question of whether there is an effect of the maternal microbiome on early life programming of microglial development.

Microglia from adult GF mice were also functionally impaired in response to challenge with lipopolysaccharide (LPS) or lymphocytic choriomeningitis virus (LCMV), maintaining altered morphology and exhibiting attenuated immune activation, including impaired induction of pro-inflammatory cytokines Interleukin-1β (IL-1β), interleukin-6 (IL-6) and tumor necrosis factor α (TNFα)[13,19]. This functional deficit aligns with the finding that naïve adult microglia from GF mice have decreased expression of several genes relevant to interferon responses, innate responses to stimulation, viral defense and effector processes[13].

While the precise mechanisms by which gut microbes influence brain microglia remain unclear, there appears to be some specificity of microglial modulation to particular bacterial taxa of the gut microbiota. GF mice that were colonized with a minimal community of three bacterial species: *Bacteroides distasonis, Lactobacillus salivarius* and a member of Clostridium cluster XIV, maintained abnormalities in microglia. This suggests that microbial effects on microglia are not regulated by bacterial load in general, but require greater diversity of the gut microbiota or are conferred by particular microbial species and functions not represented by the minimal community tested.

Notably, GF-associated alterations in microglial morphology, abundance and gene expression were normalized by postnatal supplementation with short chain fatty acids

(SCFAs), primary products of bacterial fermentation[19,20], raising the question of whether particular SCFA-producing bacterial species specifically restore abnormalities in microglia seen in GF or antibiotic-treated mice. Consistent with a role for SCFAs in mediating effects of gut microbes on brain microglia, conventionally-colonized mice harboring a deletion in the SCFA receptor G Protein-Coupled Receptor 43 (GPR43), encoded by Free Fatty Acid Receptor 2 (*FFAR2)*, exhibited abnormalities in microglia that were analogous to those seen in microbiota-depleted mice. While microglia are known to express GPR43 directly, whether the effects of the microbiota on microglia are mediated by direct signaling of SCFAs to microglia is unclear. Indeed, SCFAs are involved in a broad array of functions that influence gastrointestinal physiology, peripheral immunity, liver metabolism and even BBB integrity, which could mediate or contribute indirectly to effects on microglia. Future studies targeting specific bacterial taxa, specific SCFAs (acetate, propionate, butyrate) and conditional microglia-specific knockout of *FFAR2* are warranted.

Whether the microbiota affects microglial function during early postnatal development is not known but could have important implications for brain development and later life behavior. During early postnatal life, microglia are integral for synaptic pruning, tagging synapses for clearance with complement proteins based on neural activity[21]. Early life exposure of conventionally-colonized mice to subtherapeutic antibiotic treatment (STAT) resulted in elevated cecal levels of SCFAs compared to controls[22], raising the possibility that such alterations in SCFAs could impact microglia during early postnatal development. Moreover, early life disruption of the microbiota by antibiotic exposure and in response to

Caesarian section are associated with chronic diseases later in life, including increased risk for neurodevelopmental diseases such as autism spectrum disorder. In addition, several neurological disorders, including Parkinson's disease (PD), multiple sclerosis (MS), anxiety disorder, depression, stroke and amyotrophic lateral sclerosis (ALS), are each associated with both dysregulated microglia and dysbiosis of the gut microbiome (**Table 1**). Whether microbial effects on microglial maturation and function contribute to the pathogenesis of neurodevelopmental and neurological diseases involving microglial disruptions are important questions for future study.

Astrocytes

Astrocytes, comprising 20-40% of cells in the brain, exhibit a diverse array of functions, including the regulation of BBB integrity, ion gradient balance, neurotransmitter turnover, cerebral blood flow and nutrient transport[23,24,25,26]. Astrocytes integrate information from numerous adjacent glial, neuronal, vascular and immune cell types to regulate neural excitability[27] and synapse formation[28]. Additionally, astrocytes are important for brain metabolism; as the main site of glycogen storage in the brain, astrocytes provide support when the brain is hypoglycemic[26]. Though they derive from neural progenitor cells (NPCs) of the neuroectoderm[27], astrocytes also perform immune-related functions, expressing pattern recognition receptors (PRRs) for detection of microbial-associated molecular patterns (MAMPs) and modulation of neuroinflammatory responses[23].

The gut microbiota modulates astrocyte activity via microbially-derived metabolites that activate astrocyte aryl hydrocarbon receptors (AHR)[29] (**Fig. 1b**). Type I interferon (IFN-I) signaling in astrocytes attenuates inflammation and symptoms of experimental autoimmune encephalomyelitis (EAE) in mice, an effect mediated in part by activation of AHRs. Tryptophan derivatives produced by dietary metabolism by the gut microbiome are natural ligands of AHRs. Consistent with this notion, depletion of the gut microbiota using the antibiotic ampicillin decreased levels of the AHR agonist indoxyl-3-sulfate (I3S) and worsened EAE disease scores[29]. Supplementation of antibiotic-treated mice with bacterial tryptophanases, which converts tryptophan to indole, or with indole itself, improved EAE recovery. Similarly, decreases in EAE clinical score were enhanced by peripheral administration of I3S, indole-3-aldehyde (IAld, another AHR agonist) or consumption of an indole-supplemented diet[29]. In human astrocytes, I3S also reduced expression of pro-inflammatory factors, including C-C Motif Chemokine Ligand 2 (*CCL2*), Tumor Necrosis Factor (*TNF*), Nitric Oxide Synthase 2 (*NOS2)*, and *IL6*[29]. While much remains to be explored with regards to particular microbial taxa that regulate astrocyte function, the gut bacterium *Lactobacillus reuteri* is of interest because it is known to produce IAld from dietary tryptophan[29,30].

Whether other functions of astrocytes are affected by the microbiome is unclear. Depletion of the gut microbiome was associated with increased permeability of the BBB and alterations in tight junction expression across the frontal cortex, striatum and hippocampus[31]. While monocolonization with the butyrate-producer *Clostridium tyrobutyriticum* or supplementation with the SCFA sodium butyrate alone sufficiently

corrected abnormalities in BBB integrity, the particular molecular and cellular signaling mechanisms remain unclear. As astrocyte endfeet are primarily responsible for forming the BBB and regulating permeability, future studies should examine whether effects of the microbiota on BBB integrity involve regulation of astrocytes via butyrate signaling.

Innate and adaptive immune cells in the CNS

Aside from microglia and astrocytes, several other innate and adaptive immune cells are resident in the CNS, including perivascular macrophages, CD4^{+} T lymphocytes, CD8^{+} T lymphocytes and mast cells[14,18,32,33]. While effects of the microbiota on these brain resident immune cells have not been described, several studies reveal that the microbiota, and in some cases particular bacterial species, modulate peripheral myeloid cells, T cells and mast cells[34], which share common hematopoietic progenitors with the brain subsets. For example, the microbiota is a major regulator of hematopoiesis, impacting myeloid development in both the embryonic yolk sac and bone marrow[35], which are sources of brain microglia and perivascular macrophages, respectively. It would be interesting to determine whether these effects on peripheral hematopoietic progenitors result in alterations in brain parenchymal, perivascular, meningeal and/or tissue-resident immune cells. Since parenchymal CNS macrophages, and choroid plexus macrophages in particular[14], localize close to the vasculature[8], future studies are needed to test whether circulating factors that are regulated by the microbiome influence these subsets of brain immune cells.

Peripheral immune cell responses and neuroimmune interactions

CNS inflammation and injury

Indigenous bacteria are potent regulators of mucosal and systemic immune responses and significantly contribute to the development of inflammatory disorders including those affecting the CNS (**Fig. 2**). In EAE, GF or antibiotic-treated mice were protected from the development of EAE compared to conventional mice[36,37], suggesting a role for the gut microbes in CNS inflammation. Studies investigating the contribution of specific members of the microbiota have revealed complex interactions between indigenous bacteria and CNS inflammation. Segmented filamentous bacteria (SFB) are epithelial-associated bacteria that promote the development of IL-17A-producing CD4$^+$ T cells in the mouse small intestine[38,39]. Colonization of GF mice with SFB alone was sufficient to promote EAE compared to GF controls[36]. Since IL-17A is a critical inflammatory component of EAE[40], these data suggest that SFB-elicited T_H17 cells are responsible for the development of EAE. Indigenous bacteria that promote immunoregulatory responses have been associated with protection against EAE. The human gut bacterium *Bacteroides fragilis* induces IL-10-producing regulatory (T_{reg}) cells in the mouse colon via the bacterial expression of polysaccharide A (PSA)[41,42]. While antibiotic-treated mice were protected from EAE, re-colonization with PSA-deficient but not wild-type *B. fragilis* restored EAE susceptibility[37,43]. Regulation of EAE development by PSA is dependent on T_{reg} cells[43]. Consistent with these findings, oral treatment of wild-type mice with PSA provided protection from CNS demyelination and inflammation through a TLR2-dependent

pathway[44, 45]. Recognition of PSA through TLR2 resulted in expression of CD39 on CD4$^+$ T cells in the cervical lymph node, which represented a subset of CD4$^+$ T cells that have enhanced immunosuppressive properties[45]. Gut microbiota-derived metabolites produced by spore-forming members of the Firmicutes phylum have also been implicated in protection from EAE. Treatment of mice with SCFAs reduced EAE and axonal damage through increased T_{reg} differentiation[46]. More recently, it was demonstrated that intestinal microbes promote a subset of autoreactive intraepithelial lymphocytes (IELs) in myelin oligodendrocyte glycoprotein (MOG)-specific T cell receptor (TCR) transgenic 2D2 mice. These MOG-specific CD4$^+$ IELs were immunosuppressive and could protect wild-type mice from EAE in a LAG-3-dependent manner when adoptively transferred[47]. Altogether, indigenous bacteria significantly influence the degree of CNS inflammation through modulation of pro- and anti-inflammatory mucosal and systemic immune responses. Despite these findings, whether antigen-specific responses or bystander activation of immune cells by indigenous bacteria is involved in regulation of CNS inflammation has not been fully explored and requires further investigation.

Probiotic administration has been demonstrated to be beneficial in treating a number of chronic inflammatory diseases. Chronic inflammatory diseases such as inflammatory bowel disease and chronic liver disease are commonly associated with impaired brain function and associated sickness behaviors. Administration of probiotics can improve these debilitating symptoms by modulating peripheral immune pathways. In the bile duct ligation model of liver inflammation, mice routinely developed social disabilities, which were ameliorated following ingestion of the VSL3 probiotic cocktail[48]. Although probiotic

treatment did not alter gut microbiota composition, it reduced the amount of circulating TNF-α and monocyte accumulation in the brain, suggesting that probiotics may regulate the ability of chronic inflammatory responses to influence brain function. Age-related deterioration of cognitive function is usually manifested by loss of neural plasticity and impaired long-term potentiation (LTP). Treatment with VSL3 altered the gut microbiota and attenuated age-related reductions in LTP[49], suggesting that modulation of the microbiota can positively influence neural function. However, whether probiotics improve brain function by modulating peripheral immune responses requires further investigation.

Besides CNS inflammation, the microbiota also plays a critical role in regulating the pathogenesis and resolution of brain injury. In a mouse model of middle cerebral artery occlusions (MCAO)-induced ischemic brain injury, mice treated with antibiotics displayed reduced infarct volume and improved sensorimotor function[50]. Neuroprotection was associated with reduced infiltration of small intestine IL-17$^+$ γδ T cells into the meninges, suggesting that indigenous bacteria control immune responses to brain injury by regulating lymphocyte trafficking from the gut to the brain. A similar study showed that MCAO resulted in intestinal dysbiosis and transfer of the MCAO microbiota to GF animals led to increased pro-inflammatory cytokine production in the intestine and brain as well as increased infarct volumes. While these data suggest that indigenous bacteria induce immune responses to promote brain injury, they may also regulate immune responses that are neuroprotective. Transfer of fecal microbiota from naïve animals to MCAO mice reduced brain lesions volumes in wild-type but not *Rag1*$^{-/-}$ animals, suggesting a critical role for the adaptive immune system in protection from stroke[51]. GF or antibiotic-treated

mice have skewed systemic type 2 immune responses such as elevated serum IgE, basophilia and Th2 cells[52,53]. Induction of RORγt$^+$ T_{reg} cells in the colon by SCFA-producing bacteria, which limits T_H2 responses, was recently proposed as a mechanism for elevated T_H2 cells in microbiota-depleted mice[52,54]. In a mouse model of spinal cord contusion injury, IL-4 derived from CD4$^+$T cells played a key role in axonal regrowth[55]. Interestingly, CD4$^+$ T cells from *Myd88$^{-/-}$* mice produced less IL-4 in this model, suggesting that bacterial ligands or IL-1 cytokine family members regulate CD4$^+$ T cell responses in the CNS. Consistent with a role for IL-1 family cytokines, it was subsequently demonstrated that IL-33 released by damaged oligodendrocytes activated a tissue-protective innate immune response[56]. Despite these data, whether indigenous bacteria directly modulate tissue-protective type 2 immune responses in the CNS remains to be determined.

The humoral immune system and CNS autoimmunity

In addition to T cell-mediated mechanisms of CNS autoimmunity, B cells also play a critical role in the generation of CNS-reactive autoantibodies and the pathogenesis of neuroinflammatory disorders[57,58]. Intestinal microbes impact the development of behavioral disorders through modulation of humoral immune responses and antigen mimicry. Streptococcal infection is often associated with the generation of CNS-reactive antibodies that lead to behavioral abnormalities collectively known as pediatric autoimmune neuropsychiatic disorders associated with streptococcal infection (PANDAS). In the PANDAS animal model where mice are immunized with group A β-

hemolytic *Streptococcus*, these mice developed a variety of behavioral abnormalities such as impaired motor coordination and repetitive rearing behavior[59]. Transfer of complete, but not IgG-depleted, sera from immunized mice was sufficient to induce behavioral deficits, suggesting that bacterial infection-induced autoantibodies are critical to the development of PANDAS. Autoantibodies have also been implicated in the development of eating disorders and indigenous bacteria appear to be involved in their generation. Antibodies produced in response to the heat-shock protein ClpB derived from the bacterium *E. coli* cross-react with the α-melanocyte-stimulating hormone (α-MSH), a peptide critically involved in food intake[60]. Oral administration of wild-type but not ClpB-deficient *E. coli* resulted in the generation of ClpB- and α-MSH-reactive antibodies and decreased food intake. These preliminary findings indicate a role for indigenous bacteria-induced autoantibodies in behavioral disorders and provide the groundwork for future studies.

Neurogenesis

Recent data indicate that indigenous bacteria play a critical role in regulating neurogenesis. Bacterial cell wall components have the capacity to cross the maternal-fetal interface in pregnant dams, and activation of TLR2 by bacterial cell wall components leads to cortical neuroproliferation and impaired cognitive function in the developing fetus[61]. These data suggest that the maternal microbiome could regulate neurogenesis and subsequent behavioral changes in the developing offspring. Studies assessing adult hippocampal neurogenesis in GF mice revealed increased proliferation in these

animals[62], indicating a role for the microbiota in regulating adult neurogenesis. However, colonization of GF mice post-weaning did not reduce neuronal cell proliferation to conventional levels, suggesting that there is a critical window in which indigenous bacteria regulate this process. In contrast, it was recently demonstrated that antibiotic treatment decreases hippocampal neurogenesis and spatial and object recognition, which could be restored by exercise and probiotic VSL3 treatment[63]. Both exercise and probiotics were associated with increased Ly6C^{hi} monocytes in the brain. Depletion of monocytes reduced neurogenesis while adoptive transfer of monocytes to antibiotic-treated mice increased neurogenesis, identifying circulating monocytes as a novel cellular mediator of gut-brain communication. Despite the discrepancy in these studies, indigenous bacteria appear to regulate neurogenesis. More studies are necessary to precisely define host-microbial interactions in the context of neurodevelopment.

Impacts on behavior and endophenotypes in neurological disorders

Social communication and autism spectrum disorder

Changes in microbiota composition are linked to the development of behavioral disorders such as anxiety, depression and autism[64,65]. Recent studies have begun to elucidate the cellular and molecular pathways by which indigenous microbes regulate the development and progression of these disorders. In the maternal immune activation (MIA) animal model of autism spectrum disorder (ASD) in which administration of the TLR3 agonist poly(I:C) in pregnant dams results in offspring with behavioral phenotypes similar to those

127

observed in autism, MIA offspring exhibited increased intestinal permeability and alterations in the composition of the gut microbiota[66]. Administration of the human gut bacterium *B. fragilis* partially improved microbiota dysbiosis and behavioral abnormalities in MIA offspring. However, PSA-deficient *B. fragilis* and some other Bacteroides members were also able to protect MIA offspring, suggesting that alterations of these behaviors was not due to PSA-specific modulation of mucosal and systemic immune responses. Instead, it was proposed that *B. fragilis* treatment altered the composition of serum metabolites and reduced the anxiety-associated molecule 4-ethylphenylsulfate (4EPS). Further support for a link between intestinal dysbiosis and these symptoms was provided by a recent study, which demonstrated that a maternal high fat diet (MHFD) resulted in significant changes to the offspring microbiota and abnormal social behavior[67]. Transfer of the control but not MHFD diet microbiota from offspring to GF mice improved their social impairments, suggesting a causal relationship between intestinal dysbiosis and these behavioral readouts. When *Lactobacillus reuteri*, a bacterial strain that was reduced in the MHFD offspring, was re-introduced, social deficits were corrected. It was proposed that behavioral abnormalities in MHFD offspring was due to reduced expression of the neuropeptide oxytocin in the hypothalamus and reduced activity of the dopaminergic reward system. Collectively, these data support the idea that the gut microbiota can impact symptoms of neurodevelopmental disorders through modulation of the host metabolome and neuropeptide production.

Despite these data, the host immune system, which is dynamically regulated by the gut microbiota, also plays a critical role in the development of these behavioral phenotypes

in MIA offspring. Poly(I:C) injection of pregnant dams resulted in elevated systemic levels of the pro-inflammatory cytokines IL-6 and IL-17A[68,69]. Consistent with a role for immune dysregulation in the MIA model, bone marrow reconstitution reduced repetitive and anxiety-like behavior in MIA offspring[69]. To identify immune signals that contribute to disease in this model, it was shown that administration of IL-6 in offspring was sufficient to trigger abnormal behaviors and that blockade of IL-6 but not IFN-γ, IL-1α and TNF-α in pregnant dams reduced behavioral phenotypes induced by MIA[70]. More recently, IL-17A was implicated as a critical inflammatory mediator in the MIA model. MIA offspring from mice lacking T cell-derived IL-17A were protected from developing these behavioral phenotypes[68]. Furthermore, intraventricular IL-17A administration in fetuses was sufficient to elicit behavioral abnormalities. Given the function of IL-6 in promoting differentiation of T_H17 cells, these data suggest that IL-6 and IL-17A act in concert to promote disease induced by MIA. Since IL-17A and T_H17 cells are immune pathways that are sensitive to changes in the composition of the gut microbiota, these findings also raise the possibility that MIA-induced immune dysregulation is linked to intestinal dysbiosis. Further studies are required to address the contribution of indigenous bacteria in immune dysregulation and disease outcome in ASD.

Stress, anxiety and depression

Depression is a mood disorder characterized by melancholy, anxiety and emotional and physical exhaustion. Although experts have long suspected that the molecular basis for depression arises from neurochemical imbalances in the brain, the precise etiology of

depression is not known and appears to involve a number of environmental factors such as exposure to physical and psychological stress, activation of the immune system, and more recently, interactions between the host and microbiome. The idea that indigenous gut microbes can influence depressive behaviors is supported by studies using GF mice and mice treated with antibiotics or probiotics. Numerous studies have reported that mice lacking a normal gut flora display reduced basal and stress-induced anxiety- or depressive-like symptoms. GF mice were less anxious and depressed compared to their conventional counterparts and these phenotypes were restored following intestinal colonization[71,72,73]. In response to a physical stressor such as dextran sodium sulfate (DSS)-induced intestinal inflammation, mice exhibited increased anxiety-like behaviors, which was ameliorated by probiotic administration of *Bifidobacterium longum*[74]. Similarly, in the maternal separation model of depression, rats displayed increased depressive-like behaviors and elevated pro-inflammatory cytokines, which were reduced following treatment with the probiotic *Bifidobacterium infantis*[75]. Some *Lactobacillus* strains exhibited anti-depressive properties in steady state animals or in response to stress[76, 77]. To begin to demonstrate a causal relationship between indigenous bacteria and depression, one recent study showed that maternal separation-induced anxiety- and depressive-like symptoms required the presence of a complete gut microbiota[78]. Furthermore, patients with major depressive disorder (MDD) harbored a distinct microbiota from healthy controls and fecal transfer of the MDD microbiota enhanced depressive-like symptoms in GF mice[73]. These results collectively support the hypothesis that indigenous bacteria have a significant impact on physical and psychological stress. However, the cellular and molecular pathways that mediate gut-brain communication are

currently unclear and appear to involve modulation of the immune system[75,79], host metabolism[73] and/or vagal nerve stimulation[74,77]. Given the potent immunomodulatory properties of indigenous bacteria and probiotics[75,79], it is likely that altered immune environments due to host-microbiome interactions can lead to changes in brain function through the hypothalamic-pituitary-adrenal (HPA) axis, a neuroendocrine, stress-sensing system that is activated by pro-inflammatory cytokines[80]. Future studies using immunodeficient animals will be necessary to define the precise functions of the immune system in gut-brain communication in models of stress, anxiety and depression.

Neurodegeneration and aging

Alzheimer's disease (AD) and Parkinson's disease (PD) are neurodegenerative disorders with complex etiologies including age, genetic and environmental components. In AD, deposition of protein aggregates comprised of amyloid-β peptide and tau in CNS tissues impairs cognitive function. However, the host-intrinsic and extrinsic factors that regulate these processes are unclear. Accumulating evidence suggests that pathogenic microbes may contribute to neurodegeneration. Bacterial[81,82], viral[83,84,85,86], fungal[87] and parasitic[88,89] infections that target the CNS are associated with increased risk for AD. These infections likely promote chronic inflammatory responses in the CNS of susceptible individuals that could contribute to hallmarks of neurodegeneration such as alterations in synaptic function, neurodegeneration and amyloidosis[90]. Bacterial infection induces amyloid-β production, which has both antimicrobial and pathologic properties, proposing the idea that infection-induced amyloidosis may drive AD[91]. Aside from externally

acquired microbes, one report demonstrated that a mouse model of AD (APPPS1-Tg mice) derived under GF conditions exhibited reduced cerebral and serum amyloid-β levels[92]. These results are consistent with reduced   plaque deposition in male APP$_{SWE}$/PS1$_{ΔE9}$ mice treated with broad-spectrum antibiotics[93]. In support of a role for indigenous microbes in promoting AD, members of the host microbiota can regulate amyloidosis by producing their own amyloid peptides[94]. Additionally, manipulating the gut microbiota by antibiotic treatment or probiotic treatment alters learning and memory[95,96,97,98]. Despite these data, the role of microbiota-directed pathways in the development of AD requires further interrogation.

PD is a neurodegenerative motor disorder that is frequently associated with impaired gastric motility[99] and elevated levels of α-synuclein in the intestine[100], raising the possibility that the intestinal environment regulates the development of PD. One study revealed that the fecal microbiome of PD patients had reduced abundance of Prevotellaceae compared to healthy controls while a subset of PD patients with severe postural instability and gait difficulty (PIGD) had elevated Enterobacteriaceae[101], suggesting that these bacteria regulate motor function. Similar findings were reported in a separate study evaluating the PD gut microbiome[102]. PD patients also exhibit increased intestinal permeability and colonic inflammation[103,104]. Altogether, these preliminary data warrant additional studies exploring the contribution of the gut microbiota to the development of PD.

The primary risk for neurodegenerative disorders like AD and PD is age. Longitudinal studies interrogating the structure of the human microbiome now indicate that the composition of our gut microbiota changes over time. From birth to adulthood, the microbiota undergoes a maturation process that is primarily due to dietary changes and exposure to environmental insults[105,106]. As a result, the adult microbiome is more diverse than both the infant[107] and elderly microbiome[108]. Given associations between the gut microbiome, immune system and neurodegeneration, age-related decline in CNS function may be explained by alteration in the gut microbiome.

Bidirectional communication with the immune system and CNS

Bacterial- and host-derived products

A growing body of evidence indicates that alterations in indigenous bacteria composition and signaling events in the gut can impact brain function and behavior through multiple mechanisms (**Fig. 3**). Activation of innate immune responses following exposure to microbial factors requires the recognition of MAMPS via PRRs. The most well characterized family of PRRs is Toll-like receptors (TLRs), which are expressed not only on innate immune cells but also CNS-resident cell populations including neurons and glial cells[109,110]. Since TLR ligands derived from the intestinal microbiota can be found systemically during chronic inflammatory disorders[111], these products may be able to directly trigger innate immune pathways to impact CNS function. Although systemic LPS administration drives CNS inflammation by activating TLR4-expressing brain-resident

cells[112,113], evidence for microbiota-derived MAMPs that trigger CNS inflammation is currently lacking. An alternative pathway may involve indirect activation of the systemic immune system and release of circulating inflammatory cytokines, which then trigger CNS inflammation and subsequent behavioral changes[114].

Indigenous bacteria colonization modulates the host metabolome, which appears to influence CNS function. Circulating metabolites can enter the CNS and directly modulate neuroactivity[66,115]. On the other hand, particular metabolites can regulate the function of peripheral immune cells[116,117], which then can influence brain function potentially through the recently described brain lymphatic network[118]. How immune cells coordinate gut-brain communication and whether microbial-derived metabolites can directly modulate the function of the CNS are currently areas of intense investigation.

Neurotransmitters are of particular interest in light of emerging studies demonstrating that the gut microbiota modulates host metabolism of neurotransmitters and that particular gut microbes can synthesize neurotransmitters *de novo*. Serotonin is a neurotransmitter that controls many physiological functions such as circadian rhythms, cognition and mood[119], and multiple neurological disorders have been associated with changes in serotonin levels. Unlike many neurotransmitters, the majority of the host's serotonin is derived from the gastrointestinal tract[120], suggesting a role for the intestinal environment in modulating its synthesis. Consistent with this idea, GF mice have reduced levels of serum and colon serotonin compared to conventional controls[121,122]. Spore-forming bacteria, in particular, activate intestinal enterochromaffin cells to produce serotonin[123]. Furthermore,

metabolites upregulated by spore-forming bacteria colonization as well as SCFAs could directly promote the production of serotonin and expression of the serotonin biosynthetic enzyme, *Tph1* in enterochromaffin cells[123,124]. Similar microbiota-dependent alterations were observed for γ-aminobutyric acid (GABA), norepinephrine (NE), dopamine and tryptamine, where particular bacterial species exhibited the capability of synthesizing or inducing host neurotransmitter metabolism.

Serotonin is also a key mediator of neuroimmune interactions. Immune cells of both myeloid and lymphoid lineages express a range of serotonin receptors and can respond to serotonin stimulation by altering their inflammatory functions[125]. Thus, serotonin may have indirect effects on the CNS through modulation of immune cell function. Indeed, spore-forming members of the gut microbiota promote T_{reg} cell differentiation in the colon primarily through SCFAs[126,127,128]. Whether immunomodulation by indigenous bacteria depends on serotonin biosynthesis remains to be determined. Nevertheless, these data highlight a critical role for the microbiota in regulating CNS function through neurotransmitter biosynthesis and suggest a potential microbial etiology to some neurological conditions. Studies interrogating how intestinal microbes impact host synthesis and release of neuroactive molecules will be essential to understanding this key communication pathway in the gut-brain axis.

Neuronal signaling

In addition to modulating intestinal production of neurochemicals, gut microbes can communicate with the CNS via stimulation of the vagus nerve, a parasympathetic neural network that provides homeostatic control of the gastrointestinal tract. The anti-depressant effects of *Lactobacillus rhamnosus* administration in healthy mice were abolished following vagotomy[77]. Anxiety-like behavior induced by DSS colitis was also dependent on the vagus nerve[74]. Further, treatment with *Bifidobacterium longum* during DSS colitis did not reduce anxiety-like behavior in vagotomized mice, identifying a critical role for afferent vagal stimulation in bacteria-mediated changes in behavior. On the other hand, the CNS transmits signals to the intestine through the efferent fibers of the vagal nerve. These neurons control intestinal motility, release of neurochemicals and the intestinal immune environment. Specifically, vagal nerve stimulation has been suggested to attenuate inflammatory responses through the neurotransmitter acetylcholine[129], raising the possibility that the immunomodulatory properties of probiotic strains like *Lactobacillus* and *Bifidobacterium* may be dependent on the vagus nerve. However, protection from DSS colitis conferred by *L. rhamnosus* and *Bifidobacterium infantis* was observed in both control and vagotomized mice[130], suggesting that gut-brain communication via this pathway may depend on specific bacterial strains and the inflammatory context. The precise role of intestinal microbes and vagal nerve activity in the gut-brain communication require additional studies.

Neuroendocrine Pathways

It has long been appreciated that biochemical changes in the brain can also lead to changes in gut physiology. One of the main pathways by which this occurs is the hypothalamic-pituitary-adrenal (HPA) axis. In response to physical or psychological stress, hormones released from the hypothalamus, pituitary and adrenal glands collectively influence multiple organ systems to allow the host to adapt to their environment. For example, activation of the stress response through CRF acting through the alterations autonomic nervous system innervating the gut[47] and the HPA axis can lead to changes in intestinal permeability[131,132,133,134,135], motility[136,137] and mucus production[138,139]. These events contribute to alterations in indigenous bacteria composition as demonstrated in mouse models of early-life and chronic stress[78,140]. Activation of the HPA axis has also been shown to impact immune cell responses. Glucocorticoids released by the HPA axis have profound anti-inflammatory properties on innate and adaptive immune cells but can also stimulate pro-inflammatory responses under certain conditions[80,141]. It is conceivable that increased intestinal permeability and systemic dissemination of microbial-derived products following stress could lead to enhanced pro-inflammatory responses that further stimulate the HPA axis. Stress-induced behavioral abnormalities may occur in a microbiota-dependent manner[78]. Although maternal separation results in elevated serum corticosterone levels and increased acetylcholine release by the colon in both GF and conventional mice, it triggered anxiety-like behaviors only in conventional mice. Furthermore, maternal separation in conventional mice was associated with intestinal dysbiosis. Similar to host-derived neuroactive molecules, neuronal signaling pathways, these findings the idea that gut-brain communication not only involves microbial modulation of brain function but also

the reverse: CNS-induced changes in intestinal biology and indigenous bacteria composition. Future research should investigate the precise mechanisms, including communication through the immune system, that control bidirectional gut-brain communication.

Therapeutic manipulation of the microbiota

Preclinical studies have established a critical role for intestinal microbes in modulating behavior and CNS biology. Therefore, the gut microbiota is an intriguing target to develop therapeutics for multiple CNS disorders (**Table 1**). Examples of approaches to manipulate the microbiota include administering probiotic strains beneficial to CNS health, eliminating CNS-detrimental strains using selective antibiotic cocktails, using formulated diets (or, prebiotics) that alter gut microbial communities and perhaps target specific metabolic pathways in the microbiota. Although human studies using these methods are scarce, preliminary evidence suggests that probiotic therapies improve mental health. In one study, healthy female participants given a fermented milk product with four probiotic strains including *Bifidobacterium*, *Strepcoccus*, *Lactobacillus* and *Lactococcus* for four weeks had altered brain activity in regions that control emotion and sensation providing a proof of concept that a microbiota-gut-brain axis is operational in humans[142]. Consistent with these findings, healthy human volunteers given a probiotic formulation of *Lactobacillus* and *Bifidobacterium* for 30 days had reduced measures of psychological distress[143]. To date, there are only a few reports suggesting that antibiotics can impact brain function[144,145]. However, there is a significant correlation between nutrition and brain

health[146]. For example, a ketogenic diet is a high-fat, low-carbohydrate diet used to effectively treat refractory epilepsy[147], although the mechanisms are currently unknown. Since diet has been demonstrated to significantly influence host physiology through gut microbial communities[148,149,150], future studies should dissect whether diet-induced cognitive effects are dependent on microbiota composition and microbiota-induced immunological changes. Collectively, microbiota targeting offers a promising therapeutic strategy for the treatment of multiple CNS disorders.

Pathology type	Condition	Associated microbiota changes	Refs.
Autoimmune disease	Multiple sclerosis	Increased: *Methanobrevibacter*, *Akkermansia* Decreased: *Butyricimonas*	135
		Increased: Desulfovibroneceae Decreased: Lachnospiraceae, Ruminococcaceae	136
		Increased: *Pseudomonas*, *Mycoplana*, *Haemophilus*, *Blautia*, *Dorea* Decreased: *Parabacteroides*, *Adlercreutzia*, *Prevotella*	137
		Increased: *Streptococcus*, *Eggerthella* Decreased: Clostridia clusters XIVa and IV, Bacteroidetes, *Faecalibacterium*	138
		Increased: *Ruminococcus* Decreased: Bacteroidaceae, *Faecalibacterium*	139
Neurodegenerative disorders	Parkinson's disease	Increased: *Blautia*, *Coprococcus*, *Roseburia*, Proteobacteria Decreased: *Faecalibacterium*, Prevotellaceae	140
		Decreased: Prevotellaceae Enterobacteriaceae correlate with motor impairments	105
	Alzheimer's disease	Association with bacterial and viral infection	141
Injury	Spinal cord injury (SCI)	SCI with upper motor neuron bowel syndrome: decreased *Pseudobutyrivibrio*, *Dialister*, *Megamonas* SCI with lower motor neuron bowel syndrome: decreased *Roseburia*, *Pseudobutyrivibrio*, *Megamonas*	142
		SCI with neuropathic bladder: increased *Klebsiella*, *Escherichia*, *Enterococcus* SCI with neuropathic bladder: decreased *Lactobacillus*, *Corynebacterium*, *Staphylococcus*, *Streptococcus*, *Prevotella*, *Veillonella*	143
Neuropsychiatric conditions	Major depressive disorder	Decreased: *Bifidobacterium*, *Lactobacillus*	144
		Increased: Actinomycineae, Coriobacterineae, Lactobacillaceae, Streptococcaceae, Clostridiales, Eubacteriaceae, Lachnospiraceae, Ruminococcaceae, Erysipelotrichaceae Decreased: Bacteroidaceae, Rikenellaceae, Lachnospiraceae, Acidaminococcaceae, Veillonellaceae, Sutterellaceae	86
		Increased: Enterobacteriaceae, *Alistipes*, Acidaminococcaceae, Fusobacteriaceae, Porphyromonadaceae, Rikenellaceae Decreased: Bacteroidaceae, Erysipelotrichaceae, Lachnospiraceae, Prevotellaceae, Ruminococcaceae and Veillonellaceae *Faecalibacterium* negatively correlated with depressive symptoms	145
	Anxiety disorder	Probiotic administration of *B. longum* and *Lactobacillus helveticus* decreased anxiety	146
		Probiotic administration of *Lactobacillus casei*, *Lactobacillus acidophilus*, *L. rhamnosus*, *Lactobacillus bulgaricus*, *Bifidobacterium breve*, *B. longum*, *Streptococcus thermophilus* and *Bifidobacterium lactis* decreased anxiety	147
Autism		Increased: *Lactobacillus*, *Desulfovibrio*, *Clostridium*, cluster 1 Decreased: *Bacteroides/Firmicutes*, ratio	148
		Increased: *Sutterella*	149
		Increased: *Clostridium*, *Bacteroides*, *Porphyromonas*, *Prevotella*, *Pseudomonas*, *Aeromonas*, Enterobacteriaceae Decreased: *Enterococcus*, *Lactobacillus*, *Streptococcus*, *Lactococcus*, *Staphylococcus*, Bifidobacteria	150
		Increased: *Lactobacillus* Decreased: *Prevotella*, *Coprococcus*, Veillonellaceae	151
		Increased: *Sutterella*, Lachnospiraceae, Ruminococcaceae	152
		Increased: *Lactobacillus* Decreased: *Bifidobacterium*, *Enterococcus*	153
		Increased: *Bacteroidetes*, *Proteobacterium* Decreased: *Actinobacterium*, *Bifidobacterium*	154
		Increased: *Clostridium* clusters I and II	155

Table 4: Reported alterations in the gut microbiota in neurological and psychiatric disorders
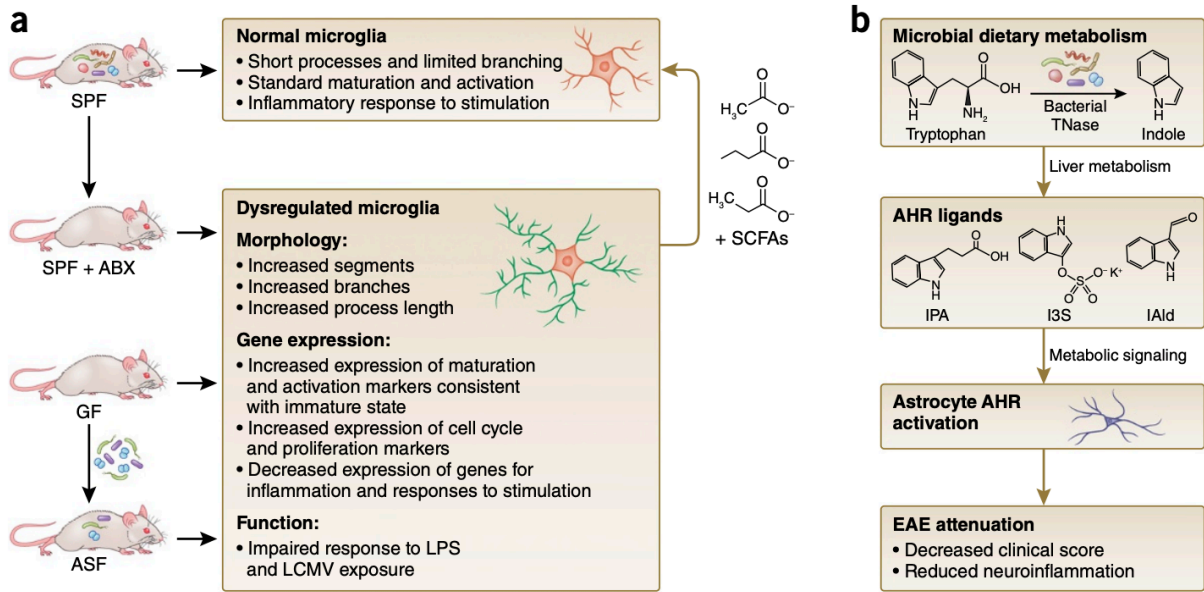
Figure 4. Effects of the microbiota on microglia and astrocyte biology. (**A**) Microglial maturation and function are affected by the presence or absence of complex microbiome. Compared to conventionally-colonized (specific pathogen-free, SPF) controls, mice reared in the absence of microbial colonization (germ free, GF) have microglia with abnormal morphology, altered gene expression and impaired functional response to stimulation. Similar microglial abnormalities are seen in microbiome-depleted mice, by antibiotic treatment of SPF mice (ABX), or restricted colonization with three bacterial taxa from a limited Altered Schaedler Flora consortia (ASF: B. distasonis, L. salivarius, and Clostridium cluster XIV). Microglial abnormalities in GF mice are corrected by supplementation with short-chain fatty acids (SCFAs), products of bacterial fermentation. (**B**) Microbial metabolites bind to the aryl hydrocarbon receptor (AHR) in astrocytes, reducing symptoms of experimental autoimmune encephalomyelitis (EAE). Type I interferon signaling (IFN-I) in astrocytes diminishes inflammation and decreases

EAE clinical scores, and this effect is reversed by antibiotic treatment. Particular

tryptophan metabolites produced by the microbiome stimulate AHR and reduce EAE

clinical score. This suggests that the microbiome has a direct effect on AHR signaling

and inflammation in astrocytes, which may have relevance to multiple sclerosis (MS),

where patients present with decreased tryptophan-derived metabolites in sera.

TnAse=tryptophanase, IPA=indole-3-propionic acid, IAld=indole-3-aldehyde,
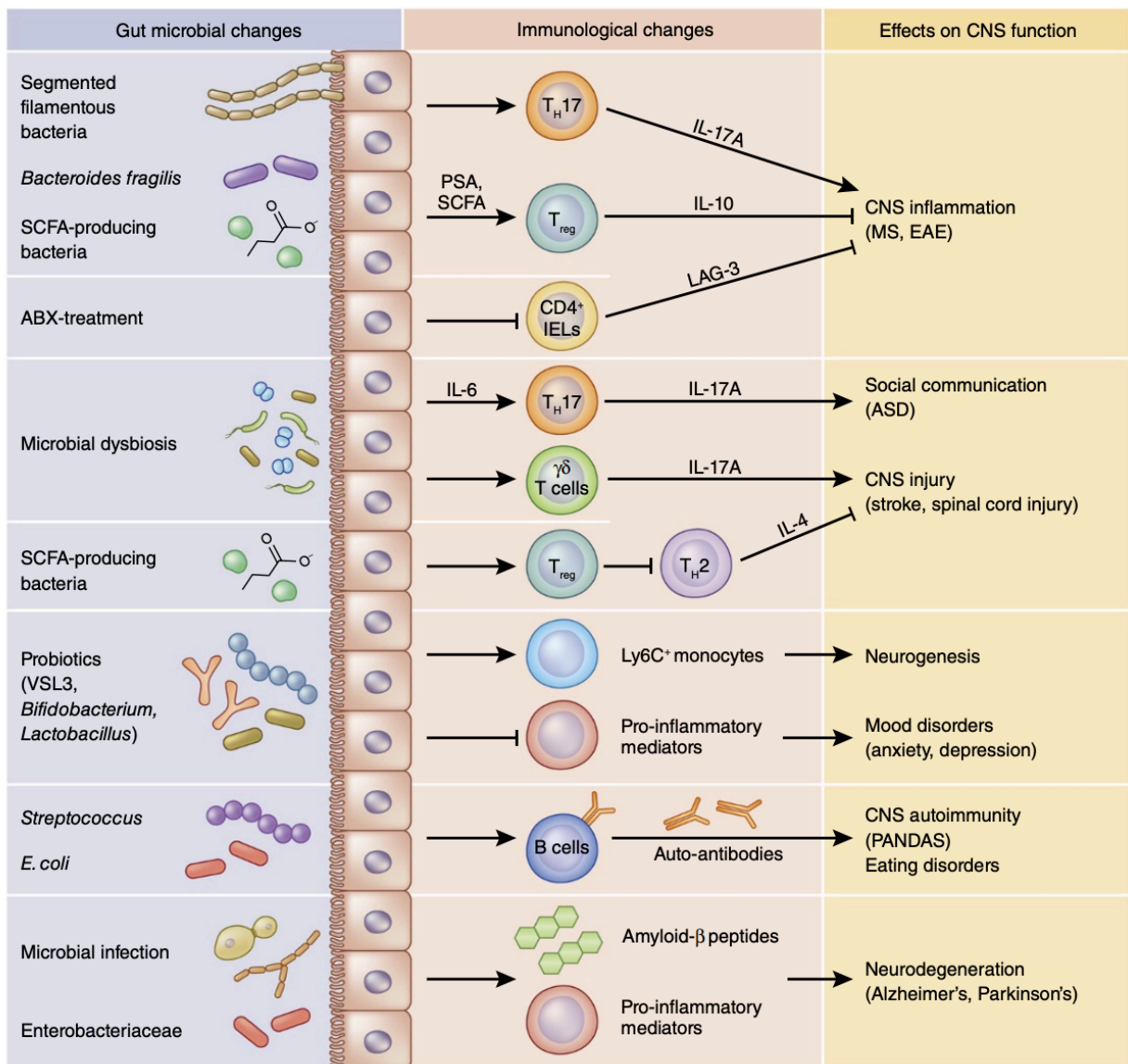
I3S=indoxyl-3-sulfate

Figure 5: The microbiome impacts peripheral immune cells and CNS function.

Indigenous microbes in the gastrointestinal tract and environmental microbial exposure regulate peripheral immune responses in the host. Emerging evidence suggest that microbes significantly impacts CNS function and behavior through the peripheral immune system. Intestinal colonization by segmented filamentous bacteria (SFB) is associated with T_H17-mediated CNS inflammation during the multiple sclerosis (MS) mouse model, experimental autoimmune encephalomyelitis (EAE)[36], while colonization by polysaccharide A (PSA)-expressing Bacteroides fragilis[37, 43, 44, 45] or short-chain fatty acid (SCFA)-producing bacteria[46] promotes regulatory T cell responses that suppress EAE. The microbiota also appears to induce anti-inflammatory CD4$^+$ IELs that protect from EAE[47]. The material immune activation (MIA) model of autism spectrum disorder leads to microbial dysbiosis that is associated with elevated T_H17 cell responses[66, 67, 68], which were sufficient to trigger social and behavioral defects[66, 67, 68]. Similar to the MIA model, middle cerebral artery occlusions (MCAO)-induced brain injury appears to be mediated by a dysbiotic microbiota[51], which induces a population of pathogenic IL-17A-producing γδ T cells[50]. In mouse models of spinal cord injury, IL-4-producing CD4$^+$ T cells have been demonstrated to restore neuronal tissue homeostasis[55]. Whether the intestinal microbiota can regulate T_H2 cell-mediated CNS tissue repair remains to be defined. Oral administration of probiotics can elicit a population of Ly6C$^+$ monocytes that increase hippocampal neurogenesis and enhance memory responses[63]. Probiotics such as Bifidobacterium and Lactobacillus have potent anti-inflammatory properties. One mechanism by which these strains reduce anxiety and depression behaviors may be through induction of anti-inflammatory responses. Preliminary findings suggest that

exposure to Streptococcus and E. coli can trigger the production of self-reactive auto-antibodies that lead to cognitive dysfunction in pediatric autoimmune neuropsychiatic disorders associated with streptococcal infection (PANDAS) and eating disorders, respectively[59, 60]. Bacterial[81, 82], viral[83, 84, 85, 86], fungal[87] and parasitic[88, 89] infections have all been associated with the development of Alzheimer's disease (AD). Infection-induced β-amyloidosis has been suggested as a potential link between microbial threats and the onset of AD[91]. Patients with Parkinson's disease (PD) exhibit gut microbial changes such as elevated levels of Enterobacteriaceae[101], suggesting a gut microbial etiology to the pathogenesis of PD. Collectively, regulation of peripheral immune responses is a critical pathway by which the indigenous microbiota and exogenous microbial challenges influence CNS function and behavior.
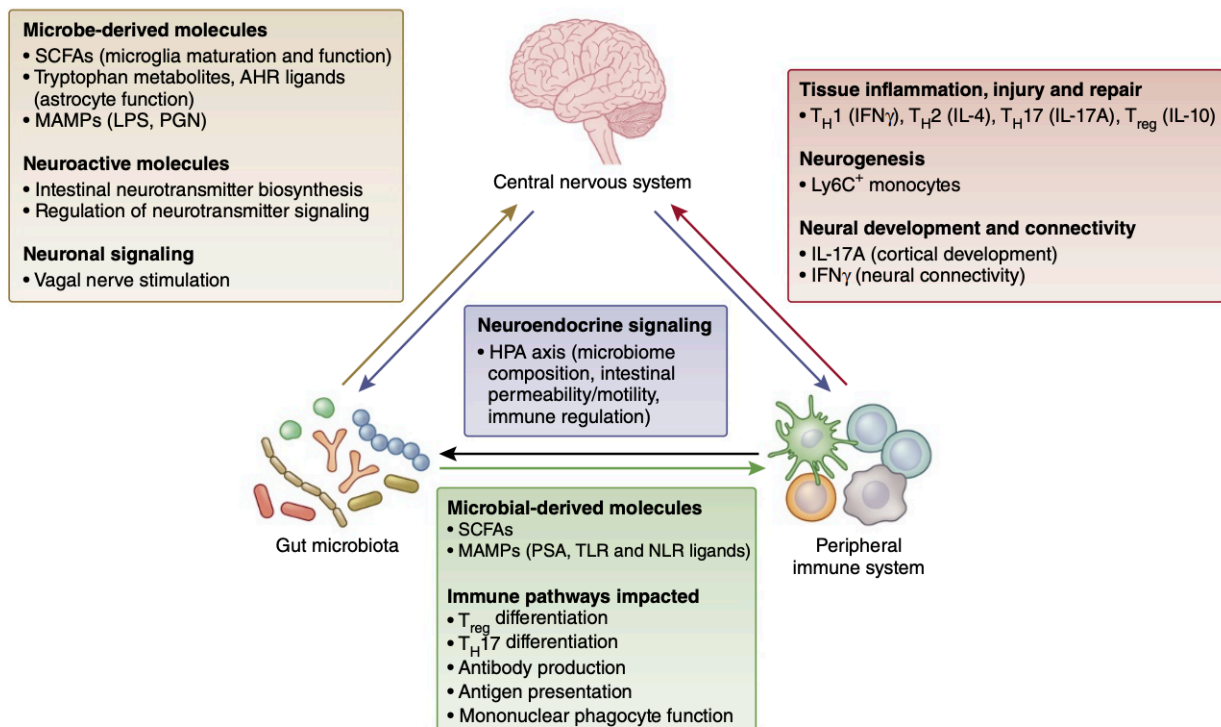

Microbe-derived molecules
- SCFAs (microglia maturation and function)
- Tryptophan metabolites, AHR ligands (astrocyte function)
- MAMPs (LPS, PGN)

Neuroactive molecules
- Intestinal neurotransmitter biosynthesis
- Regulation of neurotransmitter signaling

Neuronal signaling
- Vagal nerve stimulation

Central nervous system

Tissue inflammation, injury and repair
- T_H1 (IFNγ), T_H2 (IL-4), T_H17 (IL-17A), T_{reg} (IL-10)

Neurogenesis
- Ly6C$^+$ monocytes

Neural development and connectivity
- IL-17A (cortical development)
- IFNγ (neural connectivity)

Neuroendocrine signaling
- HPA axis (microbiome composition, intestinal permeability/motility, immune regulation)

Gut microbiota

Peripheral immune system

Microbial-derived molecules
- SCFAs
- MAMPs (PSA, TLR and NLR ligands)

Immune pathways impacted
- T_{reg} differentiation
- T_H17 differentiation
- Antibody production
- Antigen presentation
- Mononuclear phagocyte function

Figure 6: Crosstalk between the microbiota, immune system and CNS. The microbiota is a critical modulator of local and systemic immune responses. Recognition of microbial-derived products such as TLR ligands and metabolites activate distinct immune pathways. Conversely, immune cell responses critically alter microbiota composition through anti-microbial mechanisms. Both the microbiota and immune system can also regulate the physiology of the CNS. Future studies investigating the functional outcomes of these bidirectional interactions will inform the development of novel therapeutic strategies for the treatment of CNS disorders.

References

1.   Deverman BE, Patterson PH. Cytokines and CNS development. *Neuron* 2009, **64**(1)**:** 61-78.

2.   Stephan AH, Barres BA, Stevens B. The complement system: an unexpected role in synaptic pruning during development and disease. *Annual review of neuroscience* 2012, **35:** 369-389.

3.   Elmer BM, McAllister AK. Major histocompatibility complex class I proteins in brain development and plasticity. *Trends in neurosciences* 2012, **35**(11)**:** 660-670.

4.   Weinstein LI, Revuelta A, Pando RH. Catecholamines and acetylcholine are key regulators of the interaction between microbes and the immune system. *Annals of the New York Academy of Sciences* 2015, **1351**(1)**:** 39-51.

5.   Baganz NL, Blakely RD. A Dialogue between the Immune System and Brain, Spoken in the Language of Serotonin. *ACS chemical neuroscience* 2013, **4**(1)**:** 48-63.

6.   Ahern GP. 5-HT and the immune system. *Current Opinion in Pharmacology* 2011, **11**(1)**:** 29-33.

7.   Barragan A, Weidner JM, Jin Z, Korpi ER, Birnir B. GABAergic signalling in the immune system. *Acta physiologica (Oxford, England)* 2015, **213**(4)**:** 819-827.

8.   Ben-Shaanan TL, Azulay-Debby H, Dubovik T, Starosvetsky E, Korin B, Schiller M*, et al.* Activation of the reward system boosts innate and adaptive immunity. *Nature Medicine* 2016.

9.   Erickson MA, Dohi K, Banks WA. Neuroinflammation: A Common Pathway in CNS Diseases as Mediated at the Blood-Brain Barrier. *Neuroimmunomodulation* 2012, **19**(2)**:** 121-130.

10.   Banks WA. The blood-brain barrier in neuroimmunology: Tales of separation and assimilation. *Brain, Behavior, and Immunity* 2015, **44:** 1-8.

11.   Saijo K, Glass CK. Microglial cell origin and phenotypes in health and disease. *Nat Rev Immunol* 2011, **11**(11)**:** 775-787.

12.   Nayak D, Roth TL, McGavern DB. Microglia development and function. *Annual review of immunology* 2014, **32:** 367-402.

13.   Matcovitch-Natan O, Winter DR, Giladi A, Vargas Aguilar S, Spinrad A, Sarrazin S*, et al.* Microglia development follows a stepwise program to regulate brain homeostasis. *Science* 2016.

14.   Nayak D, Zinselmeyer BH, Corps KN, McGavern DB. In vivo dynamics of innate immune sentinels in the CNS. *Intravital* 2012, **1**(2)**:** 95-106.

15.   Nimmerjahn A, Kirchhoff F, Helmchen F. Resting microglial cells are highly dynamic surveillants of brain parenchyma in vivo. *Science* 2005, **308**(5726)**:** 1314-1318.

16.   Bilbo SD, Schwarz JM. The immune system and developmental programming of brain and behavior. *Frontiers in Neuroendocrinology* 2012, **33**(3)**:** 267-286.

17.   Hu X, Leak RK, Shi Y, Suenaga J, Gao Y, Zheng P*, et al.* Microglial and macrophage polarization[mdash]new prospects for brain repair. *Nat Rev Neurol* 2015, **11**(1)**:** 56-64.

18.   Bogie JFJ, Stinissen P, Hendriks JJA. Macrophage subsets and microglia in multiple sclerosis. *Acta Neuropathologica* 2014, **128**(2)**:** 191-213.

19.   Erny D, Hrabe de Angelis AL, Jaitin D, Wieghofer P, Staszewski O, David E*, et al.* Host microbiota constantly control maturation and function of microglia in the CNS. *Nature neuroscience* 2015, **18**(7)**:** 965-977.

20.   Borre YE, O'Keeffe GW, Clarke G, Stanton C, Dinan TG, Cryan JF. Microbiota and neurodevelopmental windows: implications for brain disorders. *Trends in Molecular Medicine* 2014, **20**(9)**:** 509-518.

21.   Schafer DP, Lehrman EK, Kautzman AG, Koyama R, Mardinly AR, Yamasaki R*, et al.* Microglia sculpt postnatal neural circuits in an activity and complement-dependent manner. *Neuron* 2012, **74**(4)**:** 691-705.

22.   Cho I, Yamanishi S, Cox L, Methe BA, Zavadil J, Li K*, et al.* Antibiotics in early life alter the murine colonic microbiome and adiposity. *Nature* 2012, **488**(7413)**:** 621-626.

23.   Seo JW, Yang EJ, Kim SH, Choi IH. An inhibitory alternative splice isoform of Toll-like receptor 3 is induced by type I interferons in human astrocyte cell lines. *BMB reports* 2015, **48**(12)**:** 696-701.

24.   Khakh BS, Sofroniew MV. Diversity of astrocyte functions and phenotypes in neural circuits. *Nature neuroscience* 2015, **18**(7)**:** 942-952.

25.   Freeman MR. Specification and Morphogenesis of Astrocytes. *Science* 2010, **330**(6005)**:** 774-778.

26.   Jensen CJ, Massie A, De Keyser J. Immune Players in the CNS: The Astrocyte. *Journal of Neuroimmune Pharmacology* 2013, **8**(4)**:** 824-839.

27.   Rossi D. Astrocyte physiopathology: At the crossroads of intercellular networking, inflammation and cell death. *Progress in Neurobiology* 2015, **130:** 86-120.

28.   Barres BA. The Mystery and Magic of Glia: A Perspective on Their Roles in Health and Disease. *Neuron* 2008, **60**(3)**:** 430-440.

29.   Rothhammer V, Mascanfroni ID, Bunse L, Takenaka MC, Kenison JE, Mayo L*, et al.* Type I interferons and microbial metabolites of tryptophan

modulate astrocyte activity and central nervous system inflammation via the aryl hydrocarbon receptor. *Nat Med* 2016, **22**(6)**:** 586-597.

30.   Zelante T, Iannitti RG, Cunha C, De Luca A, Giovannini G, Pieraccini G*, et al.* Tryptophan catabolites from microbiota engage aryl hydrocarbon receptor and balance mucosal reactivity via interleukin-22. *Immunity* 2013, **39**(2)**:** 372-385.

31.   Braniste V, Al-Asmakh M, Kowal C, Anuar F, Abbaspour A, Toth M*, et al.* The gut microbiota influences blood-brain barrier permeability in mice. *Science translational medicine* 2014, **6**(263)**:** 263ra158.

32.   Radjavi A, Smirnov I, Derecki N, Kipnis J. Dynamics of the meningeal CD4+ T-cell repertoire are defined by the cervical lymph nodes and facilitate cognitive task performance in mice. *Mol Psychiatry* 2014, **19**(5)**:** 531-532.

33.   Ribatti D. The crucial role of mast cells in blood-brain barrier alterations. *Experimental cell research* 2015, **338**(1)**:** 119-125.

34.   Forsythe P. Microbes taming mast cells: Implications for allergic inflammation and beyond. *European Journal of Pharmacology* 2016, **778:** 169-175.

35.   Khosravi A, Yanez A, Price JG, Chow A, Merad M, Goodridge HS*, et al.* Gut microbiota promote hematopoiesis to control bacterial infection. *Cell host & microbe* 2014, **15**(3)**:** 374-381.

36.   Lee YK, Menezes JS, Umesaki Y, Mazmanian SK. Proinflammatory T-cell responses to gut microbiota promote experimental autoimmune encephalomyelitis. *Proceedings of the National Academy of Sciences of the United States of America* 2011, **108 Suppl 1:** 4615-4622.

37.   Ochoa-Reparaz J, Mielcarz DW, Ditrio LE, Burroughs AR, Foureau DM, Haque-Begum S*, et al.* Role of gut commensal microflora in the development of experimental autoimmune encephalomyelitis. *Journal of immunology (Baltimore, Md : 1950)* 2009, **183**(10)**:** 6041-6050.

38.   Gaboriau-Routhiau V, Rakotobe S, Lecuyer E, Mulder I, Lan A, Bridonneau C*, et al.* The key role of segmented filamentous bacteria in the coordinated maturation of gut helper T cell responses. *Immunity* 2009, **31**(4)**:** 677-689.

39.   Ivanov, II, Atarashi K, Manel N, Brodie EL, Shima T, Karaoz U*, et al.* Induction of intestinal Th17 cells by segmented filamentous bacteria. *Cell* 2009, **139**(3)**:** 485-498.

40.   Komiyama Y, Nakae S, Matsuki T, Nambu A, Ishigame H, Kakuta S, *et al.* IL-17 plays an important role in the development of experimental autoimmune encephalomyelitis. *Journal of immunology (Baltimore, Md : 1950)* 2006, **177**(1)**:** 566-573.

41.   Round JL, Lee SM, Li J, Tran G, Jabri B, Chatila TA, *et al.* The Toll-like receptor 2 pathway establishes colonization by a commensal of the human microbiota. *Science* 2011, **332**(6032)**:** 974-977.

42.   Round JL, Mazmanian SK. Inducible Foxp3+ regulatory T-cell development by a commensal bacterium of the intestinal microbiota. *Proceedings of the National Academy of Sciences of the United States of America* 2010, **107**(27)**:** 12204-12209.

43.   Ochoa-Reparaz J, Mielcarz DW, Ditrio LE, Burroughs AR, Begum-Haque S, Dasgupta S, *et al.* Central nervous system demyelinating disease protection by the human commensal Bacteroides fragilis depends on polysaccharide A expression. *Journal of immunology (Baltimore, Md : 1950)* 2010, **185**(7)**:** 4101-4108.

44.   Ochoa-Reparaz J, Mielcarz DW, Wang Y, Begum-Haque S, Dasgupta S, Kasper DL, *et al.* A polysaccharide from the human commensal Bacteroides

fragilis protects against CNS demyelinating disease. *Mucosal immunology* 2010, **3**(5)**:** 487-495.

45.   Wang Y, Telesford KM, Ochoa-Reparaz J, Haque-Begum S, Christy M, Kasper EJ*, et al.* An intestinal commensal symbiosis factor controls neuroinflammation via TLR2-mediated CD39 signalling. *Nature communications* 2014, **5:** 4432.

46.   Haghikia A, Jorg S, Duscha A, Berg J, Manzel A, Waschbisch A*, et al.* Dietary Fatty Acids Directly Impact Central Nervous System Autoimmunity via the Small Intestine. *Immunity* 2015, **43**(4)**:** 817-829.

47.   Kadowaki A, Miyake S, Saga R, Chiba A, Mochizuki H, Yamamura T. Gut environment-induced intraepithelial autoreactive CD4(+) T cells suppress central nervous system autoimmunity via LAG-3. *Nature communications* 2016, **20**(7).

48.   D'Mello C, Ronaghan N, Zaheer R, Dicay M, Le T, MacNaughton WK*, et al.* Probiotics Improve Inflammation-Associated Sickness Behavior by Altering Communication between the Peripheral Immune System and the Brain. *The Journal of neuroscience : the official journal of the Society for Neuroscience* 2015, **35**(30)**:** 10821-10830.

49.   Distrutti E, O'Reilly JA, McDonald C, Cipriani S, Renga B, Lynch MA*, et al.* Modulation of intestinal microbiota by the probiotic VSL#3 resets brain gene expression and ameliorates the age-related deficit in LTP. *PloS one* 2014, **9**(9)**:** e106503.

50.   Benakis C, Brea D, Caballero S, Faraco G, Moore J, Murphy M*, et al.* Commensal microbiota affects ischemic stroke outcome by regulating intestinal gammadelta T cells. *Nature medicine* 2016, **22**(5)**:** 516-523.

51.   Singh V, Roth S, G. L, R. S, D. G, B. S*, et al.* Microbiota Dysbiosis Controls the Neuroinflammatory Response after Stroke. *The Journal of neuroscience : the official journal of the Society for Neuroscience* 2016, **36**(28)**:** 7428-7440.

52.   Ohnmacht C, Park JH, Cording S, Wing JB, Atarashi K, Obata Y*, et al.* MUCOSAL IMMUNOLOGY. The microbiota regulates type 2 immunity through RORgammat(+) T cells. *Science* 2015, **349**(6251)**:** 989-993.

53.   Hill DA, Siracusa MC, Abt MC, Kim BS, Kobuley D, Kubo M*, et al.* Commensal bacteria-derived signals regulate basophil hematopoiesis and allergic inflammation. *Nature medicine* 2012, **18**(4)**:** 538-546.

54.   Sefik E, Geva-Zatorsky N, Oh S, Konnikova L, Zemmour D, McGuire AM*, et al.* MUCOSAL IMMUNOLOGY. Individual intestinal symbionts induce a distinct population of RORgamma(+) regulatory T cells. *Science* 2015, **349**(6251)**:** 993-997.

55.   Walsh JT, Hendrix S, Boato F, Smirnov I, Zheng J, Lukens JR*, et al.* MHCII-independent CD4+ T cells protect injured CNS neurons via IL-4. *The Journal of clinical investigation* 2015, **125**(6)**:** 2547.

56.   Gadani SP, Walsh JT, Smirnov I, Zheng J, Kipnis J. The glia-derived alarmin IL-33 orchestrates the immune response and promotes recovery following CNS injury. *Neuron* 2015, **85**(4)**:** 703-709.

57.   Matsushita T, Yanaba K, Bouaziz JD, Fujimoto M, Tedder TF. Regulatory B cells inhibit EAE initiation in mice while other B cells promote disease progression. *The Journal of clinical investigation* 2008, **118**(10)**:** 3420-3430.

58.   Pollinger B, Krishnamoorthy G, Berer K, Lassmann H, Bosl MR, Dunn R*, et al.* Spontaneous relapsing-remitting EAE in the SJL/J mouse: MOG-reactive transgenic T cells recruit endogenous MOG-specific B cells. *The Journal of experimental medicine* 2009, **206**(6)**:** 1303-1316.

59.   Yaddanapudi K, Hornig M, Serge R, De Miranda J, Baghban A, Villar G, *et al.* Passive transfer of streptococcus-induced antibodies reproduces behavioral disturbances in a mouse model of pediatric autoimmune neuropsychiatric disorders associated with streptococcal infection. *Molecular psychiatry* 2010, **15**(7)**:** 712-726.

60.   Tennoune N, Chan P, Breton J, Legrand R, Chabane YN, Akkermann K, *et al.* Bacterial ClpB heat-shock protein, an antigen-mimetic of the anorexigenic peptide alpha-MSH, at the origin of eating disorders. *Translational psychiatry* 2014, **4:** e458.

61.   Humann J, Mann B, Gao G, Moresco P, Ramahi J, Loh LN, *et al.* Bacterial Peptidoglycan Transverses the Placenta to Induce Fetal Neuroproliferation and Aberrant Postnatal Behavior. *Cell host & microbe* 2016, **19**(3)**:** 388-399.

62.   Ogbonnaya ES, Clarke G, Shanahan F, Dinan TG, Cryan JF, O'Leary OF. Adult Hippocampal Neurogenesis Is Regulated by the Microbiome. *Biological psychiatry* 2015, **78**(4)**:** e7-9.

63.   Mohle L, Mattei D, Heimesaat MM, Bereswill S, Fischer A, Alutis M, *et al.* Ly6C(hi) Monocytes Provide a Link between Antibiotic-Induced Changes in Gut Microbiota and Adult Hippocampal Neurogenesis. *Cell reports* 2016, **15**(9)**:** 1945-1956.

64.   Collins SM, Surette M, Bercik P. The interplay between the intestinal microbiota and the brain. *Nature reviews Microbiology* 2012, **10**(11)**:** 735-742.

65.   Cryan JF, Dinan TG. Mind-altering microorganisms: the impact of the gut microbiota on brain and behaviour. *Nature reviews Neuroscience* 2012, **13**(10)**:** 701-712.

66.   Hsiao EY, McBride SW, Hsien S, Sharon G, Hyde ER, McCue T*, et al.* Microbiota modulate behavioral and physiological abnormalities associated with neurodevelopmental disorders. *Cell* 2013, **155**(7)**:** 1451-1463.

67.   Buffington SA, Di Prisco GV, Auchtung TA, Ajami NJ, Petrosino JF, Costa-Mattioli M. Microbial Reconstitution Reverses Maternal Diet-Induced Social and Synaptic Deficits in Offspring. *Cell* 2016, **165**(7)**:** 1762-1775.

68.   Choi GB, Yim YS, Wong H, Kim S, Kim H, Kim SV*, et al.* The maternal interleukin-17a pathway in mice promotes autism-like phenotypes in offspring. *Science* 2016, **351**(6276)**:** 933-939.

69.   Hsiao EY, McBride SW, Chow J, Mazmanian SK, Patterson PH. Modeling an autism risk factor in mice leads to permanent immune dysregulation.

Proceedings of the National Academy of Sciences of the United States of America 2012, **109**(31)**:** 12776-12781.

70.   Smith SE, Li J, Garbett K, Mirnics K, Patterson PH. Maternal immune activation alters fetal brain development through interleukin-6. *The Journal of neuroscience : the official journal of the Society for Neuroscience* 2007, **27**(40)**:** 10695-10702.

71.   Clarke G, Grenham S, Scully P, Fitzgerald P, Moloney RD, Shanahan F*, et al.* The microbiome-gut-brain axis during early life regulates the hippocampal serotonergic system in a sex-dependent manner. *Molecular psychiatry* 2013, **18**(6)**:** 666-673.

72.   Neufeld KM, Kang N, Bienenstock J, Foster JA. Reduced anxiety-like behavior and central neurochemical change in germ-free mice. *Neurogastroenterology and motility : the official journal of the European Gastrointestinal Motility Society* 2011, **23**(3)**:** 255-264, e119.

73.   Zheng P, Zeng B, Zhou C, Liu M, Fang Z, Xu X*, et al.* Gut microbiome remodeling induces depressive-like behaviors through a pathway mediated by the host's metabolism. *Molecular psychiatry* 2016, **21**(6)**:** 786-796.

74.	Bercik P, Park AJ, Sinclair D, Khoshdel A, Lu J, Huang X*, et al.* The anxiolytic effect of Bifidobacterium longum NCC3001 involves vagal pathways for gut-brain communication. *Neurogastroenterology and motility : the official journal of the European Gastrointestinal Motility Society* 2011, **23**(12)**:** 1132-1139.

75.	Desbonnet L, Garrett L, Clarke G, Kiely B, Cryan JF, Dinan TG. Effects of the probiotic Bifidobacterium infantis in the maternal separation model of depression. *Neuroscience* 2010, **170**(4)**:** 1179-1188.

76.	Arseneault-Breard J, Rondeau I, Gilbert K, Girard SA, Tompkins TA, Godbout R*, et al.* Combination of Lactobacillus helveticus R0052 and Bifidobacterium longum R0175 reduces post-myocardial infarction depression symptoms and restores intestinal permeability in a rat model. *The British journal of nutrition* 2012, **107**(12)**:** 1793-1799.

77.	Bravo JA, Forsythe P, Chew MV, Escaravage E, Savignac HM, Dinan TG*, et al.* Ingestion of Lactobacillus strain regulates emotional behavior and central GABA receptor expression in a mouse via the vagus nerve. *Proceedings of the National Academy of Sciences of the United States of America* 2011, **108**(38)**:** 16050-16055.

78.   De Palma G, Blennerhassett P, Lu J, Deng Y, Park AJ, Green W, *et al.* Microbiota and host determinants of behavioural phenotype in maternally separated mice. *Nature communications* 2015, **6:** 7735.

79.   Desbonnet L, Garrett L, Clarke G, Bienenstock J, Dinan TG. The probiotic Bifidobacteria infantis: An assessment of potential antidepressant properties in the rat. *Journal of psychiatric research* 2008, **43**(2)**:** 164-174.

80.   Bellavance MA, Rivest S. The HPA - Immune Axis and the Immunomodulatory Actions of Glucocorticoids in the Brain. *Frontiers in immunology* 2014, **5:** 136.

81.   Hammond CJ, Hallock LR, Howanski RJ, Appelt DM, Little CS, Balin BJ. Immunohistological detection of Chlamydia pneumoniae in the Alzheimer's disease brain. *BMC neuroscience* 2010, **11:** 121.

82.   Huang WS, Yang TY, Shen WC, Lin CL, Lin MC, Kao CH. Association between Helicobacter pylori infection and dementia. *Journal of clinical neuroscience : official journal of the Neurosurgical Society of Australasia* 2014, **21**(8)**:** 1355-1358.

83.   Borjabad A, Volsky DJ. Common transcriptional signatures in brain tissue from patients with HIV-associated neurocognitive disorders, Alzheimer's disease,

and Multiple Sclerosis. *Journal of neuroimmune pharmacology : the official journal of the Society on NeuroImmune Pharmacology* 2012, **7**(4)**:** 914-926.

84.   Itzhaki RF, Wozniak MA. Herpes simplex virus type 1 in Alzheimer's disease: the enemy within. *Journal of Alzheimer's disease : JAD* 2008, **13**(4)**:** 393-405.

85.   Karim S, Mirza Z, Kamal MA, Abuzenadah AM, Azhar EI, Al-Qahtani MH*, et al.* An association of virus infection with type 2 diabetes and Alzheimer's disease. *CNS & neurological disorders drug targets* 2014, **13**(3)**:** 429-439.

86.   Lurain NS, Hanson BA, Martinson J, Leurgans SE, Landay AL, Bennett DA*, et al.* Virological and immunological characteristics of human cytomegalovirus infection associated with Alzheimer disease. *The Journal of infectious diseases* 2013, **208**(4)**:** 564-572.

87.   Pisa D, Alonso R, Rabano A, Rodal I, Carrasco L. Different Brain Regions are Infected with Fungi in Alzheimer's Disease. *Scientific reports* 2015, **5:** 15015.

88.   Kusbeci OY, Miman O, Yaman M, Aktepe OC, Yazar S. Could Toxoplasma gondii have any role in Alzheimer disease? *Alzheimer disease and associated disorders* 2011, **25**(1)**:** 1-3.

89.   Prandota J. Possible link between Toxoplasma gondii and the anosmia associated with neurodegenerative diseases. *American journal of Alzheimer's disease and other dementias* 2014, **29**(3)**:** 205-214.

90.   Glass CK, Saijo K, Winner B, Marchetto MC, Gage FH. Mechanisms underlying inflammation in neurodegeneration. *Cell* 2010, **140**(6)**:** 918-934.

91.   Kumar DK, Choi SH, Washicosky KJ, Eimer WA, Tucker S, Ghofrani J*, et al.* Amyloid-beta peptide protects against microbial infection in mouse and worm models of Alzheimer's disease. *Science translational medicine* 2016, **8**(340)**:** 340ra372.

92.   Harach T, Marungruang N, Dutilleul N, Cheatham V, Mc Coy KD, Neher JJ*, et al.* Reduction of Alzheimer's disease beta-amyloid pathology in the absence of gut microbiota. *ArXiv e-prints*; 2015.

93.   Minter MR, Zhang C, Leone V, Ringus DL, Zhang X, Oyler-Castrillo P*, et al.* Antibiotic-induced perturbations in gut microbial diversity influences neuro-inflammation and amyloidosis in a murine model of Alzheimer's disease. *Scientific reports* 2016, **6:** 30028.

94.   Chapman MR, Robinson LS, Pinkner JS, Roth R, Heuser J, Hammar M*, et al.* Role of Escherichia coli curli operons in directing amyloid fiber formation. *Science* 2002, **295**(5556)**:** 851-855.

95.   Frohlich EE, Farzi A, Mayerhofer R, Reichmann F, Jacan A, Wagner B*, et al.* Cognitive impairment by antibiotic-induced gut dysbiosis: Analysis of gut microbiota-brain communication. *Brain, behavior, and immunity* 2016, **56:** 140-155.

96.   Savignac HM, Tramullas M, Kiely B, Dinan TG, Cryan JF. Bifidobacteria modulate cognitive processes in an anxious mouse strain. *Behavioural brain research* 2015, **287:** 59-72.

97.   Smith CJ, Emge JR, Berzins K, Lung L, Khamishon R, Shah P*, et al.* Probiotics normalize the gut-brain-microbiota axis in immunodeficient mice. *American journal of physiology Gastrointestinal and liver physiology* 2014, **307**(8)**:** G793-802.

98.   Wang T, Hu X, Liang S, Li W, Wu X, Wang L*, et al.* Lactobacillus fermentum NS9 restores the antibiotic induced physiological and psychological abnormalities in rats. *Beneficial microbes* 2015, **6**(5)**:** 707-717.

99.   Fasano A, Visanji NP, Liu LW, Lang AE, Pfeiffer RF. Gastrointestinal

dysfunction in Parkinson's disease. *The Lancet Neurology* 2015, **14**(6)**:** 625-639.

100.   Shannon KM, Keshavarzian A, Mutlu E, Dodiya HB, Daian D, Jaglin JA*, et

al.* Alpha-synuclein in colonic submucosa in early untreated Parkinson's disease.

Movement disorders : official journal of the Movement Disorder Society 2012,

27(6)**:** 709-715.

101.   Scheperjans F, Aho V, Pereira PA, Koskinen K, Paulin L, Pekkonen E*, et

al.* Gut microbiota are related to Parkinson's disease and clinical phenotype.

Movement disorders : official journal of the Movement Disorder Society 2015,

30(3)**:** 350-358.

102.   Keshavarzian A, Green SJ, Engen PA, Voigt RM, Naqib A, Forsyth CB*, et

al.* Colonic bacterial composition in Parkinson's disease. *Movement disorders :

official journal of the Movement Disorder Society* 2015, **30**(10)**:** 1351-1360.

103.   Devos D, Lebouvier T, Lardeux B, Biraud M, Rouaud T, Pouclet H*, et al.*

Colonic inflammation in Parkinson's disease. *Neurobiology of disease* 2013, **50:**

42-48.

104.   Forsyth CB, Shannon KM, Kordower JH, Voigt RM, Shaikh M, Jaglin JA*,

et al.* Increased intestinal permeability correlates with sigmoid mucosa alpha-

synuclein staining and endotoxin exposure markers in early Parkinson's disease. *PloS one* 2011, **6**(12)**:** e28032.

105.   Claesson MJ, Jeffery IB, Conde S, Power SE, O'Connor EM, Cusack S*, et al.* Gut microbiota composition correlates with diet and health in the elderly. *Nature* 2012, **488**(7410)**:** 178-184.

106.   Spor A, Koren O, Ley R. Unravelling the effects of the environment and host genotype on the gut microbiome. *Nature reviews Microbiology* 2011, **9**(4)**:** 279-290.

107.   Yatsunenko T, Rey FE, Manary MJ, Trehan I, Dominguez-Bello MG, Contreras M*, et al.* Human gut microbiome viewed across age and geography. *Nature* 2012, **486**(7402)**:** 222-227.

108.   Claesson MJ, Cusack S, O'Sullivan O, Greene-Diniz R, de Weerd H, Flannery E*, et al.* Composition, variability, and temporal stability of the intestinal microbiota of the elderly. *Proceedings of the National Academy of Sciences of the United States of America* 2011, **108 Suppl 1:** 4586-4591.

109.   Crack PJ, Bray PJ. Toll-like receptors in the brain and their potential roles in neuropathology. *Immunology and cell biology* 2007, **85**(6)**:** 476-480.

110. van Noort JM, Bsibsi M. Toll-like receptors in the CNS: implications for neurodegeneration and repair. *Progress in brain research* 2009, **175:** 139-148.

111. Brenchley JM, Douek DC. Microbial translocation across the GI tract. *Annual review of immunology* 2012, **30:** 149-173.

112. Chakravarty S, Herkenham M. Toll-like receptor 4 on nonhematopoietic cells sustains CNS inflammation during endotoxemia, independent of systemic cytokines. *The Journal of neuroscience : the official journal of the Society for Neuroscience* 2005, **25**(7)**:** 1788-1796.

113. Qin L, Wu X, Block ML, Liu Y, Breese GR, Hong JS*, et al.* Systemic LPS causes chronic neuroinflammation and progressive neurodegeneration. *Glia* 2007, **55**(5)**:** 453-462.

114. Jespersen S, Pedersen KK, Anesten B, Zetterberg H, Fuchs D, Gisslen M*, et al.* Soluble CD14 in cerebrospinal fluid is associated with markers of inflammation and axonal damage in untreated HIV-infected patients: a retrospective cross-sectional study. *BMC infectious diseases* 2016, **16**(1)**:** 176.

115. Rothhammer V, Mascanfroni ID, Bunse L. Type I interferons and microbial metabolites of tryptophan modulate astrocyte activity and central nervous system inflammation via the aryl hydrocarbon receptor. 2016.

116.   Koh A, De Vadder F, Kovatcheva-Datchary P, Backhed F. From Dietary Fiber to Host Physiology: Short-Chain Fatty Acids as Key Bacterial Metabolites. *Cell* 2016, **165**(6)**:** 1332-1345.

117.   Rooks MG, Garrett WS. Gut microbiota, metabolites and host immunity. *Nature reviews Immunology* 2016, **16**(6)**:** 341-352.

118.   Louveau A, Smirnov I, Keyes TJ, Eccles JD, Rouhani SJ, Peske JD*, et al.* Structural and functional features of central nervous system lymphatic vessels. *Nature* 2015, **523**(7560)**:** 337-341.

119.   Berger M, Gray JA, Roth BL. The expanded biology of serotonin. *Annual review of medicine* 2009, **60:** 355-366.

120.   Gershon MD, Tack J. The serotonin signaling system: from basic understanding to drug development for functional GI disorders. *Gastroenterology* 2007, **132**(1)**:** 397-414.

121.   Sjogren K, Engdahl C, Henning P, Lerner UH, Tremaroli V, Lagerquist MK*, et al.* The gut microbiota regulates bone mass in mice. *Journal of bone and mineral research : the official journal of the American Society for Bone and Mineral Research* 2012, **27**(6)**:** 1357-1367.

122. Wikoff WR, Anfora AT, Liu J, Schultz PG, Lesley SA, Peters EC*, et al.* Metabolomics analysis reveals large effects of gut microflora on mammalian blood metabolites. *Proceedings of the National Academy of Sciences of the United States of America* 2009, **106**(10)**:** 3698-3703.

123. Yano JM, Yu K, Donaldson GP, Shastri GG, Ann P, Ma L*, et al.* Indigenous bacteria from the gut microbiota regulate host serotonin biosynthesis. *Cell* 2015, **161**(2)**:** 264-276.

124. Reigstad CS, Salmonson CE, Rainey JF, 3rd, Szurszewski JH, Linden DR, Sonnenburg JL*, et al.* Gut microbes promote colonic serotonin production through an effect of short-chain fatty acids on enterochromaffin cells. *FASEB journal : official publication of the Federation of American Societies for Experimental Biology* 2015, **29**(4)**:** 1395-1403.

125. Baganz NL, Blakely RD. A dialogue between the immune system and brain, spoken in the language of serotonin. *ACS chemical neuroscience* 2013, **4**(1)**:** 48-63.

126. Atarashi K, Tanoue T, Oshima K, Suda W, Nagano Y, Nishikawa H*, et al.* Treg induction by a rationally selected mixture of Clostridia strains from the human microbiota. *Nature* 2013, **500**(7461)**:** 232-236.

127.   Furusawa Y, Obata Y, Fukuda S, Endo TA, Nakato G, Takahashi D*, et al.* Commensal microbe-derived butyrate induces the differentiation of colonic regulatory T cells. *Nature* 2013, **504**(7480)**:** 446-450.

128.   Smith PM, Howitt MR, Panikov N, Michaud M, Gallini CA, Bohlooly YM*, et al.* The microbial metabolites, short-chain fatty acids, regulate colonic Treg cell homeostasis. *Science* 2013, **341**(6145)**:** 569-573.

129.   Borovikova LV, Ivanova S, Zhang M, Yang H, Botchkina GI, Watkins LR*, et al.* Vagus nerve stimulation attenuates the systemic inflammatory response to endotoxin. *Nature* 2000, **405**(6785)**:** 458-462.

130.   van der Kleij H, O'Mahony C, Shanahan F, O'Mahony L, Bienenstock J. Protective effects of Lactobacillus rhamnosus [corrected] and Bifidobacterium infantis in murine models for colitis do not involve the vagus nerve. *American journal of physiology Regulatory, integrative and comparative physiology* 2008, **295**(4)**:** R1131-1137.

131.   Ait-Belgnaoui A, Durand H, Cartier C, Chaumaz G, Eutamene H, Ferrier L*, et al.* Prevention of gut leakiness by a probiotic treatment leads to attenuated HPA response to an acute psychological stress in rats. *Psychoneuroendocrinology* 2012, **37**(11)**:** 1885-1895.

132.   Demaude J, Salvador-Cartier C, Fioramonti J, Ferrier L, Bueno L. Phenotypic changes in colonocytes following acute stress or activation of mast cells in mice: implications for delayed epithelial barrier dysfunction. *Gut* 2006, **55**(5)**:** 655-661.

133.   Lennon EM, Maharshak N, Elloumi H, Borst L, Plevy SE, Moeser AJ. Early life stress triggers persistent colonic barrier dysfunction and exacerbates colitis in adult IL-10-/- mice. *Inflammatory bowel diseases* 2013, **19**(4)**:** 712-719.

134.   Moussaoui N, Braniste V, Ait-Belgnaoui A, Gabanou M, Sekkal S, Olier M*, et al.* Changes in intestinal glucocorticoid sensitivity in early life shape the risk of epithelial barrier defect in maternal-deprived rats. *PloS one* 2014, **9**(2)**:** e88382.

135.   Smith F, Clark JE, Overman BL, Tozel CC, Huang JH, Rivier JE*, et al.* Early weaning stress impairs development of mucosal barrier function in the porcine intestine. *American journal of physiology Gastrointestinal and liver physiology* 2010, **298**(3)**:** G352-363.

136.   Gue M, Junien JL, Bueno L. Conditioned emotional response in rats enhances colonic motility through the central release of corticotropin-releasing factor. *Gastroenterology* 1991, **100**(4)**:** 964-970.

137. Gue M, Peeters T, Depoortere I, Vantrappen G, Bueno L. Stress-induced changes in gastric emptying, postprandial motility, and plasma gut hormone levels in dogs. *Gastroenterology* 1989, **97**(5)**:** 1101-1107.

138. Rubio CA, Huang CB. Quantification of the sulphomucin-producing cell population of the colonic mucosa during protracted stress in rats. *In vivo (Athens, Greece)* 1992, **6**(1)**:** 81-84.

139. Da Silva S, Robbe-Masselot C, Ait-Belgnaoui A, Mancuso A, Mercade-Loubiere M, Salvador-Cartier C*, et al.* Stress disrupts intestinal mucus barrier in rats via mucin O-glycosylation shift: prevention by a probiotic treatment. *American journal of physiology Gastrointestinal and liver physiology* 2014, **307**(4)**:** G420-429.

140. Park AJ, Collins J, Blennerhassett PA, Ghia JE, Verdu EF, Bercik P*, et al.* Altered colonic function and microbiota profile in a mouse model of chronic depression. *Neurogastroenterology and motility : the official journal of the European Gastrointestinal Motility Society* 2013, **25**(9)**:** 733-e575.

141. Hueston CM, Deak T. The inflamed axis: the interaction between stress, hormones, and the expression of inflammatory-related genes within key structures comprising the hypothalamic-pituitary-adrenal axis. *Physiology & behavior* 2014, **124:** 77-91.

142.   Tillisch K, Labus J, Kilpatrick L, Jiang Z, Stains J, Ebrat B*, et al.*

Consumption of fermented milk product with probiotic modulates brain activity.

Gastroenterology 2013, **144**(7)**:** 1394-1401, 1401.e1391-1394.

143.   Messaoudi M, Lalonde R, Violle N, Javelot H, Desor D, Nejdi A*, et al.*

Assessment of psychotropic-like properties of a probiotic formulation

(Lactobacillus helveticus R0052 and Bifidobacterium longum R0175) in rats and

human subjects. *The British journal of nutrition* 2011, **105**(5)**:** 755-764.

144.   Ahluwalia V, Wade JB, Heuman DM, Hammeke TA, Sanyal AJ, Sterling

RK*, et al.* Enhancement of functional connectivity, working memory and inhibitory

control on multi-modal brain MR imaging with Rifaximin in Cirrhosis: implications

for the gut-liver-brain axis. *Metabolic brain disease* 2014, **29**(4)**:** 1017-1025.

145.   Ranjan A, Praharaj SK. Ciprofloxacin-induced psychosis. *The Journal of

neuropsychiatry and clinical neurosciences* 2014, **26**(1)**:** E36-37.

146.   Gomez-Pinilla F. Brain foods: the effects of nutrients on brain function.

Nature reviews Neuroscience 2008, **9**(7)**:** 568-578.

147.   Stafstrom CE, Rho JM. The ketogenic diet as a treatment paradigm for

diverse neurological disorders. *Frontiers in pharmacology* 2012, **3:** 59.

148.   Macia L, Tan J, Vieira AT, Leach K, Stanley D, Luong S*, et al.* Metabolite-sensing receptors GPR43 and GPR109A facilitate dietary fibre-induced gut homeostasis through regulation of the inflammasome. *Nature communications* 2015, **6:** 6734.

149.   Smith MI, Yatsunenko T, Manary MJ, Trehan I, Mkakosya R, Cheng J*, et al.* Gut microbiomes of Malawian twin pairs discordant for kwashiorkor. *Science* 2013, **339**(6119)**:** 548-554.

150.   Turnbaugh PJ, Ley RE, Mahowald MA, Magrini V, Mardis ER, Gordon JI. An obesity-associated gut microbiome with increased capacity for energy harvest. *Nature* 2006, **444**(7122)**:** 1027-1031.

Chapter 5

The gut microbiota mediates the anti-seizure effects of the ketogenic diet in mice

Christine A. Olson, Helen E. Vuong, Jessica M. Yano, Qingxing Y. Liang, David J. Nusbaum, and Elaine Y. Hsiao

SUMMARY

The ketogenic diet (KD) is used to treat refractory epilepsy and an increasing number of medical conditions, but the specific mechanisms underlying its neuroprotective effects remain unclear. Here we show that the gut microbiota is altered by the KD and is required for protection against acute electrically-induced seizures and spontaneous tonic-clonic seizures in two mouse models. Depletion of the microbiota via antibiotic treatment or germ-free rearing abrogates the seizure protective effects of the KD. Both enrichment of, and gnotobiotic co-colonization with, the KD-associated bacteria *Akkermansia muciniphila*, *Parabacteroides merdae* and *P. distasonis* mediate the anti-seizure effects of the KD. Moreover, transplantation of the KD gut microbiota and bacterial treatment with *A. muciniphila* and *Parabacteroides* spp. each confer seizure protection to mice fed a control diet. KD- and microbiota-dependent alterations in colonic lumenal, serum and hippocampal metabolomic profiles correlate with seizure protection, including systemic reductions in gamma-glutamylated ketogenic amino acids and elevated hippocampal GABA/glutamate ratios. Cross-feeding between *A. muciniphila* and *Parabacteroides* spp. decreases bacterial gamma-glutamyltranspeptidase activity, and inhibiting amino acid gamma-glutamylation promotes seizure protection *in vivo*. Overall, this study reveals a novel role for specific gut bacterial interactions in modulating host metabolism and seizure susceptibility in mice.

HIGHLIGHT

- Alterations in the gut microbiota are required for the anti-seizure effects of the KD.

- Specific KD-associated bacteria sufficiently restore and confer anti-seizure effects of the KD.

- The KD microbiota regulates amino acid g-glutamylation and hippocampal GABA/glutamate.

INTRODUCTION

The low-carbohydrate, high-fat ketogenic diet (**KD**) is an effective treatment for refractory epilepsy, a condition affecting more than one-third of epileptic individuals and defined by a failure to respond to existing anticonvulsant medications (Kwan and Brodie, 2000). However, despite its value for treating epilepsy and its increasing application to other disorders, including autism spectrum disorder, Alzheimer's disease, metabolic syndrome and cancer (Stafstrom and Rho, 2012), use of the KD remains low due to difficulties with implementation, dietary compliance and adverse side effects (Freeman and Kossoff, 2010). Molecular targets are needed to develop viable clinical interventions for intractable epilepsy and other disorders for which the KD is beneficial. Many studies have proposed roles for ketone bodies, gamma-aminobutyric acid (**GABA**) modulation, and mitochondrial anaplerosis in mediating the neurological effects of the KD (Rogawski et al., 2016), but exactly how the KD confers beneficial effects on brain activity and behavior remains unclear.

The gut microbiota is a key intermediary between diet and host physiology; the species composition and function of the gut microbiota is critically shaped by diet (Xu and Knight, 2015), and nutrients made available to the host depend on microbial metabolism (Sonnenburg and Backhed, 2016). Diet-induced changes in the gut microbiota are reproducible and persistent (David et al., 2014), and as such, have lasting impacts on the host. Several diet-induced host pathologies are mediated by changes in the gut microbiota in mouse models, including symptoms of atherosclerosis in response to the carnitine-rich diet, undernutrition in response to the Malawian diet and abnormal social behavior in response to maternal high-fat diet (Buffington et al., 2016; Koeth et al., 2013; Smith et al., 2013).

The gut microbiota modulates several metabolic and neurological pathways in the host that could be relevant to KD-mediated seizure protection. The KD alters the composition of the gut microbiota in mice (Klein et al., 2016a; Newell et al., 2016), and ketosis is associated with altered gut microbiota in humans (David et al., 2014; Duncan et al., 2008). Interestingly, fasted mice that lack microbiota exhibit impaired hepatic ketogenesis and altered myocardial ketone metabolism compared to fasted mice that are conventionally-colonized (Crawford et al., 2009). The microbiota is also increasingly associated with changes in factors relevant to neurotransmission, including neurotransmitter signaling, synaptic protein expression, long term-potentiation and myelination (Vuong et al., 2017), as well as a variety of complex host behaviors, including stress-induced, social and cognitive behaviors (Collins et al., 2012; Sandhu et al., 2017; Vuong et al., 2017). Notably, several clinical studies report that antibiotic treatment increases risk of status epilepticus or symptomatic seizures in epileptic

individuals (Sutter et al., 2015), suggesting a possible role for the microbiota in mitigating seizure likelihood.

Based on emerging studies linking the gut microbiota to host responses to diet, metabolism, neural activity and behavior, we hypothesized that the gut microbiota plays an important role in mediating the anti-seizure effects of the KD. We aimed to characterize how the microbiota is altered by the KD, to determine whether the microbiota contributes to the anti-seizure effects of the KD and to further identify molecular and cellular mechanisms that may be involved. We show herein that the gut microbiota is necessary and sufficient for seizure protection in two mouse models of intractable epilepsy, and further identify cooperative interactions between two diet-associated bacteria that regulate levels of circulating dietary metabolites, brain neurotransmitters, and seizure incidence in mice. Findings from this study reveal that the gut microbiota modulates seizure susceptibility and suggests that metabolic functions of specific gut bacteria may be important for mediating the anti-seizure effects of the ketogenic diet.

RESULTS

The Ketogenic Diet Alters the Gut Microbiota

The KD reduces seizure susceptibility and confers neuroprotective effects in several mouse models of epilepsy (Lutas and Yellen, 2013). To test whether the microbiota

plays a role in KD-mediated seizure protection, we first utilize the 6-Hz induced

psychomotor seizure model of refractory epilepsy. The 6-Hz model involves low-

frequency corneal stimulation to induce complex partial seizures reminiscent of human

temporal lobe epilepsy (Hartman et al., 2008). Importantly, the 6-Hz model is resistant

to several anti-epileptic drugs and, as such, is widely used as a model of refractory

epilepsy for investigational drug screening (Barton et al., 2001). The KD protects

against 6-Hz seizures (Hartman et al., 2010; Samala et al., 2008), as indicated by the

increased current intensity required to elicit a seizure in 50% of the subjects tested

(**CC50**, seizure threshold).

We fed conventionally-colonized (specific pathogen-free, **SPF**) Swiss Webster mice a

6:1 fat:protein KD or a vitamin- and mineral-matched control diet (**CD**) (Samala et al.,

2008) (**Figure S2A and Table S1**). Compared to CD controls, mice fed the KD exhibit

elevated seizure thresholds in response to 6-Hz stimulation (**Figure 1A**), decreased

serum glucose (**Figure 1B**) and increased serum β-hydroxybutyrate (**BHB; Figure 1C,

right**), as previously described (Hartman et al., 2010; Samala et al., 2008). There were

no significant differences in food consumption or weight gain across CD vs. KD groups

(**Figure S2B**).

In addition to raising seizure thresholds, the KD alters the composition of the gut

microbiota (**Figure 1D and Table S2**), as measured by 16S rDNA sequencing, where

fecal samples from independent cages of mice reveal substantial shifts in microbiota

profiles based on weighted and unweighted UniFrac distance matrices, by 4 days and

through 14 days post-dietary treatment (**Figure 1D** and **Table S2**). Decreased alpha

diversity is observed at each time point post-dietary treatment (**Figure 1E**) suggesting

KD-induced losses of particular bacterial taxa. Notably, the KD substantially increases

the relative abundance of *Akkermansia muciniphila*, from 2.8 ± 0.4% to 36.3 ± 2.8%

(mean ± SEM), by 4 days and through 14 days of dietary treatment (**Figures 1F, S1A

and S1B**). *Parabacteroides*, *Sutterella* and Erysipelotrichaceae spp. are also

significantly increased in KD-fed mice, whereas *Allobaculum*, *Bifidobacterium* and

Desulfovibrio spp. are increased in CD-fed mice (**Figures 1F, S1A and S1B)**. While

there is minor temporal variation in bacterial taxonomic membership after dietary

treatment, shifts the microbiota remain through 28 days on the KD vs CD (**Figure S4A**).

Imputed metagenomes predict KD-induced changes in microbial genes relevant for lipid

and protein metabolism, suggesting that the KD alters these microbial metabolic

pathways (**Table S3 and Figure S7**). These results reveal that the composition of the

gut microbiota is rapidly and significantly altered in response to the KD.

The Gut Microbiota is Necessary and Sufficient for the Anti-Seizure Effects of the

KD

To determine whether the gut microbiota is necessary for the anti-seizure effects of the

KD, we measured the 6-Hz psychomotor seizure threshold for germ-free (**GF**) and

antibiotic (**Abx**)-treated SPF mice. Compared to CD controls (SPF CD), SPF mice fed

the KD (SPF KD) for 14 days exhibit increased seizure thresholds and altered

microbiota (**Figures 2A and 1D**). This is abrogated in GF mice (**Figure 2C**) and Abx-

treated SPF mice (**Figure 2C**), indicating that the gut microbiota is required for KD-

mediated increases in seizure protection. Conventionalization of GF mice with the SPF

gut microbiota restores KD-associated seizure protection to levels seen in native SPF

KD mice (**Figure 2A**), suggesting that microbial mediation of KD seizure resistance is

not dependent on pre-weaning microbiota colonization and that the microbiota actively

mediates seizure protection by the KD. Notably, microbial modulation of KD-related

seizure resistance does not correlate with changes in serum BHB or glucose levels

(**Figures 2B and 2D**). There are also no significant differences between groups in

levels of intestinal, liver, or brain BHB (**Figures S2C and S2E**). Consistent with this,

previous studies report that BHB concentrations do not necessarily correlate with

seizure protection, and ketosis may be necessary but not sufficient for KD-mediated

seizure control (Bough and Rho, 2007). Overall, these data demonstrate that the gut

microbiota is required for anti-seizure effects of the KD in the 6-Hz seizure model and

further suggest that gut microbes modulate seizure susceptibility through mechanisms

that do not involve alterations in BHB levels.

To determine whether specific bacterial taxa mediate seizure protection in response to

the KD, Abx-treated SPF mice were colonized with select KD-associated bacteria, fed

the KD and then tested for 6-Hz seizures. Based on results from 16S rDNA sequencing

(**Figure S1C**), *A. muciniphila* and *Parabacteroides* spp. were selected as the taxa most

highly enriched by the KD. Mice were gavaged with 10^9 cfu bacteria: i) *A. muciniphila*; ii)

1:1 ratio of *Parabacteroides merdae* and *P. distasonis*, as representative intestinal

Parabacteroides spp. from the human microbiota with highest homology to the

Parabacteroides operational taxonomic unit reads that were enriched by the KD (**Figure

1D and Table S2**); or iii) 2:1:1 ratio of *A. muciniphila*, *P. merdae* and *P. distasonis*. At

14 days after oral gavage, 16S rDNA sequencing of colonic lumenal contents revealed that mice treated with *A. muciniphila* harbored 43.7 ± 0.4% relative abundance of *A. muciniphila* (**Figure S3A**). Mice gavaged with *Parabacteroides* spp. harbored 70.9 ± 4.0% relative abundance, and mice gavaged with both taxa harbored 49.0 ± 4.1% *A. muciniphila* and 22.5 ± 5.4% *Parabacteroides*. Consistent with this, fluorescence *in situ* hybridization (FISH) staining of colonic sections from mice treated with *A. muciniphila* and *Parabacteroides* spp. exhibit increased hybridization of the *A. muciniphila* probe MUC1437 (Derrien et al., 2008) and the *Bacteroides* and *Parabacteroides* spp. probe BAC303 (Manz et al., 1996) (**Figure 3B**), where the average distance from a BAC303-positive cell to the nearest MUC1437-positive cell is 0.64 ± 0.09 microns. Consistent with previous reports, both *A. muciniphila* and *Parabacteroides* spp. localized to the lumen of the mouse colon, not the mucus layer (Earle et al., 2015). There were no significant differences in weight, serum glucose levels, or enrichment of *A. muciniphila* and *Parabacteroides* spp. across mice fed CD vs. KD (**Figures S3A-S3C**). Consistent with our previous observation (**Figures 2B, 2D**), BHB was similarly induced in KD-fed groups, independent of colonization status (**Figure S3C**). These data reveal that microbiota depletion by Abx treatment followed by oral gavage of exogenous bacteria results in their persistent intestinal enrichment by 14 days post-inoculation.

We next examined seizure susceptibility in mice with selective enrichment of KD-associated gut bacteria. Treatment with the KD alone elevated seizure thresholds by 24.5% from 19.4 ± 0.8 mA, in SPF CD mice, to 24.2 ± 0.3 mA, in SPF KD mice (Figure 3A), whereas Abx treatment of KD-fed mice prevented this anti-seizure effect (**Figure**

3A). Co-administration of *A. muciniphila* and *Parabacteroides* spp. restores protection against 6-Hz seizures in Abx-treated mice fed the KD, raising thresholds by 36.0%, from 19.9 ± 0.3 mA, in Abx KD mice, to 27.0 ± 0.5 mA, in AkkPb KD mice (**Figure 3A**). The seizure protective effect of bacterial enrichment is specific to *A. muciniphila* with *P. merdae*, as mice gavaged with *A. muciniphila* and *P. distasonis* exhibited no restoration of seizure protection (**Figure S3D**). There is no significant increase in seizure threshold after enrichment of either *A. muciniphila* or *Parabacteroides* spp. alone (**Figure 3A**), indicating that both taxa are required for mediating the anti-seizure effects of the KD. There is also no effect of treatment with *Bifidobacterium longum* (**Figure 3A**), as a negative control taxon that was enriched in CD-fed mice (**Figures 1F and S1C**). Moreover, co-colonization of *A. muciniphila* and *Parabacteroides* spp. in GF mice promotes seizure protection in response to the KD, when compared to GF, *Parabacteroides*-monocolonized or *A. muciniphila*-monocolonized mice (**Figure 3C**), suggesting that *A. muciniphila* and *Parabacteroides* spp together raise seizure thresholds in the absence of other indigenous gut microbes. Overall, these findings reveal that *A. muciniphila* and *Parabacteroides* spp. increase in response to the KD and mediate its protective effect in the 6-Hz seizure model.

The Gut Microbiota Confers Seizure Protection to Mice Fed the CD

The previous experiments examine microbial mediation of seizure protection in mice fed the KD. To determine whether KD-associated gut microbes also confer anti-seizure effects to mice fed the CD, Abx-treated mice were transplanted with CD vs. KD

183

microbiota from SPF mice, fed the CD or KD and tested for their susceptibility to 6-Hz

seizures after 4 days of dietary treatment. Abx-treated mice were used to mimic clinical

fecal transplant approaches that involve pre-treatment with Abx to deplete the native

microbiota (Seekatz et al., 2014). Day 4 was selected based on i) the ability of the KD to

induce significant microbiota changes by that time (**Figures 1D-1F and 4A**) and ii)

evidence that the KD microbiota exhibits incomplete reversion to CD profiles at 4 days

after switching from KD to CD (**Figure S4A**). Mice transplanted with a CD microbiota

and fed KD for 4 days display increased seizure threshold compared to CD-fed controls

(**Figure 4A**). Abx-treated mice transplanted with a KD microbiome but fed CD for 4 days

exhibit seizure protection as well, suggesting that colonization with the KD microbiota

raises seizure thresholds in mice fed CD. Notably, however, seizure protection is

abrogated after complete reversion of the KD microbiota to CD profiles on day 28

(**Figure S4B**), suggesting that persistent interactions between the KD microbiota, diet

and neuronal activity are required. Similar anti-seizure effects are seen after enriching

A. muciniphila and *Parabacteroides* spp. in Abx-treated SPF mice fed CD as compared

to *Parabacteroides* spp., *A. muciniphila* or *B. longum* controls (**Figure 4B and S3A**).

However, increases in seizure threshold in SPF CD mice treated with Abx alone relative

to SPF CD controls confound interpretation of these results (**Figure 4B**).

To clarify this uncertainty, we applied a bacterial treatment approach to investigate

whether exogenous treatment with *A. muciniphila* and *Parabacteroides* spp. confers

anti-seizure effects in mice fed CD. SPF CD mice were gavaged bi-daily for 28 days

with 10^9 cfu *A. muciniphila* and *Parabacteroides* spp. or with vehicle. This bacterial

treatment increased seizure thresholds relative to vehicle-gavaged controls (**Figure 4C**). Consistent with our experiments on mice fed the KD (**Figure 3**), this seizure protection is not observed in animals treated with *A. muciniphila* alone, revealing that co-administration of *A. muciniphila* and *Parabacteroides* spp. is required for seizure protection (**Figure 4C**). Moreover, treatment with heat-killed bacteria decreases seizure thresholds compared to vehicle-treated controls, suggesting that viable bacteria are necessary for conferring anti-seizure effects and release of bacterial cell surface and/or intracellular factors promotes sensitivity to 6-Hz seizures. Persistent exposure to *A. muciniphila* and *Parabacteroides* spp. is required, as increases in seizure thresholds were lost after ceasing treatment for 21 days (**Figure S4C**). In addition, seizure protection was not observed in mice treated for only 4 days (**Figure S4D**), suggesting that long-term exposure is required. Taken together, these findings reveal that fecal transplant of the KD microbiota and bacterial treatment with the KD-associated taxa *A. muciniphila* and *Parabacteroides* spp. confer protection against 6-Hz psychomotor seizures in mice fed the CD.

KD-Associated Bacteria Reduce Tonic-Clonic Seizures in *Kcna1*^{-/-} Mice

Epilepsy is a heterogeneous disorder with diverse clinical presentations. The 6-Hz seizure model for pharmacoresistant epilepsy examines acute, electrically-induced seizures and is widely used for testing the efficacy of the KD (Hartman et al., 2010; Samala et al., 2008) and new anti-epileptic drugs (Barton et al., 2001). While a powerful tool for studying fundamental influences on seizure susceptibility, the model exhibits low

construct validity for human epilepsy and conveys limited information on seizure severity and form. In addition, despite statistically significant effects of the KD on raising seizure thresholds in the 6-Hz model, the effect sizes are relatively small for treatments known to be efficacious in humans. To determine whether our findings from the 6-Hz model also apply to different seizure types and etiologies, we further tested roles for the microbiota in modulating generalized tonic-clonic seizures in the $Kcna1^{-/-}$ mouse model for temporal lobe epilepsy and sudden unexpected death in epilepsy (**SUDEP**). $Kcna1^{-/-}$ mice harbor a null mutation in the voltage-gated potassium channel Kv1.1 alpha subunit, mimicking associations of human *KCNA1* gene variants with epilepsy, episodic ataxia and SUDEP (Browne et al., 1994; Eunson et al., 2000; Scheffer et al., 1998; Zuberi et al., 1999). $Kcna1^{-/-}$ mice develop severe spontaneous recurrent seizures, which are reduced 54% by the KD (Fenoglio-Simeone et al., 2009).

$Kcna1^{-/-}$ SPF C3HeB/FeJ mice were treated with Abx or vehicle for 1 week, gavaged with vehicle or *A. muciniphila* and *Parabacteroides* spp., and fed KD or CD for 3 weeks. Seizure frequency and duration were recorded by EEG over 3 days, where electrographic seizures were identified based on characteristic epileptiform spike patterns consisting of 5 phases (**Figure 5C**): A) low-frequency background, with low-voltage spiking, B) synchronized high-frequency, high-voltage spiking, C) high-frequency, low-voltage spiking, D) unsynchronized high-frequency, high-voltage spiking, and E) high-frequency, burst spiking. Furthermore, EEG seizure patterns were corroborated by detection of stereotyped seizure behaviors identified by 5 stages as previously described (Simeone et al., 2016) (**Supplementary Video 1**). Compared to

CD-fed *Kcna1*^{-/-} controls, KD-fed *Kcna1*^{-/-} mice exhibit altered gut microbiota profiles (**Figure 5A**). Consistent with findings from the 6-Hz seizure model (**Figure 1F**), the KD significantly increases both *A. muciniphila* and *Parabacteroides* spp. in *Kcna1*^{-/-} mice. The degree of diet-induced enrichment of these taxa is less than that seen in the 6-Hz model (**Figure 1F**), which could be due to an effect of host genotype and mouse strain on baseline microbiota composition and responses to KD (Klein et al., 2016b). Nonetheless, we observed decreases in seizure incidence and duration in KD-fed *Kcna1*^{-/-} mice compared to CD-fed *Kcna1*^{-/-} controls (**Figure 5D**), consistent with KD-mediated seizure protection as previously described (Fenoglio-Simeone et al., 2009). Interestingly, *Kcna1*^{-/-} mice that were pre-treated with Abx to deplete the gut microbiota exhibit a significant increase in seizures per day and total seizure duration compared to vehicle-treated, KD-fed *Kcna1*^{-/-} controls (**Figure 5D**). There is no significant difference in interspike frequency, interspike interval, and average duration per seizure (**Figure S5C**) suggesting a primary effect of Abx treatment and depletion of the gut microbiota on spontaneous seizure occurrence rather than seizure form. Moreover, colonization of Abx-treated *Kcna1*^{-/-} mice with *A. muciniphila* and *Parabacteroides* spp. reduces seizure frequency and total duration of seizures toward levels seen in vehicle-treated, KD-fed *Kcna1*^{-/-} controls (**Figure 5D**). This suggests that treatment with *A. muciniphila* and *Parabacteroides* spp. similarly confers seizure protection in the Kcna1-/- SUDEP model, as well as the WT 6-Hz seizure model. There were no significant differences in weight gain or food consumption between mice fed the KD vs. CD (**Figure S5A**). In contrast to a previous report that used a different KD formulation (Simeone et al., 2016), we observed no differences in survival across groups (**Figure S5B**). Taken together, these

findings support the notion that the gut microbiota mediates the anti-seizure effects of the KD across varied seizure types and mouse models.

The Microbiota Modulates Gut, Serum and Brain Metabolomes

Based on the role of the gut microbiota in modulating effects of the KD on seizure occurrence, we hypothesized that microbial dietary metabolism regulates secondary metabolites that impact seizure susceptibility. We utilized metabolomic profiling to identify candidate microbiota-dependent molecules in colonic lumenal contents and sera of SPF mice fed CD, and SPF, Abx-treated SPF, and *A. muciniphila*- and *Parabacteroides* spp.-enriched mice fed KD (**Figures 6A and S6A**). 622 metabolites, spanning amino acid, carbohydrate, lipid, nucleotide, peptide and xenobiotic supergroups, were detected in mouse colonic contents, and 670 metabolites were detected in mouse sera (**Tables S4 and S5**). Metabolomic profiles in colonic lumenal contents and sera discriminate seizure-protected (vehicle-treated SPF mice fed KD and *A. muciniphila* with *Parabacteroides* spp.– enriched mice fed KD) from seizure-susceptible (vehicle-treated SPF mice fed CD and Abx-treated SPF mice fed KD) groups, with a predictive accuracy of 94% for colonic lumenal metabolites and 87.5% for serum metabolites (**Figure 6B**). Interestingly, the majority of metabolites that contribute highly to group discrimination are relevant to amino acid metabolism, including derivatives of lysine, tyrosine and threonine (**Figure 6B**). In addition, we observed widespread decreases in subsets of ketogenic gamma-glutamylated amino acids— gamma-glutamyl (GG)-leucine, GG-lysine, GG-threonine, GG-tryptophan and GG-tyrosine— in both colonic lumenal contents (**Figure 6C**) and sera (**Figure 6D**) from

188

seizure-protected compared to seizure-susceptible groups. Gamma-glutamylated forms

of the amino acids were particularly affected (**Figures 6C and 6D**), as compared to their

unmodified counterparts (**Figures S6D and S6E**). This suggests that the gut microbiota

modulates gamma-glutamylation itself or selective metabolism of ketogenic GG-amino

acids and that increased ketogenic GG-amino acids are associated with seizure

susceptibility. Supporting this notion, imputed metagenomes predict KD-associated

alterations in bacterial genes relevant to amino acid metabolism (**Figure S7C**). Overall,

these findings reveal significant effects of the gut microbiota on intestinal and systemic

metabolomic responses to the KD, and further reveal an association between KD-

induced seizure protection and microbiota-dependent alterations in levels of ketogenic

GG-amino acids.

The brain relies on active import of essential amino acids to fuel neurotransmitter

biosynthesis, and as such, is sensitive to fluctuations in peripheral amino acid

bioavailability (Smith, 2000). Peripheral amino acids serve as substrates for the

synthesis of GABA and glutamate through anaplerotic refilling of Kreb's cycle

intermediates, or indirectly through carbon dioxide fixation stimulated by

hyperammonemia (Cooper and Jeitner, 2016). GG-amino acids, in particular, are

hypothesized to exhibit increased transport properties compared to non-gamma-

glutamylated forms (Castellano and Merlino, 2012; Sakai et al., 2004). Based on our

data revealing diet- and microbiota-dependent alterations in serum ketogenic amino

acids, links between amino acids importation and brain GABA levels (Samuels et al.,

1983; Yudkoff et al., 2001b), and prevailing theories that GABA contributes to the anti-

189

seizure effects of the KD (Bough, 2008; Calderon et al., 2017; Yudkoff et al., 2001a), we examined bulk levels of GABA and glutamate in the brain. Though many brain regions contribute to seizure activity, we focused specifically on the hippocampus, based on existing literature demonstrating its key involvement in the propagation of seizure activity across several seizure models (Gautier and Glasscock, 2015; Giordano et al., 2016). In particular, abnormal hippocampal activation is seen in the 6-Hz seizure model, and *Kcna1*^{-/-} mice exhibit abnormal hippocampal electrical discharge and cell loss (Lopantsev et al., 2003; Wenzel et al., 2007). Hippocampal metabolite profiles distinguished samples from seizure-protected vs. seizure-susceptible mice (**Figure 6E**). Hippocampal GABA/glutamate ratios are significantly increased in KD-fed SPF mice compared to CD-fed controls (**Figure 6F, left, and Table S6**). These increases are abrogated in Abx-treated mice fed KD and restored after enrichment of Abx-treated mice with *A. muciniphila* and *Parabacteroides* spp. (**Figure 6F**). Similar changes are seen for hippocampal levels of glutamine, a precursor of glutamate and GABA (**Figure 6F, right**). Overall, these results reveal diet- and microbiota-dependent regulation in the bioavailability of glutamine, as well as an increase in bulk hippocampal GABA levels relative to glutamate in seizure-protected mice.

Bacterial Gamma-Glutamylation Impacts Seizure Susceptibility

Based on our finding that essential ketogenic GG-amino acids are reduced in colonic lumen and serum of seizure-protected vs. seizure-susceptible experimental groups, we hypothesized that microbiota-dependent restriction of ketogenic GG-amino acids is

190

important for mediating the anti-seizure effects of the KD. Gamma-glutamylated forms of amino acids are generated by transpeptidation of GG moieties from glutathione onto amino acids. To determine whether gamma-glutamylation of amino acids impacts seizure susceptibility, we gavaged SPF CD mice for 3 days with GGsTop, a selective irreversible inhibitor of GGT. SPF CD mice treated with GGsTop exhibit increases in 6-Hz seizure thresholds toward levels seen in SPF KD mice (**Figure 7A**). Similarly, EEG recordings of CD-fed SPF *Kcna1-/-* mice treated with GGsTop display a significant decrease in seizures per day (**Figure 5E**). This reveals that peripheral inhibition of gamma-glutamylation and restriction of GG-amino acids promotes seizure protection, consistent with observed metabolomic decreases of ketogenic GG-amino acids in colonic lumenal content and sera from seizure-protected groups compared to seizure-susceptible controls. Importantly, to determine whether restriction of amino acids, rather than catabolism of glutathione, is necessary for the anti-seizure effects of the KD microbiota, we supplemented KD-fed *A. muciniphila* and *Parabacteroides* spp.-enriched mice by bi-daily intraperitoneal injection for 3 days with combined leucine, lysine, threonine, tryptophan and tyrosine, and then tested for 6-Hz seizures. Physiologically-relevant concentrations of amino acids were calculated based on serum metabolomic data (**Table S5**), such that dosages for each were projected to restore blood levels to that seen in vehicle-treated SPF CD controls. Elevating systemic levels of ketogenic amino acids decreases seizure thresholds to levels seen in vehicle-treated SPF CD controls (**Figure 7B**). This suggests that restriction of peripheral ketogenic amino acids is necessary for mediating microbiota- and KD-dependent increases in seizure resistance.

Both host cells and particular bacterial species exhibit GGT activity (van der Stel et al., 2015; Zhang et al., 2015). To gain insight into whether the KD and interactions between *A. muciniphila* and *Parabacteroides* spp. suppress bacterial gamma-glutamylation *in vivo,* we measured GGT activity in fecal samples collected from SPF or *A. muciniphila* and *Parabacteroides* spp.-enriched mice fed the CD or KD. Feeding SPF mice with KD decreases fecal GGT activity compared to CD controls (**Figure 7C**). Similar reduction in fecal GGT activity is seen after enriching *A. muciniphila* and *Parabacteroides* spp. in CD-fed mice. Moreover, enriching *A. muciniphila* and *Parabacteroides* spp. and feeding with KD further decreases fecal GGT activity relative to that seen in SPF KD and SPF CD mice. Exposing all fecal samples to the GGT inhibitor GGsTop eliminates the detected signals, confirming that the measurements reflect GGT activity. Consistent with this, treatment of CD-fed SPF mice with *A. muciniphila* and *Parabacteroides* spp. decreases fecal GGT activity relative to vehicle-treated controls and mice treated with heat-killed bacteria (**Figure 7D**). Overall, these data reveal that enriching for or exogenous treatment with *A. muciniphila* and *Parabacteroides* spp. reduces fecal GGT activity, which could explain the low levels of colonic and serum GG-amino acids observed in seizure-protected mice.

To explore whether bacterial gamma-glutamylation is affected by interactions between *A. muciniphila* and *Parabacteroides* spp., we measured GGT activity in bacteria grown in an *in vitro* cross-feeding system (Flynn et al., 2016). Since *A. muciniphila* does not exhibit GGT activity, we focused particularly on *P. merdae*, where GGT activity was

192

ablated by GGsTop (**Figure S7A**). When *A. muciniphila* is embedded in a CD- or KD-based agar, and *P. merdae* is overlaid in M9 minimal media over the agar, both bacteria exhibit enhanced growth (**Figures 7E and 7F**), suggesting that *A. muciniphila* liberates soluble factors to enable *P. merdae* growth and in turn *P. merdae* enhances *A. muciniphila* growth. This cooperative interaction could contribute to the endogenous enrichment of both *A. muciniphila* and *Parabacteroides* spp. in KD-fed mice (**Figure 1F**). Pilot experiments revealed no growth of *A. muciniphila* in M9 media when overlaid on *P. merdae* embedded in KD or CD agar, suggesting that *A. muciniphila* cannot rely solely on cross-feeding from *P. merdae* to persist. Interestingly, *P. merdae* exhibits high GGT activity that is eliminated by the addition of *A. muciniphila* embedded in CD or KD agar (**Figures 7G and 7H**), which aligns with the decreases in fecal GGT activity and GG amino acid levels observed after KD bacterial enrichment *in vivo.* Findings from these experiments raise the question of whether there is physiological function of restricting GGT activity in abundant *P. merdae* as opposed to restricting overall growth of *P. merdae*. To determine whether reduction of GGT activity in *P. merdae* affects *A. muciniphila* growth, we pre-treated *P. merdae* with vehicle or GGsTop to pharmacologically inhibit GGT activity prior to testing in the cross-feeding assay. *A. muciniphila* exposed to *P. merdae* that was pre-treated with GGsTop exhibits increased growth at 24 hours after incubation as compared to *A. muciniphila* exposed to vehicle-treated *P. merdae* (**Figure S7B**). Taken together, these findings suggest that *A. muciniphila* is capable of metabolizing components from the KD and CD diet to support *P. merdae* growth, and that this cooperative interaction reduces GGT activity. In turn, reductions in GGT activity in *P. merdae* promote *A. muciniphila* growth. This is

consistent with our finding that the KD increases intestinal relative abundance of both *A. muciniphila* and *Parabacteroides* spp., and that enrichment of *A. muciniphila* and *Parabacteroides* spp. reduces fecal GGT activity, colonic lumenal GG-amino acids and serum GG-amino acids *in vivo*. Overall, results from this study reveal that the KD alters the gut microbiota, promoting select microbial interactions that reduce bacterial gamma-glutamylation activity, decrease peripheral GG-amino acids, elevate bulk hippocampal GABA/glutamate ratios and protect against seizures (**Figure 8**).

DISCUSSION

The microbiota plays a key role in host digestion, metabolism and behavior, but whether microbial responses to diet also impact neuronal activity is poorly understood. Here we demonstrate that the KD alters the gut microbiota across two seizure mouse models and that changes in the microbiota are necessary and sufficient for conferring seizure protection. Though studies examining the microbiota in human epilepsy are lacking, several clinical studies link antibiotic treatment to increased risk of status epilepticus or symptomatic seizures in epileptic individuals (Misra et al., 2013; Sutter et al., 2015). Prolonged treatment with metronidazole can provoke convulsions (Beloosesky et al., 2000), and ampicillin exposure is associated with elevated seizure risk (Hodgman et al., 1984; Hornik et al., 2016). Penicillin and other b-lactams are hypothesized to directly reduce GABAergic inhibition, but whether microbiota depletion, as opposed to bacterial infection, mediates increases in seizure frequency is not clear (Wong and Prince, 1979). Results from our study reveal that microbiota depletion via high-dose antibiotic

194

treatment raises seizure susceptibility and incidence in response to the KD in WT and

Kcna1-/- mice. These effects of antibiotic treatment are abrogated by re-colonization with

gut bacteria, suggesting that links between antibiotic use and seizure incidence in

humans could be mediated by the microbiota. These pre-clinical studies suggest that

future investigation is warranted to determine whether human epilepsy is associated

with microbial dysbiosis and whether antibiotic exposure in epileptic individuals impacts

response to the KD.

Consistent with previous studies (Crawford et al., 2009; Klein et al., 2016b), we observe

that mice fed the KD exhibit significant reductions in bacterial alpha diversity (**Figure

1E**). In particular, the KD elevates *A. muciniphila* and *Parabacteroides* spp. in both

Taconic Swiss Webster and Jackson C3HeB/FeJ Kcna1-/- mice (**Figures 1, S1 and 5**).

Similar diet-induced increases in *A. muciniphila* are reported in response to caloric

restriction and fish oil-based diets (high in saturated and polyunsaturated lipids) (Caesar

et al., 2015; Dao et al., 2016a). Increases in *A. muciniphila* were similarly observed

during fasting in humans (Dao et al., 2016a; Remely et al., 2015), hamsters (Sonoyama

et al., 2009), squirrels, and pythons (Costello et al., 2010) and in response to caloric

restriction and high polyunsaturated fat diets in mice (Caesar et al., 2015; Dao et al.,

2016a). *A. muciniphila* and *Parabacteroides* spp. are also associated with increased

ketosis (David et al., 2014) and metabolic improvement in humans (Everard et al., 2013;

Haro et al., 2016). One study also reports changes in the gut microbiota in response to

the KD in BTBR[T+tf/] and C57Bl/6J mice, where levels of *Akkermansia* were correlated

with levels of serum glutamate, lactate, taurine and sarcosine (Klein et al., 2016b).

However, different taxonomic shifts were observed, highlighting that the KD-induced

microbiota likely depends on host genetics and baseline microbiota profiles. Indeed,

different species, strains and even cohorts of animals are known to exhibit microbiota

profiles that vary in taxonomic membership (Godon et al., 2016; Hufeldt et al., 2010) but

are functionally redundant (Lozupone et al., 2012; Moya and Ferrer, 2016), raising the

question of whether there are additional taxa that also perform similarly to *A.*

muciniphila and *Parabacteroides* spp. in our study. Further research is needed to

determine effects of the KD on microbiome profiles in individuals with refractory epilepsy

and whether particular taxonomic changes correlate with seizure severity.

Cross-feeding is a common microbial phenomenon that typically occurs under nutrient

deprivation, which places evolutionary pressure on cooperation over competition

(Gudelj et al., 2016). Our study demonstrates that *A. muciniphila* and *P. merdae*

together can mediate seizure protection in mice fed the KD (**Figure 3**) and also confer

seizure protection to mice fed the CD (**Figure 4**). This suggests that cooperative

microbe-microbe interactions or additive but independent host-microbial interactions

may be involved. We observed evidence for microbial cross-feeding, where growth of

either species alone was enhanced by exposure to soluble factors derived from the

interaction partner (**Figure 2C**). Moreover, both the KD and exposure to *A. muciniphila*

substantially decreased GGT activity in *P. merdae* (**Figure 7D-F**), suggesting that

cooperative interactions between *A. muciniphila* and *P. merdae* could explain the

reduced levels of colonic and serum GG-amino acids observed in seizure-protected

mice. Consistent with this, low GGT activity was detected in fecal samples from mice

fed KD and enriched with *A. muciniphila* and *Parabacteroides* spp. (**Figure 7G**). These findings align with a prior report that low GGT activity is associated with increased relative abundance of *A. muciniphila* in humans (Dao et al., 2016b). In addition, one animal study revealed that dietary composition modulates gut GGT activity (Sobiech and Szewczuk, 1979). Future studies are needed to identify key molecules and response elements for cross-feeding between *A. muciniphila* and *P. merdae* and to reveal additional interactions fundamental to select bacteria from the gut microbiota. Amino acids are transported across the blood-brain barrier (BBB) (Sakai et al., 2004) and serve as nitrogen donors for glutamate and GABA biosynthesis (Yudkoff et al., 2001a). GG-amino acids, in particular, are believed to exhibit increased transport properties, where the gamma-glutamyl moiety promotes translocation across lipid barriers (Castellano and Merlino, 2012). We found that many amino acids, including the ketogenic GG-amino acids lysine, leucine, threonine, tyrosine, and tryptophan, were decreased in serum and colonic lumenal contents of seizure-protected vs. seizure-susceptible mice (**Figures 6C, S6D and S6E and Tables S4 and S5**). We further demonstrate that amino acid restriction is required for seizure protection and that inhibition of GGT promotes seizure protection (**Figures 7A and 7B**). These findings align with previous studies linking GGT activity to altered seizure severity. In a study of 75 epileptic patients, high serum GGT activity was observed in 84.5% of the patients compared to controls (Ewen and Griffiths, 1973). In a rat seizure model, GGT activity was increased after 5 consecutive daily electroshock deliveries (Eraković et al., 2001). Decreases in various peripheral amino acids are associated with KD-mediated seizure suppression in animals and humans (Dahlin et al., 2005; Sariego-Jamardo et al., 2015;

van Karnebeek et al., 2012). Previous studies also highlight KD-induced increases in brain GABA in animal models (Bough, 2008; Calderon et al., 2017; Roy et al., 2015) and in humans, where elevated GABA levels are observed in patients fed a KD and correlate with seizure reductions (Dahlin et al., 2005; Wang et al., 2003). Findings from our study, as well as existing associations of KD-mediated seizure protection with elevated brain GABA and decreased peripheral amino acids, suggest that future studies are needed to determine whether peripheral amino acid restriction alters brain GABA/glutamate metabolism.

The gut microbiota can impact levels of various neuroactive molecules in the periphery and in the brain itself, including select neurotransmitters, neuropeptides and neurotrophic factors, such as hippocampal serotonin, hypothalamic oxytocin and amygdalar brain-derived neurotrophic factor (BDNF) (Vuong et al., 2017). We find that diet- and microbiota-dependent seizure protection is associated with elevations in bulk GABA relative to glutamate content in the hippocampus (**Figure 6F**). Future studies are needed to determine whether other brain regions are similarly affected, and whether GABA localized particularly to neuronal synapses or intracellular vesicles are also modulated by the gut microbiota. Consistent with a role for the gut microbiota in modulating brain GABA levels, a previous study reveals that dietary fermentation by the gut microbiota modulates GABA levels in hypothalamic extracts (Frost et al., 2014). In addition, chronic *Lactobacillus* treatment elevates GABA levels in hippocampal and prefrontal cortex as detected by magnetic resonance spectroscopy (Janik et al., 2016). While several gut bacteria are reported to synthesize GABA *de novo* (Barrett et al.,

198

2012; Dagorn et al., 2013; Higuchi et al., 1997), circulating GABA exhibits limited transport across the BBB (Frey et al., 1979; Perry and Hansen, 1973; Roberts and Kuriyama, 1968). While our study examines microbial and metabolic mechanisms underlying how the gut microbiota influences seizure outcomes, future interrogation of the precise neurological mechanisms underlying the anti-seizure effects of the KD and KD-associated microbiota is needed. Of particular interest is the question of whether the gut microbiota modulates seizure susceptibility and incidence via alterations in excitatory/inhibitory balance and neurotransmission in particular neural circuits. Overall, our study reveals a novel role for the gut microbiota in mediating and conferring seizure protection in two mouse models for refractory epilepsy. While the results lend credence to future research examining the gut microbiota in human epilepsy, several additional studies are needed to determine whether microbe-based treatments can be safely and effectively applied for clinical amelioration of seizure severity and incidence.

Chapter Figures:
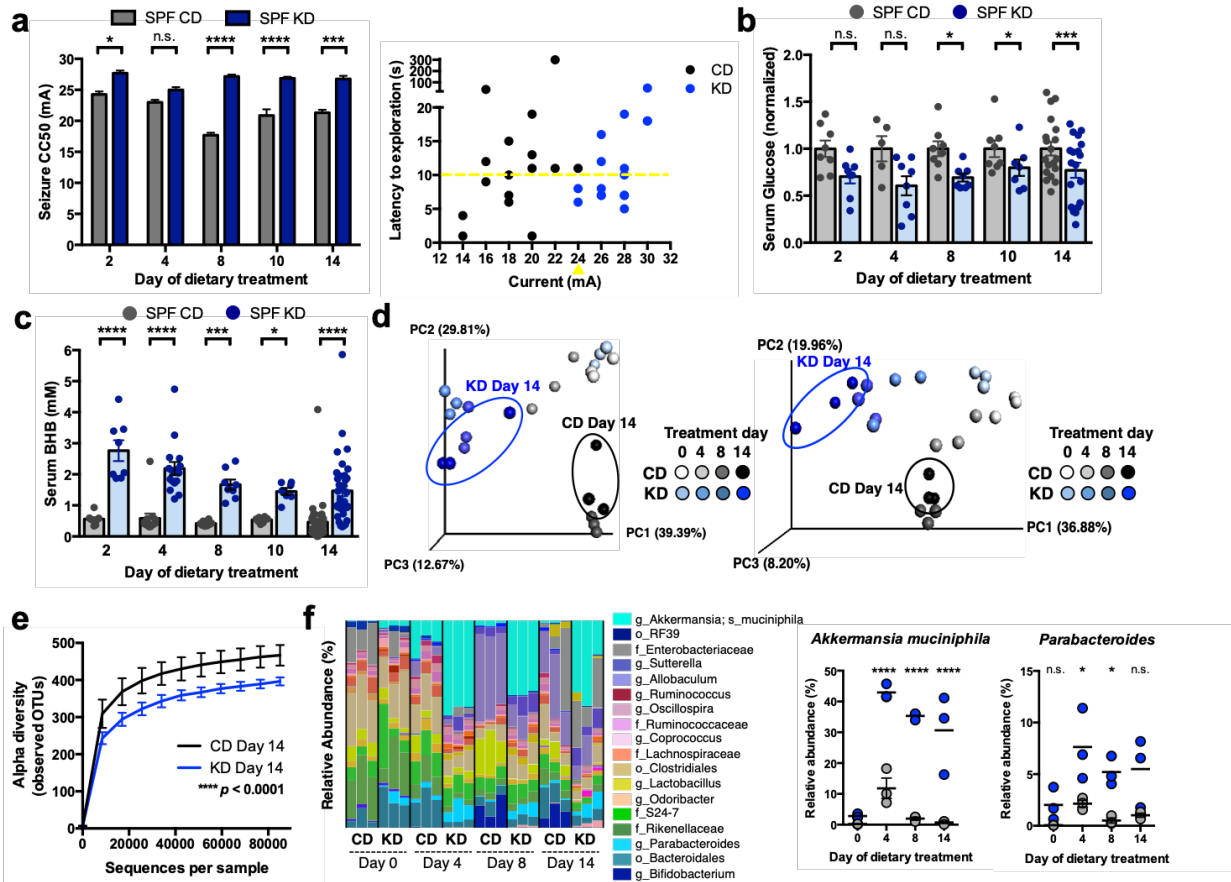
Figure 7 The Ketogenic Diet Alters the Microbiota and Protects Against 6-Hz Psychomotor Seizures. a, Seizure thresholds in response to 6-Hz stimulation in independent cohorts of mice fed the control diet (CD) or ketogenic diet (KD) for 2, 4, 8, 10 or 14 days (left). n = 8, 6, 9, 20, 6 (CD); 8, 7, 12, 21, 5 (KD). Behavior in representative cohort of seizure-tested mice at 14 days post dietary treatment (right). Yellow line at y=10 seconds represents threshold for scoring seizures, and yellow triangle at 24 mA denotes starting current per experimental cohort. n = 16. b, Levels of serum glucose in independent cohorts of mice fed CD or KD for 2, 4, 8, 10 or 14 days. Data are normalized to serum glucose levels seen in SPF CD mice for each time point. n = 8, 5, 8, 8, 19 (CD); 8, 8, 8, 7, 19 (KD). c, Levels of serum beta-hydroxybutyrate (BHB) in independent cohorts of mice fed CD or KD for 2, 4, 8, 10 or 14 days. n = 8, 13,

8, 8, 37 (CD); 8, 16, 8, 7, 38 (KD). d, Principal coordinates analysis (PCoA) of weighted (left) and unweighted (right) UniFrac distance matrices based on 16S rDNA profiling of feces from independent cohorts of mice fed CD or KD for 0, 4, 8 or 14 days. n = 3 cages/group. e, Alpha diversity of fecal 16S rDNA sequencing data from mice fed CD or KD for 14 days. n = 3 cages/group. f, Taxonomic distributions of bacteria from fecal 16S rDNA sequencing data (left). n = 3 cages/group. Relative abundances of Akkermansia muciniphila and Parabacteroides spp. from fecal 16S rDNA sequencing data (right). n = 3 cages/group. Data are presented as mean ± s.e.m. Two-way ANOVA with Bonferroni (a-c, e), Kruskal-Wallis with Bonferroni (f): P < 0.05, **P < 0.01, ***P < 0.001, ****P < 0.0001. n.s.=not statistically significant. SPF=specific pathogen-free (conventionally-colonized), CD=control diet, KD=ketogenic diet, CC50=current intensity producing seizures in 50% of mice tested, BHB=beta-hydroxybutyrate, OTUs=operational taxonomic units.
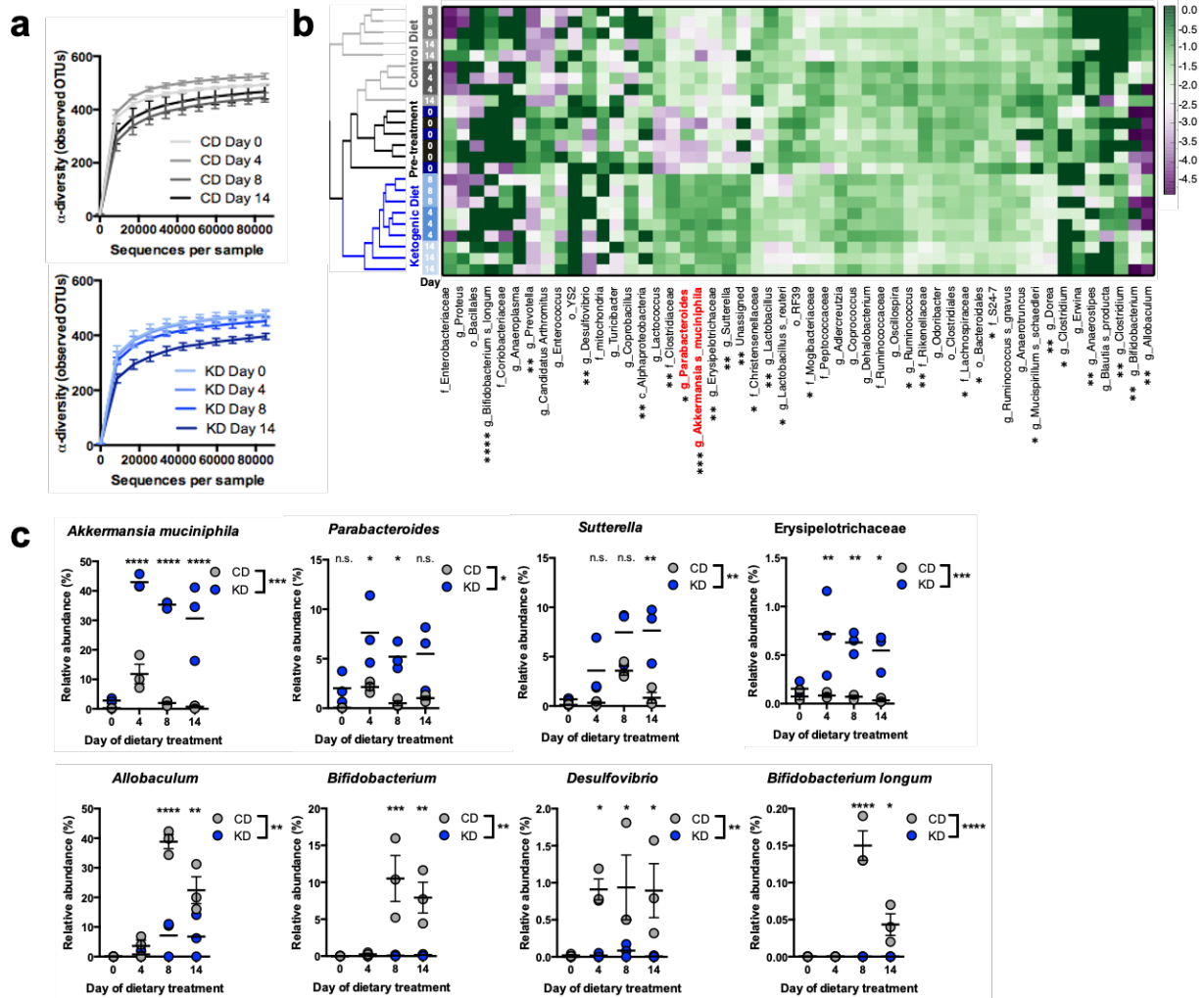
Figure 8 The Ketogenic Diet Alters Relative Abundances of Particular Bacterial Taxa from the Gut Microbiota. a, Alpha diversity based on 16S rDNA sequencing of the fecal gut microbiota on days 0, 4, 8 and 14 after treatment with the control diet (CD, top) vs. ketogenic diet (KD, bottom) n = 3 per time point. b, Heatmap of 16S rDNA sequencing data, where columns represent bacterial taxa indicated by their lowest resolved taxonomic levels. Rows represent fecal samples collected from CD or KD-fed mice at Day 0 (pre-treatment), 4, 8 or 14, where gray fields indicate mice fed CD and blue indicate mice fed KD. Phylogenetic classifications are based on weighted UniFrac

data. Asterisks denote statistical significance between CD and KD groups (excluding

Day 0). Red text highlights A. muciniphila and Parabacteroides spp. n = 3. c, Relative

abundances of select bacterial taxa that are enriched in SPF mice fed KD (top row) or

CD (bottom row). n = 3. Data are presented as mean ± s.e.m. Kruskal-Wallis with

Bonferroni: *P < 0.05, **P < 0.01, ***P < 0.001, ****P < 0.0001. n.s.=not statistically

significant. CD=control diet, KD=ketogenic diet.
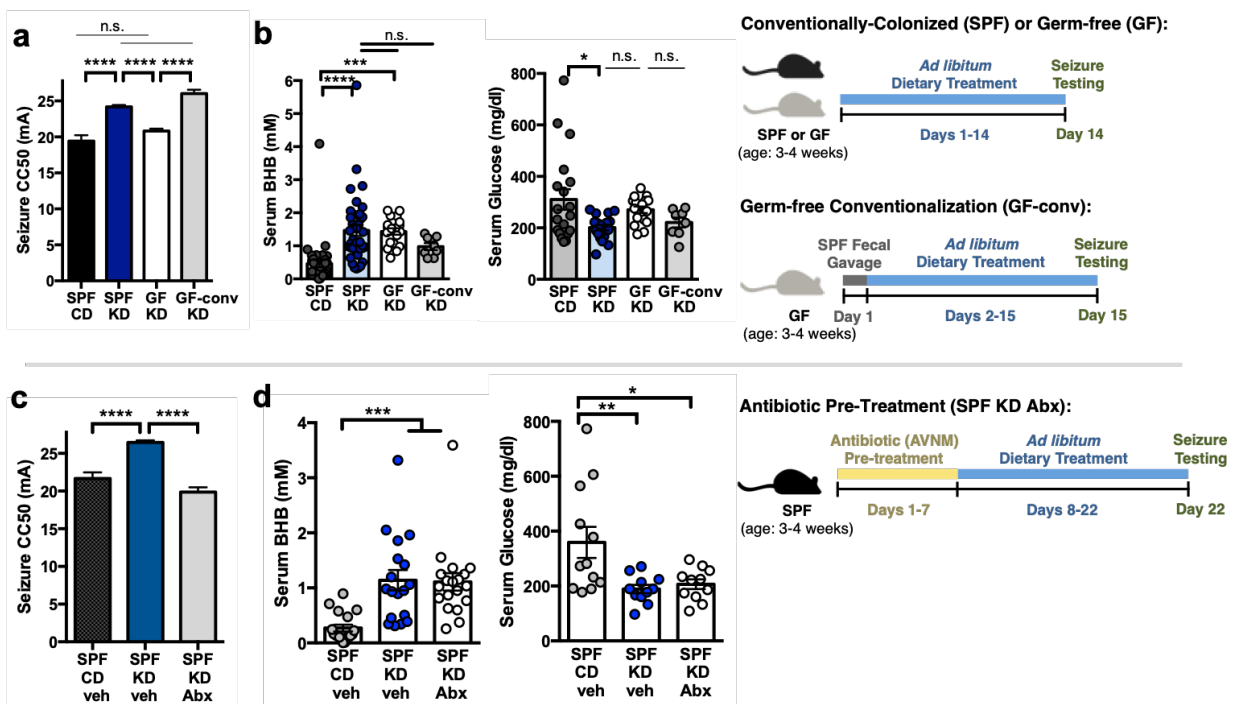
Figure 9 The Microbiota is Required for the Anti-Seizure Effects of the Ketogenic

Diet. a, Seizure thresholds in response to 6-Hz stimulation in SPF, GF or

conventionalized GF mice fed CD or KD. n = 13, 18, 12, 6. b, Serum BHB (left) and

glucose (right) levels in SPF, GF or conventionalized GF mice fed CD or KD. n = 37, 38,

19, 8. c, Seizure thresholds in response to 6-Hz stimulation in SPF mice treated with

vehicle or Abx pre-dietary treatment. n = 13, 18, 13. d, Serum BHB (left) and glucose

(right) levels in SPF mice treated with vehicle or Abx pre-dietary treatment. n = 18, 18,

19 (BHB); n = 12, 11, 11 (glucose). Data are presented as mean ± s.e.m. One-way

ANOVA with Bonferroni: *P < 0.05, **P < 0.01, ***P < 0.001, ****P < 0.0001. n.s.=not

statistically significant. SPF=specific pathogen-free (conventionally-colonized),

GF=germ-free, GF-conv=germ-free conventionalized with SPF microbiota, CD=control

diet, KD=ketogenic diet, CC50=current intensity producing seizures in 50% of mice

tested. BHB=betahydroxybutyrate, veh=vehicle, Abx=antibiotics (ampicillin, vancomycin,

neomycin, metronidazole [AVNM]).

Figure 10: The Microbiota is Required for the Anti-Seizure Effects of the Ketogenic Diet. a, Seizure thresholds in response to 6-Hz stimulation in SPF, GF or conventionalized GF mice fed CD or KD. n = 13, 18, 12, 6. **b**, Serum BHB (left) and glucose (right) levels in SPF, GF or conventionalized GF mice fed CD or KD. n = 37, 38, 19, 8. **c**, Seizure thresholds in response to 6-Hz stimulation in SPF mice treated with vehicle or Abx pre-dietary treatment. n = 13, 18, 13. **d**, Serum BHB (left) and glucose (right) levels in SPF mice treated with vehicle or Abx pre-dietary treatment. n = 18, 18,

19 (BHB); n = 12, 11, 11 (glucose). Data are presented as mean ± s.e.m. One-way ANOVA with Bonferroni: *$P < 0.05$, **$P < 0.01$, ***$P < 0.001$, ****$P < 0.0001$. n.s.=not statistically significant. SPF=specific pathogen-free (conventionally-colonized), GF=germ-free, GF-conv=germ-free conventionalized with SPF microbiota, CD=control diet, KD=ketogenic diet, CC50=current intensity producing seizures in 50% of mice tested. BHB=betahydroxybutyrate, veh=vehicle, Abx=antibiotics (ampicillin, vancomycin, neomycin, metronidazole [AVNM]).

Figure 11: KD-Associated Bacteria Sufficiently Mediate the Anti-Seizure Effects of the Ketogenic Diet. a, Seizure thresholds in response to 6-Hz stimulation in SPF mice pre-treated with vehicle or Abx, and colonized with Parabacteroides spp. (P. merdae

and P. distasonis), Akkermansia muciniphila, both, or Bifidobacterium longum (left). n =
13, 18, 15, 6, 8, 5, 5. Behavior in representative cohort of seizure-tested mice (right).
Yellow line at y=10 seconds represents threshold for scoring seizures, and yellow
triangle at 24 mA denotes starting current per experimental cohort. n = 12, 16, 8, 25. **b**,
Fluorescence in situ hybridization for A. muciniphila (MUC1437) and select Bacteroides,
including P. merdae and P. merdae (BAC303) in colonic lumen from SPF mice fed CD,
SPF mice fed KD or A. muciniphila and Parabacteroides-enriched mice fed KD. Scale
bar indicates 25 um. Dotted lines indicate the borders of the intestinal epithelium. n = 3.
c, Seizure thresholds in response to 6-Hz stimulation in GF mice colonized with
Parabacteroides spp. (P. merdae and P. distasonis) and Akkermansia muciniphila (top).
n = 15, 4, 9, 9. Behavior in seizure-tested mice (bottom). Yellow line at y=10 seconds
represents threshold for scoring seizures, and yellow triangle at 24 mA denotes starting
current per experimental cohort. n = 17, 19. Data are presented as mean ± s.e.m. One-
way ANOVA with Bonferroni: **$P < 0.01$, ***$P < 0.001$, ****$P < 0.0001$. SPF=specific
pathogen-free (conventionally-colonized), GF=germ-free, CD=control diet,
KD=ketogenic diet, CC50=current intensity producing seizures in 50% of mice tested,
veh=vehicle, Abx=pre-treated with antibiotics (ampicillin, vancomycin, neomycin,
metronidazole [AVNM]), Pb=Parabacteroides spp. (P. merdae and P. distasonis),
Akk=Akkermansia muciniphila, AkkPb=A. muciniphila, P. merdae and P. distasonis,
Bf=Bifidobacterium longum.
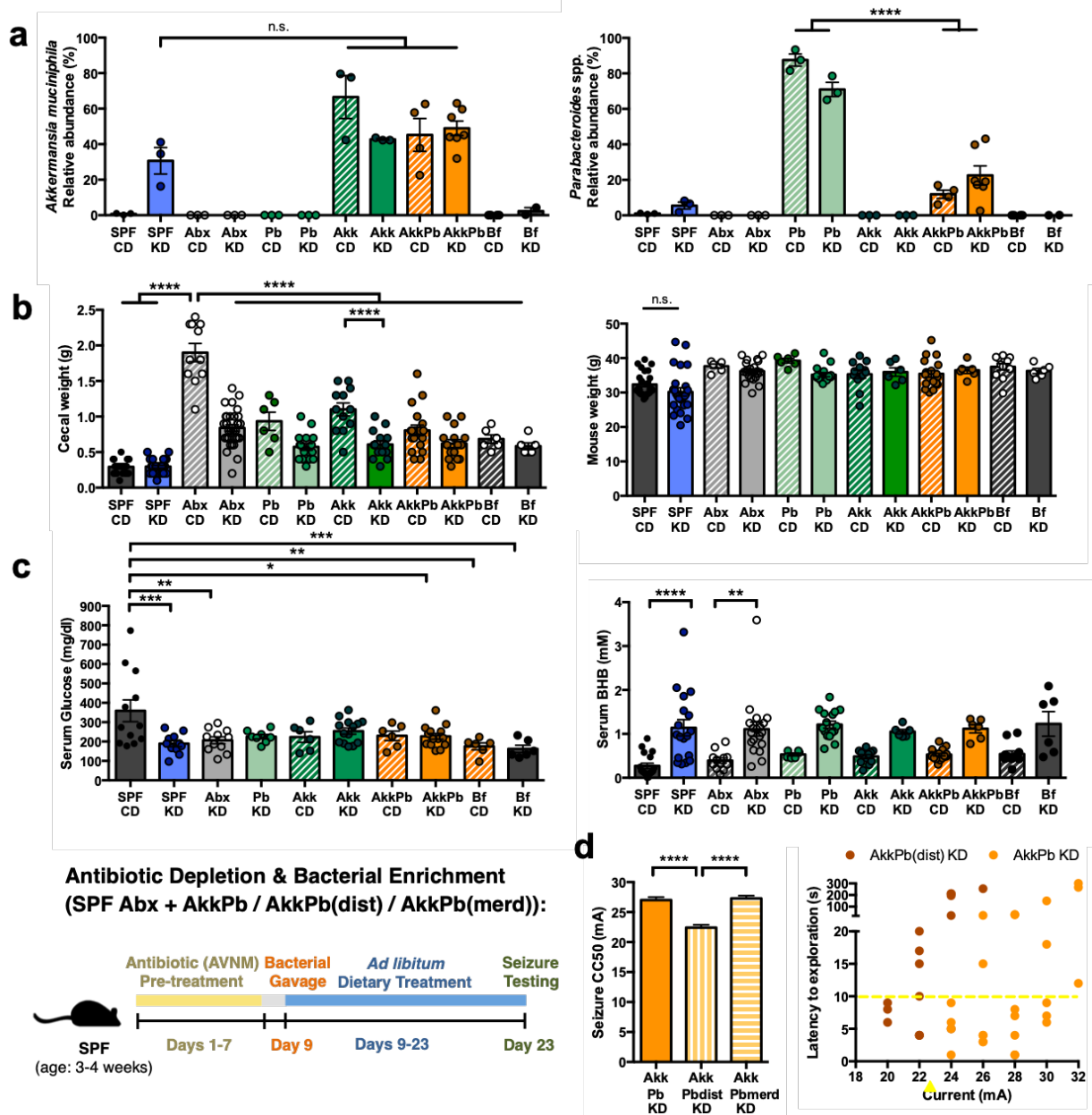
Figure 12: Colonization, Weight, Glucose and BHB Levels After Abx Treatment. a, Relative abundance of Akkermansia muciniphila (left) and Parabacteroides spp. (right), measured by 16S rDNA sequencing, after colonization of Abx-treated SPF mice. n = 3, 3, 3, 3, 3, 3, 4, 7, 4, 3, 3, 3 cages. **b,** Cecal weight (left) and mouse weight (right) at 14 days after dietary treatment in Abx-treated SPF mice colonized with different bacterial taxa. n = 28, 28, 12, 32, 6, 16, 12, 14, 18, 15, 6, 6. **c,** Serum glucose (left) and BHB

(right) concentrations at 14 days after dietary treatment in Abx-treated SPF mice colonized with different bacterial taxa. n = 12, 11, 11, 8, 6, 14, 6, 14, 6 (glucose); n = 18, 18, 12, 19, 6, 16, 12, 6, 18, 6, 12, 6 (BHB). **d**, Seizure thresholds in response to 6-Hz stimulation in SPF mice pre-treated with vehicle or Abx, and colonized with A. muciniphila and Parabacteroides merdae (Pbmerd), Parabacteroides distasonis (Pbdist), or both (left). n = 8, 5, 6. Behavior in representative cohort of seizure-tested mice (right). Yellow line at y=10 seconds represents threshold for scoring seizures, and yellow triangle at 24 mA denotes starting current per experimental cohort. n = 16, 25. Data are presented as mean ± s.e.m. One-way ANOVA with Bonferroni: *P < 0.05, **P < 0.01, ***P < 0.001, ****P < 0.0001. SPF=specific pathogen-free (conventionally-colonized), GF=germ-free, CD=control diet, KD=ketogenic diet, CC50=current intensity producing seizures in 50% of mice tested, veh=vehicle, Abx=pre-treated with antibiotics (ampicillin, vancomycin, neomycin, metronidazole [AVNM]), Pb=Parabacteroides spp. (P. merdae and P. distasonis), Akk=Akkermansia muciniphila, AkkPb=A. muciniphila, P. merdae and P. distasonis, Bf=Bifidobacterium longum.
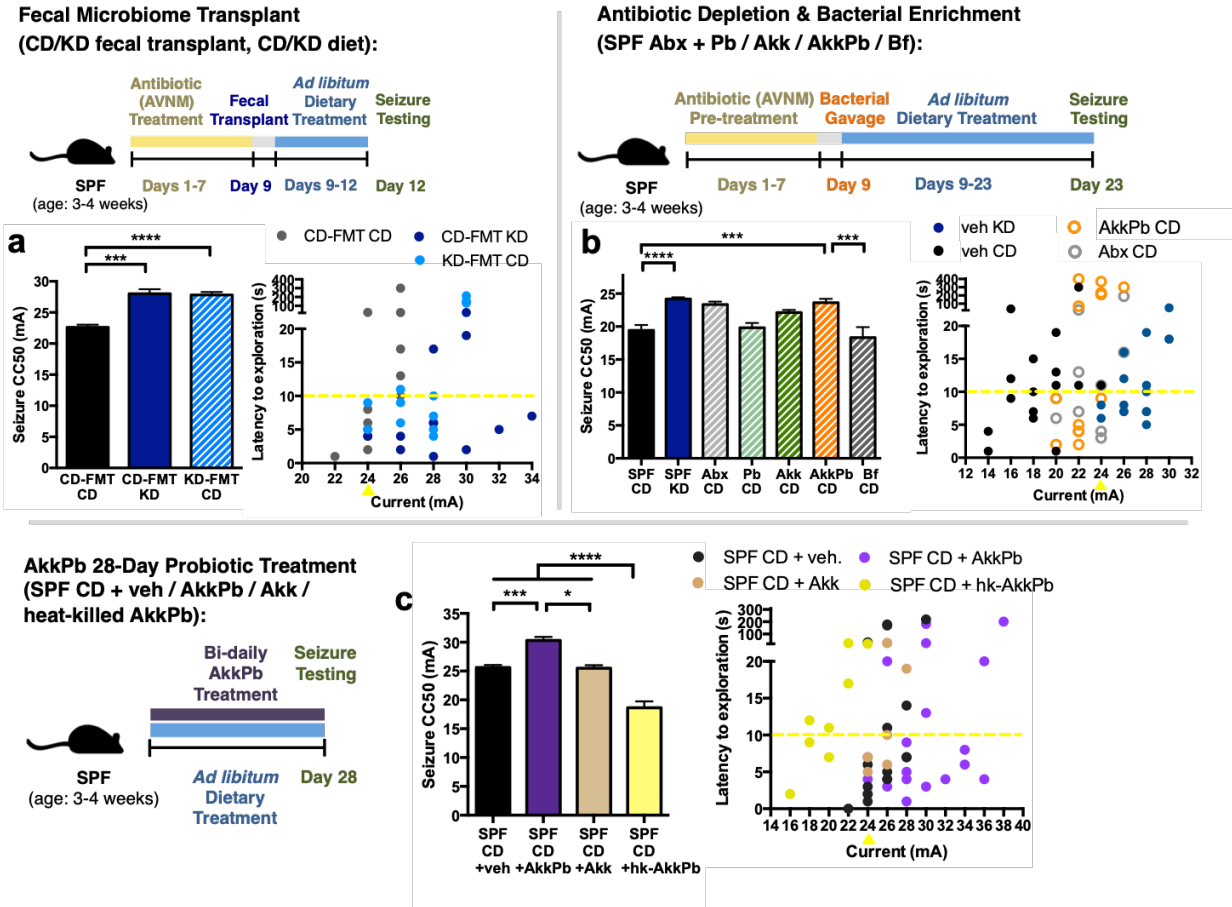
Figure 13: KD-Associated Bacteria Sufficiently Confer Seizure Protection in Mice Fed the Control Diet. a, Seizure thresholds in response to 6-Hz stimulation in Abx-treated SPF transplanted with the CD microbiota (CD-FMT) or KD microbiota (KD-FMT) and fed the CD or KD (left). n = 6, 5, 5. Behavior in representative cohort of seizure-tested mice (right). Yellow line at y=10 seconds represents threshold for scoring seizures, and yellow triangle at 24 mA denotes starting current per experimental cohort. n = 12. b, Seizure thresholds in response to 6-Hz stimulation in SPF mice pre-treated with vehicle or Abx, and colonized with Parabacteroides spp. (P. merdae and P. distasonis), Akkermansia muciniphila, both, or Bifidobacterium longum (left). n = 13, 18, 9, 8, 6, 6. Behavior in representative cohort of seizure-tested mice (right). Yellow line at y=10 seconds represents threshold for scoring seizures, and yellow triangle at 24 mA

denotes starting current per experimental cohort. n = 16, 16, 12, 12. c, Seizure

thresholds in response to 6-Hz stimulation in SPF mice orally gavaged with

Akkermansia muciniphila, P. merdae and P. distasonis (AkkPb), A. muciniphila alone

(Akk), or heat-killed Akkermansia muciniphila and Parabacteroides spp (hk-AkkPb).

(left). n = 6, 6, 4, 3. Behavior in seizure-tested mice (right). Yellow line at y=10 seconds

represents threshold for scoring seizures, and yellow triangle at 24 mA denotes starting

current per experimental cohort. n = 15, 20, 8, 8. Data are presented as mean ± s.e.m.

One-way ANOVA with Bonferroni: *P < 0.05, ***P < 0.001, ****P < 0.0001. SPF=specific

pathogen-free (conventionally-colonized), CD=control diet, KD=ketogenic diet,

CC50=current intensity producing seizures in 50% of mice tested, CD-

FMT=transplanted with CD microbiota, KD-FMT=transplanted with KD microbiota,

veh=vehicle, Abx=pre-treated with antibiotics (ampicillin, vancomycin, neomycin,

metronidazole [AVNM]), Pb=Parabacteroides spp. (P. merdae and P. distasonis),

Akk=Akkermansia muciniphila, AkkPb=A. muciniphila, P. merdae and P. distasonis,

Bf=Bifidobacterium longum, hk-AkkPb=heat-killed A. muciniphila, P. merdae and P.

distasonis.
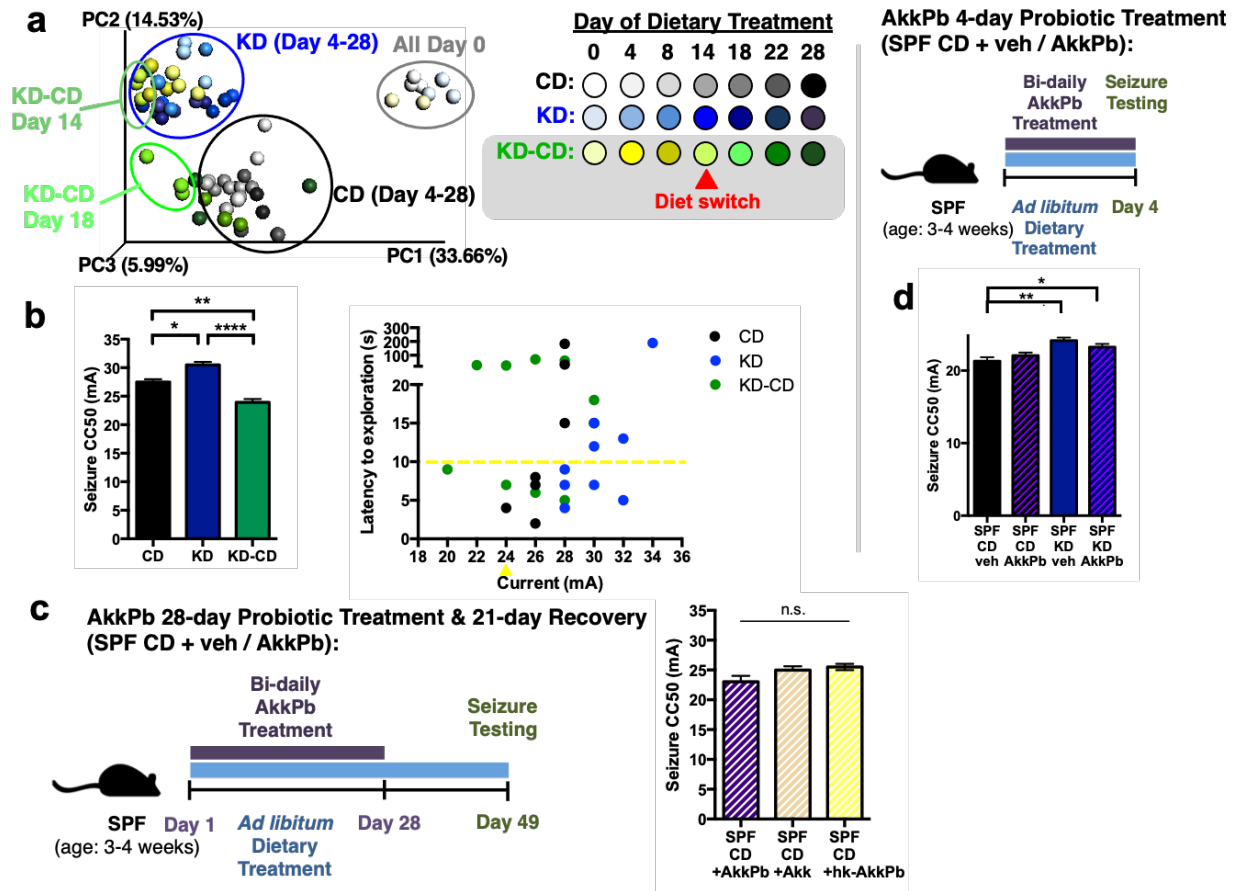
Figure 14

Reversion of the KD Microbiota and KD-Associated Seizure Protection in

Response to the Control Diet. a, Principal coordinates analysis (PCoA) of weighted

UniFrac distance matrices based on longitudinal 16S rDNA profiling of feces from SPF

mice fed CD for 28 days (CD), mice fed KD for 28 days (KD), or mice fed KD for 14

days followed by CD for 14 days (KD-CD). *n* = 3 cages/group. **b**, Seizure thresholds in

response to 6-Hz stimulation in SPF mice fed CD for 28 days (CD), mice fed KD for 28

days (KD), or mice fed KD for 14 days followed by CD for 14 days (KD-CD) (left). *n* = 4.

Behavior in representative cohort of seizure-tested mice (right). Yellow line at y=10

seconds represents threshold for scoring seizures, and yellow triangle at 24 mA

denotes starting current per experimental cohort. *n* = 8, 9, 9. **c**, Seizure thresholds in

212

response to 6-Hz stimulation in SPF mice at 21 days after probiotic treatment with

Akkermansia muciniphila, P. merdae and P. distasonis (AkkPb), *A. muciniphila* alone

(Akk), or heat-killed *Akkermansia muciniphila* and *Parabacteroides* spp (hk-AkkPb).

(left). *n* = 8. **d**, Seizure thresholds in response to 6-Hz stimulation in SPF mice orally

gavaged for 4 days with vehicle or *Akkermansia muciniphila, P. merdae and P.*

distasonis (AkkPb). *n* = 6, 7, 7, 7. Data are presented as mean ± s.e.m. One-way

ANOVA with Bonferroni: **P* < 0.05, ***P* < 0.01, *****P* < 0.0001, n.s.=not statistically

significant. SPF=specific pathogen-free (conventionally-colonized), CD=control diet,

KD=ketogenic diet, KD-CD=fed KD for 14 days followed by CD for 14 days.

CC50=current intensity producing seizures in 50% of mice tested, veh=vehicle,

Akk=*Akkermansia muciniphila,* AkkPb=*A. muciniphila, P. merdae* and *P. distasonis*, hk-

AkkPb=heat-killed *A. muciniphila, P. merdae* and *P. distasonis.*
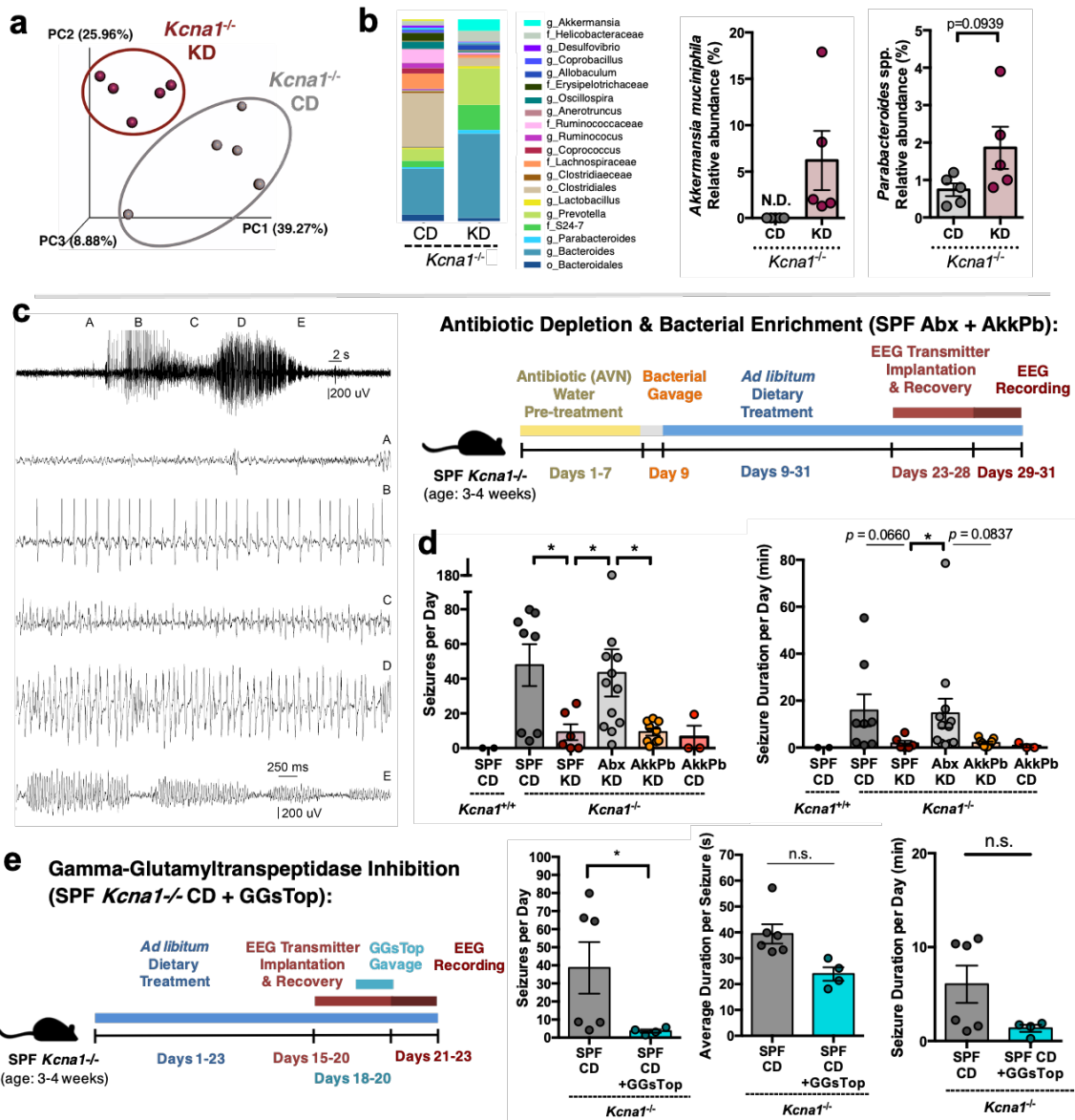
Figure 15: KD-Associated Bacteria Mediate Protection Against Tonic-Clonic Seizures in Response to the Ketogenic Diet. a, Principal coordinates analysis (PCoA) of weighted UniFrac distances based on 16S rDNA profiling of feces Kcna1-/- mice fed CD or KD for 14 days. n = 5 cages/group. b, Average taxonomic distributions of bacteria from fecal 16S rDNA sequencing data (left). Relative abundances of Akkermansia muciniphila and Parabacteroides spp. From fecal 16S rDNA sequencing data (right). n = 5 cages/group. c, Representative EEG trace showing stages used to

define seizures quantified in d. d, Average number of seizures per day (left) and total duration of seizures per day (right) in SPF Kcna1-/- mice treated with vehicle or Abx, colonized with A. muciniphila and Parabacteroides spp. or nothing, and fed CD or KD. n = 2, 6, 6, 12, 9, 3. e, Average number of seizures per day (left), average duration per seizure (middle) and total duration of seizures per day (right) in SPF CD Kcna1-/- mice treated with GGsTop. Data for SPF CD mice are as in (d). n = 6, 4. Data are presented as mean ± s.e.m. Kruskal-Wallis with Bonferroni (a,b), non-parametric one-way nested ANOVA with Dunn (d), non-parametric Kolgomorov-Smirnov t test (e). SPF=specific pathogen-free (conventionally-colonized), CD=control diet, KD=ketogenic diet, veh=vehicle, Abx=pre-treated with antibiotics (ampicillin, vancomycin, neomycin, metronidazole [AVNM]), AkkPb=A. muciniphila, P. merdae and P. distasonis.
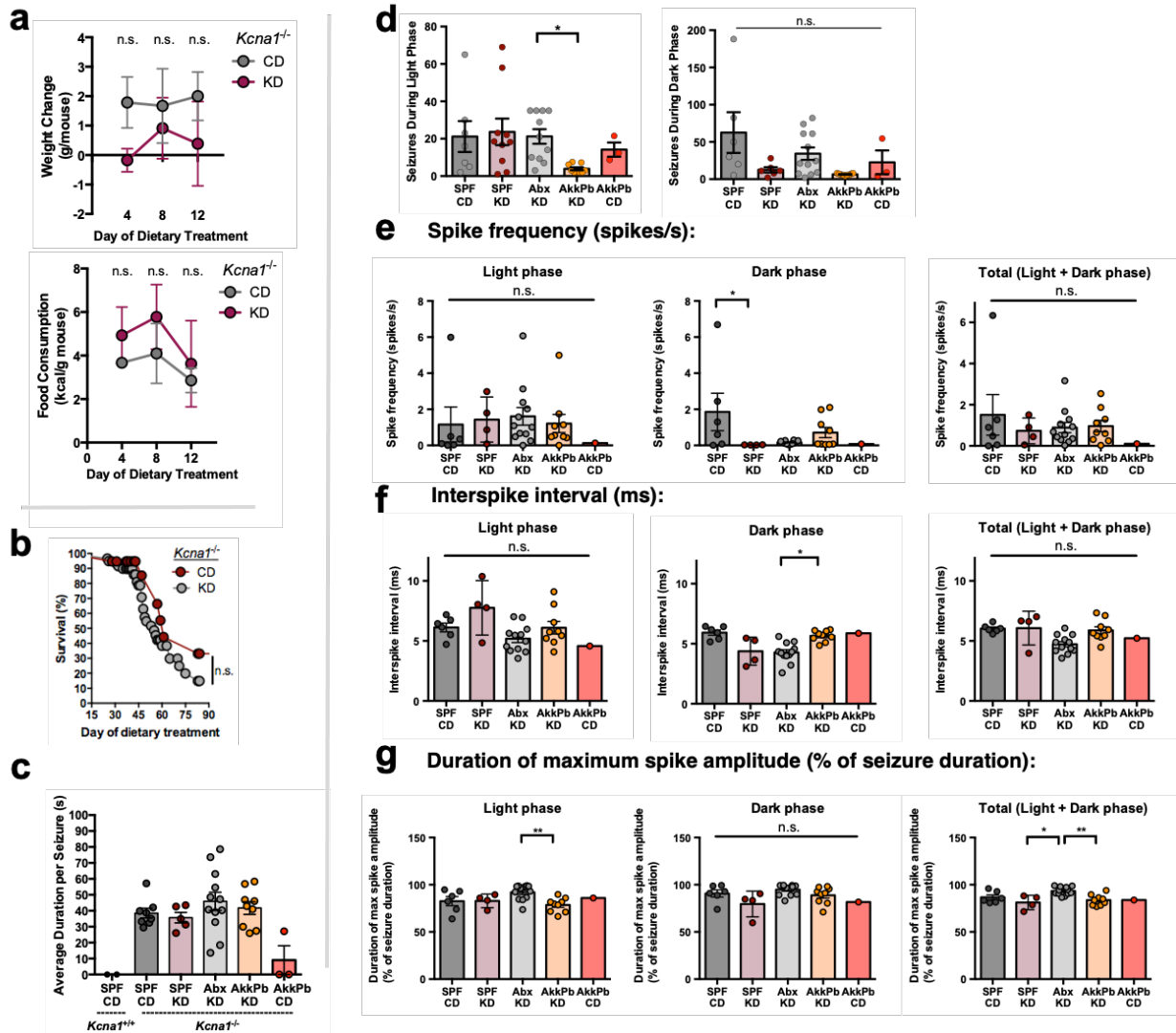
Figure 16: Weight, Food Consumption, Survival and Seizure Properties in the KCNA1 Mouse Line. a, Weight gain (top) and food consumption (bottom) in Kcna1-/- mice fed CD vs KD. n = 8 (weight); n = 6 (food). **b**, Survival curves in Kcna1-/- mice fed CD vs KD. n = 13. **c,** Average duration per seizure (right) in SPF Kcna1-/- mice treated with vehicle or Abx, colonized with A. muciniphila and Parabacteroides spp. or nothing, and fed CD or KD. n = 2, 6, 5, 12, 9, 1. Average seizure frequency per day (d), average seizure spike frequency per seizure (e), average interspike interval per seizure (f) and relative duration of maximum spike amplitude per seizure (g) for seizures observed

216

during the light phase (0600-1800), dark phase (1800-0600) or total duration. n = 6, 4, 12, 9, 1. Data are presented as mean ± s.e.m. Two-way ANOVA with Bonferroni (a,b), non-parametric one-way ANOVA with Dunn (c-g). n.s.=not statistically significant. SPF=specific pathogen-free (conventionally-colonized), CD=control diet, KD=ketogenic diet, CC50=current intensity producing seizures in 50% of mice tested.
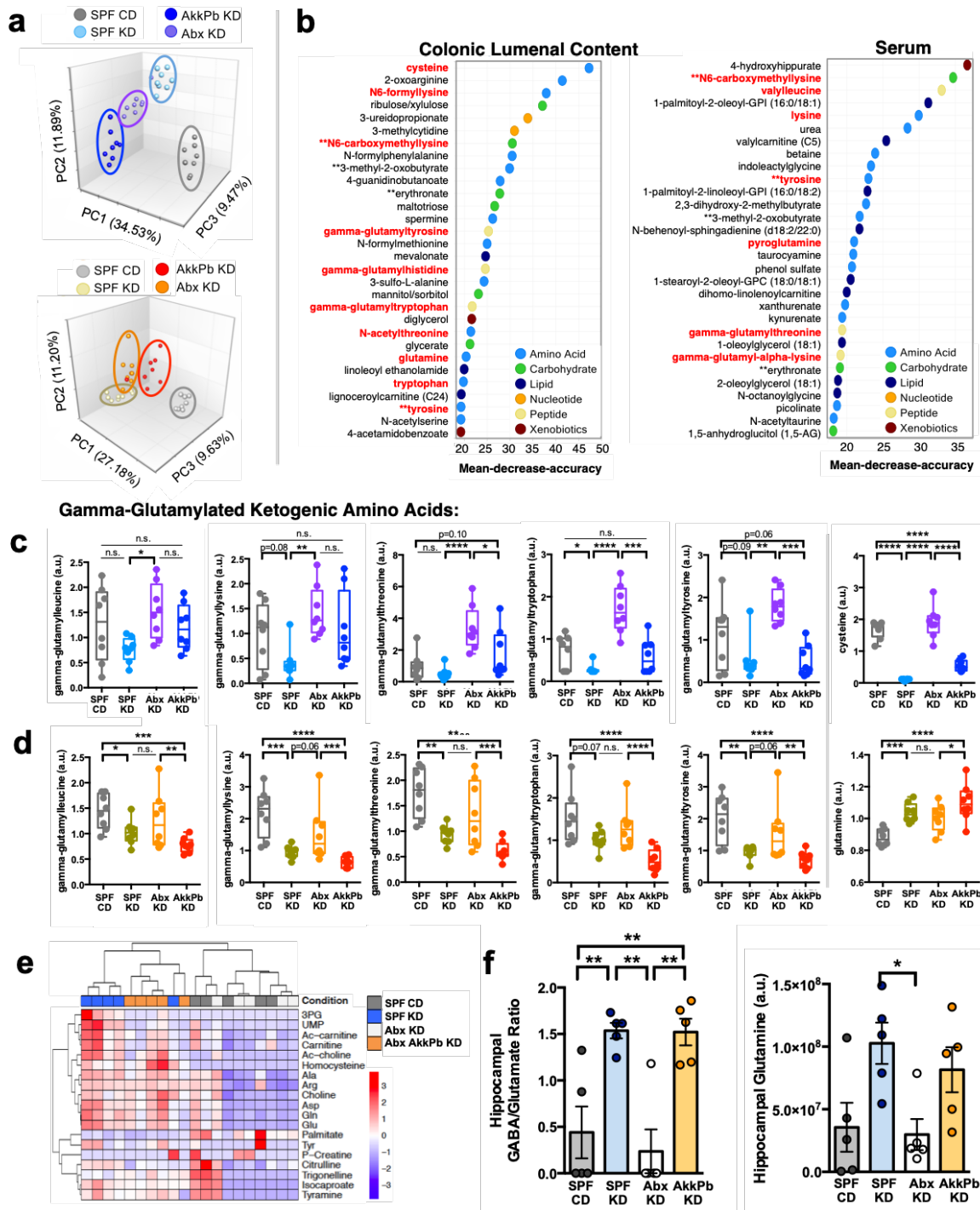
Figure 17 The Colonic Lumenal and Serum Metabolomes are Modulated by the Ketogenic Diet and Microbiota Status. a, Number of statistically significant alterations in metabolites out of the 622 detected in colonic lumen and 670 detected in serum. Values noted in black text are total number of metabolites altered, with values in green

218

denoting upregulation and values in red denoting downregulation. n = 8 cages/group. **b**,

Levels of glucose (left) and BHB (right) detected by metabolomics screening of colonic

lumen (top) and serum (bottom). n = 8 cages/group. **c**, Biochemicals, identified by

Random Forests classification of colonic lumenal (top) and serum (bottom)

metabolomes, that contribute most highly to the discrimination of CD-fed (SPF CD) from

KD-fed (Abx KD, SPF KD, AkkPb KD) groups. n = 8 cages/group. **d**, Levels of non-

gamma glutamylated amino acids in colonic lumenal contents from SPF mice fed CD,

SPF mice fed KD, Abx-treated mice fed KD, and AkkPb-colonized mice fed KD. n = 8

cages/group. **e**, Levels of non-gamma glutamylated amino acids in sera from SPF mice

fed CD, SPF mice fed KD, Abx-treated mice fed KD, and AkkPb-colonized mice fed KD.

n = 8 cages/group. Data are presented as mean ± s.e.m. Two-way ANOVA contrasts:

*$P < 0.05$, **$P < 0.01$, ***$P < 0.001$, ****$P < 0.0001$. n.s.=not statistically significant.

CD=control diet, KD=ketogenic diet, SPF=specific pathogen-free (conventionally-

colonized), veh=vehicle, Abx=pre-treated with antibiotics (ampicillin, vancomycin,

neomycin, metronidazole [AVNM]), AkkPb=A. muciniphila, P. merdae and P. distasonis,

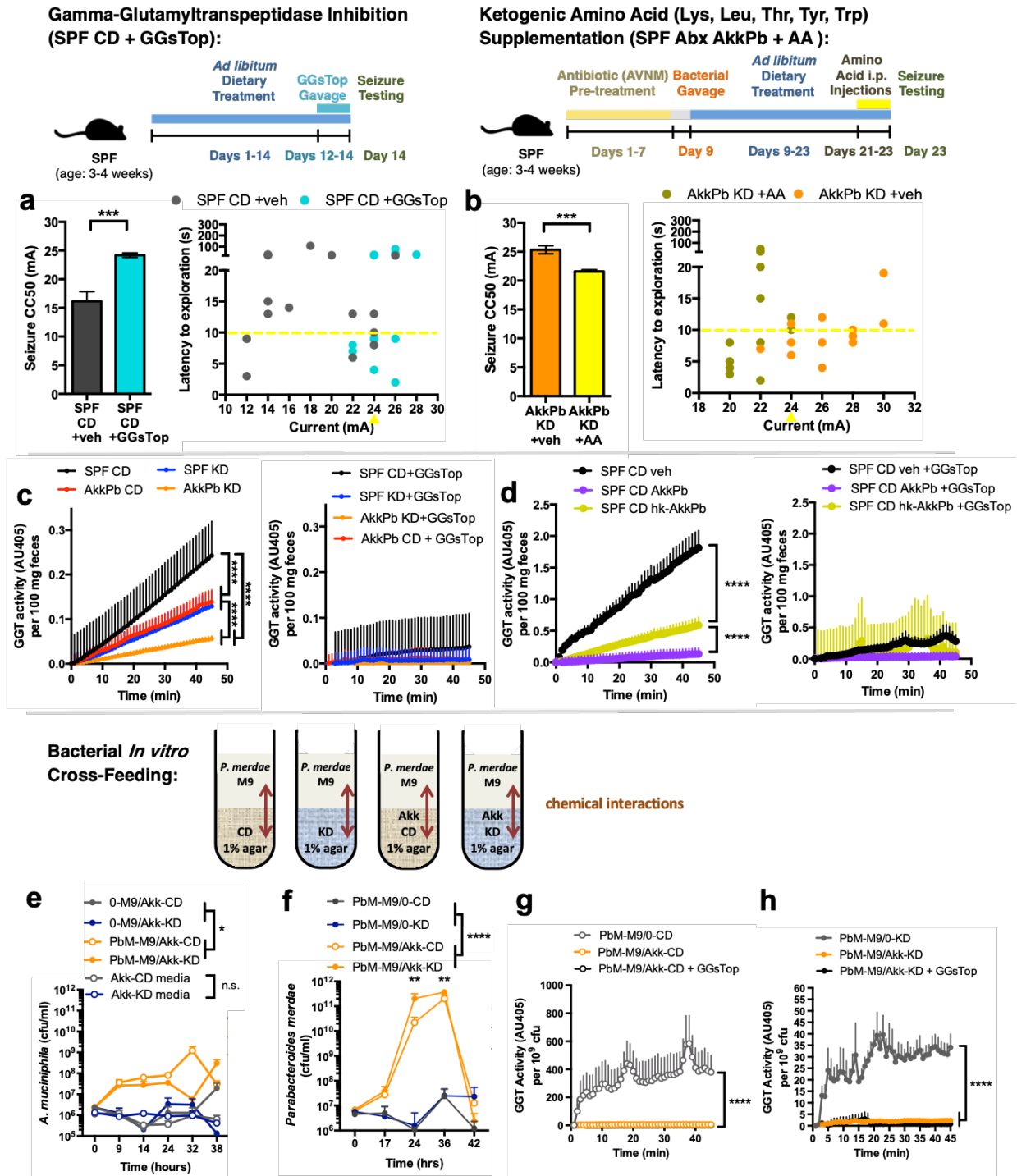a.u.=arbitrary units, BHB=beta-hydroxybutyrate.

Figure 18: The Colonic Lumenal and Serum Metabolomes are Modulated by the Ketogenic Diet and Microbiota Status. a, Number of statistically significant alterations in metabolites out of the 622 detected in colonic lumen and 670 detected in serum. Values noted in black text are total number of metabolites altered, with values in green denoting upregulation and values in red denoting downregulation. n = 8 cages/group. **b**, Levels of glucose (left) and BHB (right) detected by metabolomics screening of colonic lumen (top) and serum (bottom). n = 8 cages/group. **c**, Biochemicals, identified by Random Forests classification of colonic lumenal (top) and serum (bottom) metabolomes, that contribute most highly to the discrimination of CD-fed (SPF CD) from KD-fed (Abx KD, SPF KD, AkkPb KD) groups. n = 8 cages/group. **d**, Levels of non-gamma glutamylated amino acids in colonic lumenal contents from SPF mice fed CD, SPF mice fed KD, Abx-treated mice fed KD, and AkkPb-colonized mice fed KD. n = 8

cages/group. **e**, Levels of non-gamma glutamylated amino acids in sera from SPF mice

fed CD, SPF mice fed KD, Abx-treated mice fed KD, and AkkPb-colonized mice fed KD.

n = 8 cages/group. Data are presented as mean ± s.e.m. Two-way ANOVA contrasts:

*P < 0.05, **P < 0.01, ***P < 0.001, ****P < 0.0001. n.s.=not statistically significant.

CD=control diet, KD=ketogenic diet, SPF=specific pathogen-free (conventionally-

colonized), veh=vehicle, Abx=pre-treated with antibiotics (ampicillin, vancomycin,

neomycin, metronidazole [AVNM]), AkkPb=A. muciniphila, P. merdae and P. distasonis,

a.u.=arbitrary units, BHB=beta-hydroxybutyrate.

Figure 19: The Ketogenic Diet and Bacterial Cross-Feeding Reduces Gamma Glutamyltranspeptidase (GGT) Activity, and GGT Inhibition Sufficiently Confers Seizure Protection. a, 6-Hz seizure thresholds in response to oral gavage with the

GGT inhibitor, GGsTop, in SPF mice fed CD (left). n = 6, 9. Behavior in seizure-tested mice (right). Yellow line at y=10 seconds represents threshold for scoring seizures, and yellow triangle at 24 mA denotes starting current per experimental cohort. n = 16. **b,** 6-Hz seizure thresholds in response to supplementation with ketogenic amino acids in Abx-treated SPF mice enriched for A. muciniphila and Parabacteroides spp (left). n = 5, 6. Behavior in seizure-tested mice (right). Yellow line at y=10 seconds represents threshold for scoring seizures, and yellow triangle at 24 mA denotes starting current per experimental cohort. n = 12. **c,** Total GGT activity per 100 mg feces from SPF CD, SPF KD, AkkPb KD, or AkkPb CD mice (left), and inhibition by GGsTop (right). n = 5. **d,** Total GGT activity per 100 mg feces from SPF CD animals treated with vehicle, A. muciniphila and Parabacteroides spp. probiotic, or heat-killed bacteria for bi-daily for 28 days (left), and inhibition by GGsTop (right). n = 5. **e,** (left) Levels of live A. muciniphila (Akk) after incubation in CD vs KD culture media or in CD or KD agar overlaid with M9 minimal media containing live Parabacteroides merdae (PbM) or no bacteria (0). n = 3. **f,** Levels of live PbM after incubation in M9 minimal media overlaid on CD or KD agar containing Akk or no bacteria (0). n = 5. **g,** GGT activity in P. merdae grown in M9 media overlaid on CD agar containing A. muciniphila or no bacteria at t=24 hrs, and inhibition of GGT activity by GGsTop. n = 5. **h,** GGT activity in P. merdae grown in M9 media overlaid on KD agar containing A. muciniphila or no bacteria at t=24 hrs, and inhibition of GGT activity by GGsTop. n = 5. Data are presented as mean ± s.e.m. Students' t-test (**a,b**), Two-way ANOVA with Bonferroni (**c, d**), One-way ANOVA with Bonferroni (**e-h**): **P < 0.01, ***P < 0.001, ****P < 0.0001. SPF=specific pathogen-free (conventionally-colonized), CD=control diet, KD=ketogenic diet, CC50=current intensity

223

producing seizures in 50% of mice tested, AA=amino acids, veh=vehicle, Abx=pre-treated with antibiotics (ampicillin, vancomycin, neomycin, metronidazole [AVNM]), AkkPb=A. muciniphila, P. merdae and P. distasonis, GGsTop=GGT inhibitor, PbM=Parabacteroides merdae, Akk=Akkermansia muciniphila, M9=minimal media, GGT=gamma-glutamyltranspeptidase, AU=absorbance units.
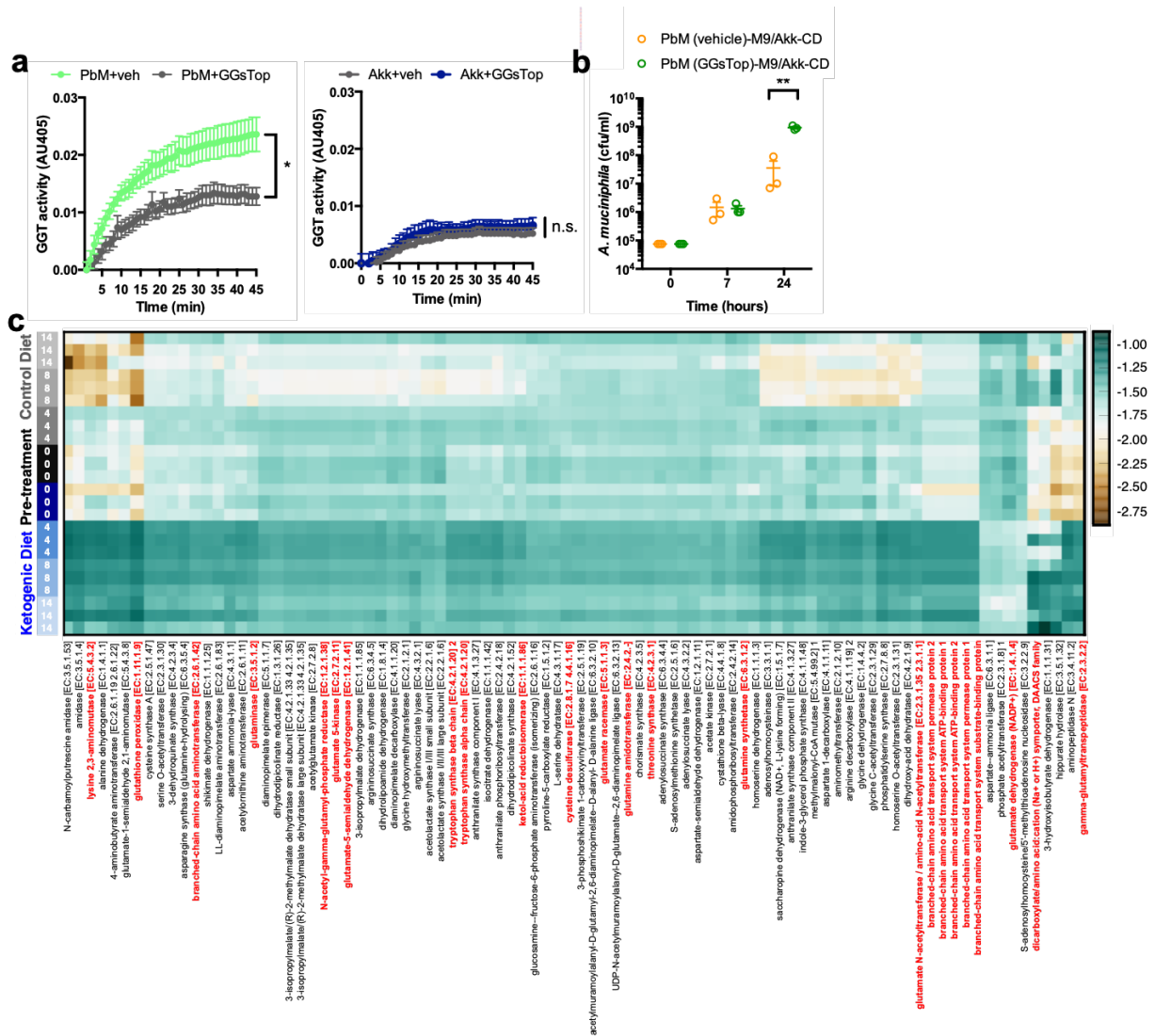

Figure 20: Amino Acid Effects on Seizures, Bacterial GGT Activity and Dietary Modulation of Bacterial Genes for Amino Acid Metabolism. a, GGT activity in

conventionally-cultured Parabacteroides merdae (left) and A. muciniphila (right), treated with GGsTop or vehicle. n = 5. b, Levels of A. muciniphila (Akk) after 0, 7, or 24 hours incubation in CD agar overlaid with P. merdae (PbM) that was pre-treated with vehicle or GGsTop in M9 minimal media. n=3. c, Inferred content of genes relevant to amino acid metabolism based on 16S rDNA sequencing of microbiomes from SPF mice fed CD or KD for 0, 4, 8, and 14 days. Genes in red text denote relevance to ketogenic amino acid metabolism and gamma-glutamylation. n = 3 cages/group. Data are presented as mean ± s.e.m. One-way ANOVA with Bonferroni (a): *P < 0.05, Two-way ANOVA with Bonferroni (b): **P < 0.01, PbM=Parabacteroides merdae, Akk=Akkermansia muciniphila, GGsTop=GGT inhibitor, GGT=gamma-glutamyltranspeptidase, AU=absorbance units.
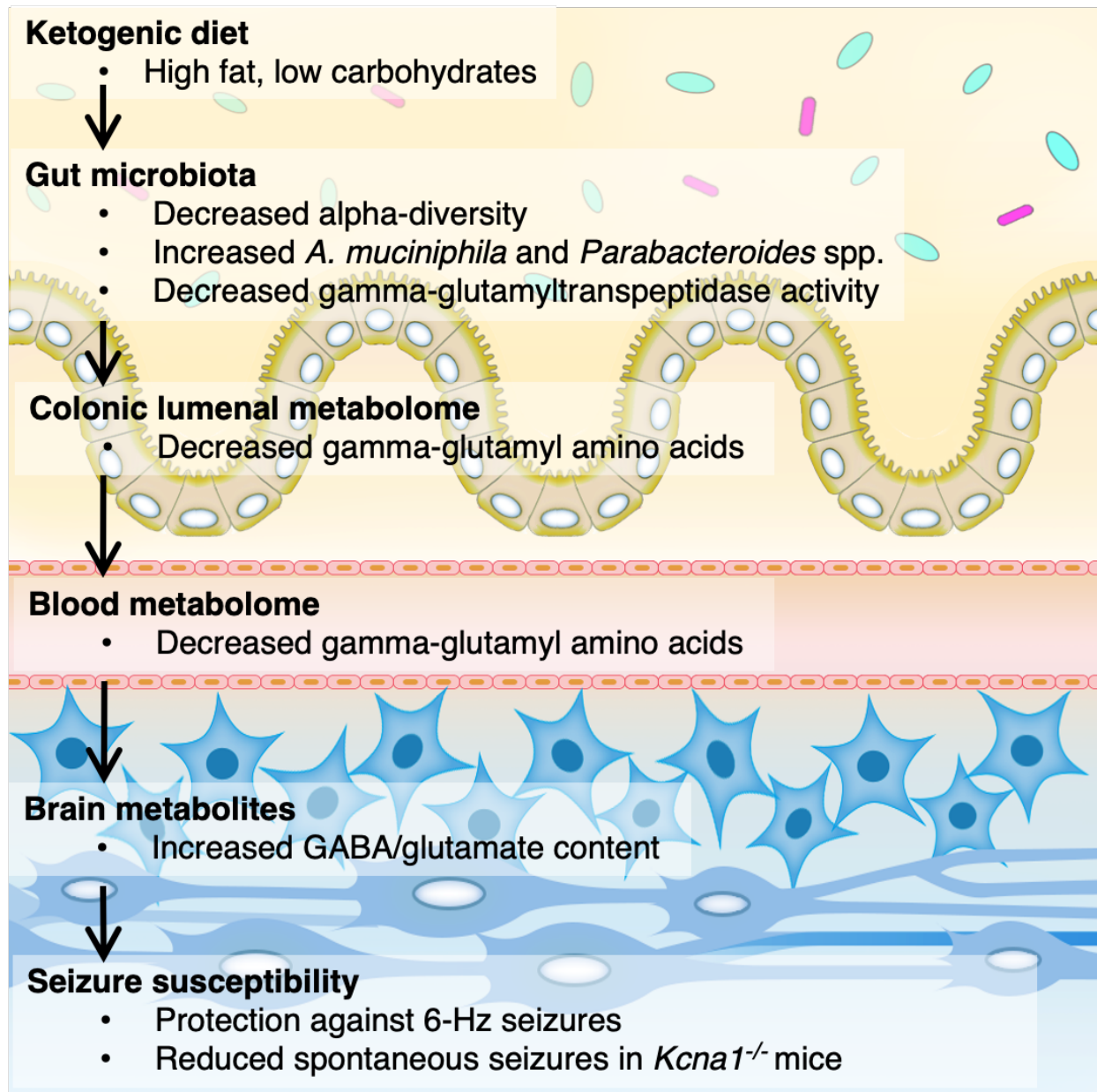
Figure 21: **Model for Effects of the Ketogenic Diet (KD) on the Gut Microbiome and Seizure Protection.** The high fat, low carbohydrate KD decreases alpha-diversity of the gut microbiota, while enriching relative abundance of particular bacterial taxa that can subsist in polysaccharide-restricted environments, including A. muciniphila and Parabacteroides spp. The KD and cross-feeding between bacteria, including A.

muciniphila and Parabacteroides spp., decreases gamma-glutamyltranspeptidase

activity of the gut microbiota. As a result, decreased levels of gamma-glutamyl amino

acids are detected in the colonic lumen and the blood, among many other microbiota-

related metabolomic alterations. Gamma-glutamyl amino acids exhibit altered transport

properties, where the brain relies on peripheral amino acid transport for regulation of

central metabolism of neurochemicals, including GABA and glutamate. The KD

microbiota, and A. muciniphila and Parabacteroides spp. in particular, sufficiently raise

hippocampal GABA/glutamate ratios and protect against induced 6-Hz psychomotor

seizures in wild-type mice as well as spontaneous tonic-clonic seizures in Kcna1

deficient mice.

STAR★METHODS

Detailed methods are provided and include the following:

- · KEY RESOURCES TABLE
- · CONTACT FOR REAGENT AND RESOURCE SHARING
- · EXPERIMENTAL MODELS AND SUBJECT DETAILS
  - o Mice
  - o Bacteria
- · METHOD DETAILS
  - o 6-Hz Psychomotor Seizure Assay
  - o Glucose Measurements

- o Beta-hydroxybutyrate Measurements

- o 16S rDNA Microbiota Profiling

- o Microbiota Conventionalization

- o Antibiotic Treatment

- o Gnotobiotic Colonization and Bacterial Enrichment

- o Bacterial Fluorescence *In Situ* Hybridization (FISH)

- o Fecal Microbiota Transplant

- o Bacterial Treatment

- o *Kcna1* Seizure EEG Recordings

- o Colonic Lumenal and Serum Metabolomics

- o Hippocampal Metabolomics

- o Amino Acid Supplementation

- o GGsTop Treatment

- o Cross-Feeding *in vitro* Assay

- o GGT Activity Assay

- o Intestinal Permeability Assay

- · QUANTIFICATION AND STATISTICAL ANALYSIS

- · DATA AND SOFTWARE AVAILABILITY

REAGENT or RESOURCE	SOURCE	IDENTIFIER
Bacterial and Virus Strains		
Akkermansia muciniphila	ATCC	ATCC BAA845

Parabacteroides merdae	ATCC	ATCC 43184
Parabacteroides distasonis	ATCC	ATCC 8503
Bifidobacterium longum	ATCC	ATCC 15707
Chemicals, Peptides, and Recombinant Proteins		
GGsTop, 3-[[(3-amino-3-carboxypropyl) methoxyphosphinyl]oxy]benzen eacetic acid	Tocris Bioscience	4452; CAS: 926281-37-0
Mucin from porcine stomach, type III	Sigma-Aldrich	· M1778; CAS: 84082-64-4
L-gamma-glutamyl-3-carboxy-4-nitroanilide	Gold Bio	G-380-1; CAS: 63699-78-5
4 kDa FITC-dextran	Sigma-Aldrich	46944; CAS: 60842-46-8
Critical Commercial Assays		
Glucose Colorimetric Assay Kit	Cayman Chemical	Cat# 10009582
Beta-hydroxybutyrate Colorimetric Assay Kit	Cayman Chemical	Cat# 700190
MoBio PowerSoil Kit	Mo Bio	Cat# 12888-100
Deposited Data		
16S rDNA sequences	This paper	https://qiita.ucsd.edu, 11566
Experimental Models: Organisms/Strains		
Mouse: Swiss Webster, germ-free	Taconic	Taconic: SW GF

Mouse: Swiss Webster, specific pathogen-free	Taconic	Taconic: SW MPF
Mouse: Kcna1-/-: C3HeB.129S7-Kcna1^{tm1Tem}/J	Dr. Bruce Tempel	JAX: 003532
Oligonucleotides		
MUC1437: 6FAM-CCTTGCGGTTGGCTTA	Derrien, et al., 2008	Sigma Aldrich: custom oligo
BAC303: Texas Red-CCAATGTGGGGGACCTT	Manz, et al., 1996	Sigma Aldrich: custom oligo
Software and Algorithms		
Ethovision XT 11	Noldus	Cat # EX11-MAMBP-E
QIIME1.8.0	Caporaso et al., 2010	http://qiime.org/
Greengenes	Lawrence Berkeley National Labs	http://greengenes.lbl.gov/cgi-bin/nphindex.cgi
PICRUSt	Langille et al., 2013	http://picrust.github.io/picrust/
Ponemah V5.1	Data Sciences International	https://www.datasci.com/products/software/ponemah
Neuroscore	Data Sciences International	https://www.datasci.com/products/software/neuroscore
TraceFinder 3.3	ThermoFisher Scientific	OPTON-30491

ImageJ	National Institutes of Health	https://imagej.nih.gov/ij/
Other		
Ketogenic Diet Mouse Chow	Envigo	TD.07797.PWD
Control Diet Mouse Chow	Envigo	TD.150300
Standard Diet Mouse Chow	LabDiet	# 5010
ECT Unit	Ugo Basile	Model # 57800
EEG transmitters	Data Sciences International	PhysioTel ETA-F10

Table 5 KEY RESOURCES TABLE

CONTACT FOR REAGENT AND RESOURCE SHARING

Further information and requests for resources and reagents should be directed to and
will be fulfilled by the Lead Contact, Elaine Hsiao (ehsiao@ucla.edu)

EXPERIMENTAL MODELS AND SUBJECT DETAILS

Mice

3-4 week old SPF wildtype Swiss Webster mice (Taconic Farms), GF wildtype Swiss
Webster mice (Taconic Farms) and SPF C3HeB/FeJ *KCNA1* KO mice (Jackson
Laboratories) were bred in UCLA's Center for Health Sciences Barrier Facility. Breeding
animals were fed "breeder" chow (Lab Diets 5K52). Experimental animals were fed

standard chow (Lab Diet 5010), 6:1 ketogenic diet (Harlan Teklad TD.07797.PWD; Supplementary Table 1) or vitamin- and mineral-matched control diet (Harlan Teklad TD.150300; Supplementary Table 1). Juvenile mice were used to i) mimic the typical use of the KD to treat pediatric and adolescent epileptic patients, ii) align the timing of mouse brain development to early human brain development, where neurodevelopmental milestones in 3-week old mice are comparable to those of the 2-3 year old human brain (Semple et al., 2013),, and iii) preclude pre-weaning dietary treatment, where effects of the diet on maternal behavior and physiology would confound direct effects of the diet on offspring. Mice were randomly assigned to an experimental group. Experiments include age- and sex-matched cohorts of males and females. Consistent with prior reports (Dutton et al., 2011), we observed no significant differences in seizure threshold or BHB levels in male vs. female WT mice. All animal experiments were approved by the UCLA Animal Care and Use Committee.

Bacteria

A. muciniphila (ATCC BAA845) was cultured under anaerobic conditions at 37°C in Brain Heart Infusion (BHI) media supplemented with 0.05% hog gastric mucin type III (Sigma Aldrich). *P. merdae* (ATCC 43184) and *P. distasonis* (ATCC 8503) were grown in anaerobic conditions at 37°C in Reinforced Clostridial Media (RCM). Cultures were authenticated by full-length 16S rDNA sequencing.

METHOD DETAILS

6-Hz Psychomotor Seizure Assay

The 6-Hz test was conducted as previously described (Samala et al., 2008). Pilot studies revealed no sexual dimorphism in seizure threshold. All subsequent experimental cohorts contained male mice. One drop (~50 ul) of 0.5% tetracaine hydrochloride ophthalmic solution was applied to the corneas of each mouse 10-15 min before stimulation. Corneal electrodes were coated with a thin layer of electrode gel (Parker Signagel). A constant-current current device (ECT Unit 57800, Ugo Basile) was used to deliver current at 3 sec duration, 0.2 ms pulse-width and 6 pulses/s frequency. CC50 (the intensity of current required to elicit seizures in 50% of the experimental group) was measured as a metric for seizure susceptibility. Pilot experiments were conducted to identify 24 mA as the CC50 for SPF wild-type Swiss Webster mice. Each mouse was seizure-tested only once, and thus at least $n > 6$ mice were used to adequately power each experiment group. To determine CC50s for each experimental group, 24 mA currents were administered to the first mouse per experimental group per cohort, followed by fixed increases or decreases by 2 mA intervals. Mice were restrained manually during stimulation and then released into a new cage for behavioral observation. Locomotor behavior was recorded using Ethovision XT software (Noldus) and quantitative measures for falling, tail dorsiflexion (Straub tail), forelimb clonus, eye/vibrissae twitching and behavioral remission were scored manually. For each behavioral parameter, we observed no correlation between percentage incidence during 24 mA seizures and microbiota status or group seizure susceptibility, suggesting a primary effect of the microbiota on seizure incidence rather than presentation or form. Latency to exploration (time elapsed from when an experimental mouse is released into

233

the observation cage (after corneal stimulation) to its first lateral movement) was scored using Ethovision and manually with an electronic timer. Mice were blindly scored as protected from seizures if they did not show seizure behavior and resumed normal exploratory behavior within 10 s. Seizure threshold (CC50) was determined as previously described (Kimball et al., 1957), using the average log interval of current steps per experimental group, where sample n is defined as the subset of animals displaying the less frequent seizure behavior. Data used to calculate CC50 are also displayed as latency to explore for each current intensity, where n represents the total number of biological replicates per group regardless of seizure outcome.

Glucose Measurements

Blood samples were collected by cardiac puncture and spun through SST vacutainers (Becton Dickinson) for serum separation. Glucose levels were detected in sera by colorimetric assay according to the manufacturer's instructions (Cayman Chemical). Data compiled across multiple experiments are expressed as glucose concentrations normalized to SPF controls within each experiment.

Beta-hydroxybutyrate (BHB) Measurements

Blood was collected by cardiac puncture and spun through SST vacutainers (Becton Dickinson) for serum separation. The colon was washed and flushed with PBS to remove lumenal contents. Frontal cortex, hippocampus, hypothalamus and cerebellum were microdissected and livers were harvested and washed in PBS. Tissue samples were sonicated on ice in 10 s intervals at 20 mV in RIPA lysis buffer (Thermo Scientific). BHB levels were detected in sera by colorimetric assay according to the manufacturer's

234

instructions (Cayman Chemical). Data were normalized to total protein content as detected by BCA assay (Thermo Pierce). Data compiled across multiple experiments are expressed as BHB concentrations normalized to SPF controls within each experiment.

16S rDNA Microbiota Profiling

Bacterial genomic DNA was extracted from mouse fecal samples or colonic lumenal contents using the MoBio PowerSoil Kit, where the sample *n* reflects independent cages containing 3 mice per cage. The library was generated according to methods adapted from (Caporaso et al., 2011). The V4 regions of the 16S rDNA gene were PCR amplified using individually barcoded universal primers and 30 ng of the extracted genomic DNA. The PCR reaction was set up in triplicate, and the PCR product was purified using the Qiaquick PCR purification kit (Qiagen). The purified PCR product was pooled in equal molar concentrations quantified by the Kapa library quantification kit (Kapa Biosystems, KK4824) and sequenced by Laragen, Inc. using the Illumina MiSeq platform and 2 x 250bp reagent kit for paired-end sequencing. Operational taxonomic units (OTUs) were chosen by open reference OTU picking based on 97% sequence similarity to the Greengenes 13_5 database. Taxonomy assignment and rarefaction were performed using QIIME1.8.0 (Caporaso et al., 2010) using 85,134 reads per sample. Metagenomes were inferred from closed reference OTU tables using PICRUSt (Langille et al., 2013). Results were filtered to display the top 72 genes relevant to amino acid metabolism in Figure S7C.

Microbiota Conventionalization

Fecal samples were freshly collected from adult SPF Swiss Webster mice and homogenized in pre-reduced PBS at 1 ml per pellet. 100 ul of the settled suspension was administered by oral gavage to recipient GF mice. For mock treatment, mice were gavaged with pre-reduced PBS.

Antibiotic Treatment

SPF mice were gavaged with a solution of vancomycin (50mg/kg), neomycin (100 mg/kg) and metronidazole (100 mg/kg) every 12 hours daily for 7 days, according to methods previously described (Reikvam et al., 2011), using dosages typically greater than those used for clinical therapeutic treatment. Ampicillin (1 mg/ml) was provided *ad libitum* in drinking water. For mock treatment, mice were gavaged with normal drinking water every 12 hours daily for 7 days. For $Kcna1^{-/-}$ mice, drinking water was supplemented with vancomycin (500 mg/ml), neomycin (1 mg/ml) and ampicillin (1 mg/ml) for 1 week to preclude the stress of oral gavage in seizure-prone mice. Antibiotic-treated mice were maintained in sterile caging with sterile food and water and handled aseptically for the remainder of the experiments.

Gnotobiotic Colonization and Bacterial Enrichment

10^9 cfu bacteria were suspended in 200 ul pre-reduced PBS and orally gavaged into antibiotic-treated mice or germ-free mice. When co-administered as "*A. muciniphila* and *Parabacteroides* spp.", a ratio of 2:1:1 was used for *A. muciniphila*: *P. merdae*: *P. distasonis*. For mock treatment, mice were gavaged with pre-reduced PBS. Pilot studies

revealed no significant differences between colonization groups in fecal DNA concentration or 16S rDNA amplification, as measures relevant to bacterial load. Mice were maintained in microisolator cages and handled aseptically. Mice were seizure tested at 14 days after colonization.

Bacterial Fluorescence *In Situ* Hybridization (FISH)

Mouse colon was cut into distal, medial and proximal sections and fixed in 4% paraformaldehyde solution overnight at 4°C, washed and passed through 15% and 30% sucrose solutions. Colon tissues were then embedded in optimal cutting temperature (OCT) compound (Tissue-Tek) and cryosectioned into 5 um longitudinal sections (Leica CM1950). Slides were equilibrated in hybridization buffer (0.9 M NaCl, 20 mM Tris-HCl, 0.01% sodium dodecyl sulfate, 10% formamide) and incubated in 10 ng/ul FISH probe (Sigma Aldrich) for 15 hr at 47°C in a humidified chamber. The probes were BAC303 (Manz et al., 1996): 5' Texas Red-CCAATGTGGGGGACCTT. MUC1437 (Derrien et al., 2008): 5' 6FAM-CCTTGCGGTTGGCTTA. Slides were then incubated for 20 min in wash buffer (0.9 M NaCl, 20 mM Tris-HCl) pre-heated to 47°C and washed gently three times in PBS. Samples were then incubated in the dark with 10mg/ml DAPI in PBS for 1 hour at 4°C, washed three times in PBS and mounted in Vectashield mounting medium (Vector Labs). Images were acquired on a Leica TCS Sp5 confocal microscope using LAS AF software (Leica). A 63X oil-immersion objective was used for imaging. Stacks spanning 10 um thickness were compressed using Fiji software (NIH).

Fecal Microbiota Transplant

Fecal samples were freshly collected from donor mice fed KD or CD for 14 days and suspended at 50 mg/ml in pre-reduced PBS. Antibiotic-treated mice were colonized by oral gavage of 100 ul suspension. For mock treatment, mice were gavaged with pre-reduced PBS. Mice were housed in microisolator cages and handled aseptically. Seizure testing was conducted at 4 days after transplant.

Bacterial Treatment

A. muciniphila, P. merdae and *P. distasonis* were freshly cultured in anaerobic conditions as described above, and then washed, pelleted and re-suspended at 5×10^9 cfu/ml in pre-reduced PBS. *A. muciniphila* with *Parabacteroides* spp. were prepared at a 2:1:1 ratio. For heat-killing, bacteria were placed at 95°C for 10 min. Mice were gavaged every 12 hours for 28 days with 200 ul bacterial suspension or sterile pre-reduced PBS as vehicle control.

***Kcna1* Seizure Recordings**

EEG Implantation and Recovery. EEGs were recorded from male and female *Kcna1*^{-/-} mice at 6-7 weeks of age. *Kcna1*^{+/+} littermates were used as controls. We observed no significant differences between males and females in seizure frequency and duration. Data presented include both sexes. Mice were anesthetized with isoflurane (5% induction, 2% maintenance) and eye ointment applied to each eye. Fur was removed along the head, and the area was cleaned with three alternative scrubs of chlorohexidine and 70% isopropanol. In a biosafety cabinet, mice were positioned in a stereotaxic apparatus (Harvard Biosciences) and 1 mg/kg lidocaine + 1 mg/kg

bupivacaine was applied locally along the incision site. Using sterile surgical tools, a 2 cm incision was made along the dorsal midline from the posterior margin of the eyes to a point midway between the scapulae. A subcutaneous pocket along the dorsal flank was created and the pocket irrigated with sterile saline. A wireless telemetry transmitter was inserted with bi-potential leads oriented cranially. The skull was cleaned with 3% hydrogen peroxide followed by 70% isopropanol. Using a 1.0 mm micro drill bit, the skull was perforated to generate two small holes halfway between the bregma and lambda, and 1-2 mm from the sagittal suture. Bilateral EEG recording electrodes (Data Sciences International (DSI) PhysioTel, ETA-F10) were epidurally implanted over the frontoparietal cortex. Sterile acrylic was applied to the dried area. The incision site was closed with absorbable 5-0 sutures and cleaned with 3% hydrogen peroxide followed by 70% ethanol. Animals were housed individually in autoclaved microisolator cages and allowed to recover for 3-5 days before recordings were initiated.

Data Acquisition and Analysis. During EEG recordings animals were freely moving and maintained on experimental diet. EEG traces were acquired over 3 days using the DSI Ponemah V5.1 data acquisition system. Simultaneous video recordings of behavioral seizures were correlated with EEG recordings and scored based on an adapted Racine scale and defined by 5 stages: 1) myoclonic jerk, 2) head stereotypy and facial clonus, 3) bilateral and alternating forelimb/hindlimb clonus, 4) rearing and falling, and 5) generalized tonic-clonic episodes (Fenoglio-Simeone et al., 2009; Simeone et al., 2016). Data were analyzed by a blinded researcher using Neuroscore CNS Software (DSI). EEG signals were filtered using a 10 Hz high pass filter, and seizure events were

detected by blinded manual scoring. Seizures were defined as patterns of high-frequency, high-voltage synchronized heterogeneous spike wave forms with amplitudes at least 2-fold greater than background with more than 6 s duration (Baraban et al., 2009). The spike frequency was determined as number of spikes occurring above baseline in a given seizure, and the interspike interval was analyzed as a function of the time between spikes for five representative seizures in each phase per mouse. The duration of maximum spike amplitude was determined as the percent time spent in spikes that were three times as large as the baseline for five representative seizures in each phase per mouse (Sato and Woolley, 2016).

Colonic Lumenal and Serum Metabolomics

Samples were collected from mice housed across independent cages, with at least 2 mice per cage. Colonic lumenal contents were collected from terminal mouse dissections, immediately snap frozen in liquid nitrogen and stored at -80°C. Serum samples were collected by cardiac puncture, separated using SST vacutainer tubes and frozen at -80°C. Samples were prepared using the automated MicroLab STAR system (Hamilton Company) and analyzed on GC/MS, LC/MS and LC/MS/MS platforms by Metabolon, Inc. Protein fractions were removed by serial extractions with organic aqueous solvents, concentrated using a TurboVap system (Zymark) and vacuum dried. For LC/MS and LC-MS/MS, samples were reconstituted in acidic or basic LC-compatible solvents containing >11 injection standards and run on a Waters ACQUITY UPLC and Thermo-Finnigan LTQ mass spectrometer, with a linear ion-trap front-end and a Fourier transform ion cyclotron resonance mass spectrometer back-end. For

GC/MS, samples were derivatized under dried nitrogen using bistrimethyl-silyl-trifluoroacetamide and analyzed on a Thermo-Finnigan Trace DSQ fast-scanning single-quadrupole mass spectrometer using electron impact ionization. Chemical entities were identified by comparison to metabolomic library entries of purified standards. Following log transformation and imputation with minimum observed values for each compound, data were analyzed using one-way ANOVA to test for group effects. P and q-values were calculated based on two-way ANOVA contrasts. Principal components analysis was used to visualize variance distributions. Supervised Random Forest analysis was conducted to identify metabolomics prediction accuracies.

Hippocampal Metabolomics

Hippocampal tissues were homogenized in 1 ml cold 80% MeOH and vigorously mixed on ice followed by centrifugation ($1.3*10^4$ rpm, 4 °C). 5 ug supernatant was transferred into a glass vial, supplemented with 5 nmol D/L-norvaline, dried down under vacuum, and finally re-suspended in 70% acetonitrile. For the mass spectrometry-based analysis of the sample, 5 l were injected onto a Luna NH2 (150 mm x 2 mm, Phenomenex) column. The samples were analyzed with an UltiMate 3000RSLC (Thermo Scientific) coupled to a Q Exactive mass spectrometer (Thermo Scientific). The Q Exactive was run with polarity switching (+4.00 kV / -4.00 kV) in full scan mode with an m/z range of 70-1050. Separation was achieved using A) 5 mM NH_4AcO (pH 9.9) and B) ACN. The gradient started with 15% A) going to 90% A) over 18 min, followed by an isocratic step for 9 min. and reversal to the initial 15% A) for 7 min. Metabolites were quantified with TraceFinder 3.3 using accurate mass measurements ($\leq$ 3 ppm), retention times of pure

241

standards and MS2 fragmentation patterns. Data analysis, including principal

component analysis and hierarchical clustering was performed using R.

Amino Acid Supplementation

4-week old Swiss Webster SPF mice were treated with antibiotics, colonized with *A.*

muciniphila and *Parabacteroides* spp., and fed KD for 14 days, as described in methods

above. Beginning on the evening of day 11, mice were injected intraperitoneally every

12 hours for 3 days with ketogenic amino acid cocktail (Sigma Aldrich)-- L-leucine (2.0

mg/kg), L-lysine (2.0 mg/kg), L-tyrosine (2.4 mg/kg), L-tryptophan (1.6 mg/kg), and L-

threonine (3.1 mg/kg) in sterile PBS. Concentrations are based on physiological levels

reported for each amino acid in mouse blood (Smith, 2000) and on fold-changes

observed in our metabolomics dataset for each amino acid between control SPF CD

and AkkPb KD mice (Table S4). Vehicle-treated mice were injected with PBS (200 ul/

30 g mouse). On day 14, mice were tested for 6-Hz seizures 2 hours after the final

morning amino acid injection, with a prior 1-hour acclimation period in the behavioral

testing room.

GGsTop Treatment

For wildtype mice: 4-week old SPF Swiss Webster mice were fed CD *ad libitum* for 14

days. Beginning on the evening of day 11, mice were orally gavaged every 12 hours

with 13.3 mg/kg 3-[[(3-amino-3-carboxypropyl)methoxyphosphinyl]oxy]benzeneacetic

acid (GGsTop, Tocris Bioscience) in sterile water. Vehicle-treated mice were gavaged

with sterile water (200 ul/ 30 g mouse). On day 14, mice were tested for 6-Hz seizures 2

hours after the final morning GGsTop gavage, with a prior 1-hour acclimation period in the behavioral testing room. For Kcna1 mice: 3-4 week old Kcna1-/- mice were fed the CD *ad libitum* for 23 days. On Day 15, EEG transmitters were implanted as described in the *Kcna1 Seizure Recordings* section above. On the evening of day 18, mice were orally gavaged every 12 hours with 13.3 mg/kg GGsTop through the morning of day 21. Seizures were recorded over 3 days by EEG beginning 2 hours after the final gavage.

Cross-Feeding *in vitro* Assay

Cross-feeding was measured as previously described (Flynn et al., 2016). *A. muciniphila* was embedded at 2×10^6 cfu/ml in 5 ml pre-reduced CD or KD-based liquid media supplemented with 1% agar at the bottom of an anaerobic tube, and *P. merdae* was overlaid above it at 6×10^6 cfu/ml in 5 ml pre-reduced M9 minimal media. Diet-based media were generated by aseptically suspending mouse KD vs. CD diets, described above, to 2 kcal/ml in M9 media. Pilot experiments confirmed no ectopic translocation of embedded *A. muciniphila* from the agar compartment into the above M9 liquid compartment. For each time point, aliquots were taken from the top and bottom compartments, plated in a dilution series in rich media (RCM for *P. merdae* and BHI + 0.05% mucins for *A. muciniphila*), and colonies were counted. For GGsTop pre-treatment experiments, *P. merdae* was incubated with 500 uM GGsTop vs vehicle in RCM media at 37°C for 2 hours and then washed with sterile media. Pilot experiments revealed no significant effect of GGsTop pre-treatment on *P. merdae* viability.

GGT Activity Assay

GGT activity was measured as previously described (van der Stel et al., 2015). For anaerobic cultures, bacteria were seeded at 3 x 10^5 cfu/ml in CD- and KD-based media. 1 ml bacterial suspension was pelleted and frozen at -80°C for 1 hr. Separate aliquots of the same suspension were plated in BHI mucin agar media or RCM and incubated at 37°C in a Coy anaerobic chamber for later data normalization by bacterial cfu. Pellets were then resuspended in 250 ul lysis buffer (50 mM Tris-HCl with 1 ug/ml lysozyme) and incubated on ice for 30 min. For fecal samples, one pellet was weighed and homogenized in 1 ml lysis buffer. Bacterial and fecal suspensions were then sonicated (QSonica 125) and centrifuged at 12000 xg for 10 min at 4°C. 20 ul supernatant was mixed with 180 ul substrate buffer (2.9 mM L-gamma-glutamyl-3-carboxy-4-nitroanilide (Gold Bio), 100 mM of glycylglycine (Sigma Aldrich), 100 mM Tris-HCl), and 500 uM GGsTop (if noted). Absorbance at 405 nm denoting production of 3-carboxy-4-nitroaniline was measured every minute for 1 hr at 37° C using an automated multimode plate reader (Biotek Synergy H1).

Intestinal Permeability Assay

Mice were fasted for 4 hr beginning at 7am before gavage with 0.6 g/kg 4 kDa FITC-dextran (Sigma Aldrich). 4 hours after gavage, serum samples were collected by cardiac puncture, diluted 3-fold in water and read in duplicate for fluorescence intensity at 521 nm using a Synergy H9 multimode plate reader (Biotek) against a standard dilution series of stock FITC-dextran in 3-fold diluted normal mouse serum in water.

QUANTIFICATION AND STATISTICAL ANALYSIS

Statistical analysis was performed using Prism software (GraphPad). Data were assessed for normal distribution and plotted in the figures as mean ± SEM. For each figure, n = the number of independent biological replicates. No samples or animals were excluded from the analyses. Differences between two treatment groups were assessed using two-tailed, unpaired Student t test with Welch's correction. Differences among >2 groups with only one variable were assessed using one-way ANOVA with Bonferroni post hoc test. Taxonomic comparisons from 16S rDNA sequencing analysis were analyzed by Kruskal-Wallis test with Bonferroni post hoc test. Data for *Kcna1* mice were analyzed by non-parametric one-way ANOVA with Dunn's post hoc test. Two-way ANOVA with Bonferroni post-hoc test was used for ≥ 2 groups with two variables (e.g. seizure time course, BHB time course, metabolomics data, bacterial growth curves). One-way ANOVA with repeated measures and Bonferroni post-hoc test was used for GGT assays. Significant differences emerging from the above tests are indicated in the figures by $*p < 0.05$, $**p < 0.01$, $***p < 0.001$, $****p < 0.0001$ Notable near-significant differences ($0.5 < p < 0.1$) are indicated in the figures. Notable non-significant (and non-near significant) differences are indicated in the figures by "n.s.".

DATA AND SOFTWARE AVAILABILITY

16S rDNA sequencing data and metadata are available online through the QIITA website (https://qiita.ucsd.edu/) with the study accession #11566.

SUPPLEMENTAL INFORMATION

Supplemental Information includes seven figures and six tables and can be found with this article.

AUTHOR CONTRIBUTIONS

DECLARATION OF INTERESTS

ACKNOWLEDGMENTS

REFERENCES

Baraban, S.C., Southwell, D.G., Estrada, R.C., Jones, D.L., Sebe, J.Y., Alfaro-Cervello, C., Garcia-Verdugo, J.M., Rubenstein, J.L., and Alvarez-Buylla, A. (2009). Reduction of seizures by transplantation of cortical GABAergic interneuron precursors into Kv1.1 mutant mice. Proceedings of the National Academy of Sciences of the United States of America *106*, 15472-15477.

Barrett, E., Ross, R.P., O'Toole, P.W., Fitzgerald, G.F., and Stanton, C. (2012). gamma-Aminobutyric acid production by culturable bacteria from the human intestine. J Appl Microbiol *113*, 411-417.

Barton, M.E., Klein, B.D., Wolf, H.H., and White, H.S. (2001). Pharmacological characterization of the 6 Hz psychomotor seizure model of partial epilepsy. Epilepsy research *47*, 217-227.

Beloosesky, Y., Grosman, B., Marmelstein, V., and Grinblat, J. (2000). Convulsions induced by metronidazole treatment for Clostridium difficile-associated disease in chronic renal failure. The American journal of the medical sciences *319*, 338-339.

Bough, K. (2008). Energy metabolism as part of the anticonvulsant mechanism of the ketogenic diet. Epilepsia *49 Suppl 8*, 91-93.

Bough, K.J., and Rho, J.M. (2007). Anticonvulsant mechanisms of the ketogenic diet. Epilepsia *48*, 43-58.

Browne, D.L., Gancher, S.T., Nutt, J.G., Brunt, E.R., Smith, E.A., Kramer, P., and Litt, M. (1994). Episodic ataxia/myokymia syndrome is associated with point mutations in the human potassium channel gene, KCNA1. Nat Genet *8*, 136-140.

Buffington, S.A., Di Prisco, G.V., Auchtung, T.A., Ajami, N.J., Petrosino, J.F., and Costa-Mattioli, M. (2016). Microbial Reconstitution Reverses Maternal Diet-Induced Social and Synaptic Deficits in Offspring. Cell *165*, 1762-1775.

Caesar, R., Tremaroli, V., Kovatcheva-Datchary, P., Cani, P.D., and Backhed, F. (2015). Crosstalk between Gut Microbiota and Dietary Lipids Aggravates WAT Inflammation through TLR Signaling. Cell metabolism *22*, 658-668.

Calderon, N., Betancourt, L., Hernandez, L., and Rada, P. (2017). A ketogenic diet modifies glutamate, gamma-aminobutyric acid and agmatine levels in the hippocampus of rats: A microdialysis study. Neurosci Lett *642*, 158-162.

Caporaso, J.G., Kuczynski, J., Stombaugh, J., Bittinger, K., Bushman, F.D., Costello, E.K., Fierer, N., Pena, A.G., Goodrich, J.K., Gordon, J.I.*, et al.* (2010). QIIME allows analysis of high-throughput community sequencing data. Nature methods *7*, 335-336.

Caporaso, J.G., Lauber, C.L., Walters, W.A., Berg-Lyons, D., Lozupone, C.A., Turnbaugh, P.J., Fierer, N., and Knight, R. (2011). Global patterns of 16S rRNA diversity at a depth of millions of sequences per sample. Proceedings of the National Academy of Sciences of the United States of America *108 Suppl 1*, 4516-4522.

Castellano, I., and Merlino, A. (2012). gamma-Glutamyltranspeptidases: sequence, structure, biochemical properties, and biotechnological applications. Cellular and molecular life sciences : CMLS *69*, 3381-3394.

Collins, S.M., Surette, M., and Bercik, P. (2012). The interplay between the intestinal microbiota and the brain. Nature reviews Microbiology *10*, 735-742.

Cooper, A.J., and Jeitner, T.M. (2016). Central Role of Glutamate Metabolism in the Maintenance of Nitrogen Homeostasis in Normal and Hyperammonemic Brain. Biomolecules *6*.

Costello, E.K., Gordon, J.I., Secor, S.M., and Knight, R. (2010). Postprandial remodeling of the gut microbiota in Burmese pythons. The ISME journal *4*, 1375-1385.

Crawford, P.A., Crowley, J.R., Sambandam, N., Muegge, B.D., Costello, E.K., Hamady, M., Knight, R., and Gordon, J.I. (2009). Regulation of myocardial ketone body metabolism by the gut microbiota during nutrient deprivation. Proceedings of the National Academy of Sciences of the United States of America *106*, 11276-11281.

Dagorn, A., Chapalain, A., Mijouin, L., Hillion, M., Duclairoir-Poc, C., Chevalier, S., Taupin, L., Orange, N., and Feuilloley, M.G. (2013). Effect of GABA, a bacterial metabolite, on Pseudomonas fluorescens surface properties and cytotoxicity. Int J Mol Sci *14*, 12186-12204.

Dahlin, M., Elfving, A., Ungerstedt, U., and Amark, P. (2005). The ketogenic diet influences the levels of excitatory and inhibitory amino acids in the CSF in children with refractory epilepsy. Epilepsy research *64*, 115-125.

Dao, M.C., Everard, A., Aron-Wisnewsky, J., Sokolovska, N., Prifti, E., Verger, E.O., Kayser, B.D., Levenez, F., Chilloux, J., Hoyles, L.*, et al.* (2016a). Akkermansia

muciniphila and improved metabolic health during a dietary intervention in obesity: relationship with gut microbiome richness and ecology. Gut *65*, 426-436.

Dao, M.C., Everard, A., Aron-Wisnewsky, J., Sokolovska, N., Prifti, E., Verger, E.O., Kayser, B.D., Levenez, F., Chilloux, J., Hoyles, L.*, et al.* (2016b). Akkermansia muciniphila and improved metabolic health during a dietary intervention in obesity: relationship with gut microbiome richness and ecology. Gut *65*, 426-436.

David, L.A., Maurice, C.F., Carmody, R.N., Gootenberg, D.B., Button, J.E., Wolfe, B.E., Ling, A.V., Devlin, A.S., Varma, Y., Fischbach, M.A.*, et al.* (2014). Diet rapidly and reproducibly alters the human gut microbiome. Nature *505*, 559-563.

Derrien, M., Collado, M.C., Ben-Amor, K., Salminen, S., and de Vos, W.M. (2008). The Mucin degrader Akkermansia muciniphila is an abundant resident of the human intestinal tract. Applied and environmental microbiology *74*, 1646-1648.

Duncan, S.H., Lobley, G.E., Holtrop, G., Ince, J., Johnstone, A.M., Louis, P., and Flint, H.J. (2008). Human colonic microbiota associated with diet, obesity and weight loss. International journal of obesity *32*, 1720-1724.

Dutton, S.B., Sawyer, N.T., Kalume, F., Jumbo-Lucioni, P., Borges, K., Catterall, W.A., and Escayg, A. (2011). Protective effect of the ketogenic diet in Scn1a mutant mice. Epilepsia *52*, 2050-2056.

Earle, K.A., Billings, G., Sigal, M., Lichtman, J.S., Hansson, G.C., Elias, J.E., Amieva, M.R., Huang, K.C., and Sonnenburg, J.L. (2015). Quantitative Imaging of Gut Microbiota Spatial Organization. Cell Host Microbe *18*, 478-488.

Eraković, V., Župan, G., Varljen, J., Laginja, J., and Simonić, A. (2001). Altered Activities of Rat Brain Metabolic Enzymes in Electroconvulsive Shock—Induced Seizures. Epilepsia *42*, 181-189.

Eunson, L.H., Rea, R., Zuberi, S.M., Youroukos, S., Panayiotopoulos, C.P., Liguori, R., Avoni, P., McWilliam, R.C., Stephenson, J.B., Hanna, M.G*., et al.* (2000). Clinical, genetic, and expression studies of mutations in the potassium channel gene KCNA1 reveal new phenotypic variability. Ann Neurol *48*, 647-656.

Everard, A., Belzer, C., Geurts, L., Ouwerkerk, J.P., Druart, C., Bindels, L.B., Guiot, Y., Derrien, M., Muccioli, G.G., Delzenne, N.M*., et al.* (2013). Cross-talk between Akkermansia muciniphila and intestinal epithelium controls diet-induced obesity. Proceedings of the National Academy of Sciences *110*, 9066-9071.

Ewen, L.M., and Griffiths, J. (1973). γ-Glutamyl Transpeptidase: Elevated Activities in Certain Neurologic Diseases. American Journal of Clinical Pathology *59*, 2-9.

Fenoglio-Simeone, K.A., Wilke, J.C., Milligan, H.L., Allen, C.N., Rho, J.M., and Maganti, R.K. (2009). Ketogenic diet treatment abolishes seizure periodicity and improves diurnal rhythmicity in epileptic Kcna1-null mice. Epilepsia *50*, 2027-2034.

Flynn, J.M., Niccum, D., Dunitz, J.M., and Hunter, R.C. (2016). Evidence and Role for Bacterial Mucin Degradation in Cystic Fibrosis Airway Disease. PLoS Pathog *12*, e1005846.

Freeman, J.M., and Kossoff, E.H. (2010). Ketosis and the ketogenic diet, 2010: advances in treating epilepsy and other disorders. Advances in pediatrics *57*, 315-329.

Frey, H.H., Popp, C., and Loscher, W. (1979). Influence of inhibitors of the high affinity GABA uptake on seizure thresholds in mice. Neuropharmacology *18*, 581-590.

Frost, G., Sleeth, M.L., Sahuri-Arisoylu, M., Lizarbe, B., Cerdan, S., Brody, L., Anastasovska, J., Ghourab, S., Hankir, M., Zhang, S*., et al.* (2014). The short-chain fatty acid acetate reduces appetite via a central homeostatic mechanism. Nat Commun *5*, 3611.

Gautier, N.M., and Glasscock, E. (2015). Spontaneous seizures in Kcna1-null mice lacking voltage-gated Kv1.1 channels activate Fos expression in select limbic circuits. Journal of neurochemistry *135*, 157-164.

Giordano, C., Costa, A.M., Lucchi, C., Leo, G., Brunel, L., Fehrentz, J.A., Martinez, J., Torsello, A., and Biagini, G. (2016). Progressive Seizure Aggravation in the Repeated 6-Hz Corneal Stimulation Model Is Accompanied by Marked Increase in Hippocampal p-ERK1/2 Immunoreactivity in Neurons. Frontiers in cellular neuroscience *10*, 281.

Godon, J.J., Arulazhagan, P., Steyer, J.P., and Hamelin, J. (2016). Vertebrate bacterial gut diversity: size also matters. BMC Ecol *16*, 12.

Gudelj, I., Kinnersley, M., Rashkov, P., Schmidt, K., and Rosenzweig, F. (2016). Stability of Cross-Feeding Polymorphisms in Microbial Communities. PLoS computational biology *12*, e1005269.

Haro, C., Garcia-Carpintero, S., Alcala-Diaz, J.F., Gomez-Delgado, F., Delgado-Lista, J., Perez-Martinez, P., Rangel Zuniga, O.A., Quintana-Navarro, G.M., Landa, B.B., Clemente, J.C*., et al.* (2016). The gut microbial community in metabolic syndrome patients is modified by diet. J Nutr Biochem *27*, 27-31.

Hartman, A.L., Lyle, M., Rogawski, M.A., and Gasior, M. (2008). Efficacy of the ketogenic diet in the 6-Hz seizure test. Epilepsia *49*, 334-339.

Hartman, A.L., Zheng, X., Bergbower, E., Kennedy, M., and Hardwick, J.M. (2010). Seizure tests distinguish intermittent fasting from the ketogenic diet. Epilepsia *51*, 1395-1402.

Higuchi, T., Hayashi, H., and Abe, K. (1997). Exchange of glutamate and gamma-aminobutyrate in a Lactobacillus strain. J Bacteriol *179*, 3362-3364.

Hodgman, T., Dasta, J.F., Armstrong, D.K., Visconti, J.A., and Reilley, T.E. (1984). Ampicillin-associated seizures. Southern medical journal *77*, 1323-1325.

Hornik, C.P., Benjamin, D.K., Jr., Smith, P.B., Pencina, M.J., Tremoulet, A.H., Capparelli, E.V., Ericson, J.E., Clark, R.H., and Cohen-Wolkowiez, M. (2016). Electronic Health Records and Pharmacokinetic Modeling to Assess the Relationship between Ampicillin Exposure and Seizure Risk in Neonates. The Journal of pediatrics *178*, 125-129.e121.

Hufeldt, M.R., Nielsen, D.S., Vogensen, F.K., Midtvedt, T., and Hansen, A.K. (2010). Variation in the gut microbiota of laboratory mice is related to both genetic and environmental factors. Comp Med *60*, 336-347.

Janik, R., Thomason, L.A.M., Stanisz, A.M., Forsythe, P., Bienenstock, J., and Stanisz, G.J. (2016). Magnetic resonance spectroscopy reveals oral Lactobacillus promotion of increases in brain GABA, N-acetyl aspartate and glutamate. Neuroimage *125*, 988-995.

Kimball, A.W., Burnett, W.T., Jr., and Doherty, D.G. (1957). Chemical protection against ionizing radiation. I. Sampling methods for screening compounds in radiation protection studies with mice. Radiation research *7*, 1-12.

Klein, M.S., Newell, C., Bomhof, M.R., Reimer, R.A., Hittel, D.S., Rho, J.M., Vogel, H.J., and Shearer, J. (2016a). Metabolomic Modeling To Monitor Host Responsiveness to

Gut Microbiota Manipulation in the BTBR(T+tf/j) Mouse. Journal of proteome research *15*, 1143-1150.

Klein, M.S., Newell, C., Bomhof, M.R., Reimer, R.A., Hittel, D.S., Rho, J.M., Vogel, H.J., and Shearer, J. (2016b). Metabolomic Modeling To Monitor Host Responsiveness to Gut Microbiota Manipulation in the BTBRT+tf/j Mouse. Journal of proteome research *15*, 1143-1150.

Koeth, R.A., Wang, Z., Levison, B.S., Buffa, J.A., Org, E., Sheehy, B.T., Britt, E.B., Fu, X., Wu, Y., Li, L.*, et al.* (2013). Intestinal microbiota metabolism of L-carnitine, a nutrient in red meat, promotes atherosclerosis. Nature medicine *19*, 576-585.

Kwan, P., and Brodie, M.J. (2000). Early identification of refractory epilepsy. The New England journal of medicine *342*, 314-319.

Langille, M.G., Zaneveld, J., Caporaso, J.G., McDonald, D., Knights, D., Reyes, J.A., Clemente, J.C., Burkepile, D.E., Vega Thurber, R.L., Knight, R.*, et al.* (2013). Predictive functional profiling of microbial communities using 16S rRNA marker gene sequences. Nat Biotechnol *31*, 814-821.

Lopantsev, V., Tempel, B.L., and Schwartzkroin, P.A. (2003). Hyperexcitability of CA3 pyramidal cells in mice lacking the potassium channel subunit Kv1.1. Epilepsia *44*, 1506-1512.

Lozupone, C.A., Stombaugh, J.I., Gordon, J.I., Jansson, J.K., and Knight, R. (2012). Diversity, stability and resilience of the human gut microbiota. Nature *489*, 220-230.

Lutas, A., and Yellen, G. (2013). The ketogenic diet: metabolic influences on brain excitability and epilepsy. Trends in neurosciences *36*, 32-40.

Manz, W., Amann, R., Ludwig, W., Vancanneyt, M., and Schleifer, K.H. (1996). Application of a suite of 16S rRNA-specific oligonucleotide probes designed to investigate bacteria of the phylum cytophaga-flavobacter-bacteroides in the natural environment. Microbiology *142 (Pt 5)*, 1097-1106.

Misra, U.K., Kalita, J., Chandra, S., and Nair, P.P. (2013). Association of antibiotics with status epilepticus. Neurological sciences : official journal of the Italian Neurological Society and of the Italian Society of Clinical Neurophysiology *34*, 327-331.

Moya, A., and Ferrer, M. (2016). Functional Redundancy-Induced Stability of Gut Microbiota Subjected to Disturbance. Trends Microbiol *24*, 402-413.

Newell, C., Bomhof, M.R., Reimer, R.A., Hittel, D.S., Rho, J.M., and Shearer, J. (2016). Ketogenic diet modifies the gut microbiota in a murine model of autism spectrum disorder. Mol Autism *7*, 37.

Perry, T.L., and Hansen, S. (1973). Sustained drug-induced elevation of brain GABA in the rat. Journal of neurochemistry *21*, 1167-1175.

Reikvam, D.H., Erofeev, A., Sandvik, A., Grcic, V., Jahnsen, F.L., Gaustad, P., McCoy, K.D., Macpherson, A.J., Meza-Zepeda, L.A., and Johansen, F.E. (2011). Depletion of murine intestinal microbiota: effects on gut mucosa and epithelial gene expression. PloS one *6*, e17996.

Remely, M., Hippe, B., Geretschlaeger, I., Stegmayer, S., Hoefinger, I., and Haslberger, A. (2015). Increased gut microbiota diversity and abundance of Faecalibacterium prausnitzii and Akkermansia after fasting: a pilot study. Wiener klinische Wochenschrift *127*, 394-398.

Roberts, E., and Kuriyama, K. (1968). Biochemical-physiological correlations in studies of the gamma-aminobutyric acid system. Brain Res *8*, 1-35.

Rogawski, M.A., Loscher, W., and Rho, J.M. (2016). Mechanisms of Action of Antiseizure Drugs and the Ketogenic Diet. Cold Spring Harbor perspectives in medicine *6*.

Roy, M., Beauvieux, M.C., Naulin, J., El Hamrani, D., Gallis, J.L., Cunnane, S.C., and Bouzier-Sore, A.K. (2015). Rapid adaptation of rat brain and liver metabolism to a ketogenic diet: an integrated study using (1)H- and (13)C-NMR spectroscopy. J Cereb Blood Flow Metab *35*, 1154-1162.

Sakai, R., Cohen, D.M., Henry, J.F., Burrin, D.G., and Reeds, P.J. (2004). Leucine-nitrogen metabolism in the brain of conscious rats: its role as a nitrogen carrier in glutamate synthesis in glial and neuronal metabolic compartments. Journal of neurochemistry *88*, 612-622.

Samala, R., Willis, S., and Borges, K. (2008). Anticonvulsant profile of a balanced ketogenic diet in acute mouse seizure models. Epilepsy research *81*, 119-127.

Samuels, S., Fish, I., and Schwartz, S.A. (1983). Anticonvulsant activity of glycylglycine and delta-aminovaleric acid: evidence for glutamine exchange in amino acid transport. J Neurochem *40*, 1063-1068.

Sandhu, K.V., Sherwin, E., Schellekens, H., Stanton, C., Dinan, T.G., and Cryan, J.F. (2017). Feeding the microbiota-gut-brain axis: diet, microbiome, and neuropsychiatry. Translational research : the journal of laboratory and clinical medicine *179*, 223-244.

Sariego-Jamardo, A., Garcia-Cazorla, A., Artuch, R., Castejon, E., Garcia-Arenas, D., Molero-Luis, M., Ormazabal, A., and Sanmarti, F.X. (2015). Efficacy of the Ketogenic

Diet for the Treatment of Refractory Childhood Epilepsy: Cerebrospinal Fluid Neurotransmitters and Amino Acid Levels. Pediatric neurology *53*, 422-426.

Sato, S.M., and Woolley, C.S. (2016). Acute inhibition of neurosteroid estrogen synthesis suppresses status epilepticus in an animal model. Elife *5*.

Scheffer, H., Brunt, E.R., Mol, G.J., van der Vlies, P., Stulp, R.P., Verlind, E., Mantel, G., Averyanov, Y.N., Hofstra, R.M., and Buys, C.H. (1998). Three novel KCNA1 mutations in episodic ataxia type I families. Hum Genet *102*, 464-466.

Seekatz, A.M., Aas, J., Gessert, C.E., Rubin, T.A., Saman, D.M., Bakken, J.S., and Young, V.B. (2014). Recovery of the gut microbiome following fecal microbiota transplantation. MBio *5*, e00893-00814.

Semple, B.D., Blomgren, K., Gimlin, K., Ferriero, D.M., and Noble-Haeusslein, L.J. (2013). Brain development in rodents and humans: Identifying benchmarks of maturation and vulnerability to injury across species. Progress in neurobiology *106-107*, 1-16.

Simeone, K.A., Matthews, S.A., Rho, J.M., and Simeone, T.A. (2016). Ketogenic diet treatment increases longevity in Kcna1-null mice, a model of sudden unexpected death in epilepsy. Epilepsia *57*, e178-182.

Smith, M.I., Yatsunenko, T., Manary, M.J., Trehan, I., Mkakosya, R., Cheng, J., Kau, A.L., Rich, S.S., Concannon, P., Mychaleckyj, J.C.*, et al.* (2013). Gut microbiomes of Malawian twin pairs discordant for kwashiorkor. Science *339*, 548-554.

Smith, Q.R. (2000). Transport of glutamate and other amino acids at the blood-brain barrier. The Journal of nutrition *130*, 1016S-1022S.

Sobiech, K.A., and Szewczuk, A. (1979). Effect of intestinal gamma-glutamyl transferase inhibitor on the amount of gamma-glutamyl metabolites in mouse. Folia Histochem Cytochem (Krakow) *17*, 147-152.

Sonnenburg, J.L., and Backhed, F. (2016). Diet-microbiota interactions as moderators of human metabolism. Nature *535*, 56-64.

Sonoyama, K., Fujiwara, R., Takemura, N., Ogasawara, T., Watanabe, J., Ito, H., and Morita, T. (2009). Response of gut microbiota to fasting and hibernation in Syrian hamsters. Applied and environmental microbiology *75*, 6451-6456.

Stafstrom, C.E., and Rho, J.M. (2012). The ketogenic diet as a treatment paradigm for diverse neurological disorders. Front Pharmacol *3*, 59.

Sutter, R., Ruegg, S., and Tschudin-Sutter, S. (2015). Seizures as adverse events of antibiotic drugs: A systematic review. Neurology *85*, 1332-1341.

van der Stel, A.X., van Mourik, A., Laniewski, P., van Putten, J.P., Jagusztyn-Krynicka, E.K., and Wosten, M.M. (2015). The Campylobacter jejuni RacRS two-component system activates the glutamate synthesis by directly upregulating gamma-glutamyltranspeptidase (GGT). Frontiers in microbiology *6*, 567.

van Karnebeek, C.D., Hartmann, H., Jaggumantri, S., Bok, L.A., Cheng, B., Connolly, M., Coughlin, C.R., 2nd, Das, A.M., Gospe, S.M., Jr., Jakobs, C.*, et al.* (2012). Lysine restricted diet for pyridoxine-dependent epilepsy: first evidence and future trials. Molecular genetics and metabolism *107*, 335-344.

Vuong, H.E., Yano, J.M., Fung, T.C., and Hsiao, E.Y. (2017). The Microbiome and Host Behavior. Annual review of neuroscience.

Wang, Z.J., Bergqvist, C., Hunter, J.V., Jin, D., Wang, D.J., Wehrli, S., and Zimmerman, R.A. (2003). In vivo measurement of brain metabolites using two-dimensional double-quantum MR spectroscopy--exploration of GABA levels in a ketogenic diet. Magn Reson Med *49*, 615-619.

Wenzel, H.J., Vacher, H., Clark, E., Trimmer, J.S., Lee, A.L., Sapolsky, R.M., Tempel, B.L., and Schwartzkroin, P.A. (2007). Structural consequences of Kcna1 gene deletion and transfer in the mouse hippocampus. Epilepsia *48*, 2023-2046.

Wong, R.K., and Prince, D.A. (1979). Dendritic mechanisms underlying penicillin-induced epileptiform activity. Science (New York, NY) *204*, 1228-1231.

Xu, Z., and Knight, R. (2015). Dietary effects on human gut microbiome diversity. The British journal of nutrition *113 Suppl*, S1-5.

Yudkoff, M., Daikhin, Y., Nissim, I., Lazarow, A., and Nissim, I. (2001a). Ketogenic diet, amino acid metabolism, and seizure control. Journal of neuroscience research *66*, 931-940.

Yudkoff, M., Daikhin, Y., Nissim, I., Lazarow, A., and Nissim, I. (2001b). Ketogenic diet, amino acid metabolism, and seizure control. Journal of Neuroscience Research *66*, 931-940.

Zhang, G., Ducatelle, R., De Bruyne, E., Joosten, M., Bosschem, I., Smet, A., Haesebrouck, F., and Flahou, B. (2015). Role of gamma-glutamyltranspeptidase in the pathogenesis of Helicobacter suis and Helicobacter pylori infections. Veterinary research *46*, 31.

Zuberi, S.M., Eunson, L.H., Spauschus, A., De Silva, R., Tolmie, J., Wood, N.W., McWilliam, R.C., Stephenson, J.B., Kullmann, D.M., and Hanna, M.G. (1999). A novel

mutation in the human voltage-gated potassium channel gene (Kv1.1) associates with episodic ataxia type 1 and sometimes with partial epilepsy. Brain *122 (Pt 5)*, 817-825.

Chapter 6

The gut microbiota modulates environmental risk for cognitive impairment

Christine A. Olson[1], Alonso J. Iñiguez[1], Grace E. Yang[1], Ping Fang[1], Geoffrey N. Pronovost[1], Kelly G. Jameson[1], Tomiko K. Rendon[1], Jorge Paramo[1], Jacob T. Barlow[2], Rustem F. Ismagilov[2], and Elaine Y. Hsiao[1]

[1] Department of Integrative Biology & Physiology, University of California, Los Angeles, Los Angeles, CA 90095, USA

[2] Division of Chemistry & Chemical Engineering, California Institute of Technology, Pasadena, CA 91108, USA

SUMMARY

Cognitive impairment (**CI**) is a prevalent neurological condition characterized by deficient attention, causal reasoning, learning and memory. Many genetic and environmental factors increase susceptibility to CI, and the gut microbiome is increasingly implicated. However, the identity of gut microbes associated with CI risk, their effects on CI, and their mechanisms of action remain unclear. Here, we examine the gut microbiome in response to restricted diet and intermittent hypoxia, known environmental risk factors for CI. Modeling these environmental risk factors together in mice potentiates CI and alters the gut microbiota. Depleting the microbiome by antibiotic treatment or germ-free rearing prevents the adverse effects of combined environmental risk on CI, whereas transplantation of the risk-associated microbiome into naïve mice confers CI. Parallel sequencing and gnotobiotic approaches identify the pathobiont *Bilophila wadsworthia* as enriched by the environmental risk factors for CI and sufficient to induce CI. Consistent with CI-related behavioral abnormalities, *B. wadsworthia* and the risk-associated microbiome disrupt hippocampal synaptic transmission and plasticity, neurogenesis, and gene expression. The CI induced by *B. wadsworthia* and by environmental risk factors is associated with microbiome-dependent increases in intestinal interferon-gamma (**IFNg**)-producing Th1 cells. Inhibiting Th1 cell development abrogates the adverse effects of both *B. wadsworthia* and environmental risk factors on CI. Together, these findings identify select gut bacteria that contribute to environmental risk for CI in mice by promoting inflammation and hippocampal dysfunction.

- Exposure to the ketogenic diet and intermittent hypoxia synergistically impair cognitive behavior in mice.

- Cognitive impairment is prevented by clearance of the risk-associated gut microbiota and conferred by transplantation of the risk-associated microbiota into naïve mice.

- *Bilophila wadsworthia* is enriched in the risk-associated microbiota and sufficiently disrupts cognitive behavior and hippocampal physiology.

- Elevations in IFNg-producing Th1 cells contribute to microbiota-mediated impairments in cognitive behavior.

INTRODUCTION

Cognitive impairment (**CI**) characterized by deficient attention, causal reasoning, and learning and memory, afflicts more than 50 million people worldwide (Guzik-Makaruk et al., 2019). With increasing lifespan, it is predicted that by 2050 an estimated 115.4 million people will have dementia, making aging-related CI a pressing global health concern (Prince et al., 2013). Genetic, environmental, and behavioral factors together mediate CI, and many biological pathways are implicated, including neuroinflammation, mitochondrial dysfunction, and blood brain barrier integrity (Han et al., 2020; Sweeney et al., 2018). However, exactly how environmental factors, such as diet and physical stress, modify risk for CI remains poorly understood.

The gut microbiome is emerging as an important mediator of environmental contributions to host health and disease. The composition of the gut microbiota is shaped by external factors, including diet, stress, and age (Marques et al., 2010; O'Toole and Jeffery, 2015; Rea et al., 2016). In animal models, alterations in the gut microbiome mediate effects of environmental challenges on various behavioral abnormalities, including impaired communication in response to maternal immune activation, anxiety-related behavior in response to stress, and reduced sociability in response to high-fat diet (Bravo et al., 2011; Buffington et al., 2016; Gareau et al., 2011; Hsiao et al., 2013; Savignac et al., 2015). Moreover, depleting the microbiome by germ-free rearing or antibiotic treatment disrupts cognitive performance across various tasks for working and spatial memory, when compared to controls raised with conventional microbiomes (Chu et al., 2019; D'Amato et al., 2020; Frohlich et al., 2016; Gareau et al., 2011; Hoban et al., 2016; Sampson and Mazmanian, 2015; Vuong et al., 2017a; Yu et al., 2019). These animal studies provide fundamental proof-of-concept that investigating interactions between the gut microbiome and environmental risk factors for CI may reveal previously uncharacterized cellular and molecular signaling pathways that regulate CI.

Herein, we examine the effects of two environmental risk factors for CI—the ketogenic diet and intermittent hypoxia—on the gut microbiota, neurophysiology and cognitive behavior. We evaluate causal roles for the gut microbiome in promoting CI, and further identify specific microbial taxa that contribute to environmental risk for impaired hippocampal function and cognitive deficits. Finally, we interrogate functional effects of

264

risk-associated microbes to reveal that microbial stimulation of type 1 immune responses contribute to microbiome-mediated environmental susceptibility to CI.

RESULTS

The Ketogenic Diet Exacerbates Hypoxia-Induced Cognitive Impairment

Hypoxia is an environmental risk factor for CI associated with high altitude exposure, sleep apnea, vascular dementia, and Alzheimer's disease, among many other pathological conditions (Biswal et al., 2016; de Aquino Lemos et al., 2012; Desbonnet et al., 2014; Giuliani et al., 2019; Qaid et al., 2017). To determine the impact of acute intermittent hypoxia impact on cognitive behavior, conventional mice (specific pathogen-free, **SPF**) consuming a control diet (**CD, Table S1**) were subjected to 6 hours of restricted 12% oxygen (normobaric hypoxia, **Hyp**) or ambient 21% oxygen (normoxia, **Mock**) daily for five days. Following a 4-day recovery period, mice were then evaluated for cognitive behavior in the Barnes maze task (**Figure 1A**). Consistent with prior literature (Aubrecht et al., 2015; Mei et al., 2020), mice exposed to Hyp exhibited impaired cognitive behavior in the Barnes maze, as indicated by increased latency to enter the escape box, errors made, and use of random search strategy as compared to Mock controls (**Figures 1B-1F**). These impairments were observed even on the first trial of testing, suggesting cognitive impairment that can include disrupted learning and memory, in addition to deficits in other underlying cognitive processes (Li et al., 2013; Shen et al., 2020). There were no significant differences in velocity or total distance travelled in the Barnes maze (**Figures S1A and S1B**), suggesting no confounding abnormalities in motor function. There were also no differences in performance in the open field test and prepulse

inhibition task, suggesting no alterations in anxiety-related exploration or sensorimotor gating (**Figure S2**). These results indicate that acute intermittent hypoxia impairs cognitive behavior in mice, which is consistent with previous reports (Aubrecht et al., 2015; Mei et al., 2020).

High dietary fat intake modifies cognitive behavior in humans and animal models, where both the high-fat, high-sugar Western diet and high-fat, low-carbohydrate ketogenic diet (**KD, Table S1**) alter working memory, particularly in response to physical or psychosocial stress (Arcego et al., 2018; Kesby et al., 2015). To determine effects of the KD on cognitive behavior, SPF mice were pre-treated with the KD and subjected to Mock or Hyp as described above (**Figure 1G**). Mice fed the KD exhibited no significant differences in cognitive behavior in the Barnes maze**,** as compared to mice fed the vitamin and mineral-matched CD (**Figure 1**, **SPF CD Mock** vs. **SPF KD Mock**), indicating that the KD alone has no overt effect on cognitive behavior in the Barnes maze. Notably, however, mice fed the KD and exposed to Hyp (**SPF KD Hyp**) exhibited a substantial increase in latency to enter the escape box, errors made, and random search strategy as compared to Mock controls fed the KD (**SPF KD Mock**) (**Figures 1H-1L**). The Hyp-induced behavioral impairment was significantly more severe in KD-fed mice than in CD-fed mice (**Figures 1 and S3**). There was no significant difference across experimental groups in velocity or total distance traveled in the Barnes maze (**Figures S1C and S1D**), or in performance in the open field and prepulse inhibition tasks (**Figure S2**). These results indicate that the KD potentiates the adverse effects of Hyp on cognitive behavior in mice, and further

266

highlight synergistic interactions between diet and hypoxic stress as environmental risk factors for cognitive impairment.

Ketogenic Diet- and Hypoxia-Associated Alterations in the Gut Microbiota Impair Cognitive Behavior

Environmental factors, including diet and stress, play important roles in shaping the composition and function of the gut microbiota (David et al., 2014; Lobionda et al., 2019; Sbihi et al., 2019; Tripathi et al., 2018; van de Wouw et al., 2018). To gain insight into whether the gut microbiota contributes to KD- and Hyp-induced disruptions in cognitive behavior, SPF mice were pre-treated with broad-spectrum antibiotics (**Abx**) to deplete the gut microbiota prior to KD and Hyp exposure (**Figure 2A**) (Reikvam et al., 2011). Compared to vehicle-treated controls, KD- and Hyp-exposed mice that were pre-treated with Abx exhibited improved cognitive performance, as indicated by decreased latency to enter the escape box, errors made, and use of random search strategy (**Figures 2B-2F, SPF KD Hyp** vs. **Abx KD Hyp**). Results for each of these behavioral parameters were comparable to those seen in Mock controls fed the KD (**Figures 2B-2F, S1E and S1F**; **Abx KD Hyp** vs. **SPF KD Mock**), suggesting that depletion of the microbiota abrogated KD and Hyp-induced impairments in cognitive behavior. Consistent with this, germ-free (**GF**) mice fed the KD were resistant to Hyp-induced cognitive impairments in the Barnes maze (**Figure S4**). Compared to KD-fed SPF mice, however, GF mice fed the KD exhibited worse cognitive behavior at baseline, suggesting detrimental effects of KD particularly in mice raised GF (Gareau et al., 2011). These data suggest that depletion of the gut microbiota prevents the synergistic effects of KD and Hyp on cognitive impairment in mice.

To further test whether microbiota alterations in response to KD and Hyp contribute to disruptions in cognitive behavior, GF mice fed standard chow were transplanted with fecal microbiota from donor SPF mice fed KD and exposed to either Hyp or Mock (**GF + Hyp** and **GF + Mock,** respectively) (**Figure 2G**). Compared to controls colonized with the KD and Mock-associated microbiota, mice colonized with KD and Hyp-associated microbiota exhibited poor cognitive performance (**Figures 2H-2L, S1G and S1H**), akin to that seen in mice fed KD and exposed to Hyp (**Figures 1H-1L**). Relative to SPF mice, transplanted control mice exhibited impaired performance on the first trial that improved with subsequent trials of the task, which may reflect initial confounding effects of GF status on behavior. Taken together, these results indicate that i) the KD potentiates Hyp-induced impairments in cognitive behavior (**Figures 1** and **S3**), ii) depletion of the microbiota prevents the adverse synergistic effects of KD and Hyp on cognitive behavior (**Figures 2A-2F**), and iii) transplantation of the KD- and Hyp-associated microbiota into naïve GF mice impairs cognitive behavior (**Figures 2G-2L**). These results strongly suggest that changes in the gut microbiota contribute to KD- and Hyp-induced impairments in cognitive behavior in mice.

Bilophila is Enriched by the Ketogenic Diet and Hypoxia and Impairs Cognitive Behavior

To identify candidate microbial taxa that may be responsible for promoting KD- and Hyp-induced abnormalities in cognitive behavior, fecal microbiota were sequenced from SPF mice fed KD and exposed to Hyp or Mock (**Figures 1G-1L**), as well as from the mice

transplanted with the corresponding microbiota from those SPF mice (**Figures 2G-2L**). While there were no global alterations in the microbiota of mice fed KD and exposed to Hyp (**Figures 3A and S5**), select bacterial taxa were significantly altered in the Hyp group, compared to Mock controls (**Figures 3B and 3C, Table S2**). In particular, the relative abundances of *Clostridium cocleatum* were reduced in Hyp-exposed animals fed KD, while *Bilophila* species were elevated in Hyp-exposed animals fed KD (**Figures 3B and 3C**). The absolute abundance of *Bilophila* species was enriched particularly in mice exposed to both KD and Hyp, but not in mice exposed to either KD or Hyp alone (**Figure S6A**). This aligns with the observed synergistic effects of KD and Hyp on cognitive impairment (**Figures 1 and S3**), and with previous reports that dietary fat favors the growth of *Bilophila*, an obligate anaerobic pathobiont (Devkota et al., 2012). Similar reductions in *C. cocleatum* and increases in *Bilophila* were seen in mice transplanted with KD and Hyp-associated microbiota (**Figures 3D-3F, Table S2.** Overall, these results reveal that KD and Hyp together enrich *Bilophila* and impair cognitive behavior in mice.

To test whether *Bilophila* may contribute to the CI induced by KD and Hyp exposure, GF mice fed standard chow were monocolonized with *Bilophila wadsworthia* and tested for cognitive behavior, relative to mice colonized with *C. cocleatum* (**Figure 3G**). *B. wadsworthia* was selected because it exhibited the highest sequence identity to the *Bilophila* operational taxonomic units elevated in mice fed KD and exposed to Hyp (**Figures 3B and 3C**). Mice colonized with *B. wadsworthia* exhibited impaired cognitive behavior compared to GF and *C. cocleatum*-colonized controls, with no overt deficits in motor ability (**Figures 3I-3L, S1I and S1J**). The effect of *B. wadsworthia* on cognitive

269

impairment during the probe trial of the Barnes maze assay was comparable to that seen with exposure to KD and Hyp and with transplantation of the KD- and Hyp-associated microbiota (**Figure 3M**). These data reveal that monocolonization with *B. wadsworthia* phenocopies the adverse effects of the KD- and Hyp-associated microbiota on cognitive behavior in mice.

The Gut Microbiota, and *Bilophila* in Particular, Modulates Hippocampal Activity

The hippocampus is sensitive to alterations in diet and hypoxic stress and is a critical site for learning and memory (Goldbart et al., 2006; Gozal et al., 2002; Kanoski and Davidson, 2011; Kanoski et al.; Kanoski et al., 2010; Titus et al., 2007). To study effects of the KD and Hyp, and potential roles for the microbiota, on hippocampal physiology, field potential recordings were acquired from acute hippocampal slices from SPF mice fed KD and exposed to Hyp or Mock, as well as from GF mice colonized with *B. wadsworthia* or *C. cocleatum*. Compared to Mock-exposed controls, KD-fed mice that were exposed to Hyp exhibited significant reductions in hippocampal long-term potentiation (**LTP**, **Figures 4A and 4B**), population spike relative to field excitatory postsynaptic potential (**fEPSP**) slope, as a measure of excitatory postsynaptic potential- spike coupling (**Figure 4C**) and paired-pulse facilitation (**Figure 4D**). Pre-treatment with Abx diminished these abnormalities in hippocampal synaptic physiology (**Figure S7**), suggesting that the gut microbiome contributes to the adverse effects of KD and Hyp on hippocampal physiology. Consistent with this, mice monocolonized with *B. wadsworthia* exhibited reduced hippocampal LTP (**Figures 4E and 4F**), reduced fiber volley amplitude vs. fEPSP slope (**Figure 4G**) and reduced paired-pulse facilitation (**Figure 4H**) when compared to *C. cocleatum*-colonized

controls. The disruptions in hippocampal activity induced by *B. wadsworthia* were comparable to those seen in mice exposed to KD and Hyp, suggesting that colonization with *B. wadsworthia* phenocopies the adverse effects of KD and Hyp on hippocampal synaptic transmission and plasticity. The microbiota-dependent alterations in hippocampal activity were further associated with microbiota-dependent changes in hippocampal gene expression (**Figure S8, Table S3**). In particular, colonization with *B. wadsworthia* resulted in widespread transcriptomic alterations in the hippocampus relative to *C. cocleatum*-colonized controls (**Figure 4I**). Particular genes that were differentially expressed in response to *B. wadsworthia* colonization included subsets related to neuronal excitation (*CBLN1, CC2D1A, GRIK4, SYT2, SYT9*), mitochondrial processes (*DNAJA3*, *SLC25A16*, *ALDH4A1*, *NDUFAF1*), neuronal interactions (*KCNN3*, *SEMA3C*, *TTR*, *MOV10*, *PLK5*), ubiquitination (*BAP1, COPS6, FBXO4, FBXO42, NDUFAF5, USP53*), and immune response (*LCK*, *HMGB1, NFKBID, TRAFD1, SPG21*) (**Figure 4J**). Moreover, immunofluorescence staining for doublecortin (**DCX**), a marker for the central phase of hippocampal neurogenesis (von Bohlen und Halbach, 2011)) revealed reduced density of DCX-positive cells in the dentate gyrus of mice colonized with *B. wadsworthia* compared with *C. cocleatum*-colonized controls (**Figure 4K**), adding to prior results demonstrating the microbiota regulates hippocampal neurogenesis (Ogbonnaya et al., 2015). Overall, these results indicate that colonization with *B. wadsworthia* alters hippocampal physiology, and further suggest that microbiota-dependent impairments in cognitive behavior may be due, at least in part, to microbiota-dependent disruptions in hippocampal function.

Th1 Cell Expansion Contributes to *Bilophila*-Induced Impairments in Cognitive Behavior

B. wadsworthia colonization promotes the expansion of IFNg-producing T helper type I (**Th1**) cells, and IFNg is associated with impairments in cognitive behavior and hippocampal physiology during homeostasis and in response to chronic stress (Devkota et al., 2012; Kim et al., 2011; Litteljohn et al., 2014). We hypothesized that Th1 induction may contribute to the detrimental effects of *B. wadsworthia* and of environmental risk factors, KD and Hyp, on cognitive behavior. To first confirm that *B. wadsworthia* increases Th1 cells, GF mice were monocolonized with either *C. cocleatum* or *B. wadsworthia*, and Th1 levels were measured in the intestine. Indeed, *B. wadsworthia*-colonized mice exhibited increased levels of CD3+CD4+IFNg+IL17a- Th1 cells in the colonic lamina propria relative to GF and *C. cocleatum*-colonized controls (**Figures S9A and S9B**). Similar increases in levels of Th1 cells were seen by colonization of Abx-treated mice with *B. wadsworthia*, indicating that the Th1-promoting effects of *B. wadsworthia* are observed in response to bacterial enrichment, as well as bacterial monocolonization (**Figures S9C and S9D**). To determine if Th1 cells are required for the adverse effects of *B. wadsworthia* on cognitive behavior, mice were reared in the absence of Th1 cells (T-bet knockout, **T-bet-/-**) or as genetically wildtype (**WT**) and colonized with *B. wadsworthia* (**Figures 5A, S9C and S9D**). Consistent with prior monocolonization experiments conducted with GF Swiss Webster mice (**Figure 3**), Abx-treated WT C57Bl/6J mice colonized with *B. wadsworthia* exhibited impaired cognitive behavior in the Barnes maze, as denoted by elevated errors made and increased random search strategy relative to non-colonized Abx-treated WT controls (**Figures 5B-5F**). In contrast to results from prior

272

monocolonization experiments (**Figure 3I**), there were no statistically significant differences in latency to enter the escape box (**Figure 5C**), which may point to effects of *B. wadsworthia* on this particular behavioral parameter that are dependent on bacterial load, prior colonization status, and/or genetic background of the host. Notably, preventing Th1 induction via T-bet deficiency abrogated the adverse effects of *B. wadsworthia* on cognitive behavior, as denoted by reductions in errors made and use of random search strategy to levels comparable to those seen in colonized WT controls (**Figures 5D-F**). These results support previous findings that *B. wadsworthia* promotes IFNg-producing Th1 cells in the intestine, and further reveal that Th1 cells are necessary for the ability of *B. wadsworthia* to impair cognitive behavior in mice.

To further determine if Th1 cells contribute to the adverse effects of KD and Hyp on cognitive behavior, mice were reared as T-bet-/- or genetically WT, then exposed to both KD and Hyp (**Figure 5G**). Consistent with prior experiments using Swiss Webster mice (**Figure 1**), C57Bl/6J WT SPF mice exposed to both KD and Hyp exhibited impaired performance in the Barnes maze relative to Mock-exposed controls (**Figures 5H-5L**). Notably, CI induced by KD and Hyp was associated with significant increases in serum IFNg levels (**Figure S9G**), and modest, but not statistically significant, increases in levels of IFNg-producing Th1 cells in the colonic lamina propria (**Figures S9E-F**). Inhibiting Th1 induction through T-bet deficiency abrogated the adverse effects of KD and Hyp on cognitive behavior, as denoted by decreases in latency to enter the escape box, errors made and use of random search strategy, relative to exposed WT controls (**Figures 5H-5L**). Altogether, these results implicate that *B. wadsworthia* impairs cognitive behavior by

increasing Th1 cells, and further suggest that microbiota-dependent increases in Th1 cells contribute to the adverse effects of KD and Hyp on cognitive behavior.

DISCUSSION

Proof-of-concept studies have reported that complete absence or severe depletion of the microbiota results in widespread alterations in complex animal behaviors, including learning and memory (Chu et al., 2019; Desbonnet et al., 2014; Frohlich et al., 2016; Gareau et al., 2011; Liu et al., 2020; Mohle et al., 2016; Vuong et al., 2017b; Yu et al., 2019). However, whether the microbiota is altered by physiologically relevant risk factors for cognitive dysfunction and whether there are select microbial species that are causally linked to cognitive impairment has been poorly understood. Results from this study reveal that the gut microbiota is shaped by synergistic interactions between environmental risk factors for cognitive impairment. They further demonstrate that select diet- and hypoxic stress-responsive bacteria from the gut microbiota disrupt hippocampal function and cognitive behavior, likely via the induction of pro-inflammatory immune cells.

In particular, we find that the high-fat, low carbohydrate KD exacerbates the detrimental effects of acute intermittent Hyp on cognitive behavior. This aligns with the so-called "two-hit" or "multiple-hit" hypotheses for neurological and neurodegenerative diseases (Heinemann et al., 2016), wherein multiple genetic and/or environmental risk factors interact to accelerate or predispose to symptoms of disease, including age-related cognitive decline (Zhu et al., 2007). Indeed, both high-fat diet and hypoxia are associated with cognitive impairment across studies of humans and animal models (Arias-Cavieres

et al., 2020; Beilharz et al., 2015; Jha et al., 2018). However, the ketogenic diet and select ketone bodies, such as beta-hydroxybutyrate, have been recently explored as potential treatments for behavioral symptoms of Alzheimer's disease (Rusek et al., 2019). Results from this study suggest that when combined with other environmental stressors, the KD can be detrimental to hippocampal function and cognitive behavior. This is consistent with one recent report that KD administration in a rat model of Alzheimer's disease worsened cognitive performance in the Morris water maze (Park et al., 2020). Further research is warranted to uncover the molecular bases for interactions between varied genetic and environmental risk factors for CI.

Data from this study indicate that alterations in the gut microbiota contribute to the adverse effects of the KD and Hyp on cognitive behavior in the Barnes maze task. One important consideration is the biological bases of the abnormalities observed in the behavioral task. Adverse effects of the KD and Hyp are seen even during the first trial of the Barnes maze assay that persist through the sixth and last trial. While we observe no overt differences in anxiety-related exploration in the open field, acoustic startle response, and sensorimotor gating in the prepulse inhibition task, the early abnormalities in the Barnes maze suggest that the KD and Hyp together induce cognitive issues that extend beyond disruptions in learning and working memory. Indeed, depletion of the risk-associated microbiota diminishes the cognitive behavioral abnormalities, even in the first trial of testing, and also improves hippocampal LTP, suggesting that the microbiome may modify hippocampal-dependent learning and memory as well other aspects of cognitive performance. Overall, while the data reveal an influence of the gut microbiota in

modulating cognitive behavior, the complexity of the behavioral phenotypes leave open the likely possibility that there are multiple microbiota-independent effects of diet and hypoxic stress that also contribute to the observed cognitive phenotypes.

In addition to identifying a synergistic effect of KD and Hyp on impairing cognitive behavior, we also reveal an interaction between KD and Hyp in enriching *Bilophila* species in the gut microbiota. While the exact mechanisms remain unknown, one study reported particular alterations in the gut microbiota that were seen when rats were exposed to both the high-fat, high-sugar diet and hypoxia in a model of obstructive sleep apnea (**OSA**) (Durgan et al., 2016). A separate paper studying intermittent hypoxia as a model of OSA found that fecal microbiome transplantation of hypoxia-associated samples sufficiently promoted murine sleep disturbances and that the microbial family *Desulfovibrionaceae* (OTU147), of which *Bilophila* is a member, was increased in hypoxia-associated samples and in children with OSA (Badran et al., 2020; Valentini et al., 2020). In a similar paradigm where atherosclerosis-prone *Ldlr-/-* mice were fed a high-fat diet, additional exposure to hypoxia and hypercapnia increased levels of select bile acids, particularly taurodeoxycholic acid (Tripathi et al., 2018). This may be relevant, as a separate study reported that a high-saturated fat diet promoted taurine conjugation of bile acids, and that taurocholic acid in particular promoted levels of *B. wadsworthia* (Devkota et al., 2012). Based on these studies and the finding that *B. wadsworthia* is an obligate anaerobe (Devkota et al., 2012; Summanen et al., 1995), we speculate that the KD and Hyp together enrich *Bilophila* through combined modulation of bile acid profiles and increased anaerobicity of the intestinal microenvironment. Future co-culture and

276

metabolic modeling experiments are needed to dissect how various environmental factors differentially influence microbial community structures.

Consistent with the finding that KD and Hyp together impair cognitive behavior and enrich *Bilophila* in the gut microbiota, we observe that colonization with *B. wadsworthia* leads to disrupted hippocampal physiology and cognitive deficits. These findings align with studies linking *B. wadsworthia* to increases in IFNg (Devkota et al., 2012), and separately, increases in IFNg to cognitive impairment (Monteiro et al., 2016). Notably, while results from our study highlight a likely role for *Bilophila* in contributing to environmental risk for CI (as induced by KD and Hyp in mice), they do not the preclude the possibility that other members of the microbiota may also modify cognitive behavior. In particular, 16S rRNA gene sequences from *Bilophila* are reported to comprise approximately 0.004-0.3% of 16S rRNA loads from the fecal microbiota of SPF mice (Caesar et al.; Caesar et al., 2015). In our experiments, KD and Hyp together increase the absolute abundance of *Bilophila* 16S rRNA gene copies in feces by ~1000X. As such, the physiological loads of *B. wadsworthia* in the presence of a complex SPF microbiota, even after increases seen in response to KD and Hyp, are much lower than those achieved by subsequent experiments involving bacterial monocolonization of GF mice or enrichment in Abx-treated mice. Results from our study indicate that gnotobiotic colonization with *B. wadsworthia* largely phenocopies the cognitive behavioral impairment, hippocampal dysfunction and Th1 induction seen in response to KD and Hyp (and their associated physiological increases in *Bilophila*). While we did not observe other bacterial taxa, aside from *Bilophila*, that were significantly elevated in response to KD and Hyp, future studies

of various risk factors for CI may reveal additional microbial taxa and signaling pathways that modify hippocampal function and cognitive behavior.

Consistent with previous literature indicating that *B. wadsworthia* promotes Th1 cell expansion (Devkota et al., 2012), we observe that T-bet deficiency prevents *B. wadsworthia*-induced increases in intestinal Th1 cells, as well as the cognitive behavioral impairments seen in *B. wadsworthia*-colonized mice. Precisely how intestinal Th1 cells promote cognitive behavioral abnormalities remains poorly understood. However, increases in Th1 cells and Th1 responses are commonly associated with aging-associated cognitive decline and cognitive impairments in Alzheimer's disease (Browne et al., 2013; Dulken et al., 2019). In particular, IFNg production by Th1 cells promotes microglial activation (Mount et al., 2007; Takeuchi et al., 2006; Zhou et al., 2015) and hippocampal-dependent cognitive dysfunction (Litteljohn et al., 2014; Monteiro et al., 2016; Zhang et al., 2020). Additionally, peripheral and hippocampal IFNg corresponds with impaired Barnes maze performance due to chronic mild stress (Palumbo et al., 2018). In aged murine brains, T cell infiltration occurs in neurogenic niches and IFNg corresponds with reduced neural stem cell function and proliferation (Dulken et al., 2019). Indeed, IFNg directly suppresses hippocampal neural stem/precursor cell proliferation and provokes neuronal apoptosis (Zhang et al., 2020). *B. wadsworthia* has also been identified in several human microbiome association studies as associating with neurodegenerative disorders (Baldini et al., 2020; Baldini et al.; Lin et al., 2019; Vogt et al., 2017). Further studies are needed to determine how microbiota-dependent neuroimmune interactions may influence cognitive health.

As the prevalence of cognitive dysfunction continues to increase (Hale et al., 2020), identifying early and modifiable risk factors is critical to enabling early detection and intervention for CI. Results from this study reveal that the gut microbiota is altered by modeling environmental risk factors for CI in mice and that changes in the gut microbiota, and *Bilophila* in particular, contribute to disruptions in hippocampal physiology and cognitive behavior. We propose that understanding the biological bases for how complex genetic, environmental and psychosocial factors together predispose to CI requires consideration of the gut microbiome, as an important interface between host genetics and environmental exposures and an integral regulator of nutrition, immunity, metabolism and behavior.

STAR★METHODS

Detailed methods are provided and include the following:

- KEY RESOURCES TABLE
- CONTACT FOR REAGENT AND RESOURCE SHARING
- EXPERIMENTAL MODELS AND SUBJECT DETAILS
  - Mice
  - Bacteria
- METHOD DETAILS
  - Dietary Treatment
  - Acute Intermittent Hypoxia

- Barnes Maze Testing

- Open Field Testing

- Prepulse Inhibition Testing

- Antibiotic Treatment

- Fecal Microbiota Transplant

- 16S rRNA Gene Sequencing

- Gnotobiotic Colonization

- Hippocampal Electrophysiology

- Hippocampal Transcriptomic Profiling

- Hippocampal Immunofluorescence Staining and Imaging

- Lymphocyte Isolation and Flow Cytometry

- Digital PCR

- IFNg Serum Quantification

- QUANTIFICATION AND STATISTICAL ANALYSIS

- DATA AND SOFTWARE AVAILABILITY

REAGENT or RESOURCE	SOURCE	IDENTIFIER
Antibodies		

anti-DCX (Guinea Pig Polyclonal)	Millipore	AB2253
IL-17A Monoclonal Antibody (eBio17B7), FITC	ThermoFisher	11-7177-81
IFN gamma Monoclonal Antibody, (XMG1.2), PE	ThermoFisher	12-7311-81
CD3 Monoclonal Antibody, (17A2), APC	BioLegend	100236
CD4 Monoclonal Antibody, (GK1.5), PE-eFluor 610	ThermoFisher	61-0041-80
CD45 Monoclonal Antibody, (30-F11), BV605	BioLegend	103140
Bacterial and Virus Strains		
Clostridium cocleatum	Deutsche Sammlung von Mikroorganismen und Zellkulturen (DSMZ)	DSMZ 1551

Bilophila wadsworthia	Murine-associated strain gifted from Drs. Connie Ha and Suzanne Devkota	strain WAL7959
Chemicals, Peptides, and Recombinant Proteins		
Vancomycin hydrochloride	Chem-Impex International	00315
Neomycin trisulfate salt hydrate	Sigma-Aldrich	N1876
Metronidazole	Sigma-Aldrich	M1547
Ampicillin sodium salt	Sigma-Aldrich	A9518
NaCl	Sigma-Aldrich	S7653
KCl	Sigma-Aldrich	P3911
$NaHCO_3$	Sigma-Aldrich	S5761
NaH_2PO_4	Sigma-Aldrich	S0751
$CaCl_2$	Sigma-Aldrich	C1016
$MgSO_4$	Sigma-Aldrich	M7506

Glucose	Sigma-Aldrich	47829
Brucella media	Hardy Diagnostics	C5311
Ferric ammonium citrate	Fisher Scientific	172-500
DAKO antigen retrieval solution	Agilent	S1699
RPMI 1640	Sigma-Aldrich	11875093
EDTA	ThermoFisher	15575020
HEPES	ThermoFisher	15630080
HBSS	ThermoFisher	14170112
Collagenase D	Sigma Aldrich	11088866 001
DNAse I, Grade II	Sigma Aldrich	10104159 001
Dispase	Gibco	17105041
Ionomycin calcium salt	Sigma Aldrich	I3909

PMA	Sigma Aldrich	P1585
Brefeldin A	Sigma Aldrich	B7651
MEM NEAA	ThermoFisher	10370021
Penicillin-streptomycin (Pen/strep)	ThermoFisher	15070063
Ultrapure water	ThermoFisher	10977015
DNA intercalating dye (EvaGreen)	Biotium	31000
Sodium pyruvate	Gibco	11360070
Critical Commercial Assays		
DNeasy PowerSoil Kit	Qiagen	12888-50
Qiaquick PCR purification kit	Qiagen	28104

RNEasy Mini Kit	Qiagen	74104
QuantSeq FWD' mRNA-Seq Library Prep Kit	Lexogen	N/A
LIVE/DEAD™ Fixable Aqua Dead Cell Stain Kit	ThermoFisher	L34957
Intracellular Fixation & Permeabilization Buffer Set	ThermoFisher	88-8824-00
QX200 ddPCR EvaGreen Supermix	Bio-Rad Laboratories	186-4033
V-PLEX Proinflammatory Panel 1 Mouse Kit	Meso Scale Diagnostics	K15048D
Deposited Data		
16S rRNA gene sequencing	https://qiita.ucsd.edu	13510

Hippocampal transcriptomic data	Gene Expression Omnibus	GSE163099
Experimental Models: Organisms/Strains		
Swiss Webster mice	Taconic Farms	Tac:SW
C57BL6/J mice	Jackson Laboratories	000664
T-bet TBX21 knockout mice (B6.129S6-*Tbx21tm1Glm*/J)	Jackson Laboratories	004648
Oligonucleotides		
Forward primer for digital PCR: UN00F2, 5′-CAGCMGCCGCGGTAA-3	Integrated DNA Technologies	N/A
Reverse primer for digital PCR: UN00R0, 5′-GGACTACHVGGGTWTCTAAT-3′ [1, 3])	Integrated DNA Technologies	N/A

Software and Algorithms		
EthoVision XT	Noldus	
Deblur	https://github.com/biocore/deblur	Amir et al., 2017
QIIME2-2018.6	https://qiime2.org/	Bolyen et al.
FastQC v. 0.11.9	https://github.com/s-andrews/FastQC/releases/tag/v0.11.9	Andrews, 2010
Trimmomatic	https://github.com/timflutre/trimmomatic	Bolger et al.
HISAT2	http://daehwankimlab.github.io/hisat2/	Kim et al.
HTSeq-count	https://github.com/htseq/htseq	Anders et al.
DESeq2	https://bioconductor.org/packages/release/bioc/html/DESeq2.html	Love et al.
R package	https://www.r-project.org/	Team, 2013

DAVID	https://david.ncifcrf.gov/gene2gene.jsp	(Huang da et al., 2009a, b
STRING	https://string-db.org/	Szklarczyk et al., 2019
QuantaSoft Software	Bio-Rad Laboratories	1864011
Prism software version 8.2.1	GraphPad	
Other		
"Breeder" chow	Lab Diets	5K52
Standard chow	Lab Diets	5010
Ketogenic diet	Harlan Teklad	TD.1150300
Control diet	Harlan Teklad	TD.150300
O2 Control InVivo cabinet	Coy Laboratories	Model 30

GigE camera	Basler	acA1280-60gc
4200 Tapestation System	Agilent	G2991AA
QX200 Droplet Generator	Bio-Rad Laboratories	1864002

Table 6 KEY RESOURCES TABLE

data are available on through Gene Expression Omnibus repository with the

identification number #

GSE163099.

EXPERIMENTAL MODELS AND SUBJECT DETAILS

Mice

4–6-week-old SPF wild-type Swiss Webster mice (Taconic Farms), GF wild-type Swiss

Webster mice (Taconic Farms), SPF wild-type C57BL6/J mice (Jackson Laboratories),

GF wild-type C57BL6/J (Jackson Laboratories), and SPF T-bet TBX21 knockout mice

(B6.129S6-*Tbx21tm1Glm*/J, Jackson Laboratories) were bred in UCLA's Center for

Health Sciences Barrier Facility. Mice were randomly assigned to an experimental group.

Experiments include age- and sex-matched cohorts of males and females. All animal

experiments were approved by the UCLA Animal Care and Use Committee.

Bacteria

Bilophila wadsworthia (strain WAL7959), generously provided by Drs. Connie Ha and

Suzanne Devkota (Cedars-Sinai Medical Center, Los Angeles, CA), was cultured under

anoxic conditions (2-3% H2, 20% CO2, and the balance N2) at 37°C in Modified

Brucella media supplemented with 1% taurine, iron, hemin, and vitamin K (Hardy

Diagnostics). *Clostridium cocleatum* (DSMZ 1551) was grown under anoxic conditions

(2-3% H2, 20% CO2, and the balance N2) at 37°C in Sweet E. Broth for Anaerobes

(ATCC medium 1004). Cultures were authenticated by full-length 16S rRNA gene

sequencing (Laragen, Inc.).

METHOD DETAILS

Dietary Treatment

Breeding GF mice were fed "breeder" chow (Lab Diets 5K52). Experimental animals were either fed standard chow (Lab Diets 5010), 6:1 ketogenic diet (Harlan Teklad TD.1150300), or vitamin- and mineral- matched control diet (Harlan Teklad TD.150300).

Acute Intermittent Hypoxia

Mice housed in the home cage were placed in an O2 Control InVivo cabinet (Coy Laboratories) and exposed to 12% oxygen for 6 hours per day for 5 consecutive days. Mock-treated mice were placed in the same chamber and exposed to ambient 21% oxygen for 6 hours per day for 5 consecutive days.

Barnes Maze Testing

Mice were tested for cognitive behavior in the Barnes maze (92 cm diameter, 5 cm hole diameter, 95 cm height; Noldus) using procedures adapted from a previously published protocol (Attar et al., 2013). Briefly, mice were acclimated for at least 1 hour before testing to the behavioral room, which featured consistent visual cues that varied in shape, color and placement. The maze was cleaned before and after each testing trial with 70% ethanol, followed by Accel disinfectant. All sessions were recorded using a Basler Gig3 camera and EthoVision XT (Noldus). For the habituation phase (day 1), mice were placed in a clear glass beaker in the center of the maze for 30 seconds, then slowly guided to the target hole and gently pushed into the escape box if they did not enter on their own

accord. Mice were kept in the escape box for 1 minute and then allowed to explore the maze freely for 5 minutes before being returned to their home cages. During the training phase (Day 2-3), mice were tested for 3 trials on the first day, and 2 trials for the second day. For each trial, mice were first placed under an opaque cup in the center of the maze for 15 seconds. Then, the cylinder was removed, and mice were allowed to explore the maze for 5 minutes. Latency to enter was defined as the time elapsed for mice to identify the target hole correctly for the first time. Errors made were defined as nose pokes over incorrect holes. Distance traveled, velocity, and time in each quadrant were other recorded for every trial. Search strategy was also analyzed, where a "random" strategy was coded as greater than 3 errors in non-consecutive holes, a "serial" strategy was coded as errors occurring in consecutive holes, and a "random" strategy was coded as greater than 3 non-consecutive hole errors. The probe trial (Day 4) was performed 24 hours after the final training trial. The escape box was removed, and mice were allowed to explore the maze for 5 minutes while latency to enter, distance traveled, errors made, velocity, search strategy and time in target were recorded.

Open Field Testing

The open field test is widely used to measure anxiety-like and locomotor behavior in rodents. Mice were placed in the center of a 50 cm x 50 cm arena for 10 min, during which an overhead Basler Gig3 camera and EthoVision XT (Noldus) software was used to measure distance traveled, and the number of entries and duration of time spent in the central 17 cm square area. The boxes were cleaned with 70% ethanol and Accel disinfectant before and after each session.

Prepulse Inhibition Testing

Prepulse inhibition is used to measure sensorimotor gating and acoustic startle and was performed according to protocols adapted from (Hsiao et al., 2013; Swerdlow and Geyer, 1998) in the UCLA Behavioral Testing Core (Franz Hall). Mice were acclimated to an SR-LAB testing chamber (SD Instruments) for 5 min, presented with six 120-dB pulses of white noise (startle stimulus), and then subjected to 14 randomized blocks of either no startle, 5-dB prepulse + startle, or 15-dB prepulse + startle. The startle response was recorded by a piezo-electric sensor and prepulse inhibition was defined as (startle stimulus only -5 or 15 dB prepulse + startle)/ startle stimulus only x 100.

Antibiotic Treatment

SPF mice were gavaged every 12 hours daily for 7 consecutive days with a solution of vancomycin (50mg/kg), neomycin (100 mg/kg) and metronidazole (100 mg/kg), as previously described (Reikvam et al., 2011). Ampicillin (1 mg/ml) was provided *ad libitum* in sterile drinking water. For mock treatment, mice were gavaged with normal drinking water every 12 hours daily for 7 days. Antibiotic-treated mice were maintained in sterile caging with sterile food and water and handled aseptically for the remainder of the experiments.

Fecal Microbiota Transplant

Fresh fecal samples were obtained from adult SPF Swiss Webster homogenized in 1 mL pre-reduced phosphate-buffered saline (PBS, pH = 7.4) per pellet. 100 µL of the

suspension was immediately administered via oral gavage to recipient GF mice. For mock treatment, mice were gavaged with pre-reduced PBS.

16S rRNA Gene Sequencing

Total bacterial genomic DNA was extracted from mouse fecal samples using the Qiagen DNeasy PowerSoil Kit, where sample n reflects separate cages containing 2 mice per cage to reduce cage-dependent effects of variation and focus on biological variation. The library was prepared following previously published and validated methods (Caporaso et al., 2011). The V4 regions of the 16S rDNA gene were PCR amplified using individually barcoded universal primers and 30 ng of the extracted genomic DNA. The PCR reaction was set up in triplicate, and the PCR products were purified using the Qiaquick PCR purification kit (Qiagen). The purified PCR product was pooled in equal molar concentrations quantified by nanodrop and sequenced by Laragen, Inc. using the Illumina MiSeq platform and 2 x 250bp reagent kit for paired-end sequencing. Amplicon sequence variants (ASVs) were chosen after denoising with Deblur (Amir et al., 2017). Taxonomy assignment and rarefaction were performed using QIIME2-2018.6 (Bolyen et al., 2019).

Gnotobiotic Colonization and Antibiotic Enrichment

10^9 cfu bacteria were suspended in 200 µL pre-reduced PBS and orally gavaged into GF mice or Abx-treated mice. For mock treatment, mice were gavaged with pre-reduced PBS. Mice were maintained in microisolator cages and handled aseptically. Mice were behaviorally tested 7 days post-colonization. Colonization was confirmed via fecal plating on modified Brucella agar supplemented with 0.5 g/L ferric ammonium citrate.

Hippocampal Electrophysiology

Mice were first deeply anesthetized with isoflurane, and following cervical dislocation, the brain was rapidly removed and submerged in ice-cold, oxygenated (95% O2/5% CO2) artificial cerebrospinal fluid (ACSF) containing (in mM) as follows: 124 NaCl, 4 KCl, 25 $NaHCO_3$, 1 NaH_2PO_4, 2 $CaCl_2$, 1.2 $MgSO_4$, and 10 glucose (Sigma-Aldrich). While iced, the brain was hemisected, and the hippocampi removed. Slice were made using a tissue chopper in 400 μM sections and maintained at 30°C in interface-type chambers that were continuously perfused (2–3 ml/min) with ACSF and allowed to recover for at least 2 h before recordings. For LTP experiments, a bipolar nichrome wire stimulating electrode was placed in stratum radiatum of the CA1 region and used to activate Schaffer collateral fiber synapses. For paired pulse facilitation and population spike measurements, the recording electrode was placed in the pyramidal cell body layer. For LTP recordings, the maximal fEPSP amplitude was determined and the intensity of stimulation was adjusted to produce fEPSPs with an amplitude 50% of the maximal amplitude. Baseline recordings were taken for at least 20 minutes, followed by two trains of 1 second long 100 Hz stimulation with 10 seconds inter-train interval, then at least an hour of recording post-tetanus. The last five minutes of recording post-tetanus were used for statistical comparison. Paired-pulse facilitation was measured at impulse distances of 10, 20, 30, 40 and 50 ms by measuring the height of the population spike.

Hippocampal Transcriptomic Profiling

Hippocampi were microdissected and RNA extracted using the Qiagen RNEasy Mini Kit. RNA quality was assessed to be RIN>8.9 using the 4200 Tapestation (Agilent). RNA libraries were prepared using the QuantSeq FWD' mRNA-Seq Library Prep Kit (Lexogen) and sequenced via the Illumina HiSeq platform by the UCLA Neuroscience Genomics Core. Sequences were filtered using FastQC v. 0.11.9 (Andrews, 2010) for quality control, followed by Trimmomatic (Bolger et al., 2014) to remove barcodes and reads with an average phred score of 33 (parameters: illuminaclip:2:30:6, slidingwindow:5:30, leading:30, trailing:30, crop:65, minlen:20). Parsed reads were then aligned to the mouse genome mm10 using HISAT2 (Kim et al., 2019). Read counts were obtained using HTSeq-count (Anders et al., 2015). Differential gene expression was determined using DESeq2 (Love et al., 2014). Heatmaps were constructed using the R package (Team, 2013) pheatmap (Kolde, 2015), GO term enrichment analysis was conducted using DAVID (Huang da et al., 2009a, b) and Protein-Protein network analysis using STRING (Szklarczyk et al., 2019).

Hippocampal Immunofluorescence Staining and Imaging

Hippocampi were microdissected, post-fixed in 4% paraformaldehyde for 24 hours, cryopreserved in 30% sucrose for 24 hours, embedded and frozen in OCT, and cryosectioned using a Leica CM1950 cryostat. 25 µm coronal sections were collected within a span of 200 µm and distributed between two slides beginning at the site of the hippocampal formation, determined in accordance to the Mouse P56 Coronal Reference Atlas of the Allen Institute (Lein et al., 2007). Slides were incubated in DAKO antigen retrieval solution (Agilent) at 90 ºC for two minutes, washed, and then blocked (0.3%PBS-

296

T, 5% BSA, 10% normal goat serum) for one hour at room temperature. Sections were incubated at 4ºC for 48 hours using anti-DCX (Guinea Pig Polyclonal, 1:500, Millipore AB2253), washed and then incubated with Alexa Fluor secondaries (1:1000) for two hours at room temperature before being washed and mounted. Sections were imaged using a Zeiss LSM 780 confocal microscope at 20X magnification with 1.5 zoom across 8.4 μm section widths across 7 Z-stacks. Image optimization and orthogonal projections were performed in Zen Blue (Zeiss) and background removal was done in ImageJ (Schneider et al., 2012). Quantification of DCX was performed by tracing the granule cell layers of the DG and quantitating DCX+ within enclosed area using ImageJ (NIH) particle analysis (Schneider et al., 2012).

Lymphocyte Isolation and Flow Cytometry

Single-cell suspensions were prepared from colonic lamina propria using procedures adapted from (Takahara et al.). Colons were dissected, cut longitudinally with gentle fat removal, and contents washed away in 1 X PBS. Epithelial cell stripping was achieved through two 45-minute incubations shaking at 37 °C HBSS with 0.5M EDTA and 1M HEPES (ThermoFisher). Colonic tissue was then digested using two 45-minute incubations shaking at 37 °C in RPMI supplemented with 4% FCS, 0.5 mg/mL collagenase D (Sigma), 0.25 mg/mL DNAseI, grade II (Sigma), and 0.5 mg/mL dispase (Gibco). All lymphocytes were then collected and stimulated for two hours with 500 ng/mL PMA and 500 ng/mL ionomycin in RPMI with 10% FCS, 2% MEM NEAA, 2% Pen/strep, 2% sodium pyruvate, followed by 3-hour incubation with 500 ng/mL Brefeldin A. Cells were incubated on ice and in darkness with 1:600 viability dye for 20 min, followed by 30

min incubation on ice and in darkness with CD3-APC (Biolegend), CD4-PE (ThermoFisher), CD45-BV605 (Biolegend) at 1:200 in FACS buffer. Cells were next incubated with 100 µL of fixation buffer for 30 minutes in darkness, washed with 1X PBS, and stored in PBS at 4 °C until the next day. On the following day, cells were incubated with permeabilization buffer for 15 minutes in darkness at room temperature, followed by intracellular antibodies IL-17A- FITC (ThermoFisher) and IFNg-PE (ThermoFisher) for 30 minutes on ice in darkness at a 1:200 ratio in permeabilization buffer. Data were acquired on FACSCalibur (BD Biosciences) or the Attune NxT Flow Cytometer. All data contained within a graph were acquired on the same flow cytometer (GF data on the FACSCalibur, and Abx and SPF data on the Attune NxT, respectively). Data were analyzed using FlowJo (TreeStar) software.

Digital PCR

Briefly, each reaction was set up with 92.0 µL of DNA sample, 10 µL of ddPCR master mix (QX200 ddPCR EvaGreen Supermix, Bio-Rad Laboratories), forward (UN00F2, 5′-CGCCGGTATCGAAATCGTGACAGCMGCCGCGGTAA-3′) and reverse (UN00R0, 5′-ATTCGCGGAAGGAGCGAGAG GGACTACHVGGGTWTCTAAT-3′ [1, 3]) primers (Integrated DNA Technologies) at the final concentration of 500 nM each, and ultrapure water (Thermo Fisher Scientific) to the final volume of 20 µL. In some experiments, additional DNA intercalating dye (EvaGreen, Biotium) was added to the reactions up to ×1 final concentration (to achieve up to ×2 overall concentration). Each reaction volume was converted to droplets using a QX200 droplet generator (Bio-Rad Laboratories). Droplet samples were amplified on a thermocycler (C1000 Touch, Bio-Rad Laboratories)

with the following conditions according to the program: initial denaturation at 95°C for 5 min. followed by 40 cycles each consisting of denaturation at 95°C for 30 sec., annealing at 6552°C for 30 sec., and extension at 68°C for 60 sec.; followed by the dye stabilization step consisting of 5 min incubation at 4°C, 5 min incubation at 90°C, and incubation at 12°C for at least 5 min. Droplet samples were quantified on a QX200 Droplet Digital PCR System (Bio-Rad Laboratories). The raw data were analyzed and the target molecule Sample concentrations were extracted using the accompanying software (QuantaSoft Software, Bio-Rad Laboratories) with auto-thresholding conditions. Sample concentrations were then normalized to sample extraction mass and corrected for volume losses during extraction protocol. Lower limit of quantification of the assay was determined as 3X the no template control concentration normalized to the minimum sample extraction mass.

IFNg Quantification

Blood samples were collected by cardiac puncture and spun through serum separation tubes (SST vacutainers, Becton Dickinson). Serum IFNg concentrations were quantified using the V-PLEX Proinflammatory Panel 1 Mouse Kit (Meso Scale Diagnostics), according to the manufacturer's instructions.

QUANTIFICATION AND STATISTICAL ANALYSIS

Statistical analysis was performed using Prism software version 8.2.1 (GraphPad). Data were assessed for normal distribution and plotted in the figures as mean ± SEM. For each

figure, n = the number of independent biological replicates. No samples or animals were excluded from the analyses. Differences between two treatment groups were assessed using two-tailed, unpaired Student t test with Welch's correction. Differences among >2 groups with only one variable were assessed using one-way ANOVA with Sidak post hoc test. Taxonomic comparisons from 16S rDNA gene sequencing analysis were analyzed by Kruskal-Wallis test with Bonferroni *post hoc* test. Two-way ANOVA with Sidak *post-hoc* test was used for ≥ 2 groups with two variables (e.g. Barnes maze latency to enter, errors made over 6 trials). Significant differences emerging from the above tests are indicated in the figures by *$p < 0.05$, **$p < 0.01$, ***$p < 0.001$, ****$p < 0.0001$. Notable non-significant (and non-near significant) differences are indicated in the figures by "n.s.".

SUPPLEMENTAL INFORMATION

Supplemental Information includes nine figures, three tables and all source data, and can be found with this article.

AUTHOR CONTRIBUTIONS

C.A.O., A.J.I., G.E.Y., P.F., G.N.P., K.G.J, J.T.B., and S.R.B. performed the experiments and analyzed the data, C.A.O., A.J.I., R.F.I., W.E.B., T.J.O, and E.Y.H. designed the study, C.A.O. and E.Y.H wrote the manuscript. All authors discussed the results and commented on the manuscript.

DECLARATION OF INTERESTS

The authors declare no competing interests.

ACKNOWLEDGEMENTS

REFERENCES

Amir, A., McDonald, D., Navas-Molina, J.A., Kopylova, E., Morton, J.T., Zech Xu, Z., Kightley, E.P., Thompson, L.R., Hyde, E.R., Gonzalez, A.*, et al.* (2017). Deblur Rapidly Resolves Single-Nucleotide Community Sequence Patterns. mSystems *2*.

Anders, S., Pyl, P.T., and Huber, W. (2015). HTSeq--a Python framework to work with high-throughput sequencing data. Bioinformatics *31*, 166-169.

Andrews, S. (2010). FastQC: a quality control tool for high throughput sequence data . .

Arcego, D.M., Toniazzo, A.P., Krolow, R., Lampert, C., Berlitz, C., Dos Santos Garcia, E., do Couto Nicola, F., Hoppe, J.B., Gaelzer, M.M., Klein, C.P.*, et al.* (2018). Impact of High-Fat Diet and Early Stress on Depressive-Like Behavior and Hippocampal Plasticity in Adult Male Rats. Mol Neurobiol *55*, 2740-2753.

Arias-Cavieres, A., Khuu, M.A., Nwakudu, C.U., Barnard, J.E., Dalgin, G., and Garcia, A.J., 3rd (2020). A HIF1a-Dependent Pro-Oxidant State Disrupts Synaptic Plasticity and Impairs Spatial Memory in Response to Intermittent Hypoxia. eNeuro *7*.

Attar, A., Liu, T., Chan, W.T., Hayes, J., Nejad, M., Lei, K., and Bitan, G. (2013). A shortened Barnes maze protocol reveals memory deficits at 4-months of age in the triple-transgenic mouse model of Alzheimer's disease. PLoS One *8*, e80355.

Aubrecht, T.G., Jenkins, R., Magalang, U.J., and Nelson, R.J. (2015). Influence of gonadal hormones on the behavioral effects of intermittent hypoxia in mice. Am J Physiol Regul Integr Comp Physiol *308*, R489-499.

Badran, M., Khalyfa, A., Ericsson, A., and Gozal, D. (2020). Fecal microbiota transplantation from mice exposed to chronic intermittent hypoxia elicits sleep disturbances in naïve mice. Exp Neurol *334*, 113439.

Baldini, F., Hertel, J., Sandt, E., Thinnes, C.C., Neuberger-Castillo, L., Pavelka, L., Betsou, F., Krüger, R., and Thiele, I. (2020). Parkinson's disease-associated alterations of the gut microbiome predict disease-relevant changes in metabolic functions. BMC Biol *18*, 62.

Baldini, F., Hertel, J., Sandt, E., Thinnes, C.C., Neuberger-Castillo, L., Pavelka, L., Betsou, F., Krüger, R., Thiele, I., Aguayo, G.*, et al.* Parkinson's disease-associated alterations of the gut microbiome predict disease-relevant changes in metabolic functions.

Beilharz, J.E., Maniam, J., and Morris, M.J. (2015). Diet-Induced Cognitive Deficits: The Role of Fat and Sugar, Potential Mechanisms and Nutritional Interventions. Nutrients *7*, 6719-6738.

Biswal, S., Sharma, D., Kumar, K., Nag, T.C., Barhwal, K., Hota, S.K., and Kumar, B. (2016). Global hypoxia induced impairment in learning and spatial memory is associated with precocious hippocampal aging. Neurobiology of Learning and Memory *133*, 157-170.

Bolger, A.M., Lohse, M., and Usadel, B. (2014). Trimmomatic: a flexible trimmer for Illumina sequence data. Bioinformatics *30*, 2114-2120.

Bolyen, E., Rideout, J.R., Dillon, M.R., Bokulich, N.A., Abnet, C.C., Al-Ghalith, G.A., Alexander, H., Alm, E.J., Arumugam, M., Asnicar, F.*, et al.* (2019). Reproducible, interactive, scalable and extensible microbiome data science using QIIME 2. In Nat Biotechnol, pp. 852-857.

Bravo, J.A., Forsythe, P., Chew, M.V., Escaravage, E., Savignac, H.M., Dinan, T.G., Bienenstock, J., and Cryan, J.F. (2011). Ingestion of Lactobacillus strain regulates

emotional behavior and central GABA receptor expression in a mouse via the vagus nerve. Proc Natl Acad Sci U S A *108*, 16050-16055.

Browne, T.C., McQuillan, K., McManus, R.M., O'Reilly, J.A., Mills, K.H., and Lynch, M.A. (2013). IFN-γ Production by amyloid β-specific Th1 cells promotes microglial activation and increases plaque burden in a mouse model of Alzheimer's disease. J Immunol *190*, 2241-2251.

Buffington, S.A., Di Prisco, G.V., Auchtung, T.A., Ajami, N.J., Petrosino, J.F., and Costa-Mattioli, M. (2016). Microbial Reconstitution Reverses Maternal Diet-Induced Social and Synaptic Deficits in Offspring. Cell *165*, 1762-1775.

Caesar, R., Tremaroli, V., Kovatcheva-Datchary, P., Cani, P.D., and Bäckhed, F.

Caesar, R., Tremaroli, V., Kovatcheva-Datchary, P., Cani, P.D., and Bäckhed, F. (2015). Crosstalk between Gut Microbiota and Dietary Lipids Aggravates WAT Inflammation through TLR Signaling. Cell Metab *22*, 658-668.

Caporaso, J.G., Lauber, C.L., Walters, W.A., Berg-Lyons, D., Lozupone, C.A., Turnbaugh, P.J., Fierer, N., and Knight, R. (2011). Global patterns of 16S rRNA diversity at a depth of millions of sequences per sample. Proc Natl Acad Sci U S A *108 Suppl 1*, 4516-4522.

Chu, C., Murdock, M.H., Jing, D., Won, T.H., Chung, H., Kressel, A.M., Tsaava, T., Addorisio, M.E., Putzel, G.G., Zhou, L.*, et al.* (2019). The microbiota regulate neuronal function and fear extinction learning. Nature *574*, 543-548.

D'Amato, A., Di Cesare Mannelli, L., Lucarini, E., Man, A.L., Le Gall, G., Branca, J.J.V., Ghelardini, C., Amedei, A., Bertelli, E., Regoli, M.*, et al.* (2020). Faecal microbiota transplant from aged donor mice affects spatial learning and memory via modulating

hippocampal synaptic plasticity- and neurotransmission-related proteins in young recipients. Microbiome *8*, 140.

David, L.A., Maurice, C.F., Carmody, R.N., Gootenberg, D.B., Button, J.E., Wolfe, B.E., Ling, A.V., Devlin, A.S., Varma, Y., Fischbach, M.A.*, et al.* (2014). Diet rapidly and reproducibly alters the human gut microbiome. Nature *505*, 559-563.

de Aquino Lemos, V., Antunes, H.K., dos Santos, R.V., Lira, F.S., Tufik, S., and de Mello, M.T. (2012). High altitude exposure impairs sleep patterns, mood, and cognitive functions. Psychophysiology *49*, 1298-1306.

Desbonnet, L., Clarke, G., Shanahan, F., Dinan, T.G., and Cryan, J.F. (2014). Microbiota is essential for social development in the mouse. Mol Psychiatry *19*, 146-148.

Devkota, S., Wang, Y., Musch, M.W., Leone, V., Fehlner-Peach, H., Nadimpalli, A., Antonopoulos, D.A., Jabri, B., and Chang, E.B. (2012). Dietary-fat-induced taurocholic acid promotes pathobiont expansion and colitis in Il10-/- mice. Nature *487*, 104-108.

Dulken, B.W., Buckley, M.T., Navarro Negredo, P., Saligrama, N., Cayrol, R., Leeman, D.S., George, B.M., Boutet, S.C., Hebestreit, K., Pluvinage, J.V.*, et al.* (2019). Single-cell analysis reveals T cell infiltration in old neurogenic niches. Nature *571*, 205-210.

Durgan, D.J., Ganesh, B.P., Cope, J.L., Ajami, N.J., Phillips, S.C., Petrosino, J.F., Hollister, E.B., and Bryan, R.M., Jr. (2016). Role of the Gut Microbiome in Obstructive Sleep Apnea-Induced Hypertension. Hypertension *67*, 469-474.

Frohlich, E.E., Farzi, A., Mayerhofer, R., Reichmann, F., Jacan, A., Wagner, B., Zinser, E., Bordag, N., Magnes, C., Frohlich, E.*, et al.* (2016). Cognitive impairment by

antibiotic-induced gut dysbiosis: Analysis of gut microbiota-brain communication. Brain Behav Immun *56*, 140-155.

Gareau, M.G., Wine, E., Rodrigues, D.M., Cho, J.H., Whary, M.T., Philpott, D.J., Macqueen, G., and Sherman, P.M. (2011). Bacterial infection causes stress-induced memory dysfunction in mice. Gut *60*, 307-317.

Giuliani, A., Sivilia, S., Baldassarro, V.A., Gusciglio, M., Lorenzini, L., Sannia, M., Calzà, L., and Giardino, L. (2019). Age-Related Changes of the Neurovascular Unit in the Cerebral Cortex of Alzheimer Disease Mouse Models: A Neuroanatomical and Molecular Study. J Neuropathol Exp Neurol *78*, 101-112.

Goldbart, A.D., Row, B.W., Kheirandish-Gozal, L., Cheng, Y., Brittian, K.R., and Gozal, D. (2006). High fat/refined carbohydrate diet enhances the susceptibility to spatial learning deficits in rats exposed to intermittent hypoxia. Brain Res *1090*, 190-196.

Gozal, E., Gozal, D., Pierce, W.M., Thongboonkerd, V., Scherzer, J.A., Sachleben, L.R., Jr., Brittian, K.R., Guo, S.Z., Cai, J., and Klein, J.B. (2002). Proteomic analysis of CA1 and CA3 regions of rat hippocampus and differential susceptibility to intermittent hypoxia. J Neurochem *83*, 331-345.

Guzik-Makaruk, E.M., Pływaczewski, E.W., Laskowska, K., Filipkowski, W., Jurgielewicz-Delegacz, E., and Mroczko, P. (2019). A Comparative Analysis of the Treatment of Decision-Making by or for Patients with Neurodegenerative Diseases in Four Legal Jurisdictions. J Alzheimers Dis *70*, 1-10.

Hale, J.M., Schneider, D.C., Gampe, J., Mehta, N.K., and Myrskylä, M. (2020). Trends in the Risk of Cognitive Impairment in the United States, 1996-2014. Epidemiology *31*, 745-754.

Han, B., Chen, H., Yao, Y., Liu, X., Nie, C., Min, J., Zeng, Y., and Lutz, M.W. (2020). Genetic and non-genetic factors associated with the phenotype of exceptional longevity & normal cognition. Sci Rep *10*, 19140.

Heinemann, S.D., Posimo, J.M., Mason, D.M., Hutchison, D.F., and Leak, R.K. (2016). Synergistic stress exacerbation in hippocampal neurons: Evidence favoring the dual-hit hypothesis of neurodegeneration. Hippocampus *26*, 980-994.

Hoban, A.E., Moloney, R.D., Golubeva, A.V., McVey Neufeld, K.A., O'Sullivan, O., Patterson, E., Stanton, C., Dinan, T.G., Clarke, G., and Cryan, J.F. (2016). Behavioural and neurochemical consequences of chronic gut microbiota depletion during adulthood in the rat. Neuroscience *339*, 463-477.

Hsiao, E.Y., McBride, S.W., Hsien, S., Sharon, G., Hyde, E.R., McCue, T., Codelli, J.A., Chow, J., Reisman, S.E., Petrosino, J.F.*, et al.* (2013). Microbiota modulate behavioral and physiological abnormalities associated with neurodevelopmental disorders. Cell *155*, 1451-1463.

Huang da, W., Sherman, B.T., and Lempicki, R.A. (2009a). Bioinformatics enrichment tools: paths toward the comprehensive functional analysis of large gene lists. Nucleic Acids Res *37*, 1-13.

Huang da, W., Sherman, B.T., and Lempicki, R.A. (2009b). Systematic and integrative analysis of large gene lists using DAVID bioinformatics resources. Nat Protoc *4*, 44-57.

Jha, N.K., Jha, S.K., Sharma, R., Kumar, D., Ambasta, R.K., and Kumar, P. (2018). Hypoxia-Induced Signaling Activation in Neurodegenerative Diseases: Targets for New Therapeutic Strategies. J Alzheimers Dis *62*, 15-38.

Kanoski, S.E., and Davidson, T.L. (2011). Western Diet Consumption and Cognitive
Impairment: Links to Hippocampal Dysfunction and Obesity. Physiology & behavior *103*,
59-68.

Kanoski, S.E., Zhang, Y., Zheng, W., and Davidson, T.L. The Effects of a High-Energy
Diet on Hippocampal Function and Blood-Brain Barrier Integrity in the Rat.

Kanoski, S.E., Zhang, Y., Zheng, W., and Davidson, T.L. (2010). The effects of a high-
energy diet on hippocampal function and blood-brain barrier integrity in the rat. J
Alzheimers Dis *21*, 207-219.

Kesby, J.P., Kim, J.J., Scadeng, M., Woods, G., Kado, D.M., Olefsky, J.M., Jeste, D.V.,
Achim, C.L., and Semenova, S. (2015). Spatial Cognition in Adult and Aged Mice
Exposed to High-Fat Diet. PLoS One *10*, e0140034.

Kim, D., Paggi, J.M., Park, C., Bennett, C., and Salzberg, S.L. (2019). Graph-based
genome alignment and genotyping with HISAT2 and HISAT-genotype. Nat Biotechnol
37, 907-915.

Kim, S.J., Lee, H., Joung, H.Y., Lee, G., Lee, H.J., Shin, M.K., Kim, S.H., Shim, I., and
Bae, H. (2011). T-bet deficient mice exhibit resistance to stress-induced development of
depression-like behaviors. J Neuroimmunol *240-241*, 45-51.

Kolde, R. (2015). pheatmap: Pretty heatmaps.

Lein, E.S., Hawrylycz, M.J., Ao, N., Ayres, M., Bensinger, A., Bernard, A., Boe, A.F.,
Boguski, M.S., Brockway, K.S., Byrnes, E.J.*, et al.* (2007). Genome-wide atlas of gene
expression in the adult mouse brain. Nature *445*, 168-176.

Li, X., Redus, L., Chen, C., Martinez, P.A., Strong, R., Li, S., and O'Connor, J.C. (2013). Cognitive dysfunction precedes the onset of motor symptoms in the MitoPark mouse model of Parkinson's disease. PLoS One *8*, e71341.

Lin, C.H., Chen, C.C., Chiang, H.L., Liou, J.M., Chang, C.M., Lu, T.P., Chuang, E.Y., Tai, Y.C., Cheng, C., Lin, H.Y.*, et al.* (2019). Altered gut microbiota and inflammatory cytokine responses in patients with Parkinson's disease. J Neuroinflammation *16*, 129.

Litteljohn, D., Nelson, E., and Hayley, S. (2014). IFN-γ differentially modulates memory-related processes under basal and chronic stressor conditions. Front Cell Neurosci *8*, 391.

Liu, Z., Dai, X., Zhang, H., Shi, R., Hui, Y., Jin, X., Zhang, W., Wang, L., Wang, Q., Wang, D.*, et al.* (2020). Gut microbiota mediates intermittent-fasting alleviation of diabetes-induced cognitive impairment. Nat Commun *11*, 855.

Lobionda, S., Sittipo, P., Kwon, H.Y., and Lee, Y.K. (2019). The Role of Gut Microbiota in Intestinal Inflammation with Respect to Diet and Extrinsic Stressors. Microorganisms *7*.

Love, M.I., Huber, W., and Anders, S. (2014). Moderated estimation of fold change and dispersion for RNA-seq data with DESeq2. Genome Biol *15*, 550.

Marques, T.M., Wall, R., Ross, R.P., Fitzgerald, G.F., Ryan, C.A., and Stanton, C. (2010). Programming infant gut microbiota: influence of dietary and environmental factors. Curr Opin Biotechnol *21*, 149-156.

Mei, X., Tan, G., and Qing, W. (2020). AMPK activation increases postoperative cognitive impairment in intermittent hypoxia rats via direct activating PAK2. Behav Brain Res *379*, 112344.

Mohle, L., Mattei, D., Heimesaat, M.M., Bereswill, S., Fischer, A., Alutis, M., French, T., Hambardzumyan, D., Matzinger, P., Dunay, I.R.*, et al.* (2016). Ly6C(hi) Monocytes Provide a Link between Antibiotic-Induced Changes in Gut Microbiota and Adult Hippocampal Neurogenesis. Cell Rep *15*, 1945-1956.

Monteiro, S., Ferreira, F.M., Pinto, V., Roque, S., Morais, M., de Sá-Calçada, D., Mota, C., Correia-Neves, M., and Cerqueira, J.J. (2016). Absence of IFNγ promotes hippocampal plasticity and enhances cognitive performance. Transl Psychiatry *6*, e707.

Mount, M.P., Lira, A., Grimes, D., Smith, P.D., Faucher, S., Slack, R., Anisman, H., Hayley, S., and Park, D.S. (2007). Involvement of interferon-gamma in microglial-mediated loss of dopaminergic neurons. J Neurosci *27*, 3328-3337.

O'Toole, P.W., and Jeffery, I.B. (2015). Gut microbiota and aging. Science *350*, 1214-1215.

Ogbonnaya, E.S., Clarke, G., Shanahan, F., Dinan, T.G., Cryan, J.F., and O'Leary, O.F. (2015). Adult Hippocampal Neurogenesis Is Regulated by the Microbiome. Biological Psychiatry *78*, e7-e9.

Palumbo, M.L., Di Rosso, M.E., Simon, E.H., Gonzalez Murano, M.R., and Genaro, A.M. (2018). Altered interferon-γ expression in lymphocytes as a potential peripheral marker of chronic stress-induced cognitive deficit. Cytokine *107*, 26-34.

Park, S., Zhang, T., Wu, X., and Yi Qiu, J. (2020). Ketone production by ketogenic diet and by intermittent fasting has different effects on the gut microbiota and disease progression in an Alzheimer's disease rat model. J Clin Biochem Nutr *67*, 188-198.

Prince, M., Bryce, R., Albanese, E., Wimo, A., Ribeiro, W., and Ferri, C.P. (2013). The global prevalence of dementia: a systematic review and metaanalysis. Alzheimers Dement *9*, 63-75.e62.

Qaid, E., Zakaria, R., Sulaiman, S.F., Yusof, N.M., Shafin, N., Othman, Z., Ahmad, A.H., and Aziz, C.A. (2017). Insight into potential mechanisms of hypobaric hypoxia-induced learning and memory deficit - Lessons from rat studies. Hum Exp Toxicol *36*, 1315-1325.

Rea, K., Dinan, T.G., and Cryan, J.F. (2016). The microbiome: A key regulator of stress and neuroinflammation. Neurobiol Stress *4*, 23-33.

Reikvam, D.H., Erofeev, A., Sandvik, A., Grcic, V., Jahnsen, F.L., Gaustad, P., McCoy, K.D., Macpherson, A.J., Meza-Zepeda, L.A., and Johansen, F.E. (2011). Depletion of murine intestinal microbiota: effects on gut mucosa and epithelial gene expression. PLoS One *6*, e17996.

Rusek, M., Pluta, R., Ułamek-Kozioł, M., and Czuczwar, S.J. (2019). Ketogenic Diet in Alzheimer's Disease. Int J Mol Sci *20*.

Sampson, T.R., and Mazmanian, S.K. (2015). Control of brain development, function, and behavior by the microbiome. Cell Host Microbe *17*, 565-576.

Savignac, H.M., Tramullas, M., Kiely, B., Dinan, T.G., and Cryan, J.F. (2015). Bifidobacteria modulate cognitive processes in an anxious mouse strain. Behavioural Brain Research *287*, 59-72.

Sbihi, H., Boutin, R.C., Cutler, C., Suen, M., Finlay, B.B., and Turvey, S.E. (2019). Thinking bigger: How early-life environmental exposures shape the gut microbiome and influence the development of asthma and allergic disease. Allergy *74*, 2103-2115.

Schneider, C.A., Rasband, W.S., and Eliceiri, K.W. (2012). NIH Image to ImageJ: 25 years of image analysis. Nat Meth *9*, 671-675.

Shen, Y., Zhang, Y., Chen, L., Du, J., Bao, H., Xing, Y., Cai, M., and Si, Y. (2020). Chemokine CXCL13 acts via CXCR5-ERK signaling in hippocampus to induce perioperative neurocognitive disorders in surgically treated mice. J Neuroinflammation *17*, 335.

Stacy, A.-O., ViniciusMcCulloch, John A.Hild, BenediktOh, Ji HoonPerez-Chaparro, P. JulianaSim, Choon K.Lim, Ai IngLink, Verena M.Enamorado, MichelTrinchieri, GiorgioSegre, Julia A.Rehermann, BarbaraBelkaid, Yasmine (2021). Infection trains the host for microbiota-enhanced resistance to pathogens. Cell *184*, 1-13.

Summanen, P.H., Jousimies-Somer, H., Manley, S., Bruckner, D., Marina, M., Goldstein, E.J., and Finegold, S.M. (1995). Bilophila wadsworthia isolates from clinical specimens. Clin Infect Dis *20 Suppl 2*, S210-211.

Sweeney, M.D., Sagare, A.P., and Zlokovic, B.V. (2018). Blood-brain barrier breakdown in Alzheimer disease and other neurodegenerative disorders. Nat Rev Neurol *14*, 133-150.

Swerdlow, N.R., and Geyer, M.A. (1998). Using an animal model of deficient sensorimotor gating to study the pathophysiology and new treatments of schizophrenia. Schizophr Bull *24*, 285-301.

Szklarczyk, D., Gable, A.L., Lyon, D., Junge, A., Wyder, S., Huerta-Cepas, J., Simonovic, M., Doncheva, N.T., Morris, J.H., Bork, P.*, et al.* (2019). STRING v11: protein-protein association networks with increased coverage, supporting functional discovery in genome-wide experimental datasets. Nucleic Acids Res *47*, D607-d613.

Takahara, M., Takaki, A., Hiraoka, S., Adachi, T., Shimomura, Y., Matsushita, H., Nguyen, T.T.T., Koike, K., Ikeda, A., Takashima, S*., et al.* Berberine improved experimental chronic colitis by regulating interferon-γ- and IL-17A-producing lamina propria CD4+ T cells through AMPK activation.

Takeuchi, H., Wang, J., Kawanokuchi, J., Mitsuma, N., Mizuno, T., and Suzumura, A. (2006). Interferon-gamma induces microglial-activation-induced cell death: a hypothetical mechanism of relapse and remission in multiple sclerosis. Neurobiol Dis *22*, 33-39.

Team, R.C. (2013). R: A language and environment for statistical computing. (Vienna, Austria: R Foundation for Statistical Computing).

Titus, A.D., Shankaranarayana Rao, B.S., Harsha, H.N., Ramkumar, K., Srikumar, B.N., Singh, S.B., Chattarji, S., and Raju, T.R. (2007). Hypobaric hypoxia-induced dendritic atrophy of hippocampal neurons is associated with cognitive impairment in adult rats. Neuroscience *145*, 265-278.

Tripathi, A., Melnik, A.V., Xue, J., Poulsen, O., Meehan, M.J., Humphrey, G., Jiang, L., Ackermann, G., McDonald, D., Zhou, D*., et al.* (2018). Intermittent Hypoxia and Hypercapnia, a Hallmark of Obstructive Sleep Apnea, Alters the Gut Microbiome and Metabolome. mSystems *3*.

Valentini, F., Evangelisti, M., Arpinelli, M., Di Nardo, G., Borro, M., Simmaco, M., and Villa, M.P. (2020). Gut microbiota composition in children with obstructive sleep apnoea syndrome: a pilot study. Sleep Med *76*, 140-147.

van de Wouw, M., Boehme, M., Lyte, J.M., Wiley, N., Strain, C., O'Sullivan, O., Clarke, G., Stanton, C., Dinan, T.G., and Cryan, J.F. (2018). Short-chain fatty acids: microbial

metabolites that alleviate stress-induced brain-gut axis alterations. J Physiol *596*, 4923-4944.

Vogt, N.M., Kerby, R.L., Dill-McFarland, K.A., Harding, S.J., Merluzzi, A.P., Johnson, S.C., Carlsson, C.M., Asthana, S., Zetterberg, H., Blennow, K*., et al.* (2017). Gut microbiome alterations in Alzheimer's disease. Sci Rep *7*, 13537.

von Bohlen und Halbach, O. (2011). Immunohistological markers for proliferative events, gliogenesis, and neurogenesis within the adult hippocampus. Cell Tissue Res *345*, 1-19.

Vuong, H.E., Yano, J.M., Fung, T.C., and Hsiao, E.Y. (2017a). The Microbiome and Host Behavior. Annu Rev Neurosci *40*, 21-49.

Vuong, H.E., Yano, J.M., Fung, T.C., and Hsiao, E.Y. (2017b). The Microbiome and Host Behavior. Annual Review of Neuroscience *40*, 21-49.

Yu, F., Han, W., Zhan, G., Li, S., Xiang, S., Zhu, B., Jiang, X., Yang, L., Luo, A., Hua, F*., et al.* (2019). Abnormal gut microbiota composition contributes to cognitive dysfunction in streptozotocin-induced diabetic mice. Aging (Albany NY) *11*, 3262-3279.

Zhang, J., He, H., Qiao, Y., Zhou, T., Yi, S., Zhang, L., Mo, L., Li, Y., Jiang, W., and You, Z. (2020). Priming of microglia with IFN-γ impairs adult hippocampal neurogenesis and leads to depression-like behaviors and cognitive defects. Glia *68*, 2674-2692.

Zhou, X., Zöller, T., Krieglstein, K., and Spittau, B. (2015). TGFβ1 inhibits IFNγ-mediated microglia activation and protects mDA neurons from IFNγ-driven neurotoxicity. J Neurochem *134*, 125-134.

Zhu, X., Lee, H.G., Perry, G., and Smith, M.A. (2007). Alzheimer disease, the two-hit hypothesis: an update. Biochim Biophys Acta *1772*, 494-50
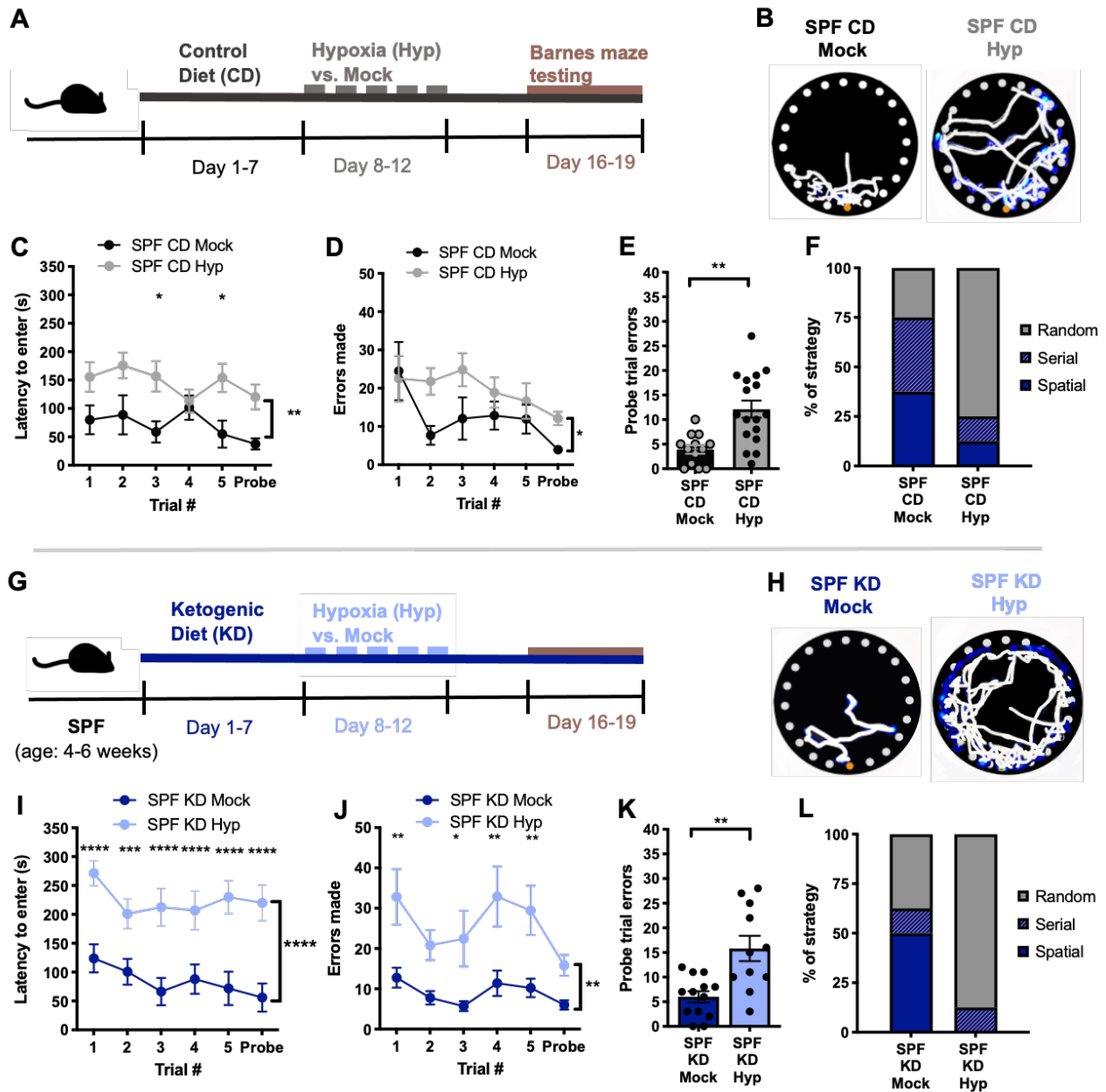
Figure 22: The Ketogenic Diet Potentiates Hypoxia-Induced Impairments in Cognitive Behavior. A) Experimental timeline: Conventionally-colonized (specific pathogen free, SPF) mice were fed a control diet (CD) for 7 days prior to intermittent hypoxia (Hyp) or normoxia (Mock) exposure for 5 days, followed by Barnes maze

315

testing 4 days later. **B)** Representative Barnes maze traces for SPF mice fed the CD and exposed to Mock or Hyp. White lines indicate movement trajectories, whereas blue hues denote increasing durations of time spent at a specific location. Orange circles indicate the escape hole. **C)** Latency to enter the escape hole of the Barnes maze across six 300-second trials for SPF mice fed the CD and exposed to Mock or Hyp. (Two-way ANOVA with Sidak, n=13-17). **D)** Errors made as measured by number of incorrect nose pokes across six Barnes maze trials for SPF mice fed the CD and exposed to Mock or Hyp. (Two-way ANOVA with Sidak, n=13-17). **E)** Errors made during the final Barnes maze trial (probe) for SPF mice fed the CD and exposed to Mock or Hyp. (Unpaired two-tailed Students t-test, n=13-17). **F)** Search strategy used during the probe trial for SPF mice fed the CD and exposed to Mock or Hyp. (n=13-17). **G)** Experimental timeline: SPF mice were fed a ketogenic diet (KD) for 7 days prior to Hyp or Mock exposure for 5 days, followed by Barnes maze testing 4 days later. (n=11-13). **H)** Representative Barnes maze traces for SPF mice fed the KD and exposed to Mock or Hyp. White lines indicate movement trajectories, whereas blue hues denote increasing durations of time spent at a particular location. Orange circles denote the escape hole. **I)** Latency to enter the escape hole across six 300-second trials for SPF mice fed the KD and exposed to Mock or Hyp. (Two-way ANOVA with Sidak, n=11-13). **J)** Errors made as measured by number of incorrect nose pokes across six Barnes maze trials for SPF mice fed the KD and exposed to Mock or Hyp. (Two-way ANOVA with Sidak, n=11-13). **K)** Errors made during the probe trial for SPF mice fed the KD and exposed to Mock or Hyp. (Unpaired two-tailed Students t-test, n=11-13). **L)** Search strategy used during the probe trial for SPF mice fed the CD and exposed to Mock or

316

Hyp. (n=11-13). Data are presented as mean ± S.E.M. * p < 0.05, **p < 0.01, ***p < 0.001, ****p < 0.0001. n.s.=not statistically significant. SPF=specific pathogen-free (conventionally-colonized), CD=control diet, KD=ketogenic diet, Mock=intermittent normoxia exposure, Hyp=intermittent hypoxia exposure.
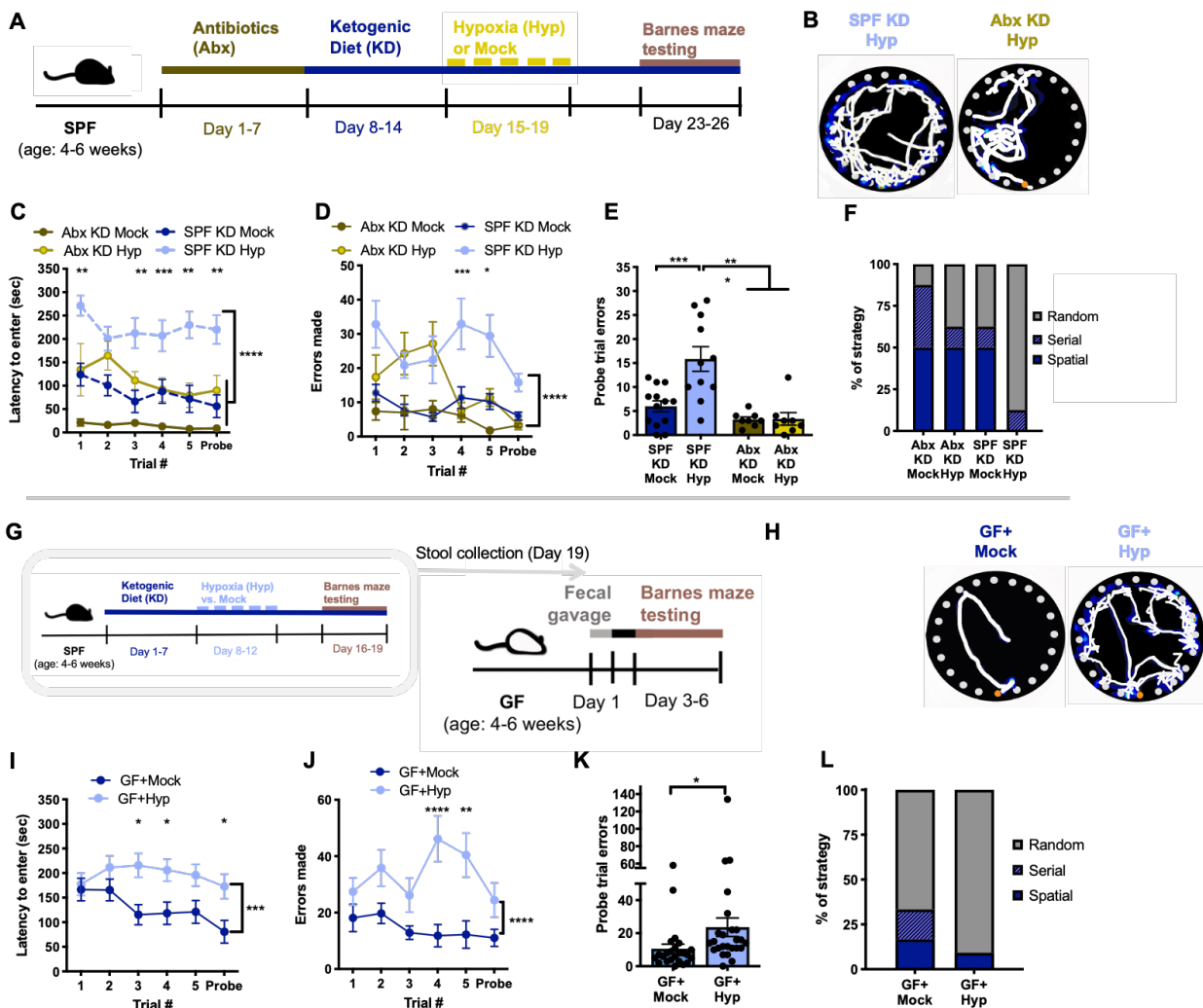
Figure 23: Alterations in the Gut Microbiota Contribute to Ketogenic Diet and Hypoxia-Induced Impairments in Cognitive Behavior. A) Experimental timeline: Conventionally-colonized (specific pathogen free, SPF) mice were pre-treated with oral

antibiotics (Abx) for 7 days prior to feeding with a ketogenic diet (KD), exposure to intermittent hypoxia (Hyp) or normoxia (Mock), and Barnes maze testing. **B)** Representative Barnes maze traces for SPF or Abx mice fed the KD and exposed to Hyp. White lines indicate movement trajectories, whereas blue hues denote increasing durations of time spent at a particular location. Orange circles indicate the escape hole. **C)** Latency to enter the escape hole of the Barnes maze across six 300-second trials for SPF or Abx mice fed the KD and exposed to Mock or Hyp. (Two-way ANOVA with Sidak, n=8 for Abx groups; SPF data are as in Fig. 1). **D)** Errors made as measured by number of incorrect nose pokes across six Barnes maze trials for SPF or Abx mice fed the KD and exposed to Mock or Hyp. (Two-way ANOVA with Sidak, n=8 for Abx groups; SPF data are as in Fig. 1). **E)** Errors made during the probe trial of the Barnes maze for SPF or Abx mice fed the KD and exposed to Mock or Hyp. (One-way ANOVA with Dunnett, n=8 for Abx groups; SPF data are as in Fig. 1). **F)** Search strategy used during probe trial of the Barnes maze for SPF or Abx mice fed the KD and exposed to Mock or Hyp. (n=8). **G)** Experimental timeline: GF mice were gavaged with fecal microbiota from SPF KD Mock or SPF KD Hyp donors (from Fig. 1) and subjected to Barnes maze testing 4 days later. **H)** Representative Barnes maze traces for GF transplanted with fecal microbiota from SPF KD Mock or SPF KD Hyp donors. Transplanted recipient mice receiving SPF KD Mock microbiota are denoted GF+Mock. Transplanted recipient mice receiving SPF KD Hyp microbiota are denoted GF+Hyp. White lines indicate movement trajectories, whereas blue hues denote increasing durations of time spent at a particular location. Orange circles denote the escape hole. **I)** Latency to enter the escape hole across six 300-second trials for GF mice transplanted with SPF KD Mock

318

or SPF KD Hyp microbiota. (Two-way ANOVA with Sidak, n=23). **J)** Errors made during

as measured by number of incorrect nose pokes across six Barnes maze trials for GF

mice transplanted with SPF KD Mock or SPF KD Hyp microbiota. (Two-way ANOVA

with Sidak, n=23). **K)** Errors made during the probe trial of the Barnes maze for GF mice

transplanted with SPF KD Mock or SPF KD Hyp microbiota. (Unpaired two-tailed

Students t-test, n=23). **L)** Search strategy used during probe trial of the Barnes maze for

GF mice transplanted with SPF KD Mock or SPF KD Hyp microbiota. (n=14-15). Data

are presented as mean ± S.E.M. * $p < 0.05$, **$p < 0.01$, ***$p < 0.001$, ****$P < 0.0001$.

n.s.=not statistically significant. SPF=specific pathogen-free (conventionally-colonized),

Abx= treated with antibiotics (ampicillin, vancomycin, metronidazole, neomycin),

KD=ketogenic diet, Mock=intermittent normoxia exposure, Hyp=intermittent hypoxia

exposure, GF=germ-free, GF+Mock = GF mice transplanted with microbiota from SPF

mice fed KD and exposed to Mock, GF+Hyp = GF mice transplanted with microbiota

from SPF mice fed KD and exposed to Hyp.
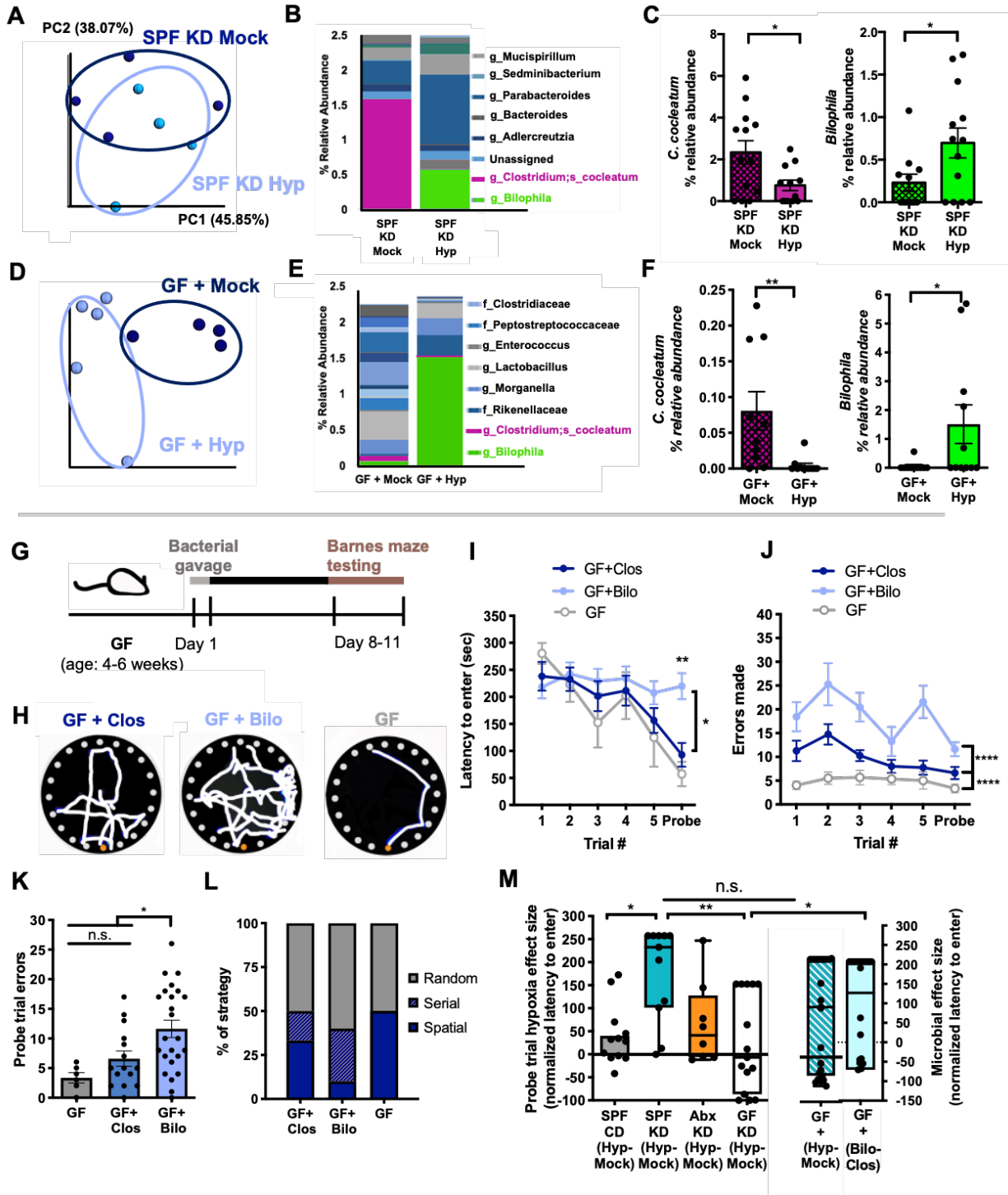
Figure 24: Bilophila is Enriched by the Ketogenic Diet and Hypoxia, and

Sufficiently Impairs Cognitive Behavior. A) Representative principal coordinates

analysis of weighted UniFrac distance based on 16S rRNA gene profiling of feces from

SPF mice fed KD and exposed to Hyp or Mock. (n=4 cages). **B)** Average taxonomic

distributions of low abundance bacteria from 16S rRNA gene sequencing data of feces

from SPF mice fed KD and exposed to Hyp or Mock. (n=13 cages). **C)** Relative

abundances of Clostridium cocleatum (left) and Bilophila spp. (right) in fecal microbiota

of SPF mice fed KD and exposed to Hyp or Mock. (Kruskal wallis with Bonferroni, n=13

cages). **D)** Representative principal coordinates analysis of unweighted UniFrac

distance based on 16S rRNA gene profiling of feces from GF mice transplanted with

fecal microbiota from SPF KD Mock or SPF KD Hyp mice (in panels A-C). (n=4-5

cages) **E)** Average taxonomic distributions of low abundance bacteria from 16S rRNA

gene sequencing data of feces from GF mice transplanted with microbiota from SPF KD

Mock or SPF KD Hyp mice (n=9 cages). **F)** Relative abundances of Clostridium

cocleatum (left) and Bilophila spp. (right) in fecal microbiota of GF mice transplanted

with microbiota from SPF KD Mock or SPF KD Hyp mice. (Kruskal wallis with

Bonferroni, n=9 cages). **G)** Experimental timeline: GF mice were gavaged with cultured

Clostridium cocleatum (Clos) or Bilophila wadsworthia (Bilo) and subjected to Barnes

maze testing 4 days later. **H)** Representative Barnes maze traces for GF mice

monocolonized with Clos or Bilo. White lines indicate movement trajectories, whereas

blue hues denote increasing durations of time spent at a particular location. Orange

circles denote the escape hole. **I)** Latency to enter the escape hole across six 300-

second trials for GF mice monocolonized with Clos or Bilo. (Two-way ANOVA with

Sidak, n=15, 24). **J)** Errors made as measured by number of incorrect nose pokes

across six Barnes maze trials for GF mice monocolonized with Clos or Bilo. (Two-way

ANOVA with Sidak, n=15, 24). **K)** Errors made during the probe trial of the Barnes maze

for GF mice monocolonized with Clos or Bilo. (Unpaired two-tailed Students t-test, n=15, 24). **L)** Search strategy used during probe trial of the Barnes maze for GF mice monocolonized with Clos or Bilo. (n=15, 24). **M)** Effect size of hypoxia on latency to enter the escape hole during the probe trial, as measured by the difference between Hyp groups and respective Mock controls for SPF, Abx, GF, microbiota-transplanted (GF+Hyp-Mock), or monocolonized (GF+Bilo-Clos) mice fed CD or KD. (Two-way ANOVA with Dunnett, n=8-24). Data are presented as mean ± S.E.M. * $p < 0.05$, **$p < 0.01$, ***$p < 0.001$. n.s.=not statistically significant. SPF=specific pathogen-free (conventionally-colonized), KD=ketogenic diet, Mock=intermittent normoxia exposure, Hyp=intermittent hypoxia exposure, GF=germ-free, GF+Mock = GF mice transplanted with SPF KD Mock microbiota, GF+Hyp = GF mice transplanted with SPF KD Hyp microbiota, GF+Clos = GF mice monocolonized with C. cocleatum. GF+Bilo = GF mice monocolonized with B. wadsworthia, Abx= treated with antibiotics (ampicillin, vancomycin, metronidazole, neomycin), CD= control diet.
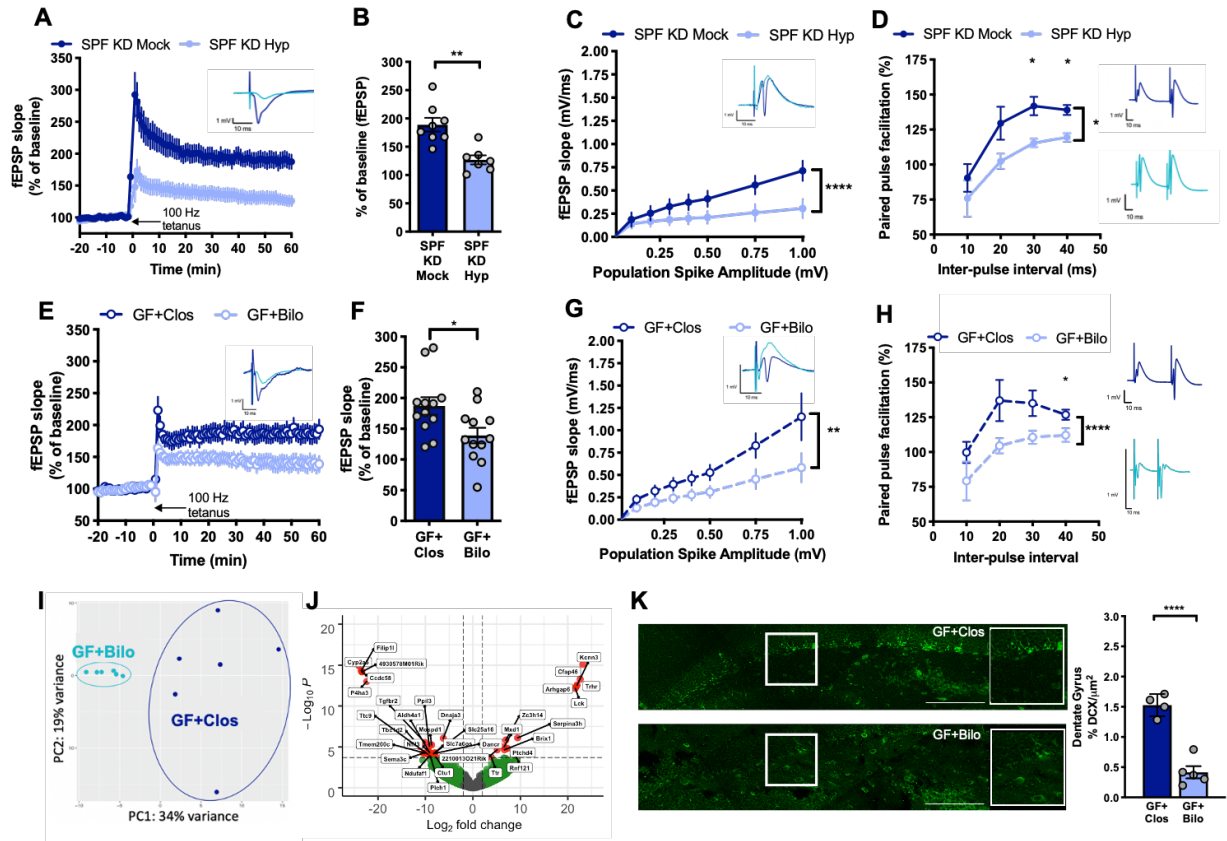
Figure 25: Bilophila Colonization Phenocopies Ketogenic Diet and Hypoxia-Induced Impairments in Hippocampal Activity. A) Hippocampal long-term

potentiation (LTP) as indicated by fEPSP slope in response to 100 Hz tetanus,

expressed as a percentage of 20-minute baseline signal, from slice electrophysiology of

brains from SPF mice fed KD and exposed to Hyp or Mock. (n=7-8). **B**) Average fEPSP

slope during the last 5 minutes of hippocampal LTP recording for SPF mice fed KD and

exposed to Hyp or Mock. (Unpaired two-tailed Students t-test, n=7-8). **C**) Hippocampal

population spike amplitude versus fEPSP slope from slice electrophysiology of brains

from SPF mice fed KD and exposed to Hyp or Mock. (Two-way ANOVA with Sidak,

n=7-8). Representative traces (inset). **D**) Hippocampal paired pulse facilitation from slice

electrophysiology of brains from SPF mice fed KD and exposed to Hyp or Mock. (Two-

323

way ANOVA with Sidak, n=7-8). Representative traces (inset). **E**) Hippocampal LTP as indicated by fEPSP slope in response to 100 Hz tetanus, expressed as a percentage of 20-minute baseline signal from slice electrophysiology of brains from GF mice monocolonized with Clos or Bilo. (n=12). **F**) Average fEPSP slope during the last 5 minutes of hippocampal LTP recording for GF mice monocolonized with Clos or Bilo. (Unpaired two-tailed Students t-test, n=12). **G**) Hippocampal population spike amplitude versus fEPSP slope from slice electrophysiology of brains from GF mice monocolonized with Clos or Bilo. (Two-way ANOVA with Sidak, n=12). Representative traces (inset). **H**) Hippocampal paired pulse facilitation from slice electrophysiology of brains from GF mice monocolonized with Clos or Bilo. (Two-way ANOVA with Sidak, n=12). Representative traces (inset). **I**) Principal components analysis of all differentially regulated genes from RNA sequencing of CA3 subfields of the hippocampus from GF mice monocolonized with Clostridium cocleatum (Clos) or Bilophila wadsworthia (Bilo). (n=6). **J**) Volcano plot labeling genes with high fold change of differential expression in hippocampal CA3 from GF mice monocolonized with Bilo relative to Clos-monocolonized controls. (Wald test, n=6). **K**) Representative image of doublecortin (DCX)-positive neurons in the dentate gyrus of GF mice monocolonized with Clos or Bilo (left). Quantitation of DCX density per area of the dentate gyrus of GF mice monocolonized with Clos or Bilo (right). (Unpaired two-tailed Students t-test, n=4-5). Data are presented as mean ± S.E.M. * $p < 0.05$, **$p < 0.01$, ***$p < 0.001$. n.s.=not statistically significant. SPF=specific pathogen-free (conventionally-colonized), Abx= treated with antibiotics (ampicillin, vancomycin, metronidazole, neomycin), GF=germ-free, KD=ketogenic diet, Hyp=intermittent hypoxia exposure, Mock=intermittent

normoxia exposure, GF+Clos = GF mice monocolonized with C. cocleatum. GF+Bilo = GF mice monocolonized with B. wadsworthia, DCX=doublecortin, LTP=long-term-potentiation, fEPSP=field excitatory post-synaptic potential.
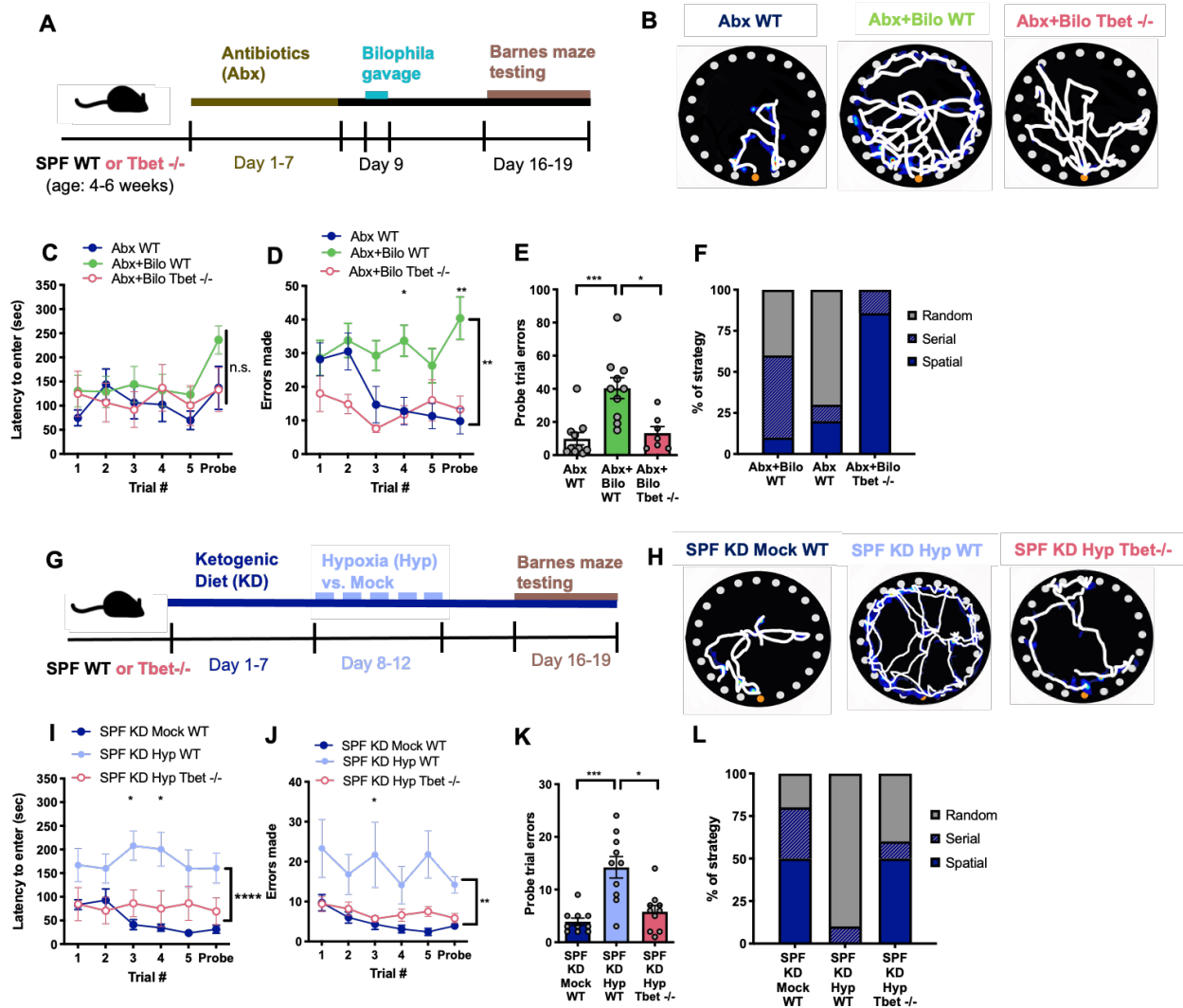
Figure 26: Th1 cell Expansion Contributes to Bilophila-induced Impairments in Cognitive Behavior. A) Experimental timeline: SPF wildtype (WT) or Tbet -/- mice were treated with a 7-day gavage of broad-spectrum antibiotics, followed by Bilophila wadsworthia (Abx+Bilo WT, Abx+Bilo Tbet -/-) or sterile, pre-reduced saline (Abx WT),

followed by Barnes maze testing. **B)** Representative Barnes maze traces for Abx+WT mice compared to Abx mice colonized with Bilophila wadsworthia with either WT or Tbet -/- background. White lines indicate movement trajectories, whereas blue hues denote increasing durations of time spent at a particular location. Orange circles denote the escape hole. **C)** Latency to enter the escape hole of the Barnes maze across six 300-second trials for male Abx WT or Tbet -/- mice colonized with Bilophila or treated with saline. (Two-way ANOVA with Sidak, n=10,7). **D)** Errors made during Barnes maze testing for Abx WT or Tbet -/- mice colonized with Bilophila or treated with saline. (Two-way ANOVA with Sidak, n=10,7). **E)** Errors made during the final Barnes maze trial (probe) for Abx WT or Tbet -/- mice colonized with Bilophila or treated with saline. (Unpaired two-tailed Students t-test, n=10,7). **F)** Search strategy used during the probe trial for Abx WT or Tbet -/- mice colonized with Bilophila or treated with saline. (n=10,7). **G)** Experimental timeline: SPF wildtype (WT) or Tbet -/- mice were fed a ketogenic diet (KD) for 7 days prior to intermittent hypoxia (Hyp) or normoxia (Mock) exposure for 5 days, followed by Barnes maze testing 4 days later. **H)** Representative Barnes maze traces for SPF KD Mock WT mice compared to SPF KD Hyp mice with either WT or Tbet -/- background. White lines indicate movement trajectories, whereas blue hues denote increasing durations of time spent at a particular location. Orange circles denote the escape hole. **I)** Latency to enter the escape hole of the Barnes maze across six 300-second trials for male SPF KD Mock WT mice compared with SPF KD Hyp WT and SPF KD Hyp Tbet -/- mice. (Two-way ANOVA with Sidak, n=10). **J)** Errors made during Barnes maze testing for SPF KD Mock WT mice compared with SPF KD Hyp WT and SPF KD Hyp Tbet -/- mice. (Two-way ANOVA with Sidak, n=10). **K)** Errors made during

326

the final Barnes maze trial (probe) for SPF KD Mock WT mice compared with SPF KD

Hyp WT and SPF KD Hyp Tbet -/- mice. (Unpaired two-tailed Students t-test, n=10). L**)**

Search strategy used during the probe trial for SPF KD Mock WT mice compared with

SPF KD Hyp WT and SPF KD Hyp Tbet -/- mice. (n=10). Data are presented as mean ±

S.E.M. * p < 0.05, **p < 0.01. n.s.=not statistically significant. SPF=specific pathogen-

free (conventionally-colonized), Abx (conventionally-colonized mice treated with broad-

spectrum antibiotics), WT= wildtype, Tbet -/-= knockout line for Tbet transcription factor,

KD=ketogenic diet, Mock=intermittent normoxia exposure, Hyp=intermittent hypoxia

exposure.

SUPPLEMENTAL FIGURES AND FIGURE LEGENDS
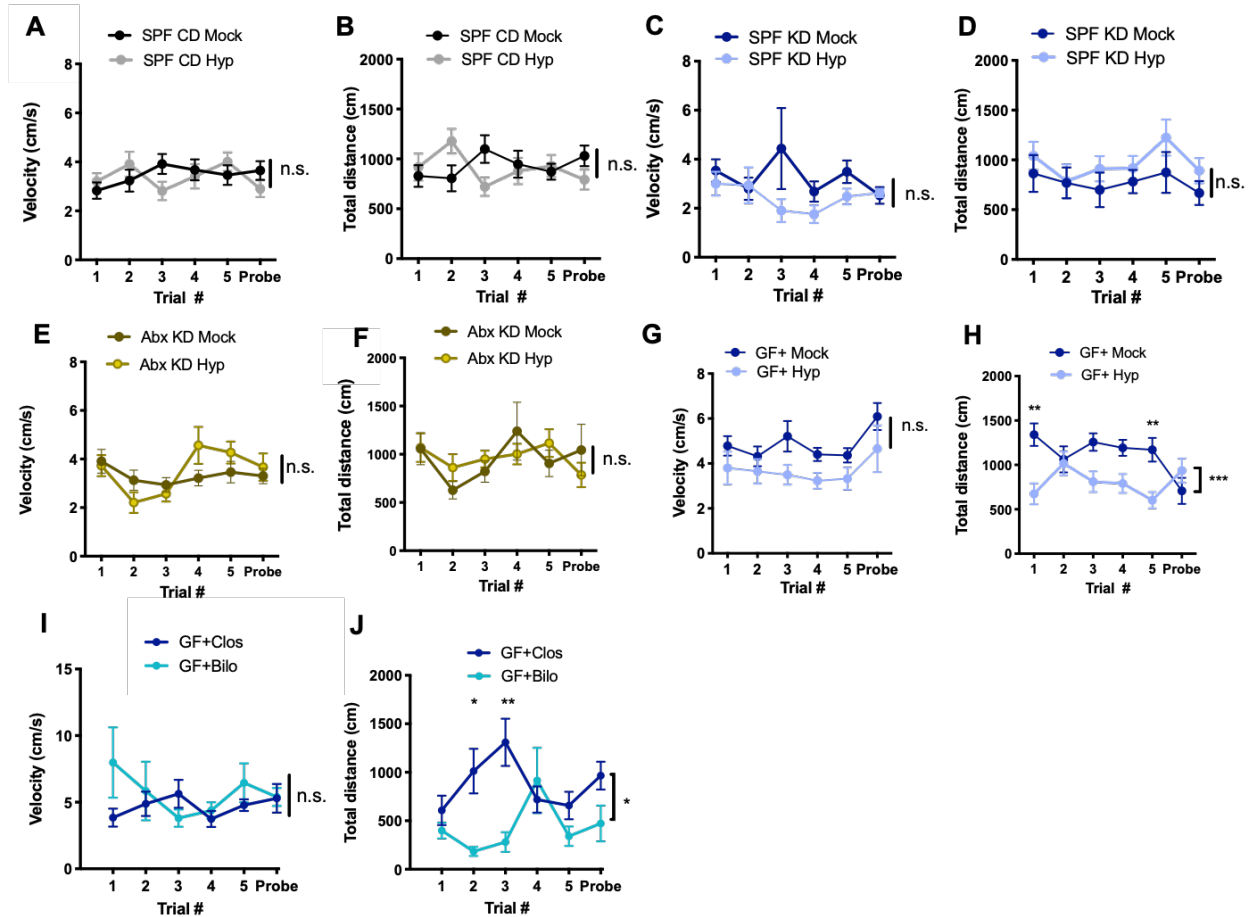
Figure 27: There is no significant effect of hypoxia or ketogenic diet on locomotion in the Barnes maze, Related to Figure 1. A) Average velocity of locomotion across trials in the Barnes maze for SPF mice fed CD and exposed to Mock or Hyp. (Two-way ANOVA with Sidak, n=12-13). **B)** Total distance travelled across trials in the Barnes maze for SPF mice fed CD and exposed to Mock or Hyp. (Two-way ANOVA with Sidak, n=12-13). **C)** Average velocity of locomotion across trials in the Barnes maze for SPF mice fed KD and exposed to Mock or Hyp. (Two-way ANOVA with Sidak, n=11-13). **D)** Total distance travelled across trials in the Barnes maze for male SPF mice fed KD and exposed to Mock or Hyp. (Two-way ANOVA with Sidak,

n=11-13). **E)** Average velocity of locomotion across trials in the Barnes maze for SPF

mice pre-treated with Abx, fed KD and exposed to Mock or Hyp. (Two-way ANOVA with

Sidak, n=8). **F)** Total distance travelled across trials in the Barnes maze for SPF mice

pre-treated with Abx, fed KD and exposed to Mock or Hyp. (Two-way ANOVA with

Sidak, n=8). **G)** Average velocity of locomotion across trials in the Barnes maze for GF

mice transplanted with SPF KD Mock or SPF KD Hyp microbiota. (Two-way ANOVA

with Sidak, n=8). **H)** Total distance travelled across trials in the Barnes maze for GF

mice transplanted with SPF KD Mock or SPF KD Hyp microbiota. (Two-way ANOVA

with Sidak, n=8). **I)** Average velocity of locomotion across trials in the Barnes maze for

GF mice monocolonized with Clos or Bilo. (Two-way ANOVA with Sidak, n=14-15). **J)**

Total distance travelled across trials in the Barnes maze for GF mice monocolonized

with Clos or Bilo. (Two-way ANOVA with Sidak, n=14-15). Data are presented as mean

± S.E.M. * $p < 0.05$, **$p < 0.01$, ***$p < 0.001$. n.s.=not statistically significant. Abx=

treated with antibiotics (ampicillin, vancomycin, metronidazole, neomycin),

KD=ketogenic diet, Mock=intermittent normoxia exposure, Hyp=intermittent hypoxia

exposure, GF=germ-free, GF+Mock = GF mice transplanted with microbiota from SPF

mice fed KD and exposed to Mock, GF+Hyp = GF mice transplanted with microbiota

from SPF mice fed KD and exposed to Hyp, GF+Clos = GF mice monocolonized with C.

cocleatum. GF+Bilo = GF mice monocolonized with B. wadsworthia.
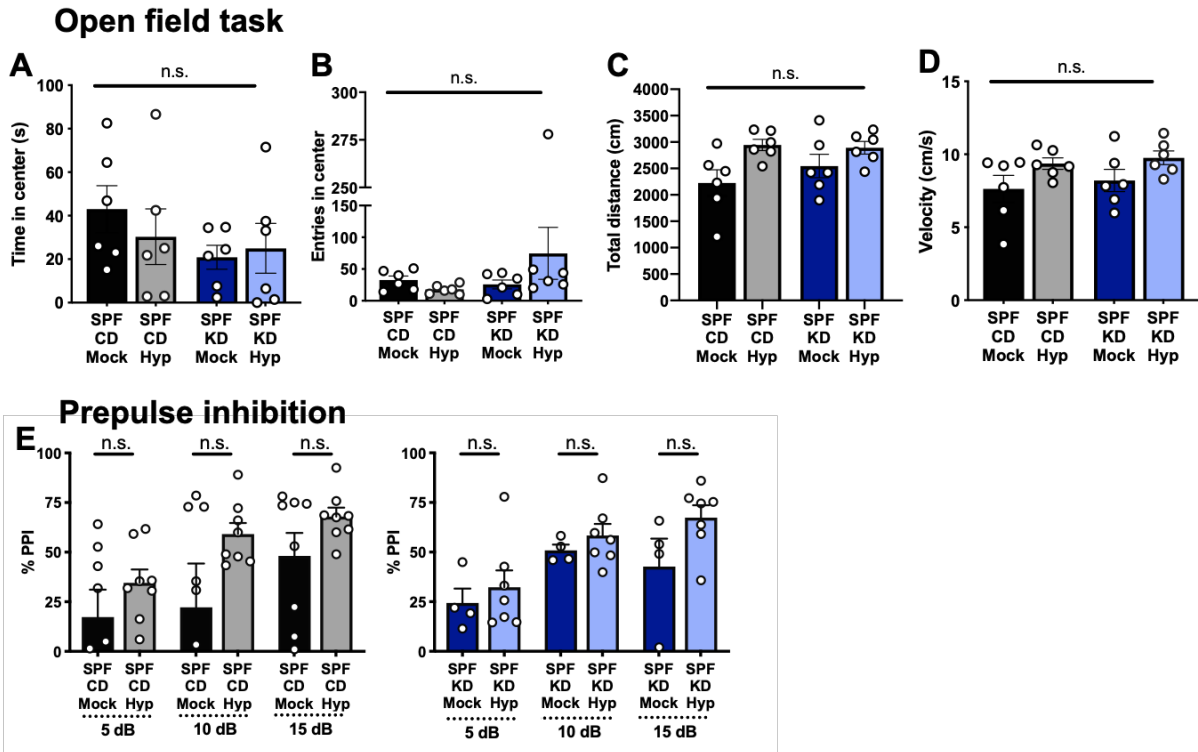
Figure 28: There is no significant effect of hypoxia or ketogenic diet on behavior of male mice in open field exploration and prepulse inhibition tasks, Related to Figure 1. A) Time spent in the center arena during the open field task for SPF mice fed CD or KD and exposed to Mock or Hyp. (One-way ANOVA with Sidak, n=6). **B)** Number of entries into the center arena during the open field task for SPF mice fed CD or KD and exposed to Mock of Hyp. (One-way ANOVA with Sidak, n=6). **C)** Total distance travelled during the open field task for SPF mice fed CD or KD and exposed to Mock of Hyp. (One-way ANOVA with Sidak, n=6). **D)** Average velocity of locomotion during the open field task for SPF mice fed CD or KD and exposed to Mock of Hyp. (One-way ANOVA with Sidak, n=6). **E)** Percent pre-pulse inhibition (PPI) in response to a 5, 10, or 15 dB pre-pulse in SPF mice fed CD or KD and exposed to Mock of Hyp. (Two-way ANOVA with Sidak, n=4-8, negative dots out of range). Data are presented as mean ±

330

S.E.M. n.s.=not statistically significant. SPF=specific pathogen-free (conventionally-colonized), CD=control diet, KD=ketogenic diet, Mock=intermittent normoxia exposure, Hyp=intermittent hypoxia exposure.
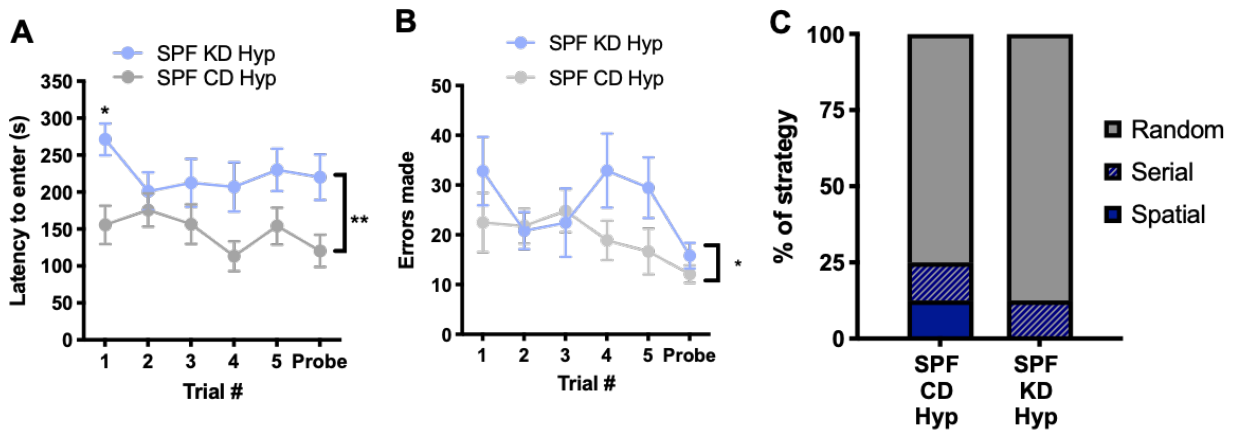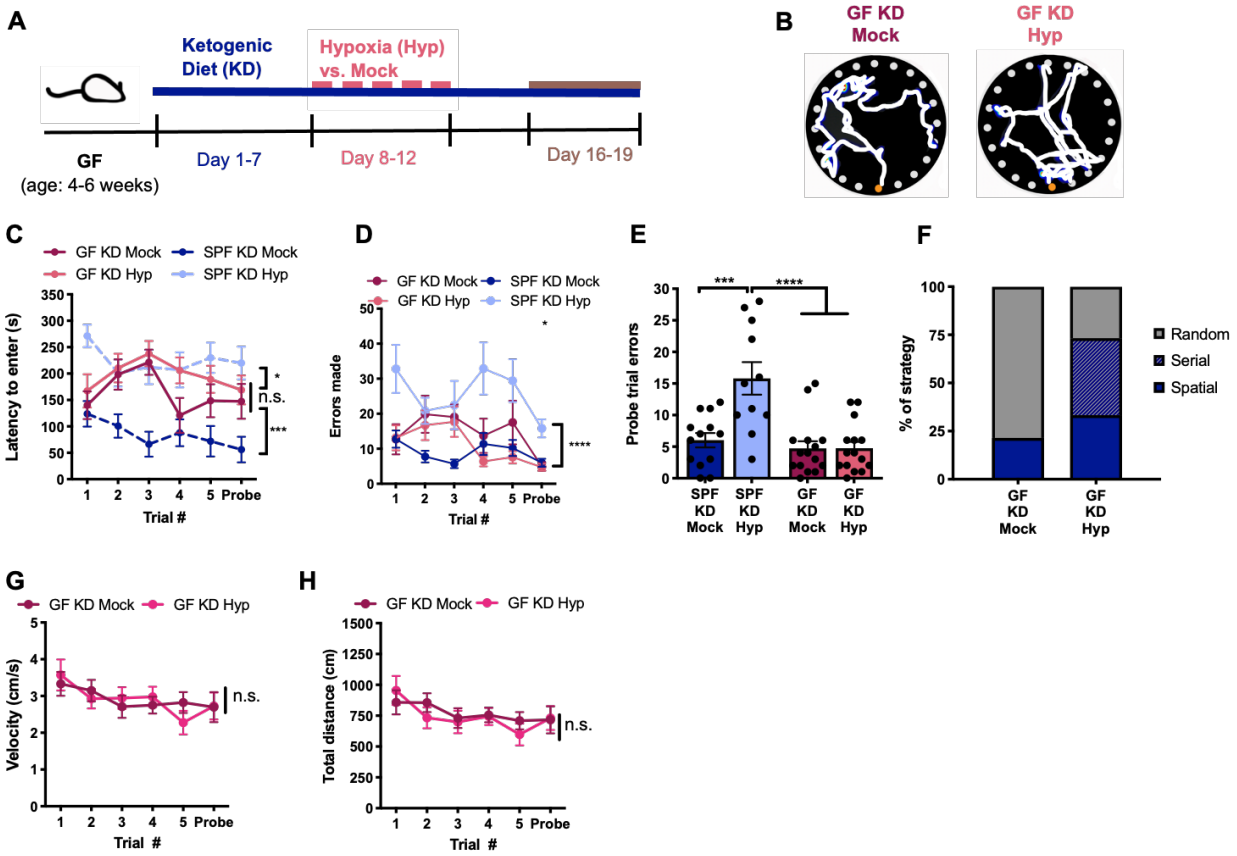

Figure 29: The ketogenic diet significantly potentiates hypoxia-induced impairments in cognitive behavior in the Barnes maze, Related to Figure 1. A) Latency to enter the escape hole of the Barnes maze across six 300-second trials for SPF mice fed the CD and exposed to Mock or Hyp. (Two-way ANOVA with Sidak, n=11-17). **B)** Errors made as measured by number of incorrect nose pokes across six Barnes maze trials for SPF mice fed the CD and exposed to Mock or Hyp. (Two-way ANOVA with Sidak, n=11-17). **C)** Search strategy used during the probe trial for SPF mice fed the CD and exposed to Mock or Hyp. (n=11-17). Data are as displayed in Figure 1. Data are presented as mean ± S.E.M. * $p < 0.05$, **$p < 0.01$. SPF=specific pathogen-free (conventionally-colonized), CD=control diet, KD=ketogenic diet, Mock=intermittent normoxia exposure, Hyp=intermittent hypoxia exposure.

Figure 30: Germ-free mice fed the ketogenic diet are resistant to hypoxia-induced impairment in cognitive behavior, Related to Figure 2. A) Experimental timeline: GF mice were fed KD for 7 days prior to Hyp or Mock exposure for 5 days, followed by Barnes maze testing 4 days later. **B)** Representative Barnes maze traces for GF mice fed the KD and exposed to Mock or Hyp. White lines indicate movement trajectories, whereas blue hues denote increasing durations of time spent at a particular location. Orange circles indicate the escape hole. **C)** Latency to enter the escape hole of the Barnes maze across six 300-second trials for male GF mice fed the KD and exposed to Mock or Hyp. (Two-way ANOVA with Sidak, n=14-15 for GF groups; SPF data are as in Fig. 1). **D)** Errors made as measured by number of incorrect nose pokes across six Barnes maze trials for GF mice fed the KD and exposed to Mock or Hyp. (Two-way

332

ANOVA with Sidak, n=14-15 for GF groups; SPF data are as in Fig. 1). **E)** Errors made during the probe trial of the Barnes maze for GF mice fed the KD and exposed to Mock or Hyp. (One-way ANOVA with Sidak, n=14-15 for GF groups; SPF data are as in Fig. 1). **F)** Search strategy used during probe trial of the Barnes maze for GF mice fed the KD and exposed to Mock or Hyp. (n=14-15). **G)** Average velocity of locomotion across trials in the Barnes maze for GF mice fed KD and exposed to Mock or Hyp. (Two-way ANOVA with Sidak, n=14-15). **H)** Total distance travelled across trials in the Barnes maze for GF mice fed KD and exposed to Mock or Hyp. (Two-way ANOVA with Sidak, n=14-15). Data are presented as mean ± S.E.M. n.s.=not statistically significant. SPF=specific pathogen-free (conventionally-colonized), GF=germ-free, KD=ketogenic diet, Mock=intermittent normoxia exposure, Hyp=intermittent hypoxia exposure.
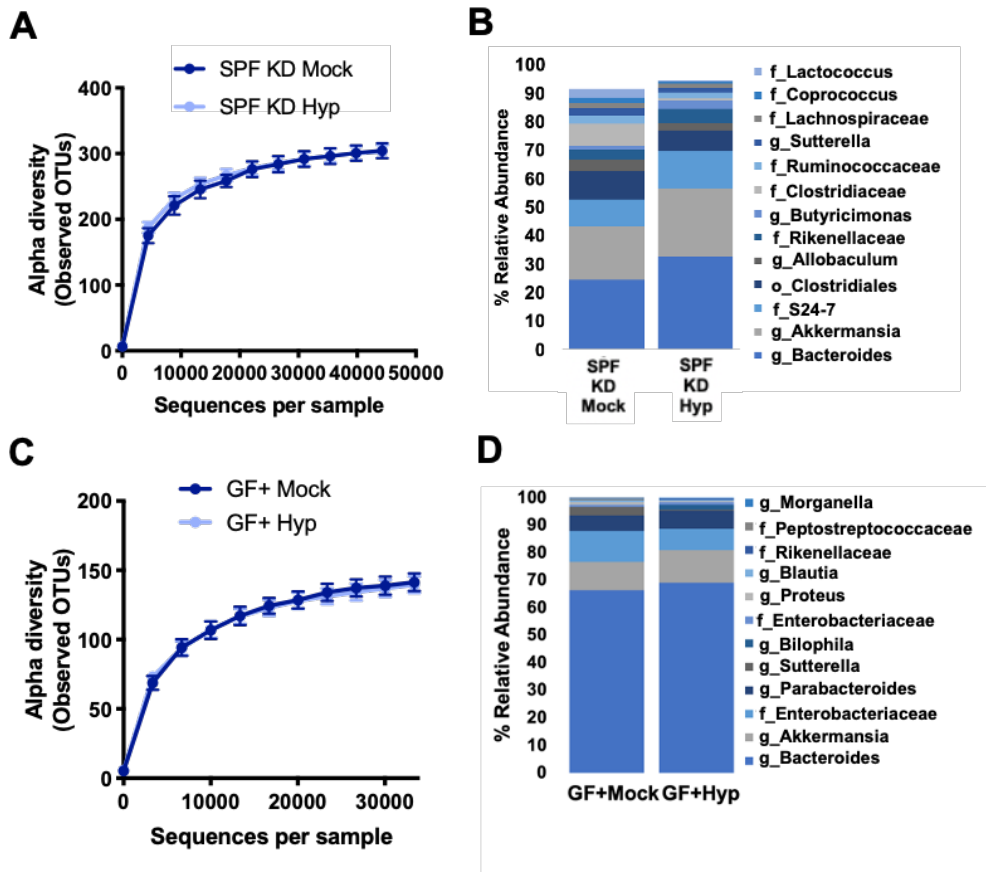
Figure 31: There is no effect of the ketogenic diet and hypoxia on alpha diversity of the fecal microbiota, Related to Figure 3. A) Number of observed operational taxonomic units (OTUs) in the gut microbiota, as measured by 16S rRNA gene sequencing data of feces from SPF mice fed the KD and exposed to Mock or Hyp. (n=8 cages). **B)** Average taxonomic distributions of abundant fecal bacteria from 16S rRNA gene sequencing of feces from SPF mice fed the KD and exposed to Mock or Hyp. (n=8 cages). **C)** Number of observed OTUs in the gut microbiota, as measured by 16S rRNA gene sequencing data of feces from GF mice transplanted with microbiota from SPF mice fed the KD and exposed to Mock or Hyp. (n=10-11 cages). **D)** Average taxonomic distributions of fecal bacteria from 16S rRNA gene sequencing of feces from GF mice

transplanted with microbiota from SPF mice fed the KD and exposed to Mock or Hyp.

(n=10-11 cages). SPF=specific pathogen-free (conventionally-colonized), KD=ketogenic

diet, Mock=intermittent normoxia exposure, Hyp=intermittent hypoxia exposure,

GF=germ-free, GF+Mock = GF mice transplanted with microbiota from SPF mice fed

KD and exposed to Mock, GF+Hyp = GF mice transplanted with microbiota from SPF

mice fed KD and exposed to Hyp.
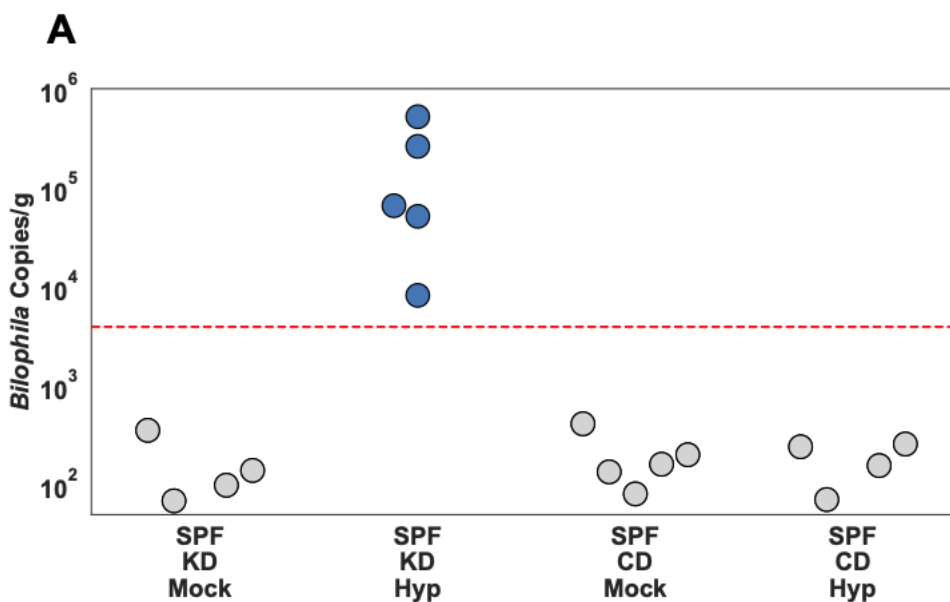
Figure 32: The absolute abundance of Bilophila in the gut microbiota is associated with cognitive impairment in the Barnes maze, Related to Figure 3. A) Digital PCR for absolute quantification of Bilophila 16S copies per gram of fecal matter for SPF KD Mock, SPF KD Hyp, SPF CD Mock, SPF CD Hyp. (n=4-5). Red-dashed line indicates the LLOQ of the assay.
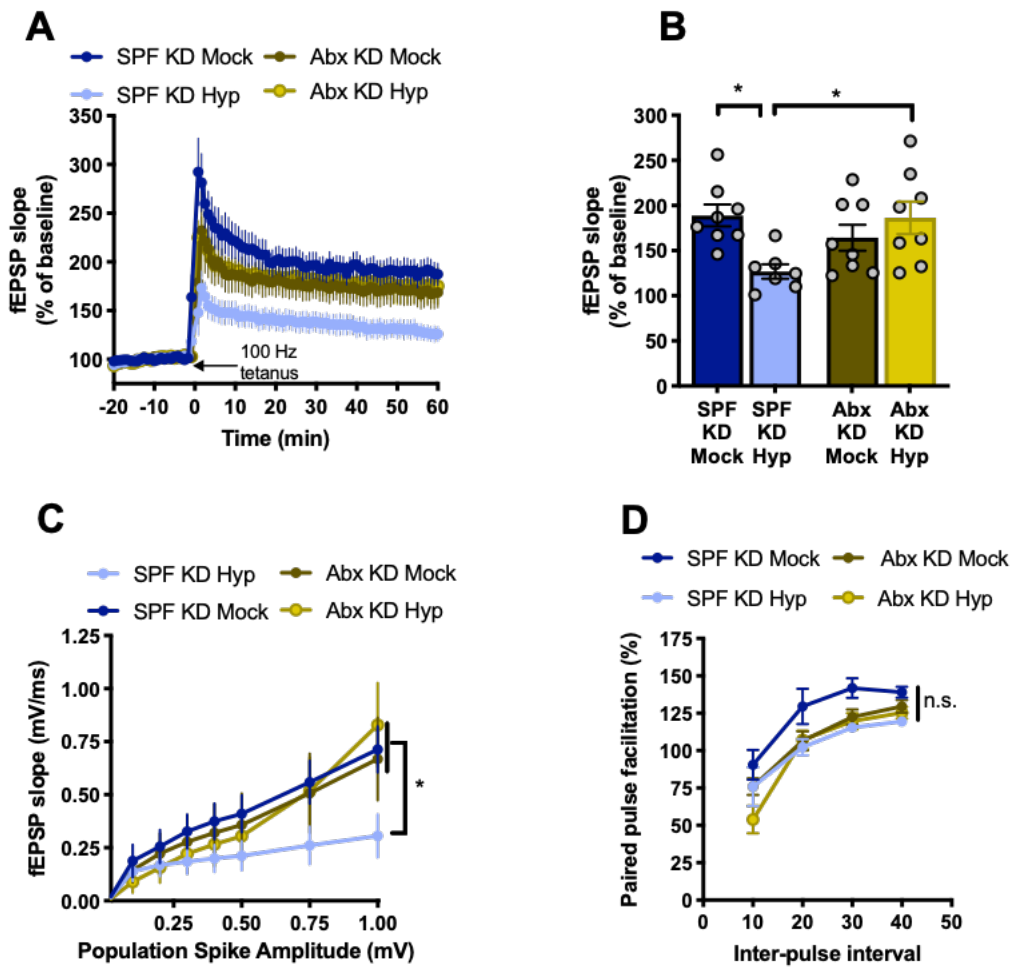
Figure 33. Microbiota depletion diminishes ketogenic diet and hypoxia-induced impairments in hippocampal physiology, Related to Figure 4. A) Hippocampal long-term potentiation (LTP) as indicated by fEPSP slope in response to 100 Hz tetanus, expressed as a percentage of 20-minute baseline signal from slice electrophysiology of brains from SPF or Abx mice fed KD and exposed to Hyp or Mock. Data for SPF groups are as in Fig. 4. (n=5-8). B) Average fEPSP slope during the last 5 minutes of hippocampal LTP recording for SPF or Abx mice fed KD and exposed to Hyp or Mock. Data for SPF groups are as in Fig. 4. (One-way ANOVA with Sidak, n=5-8). C)

Hippocampal population spike amplitude versus fEPSP slope from slice electrophysiology of brains from SPF or Abx mice fed KD and exposed to Hyp or Mock. Data for SPF groups are as in Fig. 4. (Two-way ANOVA with Sidak, n=5-8). Representative traces (inset). D) Hippocampal paired pulse facilitation from slice electrophysiology of brains from SPF or Abx mice fed KD and exposed to Hyp or Mock. Data for SPF groups are as in Fig. 4. (Two-way ANOVA with Sidak, n=5-8). Representative traces (inset). Data are presented as mean ± S.E.M. * $p < 0.05$, **$p < 0.01$. n.s.=not statistically significant. SPF=specific pathogen-free (conventionally-colonized), Abx= treated with antibiotics (ampicillin, vancomycin, metronidazole, neomycin), GF=germ-free, KD=ketogenic diet, Hyp=intermittent hypoxia exposure, Mock=intermittent normoxia exposure, LTP=long-term-potentiation, fEPSP=field excitatory post-synaptic potential.
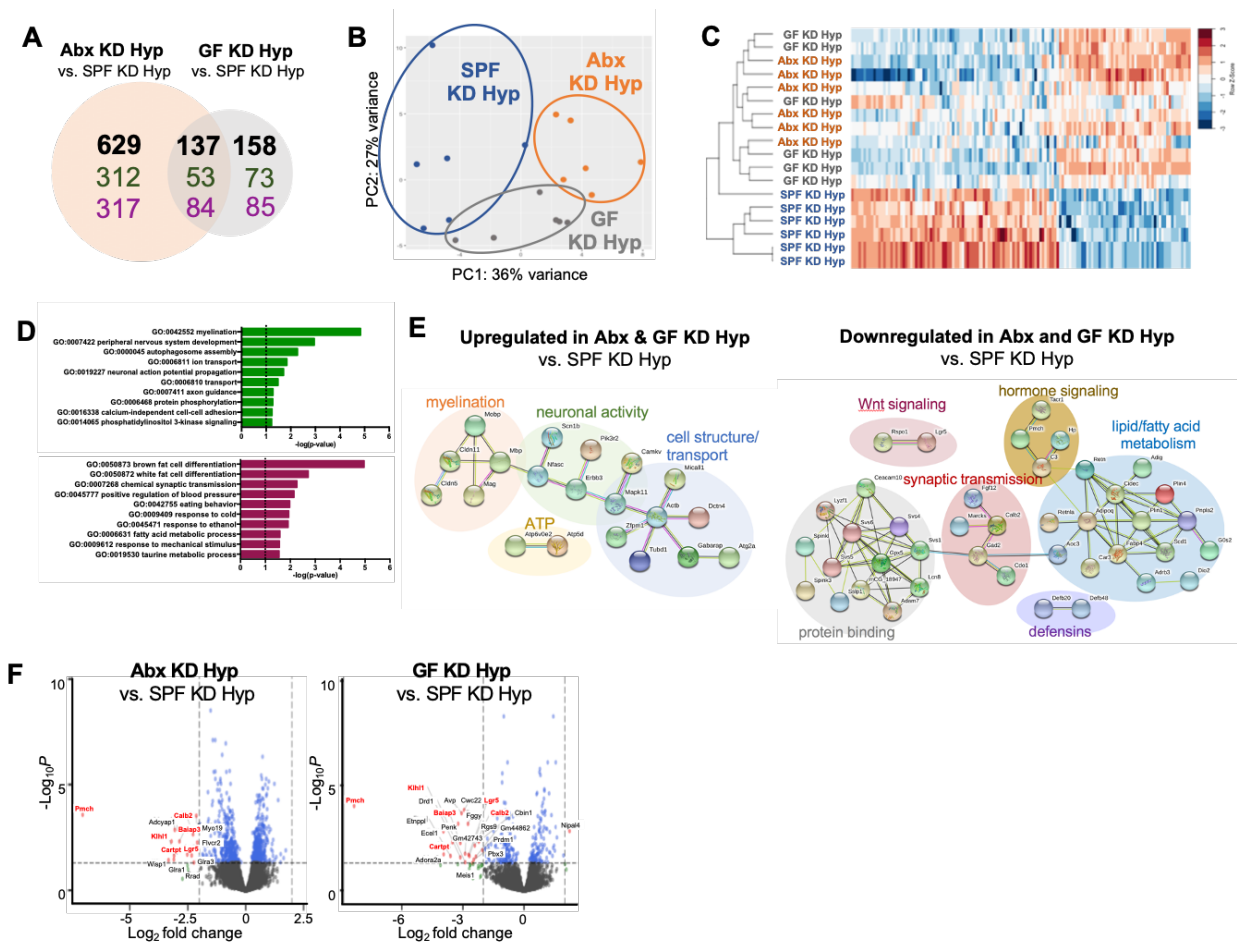
Figure 34. Microbiota depletion alters hippocampal gene expression in mice fed ketogenic diet and exposed to hypoxia, Related to Figure 4. **A)** Differentially expressed genes (q<0.05) in the CA3 of the hippocampus in Abx and GF mice relative to SPF controls, all fed KD and exposed to Hyp. Bolded numbers are the total number of genes differentially regulated by each treatment. Of these, upregulated genes are displayed in green, whereas downregulated genes are displayed in magenta. Numbers in overlapping region denote the genes similarly altered by both Abx treatment and GF rearing. (Wald test, n=6). **B)** Principal components analysis of all differentially regulated genes from RNA sequencing of CA3 subfields of the hippocampus from SPF, GF or

Abx-treated mice fed KD and exposed to Hyp. (n=6). **C)** Heatmap of the 137 genes

differentially regulated (q<0.05) in hippocampal CA3 of both GF and Abx-treated mice

relative to SPF controls fed KD and exposed to Hyp. (Wald test, n=6). **D)** Top 10

pathways from GO-Term enrichment analysis of the 53 commonly upregulated genes

(top, green) and 84 commonly downregulated genes (bottom, magenta) in hippocampal

CA3 from GF and Abx-treated mice relative to SPF controls, all fed KD and exposed to

Hyp (Fisher's exact test, n=6). **E)** STRING protein network analysis of 53 commonly

upregulated genes (left) and 84 commonly downregulated genes (right) from Abx and

GF mice relative to SPF controls, all fed KD and exposed to Hyp. (n=6). **F)** Volcano

plots of pairwise comparisons labeling differentially expressed genes (log 2 fold change

> 2) in Abx (left) and GF (right) mice relative to SPF controls, all fed KD and exposed to

Hyp. Differentially expressed genes shared by both Abx and GF conditions are labeled

in red font. (n=6). Abx= treated with antibiotics (ampicillin, vancomycin, metronidazole,

neomycin), GF= germ-free, SPF=specific pathogen-free (conventionally-colonized),

KD=ketogenic diet, Hyp=intermittent hypoxia exposure.
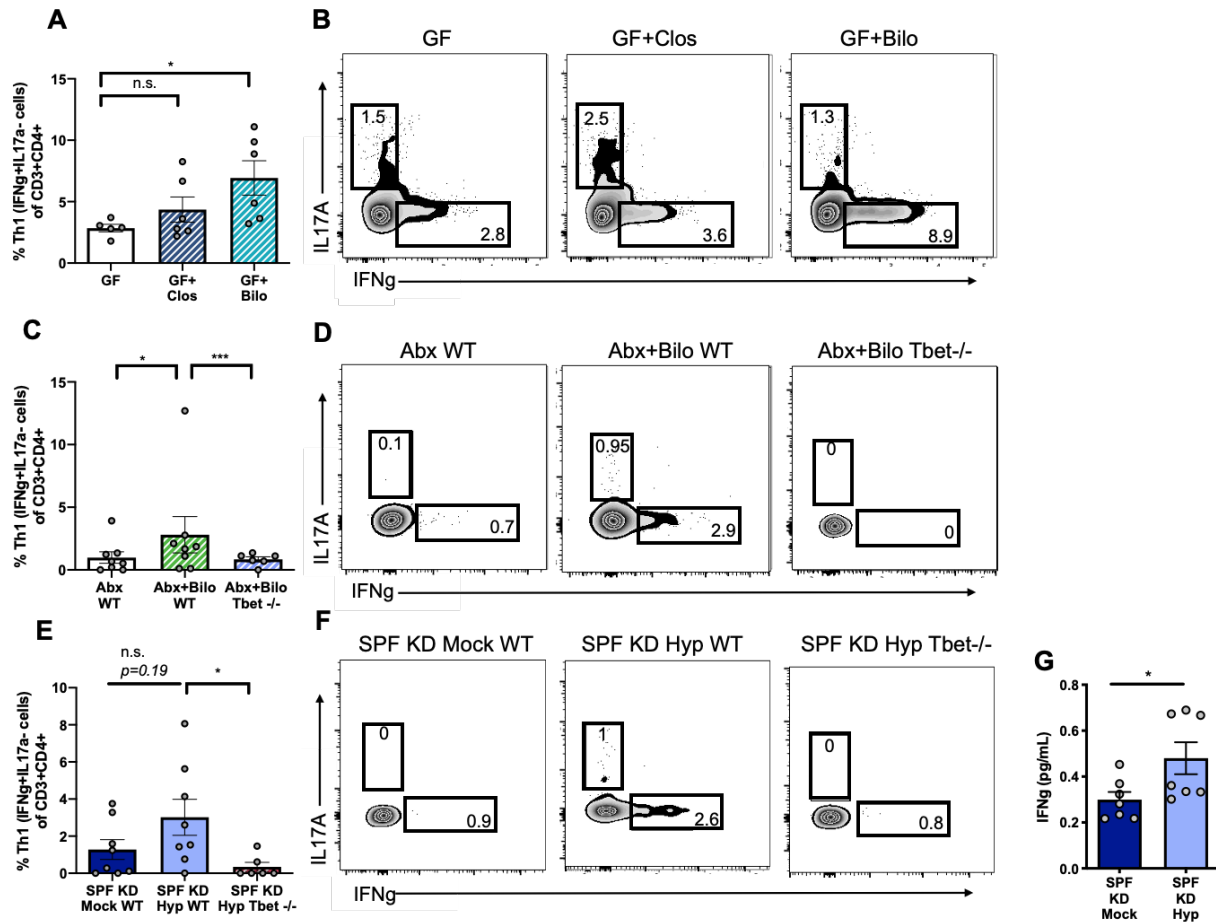
Figure 35: Th1 cell Expansion Contributes to Bilophila-induced Impairments in

Cognitive Behavior. A) Percentages of IFNg+ Th1 cells out of total CD3+CD4+ cell

counts in the lamina propria of GF, GF+Bilo, and GF+Clos mice. (One-way ANOVA with

Sidak, n=5-6). **B)** Representative flow cytometry plots of CD3+IFNg+ Th1 cells and

CD3+IL-17a+ Th17 cells in the lamina propria of GF, GF+Bilo, and GF+Clos mice. **C)**

Percentages of IFNg+ Th1 cells out of total CD3+CD4+ cell counts in the lamina propria

of Abx WT, Abx+Bilo WT, Abx+Bilo Tbet -/- mice. (One-way ANOVA with Sidak, n=6-8).

D) Representative flow cytometry plots of CD3+IFNg+ Th1 cells and CD3+IL-17a+ Th17

cells in the lamina propria of Abx WT, Abx+Bilo WT, Abx+Bilo Tbet -/- mice. **E)**

Percentages of IFNg+ Th1 cells out of total CD3+CD4+ cell counts in the lamina propria

of SPF KD Mock WT, SPF KD Hyp WT, and SPF KD Hyp Tbet -/- mice. (One-way

ANOVA with Sidak, n=6-8). **F)** Representative flow cytometry plots of CD3+IFNg+ Th1

cells and CD3+IL-17a+ Th17 cells in the lamina propria of SPF KD Mock WT, SPF KD

Hyp WT, and SPF KD Hyp Tbet -/- mice. **G)** IFNg serum concentration for SPF KD

Mock and SPF KD Hyp mice (Unpaired two-tailed Students t-test, n=7). Data are

presented as mean ± S.E.M. * $p < 0.05$, **$p < 0.01$. n.s.=not statistically significant.

SPF=specific pathogen-free (conventionally-colonized), Abx (conventionally-colonized

mice treated with broad-spectrum antibiotics), WT= wildtype, Tbet -/-= knockout line for

Tbet transcription factor, KD=ketogenic diet, Mock=intermittent normoxia exposure,

Hyp=intermittent hypoxia exposure.

Chapter 7

Host genetic background and gut microbiota contribute to differential metabolic responses to fructose consumption in mice

In Sook Ahn, Jennifer M Lang, Christine A Olson, Graciel Diamante, Guanglin Zhang, Zhe Ying, Hyae Ran Byun, Ingrid Cely, Jessica Ding, Peter Cohn, Ira Kurtz, Fernando Gomez-Pinilla, Aldons J Lusis, Elaine Y Hsiao, Xia Yang

ABSTRACT

Background: It is unclear how high fructose consumption induces disparate metabolic responses in genetically diverse mouse strains.

Objective: We aim to investigate whether the gut microbiota contributes to differential metabolic responses to fructose.

Methods: Eight-week-old male mice, namely, C57BL/6J (B6), DBA/2J (DBA), and FVB/NJ (FVB) were given 8% fructose solution or regular water (control) for 12 weeks. Gut microbiota composition in cecum and feces was analyzed using 16S rRNA gene sequencing, and PERMANOVA was used to compare community differences across mouse strains, treatments, and time points. Microbiota abundance was correlated with metabolic phenotypes and host gene expression in hypothalamus, liver and adipose tissues using Biweight midcorrelation. To test the causal role of gut microbiota in determining fructose response, we conducted fecal transplant experiments from B6 to DBA and vice versa, as well as *Akkermansia muciniphila* colonization experiments in DBA mice.

Results: Compared to B6 and FVB mice, DBA mice had significantly higher Firmicutes/Bacteroidetes ratio (*P* < 0.001 by one-way ANOVA with Sidak's test) and lower baseline levels of *Akkermansia*, S24-7 and *Turicibacter*, accompanied by metabolic dysregulation after high fructose consumption. Additionally, fructose altered specific microbial taxa in individual mouse strains, such as *Akkermansia* in B6 (7.23

fold) and Rikenellaceae in DBA (0.38 fold), which demonstrated strain-specific

correlations with host metabolic and transcriptomic phenotypes. Fecal transplant

experiments indicated that B6 microbes conferred resistance to fructose-induced weight

gain in DBA mice ($P < 0.001$), and *Akkermansia* colonization abrogated the fructose-

induced weight gain ($P < 0.001$) and glycemic dysfunctions ($P < 0.001$) in DBA mice.

Conclusions: Our findings support that differential microbiota composition between

mouse strains is partially responsible for host metabolic sensitivity to fructose, and that

Akkermansia is one of the key bacteria that confer resistance to fructose-induced

dysregulation of adiposity and glycemic traits.

Introduction

The drastic increase in fructose consumption over the past few decades has been

paralleled by the rising prevalence of metabolic syndrome and diabetes (1). Our recent

systems nutrigenomics study unraveled the impact of fructose on transcriptome,

epigenome and gene-gene interactions in the hypothalamus, which is the main

regulator of metabolism (2). Additionally, studies on the liver and adipose tissues have

also revealed fructose-induced alterations in genes involved in several aspects of

systemic metabolism (3–5). Interestingly, genetically diverse mouse strains demonstrate

disparate metabolic responses to fructose consumption, a finding reproducible across

multiple studies, including ours (5,6). However, the causal mechanisms underlying the inter-individual differences in metabolic responses to fructose have yet to be elucidated.

The gut microbiome is emerging as an important modulator of metabolism, obesity, and other metabolic disorders (7). The dynamic nature and ease of manipulating the gut microbiome have made it a suitable therapeutic target to mitigate metabolic syndrome (8). Diet influences trillions of gut microorganisms as early as one day post dietary intervention (9). The gut microbiome has been suggested to contribute to phenotypic diversity in different mouse strains on a high fat high sucrose diet (10,11). It is plausible that the gut microbiome also plays a role in determining inter-individual variability in metabolic responses to fructose consumption.

Dietary fructose is mainly absorbed in the small intestine, where it can be extensively metabolized into glucose and organic acids. However, excessive amount of fructose that is not absorbed in the small intestine due to malabsorption or high intake can undergo colonic bacterial fermentation, resulting in the production of metabolites including short-chain fatty acids (12). Fructose also has the potential to modify the microbiota community and its normal function. For instance, fructose metabolites can shape the gut environment and be an energy source for the gut microbiota (13). Fructose can also suppress gut bacterial colonization by silencing a colonization factor in a commensal bacterium (14).

Here, we investigated gut microbiota as a potential link between fructose consumption and differential metabolic phenotypes in mice with diverse genetic backgrounds. We

tested our paradigm in three mouse strains, namely C57BL/6J (B6), DBA/2J (DBA), and FVB/NJ (FVB), which have contrasting metabolic susceptibility to high caloric diets (5,6,11).

Methods

Animals and study design

To investigate the role of the gut microbiota in host responses to fructose consumption, we examined microbial composition in the context of differential metabolic and transcriptomic responses in multiple mouse strains (**Supplemental Figure 1**). Seven-week old male mice (20-25g) from three inbred strains, namely B6, DBA, and FVB, were obtained from the Jackson Laboratory (Bar Harbor, ME) and housed in a pathogen-free barrier facility with a 12-hour light/dark cycle at University of California, Los Angeles. Mice were fed Lab Rodent Diet 5001, containing 234 g/kg protein, 45 g/kg fat, 499 g/kg carbohydrate, and 2.89 kcal/g metabolizable energy (LabDiet, St Louis, MO). After one-week acclimation, mice from each strain were randomly divided into two groups. One group was provided with regular water (control group, n=8-10 mice/strain) and the other group was given 8% (w/v) fructose (3.75 kcal/g energy; NOW Real Food, Bloomingdale, IL) dissolved in regular water (fructose group, n=10-12 mice/strain) for 12 weeks *ad libitum*. Food and drink intake were monitored daily on a per-cage basis. Distinct alterations in body weight, fat mass, plasma lipids, glycemic traits, intraperitoneal glucose tolerance test (IPGTT), and the transcriptome of liver, adipose, and hypothalamus in response to fructose consumption across mouse strains were observed and previously published (5). Gut microbiota composition was analyzed from

346

cecum and feces, and was correlated with metabolic phenotypes and host gene expression in individual tissues to prioritize microbial taxa that may contribute to differential host fructose responses. Lastly, fecal microbiota transplant (FMT) and *Akkermansia muciniphila* (AM) colonization experiments were conducted to test the causal role of gut microbiota in determining mouse strain-specific fructose responses. The study was performed in accordance with National Institutes of Health Guide for the Care and Use of Laboratory Animals. All experimental protocols were approved by the Institutional Animal Care and Use Committee at the University of California, Los Angeles.

Fecal and cecal microbiota analysis

Feces were collected at 1, 2, 4, and 12-weeks of fructose treatment, and cecal contents were collected at the end of fructose treatment (12-weeks). Samples were snap frozen and then stored at -80°C until DNA isolation. Microbial DNA was isolated from samples using the MO BIO PowerSoil®-htp 96 Well Soil DNA Isolation Kit (MO BIO, Carlsbad, CA). For the fecal and cecal samples, the same lot isolation kit was used; for the fecal transplant samples a different lot kit was used. The V4 region (15,16) of the 16S rRNA gene was amplified in triplicate with barcoded primers (515f and 806r) (17). PCR products were quantified with Quant-iTTM PicoGreen® dsDNA Assay Kit (Thermo Fisher) and all samples from a specific experiment (e.g., fecal, cecal, or fecal transplant experiment) were combined in equal amounts (~250 ng per sample) into a single pooled submission to be purified with the UltraClean PCR® Clean-Up Kit (MO BIO). Single-end reads were generated on the Illumina HiSeq 2500 platform using two lanes for each

347

pool of mixed samples to create an unbiased sequencing approach. Roughly 500 samples were sequenced per submission, and each dataset of fecal, cecal, and fecal transplant samples were sequenced in different submissions. Raw sequences were processed using QIIME to produce de-multiplexed and quality-controlled sequences. Reads were binned into OTUs at 97% similarity using UCLUST against the Greengenes reference database (18). Singletons, OTUs representing less than 0.005% total relative abundance, unsuccessfully sequenced samples, and outliers were removed. Samples were normalized to a rarefied level specific for each dataset to reduce the effect of unequal sequencing depth to result in 60,000, 106,815, and 37,614 reads per sample for fecal, cecal, fecal transplant samples, respectively. A total of 180 fecal, 46 cecal, and 170 fecal transplant samples were used for downstream analysis.

Correlation analysis between gut microbiota and metabolic phenotypes or fructose signature genes

Correlation analysis was performed between the relative abundance or proportion of microbiota with metabolic phenotypes including body weight, adiposity, and area under the curve (AUC) for glucose tolerance. Microbiota proportion was also correlated with differentially expressed genes in response to fructose consumption, or "fructose signature genes", in hypothalamus, liver, and adipose tissue. The fructose signature genes correlated with bacterial abundance were classified for their biological functions in Gene Ontology, REACTOME, and KEGG using the GSEA tool (19).

Antibiotics treatment prior to fecal transplant or *Akkermansia* colonization

Six-week old B6 or DBA recipient mice were orally gavaged with a solution of vancomycin (50 mg/kg), neomycin (100 mg/kg), and metronidazole (100 mg/kg) twice daily for 7 days. Ampicillin (1 mg/mL) was provided *ad libitum* in drinking water (20). Antibiotics-treated mice were housed in sterile cages with sterile water and food throughout the experiment. Following antibiotics treatment, mice were used for fecal transplant or *Akkermansia* colonization, as described below.

Fecal transplant between B6 and DBA mice

Reciprocal fecal transplant between B6 and DBA mice was conducted, designated as B6(DBA) for B6 mice receiving DBA feces, and DBA(B6) for DBA mice receiving B6 feces. DBA mice that were transplanted with DBA feces, designated as DBA(DBA), and B6 mice that were transplanted with B6 feces, designated as B6(B6), served as control groups. Fecal transplant was performed according to previous studies with some modification (21,22). Briefly, freshly collected feces were pooled from 4 donor mice and suspended at 40mg/mL concentration in anaerobic PBS. The suspension (150 μL) was orally gavaged to the recipient mice for 4 weeks. Total time between collecting feces and delivery of microbial contents into recipients was kept as short as possible (< 15 min) to protect anaerobes. After 1 week of fecal transplant, mice from each of the four transplant experiments, namely B6(DBA), B6(B6), DBA(B6), DBA(DBA), were divided into two groups and treated with 8% fructose or regular water for 12 weeks (n = 7-14 mice/group). Body weight and IPGTT were measured using the methods described previously (5).

Akkermansia colonization in DBA mice

Akkermansia colonization was conducted according to Olson et al. (20). Antibiotics-treated DBA mice were orally gavaged with 200 μL bacterial suspension (5 x 10^9 cfu/mL in anaerobic PBS) throughout the experiment. After 1 week of bacterial gavage, DBA mice were treated with 8% fructose or regular water for 8 weeks (n = 10-14/group). DBA mice receiving anaerobic PBS served as control (n = 8-10/group). Body weight and IPGTT were measured as described previously (5).

Statistical analysis

The microbiota data was summarized into relative abundance by taxonomic level in QIIME, and communities were visualized with principal coordinates analysis (PCoA) based on the weighted UniFrac distance measure (23). Categorical groups (treatment, time, mouse strain) were confirmed to have similar multivariate homogeneity of group dispersions to allow them to be compared using the non-parametric PERMANOVA (permutational multivariate analysis of variance) test with the adonis function (24). Microbial composition was analyzed at the phylum, family, and genus taxonomic levels using the Statistical Analysis of Metagenomic Profiles (STAMP) software (25).

Linear discriminant analysis (LDA) effect size (LEfSe) was used to identify taxa differentially represented between three mouse strains using standard parameters (P < 0.05, LDA score > 2.0) (26). Using the identified features from the LEfSe analysis, we selected six fecal genera which showed contrasting patterns in their baseline levels between DBA and the other two mouse strains, B6 and FVB. To visualize the baseline differences of these six genera between the three mouse strains, boxplots were plotted

using centered log-ratio (CLR) transformed from OTU counts. The difference between strains was assessed using a one-way ANOVA followed by Sidak's post hoc test. Because *Turicibacter* was not normally distributed, the difference between strains was analyzed by Kruskal-Wallis test followed by Dunn's test.

Taxa that differed between the fructose and regular water groups were identified using White's non-parametric T-test (27), followed by Storey's false discovery rate (FDR) estimation using relative abundance data and the Statistical Analysis of Metagenomic Profiles (28). A one-way ANOVA followed by Sidak's post hoc test was used to determine the difference in Firmicutes/Bacteroidetes (F/B) ratio between three mouse strains. F/B ratio was calculated by dividing the proportion of Firmicutes and Bacteroidetes for each sample, and log-transformed to achieve normal distribution. Correlation between gut microbiota and metabolic phenotypes or fructose signature genes from individual tissues, was assessed using Biweight midcorrelation (bicor) (29). Statistical *P*-values were adjusted using the Benjamini-Hochberg approach and FDR < 0.05 was considered significant.

To analyze body weight gain and glucose tolerance data involving multiple time points in fecal transplant and *Akkermansia* colonization experiments, a three-way repeated-measures ANOVA followed by Sidak's post hoc test was used. The effects and interaction of three factors (microbial manipulation, fructose, time) on the metabolic phenotypes were tested.

To evaluate the effects of fructose under each unique microbiota manipulation (e.g., within *Akkermansia*-colonized groups or within B6 mice transplanted with DBA microbe) across multiple time points, a two-way repeated-measures ANOVA was used. Fructose

351

treatment was used as the between-group factor and time was used as the within

subject factor. To assess the effect of a given microbiota manipulation under fructose

treatment across multiple time points, a two-way repeated-measures ANOVA was used.

Microbiota manipulation was used as the between-group factor and time was used as

the within subject factor. If the interaction was significant, microbiota manipulations

within each time point were compared by Sidak's post hoc test. Statistical analyses

were performed using STATISTICA (version 7, Statsoft Inc., Tulsa, OK) and GraphPad

Prism (version 8, GraphPad Software Inc., San Diego, CA). Data were expressed as

means ± SEM. $P < 0.05$ was considered statistically significant.

Results

Strain-specific metabolic responses to fructose treatment

We have previously reported that B6, DBA, and FVB mice demonstrated striking

differences in their metabolic responses to 8% fructose treatment for 12 weeks (5). DBA

mice were more sensitive to fructose in terms of obesity and diabetes-related

phenotypes including body weight, adiposity, and glucose intolerance. In contrast, B6

mice showed significant increases while FVB mice had decreases in plasma cholesterol

levels. These results demonstrate strong inter-strain variability in fructose response in

genetically divergent mice. Importantly, the disparate metabolic responses were not due

to differences in overall energy intake (14.63 ± 0.38, 17.85 ± 0.88, or 18.02 ± 0.40

Kcal/mouse/day for B6, DBA, or FVB, respectively) (5). The differences in metabolic

responses (DBA > B6 or FVB) also did not correlate with the amount of fructose water

intake [FVB (23.62 ± 1.36 mL/mouse/day) > B6 (8.74 ± 0.19 mL/mouse/day) or DBA

(8.47 ± 0.39 mL/mouse/day)] (5), with the latter more likely driven by differences in fructose perception and preference between the mouse strains (6,30).

Overall effects of fructose on gut microbiota community

The gut microbiota in the three mouse strains was assessed using 16S rRNA sequencing. PCoA plots showed distinct clusters determined by mouse strain for both the cecum ($P < 0.001$ by PERMANOVA, **Figure 1**A) and the fecal samples ($P < 0.001$, Figure 1B). Time was also a significant factor in fecal samples ($P < 0.001$), with week 12 separating from the earlier weeks evaluating all mouse strains (Figure 1C) and within each individual mouse strain (Figure 1D-F).

Fecal microbiota differences were seen between fructose and water groups at 12 weeks in B6 ($P = 0.001$ by PERMANOVA, Figure 1G) and DBA mice ($P = 0.046$, Figure 1H) but not in FVB ($P = 0.58$, Figure 1I). In cecum, the fructose group showed separation from controls for B6 mice (Figure 1J), however, the separation was not statistically significant with PERMANOVA ($P = 0.43$). This result may be influenced by the difference in multivariate spread ($P = 0.038$) since PERMANOVA assumes equal dispersion. Fructose treatment was a significant factor for cecal microbiota composition in DBA ($P = 0.002$, Figure 1K), but not for FVB ($P = 0.44$, Figure 1L). Overall, consistent with the differential effects of fructose on metabolic phenotypes, DBA gut microbiota in both feces and cecum was sensitive to fructose treatment.

Baseline differences in gut microbiota between mouse strains show correlation with host metabolic phenotypes

Differences in baseline microbial composition can drive distinct host responses to the

same dietary manipulation (31,32). At the phylum level, there was no significant

difference in cecum Firmicutes/Bacteroidetes (F/B) ratio between three mouse strains

(**Figure 2**A**)**. However, in fecal samples, DBA had significantly higher F/B ratio (1.78 ±

0.17) than B6 (0.35 ± 0.24, $P < 0.001$ by one-way ANOVA) or FVB (0.90 ± 0.09, $P <$

0.001) (Figure 2B), agreeing with the known association of higher Firmicutes

abundance with obesity (33) and the increased adiposity in DBA (5). The microbial taxa

that accounted for the greatest differences between the three mouse strains included 21

cecal (**Supplemental Figure 2**A, B) and 14 fecal (Supplemental Figure 2C, D) microbial

genera based on the LEfSe analysis.

　　We reasoned that if any specific microbial taxon determines the differential

fructose response between the mouse strains, its abundance likely shows contrasting

patterns between the susceptible strain DBA and the two resistant strains. Out of 21

cecal genera (Supplemental Figure 2B**),** none showed contrasting patterns between

DBA and the two resistant strains. Out of the 14 fecal genera (Supplemental Figure 2D**)**,

6 showed distinct patterns in DBA mice compared to the resistant strains (Figure 2C-H).

DBA mice showed higher centered log-ratio (CLR) abundance for *Lactobacillus*,

unknown bacteria of order Clostridiales, and unknown bacteria of family

Lachnospiraceae compared to B6 and FVB. On the other hand, DBA mice had lower

CLR abundance for unknown bacteria of family S24-7, *Akkerman*sia, and *Turicibacter*.

To understand the potential role of these microbial taxa in metabolic regulation,

correlation was tested between the proportion of these taxa and adiposity gain across

strains, and all were significantly correlated with adiposity gain ($P < 0.05$) (Figure 2I-N).

Fructose-responsive microbiota and correlation with host metabolic phenotypes

Next, we explored the differentially abundant microbiota between fructose and water group in the three mouse strains at week 12. We observed more fructose responsive microbiota in feces (11 taxa) compared to cecum samples (1 taxon) across mouse strains at family level (**Table 1**).

In feces, fructose treatment had the highest impact on B6 microbiota (nine families and three genera). Significant decreases were observed in five taxa belonging to phylum Firmicutes. There were also significant increases in S24-7 of phylum Bacteroidetes and Verrucomicrobiaceae. At the genus level, *Akkermansia* showed a significant increase which has demonstrated anti-obesity effect and improved insulin sensitivity. In DBA feces, fructose altered the abundance of Rikenellaceae and Pseudomonadaceae, and their genera. These two families were also found to be fructose responsive in B6 mice, however, the response was more dramatic in DBA mice (0.37 and 33.33 fold changes in DBA compared with 0.62 and 3.33 fold changes in B6 for Rikenellaceae and Pseudomonadaceae, respectively). No fecal microbial taxa were significantly altered by fructose in FVB mice (Table 1; **Supplemental Figure 3**A, B). In DBA cecum, family Erysipelotrichaceae and its two genera (*Clostridum* and an unknown genus), and *Anaerostipes* were all significantly decreased by fructose. Fructose also significantly increased cecal *Bifidobacterium* in FVB mice, while no cecal taxa were significantly changed in B6 mice (Table 1; Supplemental Figure 3C, D).

We next correlated the abundance of these fructose-responsive taxa with metabolic phenotypes in water or fructose-treated mice. In DBA mice, cecal Erysipelotrichaceae was negatively correlated with adiposity and AUC (**Supplemental Figure 4**A, B). Fecal Rikenellaceae in DBA mice showed negative correlation with body weight and adiposity, and positive correlation with AUC in the fructose group, while no significant correlation was observed with these phenotypes in the water group (**Figure 3**A-F). No phenotypic correlation was observed for the fructose-responsive taxa in B6 and FVB mice, which is not surprising given the weaker phenotypic alterations in these mouse strains in response to fructose consumption.

Correlation of fructose-responsive microbiota with fructose signature genes in host metabolic tissues

We then analyzed the correlation between the abundance of fructose-responsive microbiota and the host fructose signature genes in liver, adipose tissue, and hypothalamus (5). We observed distinct correlation patterns in the three mouse strains: the B6 fructose-responsive taxa were correlated with only hypothalamic fructose signature genes, while the fructose-responsive taxa in DBA cecum or feces were correlated with only liver or adipose tissue signature genes, respectively (summary in **Table 2**; full list of genes correlated with fructose-responsive taxa in **Supplemental Table 1**).

In B6, *Dehalobacterium* showed positive correlation with hypothalamic genes encoding the neurotransmitter transporter *Slc6a3*, a notch signaling component *Nrarp*, and an autophagy gene *Atg3*. *Akkermansia* was correlated with several

356

neurotransmitter related genes, including *Oxt* encoding precursor of oxytocine/neurophysin 1 and *Th* encoding tyrosine hydroxylase. In DBA cecum, both *Anaerostipes* and *Clostridium* were positively correlated with *Cyp8b1* in liver, which is responsible for bile acid synthesis (34). In DBA feces, all fructose-responsive taxa were correlated with host signature genes of the adipose tissue, and these genes were involved in lipid metabolism, immune system, response to lipid, cytokines, and hormone (**Supplemental Table 2**). Adipose genes such as *Abhd3, Msr1, Ccr1, Creb,* and *Fas* were correlated with Rikenellaceae and Pseudomonadaceae as well as genera within these families (Table 2; Supplemental Table 2). Taken together, these correlations suggest that gut microbiota may interact with host genes in a mouse strain- and tissue-specific manner in response to fructose.

Alteration of gut microbiota modulates fructose response

Since B6 and DBA mice showed disparate metabolic responses to fructose, we tested whether B6 microbiota confers resistance and DBA microbiota confers vulnerability to fructose effects by transplanting B6 feces to antibiotics-treated DBA mice and vice versa (**Figure 4**A). Using 16S rRNA sequencing, we confirmed that the recipient mice gut microbiome shifted after fecal transplantation (**Supplemental Figure 5**A, B). When the main effects of FMT, fructose, and time were tested, there were significant FMT effects on weight gain in both B6 ($P < 0.001$, Figure 4B) and DBA mice ($P = 0.0015$, Figure 4C), but there was no effect of FMT on glucose tolerance in both mouse strains (Figure 4D, E). Overall, there was a significant fructose effect on weight gain in DBA mice (P = 0.025; Figure 4C), which was not observed in B6 mice (Figure 4B).

357

Under fructose treatment, body weight gain in DBA mice receiving B6 bacteria [DBA(B6)] was significantly lower compared to DBA(DBA) at 4 (P < 0.05), 6, and 8 weeks (P < 0.001). In contrast, there was no significant fructose effect in B6 mice receiving DBA bacteria [B6(DBA)] or in B6(B6) mice (Figure 4B). These results suggest that DBA microbiota failed to induce fructose sensitivity in B6 mice. On the other hand, DBA(B6) mice no longer display fructose-induced weight gain (fructose effect P = 0.66) as seen in DBA(DBA) mice (fructose effect P = 0.047, Figure 4C), supporting that B6 microbiota conferred resistance to body weight gain upon fructose consumption.

The result from FMT experiment supports a causal role of B6 microbiota in conferring fructose resistance to DBA. We next focused on prioritizing the potential microbes in B6 that may determine the fructose resistance phenotype. *Akkermansia* was found to be a highly plausible candidate to explain the dampened response to fructose in B6 for the following reasons. First, *Akkermansia* has been previously demonstrated to carry anti-obesity and insulin sensitizing effects (32,35,36). The beneficial effect of *Akkermansia* was also previously observed in mice fed a high-fat/high-sucrose diet (37). Secondly, it was depleted in the vulnerable strain DBA but was highly abundant in both resistant mouse strains, B6 and FVB (Figure 2G). Thirdly, fructose treatment caused an increase in *Akkermansia* in B6 mice (Table 1; Supplemental Figure 3A). Lastly, *Akkermansia* abundance in B6 is significantly correlated with a large number of hypothalamic genes such as *Oxt* and *Th* that regulate metabolism (Table 2; Supplemental Table 1).

To test the role of *Akkermansia* in protecting against fructose-induced metabolic dysregulation as predicted above, we gavaged DBA mice with *Akkermansia muciniphila* (AM) or PBS media along with fructose treatment for 8 weeks (**Figure 5**A). There were

358

significant effects of AM on both body weight gain ($P < 0.001$) and glucose tolerance ($P < 0.001$) (Figure 5B, C). Under fructose treatment, significantly lower weight gains were observed in DBA mice receiving *Akkermansia* [DBA(AM)] at 3 ($P < 0.05$) and 5-8 weeks ($P < 0.001$) compared to DBA(PBS), while no effect was seen under water treatment (AM effect $P = 0.14$). Within AM or PBS group, fructose had significant effects on body weight gain in control group [DBA(PBS)] ($P = 0.037$), whereas DBA mice receiving AM [DBA(AM)] no longer display fructose-induced body weight gain as seen in DBA(PBS) mice (Figure 5B). Furthermore, DBA(AM) mice significantly improved glucose intolerance compared with DBA(PBS) mice (fructose effect, $P = 0.035$) upon fructose treatment (Figure 5C). These results support that *Akkermansia* confers resistance to fructose-mediated metabolic dysregulation.

Discussion

Our previous study showed that three mouse strains representing a range of genetic diversity differed in their metabolic and transcriptomic responses to high fructose treatment (5). Since gut microbiota is an important modulator of metabolic capacity (7), here we tested the hypothesis that disparate fructose responses among mouse strains were at least partially driven by the gut microbiota. Our 16S rRNA sequencing analysis revealed that baseline microbiota composition and its response to fructose varied by mouse strains. Fecal transplant data supports that B6 mice carry microbiota that confers resistance to fructose-induced body weight gain. We next prioritized *Akkermansia* as a candidate taxon to explain the dampened response to fructose in B6 mice, which are enriched with *Akkermansia*, in comparison to DBA mice, which show depletion of

359

Akkermansia. Indeed, gavaging *Akkermansia muciniphila* to DBA mice mitigated fructose-induced obesity and glucose intolerance. These results support a causal role of gut microbiota in determining the differential metabolic responses to fructose among genetically diverse mouse strains.

As initial colonizing microbial species are important for establishing a favorable environment for bacterial growth in a particular context (38), differences in baseline microbial composition between mouse strains can lead to variations in the metabolic processes of individuals in response to diet (31,32). We found that *Akkermancia*, *Turicibacter*, and S24-7 were almost depleted in DBA mice but were abundant in B6 and FVB mice, whereas *Lactobacillus,* Clostridiales and Lachnospiraceae were at higher baseline levels in DBA mice. Previously, *Akkermansia* has been associated with obesity resistance and improved metabolic parameters in humans and mice, and beneficial effects of dietary interventions have been associated with the higher abundance of *Akkermansia* at baseline (32,36). S24–7 has protective association against diabetes whereas Lachnospiraceae promotes pathogenesis of diabetes in NOD mice (39). The observed lack of protective *Akkermansia* and S-24, along with the higher abundance in pathogenic Lachnospiraceae in DBA mice, agrees with the vulnerability of DBA mice to fructose-induced metabolic dysregulation. Therefore, these bacterial taxa that differ significantly at baseline between strains have the potential to regulate the differential response to fructose treatment.

In addition to differences in baseline microbes that can explain inter-mouse strain variability, bacteria altered by fructose may also play a role in the variability in metabolic responses to fructose. It has been suggested that fructose shifts the gut microbiota and

leads to a westernized microbiome acquisition with altered metabolic capacity, resulting in development of obesity or metabolic disorders (40). In our study, we found various microbes with significantly altered abundances in DBA and B6 but not FVB, which may relate to their differential sensitivity to fructose. Cecal Erypsipelotricaceae and *Anaerostipes* in DBA mice decreased in abundance upon fructose consumption (Table 1; Supplemental Figure 3), and they are known as butyrate-producing bacteria (41). Butyrate promotes the intestinal barrier development, and decreased butyrate production can increase intestinal permeability (42). In both the B6 and DBA feces, we also detected decreased abundance of Rikenellaceae and increased abundance of Pseudomonadaceae following fructose treatment (Table 1). Increases in Pseudomonadaceae and *Pseudomonas* were previously found in obese individuals with higher insulin resistance (43). Therefore, despite the numerous differences between B6 and DBA, there were shared microbial changes in response to fructose consumption. The weaker phenotypic responses in B6 can be a result of compensatory balancing effects of higher abundances of beneficial bacteria such as *Akkermansia* and S24-7 in B6.

We detected more fructose-responsive microbiota in B6 mice than in DBA and FVB mice (Table 1), and, interestingly, most of these B6 taxa were associated with the hypothalamic genes responsive to fructose (Table 2; Supplemental Table 1). Among them are genes that are important for energy homeostasis such as *Nrarp, Qxt*, and *Th*. *Nrarp* encodes an intracellular component of the Notch signaling pathway and regulates differentiation of mouse hypothalamic arcuate neurons responsible for feeding and energy balance. Dysregulation of this homeostatic mediator underlies diseases ranging

361

from growth failure to obesity (44). *Qxt* encodes oxytocin which is the anorexigenic peptide. Oxytocin maintains homeostasis in feeding-related behavior (45). *Th* gene encodes tyrosine hydrogenase (TH). Hypothalamic arcuate nucleus TH neurons play a role in energy homeostasis, and silencing of TH neurons reduces body weight (46). Our previous study (2) reported fructose as a powerful inducer of genomic and epigenomic variability with the capacity to reorganize gene networks critical for central metabolic regulation and neuronal processes in the hypothalamus. The current study suggests that fructose-induced changes in hypothalamic gene expression in B6 mice could be partly via fructose-responsive gut microbiota.

In contrast to B6, fructose responsive microbiota in DBA was more associated with lipid and inflammatory genes in the adipose tissue (Table 2; Supplemental Table 2). *Abhd3* is a crucial factor for insulin resistance in adipose tissue (47); *Sema3e* contributes to inflammation and insulin resistance in obese mice (48); *Msr1* is macrophage scavenger receptor 1 and provides protection from excessive insulin resistance in obese mice (49); *Creb* promotes expression of transcriptional factors of adipogenesis and insulin resistance in obesity (50); *Fas* contributes to adipose tissue inflammation, hepatic steatosis, and insulin resistance induced by obesity (51). Therefore, these adipose-tissue genes correlating with fructose-responsive bacteria in DBA are relevant to the increased adiposity and compromised insulin sensitivity seen in DBA mice. However, we acknowledge that the correlative relationship observed here does not directly imply causation, and future experiments are needed to directly test the causal role of the genes as well as the bacteria implicated.

Our fecal transplant study support that B6 mice carry gut microbes that confer resistance to fructose-induced metabolic syndrome, while DBA microbiota did not significantly induce fructose sensitivity in B6 mice. We further demonstrate that *Akkermansia* partially mediates the protective effect of B6 microbiota. This is the first time that *Akkermansia* is implicated in determining fructose response. Given the recognized therapeutic potential of modulating the gut microbiota (8), probiotic treatment with *Akkermansia* may represent a viable approach to mitigate fructose-induced metabolic abnormalities. In addition to *Akkermansia,* other microbes may also play a role in modulating the differential fructose response between individuals. Future efforts testing the pathogenic or protective role of other individual bacteria revealed, such as *Lactobacillus*, *Turicibacter*, or *Pseudomonas*, are warranted.

In summary, our multi-strain, multi-omics (gut microbiome, transcriptome, and phenome) integrative studies of inter-individual variability in fructose-induced metabolic syndrome established a causal role of gut microbiota in modulating host responses to fructose, a significant metabolic risk in modern societies. Importantly, our study identified key microbial species that may serve as preventative or therapeutic targets for metabolic syndrome. By exploring gut-host interactions, our studies also open numerous hypotheses regarding specific microbiota-host interactions to be further elucidated in the future.

363

Dr. Sana Majid, Paul Patel, Maya Sigh, Jessica Yang and Justin Yoon for helping with animal experiments.

XY, EYH, ISA, and CO designed the research; ISA, CAO, JML, ZY, IC, GD, PC, HRB and JD conducted research including animal experiments; JML, ISA, GZ, IK, JD analyzed data; ISA, XY and JML wrote the manuscript; FG-P, AL and all authors contributed to manuscript revision; XY had primary responsibility for the final content; All authors read and approved the final version of the paper.

References

1. Basciano H, Federico L, Adeli K. Fructose, insulin resistance, and metabolic dyslipidemia. Nutr Metab. 2005;2:1–14.

2. Meng Q, Ying Z, Noble E, Zhao Y, Agrawal R, Mikhail A, Zhuang Y, Tyagi E, Zhang Q, Lee JH, et al. Systems nutrigenomics reveals brain gene networks linking metabolic and brain disorders. EBioMedicine. 2016;7:157–66.

3. Koo HY, Wallig MA, Chung BH, Nara TY, Cho BHS, Nakamura MT. Dietary fructose induces a wide range of genes with distinct shift in carbohydrate and lipid metabolism in fed and fasted rat liver. Biochim Biophys Acta - Mol Basis Dis. 2008;1782:341–8.

4. Li Z, Xiong C, Mo S, Tian H, Yu M, Mao T, Chen Q, Luo H, Li Q, Lu J, et al. Comprehensive transcriptome analyses of the fructose-fed syrian golden hamster liver provides novel insights into lipid metabolism. PLoS One. 2016;11:1–19.

5.	Zhang G, Byun HR, Ying Z, Blencowe M, Zhao Y, Hong J, Shu L, Chella Krishnan K, Gomez-Pinilla F, Yang X. Differential metabolic and multi-tissue transcriptomic responses to fructose consumption among genetically diverse mice. Biochim Biophys Acta - Mol Basis Dis. Elsevier; 2020;1866:165569.

6.	J. Glendinnning, L. Breinager, E. Kyrillou, K. Lacuna, R. Rocha AS. Differential effects of sucrose and fructose on dietary obesity in four mouse strains. Physiol Behav. 2010;101:331–43.

7.	Turnbaugh PJ, Ley RE, Mahowald M a, Magrini V, Mardis ER, Gordon JI. An obesity-associated gut microbiome with increased capacity for energy harvest. Nature. 2006;444:1027–31.

8.	Fändriks L. Roles of the gut in the metabolic syndrome: an overview. J Intern Med. 2016;1–18.

9.	David LA, Maurice CF, Carmody RN, Gootenberg DB, Button JE, Wolfe BE, Ling A V, Devlin AS, Varma Y, Fischbach MA, et al. Diet rapidly and reproducibly alters the human gut microbiome. Nature. 2014;505:559–63.

10.	Carmody RN, Gerber GK, Luevano JM, Gatti DM, Somes L, Svenson KL, Turnbaugh PJ. Diet dominates host genotype in shaping the murine gut microbiota. Cell Host Microbe. Elsevier Inc.; 2015;17:72–84.

11.	Parks BW, Nam E, Org E, Kostem E, Norheim F, Hui ST, Pan C, Civelek M, Rau CD, Bennett BJ, et al. Genetic control of obesity and gut microbiota composition in response to high-fat, high-sucrose diet in mice. Cell Metab. 2013;17:141–52.

12. Oh JH, Alexander LM, Pan M, Schueler KL, Keller MP, Attie AD, Walter J, van Pijkeren JP. Dietary fructose and microbiota-derived short-chain fatty acids promote bacteriophage production in the gut symbiont Lactobacillus reuteri. Cell Host Microbe. 2019;25:273–84.

13. Ríos-Covián D, Ruas-Madiedo P, Margolles A, Gueimonde M, De los Reyes-Gavilán CG, Salazar N. Intestinal short chain fatty acids and their link with diet and human health. Front Microbiol. 2016;7:1–9.

14. Townsend GE, Han W, Schwalm ND, Raghavan V, Barry NA. Dietary sugar silences a colonization factor in a mammalian gut symbiont. 2019;116:233–8.

15. Faith JJ, Guruge JL, Charbonneau M, Subramanian S, Seedorf H, Goodman AL, Clemente JC, Knight R, Heath AC, Leibel RL, et al. The long-term stability of the human gut microbiota. Science (80-). 2013;341:1237439.

16. Zhang J, Ding X, Guan R, Zhu C, Xu C, Zhu B, Zhang H, Xiong Z, Xue Y, Tu J, et al. Evaluation of different 16S rRNA gene V regions for exploring bacterial diversity in a eutrophic freshwater lake. Sci Total Environ. 2018;618:1254–67.

17. Caporaso JG, Lauber CL, Walters WA, Berg-Lyons D, Lozupone CA, Turnbaugh PJ, Fierer N, Knight R. Global patterns of 16S rRNA diversity at a depth of millions of sequences per sample. Proc Natl Acad Sci. 2011;108.

18. Caporaso JG, Kuczynski J, Stombaugh J, Bittinger K, Bushman FD, Costello EK, Fierer N, Peña AG, Goodrich JK, Gordon JI, et al. QIIME

allows analysis of high-throughput community sequencing data. Nat Methods. 2010;7:335–6.

19.   Subramanian A, Tamayo P, Mootha VK, Mukherjee S, Ebert BL, Gillette MA, Paulovich A, Pomeroy SL, Golub TR, Lander ES, et al. Gene set enrichment analysis: A knowledge-based approach for interpreting genome-wide expression profiles. Proc Natl Acad Sci. 2005;102:15545–50.

20.   Olson C a., Vuong HE, Yano JM, Liang QY, Nusbaum DJ, Hsiao EY. The gut microbiota mediates the anti-seizure effects of the ketogenic diet. Cell. 2018;173:1728–41.

21.   Gregory JC, Buffa JA, Org E, Wang Z, Levison BS, Zhu W, Wagner MA, Bennett BJ, Li L, DiDonato JA. Transmission of atherosclerosis susceptibility with gut microbial transplantation. J Biol Chem. 2015;290:5647–60.

22.   Suez J, Korem T, Zeevi D, Zilberman-Schapira G, Thaiss CA, Maza O, Israeli D, Zmora N, Gilad S, Weinberger A, et al. Artificial sweeteners induce glucose intolerance by altering the gut microbiota. Nature. 2014;514:181–6.

23.   Lozupone C, Knight R. UniFrac: a new phylogenetic method for comparing microbial communities. Appl Environ Microbiol. 2005;71:8228–35.

24.   Oksanen J, Blanchet FG, Kindt R, Legendre P, Minchin PR, O'Hara RB, Simpson GL, Solymos P, Stevens MH, Wagner H. vegan: community ecology package. 2015.

25. Parks DH, Tyson GW, Hugenholtz P, Beiko RG. STAMP : statistical analysis of taxonomic and functional profiles. 2014;30:3123–4.

26. Segata N, Izard J, Waldron L, Gevers D, Miropolsky L, Garrett WS, Huttenhower C. Metagenomic biomarker discovery and explanation. Genome Biol. 2011;12:R60.

27. White JR, Nagarajan N, Pop M. Statistical methods for detecting differentially abundant features in clinical metagenomic samples. PLoS Comput Biol. Public Library of Science; 2009;5:e1000352.

28. Storey JDD, Taylor JE, Siegmund D. Strong control, conservative point estimation and simultaneous conservative consistency of false discovery rates: a unified approach. J R Stat Soc. 2004;66:187–205.

29. Zheng CH, Yuan L, Sha W, Sun ZL. Gene differential coexpression analysis based on biweight correlation and maximum clique. BMC Bioinformatics. 2014;15:S3.

30. Reed DR, Li S, Li X, Huang L, Tordoff MG, Starling-Roney R, Taniguchi K, West DB, Ohmen JD, Beauchamp GK, et al. Polymorphisms in the taste receptor gene (Tas1r3) region are associated with saccharin preference in 30 mouse strains. J Neurosci. 2004;24:938–46.

31. Kootte RS, Levin E, Salojärvi J, Smits LP, Hartstra A V, Udayappan SD, Hermes G, Bouter KE, Koopen AM, Holst JJ, et al. Improvement of insulin sensitivity after lean donor feces in metabolic syndrome is driven by baseline intestinal microbiota composition. Cell Metab. 2017;26:611–9.

32. Dao MC, Everard A, Aron-Wisnewsky J, Sokolovska N, Prifti E, Verger EO, Kayser BD, Levenez F, Chilloux J, Hoyles L, et al. Akkermansia muciniphila and improved metabolic health during a dietary intervention in obesity: relationship with gut microbiome richness and ecology. Gut. 2016;65:426–36.

33. Ley RE, Backhed F, Turnbaugh P, Lozupone CA, Knight RD, Gordon JI. Obesity alters gut microbial ecology. Proc Natl Acad Sci U S A. 2005;102:11070–5.

34. Wahlström A, Sayin SI, Marschall H-U, Bäckhed F. Intestinal crosstalk between bile acids and microbiota and its impact on host metabolism. Cell Metab. 2016;24:41–50.

35. Derrien M, van Baarlen P, Hooiveld G, Norin E, Muller M, de Vos W. Modulation of Mucosal Immune Response, Tolerance, and Proliferation in Mice Colonized by the Mucin-Degrader Akkermansia muciniphila. Front Microbiol. 2011;2:166.

36. Everard A, Belzer C, Geurts L, Ouwerkerk JP, Druart C, Bindels LB, Guiot Y. Cross-talk between *Akkermansia muciniphila* and intestinal epithelium controls diet-induced obesity. Proc Nati Acad Sci USA. 2013;110:9066–71.

37. Org E, Parks BW, Joo JWJ, Emert B, Schwartzman W, Kang EY, Mehrabian M, Pan C, Knight R, Gunsalus R. Genetic and environmental control of host-gut microbiota interactions. Genome Res. 2015;25:1558–69.

38. Jost T, Lacroix C, Braegger CP, Chassard C. New insights in gut microbiota establishment in healthy breast fed neonates. PLoS One. 2012;7.

39. Krych, Nielsen DS, Hansen AK, Hansen CHF. Gut microbial markers are associated with diabetes onset, regulatory imbalance, and IFN-γ level in NOD Mice. Gut Microbes. 2015;6:101–9.

40. Payne AN, Chassard C, Lacroix C. Gut microbial adaptation to dietary consumption of fructose, artificial sweeteners and sugar alcohols: implications for host–microbe interactions contributing to obesity. Obes Rev. 2012;13:799–809.

41. Levine UY, Looft T, Allen HK, Stanton TB. Butyrate-producing bacteria, including mucin degraders, from the swine intestinal tract. Appl Environ Microbiol. 2013;79:3879–81.

42. Peng L, Li Z-R, Green RS, Holzman IR, Lin J. Butyrate enhances the intestinal barrier by facilitating tight junction assembly via activation of AMP-activated protein kinase in Caco-2 cell monolayers. J Nutr. 2009;139:1619–25.

43. Moreno-Indias I, Sánchez-Alcoholado L, García-Fuentes E, Cardona F, Queipo-Ortuño MI, Tinahones FJ. Insulin resistance is associated with specific gut microbiota in appendix samples from morbidly obese patients. Am J Transl Res. 2016;8:5672–84.

44. Lamar E, Deblandre G, Wettstein D, Gawantka V, Pollet N, Niehrs C, Kintner C. Nrarp is a novel intracellular component of the Notch signaling pathway. Genes Dev. 2001;15:1885–99.

45. Olszewski PK, Klockars A, Schiöth HB, Levine AS. Oxytocin as feeding inhibitor: Maintaining homeostasis in consummatory behavior. Pharmacol Biochem Behav. 2010;97:47–54.

46. Zhang X, Van Den Pol AN. Hypothalamic arcuate nucleus tyrosine hydroxylase neurons play orexigenic role in energy homeostasis. Nat Neurosci. 2016;19:1341–7.

47. Xia W, Pessentheiner AR, Hofer DC, Amor M, Schreiber R, Schoiswohl G, Eichmann TO, Walenta E, Itariu B, Prager G, et al. Loss of ABHD15 impairs the anti-lipolytic action of insulin by altering PDE3B stability and contributes to insulin resistance. Cell Rep. 2018;23:1948–61.

48. Shimizu I, Yoshida Y, Moriya J, Nojima A, Uemura A, Kobayashi Y, Minamino T. Semaphorin3E-induced inflammation contributes to insulin resistance in dietary obesity. Cell Metab. 2013;18:491–504.

49. Cavallari, J. F., Anhe, F. F., Foley , K. P., Denou E., Chan R. W., Bowdish D. M. E. SJD. Targeting macrophage scavenger receptor 1 promotes insulin resistance in obese male mice. 2018;6:1–11.

50. Qi L, Saberi M, Zmuda E, Wang Y, Altarejos J, Dentin R, Hedrick S, Bandyopadhyay G, Hai T, Montminy M. Adipocyte CREB promote insulin resistance in obesity. Cell Metab. 2010;9:277–86.

51. Wueest S, Rapold R a., Schumann DM, Rytka JM, Schildknecht A, Nov O, Chervonsky A V., Rudich A, Schoenle EJ, Donath MY, et al. Deletion of Fas in adipocytes relieves adipose tissue inflammation and hepatic manifestations of obesity in mice. J Clin Invest. 2010;120:191–202.

Figure legends

Figure 1. Principal coordinates analysis (PCoA) of cecal and fecal microbiota of B6, DBA, and FVB mice consuming fructose or regular water. Samples grouped separated by the 3 strains in both cecum (A; n = 16/strain) and feces communities (B; n = 64/strain), but time also influenced fecal communities (C). Plot C is the same ordination as Plot B, but PC3 is presented as the x-axis to demonstrate the relationship with time. Time is overlaid on the individual strain ordinations of fecal samples from B6 (D), DBA (E), and FVB (F), and the same plots were overlaid with the fructose treatment for B6 (G), DBA (H), and FVB (I) strains. Samples within the dotted circles are for the 12-week time point, and the associated P-values refer to the differences between treatments only during the 12-week time point. Cecal plots at 12 weeks show the fructose treatment for B6 (J), DBA (K), and FVB (L). P-values were generated by PERMANOVA after testing for homogeneity of variances for unequal group dispersion. P-values with an asterisk designate significantly different dispersions, and therefore the results may be influenced by this. Percent variance explained by axes is shown in parentheses. Various colors represent different mouse strains, time points, or treatment groups. The significant P values were presented in bold. A, J-L are from cecum, and B-I are fecal samples.

Figure 2. Cecal and fecal baseline microbial composition in B6, DBA, and FVB mice and correlation with adiposity gain. Taxa bar plots of baseline cecal (A) and

fecal (B) microbiota of three mouse strains at the phylum level. Baseline abundance profiles for specific fecal microbiota of three mouse strains at the genus level (C-H). Centered log-ratio (CLR) values were used for plotting the abundance of each microbiota. Box and whiskers plots from minimum to maximum showing abundance distribution of *Lactobacillus* (C), unknown genus of Clostridiales (D), unknown genus of Lachnospiraceae (E), unknown genus of S24-7 (F), *Akkermansia (*G), *Turicibacter* (H). The center line denotes the median value. One-way ANOVA followed by Sidak's post hoc test was conducted to calculate significant differences between three mouse strains. Labeled means without a common letter differ, $P < 0.05$. n = 7-8/group. (I-N) Correlation analysis plots between microbiota baseline proportion and adiposity gain at 12 week. r = Biweight midcorrelation (*bicor*) coefficient, P = Benjamini-Hochberg adjusted P-values. n = 7-8/mouse strain.

Figure 3. Correlation analysis of fructose-responsive microbiota with metabolic phenotypes in DBA mice. Plots showing correlation of Rikenellaceae proportion to body weight (A, D), adiposity (B, E), and glucose tolerance AUC (C, F) across time points with or without fructose treatment in DBA mice. Water (A-C) or fructose (D-F) groups were analyzed separately. r = Biweight midcorrelation (*bicor*) coefficient, P = Benjamini-Hochberg adjusted P-values. n = 7-8/group/time point.

Figure 4. Metabolic phenotypes post fecal transplant in B6 and DBA mice with or without fructose consumption. Schematic design of fecal microbiota transplant (FMT,

A). Body weight gains (B, C) and glucose tolerance (D, E) of recipient B6 and DBA

mice, respectively, with or without 8% fructose water. Data are presented as means ±

SEM. (B-E) The significant effects of main factors and the interactions by three-way

repeated-measures ANOVA are shown on the top of the graph with respective *P*-

values. (C) Asterisks indicate time points at which significant differences were found

between DBA(DBA) and DBA(B6) under fructose treatment based on two-way

repeated-measures ANOVA with Sidak's post hoc test; *$P < 0.05$, **$P < 0.01$. Fructose

effects within each FMT group across time points were assessed by two-way repeated-

measures ANOVA, and significant fructose effect is indicated with *P*-values with side

bar in (C) for DBA(DBA) water vs. fructose. B6(B6), B6 mice receiving B6 feces;

DBA(DBA), DBA mice receiving DBA feces; B6(DBA), B6 mice receiving DBA feces;

DBA(B6), DBA mice receiving B6 feces. *n* = 7-14/group.

**Figure 5. Metabolic phenotypes post *Akkermansia* colonization in DBA mice with

or without fructose consumption.** Schematic design of *Akkermansia* (AM)

colonization (A). Body weight gains (B) and glucose tolerance (C) of recipient DBA mice

with or without 8% fructose water. Data are presented as means ± SEM. The significant

effects of main factors and the interactions by three-way repeated-measures ANOVA

are shown on the top of the graph with respective *P*-values. Asterisks indicate time

points at which significant differences were found between DBA(PBS) and DBA(AM)

under fructose treatment based on two-way repeated-measures ANOVA with Sidak's

post hoc test; *$P < 0.05$, **$P < 0.01$. Fructose effects within each group [DBA(PBS) or

DBA(AM)] across time points were assessed by two-way repeated-measures ANOVA,

and significant fructose effects are indicated with *P*-values with a side bar between water and fructose groups in DBA(PBS) (B, C). DBA(PBS), DBA mice receiving PBS; DBA(AM), DBA mice receiving AM. *n* = 8-14/group.

Table 7. Differentially abundant microbiota between fructose and water groups in cecal and fecal samples of B6, DBA, and FVB mice.

Mouse strain	Taxonomic level	Source	Fructose-responsive microbiota	Fold change
DBA	Family	Cecum	Erysipelotrichaceae	0.055*
B6	Family	Feces	Rikenellaceae	0.620*
	Family	Feces	S24-7	1.189*
	Family	Feces	Dehalobacteriaceae	0.600*
	Family	Feces	Lachnospiraceae	0.590*
	Family	Feces	Mogibacteriaceae	0.333*
	Family	Feces	Ruminococcaceae	0.706*
	Family	Feces	Turicibacteraceae	0.348*
	Family	Feces	Pseudomonadaceae	3.333*

	Family	Feces	Verrucomicrobiaceae	7.250**
DBA	Family	Feces	Rikenellaceae	0.374*
	Family	Feces	Pseudomonadaceae	33.33*
DBA	Genus	Cecum	*Erysipelotrichaceae (Unknown genus)*	0.004*
	Genus	Cecum	*Erysipelotrichaceae Clostridium*	0.009**
	Genus	Cecum	*Lachnospiraceae Anaerostipes*	0.025**
FVB	Genus	Cecum	*Bifidobacteriaceae Bifidobacterium*	16.500*
B6	Genus	Feces	*Dehalobacteriaceae Dehalobacterium*	0.600*
	Genus	Feces	*Mogibacteriaceae (Unknown genus)*	0.333*
	Genus	Feces	*Verrucomicrobiaceae Akkermansia*	7.271**
DBA	Genus	Feces	*Rikenellaceae (Unknown genus)*	0.374*
	Genus	Feces	*Pseudomonadaceae (Unknown genus)*	60.000*
	Genus	Feces	*Pseudomonadaceae Pseudomonas*	28.000*

[1]Fold change is calculated as the ratio of the relative abundance of microbiota between fructose and water groups (fructose/water). *n*=8/group/mouse strain, *FDR < 0.05, **FDR < 0.01.

Table 2. Correlation between fructose-responsive microbiota and host fructose signature genes in three metabolic tissues in B6 and DBA mice.

Mouse str	Fructose-responsive microbiota		Host tis	No. corr elat ed	Correlation with host fructose-responsive genes

ai n		su e	Ge ne at FD R <0. 05	Top correlated genes	Over-represented pathways
B6 (fe ce s)	Rikenellaceae	Hy po	37	*Emg1, Rpl37a, Oat, Gna13,* ***Ctsz***	RNA metabolism, Protein localization in endoplasmic reticulum, Ribosome, Amino acid metabolism, Influenza infection
	S24-7	Hy po	11	***Numbl, Cxx1c, Gnb2, 1500009L16Rik , Slc25a17***	
	Dehalobacteriaceae	Hy po	7	***Atp2b2, Slc6a3, Nefh,*** *Nrarp, Hint2*	
	Dehalobacterium	Hy po	42	***Atp2b2, Slc6a3, Nefh,*** *Nrarp,* ***Atg3,***	Ribosome, Response to alcohol, Blood circulation, Dopamine biosynthesis, Locomotory behavior
	Lachnospiraceae	Hy po	2	*Maneal, Rbm39*	
	Mogibacteriaceae	Hy po	54	*Mogs, Snrpe****,*** *Nrarp,* ***Timp3****, Sgsm1*	Ribosome, Metabolism of proteins, RNA, organonitrogen compound, Protein targeting to membrane metabolism
	Mogibacteriaceae (Unknown genus)	Hy po	130	*Mogs, Psmb4, Derl1,* ***Timp3****, Sdcbp*	Ribosome, Metabolism of protein, RNA, Protein localization to endoplasmic reticulum, Signaling by robo receptors

377

Ruminococcaceae	Hypo	12	*Trappc2l, Gnb2, Uck1, Mid1ip1,* **Itm2a**	
Pseudomonadaceae	Hypo	2	**Cxx1c, Numbl**	
Verrucomicrobiaceae	Hypo	13	**Scarna2, AW209491,** *Gja1,* **Rps9,** *Th,*	Ribosome, Protein localization to endoplasmic reticulum, mRNA activation
Akkermansia	Hypo	44	*Gja1,* **Rps9,** *Th, Bmp7,* **Oxt**	Ribosome, Protein localization to endoplasmic reticulum, Selenoamino acid metabolism, Influenza infection, Signaling by robo receptors

DBA (cecum)	*Erysipelotrichaceae (Unknown genus)*	Liver	5	**Gsdmd, Wdr82, Tmem62, S100a10, Pgk1,**
	Erysipelotrichaceae Clostridum	Liver	5	**Epha2, Mad2l2, Cyp8b1, Ero1l, Pus10**
	Lachnospiraceae Anaerostipes	Liver	4	**Rogdi, Cyp8b1, Mad2l2, Baiap2**

DBA (feces)	Rikenellaceae	Adipose	447	*Ccr1, Sema3e, Msr 1, Abhd3, Fas,*	RNA metabolism, Response to lipid, cytokines, bacterial molecule, Lipid metabolism, Immune system, Endocytosis
	Rikenellaceae (Unknown genus)	Adip	432	*Ccr1, Apobec1, Sema3e, Creb1, Fas*	RNA metabolism, Response to lipid, cytokines, bacterial

378

	os e			molecule, Lipid metabolism, Immune system, Signaling pathway
Pseudomonadaceae	Ad ip os e	77	**Sfrp4, Msr1, Sema3e, Abhd3, Fas**	
Pseudomonadaceae (Unknown genus)	Ad ip os e	209	**Creb1, Fabp3, Msr1, Sema3e, Fas**	RNA processing, Response to cytokine, lipid, Defense response, lipid metabolism, Response to hormone
Pseudomonas	Ad ip os e	43	**Ppp1r13b, Jmjd1c, Msr1, Slc25a10, Fabp3**	

[1]Fructose-responsive genes in Hypothalamus (Hypo), Liver, and Adipose which were positively or negatively correlated with microbiota were indicated in bold or non-bold font, respectively.

[2]Top five correlated genes which belong to major gene sets analyzed using GSEA software.

[3]Sample size *n*=4-6/group/mouse strain.

[4]Full lists of correlated genes are in Supplemental Table 1 and enriched pathways are in Supplemental Table 2.

Chapter 8

Gut microbial taxa elevated by dietary sugar disrupt memory function

Emily E. Noble, Christine A. Olson, Elizabeth Davis, Linda Tsan, Yen-Wei Chen, Ruth Schade, Clarissa Liu, Andrea Suarez, Roshonda B. Jones, Claire de La Serre, Xia Yang, Elaine Y. Hsiao & Scott E. Kanoski

Abstract (250 words)

The mammalian gastrointestinal tract contains a diverse ecosystem of microbial species collectively making up the gut microbiome. Emerging evidence highlights a critical relationship between gut microbiota and neurocognitive development. Consumption of unhealthy yet palatable dietary factors associated with obesity and metabolic dysfunction (e.g., saturated fat, added sugar) produces microbiota dysbiosis and negatively impacts neurocognitive function, particularly when consumed during early life developmental periods. Here we explore whether excessive early life consumption of added sugars negatively impacts neurocognitive development via the gut microbiome. Using a rodent model of habitual sugar-sweetened beverage (SSB) consumption during the adolescent stage of development, we first show that excessive early life sugar intake impairs hippocampal-dependent memory function when tested during adulthood while preserving other neurocognitive domains. Gut microbiome genomic sequencing analyses reveal that early life SSB consumption alters the abundance of various bacterial populations, including elevations in operational taxonomic units within the genus *Parabacteroides* (*P. distasonis* and *P. johnsonii)* whose abundance negatively correlated with memory task performance. Additional results reveal that in vivo *Parabacteroides* enrichment of cultured *P. distasonis* and *P. johnsonii* bacterial species in adolescent rats severely impairs memory function during adulthood. Hippocampus gene pathway enrichment sequencing analyses identify alterations in neurotransmitter synaptic signaling, intracellular kinase signaling, metabolic function, neurodegenerative disease, and dopaminergic synaptic signaling-associated pathways as potential

mechanisms linking microbiome outcomes with memory impairment. Collectively these results identify microbiota dysbiosis as a mechanism through which early life unhealthy dietary patterns negatively impact neurocognitive outcomes.

Introduction

Accumulating evidence across multiple mammalian species substantiates the importance of the gut microbiome to neurocognitive development and consequent functioning [48, 49]. Early life developmental periods represent critical windows for the impact of commensal gut microbes on the brain, as evidenced by the reversal of behavioral and neurochemical abnormalities in gnotobiotic "germ free" rodents when inoculated with specific pathogen free microbiota during early life, but not during adulthood [50, 51] [52]. Dietary factors are a critical determinant of gut microbiota diversity and can alter abundances of bacterial populations, as evident from the microbial plasticity observed in response to pre- and probiotic treatment, as well as the "dysbiosis" resulting from consuming unhealthy, yet palatable foods that are associated with obesity and metabolic disorders (e.g., "Western diet"; foods high in saturated fatty acids and added sugar) [53]. In addition to producing dysbiosis, consumption of these dietary factors also yields long-lasting memory impairments, and these effects are more pronounced when consumed during early life developmental periods vs. during adulthood [54-56]. Whether dietary-induced changes in specific bacterial populations are functionally-related to altered early life neurocognitive outcomes, however, is poorly understood.

The hippocampus, which is well known for its role in spatial and episodic memory and more recently for regulating learned and social aspects of food intake control [57-62], is particularly vulnerable to the deleterious effects of Western dietary factors [63-65].

383

During the juvenile and adolescent stage of development, a time when the brain is rapidly developing, consumption of diets high in saturated fat and sugar [66-68] or sugar alone [69-72] impairs hippocampal function while in some cases preserving memory processes that do not rely on the hippocampus. While several putative underlying mechanisms have been investigated, the precise biological pathways linking dietary factors to neurocognitive dysfunction remain largely undetermined [56]. Here we set out to determine whether sugar-induced alterations in gut microbiota during early life are causally related to hippocampal-dependent memory impairments observed in during adulthood.

Early-life sugar consumption impairs hippocampal-dependent memory function without affecting other neurocognitive domains

Results from the Novel Object in Context (NOIC) task, which measures hippocampal-dependent episodic contextual memory function[73], reveal that, while there were no differences in total exploration time of the combined objects on days 1 or 3 of the task (Fig. 1A,B), animals fed early life sugar solutions had a reduced capacity to discriminate an object that was novel to a specific context, indicating impaired hippocampal function (Fig. 1C, D). Conversely, when tested in the novel object recognition task (NOR), which tests for object recognition memory independent of context and is primarily dependent on the perirhinal cortex [73-75], animals fed early life sugar solutions performed similarly to those in the control group (Fig. 2E).

384

Elevated anxiety and altered general activity levels may influence novelty exploration independent of memory effects and may therefore confound the interpretation of behavioral results. Thus, we next tested whether early life sugar consumption affects anxiety-like behavior using two different tasks designed to measure anxiety in the rat: the elevated zero maze and the open field task, that latter of which also assesses levels of general activity [76]. Early life sugar had no effect on time spent in the open area or in the number of open area entries in the zero maze (Fig. 1F, G). Similarly, early life sugar had no effect on distance travelled or time spent in the center zone in the open field task (Fig. 1H, I). Together these data suggest that habitual early life sugar consumption did not increase anxiety-like behavior or general activity levels in the rats.

Early life sugar consumption impairs glucose tolerance without affecting total caloric intake, body weight, or adiposity

Given that excessive sugar consumption is associated with weight gain and metabolic deficits [77], we tested whether access to a sugar solution during the adolescent phase of development would affect food intake, body weight gain, adiposity, and glucose tolerance in the rat. Early life sugar consumption had no effect on body weight or total kcal intake (Fig. 1J, K), which is in agreement with previous findings [69, 78, 79]. Animals steadily increased their intake of the 11% sugar solution throughout the study but compensated for the calories consumed in the sugar solutions by reducing their intake of dietary chow (Supplemental Fig. 1A, B). There were no differences in body fat percentage during adulthood (Fig. 1L) or in total grams of body fat or lean mass.

However, animals that were fed sugar solutions during early life showed impaired glucose metabolism in an intraperitoneal glucose tolerance test (IP GTT) (Fig. 1L, Supplemental Fig 1C-E).

Gut microbiota are impacted by early life sugar consumption

Principal component analyses of 16s rRNA sequencing data revealed a separation between the fecal microbiome of rats fed early life sugar and controls (Fig. 2A). Results from Lefse Analysis show the differentially abundant bacterial taxa in fecal samples that were elevated by sugar consumption are the family *Clostridiaceae* and the genus *02d06* within *Clostridiaceae*, the family *Mogibacteriaceae*, the family *Enterobacteriaceae*, the order *Enterobacteriales*, the class of *Gammaproteobacteria*, and the genus *Parabacteroides* within the family *Porphyromonadaceae* (Fig. 2B-D). In addition to being elevated in the animals fed early life sugar, abundance of the genus *Parabacteroides* also negatively correlated with performance scores in the NOIC memory task (r^2=0.53, *P*=0.0002; Fig. 2E). Within *Parabacteroides*, levels of three operational taxonomic units (OTUs) that were elevated by sugar significantly correlated negatively with performance in the NOIC task, two of which were identified as *P. johnsonii* and *P. distasoni* (Fig. 2F). Abundance of other bacterial populations that were affected by sugar consumption were not significantly related to memory task performance.

There was a similar separation between groups in bacteria analyzed from cecal samples (Supplemental Fig. 2A). Lefse results from cecal samples show elevated

populations in *Bacilli*, *Actinobacteria*, *Erysipelotrichi*, and *Gammaproteobacteria* in rats

fed early life sugar, and elevated *Clostridia* in the controls (Supplemental Fig. 2B).

Abundances at the different taxonomic levels in fecal and cecal samples are shown in

(Supplemental Fig. 3, 4). Regression analyses did not identify these altered cecal

bacterial populations as being functionally correlated to NOIC memory performance.

Early life Parabacteroides enrichment impairs memory function

To determine whether neurocognitive outcomes due to early life sugar consumption

could be attributable to elevated levels of *Parabacteroides* in the gut, we used a recently

established method [80] to experimentally enriched the gut microbiome of naïve juvenile

rats with two *Parabacteroides* OTUs that were increased by sugar consumption and

were negatively correlated with behavioral outcomes in rats fed early life sugar. *P.

johnsonii* and *P. distasoni* species were cultured individually in anaerobic conditions and

transferred to a group of young rats in a 1:1 ratio via oral gavage using the experimental

design described in Methods and outlined in Supplemental Fig. 5A, and from [80]. All

rats treated with antibiotics showed a reduction in food intake and body weight during

the initial stages of antibiotic treatment, however, there were no differences in body

weight between the two groups of antibiotic treated animals at the time of testing

(Supplemental Fig. 5B, C).

Results from the hippocampal-dependent NOIC memory task showed that while there

were no differences in total exploration time of the combined objects on days 1 or 3 of

the task, indicating similar exploratory behavior, animals that received the *Parabacteroides* transfer showed a significantly reduced discrimination index in the NOIC task (Fig 3A-D), indicating impaired performance in hippocampal-dependent memory function. When tested in the perirhinal cortex-dependent NOR task [73], animals that received *Parabacteroides* enrichment showed impaired object recognition memory as indicated by a reduced novel object exploration index, with no differences in total exploration time (Fig 3E). These findings show that unlike sugar-fed animals, *Parabacteroides* enrichment impaired perirhinal cortex-dependent memory processes in addition to hippocampal-dependent memory.

Results from the zero maze showed a non-significant trend toward reduced time spent in the open arms and a reduced number of open arm entries for the *Parabacteroides* enriched rats (Fig 3F, G), which is indicative of increased anxiety-like behavior. However, there were no differences in distance travelled or time spent in the center arena in the open field test, which is a measure of both anxiety-like behavior and general activity in rodents (Fig. 3H, I). Together these data suggest that *Parabacteroides* enrichment negatively impacted both hippocampal-dependent perirhinal cortex-dependent memory function without impacting general activity and with only modest effects on anxiety-like behavior.

Similar to a recent report [81], *Parabacteroides* enrichment in the present study impacted body weight and glucose metabolism. Animals who received enrichment of *P. johnsonii* and *P. distasoni* showed reduced body weight 40 days after the transfer, with

significantly lower lean mass and a trend toward reduced fat mass (Fig 3J-L). There were no differences in percent body fat between groups, nor were there significant group differences in glucose metabolism in the IP GTT (Supplemental Fig. 5D, E).

Early life sugar consumption and *Parabacteroides* enrichment alter hippocampal gene expression profiles

Supplemental Fig 6A shows the results of principal component analyses revealing separation based on RNA sequencing data from the dorsal hippocampus of rats fed early life sugar compared with controls. Gene pathway enrichment analyses from RNA sequencing data revealed multiple pathways significantly affected by early life sugar consumption, including four pathways involved in neurotransmitter synaptic signaling: dopaminergic, glutamatergic, cholinergic, and serotonergic signaling pathways. Additionally, several gene pathways that also varied by group were those involved in kinase-mediated intracellular signaling: cGMP-PKG, RAS, cAMP, and MAPK signaling pathways (Fig. 4A, Supplemental Table 1). Analyses of individual genes across the entire genome using a stringent false-discovery rate criterion further identified 21 genes that were differentially expressed in rats fed early life sugar compared with controls, with 11 genes elevated in rats fed sugar and 10 genes elevated in the controls (Fig 4B). Among the genes impacted, several genes that regulate cell survival, migration, differentiation, and DNA repair were elevated by early life sugar access, including *Faap100*, which encodes an FA core complex member of the DNA damage response pathway [82], and *Eepd1*, which transcribes an endonuclease involved in repairing

389

stalled DNA replication forks, stressed from DNA damage [83]. Other genes associated with ER stress and synaptogenesis were also significantly increased by sugar consumption, including *Klf9, Dgkh, Neurod2, Ppl*, and *Kirrel1* [84][85][86][87].

Several genes were reduced by dietary sugar, including *Tns2*, which encodes tensin 2, important for cell migration [88], *RelA*, which encodes a NF/kB complex protein that regulates activity dependent neuronal function and synaptic plasticity [89], and *Grm8*, the gene for the metabotropic glutamate receptor 8 (mGluR8). Notably, reduced expression of mGluR8 receptor may contribute to the impaired neurocognitive functioning in animals fed sugar, as mGluR8 knockout mice show impaired hippocampal-dependent learning and memory [90].

Supplemental Fig 7B shows the results of principal component dorsal hippocampus RNA sequencing analyses indicating separation between rats enriched with *Parabacteroides* compared with controls. Gene pathway analyses revealed that early life *Parabacteroides* transfer, similar to effects associated with sugar consumption, significantly altered the genetic signature of dopaminergic synaptic signaling pathways. *Parabacteroides* transfer also impacted gene pathways associated with metabolic signaling. Specifically, pathways regulating fatty acid oxidation, rRNA metabolic processes, mitochondrial inner membrane, and valine, leucine, and isoleucine degradation were significantly affected by *Parabacteroides* enrichment. Other pathways that were influenced were those involved in neurodegenerative disorders, including Alzheimer's disease and Parkinson's disease (Fig. 4D, Supplemental Table 2).

At the level of individual genes, dorsal hippocampal RNA sequencing data revealed that 15 genes were differentially expressed in rats enriched with

390

Parabacteroides compared with controls, with 13 genes elevated in the *Parabacteroides* group and 2 genes elevated in the controls (Fig 4C). Consistent with results from gene pathway analyses, several individual genes involved in metabolic processes were elevated by *Parabacteroides* enrichment, such as *Hmgcs2*, which is a mitochondrial regulator of ketogenesis and provides energy to the brain under metabolically taxing conditions or when glucose availability is low [91], and *Cox6b1*, a mitochondrial regulator of energy metabolism that improves hippocampal cellular viability following ischemia/reperfusion injury [92]. *Parabacteroides* enrichment was also associated with incased expression of *Slc27A1* and *Mfrp*, which are each critical for the transport of fatty acids into the brain across capillary endothelial cells [93].[94].

Discussion

Dietary factors are a key source of gut microbiome diversity [78, 80, 95-97] and emerging evidence indicates that diet-induced alterations in the gut microbiota may be linked with altered neurocognitive development [80, 97]. Our results identify species within the genus *Parabacteroides* that are both elevated by habitual early life consumption of dietary sugar and are negatively associated with hippocampal-dependent memory performance. Further, targeted microbiome enrichment of *Parabacteroides* perturbed both hippocampal- and perirhinal cortex-dependent memory performance. These findings are consistent with previous literature in showing that early life consumption of Western dietary factors impair neurocognitive outcomes [55, 56], and further suggest that altered gut bacteria due to excessive early life sugar consumption may functionally link dietary patterns with cognitive impairment.

Gene pathway enrichment analyses from dorsal hippocampus whole genome RNA sequencing identified multiple neurobiological pathways that may functionally connect gut dysbiosis with memory impairment. Early life sugar consumption was associated with alterations in several neurotransmitter synaptic signaling pathways (e.g., glutamatergic, cholinergic) and intracellular signaling targets (e.g., cAMP, MAPK). A different profile was observed in *Parabacteroides*-enriched animals, where gene pathways involved with metabolic function (e.g., fatty acid oxidation, amino acid degradation) and neurodegenerative disease (e.g., Alzheimer's disease) were altered relative to controls. However, gene clusters involved with dopaminergic synaptic signaling were significantly influenced by both early life sugar consumption and *Parabacteroides*-enrichment, thus identifying a common pathway through which both diet-induced and gut bacterial infusion-based elevations in *Parabacteroides* may influence neurocognitive development. Though differentially expressed genes were commonly affected in opposite directions in *Parabacteroides* enriched animals compared with early life sugar treated animals, it is possible that perturbations to the dopamine system play a role in the observed cognitive dysfunction. For example, while dopamine signaling in the hippocampus has not traditionally been investigated for mediating memory processes, several recent reports have identified a role for dopamine inputs from the locus coeruleus in regulating hippocampal-dependent memory and neuronal activity [98, 99]. Interestingly, endogenous dopamine signaling in the hippocampus has recently been linked with regulating food intake and food-associated

contextual learning [100], suggesting that dietary effects on gut microbiota may also impact feeding behavior and energy balance-relevant cognitive processes.

A recent report showed that a high fructose diet (35% kcal from fructose) promotes gut microbiome dysbiosis and neuroinflammation and cell death in the hippocampus, yet without impacting cognitive function [101]. One major discrepancy between this study and our own was the use of adult vs young animals. Indeed, our previous data show that rats are not susceptible to habitual sugar consumption-induced learning and memory impairments when the sugar is consumed during adulthood, in contrast to effects observed in the present study in which the sugar is consumed during early life development [69]. Whether habitual sugar consumption differentially affects the gut microbiome when consumed during adolescence vs. adulthood is suggested by these findings and by other reports identifying early life critical periods for microbiota influences on behavioral and neurochemical endpoints in germ free mice [50, 51] [52]. However, the age-specific profile of sugar-associated microbiome dysbiosis and neurocognitive impairments remains to be determined.

While our study reveals a strong negative correlation between levels of gut *Parabacteroides* abundance and performance in the hippocampal-dependent contextual episodic memory NOIC task, as well as impaired NOIC performance in rats given access to a sugar solution during adolescence, sugar intake did not produce impairments in the perirhinal cortex-dependent NOR memory task. That early life sugar consumption negatively impacts hippocampal-dependent spatial [69] and contextual-

based learning without influencing NOR performance is consistent with previous reports using a cafeteria diet high in both fat content and sugar [102]. On the other hand, enrichment of *P. johnsonii* and *P. distasoni* OTUs in the present study impaired memory performance in both tasks, suggesting a broader impact on neurocognitive functioning with this targeted bacterial enrichment approach.

Many of the genes that were differentially upregulated in the hippocampus by targeted *Parabacteroides* enrichment were involved in fat metabolism and transport. Thus, it is possible that the high levels of *Parabacteroides* conferred an adaptation in the brain, shifting fuel preference away from carbohydrate toward lipid-derived ketones. Consistent with this framework, *Parabacteroides* abundance was previously shown to be upregulated by a ketogenic diet in which carbohydrate consumption is drastically depleted and fat is used as a primary fuel source due. Furthermore, *Parabacteroides* enrichment (specifically, *P. distasoni*), similar to a ketogenic diet, was protective against seizures in mice [80]. It is possible that *P. distasoni* reduces glucose uptake from the gut, enhances glucose clearing from the blood, and/or alter nutrient utilization in general, an idea further supported by recent finding that *P. distasoni* is associated with reduced diet- and genetic-induced obesity and hyperglycemia in mice [81].

Collective results provide mechanistic insight into the neurobiological mechanisms that link early life unhealthy dietary patters and altered gut microbiome changes with neurocognitive impairments. Currently probiotics, live microorganisms intended to confer health benefits, are not regulated with the same rigor as

394

pharmaceuticals but instead are sold as dietary supplements. Our findings suggest that gut enrichment with certain species of *Parabacteroides*, while previously shown to be beneficial for epilepsy [80], is harmful for neurocognitive mnemonic development. These results highlight the importance of conducting rigorous basic science analyses on the relationship between diet, microorganisms, brain, and behavior prior to widespread recommendations of bacterial microbiome interventions for humans.

Author Contributions

E.E.N. and S.E.K. designed the experiments. E.E.N. performed the majority of the behavioral experiments and analyzed the data. E.D. helped with the behavioral experiments and performed the RNA sequencing preparation with Y.C. and X.Y. for analyses of the RNA sequencing data. C.O. and E.H. contributed to the design of the and implementation of the bacterial enrichment procedure. R.J., M.G., R. S. and C.D.L.S., performed the gut microbiome analyses. L.T., C.L., and A.S., helped with

behavioral experiments. The paper was written by E.E.N and S.E.K. with additional editorial input from the other authors.

Competing interests

The authors declare no competing interests

References

1.   Tsavkelova, E.A., et al., *Hormones and hormone-like substances of microorganisms: A review.* Applied Biochemistry and Microbiology, 2006. **42**(3): p. 229-235.
2.   Belay, T. and G. Sonnenfeld, *Differential effects of catecholamines on in vitro growth of pathogenic bacteria.* Life Sciences, 2002. **71**(4): p. 447-456.
3.   Lyte, M. and S. Ernst, *Catecholamine induced growth of gram negative bacteria.* Life Sciences, 1992. **50**(3): p. 203-212.
4.   Strakhovskaia, M.G., E.V. Ivanova, and G. Frainkin, *[Stimulatory effect of serotonin on the growth of the yeast Candida guilliermondii and the bacterium Streptococcus faecalis].* Mikrobiologiia, 1993. **62**(1): p. 46-9.
5.   Neal, C.P., et al., *Catecholamine inotropes as growth factors for Staphylococcus epidermidis and other coagulase-negative staphylococci.* FEMS Microbiol Lett, 2001. **194**(2): p. 163-9.
6.   Freestone, P.P., R.D. Haigh, and M. Lyte, *Specificity of catecholamine-induced growth in Escherichia coli O157:H7, Salmonella enterica and Yersinia enterocolitica.* FEMS Microbiol Lett, 2007. **269**(2): p. 221-8.
7.   Pande, G.S., et al., *The catecholamine stress hormones norepinephrine and dopamine increase the virulence of pathogenic Vibrio anguillarum and Vibrio campbellii.* FEMS Microbiol Ecol, 2014. **90**(3): p. 761-9.
8.   Kendall, M.M., D.A. Rasko, and V. Sperandio, *Global effects of the cell-to-cell signaling molecules autoinducer-2, autoinducer-3, and epinephrine in a luxS mutant of enterohemorrhagic Escherichia coli.* Infect Immun, 2007. **75**(10): p. 4875-84.
9.   Bansal, T., et al., *Differential effects of epinephrine, norepinephrine, and indole on Escherichia coli O157:H7 chemotaxis, colonization, and gene expression.* Infect Immun, 2007. **75**(9): p. 4597-607.
10.   Roshchina, V.V., *New Trends and Perspectives in the Evolution of Neurotransmitters in Microbial, Plant, and Animal Cells.* Adv Exp Med Biol, 2016. **874**: p. 25-77.
11.   Freestone, P.P., et al., *Stimulation of bacterial growth by heat-stable, norepinephrine-induced autoinducers.* FEMS Microbiol Lett, 1999. **172**(1): p. 53-60.

12.   Lyte, M., et al., *Norepinephrine-induced expression of the K99 pilus adhesin of enterotoxigenic Escherichia coli.* Biochem Biophys Res Commun, 1997. **232**(3): p. 682-6.

13.   Lyte, M., B.P. Arulanandam, and C.D. Frank, *Production of Shiga-like toxins by Escherichia coli O157:H7 can be influenced by the neuroendocrine hormone norepinephrine.* J Lab Clin Med, 1996. **128**(4): p. 392-8.

14.   Clarke, M.B., et al., *The QseC sensor kinase: A bacterial adrenergic receptor.* Proceedings of the National Academy of Sciences, 2006. **103**(27): p. 10420-10425.

15.   Sperandio, V., et al., *Bacteria-host communication: the language of hormones.* Proc Natl Acad Sci U S A, 2003. **100**(15): p. 8951-6.

16.   Hegde, M., T.K. Wood, and A. Jayaraman, *The neuroendocrine hormone norepinephrine increases Pseudomonas aeruginosa PA14 virulence through the las quorum-sensing pathway.* Applied Microbiology and Biotechnology, 2009. **84**(4): p. 763-776.

17.   Cogan, T.A., et al., *Norepinephrine increases the pathogenic potential of Campylobacter jejuni.* Gut, 2007. **56**(8): p. 1060-5.

18.   Rahman, H., R. Reissbrodt, and H. Tschape, *Effect of norepinephrine on growth of Salmonella and its enterotoxin production.* Indian J Exp Biol, 2000. **38**(3): p. 285-6.

19.   Stephenson, M. and E. Rowatt, *The production of acetylcholine by a strain of Lactobacillus plantarum.* J Gen Microbiol, 1947. **1**(3): p. 279-98.

20.   Kawashima, K., et al., *Ubiquitous expression of acetylcholine and its biological functions in life forms without nervous systems.* Life Sci, 2007. **80**(24-25): p. 2206-9.

21.   Horiuchi, Y., et al., *Evolutionary study on acetylcholine expression.* Life Sci, 2003. **72**(15): p. 1745-56.

22.   Sanchez, D.G., et al., *A Pseudomonas aeruginosa PAO1 acetylcholinesterase is encoded by the PA4921 gene and belongs to the SGNH hydrolase family.* Microbiol Res, 2012. **167**(6): p. 317-25.

23.   Schafer, D.F., J.M. Fowler, and E.A. Jones, *Colonic bacteria: a source of gamma-aminobutyric acid in blood.* Proc Soc Exp Biol Med, 1981. **167**(3): p. 301-3.

24.   Minuk, G.Y., *Gamma-aminobutyric acid (GABA) production by eight common bacterial pathogens.* Scand J Infect Dis, 1986. **18**(5): p. 465-7.

25.   Barrett, E., et al., *gamma-Aminobutyric acid production by culturable bacteria from the human intestine.* J Appl Microbiol, 2012. **113**(2): p. 411-7.

26.   Dagorn, A., et al., *Effect of GABA, a bacterial metabolite, on Pseudomonas fluorescens surface properties and cytotoxicity.* Int J Mol Sci, 2013. **14**(6): p. 12186-204.

27.   Franciosi, E., et al., *Biodiversity and γ-Aminobutyric Acid Production by Lactic Acid Bacteria Isolated from Traditional Alpine Raw Cow’s Milk Cheeses.* BioMed Research International, 2015. **2015**: p. 11.

28.   Higuchi, T., H. Hayashi, and K. Abe, *Exchange of glutamate and gamma-aminobutyrate in a Lactobacillus strain.* J Bacteriol, 1997. **179**(10): p. 3362-4.

29.   Wu, Q., Y.-S. Law, and N.P. Shah, *Dairy Streptococcus thermophilus improves cell viability of Lactobacillus brevis NPS-QW-145 and its γ-aminobutyric acid biosynthesis ability in milk.* Scientific Reports, 2015. **5**: p. 12885.

30.   Strandwitz, P., et al., *Gaba Modulating Bacteria of the Human Gut Microbiome.* 2016.

31.   Capitani, G., et al., *Crystal structure and functional analysis of Escherichia coli glutamate decarboxylase.* Embo j, 2003. **22**(16): p. 4027-37.

32.   Komatsuzaki, N., et al., *Characterization of Glutamate Decarboxylase from a High γ-Aminobutyric Acid (GABA)-Producer, Lactobacillus paracasei.* Bioscience, Biotechnology, and Biochemistry, 2008. **72**(2): p. 278-285.

33.   Li, H. and Y. Cao, *Lactic acid bacterial cell factories for gamma-aminobutyric acid.* Amino Acids, 2010. **39**(5): p. 1107-1116.

34.   Yang, S.Y., et al., *Production of gamma-aminobutyric acid by Streptococcus salivarius subsp. thermophilus Y2 under submerged fermentation.* Amino Acids, 2008. **34**(3): p. 473-8.

35.   Yunes, R.A., et al., *Draft Genome Sequences of Lactobacillus plantarum Strain 90sk and Lactobacillus brevis Strain 15f: Focusing on Neurotransmitter Genes.* Genome Announcements, 2015. **3**(2).

36.   Dyachkova, M.S., et al., *Draft Genome Sequences of Bifidobacterium angulatum GT102 and Bifidobacterium adolescentis 150: Focusing on the Genes Potentially Involved in the Gut-Brain Axis.* Genome Announc, 2015. **3**(4).

37.   Guthrie, G.D. and C.S. Nicholson-Guthrie, *gamma-Aminobutyric acid uptake by a bacterial system with neurotransmitter binding characteristics.* Proceedings of the National Academy of Sciences, 1989. **86**(19): p. 7378-7381.

38.   Tsavkelova, E.A., et al., *Detection of neurotransmitter amines in microorganisms with the use of high-performance liquid chromatography.* Dokl Biochem, 2000. **372**(1-6): p. 115-7.

39.   Oleskin, A.V., G.I. El'-Registan, and B.A. Shenderov, *Role of neuromediators in the functioning of the human microbiota: "Business talks" among microorganisms and the microbiota-host dialogue.* Microbiology, 2016. **85**(1): p. 1-22.

40.   Özoğul, F., *Production of biogenic amines by Morganella morganii, Klebsiella pneumoniae and Hafnia alvei using a rapid HPLC method.* European Food Research and Technology, 2004. **219**(5): p. 465-469.

41.   Ouml, et al., *The Function of Lactic Acid Bacteria on Biogenic Amines Production by Food-Borne Pathogens in Arginine Decarboxylase Broth.* Food Science and Technology Research, 2012. **18**(6): p. 795-804.

42.   Anuchin, A.M., et al., *Effects of monoamine neuromediators on the growth-related variables of Escherichia coli K-12.* Microbiology, 2008. **77**(6): p. 674-680.

43.   Oleskin, A.V., et al., *[Effect of serotonin (5-hydroxytryptamine) on the growth and differentiation of microorganisms].* Mikrobiologiia, 1998. **67**(3): p. 305-12.

44.   Lyte, M. and P.P. Freestone, *Microbial endocrinology: interkingdom signaling in infectious disease and health.* 2010: Springer.

45.   Knecht, L.D., et al., *Serotonin Activates Bacterial Quorum Sensing and Enhances the Virulence of Pseudomonas aeruginosa in the Host.* EBioMedicine, 2016. **9**: p. 161-9.

46.   Williams, Brianna B., et al., *Discovery and Characterization of Gut Microbiota Decarboxylases that Can Produce the Neurotransmitter Tryptamine.* Cell Host & Microbe, 2014. **16**(4): p. 495-503.

47.   Tache, Y., et al., *Brain and Gut CRF Signaling: Biological Actions and Role in the Gastrointestinal Tract.* Curr Mol Pharmacol, 2018. **11**(1): p. 51-71.

48.   Vuong, H.E., et al., *The Microbiome and Host Behavior.* Annu Rev Neurosci, 2017. **40**: p. 21-49.

49. Noble, E.E., T.M. Hsu, and S.E. Kanoski, *Gut to Brain Dysbiosis: Mechanisms Linking Western Diet Consumption, the Microbiome, and Cognitive Impairment.* Front Behav Neurosci, 2017. **11**: p. 9.

50. Diaz Heijtz, R., et al., *Normal gut microbiota modulates brain development and behavior.* Proc Natl Acad Sci U S A, 2011. **108**(7): p. 3047-52.

51. Neufeld, K.A., et al., *Effects of intestinal microbiota on anxiety-like behavior.* Commun Integr Biol, 2011. **4**(4): p. 492-4.

52. Sudo, N., et al., *Postnatal microbial colonization programs the hypothalamic-pituitary-adrenal system for stress response in mice.* J Physiol, 2004. **558**(Pt 1): p. 263-75.

53. Cryan, J.F., et al., *The Microbiota-Gut-Brain Axis.* Physiol Rev, 2019. **99**(4): p. 1877-2013.

54. Kanoski, S.E. and T.L. Davidson, *Western diet consumption and cognitive impairment: links to hippocampal dysfunction and obesity.* Physiology & behavior, 2011. **103**(1): p. 59-68.

55. Noble, E.E., et al., *Early-life sugar consumption has long-term negative effects on memory function in male rats.* Nutr Neurosci, 2019: p. 1-11.

56. Noble, E.E. and S.E. Kanoski, *Early life exposure to obesogenic diets and learning and memory dysfunction.* Curr Opin Behav Sci, 2016. **9**: p. 7-14.

57. Hsu, T.M., et al., *Hippocampus ghrelin receptor signaling promotes socially-mediated learned food preference.* Neuropharmacology, 2018. **131**: p. 487-496.

58. Hsu, T.M., et al., *A hippocampus to prefrontal cortex neural pathway inhibits food motivation through glucagon-like peptide-1 signaling.* Mol Psychiatry, 2018. **23**(7): p. 1555-1565.

59. Hsu, T.M., et al., *Hippocampus ghrelin signaling mediates appetite through lateral hypothalamic orexin pathways.* Elife, 2015. **4**.

60. Kanoski, S.E., et al., *Ghrelin Signaling in the Ventral Hippocampus Stimulates Learned and Motivational Aspects of Feeding via PI3K-Akt Signaling.* Biol Psychiatry, 2013. **73**(9): p. 915-23.

61. Davidson, T.L., et al., *Contributions of the hippocampus and medial prefrontal cortex to energy and body weight regulation.* Hippocampus, 2009. **19**(3): p. 235-52.

62. Kanoski, S.E. and H.J. Grill, *Hippocampus Contributions to Food Intake Control: Mnemonic, Neuroanatomical, and Endocrine Mechanisms.* Biol Psychiatry, 2017. **81**(9): p. 748-756.

63. Kanoski, S.E. and T.L. Davidson, *Western diet consumption and cognitive impairment: links to hippocampal dysfunction and obesity.* Physiol Behav, 2011. **103**(1): p. 59-68.

64. Davidson, T.L., C.H. Sample, and S.E. Swithers, *An application of Pavlovian principles to the problems of obesity and cognitive decline.* Neurobiol Learn Mem, 2014. **108**: p. 172-84.

65. Baym, C.L., et al., *Dietary lipids are differentially associated with hippocampal-dependent relational memory in prepubescent children.* Am J Clin Nutr, 2014. **99**(5): p. 1026-32.

66. Valladolid-Acebes, I., et al., *Spatial memory impairment and changes in hippocampal morphology are triggered by high-fat diets in adolescent mice. Is there a role of leptin?* Neurobiol Learn Mem, 2013. **106**: p. 18-25.

67.   Boitard, C., et al., *Impairment of hippocampal-dependent memory induced by juvenile high-fat diet intake is associated with enhanced hippocampal inflammation in rats.* Brain Behav Immun, 2014. **40**: p. 9-17.

68.   Boitard, C., et al., *Juvenile, but not adult exposure to high-fat diet impairs relational memory and hippocampal neurogenesis in mice.* Hippocampus, 2012. **22**(11): p. 2095-100.

69.   Hsu, T.M., et al., *Effects of sucrose and high fructose corn syrup consumption on spatial memory function and hippocampal neuroinflammation in adolescent rats.* Hippocampus, 2015. **25**(2): p. 227-39.

70.   Kendig, M.D., et al., *Chronic restricted access to 10% sucrose solution in adolescent and young adult rats impairs spatial memory and alters sensitivity to outcome devaluation.* Physiol Behav, 2013. **120**: p. 164-72.

71.   Reichelt, A.C., et al., *Impact of adolescent sucrose access on cognitive control, recognition memory, and parvalbumin immunoreactivity.* Learn Mem, 2015. **22**(4): p. 215-24.

72.   Noble, E.E., et al., *Early-life sugar consumption has long-term negative effects on memory function in male rats.* Nutr Neurosci, 2019. **22**(4): p. 273-283.

73.   Balderas, I., et al., *The consolidation of object and context recognition memory involve different regions of the temporal lobe.* Learn Mem, 2008. **15**(9): p. 618-24.

74.   Aggleton, J.P. and M.W. Brown, *Contrasting hippocampal and perirhinal cortex function using immediate early gene imaging.* Q J Exp Psychol B, 2005. **58**(3-4): p. 218-33.

75.   Albasser, M.M., et al., *Magnitude of the object recognition deficit associated with perirhinal cortex damage in rats: Effects of varying the lesion extent and the duration of the sample period.* Behav Neurosci, 2009. **123**(1): p. 115-24.

76.   Sestakova, N., et al., *Determination of motor activity and anxiety-related behaviour in rodents: methodological aspects and role of nitric oxide.* Interdiscip Toxicol, 2013. **6**(3): p. 126-35.

77.   Goran, M.I., et al., *The obesogenic effect of high fructose exposure during early development.* Nat Rev Endocrinol, 2013. **9**(8): p. 494-500.

78.   Noble, E.E., et al., *Early-Life Sugar Consumption Affects the Rat Microbiome Independently of Obesity.* J Nutr, 2017. **147**(1): p. 20-28.

79.   Noble, E.E., et al., *Early-life sugar consumption has long-term negative effects on memory function in male rats.* Nutr Neurosci, 2017: p. 1-11.

80.   Olson, C.A., et al., *The Gut Microbiota Mediates the Anti-Seizure Effects of the Ketogenic Diet.* Cell, 2018. **173**(7): p. 1728-1741 e13.

81.   Wang, K., et al., *Parabacteroides distasonis Alleviates Obesity and Metabolic Dysfunctions via Production of Succinate and Secondary Bile Acids.* Cell Rep, 2019. **26**(1): p. 222-235 e5.

82.   Ling, C., et al., *FAAP100 is essential for activation of the Fanconi anemia-associated DNA damage response pathway.* EMBO J, 2007. **26**(8): p. 2104-14.

83.   Kim, H.S., et al., *Endonuclease EEPD1 Is a Gatekeeper for Repair of Stressed Replication Forks.* J Biol Chem, 2017. **292**(7): p. 2795-2804.

84.   Zucker, S.N., et al., *Nrf2 amplifies oxidative stress via induction of Klf9.* Mol Cell, 2014. **53**(6): p. 916-928.

85.   Yasuda, S., et al., *Diacylglycerol kinase eta augments C-Raf activity and B-Raf/C-Raf heterodimerization.* J Biol Chem, 2009. **284**(43): p. 29559-70.

86.   Murdoch, H., et al., *Periplakin interferes with G protein activation by the melanin-concentrating hormone receptor-1 by binding to the proximal segment of the receptor C-terminal tail.* J Biol Chem, 2005. **280**(9): p. 8208-20.

87.   Gerke, P., et al., *Neuronal expression and interaction with the synaptic protein CASK suggest a role for Neph1 and Neph2 in synaptogenesis.* J Comp Neurol, 2006. **498**(4): p. 466-75.

88.   Chen, H., et al., *Tensin1 and a previously undocumented family member, tensin2, positively regulate cell migration.* Proc Natl Acad Sci U S A, 2002. **99**(2): p. 733-8.

89.   O'Mahony, A., et al., *NF-kappaB/Rel regulates inhibitory and excitatory neuronal function and synaptic plasticity.* Mol Cell Biol, 2006. **26**(19): p. 7283-98.

90.   Gerlai, R., et al., *Performance deficits of mGluR8 knockout mice in learning tasks: the effects of null mutation and the background genotype.* Neuropharmacology, 2002. **43**(2): p. 235-49.

91.   Shao, X., et al., *HMG-CoA synthase 2 drives brain metabolic reprogramming in cocaine exposure.* Neuropharmacology, 2019. **148**: p. 377-393.

92.   Yang, S., et al., *Overexpression of COX6B1 protects against I/Rinduced neuronal injury in rat hippocampal neurons.* Mol Med Rep, 2019. **19**(6): p. 4852-4862.

93.   Ochiai, Y., et al., *The blood-brain barrier fatty acid transport protein 1 (FATP1/SLC27A1) supplies docosahexaenoic acid to the brain, and insulin facilitates transport.* J Neurochem, 2017. **141**(3): p. 400-412.

94.   Kautzmann, M.I., et al., *Membrane-type frizzled-related protein regulates lipidome and transcription for photoreceptor function.* FASEB J, 2020. **34**(1): p. 912-929.

95.   David, L.A., et al., *Diet rapidly and reproducibly alters the human gut microbiome.* Nature, 2014. **505**(7484): p. 559-63.

96.   de La Serre, C.B., et al., *Propensity to high-fat diet-induced obesity in rats is associated with changes in the gut microbiota and gut inflammation.* Am J Physiol Gastrointest Liver Physiol, 2010. **299**(2): p. G440-8.

97.   Bruce-Keller, A.J., et al., *Obese-type gut microbiota induce neurobehavioral changes in the absence of obesity.* Biol Psychiatry, 2015. **77**(7): p. 607-15.

98.   Takeuchi, T., et al., *Locus coeruleus and dopaminergic consolidation of everyday memory.* Nature, 2016. **537**(7620): p. 357-362.

99.   Kempadoo, K.A., et al., *Dopamine release from the locus coeruleus to the dorsal hippocampus promotes spatial learning and memory.* Proc Natl Acad Sci U S A, 2016. **113**(51): p. 14835-14840.

100.   Azevedo, E.P., et al., *A Role of Drd2 Hippocampal Neurons in Context-Dependent Food Intake.* Neuron, 2019. **102**(4): p. 873-886 e5.

101.   Li, J.M., et al., *Dietary fructose-induced gut dysbiosis promotes mouse hippocampal neuroinflammation: a benefit of short-chain fatty acids.* Microbiome, 2019. **7**(1): p. 98.

102.   Kendig, M.D., R.F. Westbrook, and M.J. Morris, *Pattern of access to cafeteria-style diet determines fat mass and degree of spatial memory impairments in rats.* Sci Rep, 2019. **9**(1): p. 13516.

103.   Whitehead, J.C., et al., *A clinical frailty index in aging mice: comparisons with frailty index data in humans.* J Gerontol A Biol Sci Med Sci, 2014. **69**(6): p. 621-32.

104.   Schultz, M.B., et al., *Age and life expectancy clocks based on machine learning analysis of mouse frailty.* Nat Commun, 2020. **11**(1): p. 4618.
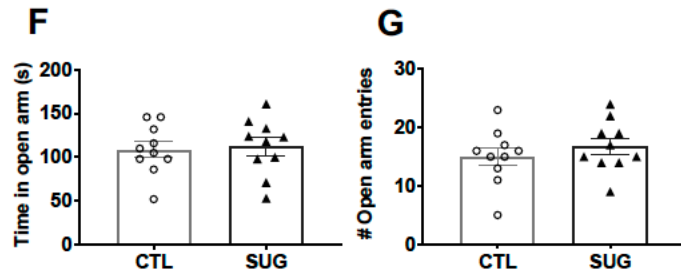
Chapter Figures

Novel Object in Context

A — Day 1: total time (s), CTL vs SUG

B — Day 3: total time (s), CTL vs SUG

C — Discrimination index (%), CTL vs SUG *

D — NOIC baseline shift, CTL vs SUG *

Novel Object Recognition

E — Exploration index, CTL vs SUG

Open Field

H — Distance (m), CTL vs SUG

I — Center time (s), CTL vs SUG

Zero Maze

F — Time in open arm (s), CTL vs SUG

G — # Open arm entries, CTL vs SUG

Energy Balance

J — Body weight (g) vs PN Day, CTL and SUG

K — Total intake (kcal) vs PN Day, CTL and SUG

L — % Body fat, CTL vs SUG
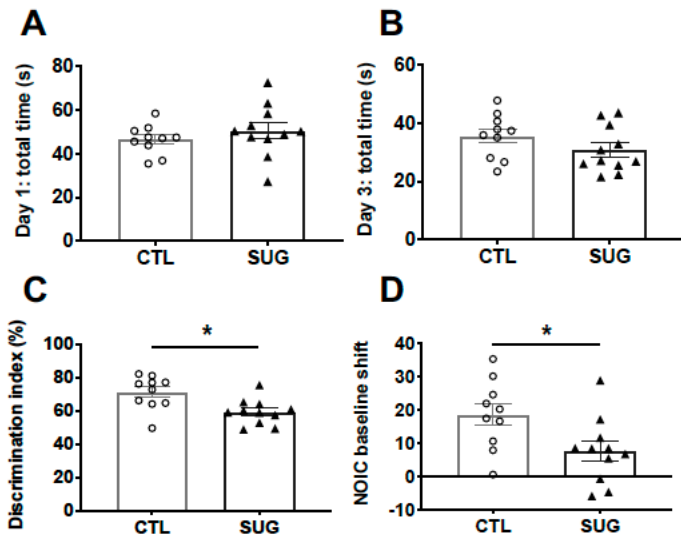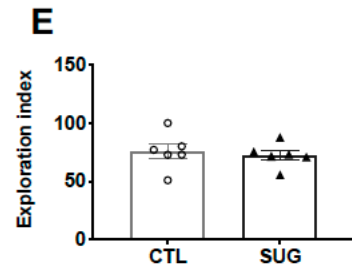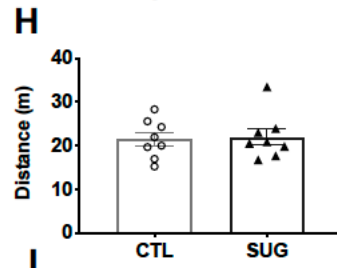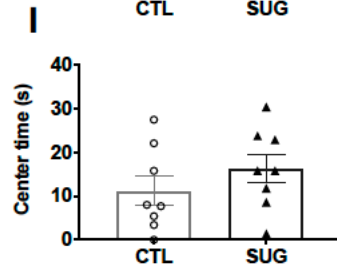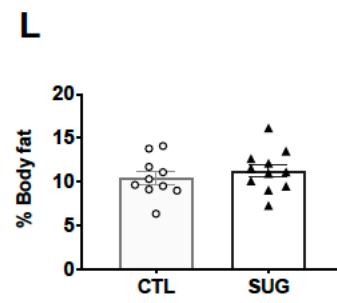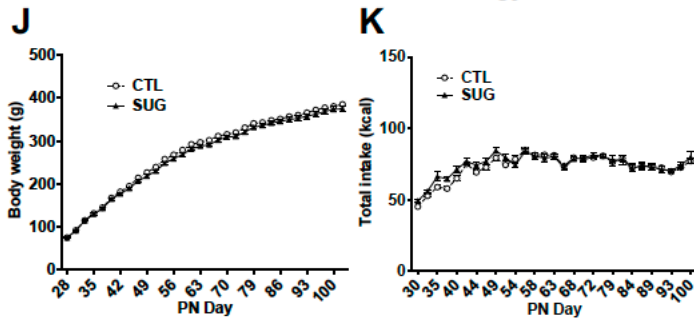
Figure 36: Early-life sugar consumption negatively impacts hippocampal-dependent memory function. (A,B) Early life sugar consumption had no effect on total exploration time in the Novel Object in Context (NOIC) task. (C,D) discrimination index and discrimination shift from baseline were significantly reduced by early life sugar consumption, indicating impaired hippocampal function ($P<.05$, n=10,11; two-tailed, type 2 Student's T-test). (E) There were no differences in exploration index in the Novel Object Recognition (NOR task) (n=6; two-tailed, type 2 Student's T-test). (F, G) There were no differences in time spent in the open arm or the number of entries into the open arm in the Zero Maze task for anxiety-like behavior (n=10,11; two-tailed, type 2 Student's T-test). (H, I) There were no differences in distance travelled or time spent in the center arena in the Open Field task (n=10,11; two-tailed, type 2 Student's T-test). (J-K) Body weights and did not differ between the groups and there was no effect of treatment on total kcal intake while animals had access to early life sugar (n=10,11; two-way repeated measures ANOVA). (L) There were no differences in body composition between rats fed early life sugar and controls (n=10,11; two-tailed, type 2 Student's T-test). CTL=control, SUG= sugar, PN= post-natal day; data shown as mean $\pm$ SEM.
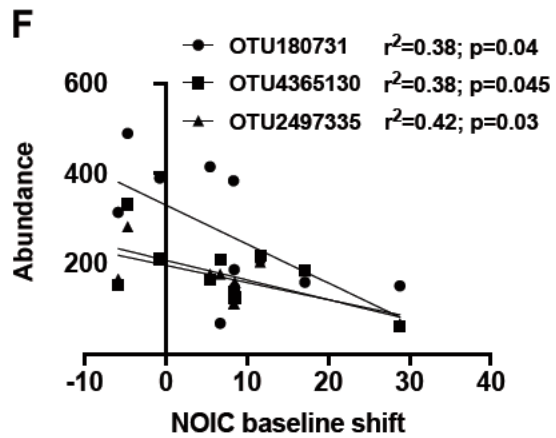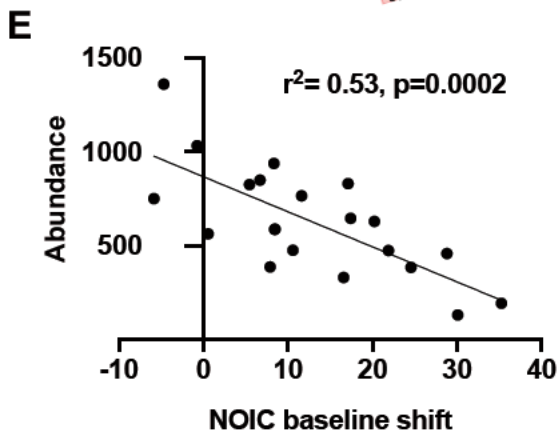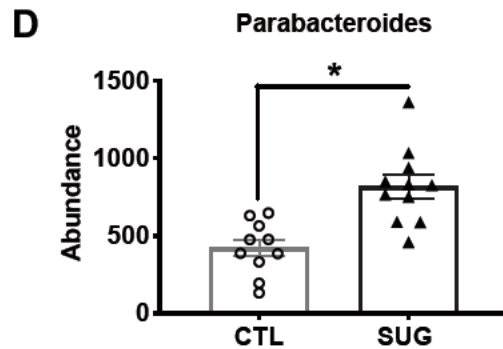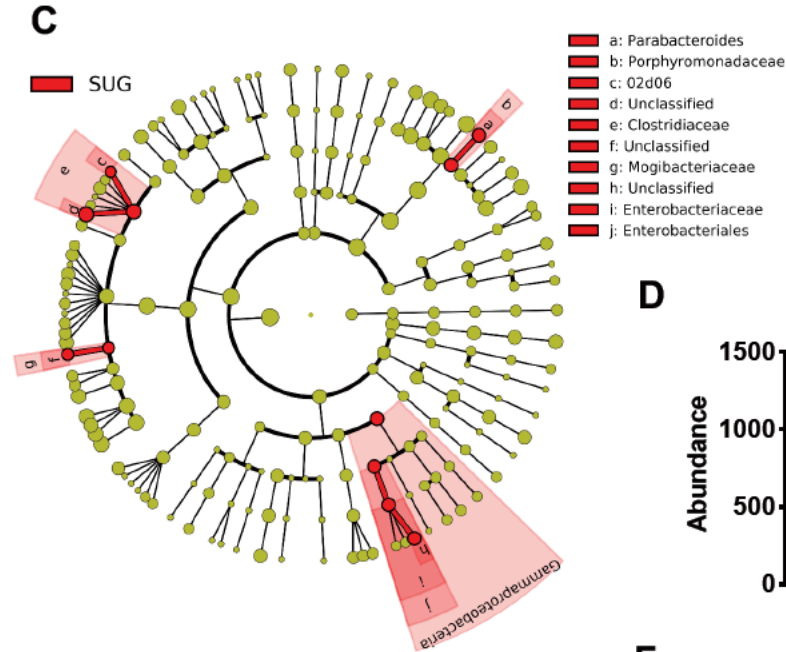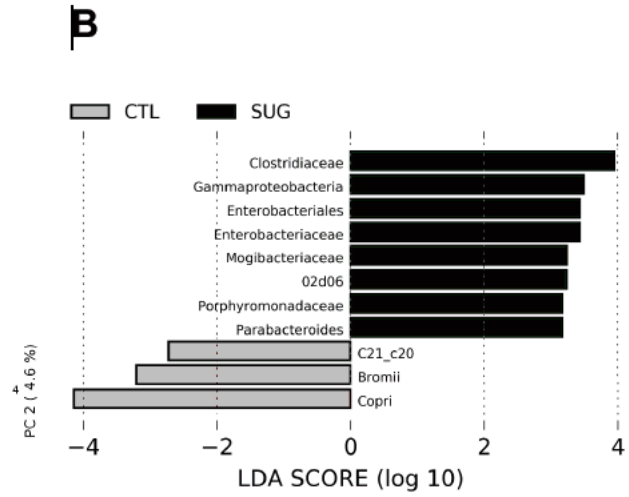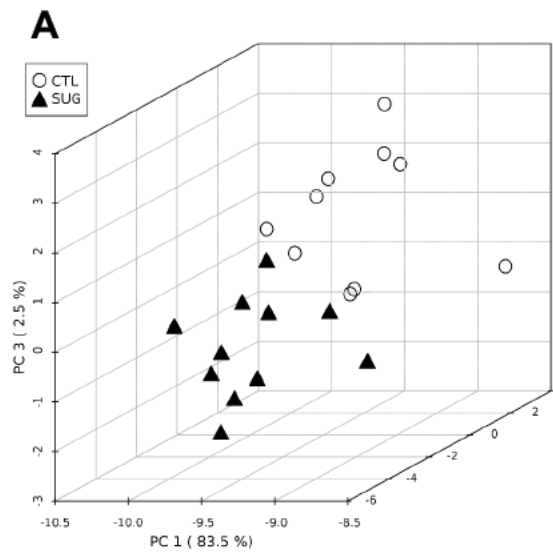
Figure 37: Effect of adolescent sugar consumption on the gut microbiome in rats

(A) Principal component analysis showing separation between fecal microbiota of rats fed early life sugar or controls (n=11, 10; dark triangles= sugar, open circles= control). (B, above) Results from LefsE analysis showing Linear Discriminate Analysis (LDA) scores for microbiome analysis of fecal samples of rats fed early life sugar or controls. (B, below) A cladogram representing the results from the LefsE analysis with class as the outer most taxonomic level and species at the inner most level. Taxa in red are elevated in the sugar group. (C) Sequence counts of fecal *Parabacteroides* w significantly elevated in rats fed early life sugar (P<.05; n=11, 10, two-tailed, type 2 Student's T-test). (D) Linear regression of fecal *Parabacteroides* counts against shift from baseline performance scores in the novel object in context task (NOIC) across all groups tested (n=21). (E) linear regression of the most abundant fecal *Parabacteroides* OTUs against shift from baseline performance scores in NOIC in animals fed sugar solutions during early life (n=11). *P<0.05; data shown as mean $\pm$ SEM.
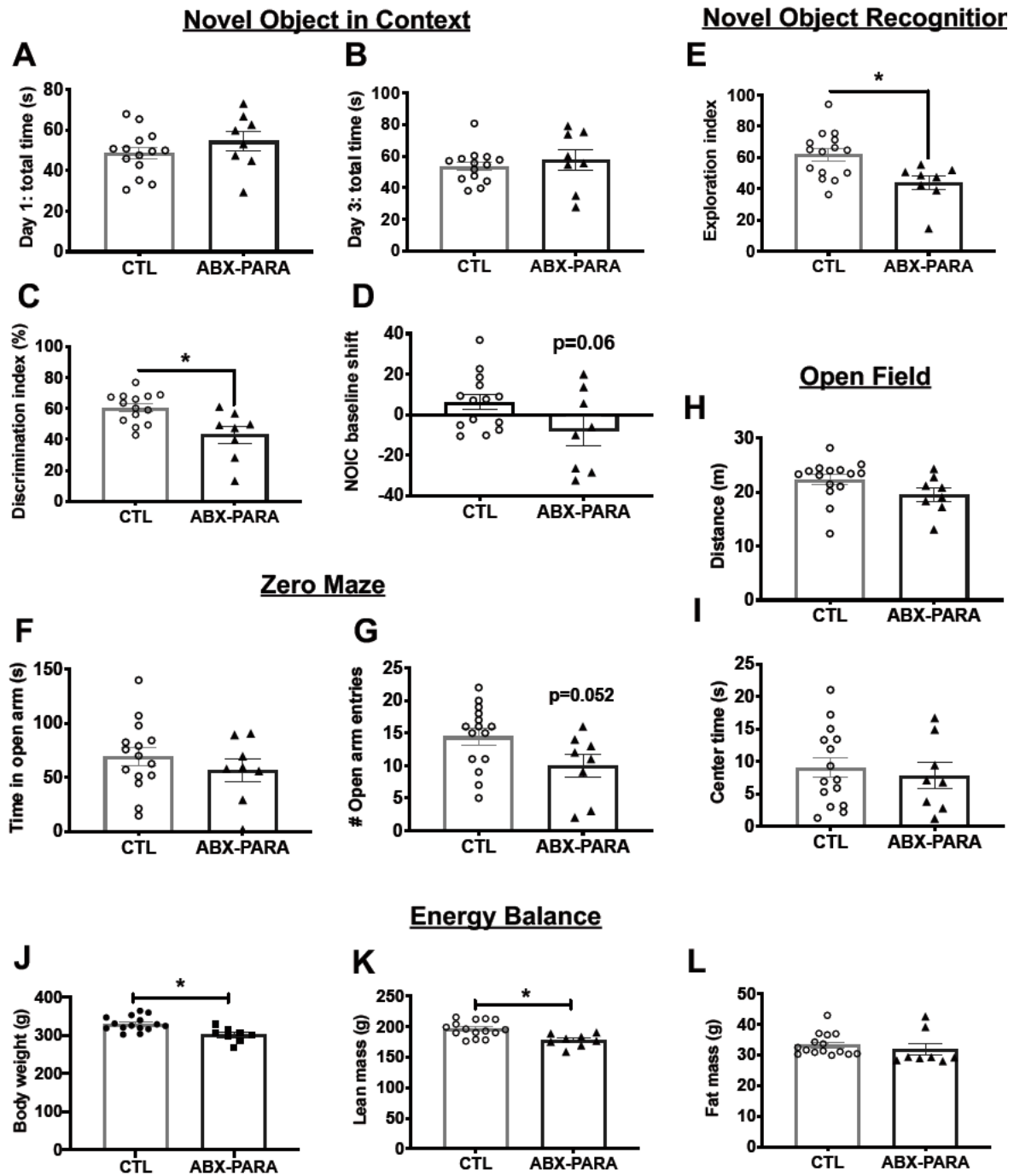
Figure 38: Early-life enrichment with Parabacteroides negatively impacts neurocognitive function (A, B) Early-life enrichment with a 1:1 ratio of P. johnsonii and P. distasoni had no effect on total exploration time in the Novel Object in Context

(NOIC) task. (C, D) Discrimination index was significantly reduced and discrimination shift from baseline tended to be reduced by enrichment with P. johnsonii and P. distasoni, indicating impaired hippocampal function (P<.05, n=14,8; two-tailed, type 2 Student's T-test). (E) There was a significant reduction in the exploration index in the Novel Object Recognition (NOR task), indicating impaired perirhinal cortex function (P<.05, n=14, 8; two-tailed, type 2 Student's T-test). (F, G) There were no differences in time spent in the open arm but there was a trend toward a reduced number of entries into the open arm by animals with P. johnsonii and P. distasoni enrichment in the Zero Maze task for anxiety-like behavior (P=.052, n=14, 8; two-tailed, type 2 Student's T-test). (H, I) There were no differences in distance travelled or time spent in the center arena in the Open Field task (n=14, 8; two-tailed, type 2 Student's T-test). (J-L) Body weights and lean mass were significantly reduced in animals enriched with P. johnsonii and P. distasoni, but body fat did not differ between the groups (P<.05, n=14, 8; two-tailed, type 2 Student's T-test). CTL=control, ABX-PARA= P. johnsonii and P. distasoni enriched, PN= post-natal day; data shown as mean ± SEM.
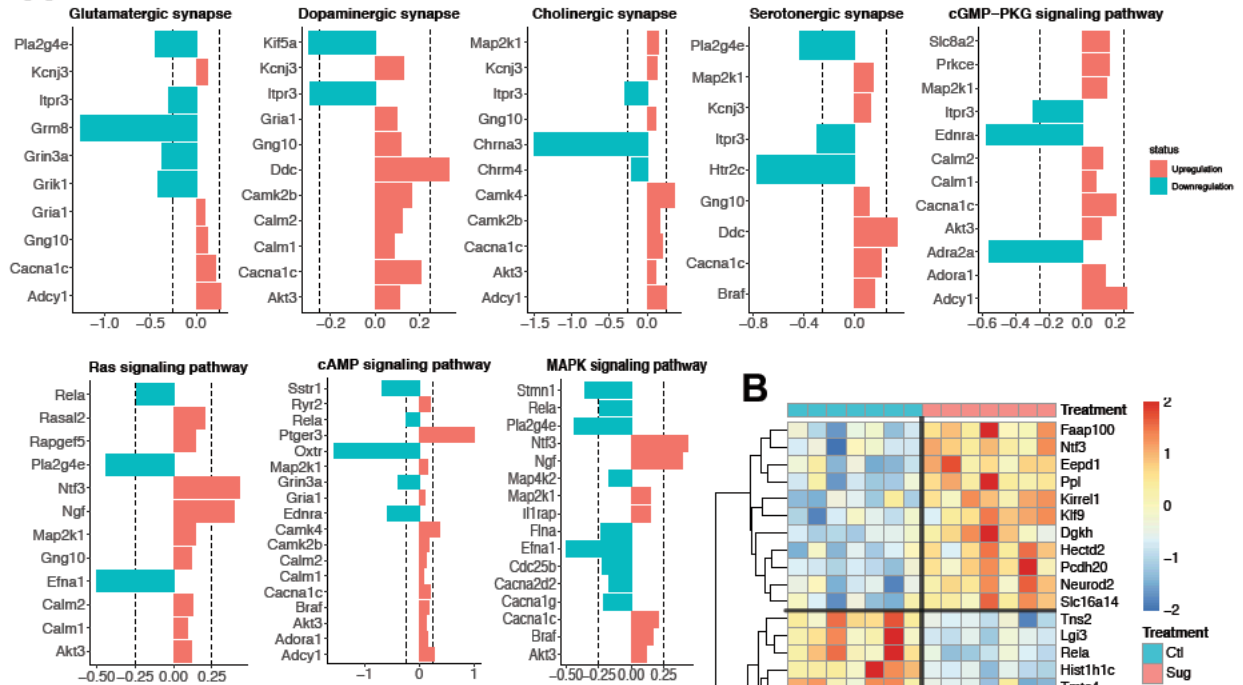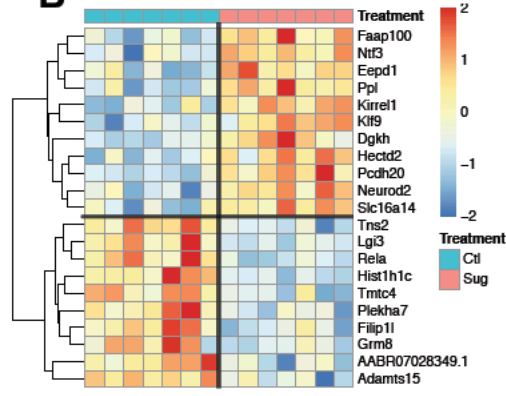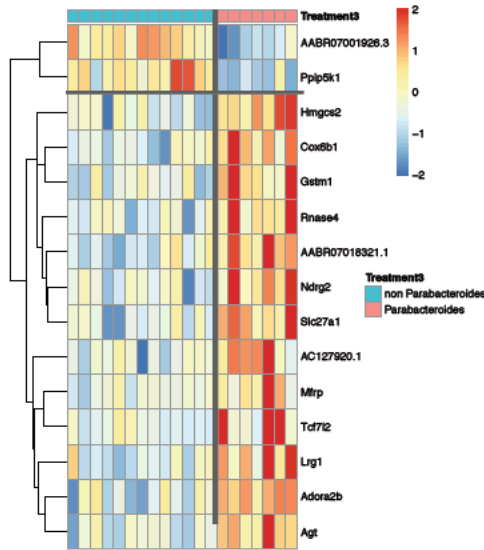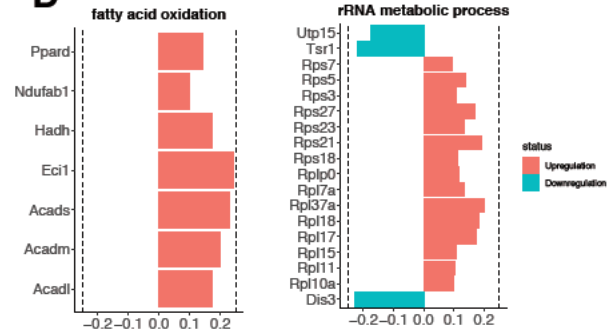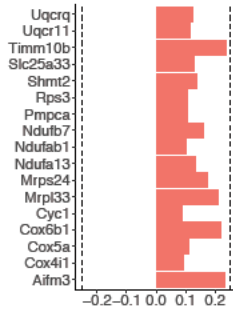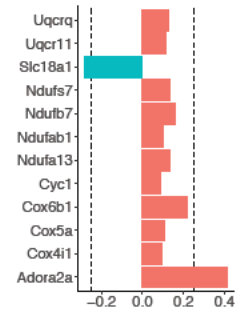
409
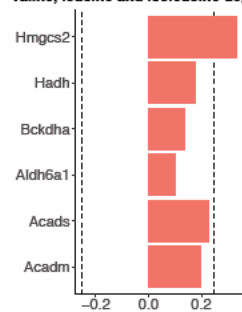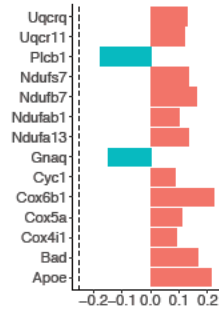
Figure 39: Effect of early life sugar or targeted Parabacteroides enrichment on hippocampal gene expression (A) Pathway analyses for differentially expressed genes (DEGs) at a p-value < 0.01 in hippocampal tissue punches from rats fed early life sugar compared with controls. Upregulation by sugar is shown in pink and downregulation by sugar in blue. (B) A heatmap depicting DEGs that survived the Benjamini-Hochberg corrected FDR of P< 0.05 in rats fed early life sugar compared with controls. Warmer colors (red) signify an increase in gene expression and cool colors (blue) a reduction in gene expression by treatment (CTL=control, SUG= early life sugar; n=7/group). (C) A heatmap depicting DEGs that survived the Benjamini-Hochberg corrected FDR of P< 0.05 in rats with early life Parabacteroides enrichment compared with controls. Warmer colors (red) signify an increase in gene expression and cool colors (blue) a reduction in gene expression by treatment (n=7, 14). (D) Pathway analyses for differentially expressed genes (DEGs) at a P-value < 0.01 in rats enriched with Parabacteroides compared with controls. Upregulation by Parabacteroides transfer is shown in pink and downregulation in blue.
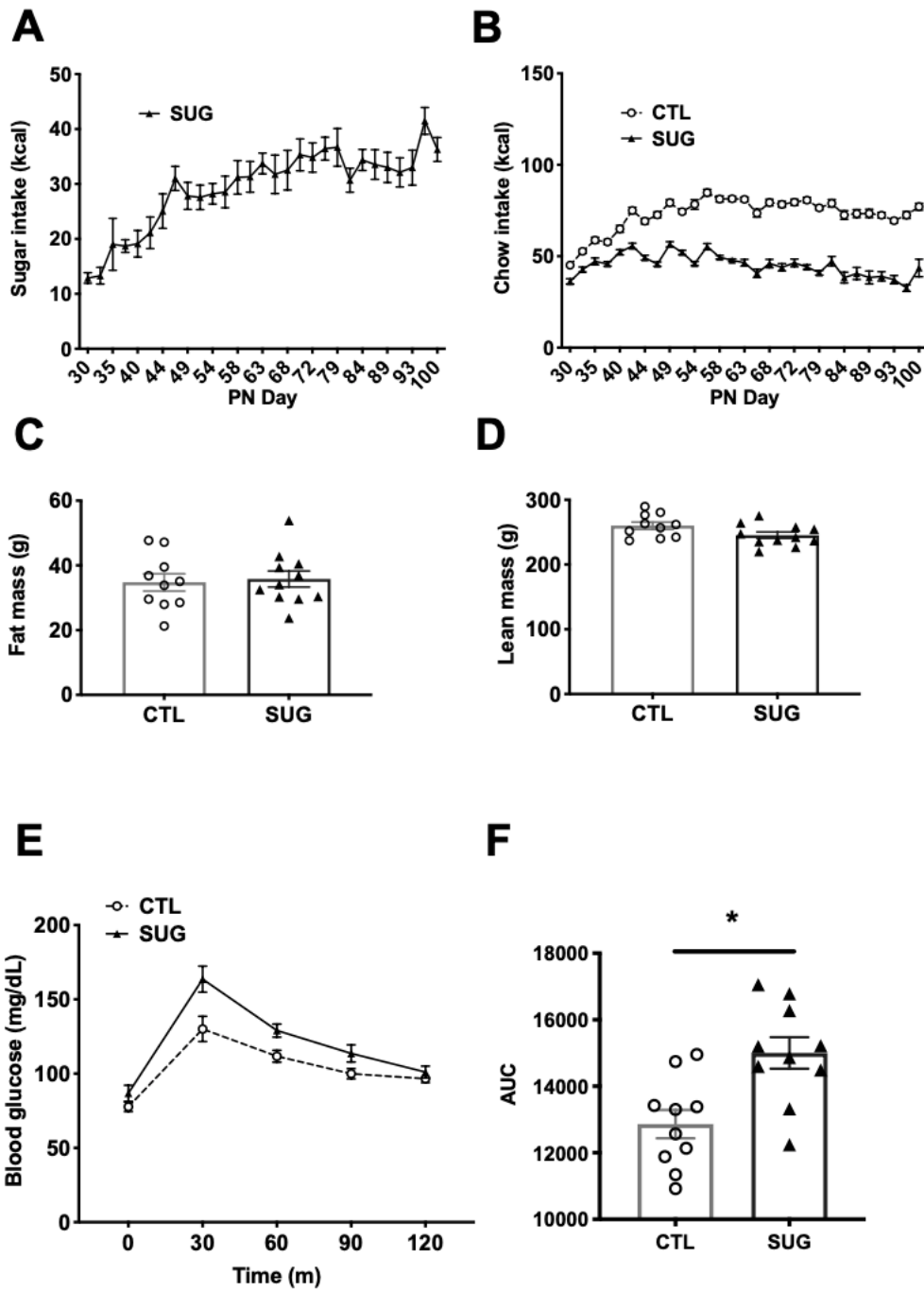
Figure 40:

Effect of early life sugar consumption on food intake and metabolic measures (A)

kcals from sugar over the feeding period beginning at post-natal day (PN) 28 with the

first measurement taken on PN 30 (n=11). (B) Kcals from chow intake were lower

throughout the feeding period in animals fed early life sugar (n=10,11). (C, D) there were no differences in fat mass or lean mass (n=10,11; two-tailed, type 2 Student's T-test). (E, F) Results from the intraperitoneal glucose tolerance test show an elevated area under the curve (AUC) in rodents fed sugar solutions during early life (n=10,11; two-tailed, type 2 Student's T-test; P<.05). CTL=control, SUG= sugar, PN= post-natal day; data shown as mean ± SEM.'
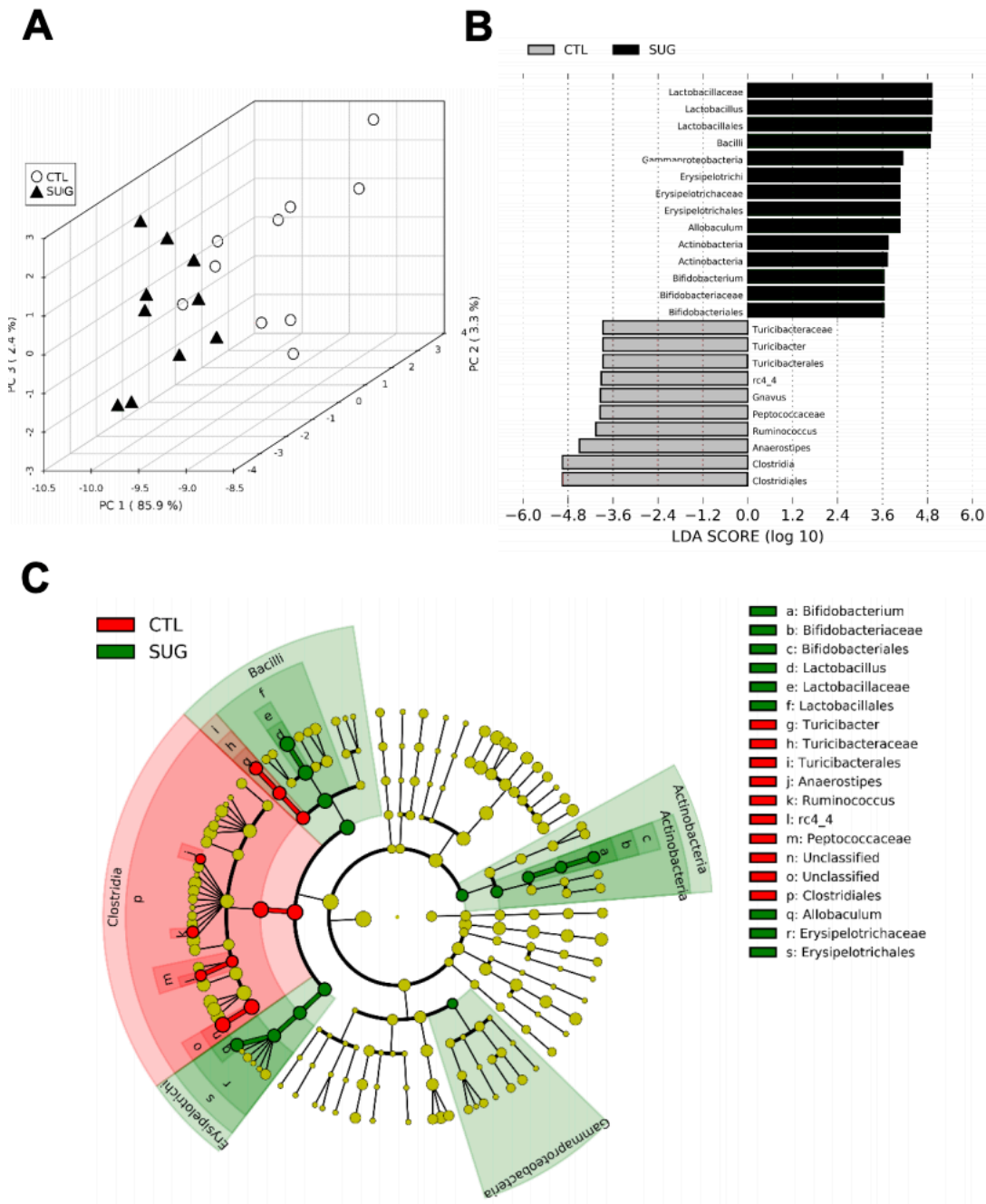
Figure 41

Effect of early life sugar consumption on the rat cecal microbiome (A) Principal

component analysis (PCA) was run using all phylogenic levels (112 normalized taxa

abundances) and shows different clustering patterns based on overall cecal microbial

profiles. (B) Linear discriminant analysis (LDA) Effect Size (LEfSe), run using the

GALAXY platform, identified characteristic features of the cecal microbiota of rats fed a

control diet or early life sugar. Relative differences among groups were used to rank the

features with the LDA score set at 2. (C) Identified taxa are displayed by scores and on

a phylogenic cladogram. CTL=control, SUG= sugar.
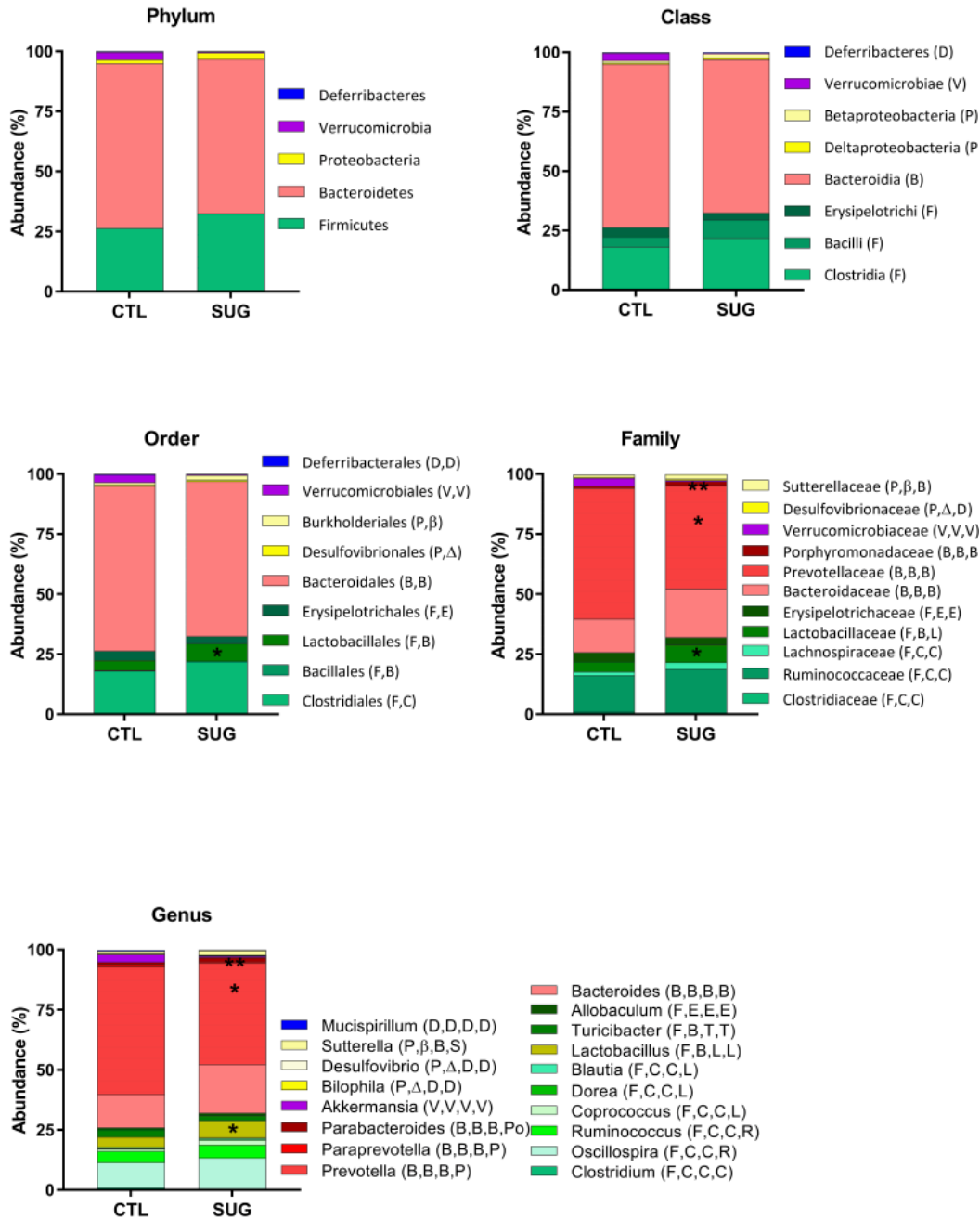
414

Abundances at the different phyla levels -FECAL

Figure 42

Effect of early life sugar consumption on the rat fecal microbiome: Filtered

bacterial abundances by taxonomic levels phylum, class, order, family, genus in fecal

samples from rats fed a control diets or early life sugar. Differences in abundances were

assessed by Mann-Whitney non-parametric test. * p<0.05, *** p<0.001. CTL=control,

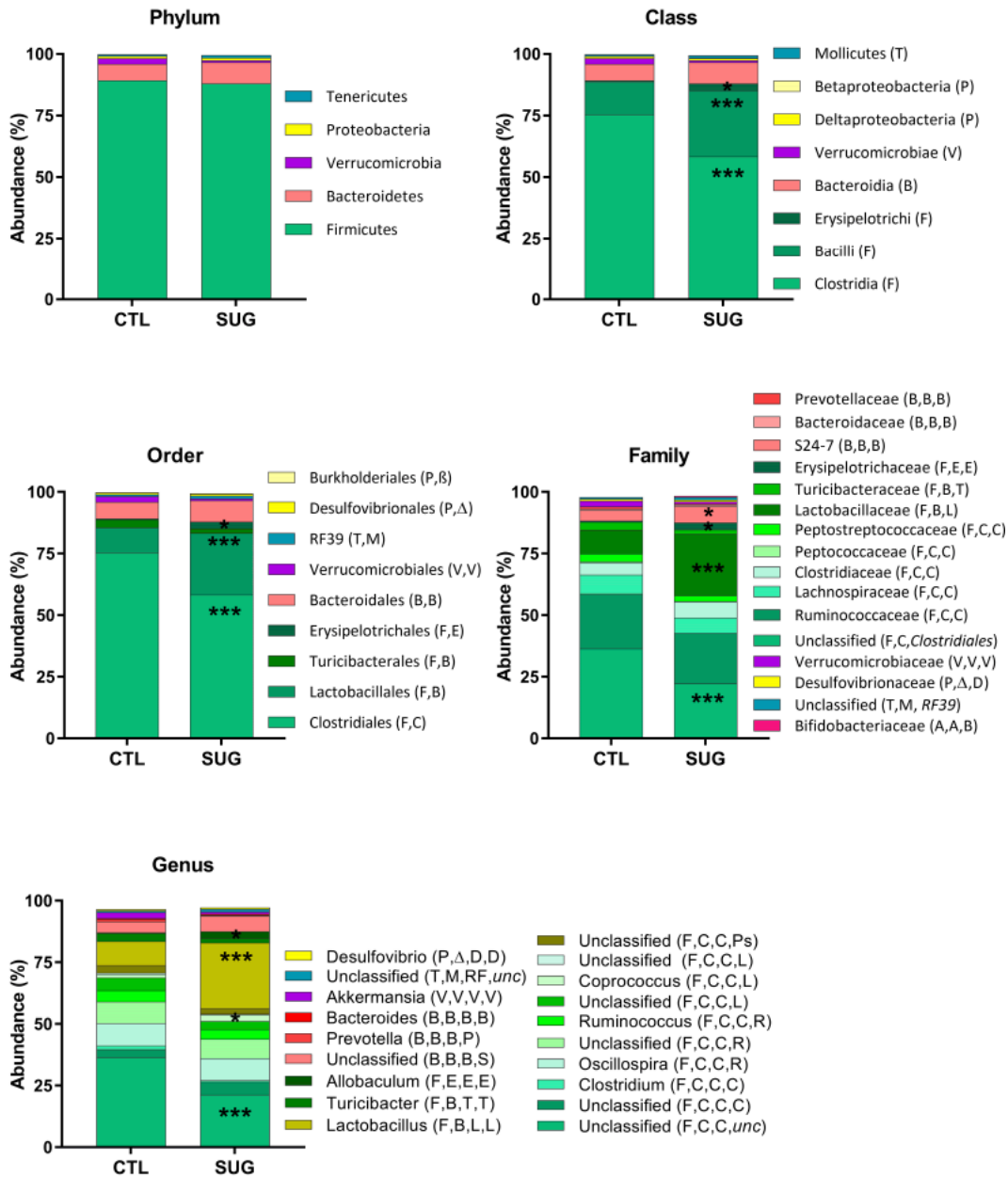SUG= sugar.

Abundances at the different phyla levels -CECAL

Figure 43

Effect of early life sugar consumption on the rat cecal microbiome: Filtered

bacterial abundances by taxonomic levels phylum, class, order, family, genus in cecal

samples from rats fed a control diets or early life sugar. Differences in abundances were

assessed by Mann-Whitney non-parametric test. * p<0.05, *** p<0.001. CTL=control,

SUG= sugar.

	Phylum		Class		Order		Family	Genus
						C	Clostridiaceae	Clostridium
						L	Lachnospiraceae	Coprococcus
								Blautia
								Dorea
		C	Clostridia	C	Clostridiales	P	Peptococcaceae	
F	Firmicutes					Ps	Peptostreptococcaceae	
						R	Ruminococcaceae	Oscillospira
								Ruminococcus
				L	Lactobacillales	L	Lactobacillaceae	Lactobacillus
		B	Bacilli	T	Turicibacterales	T	Turicibacteraceae	Turicibacter
				B	Bacillales			
		E	Erysipelotrichi	E	Erysipelotrichales	E	Erysipelotrichaceae	Allobaculum
						S	S24-7	
						B	Bacteroidaceae	Bacteroides
B	Bacteroidetes	B	Bacteroidia	B	Bacteroidales	P	Prevotellaceae	Prevotella
								Paraprevotella
						Po	Porphyromonadaceae	Parabacteroides
V	Verrucomicrobia	V	Verrucomicrobiae	V	Verrucomicrobiales	V	Verrucomicrobiaceae	Akkermansia
		β	Betaproteobacteria	B	Burkholderiales	S	Sutterellaceae	Sutterella
P	Proteobacteria	Δ	Deltaproteobacteria	D	Desulfovibrionales	D	Desulfovibrionaceae	Desulfovibrio
								Bilophila
T	Tenericutes	M	Mollicutes	RF	RF39			
D	Deferribacteres	D	Deferribacteres	D	Deferribacterales	D	Deferribacteraceae	Mucispirillum
A	Actinobacteria	A	Actinobacteria	B	Bifidobacter	B	Bifidobacteriaceae	

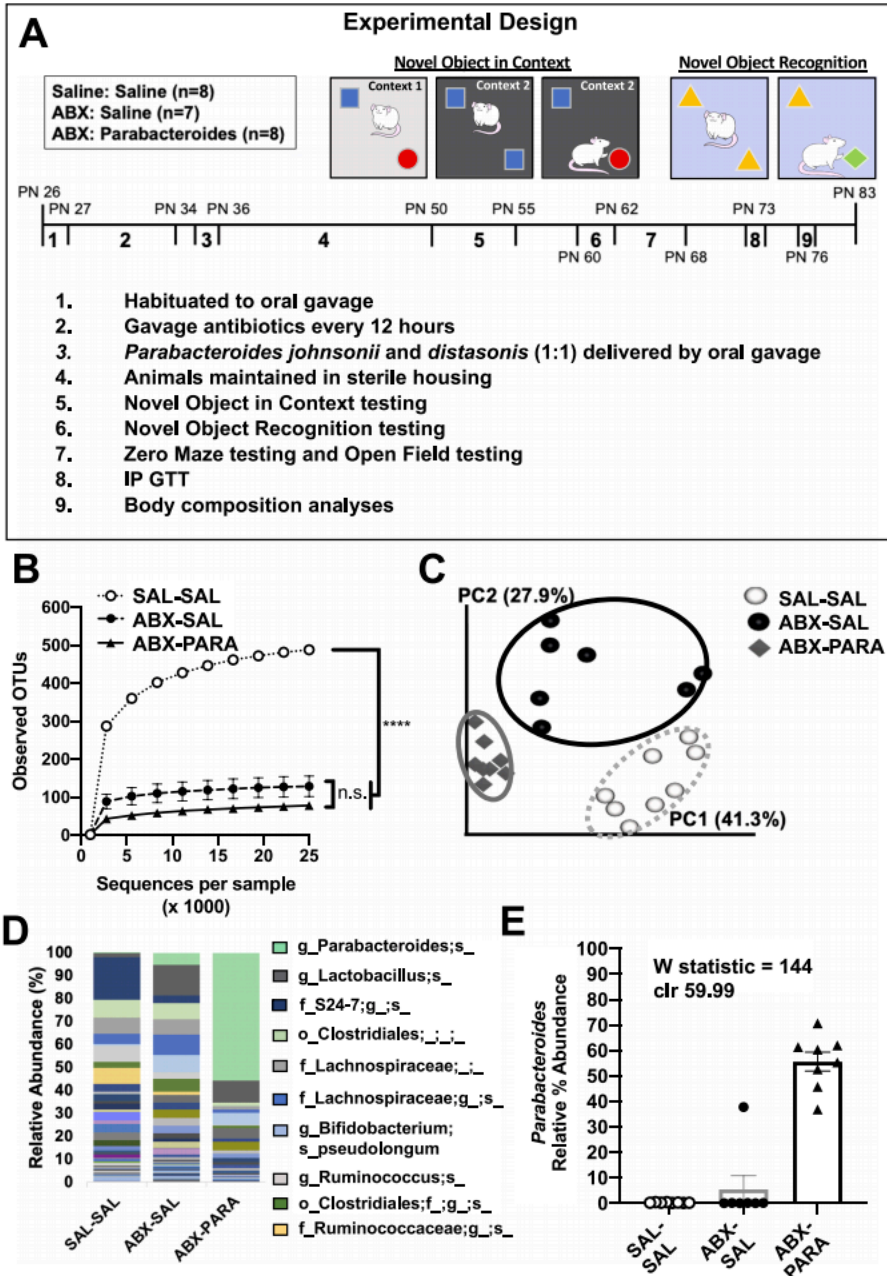**Table 8**

Associated phylogenetic tree

Figure 44

Intestinal Parabacteroides is enriched by antibiotic treatment and oral gavage of

P. distasonis and P. johnsonii. (A) Schematic showing the timeline for the

experimental design of the Parabacteroides transfer experiment. **(B)**Alpha diversity

based on 16S rRNA gene profiling of fecal matter (n = 7–8) represented by observed

operational taxonomic units (OTUs) for a given number of sample sequences. **(C)**

418

Principal coordinates analysis of weighted UniFrac distance based on 16S rRNA gene profiling of feces for SAL–SAL, ABX-SAL, and ABX-PARA enriched rats (n = 7–8). **(D)** Average taxonomic distributions of bacteria from 16S rRNA gene sequencing data of feces for SAL–SAL, ABX-SAL, and ABX-PARA enriched animals (n = 7–8). **(E)** Relative abundances of Parabacteroides in fecal microbiota for SAL–SAL, ABX-SAL, and ABX-PARA enriched animals (n = 7–8) (ANCOM). PN post-natal day, IP GTT intraperitoneal glucose tolerance test. Data are presented as mean ± S.E.M. *P < 0.05, **P < 0.01, ***P < 0.001. n.s. not statistically significant, SAL–SAL rats treated with saline, ABX-SAL rats treated with antibiotics followed by sterile saline gavage, ABX-PARA rats treated with antibiotics followed by a 1:1 gavage of Parabacteroides distasonis and Parabacteroides johnsonii.
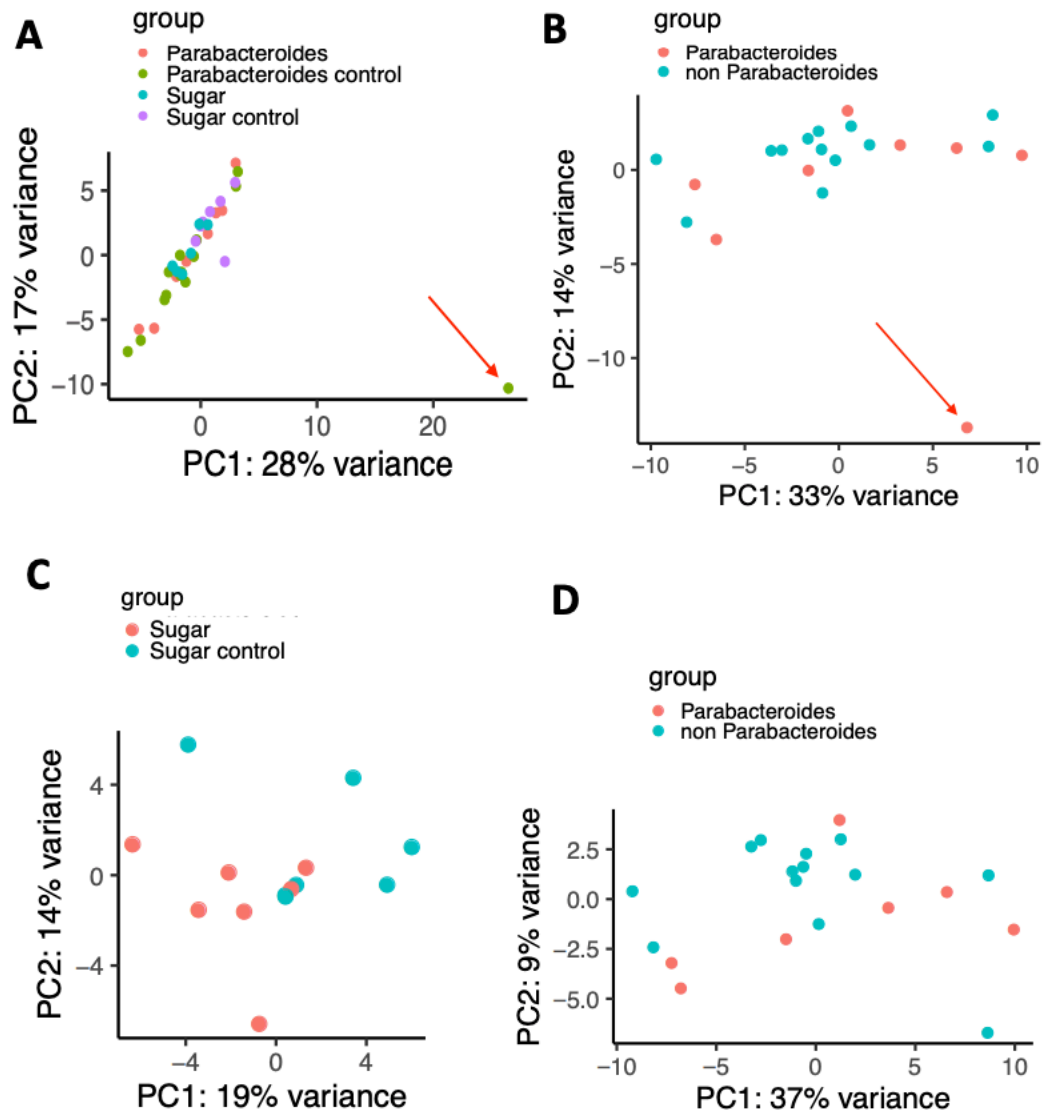
Figure 45

Principal coordinate analyses of hippocampal gene expression (A) Potential

sample outliers were detected by principle component analysis (PCA) and one control

(red arrow) and (B) one treatment sample (red arrow) from the *Parabacteroides*

experiment were deemed outliers and removed. (C) principal component analysis for

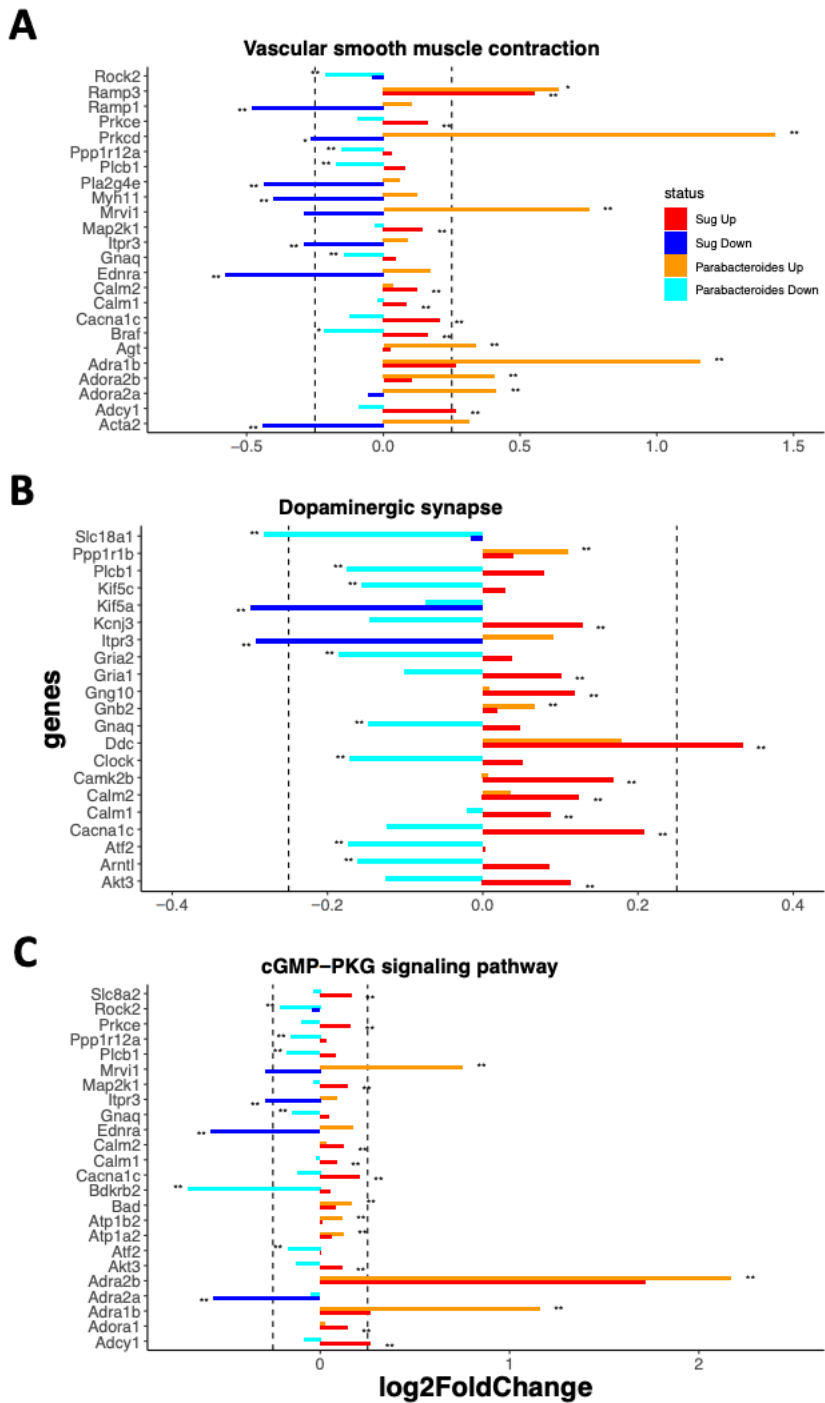the sugar (D) and *Parabacteroides* enrichment experiments.

Figure 46

Comparison of hippocampal gene expression pathways altered by sugar and

Parabacteriodes At the pathway level, three pathways overlapped in the sugar and

Parabacteroides transfer experiments including (A) vascular smooth muscle contraction

(B) dopaminergic synapse and (C) cGMP-PKG signaling pathway. Red= upregulated by

sugar, dark blue= downregulated by sugar, orange= upregulated by *Parabacteroides*,

light blue= downregulated by *Parabacteroides* * $P < 0.05$ and ** $P < 0.01$. Dotted line

indicates ±0.25 log2 fold change.

Concluding remarks

Increasing evidence implicates the gut microbiota in host neurological homeostasis and pathology. Diet and environmental stressors are primary environmental risk factors for epileptic disorders, cognitive impairment, and host metabolic dysfunction. Still unknown in this work is the extent to which microbial communities synergistically impart effects on host neurophysiology and behavior, which microbial-produced molecules can either trigger or prevent neurological disruption, and how treatments can stably target noted microbial effectors. Future work in these areas needs to further focus on precise mechanisms for how microbes affect host neurophysiology and identify candidate effectors relevant for human patients.

Appendix 1

STENSL: microbial Source Tracking with ENvironment SeLection

Ulzee, A., Shenhav, L., Olson, C.A., Hsiao, E.Y., Halperin, E., Sankararaman

Under review

Abstract

Microbial source tracking analysis has emerged as a wide-spread technique for characterizing the properties of complex microbial communities. However, this analysis is currently limited to source environments sampled in a specific study. In order to expand the scope beyond one single study, and allow the 'exploration' of source environments using large databases and repositories such as the Earth Microbiome Project, a source selection procedure is required. Such a procedure will allow differentiating between contributing environments and nuisance ones when the number of potential sources considered is high. Here we introduce STENSL (microbial Source Tracking with ENvironment SeLection), a machine learning method that extends the common microbial source tracking analysis by performing an unsupervised source selection and enabling sparse identification of latent source environments. By incorporating sparsity into the estimation of potential source environments, STENSL improves the accuracy of true source contribution, while significantly reducing the noise introduced by non-contributing ones. We therefore anticipate that source selection will augment microbial source tracking analyses, enabling an exploration of multiple source environments from publicly available repositories while maintaining high accuracy of the statistical inference.

Introduction

Complex microbial communities are present in multiple biological domains, and play far-reaching roles in various fields, from human health, through agriculture, to bioremediation. The study of these high-dimensional communities offers great opportunities for biological discovery, due to the ease of their measurement, the ability to perturb them, and their dynamic and rapidly evolving nature. These same characteristics, however, make it

425

difficult to extract informative and reproducible patterns informing the origins of these ecosystems. Specifically, as microbial community assembly strongly depends on the dispersal of microbes from a mixture of source environments, the analysis of such communities requires tailored algorithms deconvolving latent structures regarding community integration.

Over the last decade, a number of computational techniques have been described for tracking the assembly of such complex microbial communities[1–3]. By performing "microbial source tracking", methods such as FEAST[1] and SourceTracker2[2] quantify the fraction, or proportion, of different microbial samples (sources) in a target microbial community (sink), while assuming the sink is a mixture of sampled microbial environments (i.e., known sources) with the possibility of unmeasured ones, collectively referred to as the 'unknown source'. These methods have shown great promise in revealing new insights, particularly in quantifying contamination and tracking microbial community integration[4–6]. However, in many practical scenarios, the list of potential sources cannot be narrowed down to a small number, and therefore the number of contributing sources is often much smaller than the number of candidate sources considered in the analysis. Unfortunately, existing methods are suboptimal in such scenarios, hindering the concept of source exploration.

As it may be nearly impossible to obtain sequencing data for all potential source environments in a study, source exploration using public repositories may augment microbial source tracking analyses, beyond the scope of any one study. We therefore suggest that in these settings, microbial source tracking can benefit from automated source exploration and selection. Nonetheless, this process remains largely

understudied, with current methods not suitable for the task, as-is, since the estimation error increases as the number of sources considered increases. Only one previous study tried to address this limitation by exploring the utility of Aitchison distance to select "important" sources that drive community assembly[7]. However, as we demonstrate using simulations, the accuracy of this strategy in the presence of an unknown source is very low.

Here we introduce STENSL, a scalable regularization algorithm that unveils the latent structure of a given microbial community by modeling it as a convex combination of (1) contributing sources (sources observed and have nonzero contribution), (2) nuisance sources also called non-contributing sources (observed and have zero contribution) and (3) unobserved sources, collectively referred to as the unknown source. We use the term candidate sources to describe the union of the former two. STENSL enables the incorporation of multiple candidate sources from publicly available repositories without the need for manual selection. As a result, multiple sources can be considered without increasing the error in estimating the underlying mixing proportions, unlike current microbial source tracking methods.. We demonstrate that, when considering both contributing and non-contributing source environments, STENSL is significantly more accurate than state-of-the-art methods. Thus, by leveraging sources from publicly available repositories, STENSL can provide a more accurate estimation of the origin of complex microbial communities

Results

A brief description of the model. STENSL detects a core group of source environments, within a larger group of candidate environments, and quantifies their contribution to the

427

formation of complex microbial communities. STENSL takes as input a microbiome sample (called the sink) as well as a separate group of microbial samples (called the candidate sources), detects a core group of contributing sources and estimates the fraction of the sink community that was contributed by each of these core environments. By virtue of these mixing proportions summing to less than the entire sink, STENSL also reports the fraction of the sink attributed to other, unobserved, origins (Figure 1). STENSL is based on a least-squares optimization with an L1-norm regularization, acting as a source selection procedure, prior to the common microbial source tracking analysis. In STENSL we also introduce a procedure to analytically reconstruct the best representation of the unknown source. Specifically, we leverage the regularized least-squares solution of the mixture model to identify taxa which are accurately reconstructed and are thus not unlikely to originate from the unknown source (Methods). STENSL identifies three types of sources: (1) contributing sources (sources observed and have nonzero contribution), (2) nuisance sources also called non-contributing sources (observed and have zero contribution) and (3) unobserved sources, collectively referred to as the unknown source. In other words, our method explicitly differentiates between two types of known sources introduced to the model (i.e., contributing and nuisance). As we demonstrate below, these modifications are significant in denoising and exploring a cohort of candidate sources. Specifically, we show that STENSL is significantly more accurate than existing methods when considering a large number of nuisance sources, a setting in which the identification of truely contributing sources becomes non-trivial.
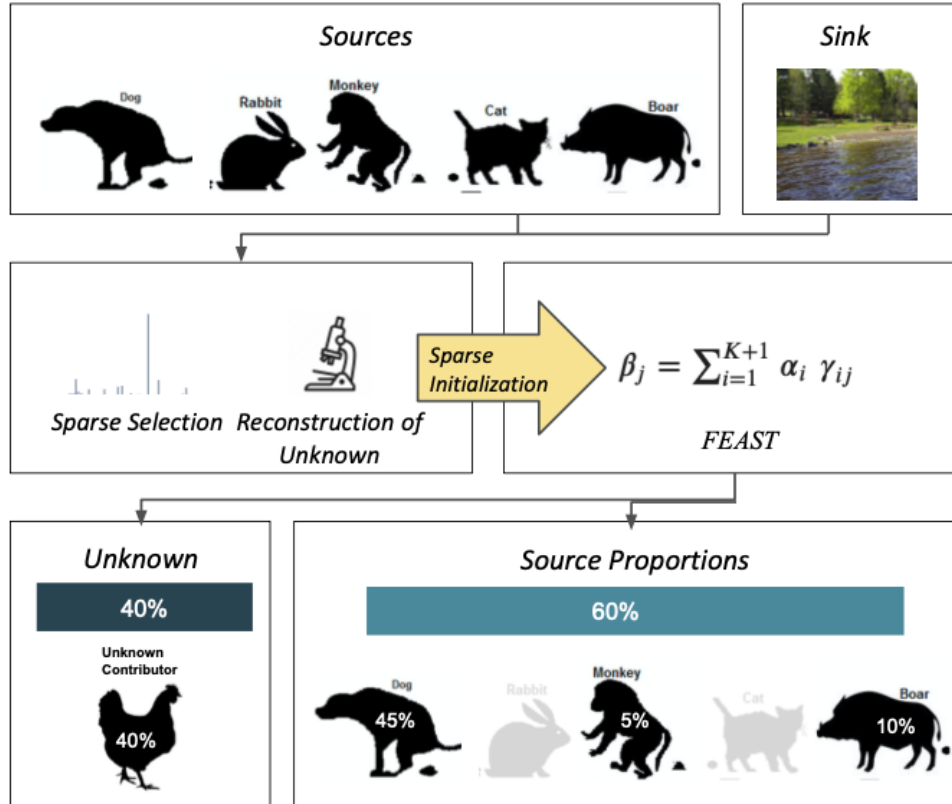
Figure 47: The procedure of STENSL. The source-tracking task describes the problem of identifying the relative presence of microbial communities from an unknown mixture. STENSL implements a sparse selection procedure to allow the use of potential sources and obtain robust measure of contamination and relative source contributions.

Model evaluation using data-driven simulations. We compared the accuracy of STENSL to FEAST, SourceTracker2 and RAD, methods previously suggested for microbial source tracking using simulations. The samples used in these simulations are based on real microbial samples documented and processed as part of the Earth Microbiome Project[8]. The synthetic sink samples were generated as a convex combination of real microbial samples (i.e., contributing sources) and an unknown source,

hidden from the algorithm. Our evaluation extends the source tracking problem by introducing to the algorithms numerous additional sources unrelated to the sink such that all methods consider both contributing and non-contributing sources. To measure accuracy, we compared the estimated mixing proportions with the true ones using mean-squared error (Figure 2a, Table S1). Overall, we found that STENSL was the only method to consistently estimate the level of real sources' contribution, with significantly lower MSE across unknown contributions 0~90% (SourceTracker2 $P<9.1310-7$, FEAST $P<1.4310-3$, RAD $P<9.1310-7$; Wilcoxon signed-rank test). The ability of each method to distinguish truly contributing sources was further assessed by summing non-zero weight attributed to non-contributing sources. We term this metric the 'false positive rate'. We found that using STENSL, the false positive rate was significantly reduced compared to the other methods (Figure 2b;SourceTracker2 $P<9.1310-7$, FEAST $P<3.9210 -5$, RAD $P<9.1310-7$; Wilcoxon ranked-sum test). We note that lower false positive rates correspond to improvements in identification of truly contributing sources as well as estimation of the unknown source proportions. Conversely, we found that for FEAST, RAD and SourceTracker2, non-contributing sources were consistently assigned positive weights and the misattributions increased with increasing number of candidate sources. Notably, in the absence of nuisance sources, STENSL is as accurate as FEAST, the state-of-the-art method.

Mean-Squared Error
(50 Candidate Sources / 10 Contributing)
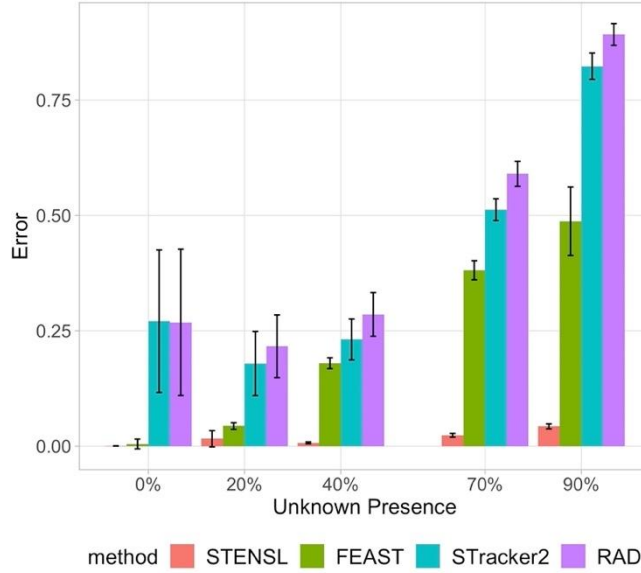
Mean-Squared Error
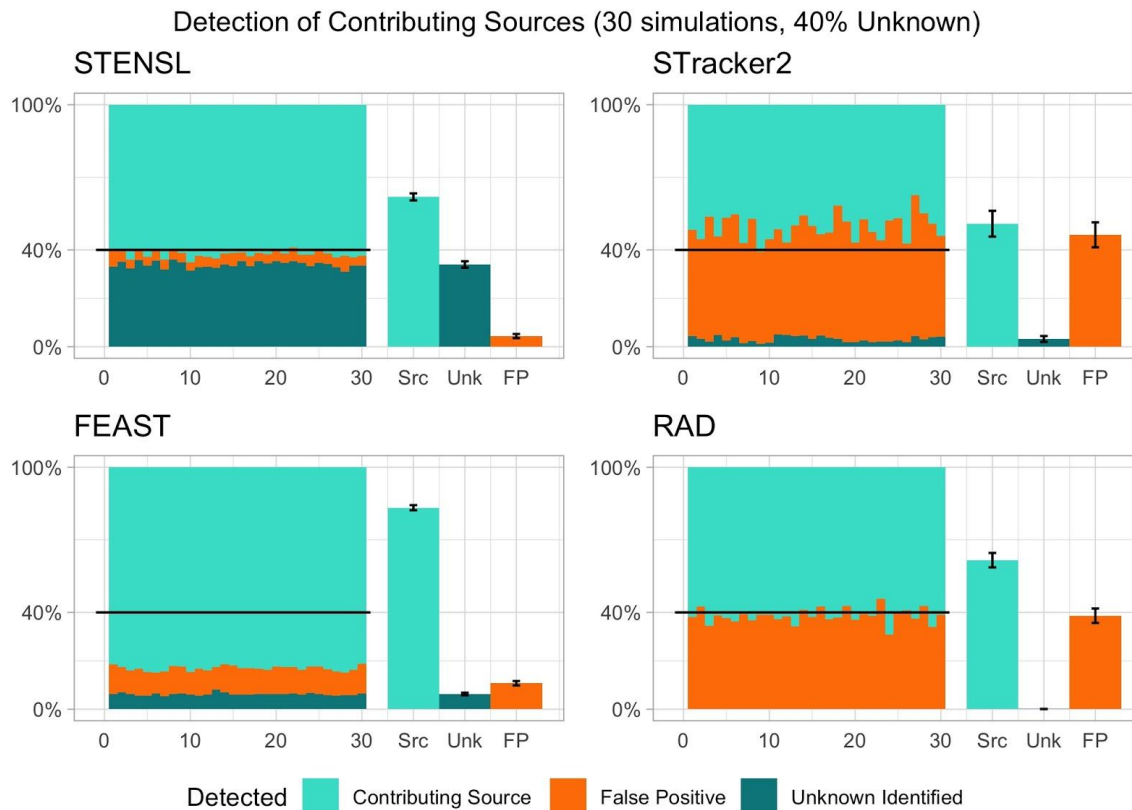(200 Candidate Sources / 20 Contributing)

Detection of Contributing Sources (30 simulations, 40% Unknown)
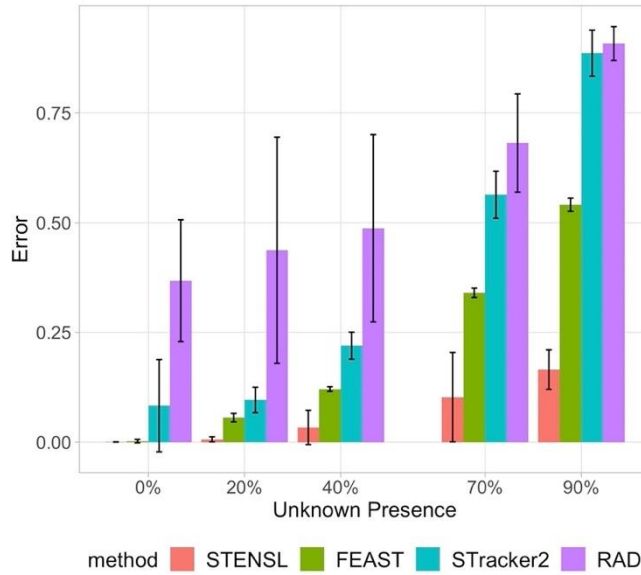
Figure 48 (a) Estimation of mixing proportions using STENSL In simulated settings of M=50,200 total candidates (K=10,20 contributing sources within respectively), mean-squared error of the estimated mixing proportion was evaluated for STENSL, SourceTracker2, FEAST, and RAD. For each environment, experiments were repeated with increasing unknown presence of 0%, 20%, 40%, 70%, and 90%. Error bars indicate standard deviation in error for tested sinks within each group. **(b) Breakdown of estimated mixing proportions** For the group of sinks where we simulated intermediate unknown proportion (40%), we label how each method attributes mixing proportion weights across truly contributing sources, false positive sources, and the unknown proportion, in the setting of 50 candidate and 10 contributing sources.

432

STENSL maintained the lowest proportion of false positive attributions in comparison to similar methods which were overwhelmed adversely by the increased number of candidates (significantly lower with $p < 7.47 \times 10^{-4}$ across all methods, Figure S1).

We next quantified the accuracy of the estimated unknown proportion through Mean Absolute Error (MAE) against the true simulated unknown proportion ranging from 0% to 90% in the sink. To visualize how unknown proportions affect estimation, we correlated the estimated unknown proportions with the true unknown proportions in Figure S4. We found that STENSL is significantly more accurate in estimating the unknown source contribution throughout the entire range of unknown source proportions (SourceTracker2 $P < 9.13 \times 10^{-7}$, FEAST $P < 3.92 \times 10 - 5$, RAD $P < 9.13 \times 10^{-7}$; Wilcoxon rank-sum test; Table S1). For the smallest simulated setting of three true sources and six total candidate sources we found that all methods were accurate in estimating the unknown source contribution (Figure S2). However, as the number of candidate sources increased, existing methods significantly underestimated the unknown proportion due to both false identification of sources and overestimation of truly contributing sources.

Real data

In vitro model validation. To validate the sparsity assumption introduced by STENSL, which models a microbial community as a convex combination of contributing sources, and to further demonstrate the utility of our method, we created an *in vitro* data set. In this data, we generated in vitro sinks as a mixture of microbial samples acquired from the digestive systems of three human subjects and three mice subjects (Methods). Twenty-four in-vitro sinks were assembled, each sink consisting of two to three microbial samples

at varying mixing proportions. When performing microbial source tracking analyses on this set of contributing sources and sinks, we added a group of 50 additional non-contributing sources (Methods). Our analysis considered STENSL, SourceTracker2, and FEAST, forgoing RAD as it does not estimate an unknown proportion. We evaluated the accuracy of these methods by using mean-squared error (MSE) between the lab-generated ground-truth and the estimated mixing proportions. As part of our analysis, for each sink we withheld one or two contributing sources to create settings in which the unknown proportions range between 0%~80%. Similarly to our simulation results, we found that in real data STENSL was significantly more accurate than other methods (Figure 3, SourceTracker2 $P<2.2\times10^{-16}$, FEAST with $P<8.596\times10^{-16}$; Wilcoxon ranked-sum test).
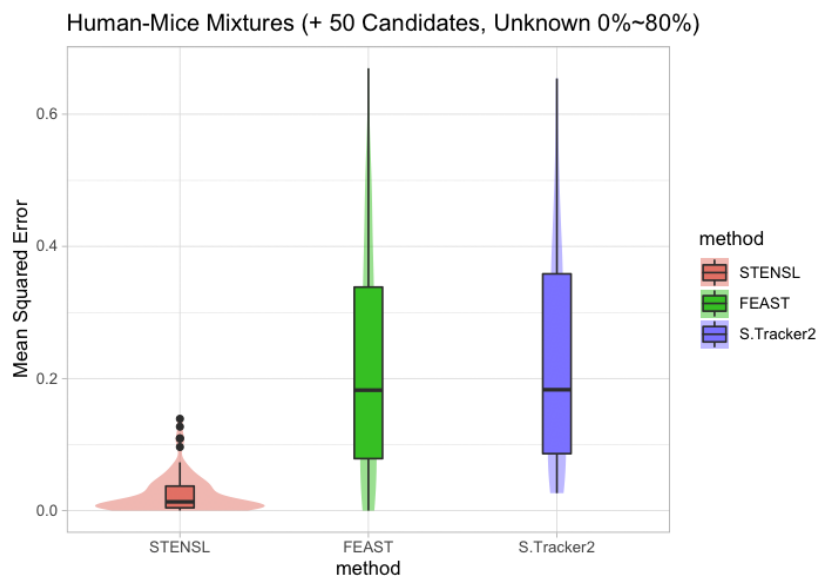

Figure 49: Analysis of in-vitro dataset of sinks created from mixture of Human and Mice Gut Samples The accuracy of STENSL, SourceTracker2, and FEAST was evaluated using mean-squared error (MSE) against the true mixing proportion used to

create in vitro sinks with unknown proportions ranging from 0%~80% and in the presence of 50 non-contributing sources.

Source selection in the Human Microbiome Project. To demonstrate the utility of STENSL when using large public repositories, we sought to assess the origins of a microbiome sample taken from a single individual found in the Human Microbiome Project[9]. To construct the source tracking problem, we defined the sink to be a saliva microbiome sample which is one of several orally acquired samples including tongue, palate, and buccal mucosa. The candidate sources were then defined to be all the microbiome samples from the focal subject from which the saliva was sampled (excluding the saliva) as well as all other available microbial samples originated from 15 body sites across 88 individuals. In Figure 4.a, we outline results of applying both STENSL and SourceTracker2 to the same source tracking problem, with a substantially higher false positive rate attributed to the latter. Specifically, STENSL attributed a total of 33.7% to other oral microbiome samples belonging to the focal subject from which the sink was sampled (Buccal Mucosa 14.3% , Tongue Dorsum 11.0% and 8.4% from Throat), while SourceTracker2 attributed only 4.3% to the other oral microbiome samples belonging to the focal subject from which the sink was sampled (Buccal Mucosa 3.3%, Tongue Dorsum 0.4% and 0.7% from Throat). In addition, STENSL estimated an unknown contribution of 26% while estimating zero contribution for most non-contributing sources originating from other individuals. In contrast, SourceTracker2 assigned non-zero weights to the majority of sources from all other individuals (i.e., non-contributing sources) and estimated a negligible unknown proportion (0.1%) . We next performed a follow-up analysis, only considering samples from the focal individual (1 individual, 15 samples across body sites)

435

and examined the results of this problem with no external individuals, a setting with little to no non-contributing sources. Both methods estimate that the oral sites would contribute largely to the saliva (STENSL estimates 19.2% Buccal Mucosa, 18.4% Tongue Dorsum, 17.9% Throat; SourceTracker2 estimates 12.4% Buccal Mucosa, 14.8% Tongue Dorsum, 10.3% Throat) and unknown proportion of 20-30% (STENSL estimates 35% unknown while SourceTracker2 estimates 19% unknown). These estimates agreed best with the results of STENSL in the full setting of 88 individuals and 997 samples. STENSL specifically highlighted Tongue, Buccal Mucosa, and Throat samples as the top contributors, which remained consistent when analysing one subject or including the entire cohort.
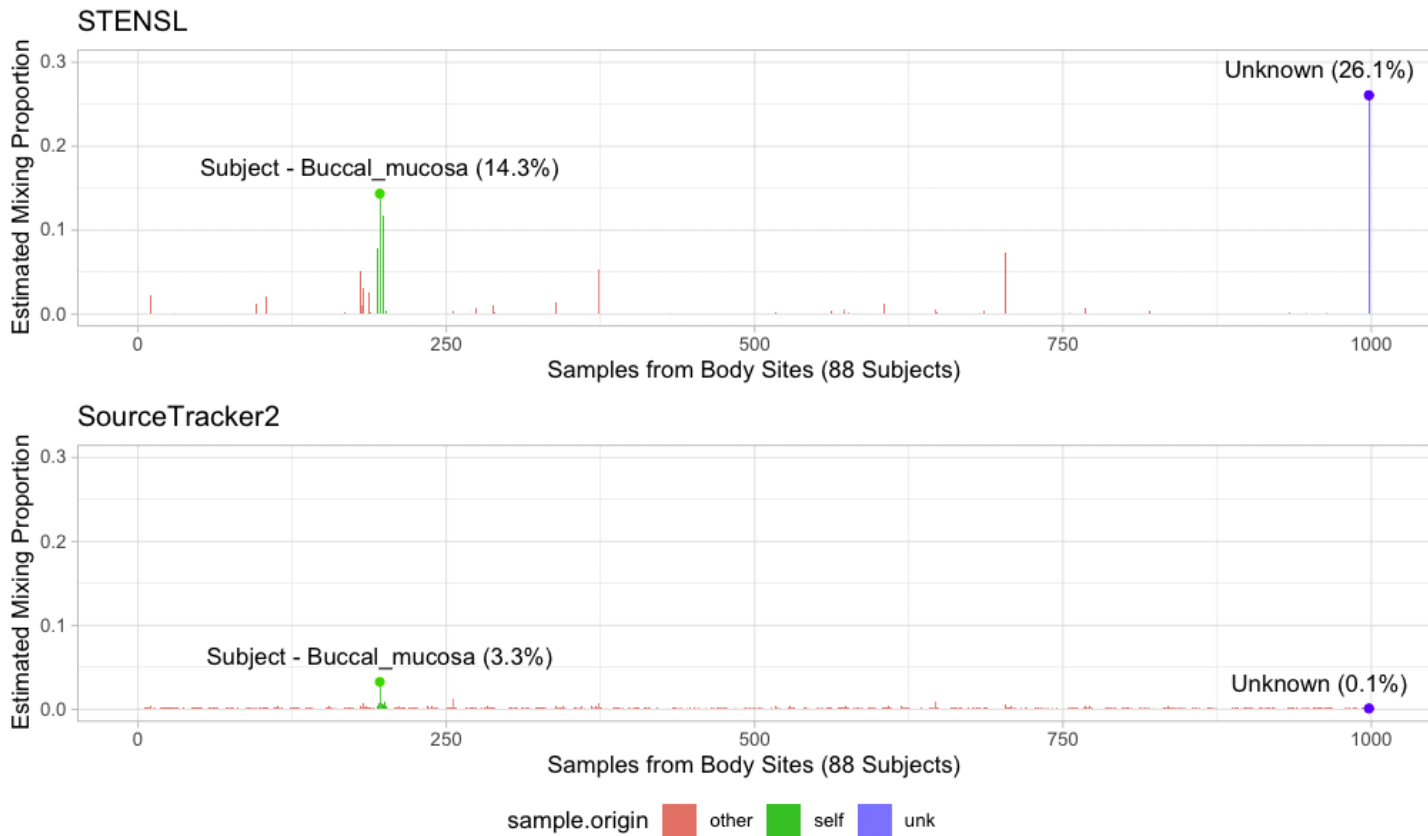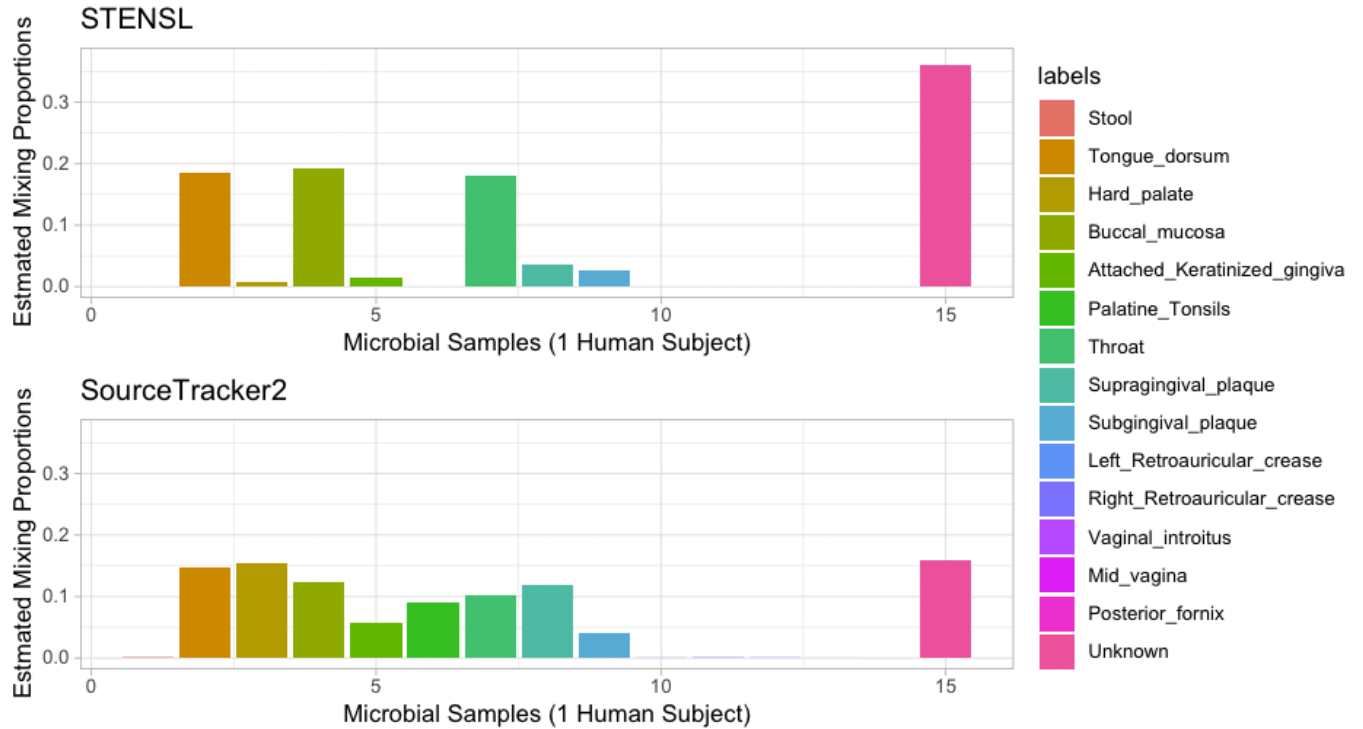
Figure 50: Single microbial samples can be strongly attributed to its original subject in a database-wide analysis of the Human Microbiome Project using STENSL. STENSL is applied in analysing a saliva sample from one Human subject as a composition of any choice of 997 samples which were collected from other body sites from the same subject and also from other human subjects. (a) Using STENSL, we identify several samples with high contribution (top-3: Buccal Mucosa 14.3%, Tongue 11.0%, Throat 8.4%) which originate from the same Human subject. This is compared to SourceTracker2 where the highest weight given to a sample from the subject diminishes to 2.9%. (b) To verify the database-wide analysis, we compared it with results of applying both methods to the set of fifteen sources belonging to the original Human subject. In this reduced setting, both methods agreed roughly in the presence of unknown proportions (STENSL 35%, SourceTracker2 19%) and the top three contributing sources to be Buccal Mucosa, Tongue, and Throat.

437

Discussion

In this work we present STENSL, a least-squares optimization with an L1-norm regularization acting as a sparse source selection procedure prior to microbial source tracking analysis. STENSL enables the identification of contributing sources amongst a large set of potential source environments while obtaining robust measures of source contributions. With the unprecedented expansion of microbiome data repositories such as the 'Earth Microbiome Project', recording over 200,000 samples from more than 50 types of categorized environments, STENSL takes first steps in performing automated source exploration and selection. Using simulations, we found that STENSL is significantly more accurate in identifying the contributing sources as well as the unknown source, even when considering hundreds of candidate sources; settings in which state-of-the-art microbial source tracking methods add considerable error.

The utility of STENSL is established using two real datasets. The first is an *in vitro* data we generated, in which we mixed six microbial environments, samples from the gut of humans and mice, and generated over two dozen sink samples. As this dataset provides the ground truth rather than a simulation, we validated, for the first time, the generative model of common microbial source tracking methods (i.e., a sink is a convex combination of known and unknown sources). Next, we demonstrated the added value of STENSL, by showing it is robust to the presence of nuisance sources (i.e., sources that didn't contribute to the formation of the sink). The second dataset is the Human Microbiome Project. In this analysis, we showed STENSL's ability to accurately identify the latent

contributing sources, even in the presence of hundreds of nuisance ones, while significantly reducing estimation error.

Overall, using simulated and real sequencing data, we demonstrated that STENSL significantly improves the accuracy of microbial source tracking analysis over comparable methods by minimizing the contribution of nuisance sources and highlighting the actual contributing one. By performing source selection that is robust to the presence of hundreds of nuisance sources, STENSL is enabling efficient source exploration using publicly available repositories thereby augmenting microbial source tracking analysis.

Methods

The STENSL Model

Consider a single sink sample represented by a vector x where x_j corresponds to the abundance of taxa j, $1 \le j \le N$. We define our model over **M** sources among which any few sources may truly contribute to the sink, and therefore refer to them as candidates. Each source is represented by a vector Y_i, where y_{ij} is the observed abundance of taxa j in source i $(1 \le i \le M)$. Additionally, we assume there is an unobserved source $(M+1)$. Let $C_i = \sum_{j=1}^{N} y_{ij}$ and $C = \sum_{j=1}^{N} X_j$ be the total taxa counts of the candidate sources and sink respectively. With this notation, the generative model is as follows: we assume that there are mixture proportions —a vector of length $M+1$—where i corresponds to the fraction of source i in the sink, hence $\sum_{i=1}^{M+1} i = 1$. We also assume that the underlying relative abundance for each of the sources is unobserved, and that Y_i are noisy realizations of these relative abundances. Formally, for each source, we have a vector i, where $\sum_{j=1}^{N} ij =$

439

1. Each **ij** represents the true relative abundance of taxa j in sourcei**.** The generative model for STENSL is given by:

$$j = \sum_{i=1}^{M+1} \alpha_i \beta_{ij}$$

$$Y_i \sim \text{Multinomial}(C_i, (\beta_{i1}, ...\beta_{iN})); i \in [M]$$

$$Y_{M+1} \sim \text{Multinomial}(C_{M+1}, (\beta_{M+1,1}, ...\beta_{M+1,N}))$$

$$x \sim \text{Multinomial}(C, (\gamma_1, ...\gamma_N))$$

As we do not observe Y_{M+1}, we use a data-driven plug-in estimate $\hat{Y}_{M+1}$ as described below. The generative model underlying STENSL is the same as the generative model of FEAST, with the exception that STENSL is explicitly assuming the unknown source was also sampled from a multinomial distribution while using a data-driven plug-in estimate $\hat{Y}_{M+1}$ that serves as an initial "observed" sample. Another notable difference between STENSL and other microbial source tracking methods, is the sparsity assumption. STENSL assumes that a sink is a convex combination of (1) contributing sources (sources observed and have nonzero contribution), (2) nuisance sources also called non-contributing sources (observed and have zero contribution) and (3) unobserved sources, collectively referred to as the unknown source. We use the term candidate sources to describe the union of the former two. In other words and as described below, STENSL assumes that only a subset of the sources introduced to the algorithm actually contribute to the formation of the sink, where this sparsity is induced by the inference framework rather than the generative model (i.e., data-driven parameter initialization).

Inference of STENSL Parameters

440

Under the STENSL model, we need to estimate the parameters, . Given the observed taxa counts in the candidate sources and sink, a number of inference algorithms could be used to estimate the parameters. A challenge in designing an accurate inference algorithm arises from the large number of parameters that need to be estimated. This challenge is further exacerbated when the number of candidate sources is large. To overcome this challenge, we perform inference in two steps. In the first step, we aim to identify the candidate sources that are likely to contribute to the sink and obtain an initial estimate of the mixing proportion at these sources. We use a constrained optimization algorithm with a sparsity assumption to obtain these initial estimates. In the second step, we focus on the sources identified as contributing to the sink in the previous step as well as approximate the taxa abundance added by unknown contribution. We leverage these initial estimates in performing expectation-maximization (EM) in an attempt to obtain improved estimates of the mixing proportions using FEAST[1]. We note that this is not a convex optimization problem (i.e., no global optimum) and therefore the initialization of the EM procedure is critical to the accuracy of the final parameter estimates.

Source Selection. STENSL assumes that only a sparse subset of the candidate sources contribute to the formation of the sink. To obtain a sparse selection of sources, we define a heuristic approach to infer the mixing proportions under a sparsity assumption. In practice, inferring the latent taxa variables depend heavily on the observed taxa counts and motivates a heuristic which uses the observed counts directly to obtain an approximation of the hidden variables, with an added benefit that the approximation leads to an optimization problem that can be efficiently solved for large numbers of sources. A

convenient choice for the initial values of γ are the observations $Y_{ij} / \sum_{j=1}^{N} Y_{ij}$, and we find

that the observations are a sufficient proxy of γ_{ij} in approximating . We next perform

inference by formulating a least-squares problem between x and Y_T while ensuring that

is sparsely approximated by L1 regularization. We specifically choose the L1

regularization (Lasso) which follows this formulation, with added constraints that each

proportion must be non-negative and $\sum_{i=1}^{M} \pi_i = 1$. In leveraging Lasso, we assume the

presence of underlying noise which is normally distributed when forming the sink. We

leverage this underlying noise to estimate the abundance profile of the unknown source.

We therefore seek to optimize the following objective function, where we determine an

optimal value for hyperparameter through cross-validation (Figure S3):

$$\min \| Y_T - X \|_2^2 + \| \|_1$$

$$\text{subject to } \sum_{i=1}^{M} \pi_i = 1, \ \pi_i \geq 0$$

The objective describes a least-squares problem which is solvable as a quadratic

program with the stated constraints. From the initial sparse approximation of , we consider

candidate source i for which contribution is positive $\pi_i > 0$ to be highly likely to be

contributing to the sink, and the result of the selection step.

Unknown source Initialization. In obtaining an initial estimate of the unknown

abundances counts Y_{M+1}, we assume that its underlying relative abundance follows a

truncated normal distribution similar to the non-negative components of the estimation

noise resulting from the selection step. In practice, in order to remove the prominent signal

stemming from the true known sources, we subtract the scaled counts of the top

contributing source, ranked based on the L-1 regularization and thus, $Y_{M+1}^{init} = \max(0, x - \max L1() Y_{argmaxL1}())$. We introduce two additional regularization methods to further improve the approximation of the unknown taxa abundance. First, we leverage the reconstruction error of taxa-j in the sink. Taxa observations which are poorly estimated are indicative of an unknown contributor, thus we measure the taxa-wise error $\epsilon_j = || \sum_{i=1}^{M} i_{ij} - j ||_2^2$ and choose an inclusion percentile **$0 \le 1$** for which top-n taxas would account for the majority of the error $\sum_{j=1}^{n} \epsilon_j / \sum_{j=1}^{N} \epsilon_j$. All taxa-j satisfying **= 0.75** was considered in the final unknown source. Next, we assessed the prevalence of taxa-j across the contributing sources. The appearance of a taxa-j is tallied to quantify the measure $\tau_j = \frac{1}{M} \sum_{i=1}^{M} \mathbb{1}_{ij} > 0; \mathbf{0 \le j \le 1}$. We assume that taxa with high τ_j are 'general' in the source environments considered and unlikely to benefit unknown estimation and should therefore be excluded from the unknown source initialization. To determine a threshold for **$\tau_1 ... \tau_N$**, we calculate the goodness-of-fit score $R = ||T - ||_2 / || ||_2$ of the least-squares source selection result. We dynamically apply the prevalence assumption, where by including taxa-j with $\tau_j < R$ are then considered as originating from an unknown contributor and the rest are excluded. For sinks which are well represented by the sparse model, the regularization step ensures that only the most uniquely present taxa are used to initialize the unknown source. For poorly reconstructed sinks, the majority of taxa will be considered. Finally, we treat this regularized taxa abundance as an initial estimate of the true taxa abundance of the unknown contributor $Y_{M+1} = 1 > \& < R Y_{M+1}^{init}$.

Microbial source Tracking

Given the estimate for the unknown source YM+1 and the initial estimates for and we use FEAST[1] to infer the model's parameters. FEAST uses the expectation maximization framework for parameter inference.

Simulation Procedure

To examine the accuracy of STENSL, we used multiple source environments with varying degrees of overlap in their distribution by randomly sampling from the Earth Microbiome Project. Each source environment was sub-sampled to contain 10,000 reads. In each iteration of the simulation we sampled $M + 1$ candidate environments and used them to build a synthetic sink with different mixing proportions. To simulate an unknown source as well as sparsity in source contribution, only K source environments are designated as contributing sources. We used 30 mixing proportions (corresponding to 30 simulated sinks) and $K = 10$, 20 contributing sources in each iteration with $M = 50$ and 200 respectively. We drew the mixing vector of length K from a Pareto distribution, which was scaled to sum to 1. Finally, the sink was generated under the model as a linear combination of the K contributing sources and the unknown source. For a detailed description of the simulation, see Supplementary Material.

In vitro data generation

To evaluate the performance of STENSL and validate the mixture model assumed by common microbial source tracking methods, we generated in vitro data, using the generative model described above following a 16S amplification protocol from Tong et al.[10]. The contributing sources were taken from the digestive systems of three human

444

subjects and three mice. Two of the human subjects were documented with a pre-Ketogenic diet and the third was sampled from the 'Human Altitude Study'. Using these sources, we assembled 27 in-vitro sinks, each sink composed of two to three microbial samples at varying mixing proportions (ranging from 20% to 80%). For a detailed description of the assembly process and protocols used, see Supplementary Material. To assess the performance of microbial source tracking methods in the presence of non-contributing sources, we next generated 50 additional synthetic sources by shuffling the abundances of the six contributing sources described above. The number of taxa expressed in each synthetic source T_i; $(1 \leq i \leq 50)$ was determined following a uniform distribution T_i Unif(min(T_{real1} ,..., T_{real6}), max(T_{real1} ,..., T_{real6})), where T_{realj}; $(1 \leq j \leq 6)$ is the number of taxa in the six contributing sources described above. Then, for each taxa-j, we randomly drew, without replacement, a count which was observed among all non-zero taxa.

Supplementary Information

Simulation procedure

We evaluated STENSL under a variety of sinks generated using real-world microbial samples found in the Earth Microbiome Project [ref]. In practice, we may encounter minimal to dominant unknown presence, so we simulated sinks for unknown percent from 0%~90%. We denote the unknown proportion according to the percentages as u. In

445

addition, we ensured similarity between sources measured in Jensen-Shannon divergence (JSD) was consistent such that sink-source relationships were not trivial. As many as M sources were gathered per sink, of which K sources randomly contributed to the sink. Accuracy for the generated sinks was measured as the Mean-Squared Error (MSE) between the estimated and true mixing proportions.

The simulation procedure to generate a single sink for chosen unknown proportion $u \in \{0.2, 0.4, 0.6, 0.7, 0.9\}$ was as follows:

1. Choose number of sources M and K, where $K \leq M$

2. Randomly generate a mixing proportion for K sources such that $m_{-1} \sim Pareto(> 0)$ where $m_{-1} = 1 - u$.

3. Draw M microbial samples $S_1, \ldots , S_K$ from the dataset. We ensure pairwise divergence $JSD(S_i, S_j) > 0.8$ for $1 \leq i \leq M, 1 \leq j \leq M$.

4. Draw the $M+1^{th}$ microbial sample S_{M+1} which is the unknown source. Ensure pairwise divergence $JSD(S_i, S_{M+1}) > 0.5$ for $1 \leq i \leq M$.

5. Draw noisy realizations of real sources $S_1, \ldots , S_{M+1}$ from the Multinomial distribution which we denote as $Y_1, \ldots , Y_{M+1}$.

6. The sink sample abundance is obtained as $\sum_{k \in \{1 \ldots K, M+1\}} m_k S_k = X$. This combines the first K randomly selected sources and the unknown source.

7. STENSL is applied to sink X and sources $Y_1, \ldots , Y_{M+1}$.

8. Calculate the MSE between the estimated and true mixing proportions.

In vitro data generation. The following materials were used: (a) 96 well plate of uniquely barcoded IL_806r primers[11], (b) ILHS_515f, (c) 10 PCR buffer (Sigma-Aldrich, cat. no. D9307) 10 mM dNTPs JumpStart Taq DNA polymerase (Sigma-Aldrich, cat. no. D9307), (d) DEPC-treated water QIAquick PCR purification kit (QIAGEN, cat. no. 28104), (e) Nanodrop spectrophotometer, (f) Thermal cycler, (g) six microbial environments: (1) Mouse SPF after 7 days of Ketogenic Diet, (2) Mouse SPF with after 7 days of standard diet, (3) Mouse SPF Kcna +/+ 1, (4) human subject 1, Pre-Ketogenic diet, (5) human subject 2, from the 'Human Altitude Study', SA2 and (6) human subject 3, Pre-Ketogenic diet. Overall, 27 synthetic sinks were assembled in vitro with varying source contributions, using two to three microbial environments per sink. We Prepared the following PCR master mix to amplify each sample in triplicate: 10× PCR buffer 3l x 3.3 x no. of samples dNTPs (10 mM) 0.6l x3.3 x no. of samples JumpStart Taq DNA polymerase 0.3l x 3.3 x no. of samples H2O 23.1l x 3.3 x no. of samples. For this step, each separate source used in a sample was amplified separately, then purified via PCR purification, then added to the final multiplexed tube in a proportion according to the outlined above so that the total amount added is 250 ng of DNA per barcode. This is to prevent sequencing bias. i.e., for Barcode number 1, if this is a sample prepared as 1a, this would mean sample number 1 and number 2 would be amplified in separate tubes using Barcode 1, then 125 ng of purified product will be used for each in the final tube (to get 50% of each).

We Added 81l master mix to every third well of a 96-well PCR plate, added 6l sample DNA (2l x 3 reactions) and 3l primer mix (1l x 3 reactions) from a well of a 96-well primer plate to each of these wells. Using a P200 pipette, we mixed each well and then

447

transferred 30l into each of the two neighboring wells, resulting in triplicate reactions for each sample. we Sealed the plate with 8-cap strips (made sure they are matched to the plate) or with plastic film. We performed PCR with the following thermal cycler settings: 1 cycle: 94 degree Celsius 3 min 35 cycles: 94 degrees Celsius 45 sec 50 degrees Celsius 1 min 72 degrees 1.5 min 1 cycle: 72 degrees Celsius 10 min 1 cycle: 72 degrees Celsius 5 min Final step: 4 degrees Celsius (hold). We Combined the PCR products from the triplicate reactions. We used the Qiagen PCR cleanup kit to purify PCR products from each sample, and elute DNA with 30l PCR grade (DEPC-treated) H2O. We quantified the amplified DNA using spectrophotometer, and then combined 250 ng of each sample amplicon into one tube to make a multiplexed library. Samples were multiplexed using the appropriate sequencing primers[11], to Laragen for sequencing. We obtained ~70,000 reads per sample. All samples were analyzed via QIIME2 using ASV and taxonomic information[12].

a. Difference in means, MSE

Unknown	0%	20%	40%	70%	90%
FEAST	Not sig.	Not sig.	p=5.40e-24	p=5.59e-31	p=1.03e-19
STracker2	Not sig.	p=0.0397	p=8.39e-17	p=1.01e-34	p=4.87e-26
RAD	Not sig.	p=7.47e-4	p=3.93e-18	p=4.39e-35	p=5.29e-27

b. Difference in means, noise amount

Unknown	0%	20%	40%	70%	90%
FEAST	p=0.0361	p=2.84e-11	p=1.39e-23	p=4.86e-26	p=2.69e-18
STracker2	p=5.96e-13	p=4.67e-23	p=3.63e-24	p=6,86e-27	p=3.41e-22
RAD	p=2.13e-31	p=2.37e-29	p=6.48e-27	p=9.61e-26	p=5.37e-13

(c) Difference in means in unknown estimation, MAE

Unknown	0%	20%	40%	70%	90%
FEAST	Not Sig.	p=2.24e-18	p=2.40e-37	p=9.50e-29	p=1.38e-19
STracker2	p=1.07e-4	p=1.36e-20	p=1.52e-41	p=3.11e-34	p=6.94e-26
RAD	Not sig.	p=2.61e-21	p=2.88e-44	p=8.77e-36	p=6.98e-27

Table 9 (a) P-values for difference in mean t-tests (paired) for MSE accuracy of STENSL to estimate the true mixing proportions against comparable methods. We observe that for any amount of positive unknown contribution that STENSL would perform favorable results in the estimation task with significance. (b) P-values for difference in mean t-tests of false positive source detections, characterized as noisy predictions. (c) P-values for difference in mean t-tests of estimation of
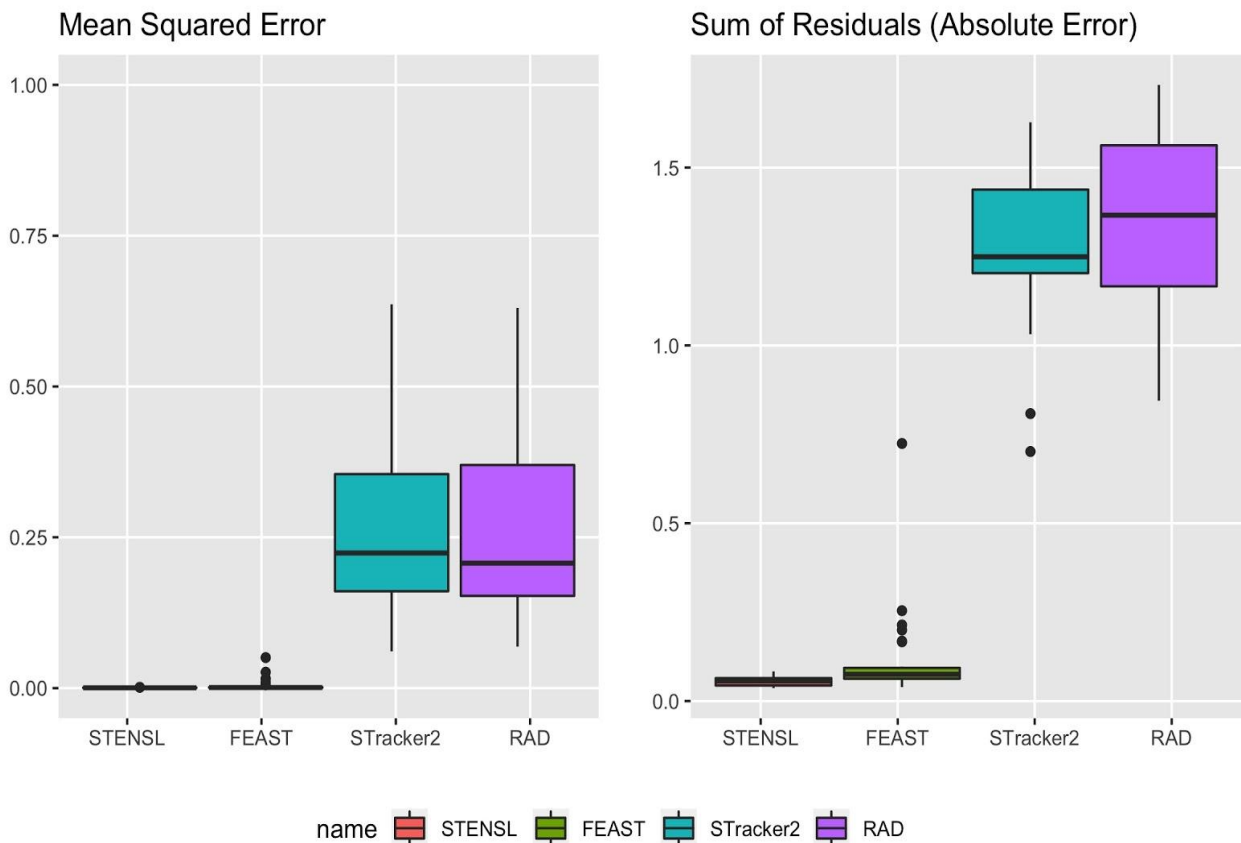
Figure 51: Performance of STENSL, FEAST, SourceTracker2, and RAD where no unknown source is present (0%) in simulations Estimation performance is measured on a simulated sink consisting of K=10 sources, with M=50 sources provided in total as potential candidates as sources in the source tracking problem. For 30 such simulated source-snik problems (a) performance is quantified as mean-squared error of known simulated mixing proportion vs estimated mixing proportion and (b) sum of residuals (absolute) of estimated mixing proportion for each set of sources where error directly corresponds to mis-attributed proportions.
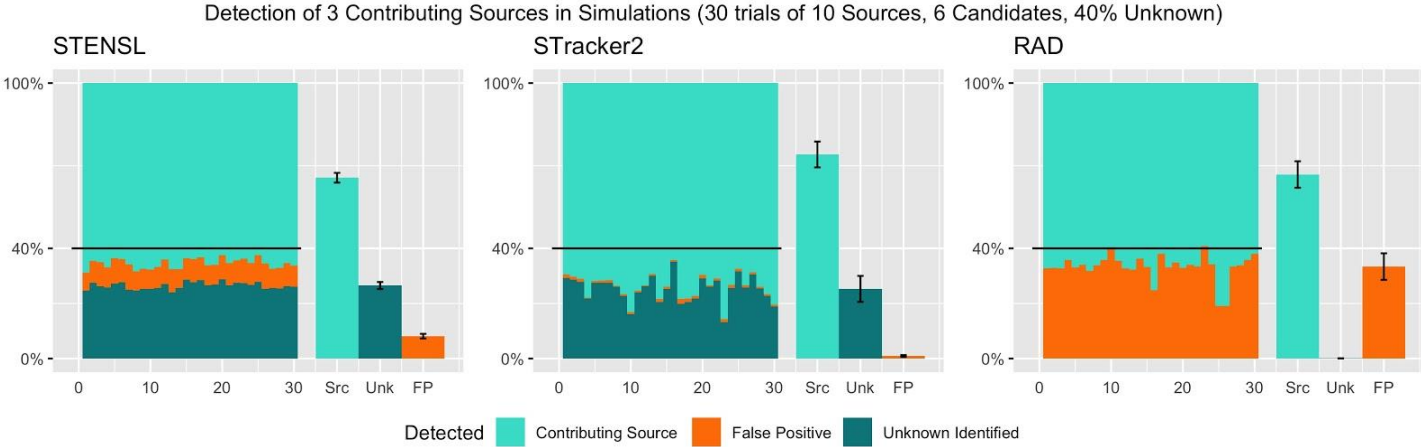

Figure 52: A small source tracking problem with sinks consisting of M=3 sources analysed using STENSL, FEAST, SourceTracker2, and RAD in simulations Sinks were simulated each consisting of M=3 sources, and 3 additional candidate sources (M=6 in total) were provided in each source tracking problem. Additionally, an unknown contributor of 40% was simulated in the sink. Mixing proportions estimated for 30 such simulations were labelled as belonging to either a Contributing, False Positive (not contributing to formation of sink), and Unknown Identified.
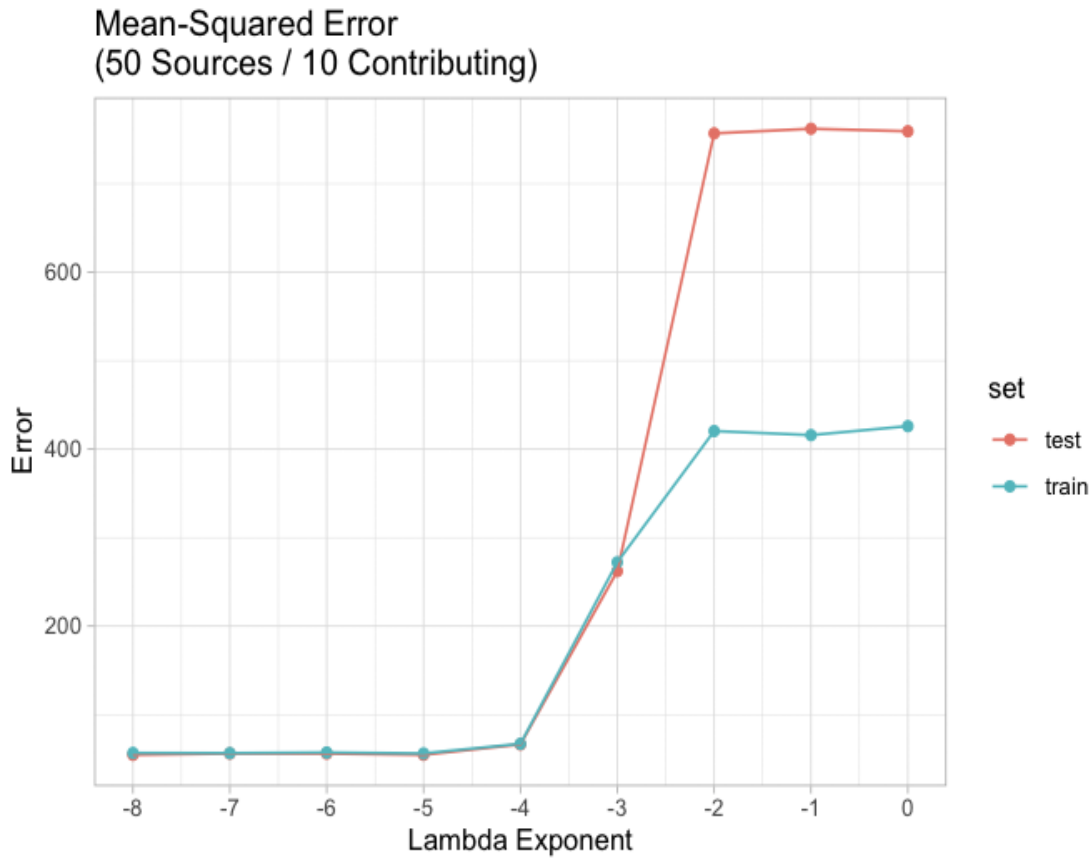
Mean-Squared Error
(50 Sources / 10 Contributing)

Figure 53: Cross-validation to determine λ STENSL utilizes Lasso as part of the

selection step, in which hyperparameter **λ** of the sparsity regularization must be

determined. We use cross-validation on a simulated dataset of sinks (and their

corresponding sources) to find an optimal **λ** for microbial data based on prediction

errors $=_1 M_{i=1} M(X-YT)2$. The dataset is split in half for sinks which will be analysed as

part of training to tune the hyperparameter, and we evaluate Lasso on the reserved test

set. In the validation plot, we show the average of the errors for each **λ** and find that

choosing a value $< 1x10^{-4}$ would be optimal. In our experiments, we choose **λ = 1x10⁻⁶**

Unknown Proportion
(50 Candidates / 10 Contributing)
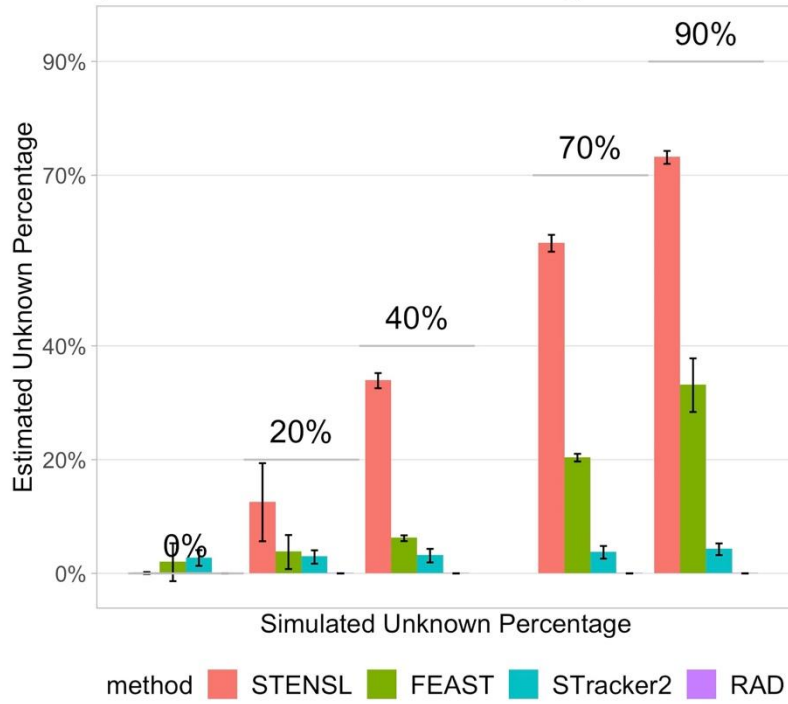
Unknown Proportion
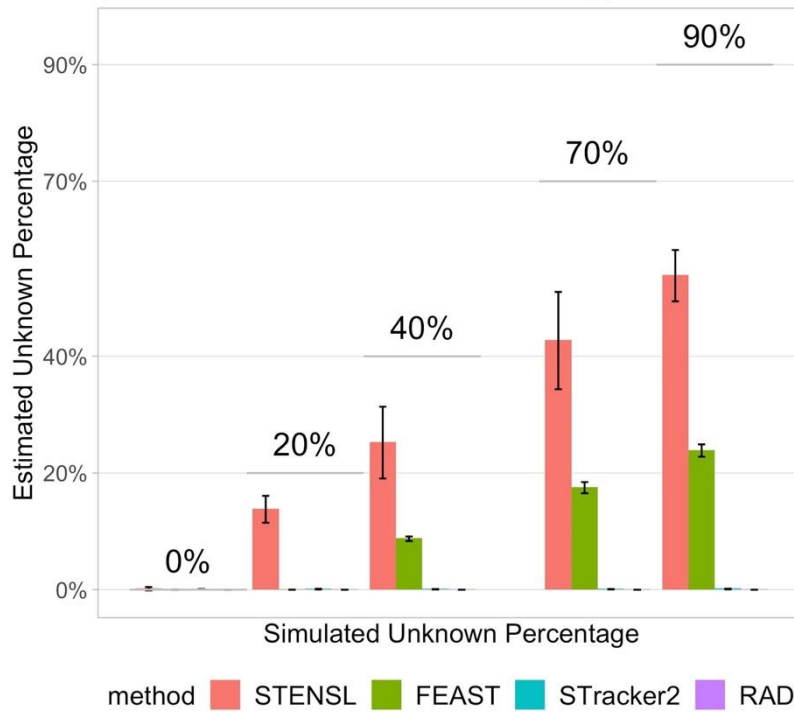## (200 Candidates / 20 Contributing)

Figure 54: Robustness to a wide range of unknown presence. For all the estimated

mixing proportions in our simulations from (a), we highlight how accurately each method

estimated the unknown proportion. We found that STENSL was the only method to

correctly estimate the simulated amount of unknown for M=50,200. For any positive

unknown proportion 20%~90%, mean absolute error (MAE) of the estimated unknown

proportion was significantly lower when using STENSL with p-value < 1.07x10-4 across

the compared methods.

Mean-Squared Error

method ■ STENSL ■ FEAST ■ S.Tracker2
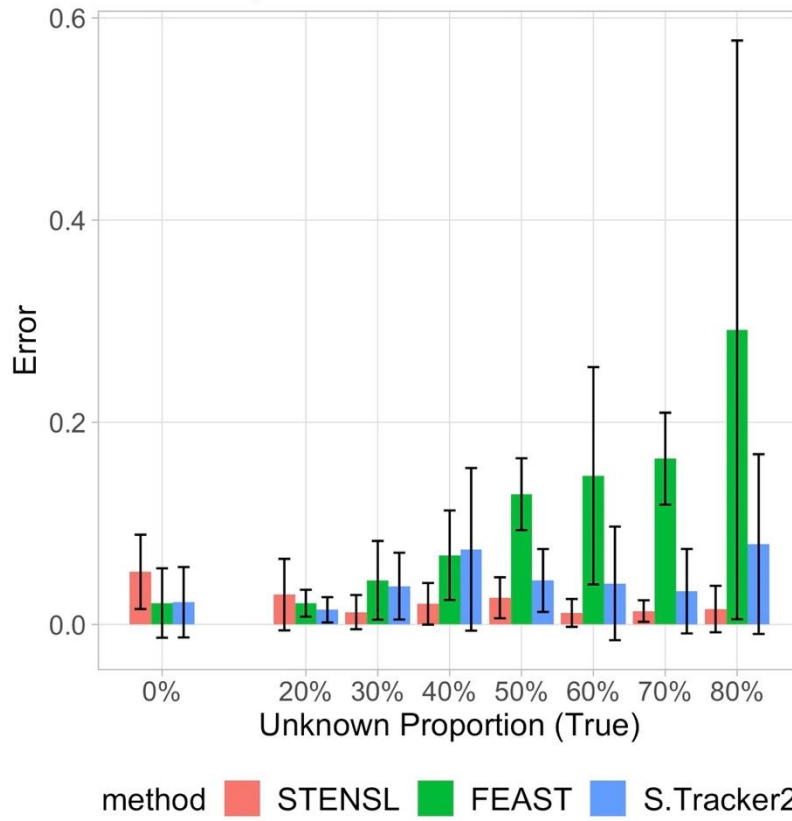
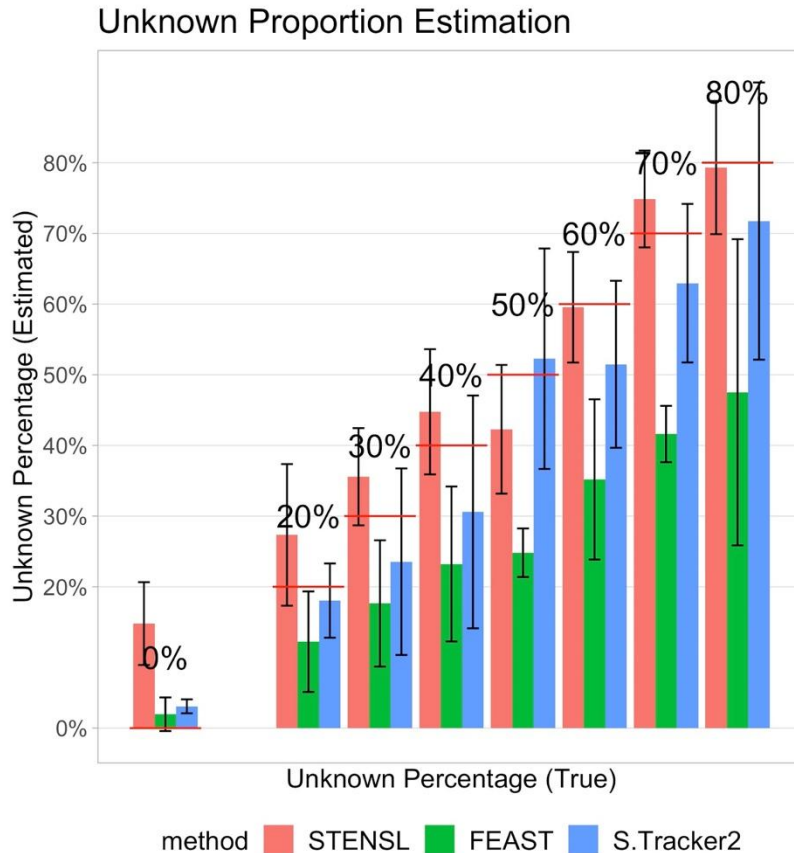**Figure 55: Analysis of in-vitro dataset of sinks created from mixture of Human and Mice Gut Samples** Known contributors to the sink mixture were withheld from the list of sources to create source tracking problems with unknown quantities between 0%~80%. The accuracy of STENSL, SourceTracker2, and FEAST was evaluated using mean-squared error (MSE) against the true mixing proportion used to create in vitro sinks with unknown proportions ranging from 0% to 80% and in the presence of 50 non-contributing sources. (a) Accuracies of STENSL, SourceTracker2, and FEAST were evaluated using mean-squared error (MSE) against the stated mixing proportion used to create the sink and are shown across 0%~80% (p-values < 0.021 for positive unknown proportions using paired t-test). (b) We visualize the estimated unknown proportion against the true unknown proportion introduced by the withheld source(s) for unknown

proportions 0%~80%. Sink mixtures ranged from consisting of two to three sources and up to two sources were withheld to create an environment with unknown quantity.

References

1. Shenhav, L. *et al.* FEAST: fast expectation-maximization for microbial source tracking. *Nature Methods* vol. 16 627–632 (2019).

2. Knights, D. *et al.* Bayesian community-wide culture-independent microbial source tracking. *Nat. Methods* **8**, 761–763 (2011).

3. Wu, C. H. *et al.* Characterization of coastal urban watershed bacterial communities leads to alternative community-based indicators. *PLoS One* **5**, e11285 (2010).

4. Lax, S. *et al.* Longitudinal analysis of microbial interaction between humans and the indoor environment. *Science* **345**, 1048–1052 (2014).

5. Dominguez-Bello, M. G. *et al.* Partial restoration of the microbiota of cesarean-born infants via vaginal microbial transfer. *Nat. Med.* **22**, 250–253 (2016).

6. Teaf, C. M., Flores, D., Garber, M. & Harwood, V. J. Toward Forensic Uses of Microbial Source Tracking. *Microbiol Spectr* **6**, (2018).

7. Carter, K. M., Lu, M., Luo, Q., Jiang, H. & An, L. Microbial community dissimilarity for source tracking with application in forensic studies. *PLoS One* **15**, e0236082 (2020).

8. Thompson, L. R. *et al.* A communal catalogue reveals Earth's multiscale microbial diversity. *Nature* vol. 551 457–463 (2017).

9. Human Microbiome Project Consortium. Structure, function and diversity of the healthy human microbiome. *Nature* **486**, 207–214 (2012).

10. Tong, M., Jacobs, J. P., McHardy, I. H. & Braun, J. Sampling of intestinal microbiota and targeted amplification of bacterial 16S rRNA genes for microbial ecologic analysis. *Curr. Protoc. Immunol.* **107**, 7.41.1–7.41.11 (2014).

11. Caporaso, J. G. *et al.* Ultra-high-throughput microbial community analysis on the Illumina HiSeq and MiSeq platforms. *ISME J.* **6**, 1621–1624 (2012).

12. Amir, A. *et al.* Deblur Rapidly Resolves Single-Nucleotide Community Sequence Patterns. *mSystems* vol. 2 (2017).

Appendix 2

The gut microbiota in aging-dependent frailty phenotypes

Christine A. Olson, Grace E. Yang, Elaine. Y. Hsiao

Unpublished

Introduction and motivation:

Aging is the main risk factor in all leading diseases for mortality after age 28 in humans[1], and is defined as "the accumulation over time of detrimental changes at the molecular and cellular levels, and ultimately at the level of tissues and organs, resulting in disease and increased risk of morbidity and mortality"[2]. It makes sense that in order to extend human life expectancy, we must target the root causes of aging[1]. The ***nine hallmarks of aging*** are as follows[3]:

1) Altered intercellular communication

2) Genomic instability

3) Telomere attrition

4) Epigenetic alteration

5) Loss of proteostasis

6) Deregulated nutrient sensing

7) Mitochondrial dysfunction

8) Cellular senescence

9) Stem cell exhaustion

The gut microbiota In the initial germ-free aging studies performed at Notre Dame University in 1966, the researchers noted that germ-free (**GF**) mice live significantly longer, on average, than mice that are conventionally reared (specific-pathogen free, **SPF**)[4]. While the gut microbiota composition has been associated with aging-related decline in humans and mice[5], precise mechanisms for how the gut microbiota regulates aging-related dysfunction is unknown. The only modern mechanistic study comparing aged GF mice to aged SPF mice[6] found that (a) a greater proportion of GF mice live to

day 600, (b) aging in SPF mice increases intestinal permeability, which reduces with GF status in aging, (c) aging in SPF increases circulating pro-inflammatory IL-6, which reduces with GF status in aging, (d) increased lung immune infiltration with aging under SPF conditions that is ameliorated with GF status in aging.

Age-related frailty is associated with a reduction in the gut microbiota diversity[7], but whether these changes are hallmarks of an aging ecosystem or direct factors which contribute to aging-associated decline is uncertain. Factors associated with acceleration of biological ageing, like chronic inflammation, are strongly affected by the gut microbiota, and indeed, aging is characterized by a low-level of inflammation, termed "inflammaging"[2,6]. The following study aims to interrogate and describe the healthspan of aged GF vs. SPF vs. ABX mice compared with young SPF controls using gross evaluation, frailty assessment, cognitive, metabolic, and 'omics sequencing and profiling technologies.

METHODS:

EXPERIMENTAL MODELS AND SUBJECT DETAILS

Mice

For the Young SPF cohorts, 6-week-old SPF wild-type C57/BL6J mice (Jackson Laboratories) were used, for the Aged SPF and Abx cohorts, 17-month-old SPF wild-type C57 BL6/J mice (National Institutes of Aging) were used, and for the Aged GF mice, 18-month-old germ-free C57 BL6/J mice (Jackson Laboratories) were used. The age discrepancy for Aged SPF/Abx mice and Aged GF mice was due to a dietary difference between Jackson Laboratories and the National Institutes of Health (NIA). All NIA-sourced mice were acclimated to the same dietary treatment utilized for Jackson

Laboratories for one month as described in the 'Dietary Treatment' section below. All Aged mice were tested for behavior and frailty metrics at 18 months of age. All mice were house in UCLA's Center for Health Sciences Barrier Facility. Mice were housed in autoclaved cages with irradiated food and sterile water and handled aseptically in a BSL2 biosafety cabinets with autoclaved gloves and sterile consumables. All animal experiments were approved by the UCLA Animal Care and Use Committee.

METHOD DETAILS

Dietary Treatment

Aged GF mice and Young SPF mice were fed sterile "breeder" chow (Lab Diets 5K52). Aged Abx and Aged SPF mice were raised on Purina LabDiet 5L79 and at 17 months of age were placed on Lab Diet 5K52 for one month, followed by behavioral testing. In the table below, we note nutrient differences between 5K52 and 5l79 respectively as follows: tyrosine (0.56% vs. 0.2%), taurine (0.03% vs. 0.01%), cholesterol (240 ppm vs. 110 ppm), linolenic acid (0.37% vs 0.1%), omega 3-fatty acids (0.46% vs. 0.2%), glucose (0.12% vs. 0.3%), fructose (0.15% vs. 0.3%), sucrose (0.62% vs. 2%), phosphorus (non-phytate) (0.68% vs. 0.28%). fluorine (37 ppm vs. 4.4 ppm), copper (11 ppm vs. 22 ppm), chromium (2 ppm vs. 0.01 ppm), Vitamin K (20 ppm vs. 3.3 ppm), thiamin hydrochloride (79 ppm vs. 500 ppm), pyridoxine (10 ppm vs. 72 ppm), B12 (50 mcg/kg vs. 130 mcg.kg), vitamin A (20 IU/gm vs. 44 IU/gm), vitamin D3 (4.3 IU/gm vs. 1.5 IU/gm).

Nutrients	Unit	5K52	5L79
Protein	%	19.3	18.4
Arginine	%	1.03	1.16
Cystine	%	0.25	0.32
Glycine	%	0.94	0.87

Histidine	%	0.44	0.49
Isolaucine	%	0.87	0.74
Leucine	%	1.52	1.44
Lysine	%	0.97	0.96
Methionine	%	0.73	0.38
Phenylalanine	%	0.85	0.84
Tyrosine	%	0.56	0.2
Threonine	%	0.68	0.66
Tryptophan	%	0.23	0.22
Valine	%	0.9	0.86
Serine	%	0.98	0.98
Aspartic Acid	%	1.8	2.03
Glyutamic Acid	%	4.52	3.94
Alanine	%	1.13	1.09
Proline	%	1.53	1.31
Taurine	%	0.03	0.01
Fat (ether extract)	%	6.2	5.7
Fat (acid hydrolysis)	%	7.2	6.8
Cholesterol	ppm	240	110
Linoleic Acid	%	2.88	1.6
Linolenic Acid	%	0.37	0.1
Arachidonic Acid	%	0.01	<0.1
Omega-3 Fatty Acids	%	0.46	0.2
Total Saturated Fatty Acids	%	1.24	1.8
Total Monosaturated Fatty Acids	%	1.37	1.9
Fiber (Crude)	%	4.3	4.4
Neutral Detergent Fiber	%	15.1	17.1
Acid Detergent Fiber	%	5.2	5.3
Nitrogen-Free Extract (by difference)	%	53.6	55.9
Starch	%	38.9	31.9

			5K52	5L79
Glucose	%		0.12	0.3
Fructose	%		0.15	0.3
Sucrose	%		0.62	2
lactose	%		0	0
Total Digestible Nutrients	%		76.3	77.1
Gross Energy	kcal/gm		4.17	4.15
Physiological Fuel Value	kcal/gm		3.47	3.48
Metabolizable Energy	kcal/gm		3.17	3.15

Minerals			5K52	5L79
Ash	%		6.5	5.6
Calcium	%		1.17	0.85
Phosphorus	%		0.93	0.61
Phosphorus (non-phytate)	%		0.68	0.28
Potassium	%		0.66	0.95
Magnesium	%		0.22	0.25
Sulfur	%		0.33	0.24
Sodium	%		0.26	0.25
Chloride	%		0.45	0.41
Fluorine	ppm		37	4.4
Iron	ppm		380	200
Zing	ppm		85	150
Manganese	ppm		160	150
Copper	ppm		11	22
Cobalt	ppm		0.8	0.56
Iodine	ppm		2.1	1.9
Chromium (added)	ppm		2	0.01
Selenium	ppm		0.3	0.46

Vitamins			5K52	5L79
Carotene	ppm		1.5	0.9
Vitamin K (as menadione)	ppm		20	3.3
Thiamin Hydrochloride	ppm		79	500

Riboflavin	ppm		9	8.1
Niacin	ppm		90	82
Panthothenic Acid	ppm		37	36
Choline Chloride	ppm		2000	1260
Folic Acid	ppm		1.9	3.5
Pyridoxine	ppm		10	72
Biotin	ppm		0.3	0.3
B12	mcg/kg		50	130
Vitamin A	IU/gm		20	44
Vitamin D3 (added)	IU/gm		4.3	1.5
Vitamin E	IU/kg		45	79
Ascorbic Acid	mg/gm		-	trace

Calories Provided By		5K52	5L79
Protein	%	22.238	21.126
Fat (ether extract)	%	16.028	14.725
Carbohydrates	%	61.734	64.149

Open Field Testing

All mice were habituated in the behavior room for an hour prior to behavioral testing. The open field test is widely used to measure anxiety-like and locomotor behavior in rodents. Mice were placed in the center of a 50 cm x 50 cm arena for 10 min, during which an overhead Basler Gig3 camera and EthoVision XT (Noldus) software was used to measure distance traveled, and the number of entries and duration of time spent in the central 17 cm square area. The boxes were cleaned with 70% ethanol and Accel disinfectant before and after each session.

Object Habituation, Novel Location and Novel Object Testing

An hour after open field testing, mice were habituated to two identical cups in opposite corners of the open field arena for 10 minutes for object habituation. The time spent in each object and the nose pokes in each object, each quantified as a 2 cm border around

the object, were analyzed to determine whether there was an initial object or size preference for any group. For the novel location task, an hour after object habituation, one of the identical cups was placed in a different corner of the arena, which represents the novel location, while the cup in the familiar location represents the familiar object. The time and entries into object were calculated for a 2 cm perimeter around each object. For the novel object task, 1 hour after the novel location task, one object was replaced with a new ball object, which represented the novel object, while the previous cup represented the familiar object. The time and entries into object were calculated for a 2 cm perimeter around each object.

Frailty Metrics

All mice were assessed for frailty using metrics as previously published [103, 104], and as listed below.

I.   Excessive barbering

II.   Alopecia

III.   Dermatitis

IV.   Loss of whiskers

V.   Coat condition

VI.   Kyphosis

VII.   Tail stiffening

VIII. Grip strength (see below)

IX.   Body condition

X.   Eye discharge and swelling

XI.   Nasal discharge

XII.   Rectal prolapse

XIII. Vaginal/uterine/penile prolapse

XIV.   Breathing rate/depth

XV.   Grimace

XVI.   Cataracts

XVII. Malocclusion

XVIII. Tumors/lumps

XIX.   Take a photo from the top of the animal and of the animal's face

RESULTS

In comparing SPF young mice to Aged SPF, Aged ABX, and Aged GF mice, for the open field task aged GF mice exhibit lower numbers of nose pokes to the center region and total distance traveled compared to other groups (**Figure 56**). In habituating mice to objects used for novel object task and novel location task, no overt object preference was demonstrated across groups (**Figure 57**). For the novel object task and location task, no overt differences were noted between groups (**Figure 58**). In comparing a battery of frailty-associated traits, we find clearance of the gut microbiota prevents aging-induced alopecia, deteriorating coat condition, and kyphosis, with no effect noted on other traits tested (**Figure 59,** example images in **Figure 60**).

Future Directions:

In the future, this project will focus on aging and microbiota-associated lipidomic profiling, metagenomics on colon contents, and hippocampal RNA sequencing to identify aging and microbiota-associated traits for each assay.

References

1.   Harman, D. The aging process: major risk factor for disease and death. *Proc. Natl. Acad. Sci. U. S. A.* **88**, 5360–5363 (1991).

2.   Jenny, N. S. Inflammation in aging: cause, effect, or both? *Discov. Med.* **13**, 451–460 (2012).

3.   López-Otín, C., Blasco, M. A., Partridge, L., Serrano, M. & Kroemer, G. The hallmarks of aging. *Cell* (2013). doi:10.1016/j.cell.2013.05.039

4.   Gordon, H. A., Bruckner-Kardoss, E. & Wostmann, B. S. Aging in germ-free mice: life tables and lesions observed at natural death. *J. Gerontol.* **21**, 380–387 (1966).

5.   Aleman, F. D. D. & Valenzano, D. R. Microbiome evolution during host aging. *PLOS Pathog.* **15**, e1007727 (2019).

6.   Thevaranjan, N. *et al.* Age-Associated Microbial Dysbiosis Promotes Intestinal Permeability, Systemic Inflammation, and Macrophage Dysfunction. *Cell Host Microbe* **21**, 455-466.e4 (2017).

7.   O'Toole, P. W. & Jeffery, I. B. Gut microbiota and aging. *Science (80-.).* **350**, 1214 LP – 1215 (2015).

8.   Bellantuono, I. *et al.* A toolbox for the longitudinal assessment of healthspan in aging mice. *Nat. Protoc.* **15**, 540–574 (2020).

9.   Hao, Z. *et al.* Motor dysfunction and neurodegeneration in a C9orf72 mouse line
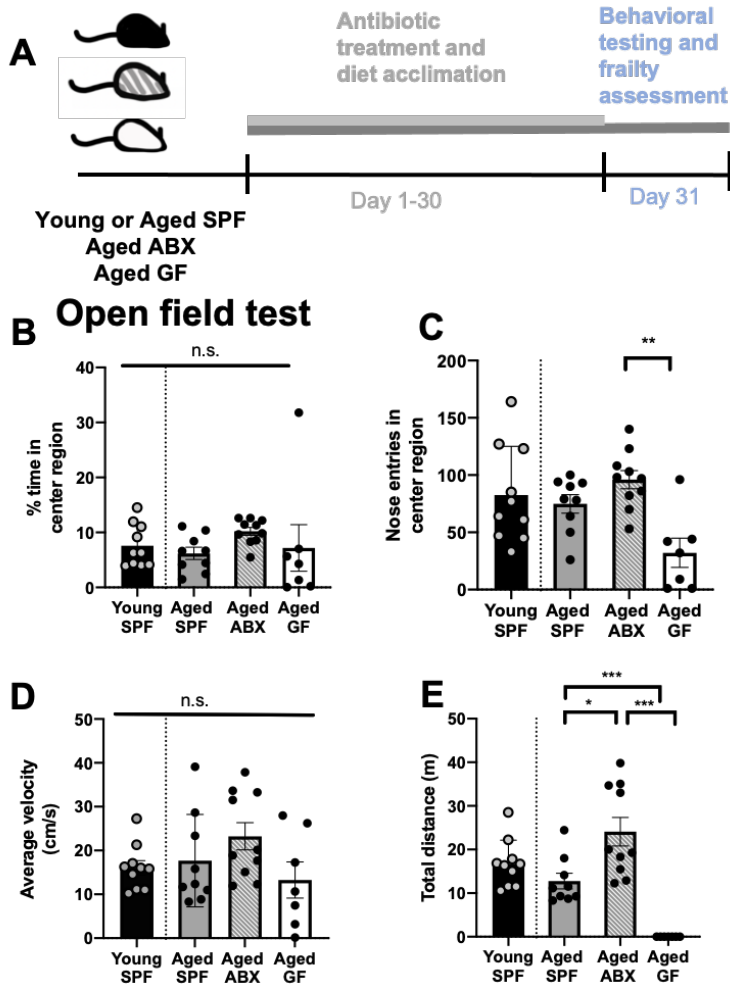
expressing poly-PR. *Nat. Commun.* **10**, 2906 (2019).

Figure 56: Open field testing. A) Experimental timeline: Conventionally-colonized (specific pathogen free, SPF) mice were aged to 17 months and treated for 30 days with antibiotics in the ABX condition (Aged ABX) compared with water controls (Aged SPF). 1.5 month old SPF mice were used for the Young SPF condition, and mice reared germ-free until 18 months of age were used for the GF Aged group. After this period, mice were subjected to behavioral testing consisting of open field testing, novel location recognition, and novel object recognition, in addition to frailty assessment and rotarod testing. **B)** Percent of time spent in the center region of the arena (n=7-10). **C)** Nose entries into the center region (n=7-10). **D)** Average velocity of mice during the open field task (cm/s) (n=7-10). **E)** Total distance traveled (m) during the open field task (n=7-10).

(Two-way ANOVA with Data are presented as mean ± S.E.M. * p < 0.05, **p < 0.01, ***p < 0.001, ****p < 0.0001. n.s.=not statistically significant. SPF=specific pathogen-free (conventionally-colonized), ABX= treated with antibiotics, GF=germ-free.
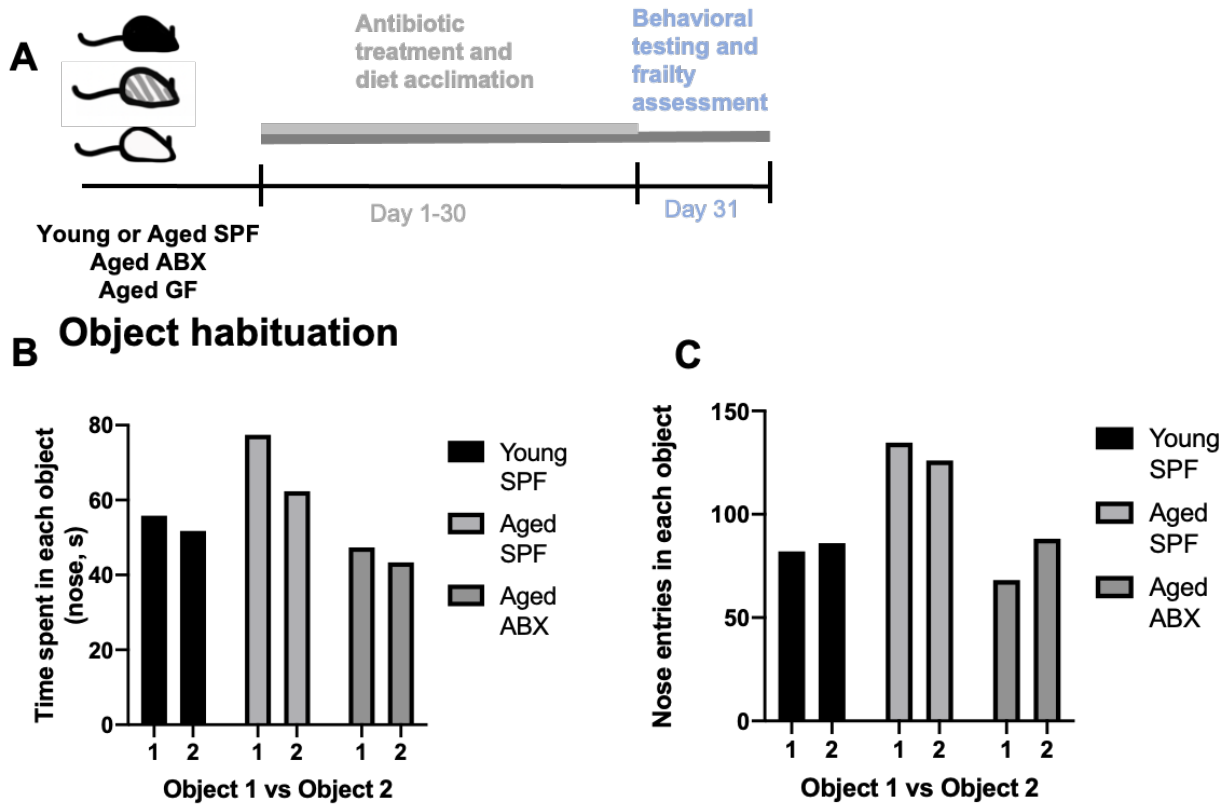

Figure 57: Clearance of the gut microbiota during aging does not affect object habituation A) Experimental timeline: Conventionally-colonized (specific pathogen free, SPF) mice were aged to 17 months and treated for 30 days with antibiotics in the ABX condition (Aged ABX) compared with water controls (Aged SPF). 1.5 month old SPF mice were used for the Young SPF condition, and mice reared germ-free until 18 months of age were used for the GF Aged group. After this period, mice were subjected

to behavioral testing consisting of open field testing, novel location recognition, and novel object recognition, in addition to frailty assessment and rotarod testing. **B)** Time spent (s) with habituating objects during task (n=7-10). **C)** Entries into each habituating object during task (n=7-10). (Two-way ANOVA with Data are presented as mean ± S.E.M. * $p < 0.05$, **$p < 0.01$, ***$p < 0.001$, ****$p < 0.0001$. n.s.=not statistically significant. SPF=specific pathogen-free (conventionally-colonized), ABX= treated with antibiotics, GF=germ-free.
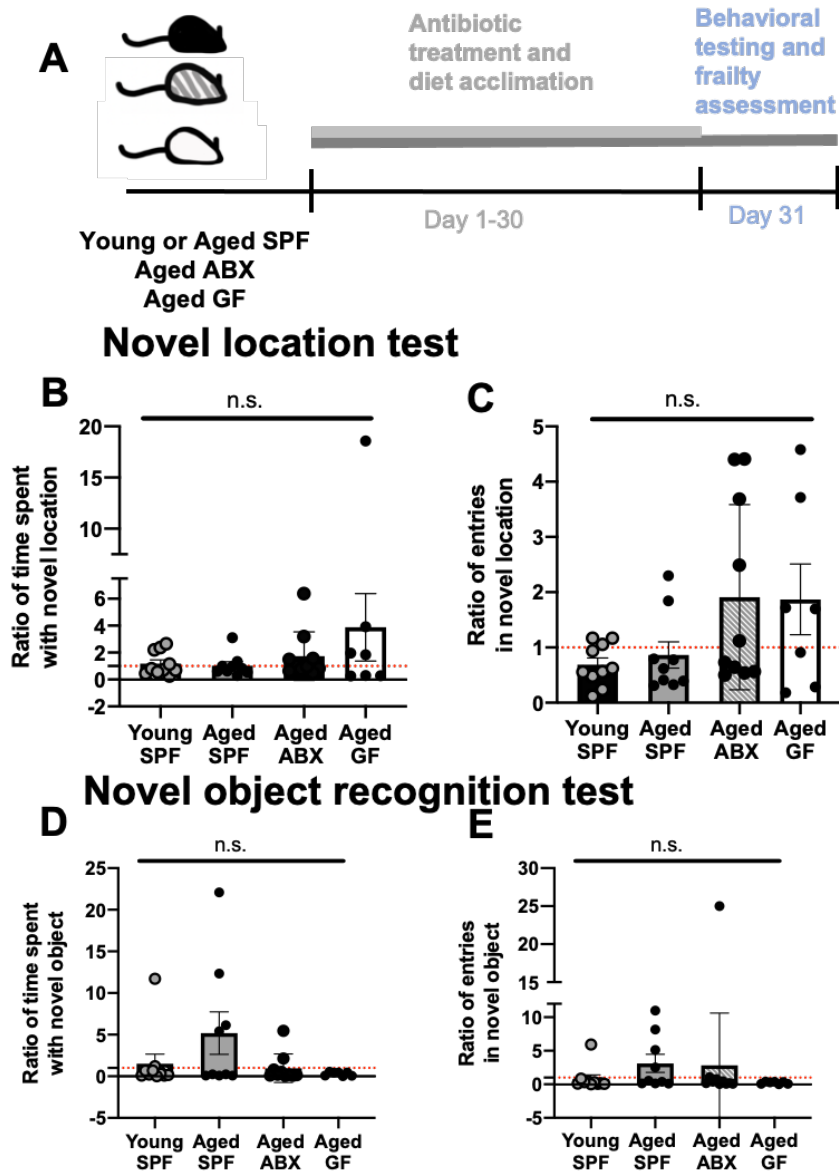
Figure 58: Clearance of the gut microbiota during aging does not affect novel object location or novel location recognition. A) Experimental timeline:

Conventionally-colonized (specific pathogen free, SPF) mice were aged to 17 months

and treated for 30 days with antibiotics in the ABX condition (Aged ABX) compared with

water controls (Aged SPF). 1.5 month old SPF mice were used for the Young SPF

condition, and mice reared germ-free until 18 months of age were used for the GF Aged

group. After this period, mice were subjected to behavioral testing consisting of open

field testing, novel location recognition, and novel object recognition, in addition to frailty

assessment and rotarod testing. **B)** Ratio of time spent with novel object location during

task (n=7-10). **C)** Ratio of entries in novel object location during task (n=7-10). **D)** Ratio

of time spent with novel object during task (n=7-10). **E)** Ratio of entries (n=7-10). (Two-

way ANOVA with Data are presented as mean ± S.E.M. * $p < 0.05$, **$p < 0.01$, ***$p <$

0.001, ****$p < 0.0001$. n.s.=not statistically significant. SPF=specific pathogen-free

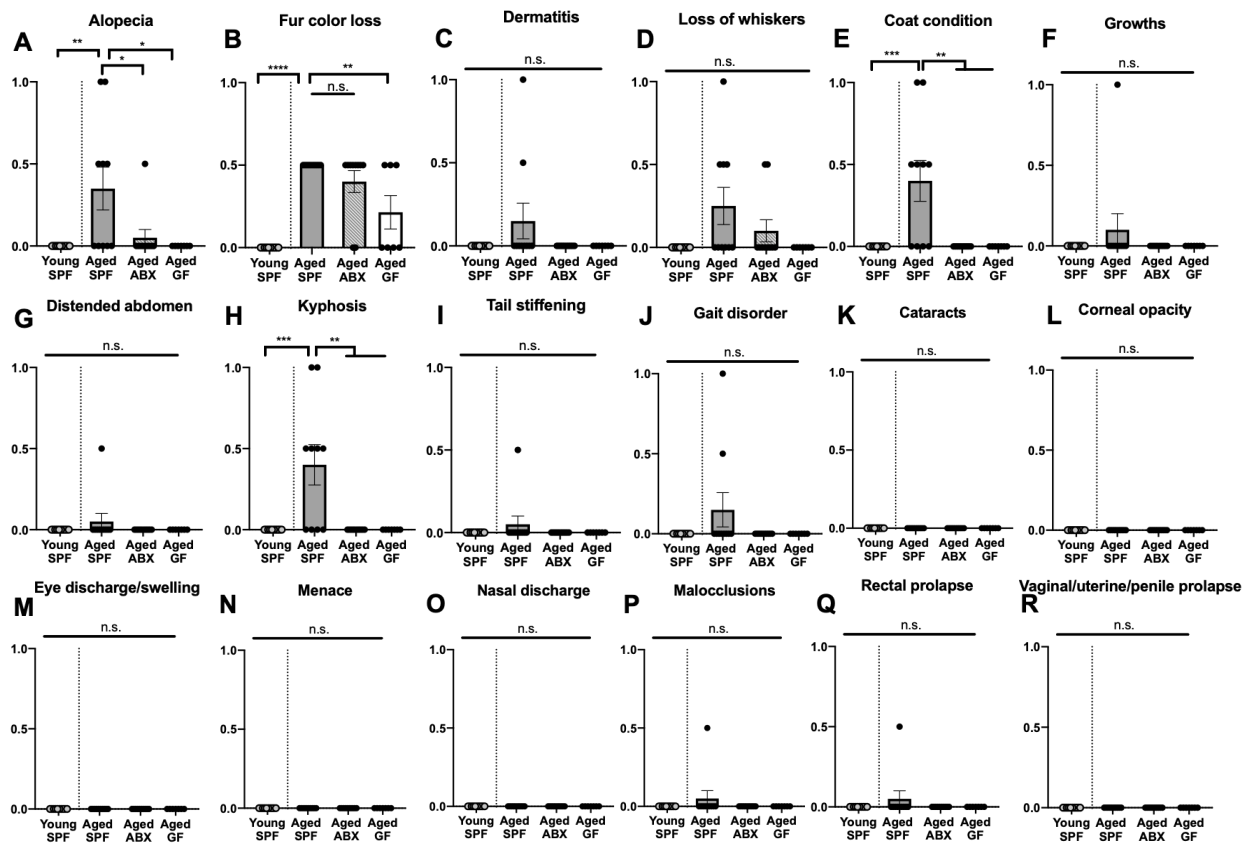(conventionally-colonized), ABX= treated with antibiotics, GF=germ-free.

Figure 59: Clearance of the gut microbiota prevents aging-induced alopecia,

deteriorating coat condition, and kyphosis. For all conditions, scoring was

performed at the time of sacrifice. Scores are given either as 0, 0.5, or 1, where 1 is the

worst subjective score. **A)** Alopecia scoring (n=7-10). **B)** Fur color loss scoring (n=7-10). **C)** Dermatitis scoring (n=7-10). **D)** Loss of whiskers scoring (n=7-10). **E)** Coat condition scoring (n=7-10). **F)** Growths scoring (n=7-10). **G)** Distended abdomen scoring (n=7-10). **H)** Kyphosis scoring (n=7-10). **I)** Tail stiffening scoring (n=7-10). **J)** Gait disorder scoring (n=7-10). **K)** Cataracts scoring (n=7-10). **L)** Corneal opacity scoring (n=7-10). **M)** Eye discharge/swelling scoring scoring (n=7-10). **N)** Menace scoring (n=7-10). **O)** Nasal discharge scoring (n=7-10). **P)** Malocclusion scoring (n=7-10). **Q)** Rectal prolapse scoring (n=7-10). **R)** Vaginal/uterine/penile prolapse scoring (n=7-10). (Two-way ANOVA with Data are presented as mean ± S.E.M. * $p < 0.05$, **$p < 0.01$, ***$p < 0.001$, ****$p < 0.0001$. n.s.=not statistically significant. SPF=specific pathogen-free (conventionally-colonized), ABX= treated with antibiotics, GF=germ-free.
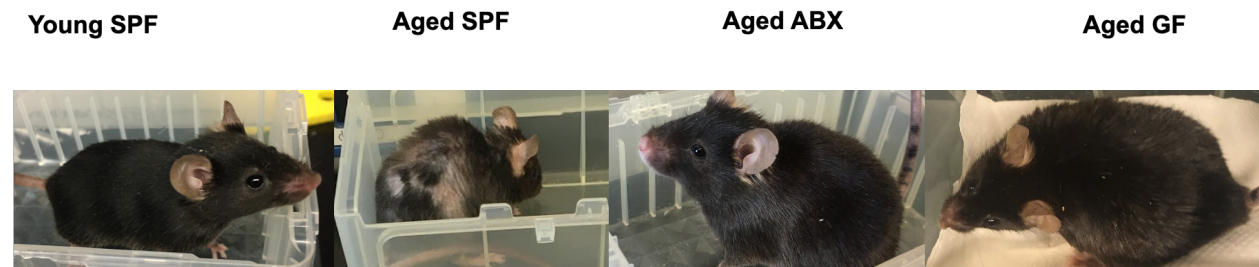

Figure 60: Example images of mice during frailty assessment. SPF=specific pathogen-free (conventionally-colonized), ABX= treated with antibiotics, GF=germ-free.